Studies on the mechanisms of acute mental stress-induced gastropathy and impairment of mitochondrial biogenesis in gastric mucosa

Thesis submitted to Jadavpur University for the degree of
Doctor of Philosophy (Science)

2025

by

Saikat Pramanik

CSIR-Indian Institute of Chemical Biology
Kolkata-700032, India

&

Jadavpur University
Kolkata-700032, India

बसु विज्ञान मन्दिर
BOSE INSTITUTE

(विज्ञान एवं प्रौद्योगिकी विभाग, भारत सरकार के एक स्वायत्त संस्था)
(An Autonomous Institute of Department of Science & Technology, Govt. of India)

मुख्य कैंपस / Main Campus :
93/1, आचार्य प्रफुल्ल चंद्र रोड, कोलकाता-700 009
93/1, Acharya Prafulla Chandra Road, Kolkata-700 009
फोन/Phone : 2350-7073 (निदेशक/Director)
इपीएबीएक्स /EPABX : 2350-6619/6702/2402/2403, 2303-0000/1111
फैक्स/Fax : 91-33-2350 6790

शतवार्षिकी भवन / Centenary Building :
पी-1/12, सी.आई.टी. स्कीम-VII-एम, कोलकाता-700 054
P-1/12, C.I.T. Scheme VII-M, Kolkata-700 054
फोन/Phone : 2355-7434 (निदेशक/Director), 2355-0595 (रजिस्ट्रार/Registrar)
इपीएबीएक्स /EPABX : 2355-9416/9219/9544, 2569-3271, फैक्स/Fax : 91-33-2355-3886

समन्वित शैक्षिक परिसर / Unified Academic Campus :
ब्लॉक-ईएन, प्लॉट नं-80, सेक्टर-V, सॉल्ट लेक सिटी, कोलकाता-700 091
Block-EN, Plot No.-80, Sector-V, Salt Lake City, Kolkata-700 091
फोन/Phone : 2569-3131 (निदेशक/Director)
इपीएबीएक्स /EPABX : 2569-3123/28, फैक्स/Fax : 91-33-2569-3127

संदर्भ सं. / Ref. No._____ दिनांक / Date :

CERTIFICATE FROM THE SUPERVISOR

This is to certify that the thesis entitled **"Studies on the mechanisms of acute mental stress-induced gastropathy and impairment of mitochondrial biogenesis in gastric mucosa"** submitted by **Sri Saikat Pramanik** who got his name registered on **27/08/2019** for the award of Ph. D. (Science) Degree of Jadavpur University, is absolutely based upon his own work under the supervision of **Prof. (Dr.) Uday Bandyopadhyay** and that neither this thesis nor any part of it has been submitted for either any degree / diploma or any other academic award anywhere before.

(Uday Bandyopadhyay) 23/7/25

Signature of the Supervisor

& date with official seal

Dr. Uday Bandyopadhyay
J.C. Bose National Fellow
Department of Biological Sciences
Bose Institute
Unified Academic Campus
Block-EN, Plot No.-80, Sector-V
Salt Lake City, Kolkata-700 091

Dedicated To My Beloved Family and All My Esteemed Teachers Who Shaped My Path

ACKNOWLEDGEMENT

*The journey toward earning the **Doctor of Philosophy (Ph.D.)** degree has been anything but linear-a path marked by exhilarating discoveries, formidable challenges, and steadfast perseverance. As I stand at the culmination of this transformative chapter, I am deeply mindful of the profound impact it has had on shaping my intellect, character, and aspirations. This work would not have come to fruition without the unwavering support and encouragement of many individuals.*

*First and foremost, I extend my deepest gratitude to my esteemed supervisor, **Prof. (Dr.) Uday Bandyopadhyay**, whose invaluable guidance, steadfast support, and profound expertise have been the cornerstone of my doctoral journey. His exceptional mentorship, marked by intellectual rigor and spiritual depth, has been pivotal in shaping both my academic and personal growth. I consider myself truly fortunate to have had the privilege of working under his mentorship, learning not only from his scholarly brilliance but also from his humility, wisdom, and unwavering passion for science. His constant encouragement and insightful feedback have continually motivated me to exceed my limits and pursue excellence with integrity. This enriching experience under his supervision has not only defined my academic trajectory but has also instilled in me a lifelong dedication to the pursuit of knowledge. I remain deeply indebted to him for his remarkable mentorship and unshakable belief in my potential, an influence I will carry with profound gratitude throughout my life.*

*I want to thank **Dr. Arun Bandyopadhyay**, former Director of CSIR-IICB, sincerely, and **Dr. Vibha Tandon**, the present Director, for providing an excellent research environment and the necessary infrastructure that enabled the smooth progression of my doctoral work.*

*Next, I would like to acknowledge the financial support provided by the **Council of Scientific & Industrial Research (CSIR), Ministry of Science & Technology, Government of India.** Their investment in my research has enabled me to carry out this study and pursue my scholarly aspirations.*

*I am deeply grateful to **Dr. Indu Bhusan Deb**, Senior Principal Scientist, CSIR-IICB, Kolkata, for his exceptional dedication, support, and commitment in overseeing our laboratory during the absence of my supervisor. His invaluable contributions were instrumental in maintaining the continuity of our research and ensuring the smooth functioning of the lab.*

*I extend my sincere thanks to **Prof. Kaushik Biswas**, Department of Biological Sciences, Bose Institute, for his kind support and willingness to help whenever needed.*

*I sincerely acknowledge **Prof. Zhumur Ghosh**, Associate Professor, Department of Biological Sciences, Bose Institute, Kolkata, for her expert guidance, insightful suggestions, and valuable contributions to the transcriptomic data analysis that greatly enriched my research work.*

*I am extremely thankful to **Dr. Subrata Adak**, **Dr. Partha Chakraborti**, **Dr. Nahid Ali**, and **Dr. Sib Sankar Roy** for providing me with the opportunity to use their laboratory instrument facilities. I am thankful to Mr. Pasupati Midya, the animal house technician, for providing us with the rats as per my animal experiment requirement.*

*I would like to express my heartfelt gratitude to **Dr. Subhashis Debsharma**, who has been far more than just a senior colleague in the lab. From my very first day, he took me under his wing-guiding me patiently through the intricacies of experimental work, helping me navigate the challenges of research life, and setting a standard of discipline and dedication that I have always aspired to follow. As a labmate, comrade, and flatmate, he has been a constant source of support, encouragement, and practical wisdom. His mentorship went beyond protocols and techniques; he led by example and offered*

guidance with the care and generosity of an elder brother. The countless hours we shared discussing science, life, and everything in between have left a lasting imprint on my journey. I will always cherish the camaraderie and brotherhood that grew between us over the years-an invaluable part of my Ph.D. experience.

I want to express my heartfelt gratitude to my seniors in the laboratory, ***Dr. Somnath Mazumder*** *and* ***Dr. Rudranil De****. From the very beginning of my doctoral journey, they have been more than just senior colleagues; they have been like elder brothers to me. Their patient guidance, hands-on training, and unwavering support in the lab have been instrumental in helping me build a strong foundation in research. Beyond scientific mentorship, their camaraderie, encouragement, and genuine care have made the challenging moments more bearable and the achievements more meaningful. I am deeply thankful for their presence in my life, both professionally and personally, and I will always cherish the bond we have shared throughout these years.*

I extend my heartfelt gratitude to ***Dr. Asim Azhar Siddiqi*** *and* ***Dr. Chinmoy Banerjee****, two of my favourite seniors, whose humble, polite, and ever-supportive approach has profoundly influenced my academic pursuit during this Ph.D. journey. They never hesitated to offer a helping hand, patiently answering my questions and providing guidance with the utmost kindness and respect. I want to thank my senior,* ***Dr. Subha Jyoti Saha,*** *for his constant support and encouragement whenever I required it.*

Additionally, I owe a debt of gratitude to ***Dr. Samik Bindu****, Assistant Professor, Cooch Behar Panchanan Barma University, for his valuable guidance and support at crucial stages of my academic path.*

I would like to extend my deepest appreciation and gratitude to my esteemed Ph.D. colleagues, ***Dr. Shiladitya Nag*** *and* ***Dr. Debanjan Saha,*** *for their exceptional support, camaraderie, and collaboration throughout our doctoral journey. The vibrant academic discussions, exchange of ideas, and mutual motivation over a cup of tea have helped push the boundaries of my research. Their presence has made this journey more enjoyable, memorable, and fulfilling. I am fortunate to have had such an exceptional colleague by my side, and I will forever cherish the memories and lessons learned from our shared experiences.*

I would like to extend my heartfelt thanks to ***Dr. Sourav Manna*** *and* ***Dr. Sumit Manna****, whose friendship and support have accompanied me since the very beginning, from our B.Sc. days through Ph.D. entrance preparations and into the core of my doctoral journey.* ***Dr. Sourav Manna****'s extensive support in metabolomics analysis significantly enriched my research, and his scientific insights were of immense value. Their unwavering encouragement, constant help, and enduring camaraderie have been a pillar of strength throughout the years. I am truly grateful for this lifelong bond of friendship that has grown stronger through every challenge and success.*

I am deeply grateful to ***Dr. Sonali Das*** *for her unwavering support, guidance, and friendship throughout my research journey. Her generosity in sharing knowledge and her constant encouragement were invaluable during the most challenging phases.*

I would like to acknowledge our lab attendant, ***Surjendu da****, for his indispensable support and assistance that ensured the smooth functioning of our lab. I am deeply grateful for his invaluable contributions.*

I would like to express my sincere appreciation to ***Dr. Troyee Das*** *for her unpaid contributions to transcriptomics data analysis. Her in-depth knowledge of bioinformatics tools and her meticulous*

approach to handling complex datasets have been invaluable in unravelling the intricate patterns within the transcriptomic data.

I sincerely thank ***Prof. Subir Dasgupta****, my M.Sc. teacher, for his continuous support, encouragement, and generous sharing of knowledge, which have greatly influenced my academic growth and motivation throughout this journey. I extend my heartfelt gratitude to all my teachers, from childhood to the present, whose guidance, encouragement, and teachings have laid the foundation of my learning and shaped the person I am today.*

In the course of my Ph.D., I was fortunate to receive unwavering support from ***Dr. Saroj Biswas*** *and* ***Dr. Milon Banik****-brothers in spirit, whose encouragement, insightful ideas, and selfless help were instrumental to this work. I remain deeply grateful for their constant motivation and the countless late-night discussions that enriched both my research and perspective.*

The successful completion of this Ph.D. thesis would not have been possible without the support and valuable contributions of several individuals from outside our lab. I would like to acknowledge ***Sumit, Puja, Yuthika, Susmita, Gourab, Namrata, Ritwick, Swastik, Saptadeepa, Monima, Sohini, Dipsikha, Pratiti, Rumela, Priti, Sudip, Shantanu, Moumita, Imtiaz, Koushik, Abhishek da, Subho, Sounak, Sanchari, Aishwarya, and Somnath Da (KB Lab).*** *I am deeply grateful for their involvement throughout this academic journey.*

I sincerely thank ***Dr. Piyali Pramanik*** *and* ***Dr. Arka Bhattacharya****, not only brilliant doctors but also cherished friends, whose warmth, wisdom, and camaraderie have been a source of joy and inspiration. Whether over coffee conversations filled with knowledge or during our shared travels, their presence has always brought clarity, laughter, and lasting memories to this journey. I am also deeply grateful to* ***Samrat Pramanik*** *and* ***Dr. Saheb Pramanik****, lifelong friends and brothers, for their unwavering support and constant encouragement.*

I would also like to express my sincere gratitude to ***Dr. Saikat Manna****, who has been like an elder brother to me. His kindness, generosity, and constant willingness to help, along with his excellence as a doctor, have been truly invaluable throughout my journey.*

I offer my deepest gratitude and respect to my music teacher, ***Pandit Anil Mukherjee****, whose timeless guidance and spiritual discipline have been a profound influence in my life. His music has been a source of healing and solace, offering strength and inner peace during the most challenging phases of my doctoral journey.*

I owe my deepest and most heartfelt gratitude to my family, especially my parents, ***Hena Pramanik*** *and* ***Alok Pramanik,*** *whose unconditional love, constant support, and silent sacrifices have made this journey possible. Their unwavering faith in me, even during the most trying moments, has been a pillar of strength and a source of quiet inspiration. Every step I have taken is built on the foundation of their blessings, values, and tireless efforts. I am also immensely grateful to* ***Meheli*** *and* ***Rima****, whose presence in my life has been nothing short of a blessing. Their unshakable support and uplifting spirit have kept me grounded and motivated. They have been my source of "free energy"-radiating warmth, joy, and encouragement even when the days were long and uncertain. This achievement is as much theirs as it is mine.*

Saikat Pramanik

PREFACE

Psychological stress has emerged as a pivotal determinant of gastrointestinal (GI) health, exerting profound influences on mucosal integrity, immune regulation, and epithelial homeostasis. Stress, in both its psychological and physiological forms, is a complex response to perceived or actual threats, mediated through intricate neuroendocrine pathways such as the hypothalamic-pituitary-adrenal (HPA) axis and the sympathetic nervous system. These systems orchestrate the release of glucocorticoids and catecholamines, chiefly cortisol and adrenaline. These hormones are evolutionarily conserved to facilitate immediate physiological adaptation through the "fight-or-flight" response. One of the principal pathways through which these stress mediators influence visceral function is the gut–brain axis (GBA), a bidirectional communication network that coordinates neural, endocrine, immune, and microbial signals between the central nervous system and the gastrointestinal tract. Despite the rising prevalence of stress-related gastric pathologies in both clinical and subclinical populations, the precise molecular mechanisms remain incompletely understood. This underscores an urgent need to investigate subcellular targets involved in stress-induced gastric damage and to identify novel therapeutic strategies aimed at restoring mitochondrial and epithelial resilience. Mitochondria, the central regulators of cellular bioenergetics and oxidative balance, are now recognized as pivotal nodes in the stress response pathway. Emerging evidence indicates that mitochondrial injury, driven by sustained oxidative stress and metabolic collapse, underpins the pathogenesis of stress-induced gastric mucosal damage.

In this context, the present thesis aims to dissect the mitochondrial involvement in acute stress-induced gastric injury, with a focus on identifying precise molecular targets and signaling nodes that mediate bioenergetic failure and oxidative collapse. The thesis is systematically divided into a literature review and an experimental investigation. The initial chapters critically review the current understanding of how stress influences gastrointestinal health, emphasizing the intricate neuroendocrine, immunological, and microbial interactions that underlie stress-induced gastric pathology. Particular attention is given to the gut–brain axis and its role in mediating stress responses through hormonal signaling, intestinal permeability modulation, and microbiota dynamics. Based on this foundation, the subsequent chapter explores the pivotal role of mitochondria in maintaining gastrointestinal homeostasis, highlighting how these organelles function as bioenergetic hubs and regulators of redox signaling, apoptosis, and cellular resilience. This section explores emerging evidence that positions mitochondrial dysfunction as a central pathogenic driver of gastrointestinal disorders, emphasizing its role in disrupting cellular energy metabolism, redox homeostasis, and epithelial integrity. By integrating insights from these two domains, the literature review constructs a cohesive framework for understanding how psychological stress precipitates molecular and cellular disturbances within the gastric mucosa. This foundation sets the stage for the experimental investigation of key mitochondrial regulatory pathways and bioenergetic processes involved in stress-induced gastropathy.

The experimental chapter presents a multi-tiered approach combining transcriptomics, metabolomics, and functional assays to establish a comprehensive mechanistic model of stress-induced mitochondrial dysfunction in gastric tissues. Acute restraint stress in rodents served as the primary model, enabling assessment of transcript-level changes in mitochondrial biogenesis, oxidative phosphorylation, and redox regulatory pathways. In particular, the mitochondrial biogenesis regulatory axis, PGC1α, NRF1, and TFAM, appears to be critically suppressed under acute psychological stress, leading to disrupted energy production and redox homeostasis. Additionally, stress-induced activation of the glucocorticoid receptor (GR) axis further exacerbates mitochondrial dysfunction through the KLF15–FBXO32 proteasomal degradation pathway, reinforcing the multifaceted and inter-organellar nature of the injury cascade. Functional validation included assays for mitochondrial membrane potential, ATP levels,

reactive oxygen species accumulation, and apoptotic markers. The role of GR-mediated transcriptional control was explored through pharmacological interventions using RU486, a GR antagonist, alongside agents such as quercetin-3-glucoside and olanzapine that target oxidative stress and central stress perception, respectively. Notably, this thesis introduces and validates a mitochondria-centric therapeutic perspective for stress-induced gastropathy. The restorative effects of quercetin-3-glucoside on mitochondrial integrity and redox status, coupled with the protective efficacy of RU486 in preserving epithelial structure through GR inhibition, underscore the therapeutic value of targeting both local and systemic mediators of stress pathology. This approach not only expands our understanding of stress biology in the gastric system but also sets the stage for the development of next-generation gastroprotective agents that integrate mitochondrial preservation with neuroendocrine modulation.

ABBREVIATIONS

- AMPK: AMP-activated protein kinase
- Ach: Acetylcholine
- ATP: Adenosine triphosphate
- ADP: Adenosine diphosphate
- Bax: Bcl-2-associated X protein
- Bcl-2: B-cell lymphoma 2
- Bcl-xL: B-cell lymphoma-extra large
- BSA: Bovine serum albumin
- CAT: Catalase
- CNS: Central nervous system
- COX: Cyclooxygenase
- CBT: Cognitive-behavioural therapy
- DAMP: Damage-associated molecular patterns
- DAPI: 4',6-diamidino-2-phenylindole
- DMSO: Dimethyl sulfoxide
- DNA: Deoxyribonucleic acid
- EGD: Esophagogastroduodenoscopy
- ED_{50}: Effective dose 50
- EDTA: Ethylenediamine tetraacetic acid
- ERRα: Estrogen-related receptor alpha
- ETC: Electron transport chain
- FD: Functional dyspepsia
- FDA: United States Food and Drug Administration
- FDR: False discovery rate
- FAO: Fatty acid oxidation
- Fe-S: Iron-Sulphur
- GC: Gastric cancer
- GEO: Gene expression omnibus
- GI: Gastrointestinal
- GERD: Gastroesophageal reflux disease
- GPx: Glutathione peroxidise
- GR: Glucocorticoid receptor
- GSH: Glutathione (reduced)
- H_2O_2: Hydrogen peroxide
- HCl: Hydrochloric acid
- HIF: Hypoxia inducible factor
- HCC: Hepatocellular carcinoma
- HMGB1: High mobility group box 1
- HO˙: Hydroxyl radical
- HO-1: Heme oxygenase-1
- HP: *Helicobacter pylori*
- HPA: Hypothalamic-pituitary-adrenal
- IBD: Inflammatory bowel disease
- IBS: Irritable bowel syndrome
- ICU: Intensive care unit
- ISC: Intestinal stem cell
- IFN-γ: Interferon gamma
- IL: Interleukin
- IMM: Inner mitochondrial membrane
- iNOS: Inducible nitric oxide synthase
- JC-1: 5,5’,6,6’-tetra-chloro-1,1’,3,3’-tetraethylbenzimidazol carbocyanine iodide
- kDa: Kilodalton
- lncRNA: Long non-coding RNAs
- MAPK: Mitogen-activated protein kinase
- MCODE: Molecular complex detection
- Mdivi-1: Mitochondrial division 1
- MFN: Mitofusin
- miRNAs: MicroRNAs
- MitoQ: Mitoquinone
- MMP: Metalloproteinase
- MOS: Mitochondrial oxidative stress
- MPP: Mitochondrial processing peptidase
- MTCO1: Mitochondrially encoded cytochrome c oxidase 1
- MTA: Mitochondrially targeted antioxidants
- MTOR: Mammalian target of rapamycin
- NAD: Nicotinamide adenine dinucleotide
- NAFLD: Non-alcoholic Fatty Liver Disease
- NADPH: Nicotinamide adenine dinucleotide phosphate
- NDUFB8: NADH:ubiquinone oxidoreductase subunit B8

- NF-κB: Nuclear factor κB
- NLRP3: nucleotide-binding domain, leucine-rich-containing family, pyrin domain-containing-3
- NO: Nitric oxide
- Nrf2: NF-E2 related factor 2
- NSAIDs: Non-steroidal anti-inflammatory drugs
- $O_2^{\cdot-}$: Superoxide anion radical
- OMM: Outer mitochondrial membrane
- OPA: Optic atrophy
- OD: Optical density
- OXPHOS: Oxidative phosphorylation
- PUD: Peptic ulcer disease
- PBS: Phosphate buffer saline
- PD: Parkinson's disease
- PVN: Paraventricular nucleus
- PGC-1α: Peroxisome proliferator-activated receptor γ coactivator-1α
- PINK1: PTEN-induced putative kinase 1
- PKA: Protein kinase A
- PKC: Protein kinase C
- PPIs: Proton pump inhibitors
- PTM: Posttranslational modification
- PTSD: Post-traumatic stress disorder
- QGL: Quercetin-3-glucoside
- ROS: Reactive oxygen species
- RT-PCR: Reverse transcriptase polymerase chain reaction
- SAM: Sympathetic-adrenomedullary
- SOD: Superoxide dismutase
- SNS: Sympathetic nervous system
- SSRI: Serotonin reuptake inhibitors
- SNRI: Serotonin-norepinephrine reuptake inhibitors
- TCA: Tricarboxylic acid
- TNF-α: Tumor necrosis factor alpha
- TOM: Translocase of the outer membrane
- UQCRC2: Ubiquinol-cytochrome c reductase core protein II
- VDAC: Voltage-dependent anion channel
- ΔΨm: Mitochondrial trans- membrane potential
- %: Percentage
- °C: Degree celcius
- µg: Microgram

CONTENTS

REVIEW OF LITERATURE

A. STRESS AND THE GUT: EXPLORING THE PATHOPHYSIOLOGY

B. ROLE OF MITOCHONDRIA IN GUT PHYSIOLOGY AND PATHOLOGY

REVIEW CHAPTER 1

Stress and the Gut: Exploring the Pathophysiology

1. INTRODUCTION

Stress is a complex physiological and psychological response triggered by perceived threats or challenges, influencing cognition, behaviour, and overall health. Psychological stress stems from emotional reactions such as anxiety and irritability, often exacerbated by major life events and persistent rumination, increasing the risk of mental disorders like anxiety and depression (1,2). Physiological stress, on the other hand, activates the body's biological defence mechanisms, such as the activation of the hypothalamic-pituitary-adrenal (HPA) axis and the sympathetic nervous system, resulting in the secretion of stress hormones like cortisol and adrenaline (3). These responses prepare the body for the "fight-or-flight" reaction, but when prolonged, can have detrimental effects on multiple organ systems. The gastrointestinal (GI) system is intricately connected to the brain via the gut–brain axis (GBA), a bidirectional communication network that integrates neural, endocrine, immune, and metabolic pathways. This axis facilitates coordinated interaction between the central nervous system (CNS) and the gut microbiota, allowing each to influence the other. The GBA plays an essential role in preserving physiological balance and regulating both gastrointestinal and mental health, as shown in Figure 1(4). Stress can disrupt gut health by increasing intestinal permeability, altering gut motility, and inducing microbial dysbiosis (5). Severe stress-related GI complications are evident in critically ill patients, including those undergoing mechanical ventilation, experiencing septic shock, or suffering from extensive burns exceeding 35% of body surface area, leading to gastric mucosal bleeding (6). Moreover, stress-related GI pathologies have been reported in COVID-19 patients, with studies indicating that nearly half of hospitalized individuals undergoing endoscopy exhibited acute mucosal damage, and over one-third of lower GI endoscopies revealed signs of ischemic colitis (7). Globally, stress-related mental health disorders have reached alarming levels. As reported by the World Health Organization, an estimated 970 million people suffered from mental illnesses in 2019, with anxiety and depression being

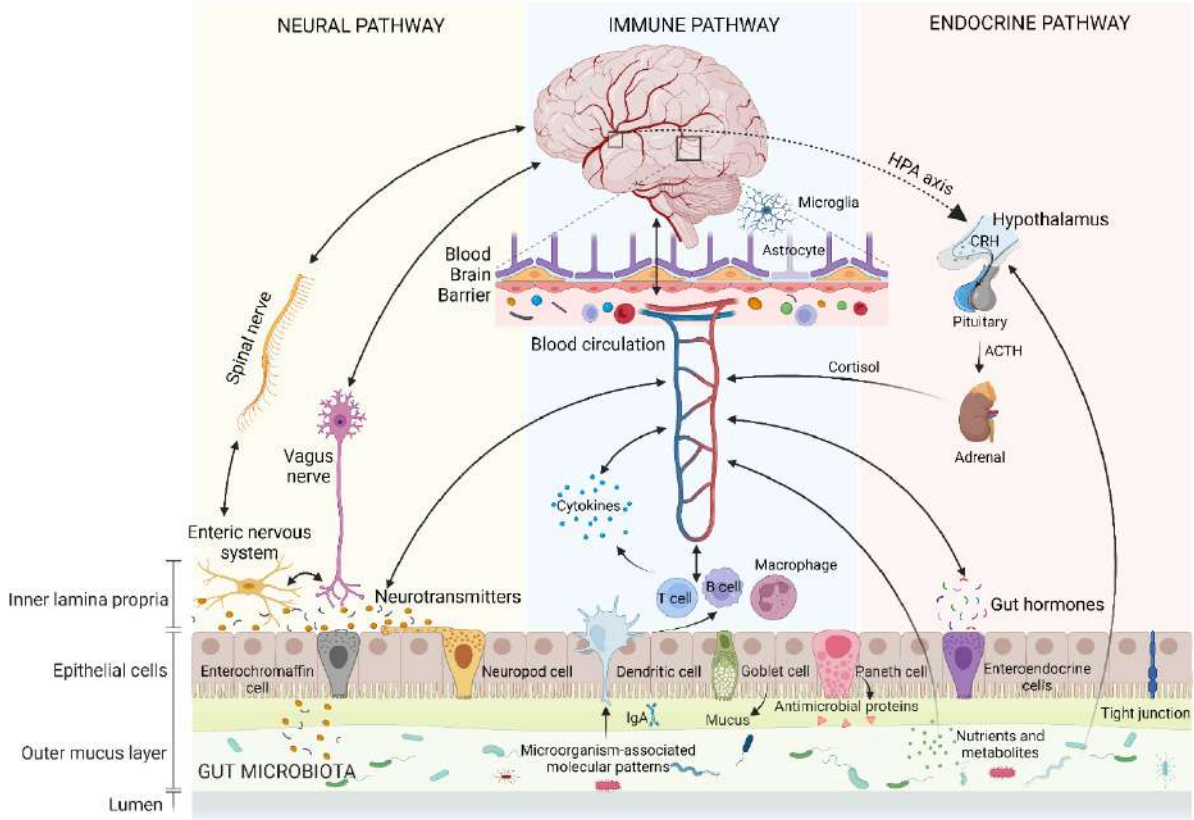

Fig. 1. Mechanisms mediating the bidirectional communication between the gut and the brain within the gut–brain axis (GBA). The mechanisms include neural, immune, and endocrine pathways. Involved mediators include neurotransmitters such as dopamine, serotonin, norepinephrine, and GABA; cytokines like interleukin (IL)-1β, IL-6, IL-10, and tumour necrosis factor-α (TNF-α); and various nutrients and metabolites including short-chain fatty acids (SCFAs), amine compounds, vitamins, and neurochemical precursors. This figure is adapted from Zheng *et. al.* (4)

the conditions that occur most frequently. The COVID-19 pandemic further intensified mental health challenges, with major depressive disorder cases increasing by 27.6% and anxiety disorders rising by 25% worldwide in 2020 (8-10). Understanding the influence of stress on gut health is crucial because the gut and brain are closely linked via the gut–brain axis, influencing both mental and physical well-being. By recognizing this connection, strategies like stress management, dietary changes, and gut-focused therapies can be implemented to enhance overall health, prevent stress-related disorders, and improve resilience against physical and emotional challenges.

2. THE NATURE AND CLASSIFICATION OF STRESS

Stress is a natural, multifaceted response to demands or threats that challenge an organism's equilibrium, referred to as "homeostasis." It is a well-documented phenomenon, recognized as far back as ancient Greece and formalized in modern biological research by figures like Claude Bernard, Walter Bradford Cannon, and Hans Selye. Claude Bernard (1865/1961) emphasized that sustaining life depends on maintaining a stable internal environment, even in the face of external fluctuations. In 1929, Cannon used the term “homeostasis” to describe this phenomenon(11). Later, in 1956, Selye introduced the concept of “stress” to define the impact of factors that significantly disrupt homeostasis(12). The term “stressor” refers to the actual or perceived threat to an organism, while the organism's reaction to the stressor is known as the “stress response.” Stress can manifest as either physical stress (direct disruptions to physiological states, like injury or infection) or psychological stress (perceived threats, such as environmental pressures or social conflicts). Physical stressors refer to external factors that disrupt the body’s balance, while psychological stressors are defined as the “anticipation justified or not, that a challenge to homeostasis looms.” (13). While stress responses originally evolved as adaptive mechanisms, Selye noted that when these responses are intense or persist for a long time, they can result in tissue damage and illness(14).

2.1. Physical stressors and their impact

Physical stressors, which encompass external conditions or internal disruptions, directly challenge the body's physiological equilibrium and elicit responses aimed at maintaining homeostasis. Physiological stress, defined as an uncomfortable sensory, emotional, and subjective experience associated with potential bodily harm or tissue damage, can result from injuries, infections, or extreme environmental conditions such as temperature fluctuations(15,16). Injuries, including cuts and fractures, trigger inflammatory responses characterized by the release of proinflammatory cytokines such as interleukin-1 (IL-1), tumour necrosis factor-alpha (TNF-α), and interleukin-6 (IL-6), which recruit immune cells to the affected area to facilitate tissue repair (17,18). Additionally, pain signals activate the hypothalamic-pituitary-adrenal (HPA) axis, resulting in cortisol secretion to modulate inflammation and prevent excessive tissue damage; however, chronic injuries may lead to prolonged inflammation and fibrosis (19). Similarly, infections caused by bacteria, viruses, or fungi serve as significant physical stressors, prompting the innate immune system to recognize pathogen-associated molecular patterns (PAMPs) via pattern recognition receptors (PRRs), such as Toll-like receptors (TLRs), to initiate immune responses

(20). Extreme temperatures also impose substantial stress on thermoregulatory mechanisms, with heat exposure promoting sweat gland activation and peripheral blood flow to dissipate heat, whereas cold exposure triggers vasoconstriction and shivering to conserve warmth(21,22). Both scenarios involve activation of the sympathetic nervous system (SNS) and HPA axis, leading to increased catecholamine and cortisol levels, yet chronic exposure may impair regulatory systems and increase susceptibility to stress-related disorders(23).

Physical stressors activate brainstem and hypothalamic regions, initiating a rapid and reflexive response via the sympathetic-adrenomedullary (SAM) system, enhancing alertness, vigilance, and situational appraisal. This immediate phase is complemented by a slower, sustained hormonal response from the hypothalamic-pituitary-adrenal (HPA) axis, which secretes cortisol to regulate energy availability and maintain homeostasis (23). Stress perception activates preganglionic autonomic neurons and hypophysiotrophic neurons in the paraventricular nucleus (PVN), triggering the HPA axis and autonomic nervous system (ANS), which includes sympathetic and parasympathetic components (11,24). The nucleus of the solitary tract (NTS), a key autonomic structure, relays sensory and visceral information and regulates cardiovascular and respiratory functions(25). The NTS modulates the HPA axis through noradrenergic and adrenergic pathways, with additional contributions from other catecholaminergic systems. Circumventricular organs, such as the subfornical organ, also regulate stress responses via angiotensin II and PVN activation, influencing blood pressure and drinking behaviours(26). Physiological responses to stress include the secretion of cortisol, adrenaline, and other neurotransmitters, affecting heart rate, blood pressure, and immune function(23). Cortisol, the "stress hormone," prepares the body for "fight or flight" by releasing glucose, raising heart rate, and suppressing immunity. Prolonged stress leads to hypercortisolism, associated with anxiety, depression, Cushing's syndrome, and menstrual irregularities in women(27). Conversely, hypocortisolism can result in Addison's disease or adrenal insufficiency. Cortisol dysregulation also underpins conditions like post-traumatic stress disorder (PTSD)(28). Together, these mechanisms underscore the intricate role of stress in health and disease.

2.2. Psychological stressors and their impact

Psychological stressors are stimuli perceived as threats, leading to emotional and psychological distress, categorized into social pressures, anticipatory threats, and perceived dangers such as predator-related cues. These stressors target cognitive and affective processes, with common models including restraint, electrical shock, loud noise, and open field exposure. Perceived threats, whether real or imagined, significantly influence stress responses, with cognitive appraisal playing a crucial role(29,30). Social pressures from relationships, cultural expectations, and societal norms can intensify stress responses, with social support serving as a buffer. Chronic social stressors may contribute to anxiety and depression(31). Failure to meet personal or societal goals can cause stress, with individuals attributing failure to inherent abilities experiencing greater distress(32). Anticipatory threats, such as concerns about job security or health, activate the hypothalamic-pituitary-adrenal (HPA) axis, increasing cortisol levels and perpetuating anxiety cycles. Evolutionarily, predator-related cues elicit strong stress responses, engaging survival-related brain regions such as the amygdala(33). Psychological stressors during childhood and adolescence, including exposure to violence, abuse, and familial conflicts, have lasting effects on mental health, leading to emotional dysregulation and attachment disturbances(34). Children of divorced parents report increased antisocial behaviour and emotional distress. Exposure to war and terrorism during childhood results in high PTSD and depressive symptom prevalence, with long-term effects persisting into adulthood(35). Chronic exposure to stressors during developmental years increases the risk of mood disorders, immune dysfunction, and early mortality(36). Lifetime exposure to trauma is high, with PTSD affecting approximately 25% of

exposed individuals(37). Trauma-related disorders such as acute stress disorder (ASD) and PTSD can lead to concurrent depression, cognitive impairment, and substance abuse. Stress-related behaviours such as smoking, alcohol use, and sleep disturbances further exacerbate health risks(38,39)

Intense psychological and socially evaluative stressors activate both physical and cognitive stress responses, primarily mediated by key brain regions such as the prefrontal cortex (PFC), amygdala, ventral tegmental area (VTA), paraventricular nucleus (PVN), hippocampus (HIPPO), and nucleus accumbens (NAc). The PFC facilitates behavioural plasticity in response to stress, with the prelimbic (PL) cortex increasing adrenocorticotropic hormone (ACTH) and corticosterone levels, whereas the infralimbic (IL) cortex reduces corticosterone secretion, demonstrating the complex interplay of PFC subdivisions. Lesions in the dorsal PFC produce anxiogenic effects, while ventral PFC lesions exert anxiolytic effects(40,41). Different brain areas associated with stress resilience are shown with a simple illustration in Figure 2 (41).

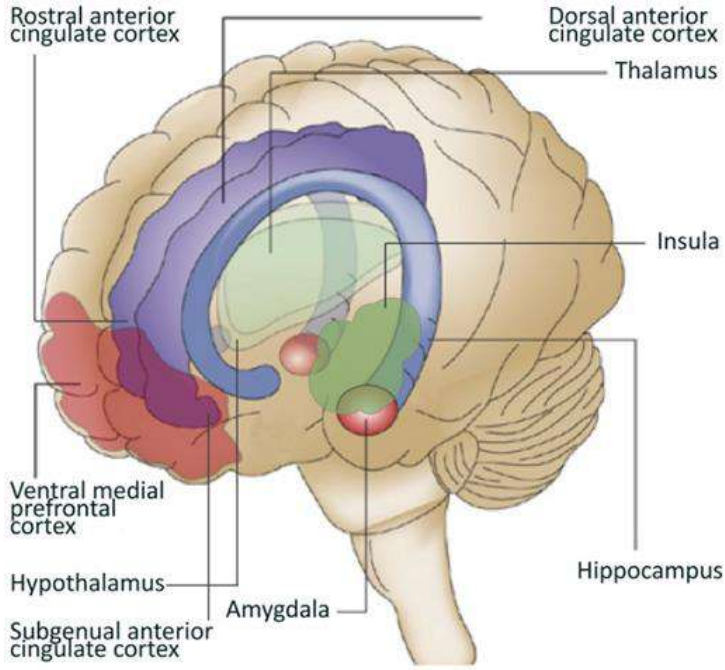

Fig. 2. Brain areas associated with stress resilience. This illustration highlights key brain regions commonly implicated in mediating resilience to stress. This figure is adapted from Schloesser *et al*. (41).

The PFC extensively projects to the amygdala, a key emotional processing center that modulates corticosteroid release, with the basolateral amygdala (BLA) playing a crucial role in anticipatory stressor processing and dendritic changes related to emotional learning (42). The central nucleus of the amygdala (CeA) is critical for long-term fear memory retrieval, whereas short-term memory retrieval relies on PFC-BLA interactions. The CeA connects to the periaqueductal gray (PAG), modulating responses to unconditioned and conditioned threats(43). The hippocampus, with projections to both the PFC and BLA, regulates stress responses through inhibitory control over the HPA axis and top-down modulation of stress, while excessive amygdala activity can shift control to bottom-up processes(40). The hippocampus and amygdala process experiences by interfacing with the hypothalamus and brainstem and interpreting environmental contexts to determine threat levels, influencing allostatic responses. The amygdala encodes fearful and emotionally charged events, whereas the hippocampus contextualizes these events within episodic and declarative memory. Lesions in the amygdala impair conditioned fear responses, whereas hippocampal lesions affect contextual conditioning(44).

Anatomical and functional links between the amygdala and hippocampus facilitate memory-related plasticity, such as long-term potentiation (LTP) in the dentate gyrus. The hippocampus generally inhibits HPA activity, while the amygdala enhances it; however, specific hippocampal regions can activate HPA responses under certain conditions(45). The medial prefrontal cortex (mPFC) further constrains HPA activity under stress-related conditions.

2.3. Stress response systems

When a stressor is perceived, two key stress-response systems are activated: the hypothalamic-pituitary-adrenal (HPA) axis and the sympathetic-adrenal-medullary (SAM) axis. The SAM axis triggers the rapid "fight-or-flight" response within seconds, initiated by the locus coeruleus in the brainstem, which activates sympathetic ganglia. Sympathetic nerve fibers targeting the adrenal medulla stimulate the release of adrenaline and, to a lesser extent, noradrenaline. These catecholamines modulate the cardiovascular, respiratory, skeletal muscle, hepatic, and immune systems, priming the body for immediate action to enhance survival(46). At the same time, the HPA axis initiates a slower response, beginning with the release of corticotropin-releasing hormone (CRH) and vasopressin from the paraventricular nucleus (PVN) of the hypothalamus. CRH prompts the anterior pituitary to secrete adrenocorticotropic hormone (ACTH) into the bloodstream, which then stimulates the adrenal cortex to produce glucocorticoid, primarily cortisol in humans and corticosterone in rodents(47). The SAM and HPA axes form a mutually reinforcing feedback loop, where the activation of one system promotes the activation of the other. Together, these systems influence multiple organs, including the gastrointestinal (GI) tract.

The Sympathetic-Adrenal-Medullary (SAM) axis rapidly responds to physical or psychological stress through the activation of the sympathetic nervous system and adrenal medulla, which release catecholamines, primarily epinephrine (Epi) and norepinephrine (NE), to facilitate immediate physiological adaptations. These neurotransmitters are released via efferent pathways from brainstem catecholaminergic neurons to preganglionic sympathetic neurons and adrenal chromaffin cells(48). Epi and NE, acting through adrenergic G-protein-coupled receptors, prepare the body for "fight-or-flight" responses by increasing heart rate, mobilizing glucose, and modulating vascular tone. NE plays a key role in activating the amygdala, enhancing memory consolidation of stress-related events in the hippocampus(49). Stress also triggers dopamine (DA) release, particularly in the ventral tegmental area, modulating behavioural responses based on stress duration and controllability. While circulating DA levels show minimal changes during stress, they contribute to blood pressure regulation and glucose homeostasis. The SAM axis interacts with the hypothalamic-pituitary-adrenal (HPA) axis for short- and long-term stress responses, balancing autonomic nervous system activity. Chronic stress, however, can dysregulate these systems, leading to potential pathologies, as the locus coeruleus and associated structures mediate cognitive and endocrine stress responses(23).

The Hypothalamus-Pituitary-Adrenal (HPA) axis serves as the body’s central stress response system, engaging multiple brain regions to regulate adaptive and maladaptive responses to stressors (Fig. 3). Glucocorticoids regulate peripheral and central systems via negative feedback mechanisms involving glucocorticoid (GR) and mineralocorticoid receptors (MR), particularly in stress-related brain regions such as the hippocampus, amygdala, PVN, and nucleus of the solitary tract(50,51). CRH neurons in the PVN’s dorsomedial parvocellular division, along with co-released peptides like vasopressin (AVP), act on the anterior pituitary through G-protein coupled CRHR1 receptors, enhancing ACTH secretion, which is further modulated by stressor-specific pathways and transcriptional regulation of proopiomelanocortin (POMC)(52).

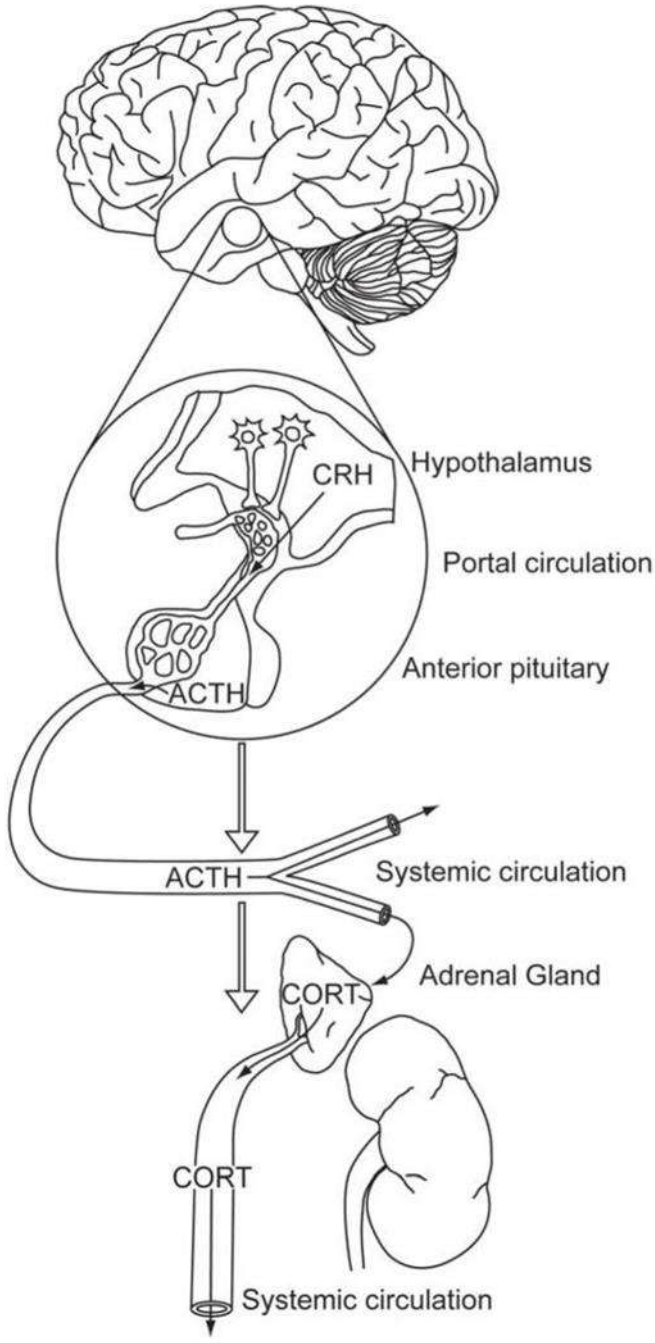

Fig. 3. Schematic Representation of HPA Axis Activation in Response to Stress. The organization of the hypothalamo-pituitary-adrenocortical (HPA) axis involves a highly regulated neuroendocrine cascade. The stress response is initiated by corticotropin-releasing hormone (CRH)-producing neurons located in the paraventricular nucleus (PVN) of the hypothalamus. In response to stressors, CRH is secreted into the hypophysial portal circulation, which delivers the hormone directly to the anterior pituitary, allowing it to act on corticotroph cells. Activation of these corticotrophs results in the release of adrenocorticotropic hormone (ACTH) into the bloodstream. ACTH then stimulates the adrenal cortex to produce and secrete glucocorticoids, cortisol in species such as humans, and corticosterone in rodents like rats and mice. Once released into the systemic circulation, glucocorticoids can bind to their specific receptors throughout the body, including within various regions of the brain. This figure is adapted from Myers et al. (51).

Anticipatory stress responses often involve GABAergic disinhibition from limbic circuits such as the amygdala, while reactive responses stem from direct noradrenergic inputs, reflecting the intricate neural control of CRH release. The HPA axis integrates environmental, genetic, and experiential factors, with glucocorticoids influencing immune, metabolic, and cognitive processes via genomic and non-genomic pathways, mediated in part by epigenetic modifications like DNA methylation and histone acetylation(53). Chronic stress alters HPA axis dynamics, causing hypersecretion, sensitization, or adrenal exhaustion, often involving limbic-hypothalamic-brainstem circuits, with individual variability shaped by age, sex, and early-life experiences. Importantly, glucocorticoids also regulate mitochondrial function, with stress-induced GR translocation affecting bioenergetic balance and promoting oxidative stress, apoptosis, and reductions in ATP synthesis via suppression of mitochondrial genes such as NADH dehydrogenases ND-1, ND-3, and ND-6(54). Pharmacological strategies targeting GR signalling, like RU486, alongside lifestyle modifications, offer promising avenues for mitigating stress-induced pathologies. However, challenges in achieving precise receptor blockade persist(54). The interplay between HPA axis activity, mitochondrial resilience, and systemic responses underscores the need for integrative therapeutic approaches to optimize stress adaptation and prevent maladaptive outcomes.

2.4. Acute stress responses overview

Acute stress, triggered by short-term events like meeting deadlines or avoiding accidents, elicits rapid physiological responses driven by the sympathetic nervous system (SNS) and hypothalamic-pituitary-adrenal (HPA) axis. This response, first described by Selye, involves the release of stress hormones such as adrenaline, noradrenaline, and cortisol, which act within seconds to modulate the brain's limbic-cortical circuits and enhance energy availability(12). These hormones promote lipolysis and glycogen breakdown to ensure an immediate energy supply. Blood pressure increases through myocardial mechanisms, which boost cardiac output, and vascular mechanisms, which constrict blood vessels(55). Acute stress also activates the immune system, causing innate immune cells, such as macrophages and natural killer cells, to migrate from lymphatic tissues into the bloodstream, resulting in leukocytosis. These immune cells concentrate in high-risk tissues, like the skin, to defend against potential pathogens during injury, thereby supporting healing(56). Although generally adaptive, this intricate stress response is designed to optimize survival during short-term challenges.

2.5. Chronic stress responses overview

Chronic stress, characterized by prolonged exposure to stressors, has far-reaching consequences on health, affecting multiple physiological systems. Persistent activation of the hypothalamic-pituitary-adrenal (HPA) axis and the sympathetic nervous system (SNS) leads to sustained elevation of stress hormones, such as cortisol, which disrupt homeostasis (Selye, 1956). Prolonged activation of the sympathetic nervous system persistently engages the cardiovascular system, leading to elevated heart rate and blood pressure, which can contribute to vascular remodelling, left ventricular hypertrophy, and an increased risk of hypertension, myocardial infarction, and stroke(57). Chronic stress also impairs the immune system by dysregulating cytokine profiles. While acute stress activates the immune system, chronic stress shifts immune function toward humoral immunity by increasing Th2 cytokines and suppressing cellular immunity, as evidenced by slower wound healing and diminished antiviral responses (58,59). This immune dysfunction, coupled with inflammation, increases vulnerability to infections and chronic diseases. In older adults, chronic stress exacerbates immunosenescence, further impairing responses to infections and vaccinations(60). Moreover, chronic stress alters brain structure and function, particularly within the limbic system, leading to dendritic reorganization in neurons, dysregulated neurotransmitter signalling, and heightened risk of neuropsychiatric disorders such as

anxiety and depression(45,61). Chronic stress also disrupts energy homeostasis, as glucocorticoid overproduction impacts glucose metabolism, increases brown adipose tissue, and promotes weight changes, metabolic disorders, and insulin resistance(62). Dysregulated gut microbiota and blood-brain barrier permeability further link chronic stress to immune and metabolic dysfunction. Together, these findings emphasize the systemic effects of chronic stress, highlighting its role in cardiovascular disease, immune impairment, neuropsychiatric disorders, and metabolic dysregulation. Understanding these mechanisms is vital for mitigating chronic stress's long-term health impacts.

3. STRESS AND GUT-BRAIN AXIS

The gut-brain axis (GBA) is a sophisticated, bidirectional communication system connecting the central nervous system (CNS) with the enteric nervous system (ENS) in the gastrointestinal (GI) tract. This network integrates neural, immune, endocrine, and microbiota-derived signals to regulate both intestinal functions and brain activity as described in (Fig.4) (63) . By linking the cognitive and emotional centres of the brain with gut physiology, the GBA plays a critical role in maintaining homeostasis and overall well-being(63,64). The CNS, comprising the brain and spinal cord, influences gut behaviour through stress responses, appetite regulation, and digestion via neural pathways. In turn, the CNS responds to gut-derived signals, such as those related to distension or microbiota activity, adapting its responses to maintain balance(64). The ENS, often termed the "second brain," independently governs GI functions through a vast network of 200–600 million neurons. It regulates processes like peristalsis, enzyme secretion, and blood flow while communicating bidirectionally with the CNS via the vagus nerve and spinal pathways(65). Recent studies emphasize the role of gut microbiota in this axis, influencing mood, cognition, and susceptibility to neurodegenerative diseases and mood disorders. The microbiota interacts with the GBA through microbial metabolites, cytokines, and neurotransmitters, further highlighting its role in health and disease. This intricate system underscores the therapeutic potential of targeting the GBA in managing gastrointestinal, neurological, and psychiatric disorders.

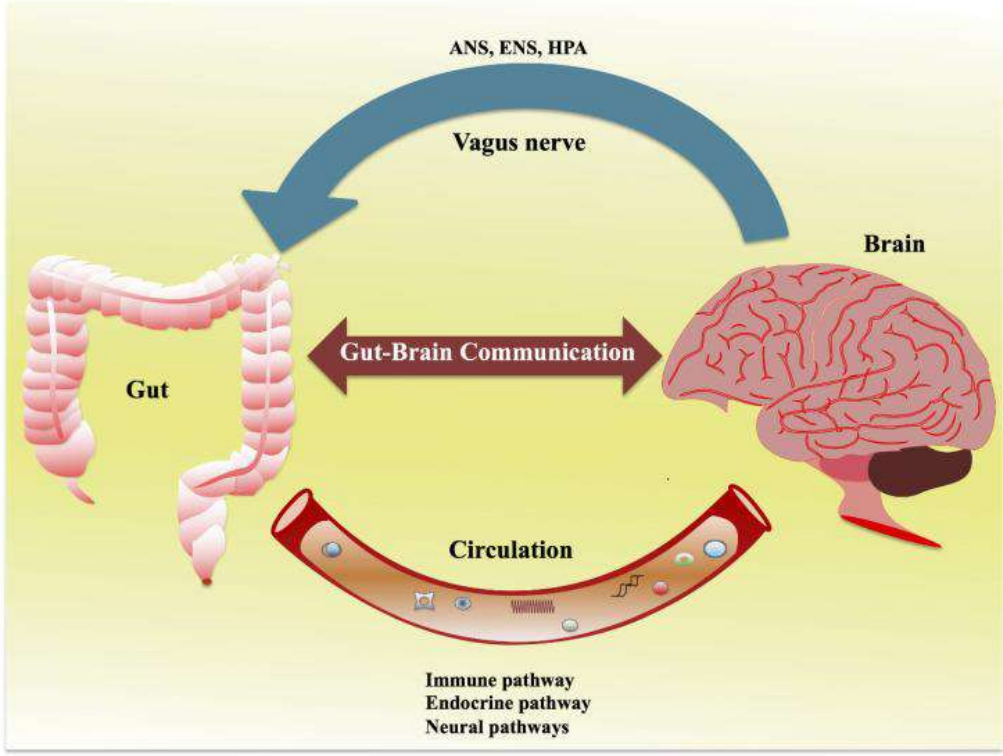

Fig. 4. Schematic illustration depicting the bidirectional communication between the gut and the brain. This interaction is regulated through multiple interconnected systems, including the autonomic nervous system (ANS), enteric nervous system (ENS), hypothalamic–pituitary–adrenal (HPA) axis, as well as immune, endocrine, and neural signalling pathways. This figure is adapted from Suganya *et al.* (63).

3.1. Involvement of the central nervous system (CNS)

The CNS regulates gut functions and homeostasis, while gut microorganisms influence CNS activity, contributing to the development and progression of various diseases, including neurological and gastrointestinal disorders(64). The GBA relies on multiple pathways to maintain systemic balance. The ENS, often called the "second brain," consists of myenteric and submucosal plexuses that integrate sensory and motor signals independently. Prevertebral ganglia mediate signals between the ENS and CNS, while the CNS itself processes inputs to regulate gut smooth muscle, glands, and blood vessels via the autonomic and neuroendocrine systems. Higher brain centres influence these responses, creating a hierarchical regulation system. Disruptions at any level can lead to GBA dysfunction, which is linked to conditions like irritable bowel syndrome (IBS), depression, and neurodegenerative diseases(66). The vagus nerve is a critical component of the GBA, providing bidirectional communication. It modulates gut motility, secretion, and immune responses, and its afferent fibres transmit sensory signals to the brain. Gut bacteria influence CNS functions through vagal pathways, but studies show that severing the vagus nerve (vagotomy) disrupts microbial regulation of behaviour, as seen in mice models where probiotics fail to impact vagotomized animals(67). The immune system also plays a significant role in the GBA. Gut microorganisms interact with immune cells, promoting homeostasis and influencing CNS functions. Microbial metabolites, such as short-chain fatty acids (SCFAs), are key mediators. SCFAs cross the blood-brain barrier, modulating neuroinflammation and cognitive function. However, certain SCFAs, like propionic acid, have been shown to induce neuroinflammatory and oxidative stress-related changes in animal models, mimicking conditions like autism(68). Neurotransmitters produced by gut microbiota, including serotonin, GABA, and melatonin, further underscore the microbiota's influence on CNS activity. Changes in gut microbiota composition have been linked to altered emotional and cognitive states, emphasizing the strong association between gastrointestinal and mood disorders. Additionally, gut microorganisms regulate adult hippocampal neurogenesis (AHN), which is essential for learning and memory. Sterile mice exhibit reduced AHN, highlighting the critical role of early microbial colonization(69). The CNS also adapts to peripheral signals, such as hormonal secretions, immune mediators, and microbial metabolites, ensuring systemic homeostasis. For example, the hypothalamic-pituitary-adrenal (HPA) axis mediates stress responses, releasing cortisol, which influences gut motility and permeability. These mechanisms illustrate the CNS's role in coordinating complex physiological and behavioural responses via the GBA. In conclusion, the CNS is a pivotal modulator of the GBA, relying on neural, immune, and endocrine pathways to maintain homeostasis. Understanding this intricate network provides insights into therapeutic approaches for neurological, psychiatric, and GI disorders.

3.2. Vagus nerve as a modulator of the gut-brain axis

The vagus nerve plays a pivotal role in mediating communication between the gastrointestinal (GI) tract and the brain, forming a central component of the gut-brain axis (GBA). This nerve not only regulates gastrointestinal functions, including gastric motility and enzyme secretion, but also influences metabolic processes, immune signalling, and behavioural responses. Through its involvement in various physiological systems, the vagus nerve significantly impacts overall health and behaviour. The vagus nerve is integral to the regulation of metabolic homeostasis by modulating pancreatic hormone secretion, such as insulin and glucagon. For instance, it has been shown to enhance the growth hormone-

releasing effects of ghrelin and reduce postprandial insulin secretion(70). Additionally, its interaction with hormones like cholecystokinin (CCK) and leptin influences energy balance, satiety, and appetite regulation. The vagus nerve carries signals related to hunger and fullness from the GI tract to the brain, coordinating long-term energy balance and food intake(71). Beyond metabolic regulation, the vagus nerve's cholinergic signalling has been implicated in reducing inflammation, particularly in obesity and metabolic syndrome. Dysregulation of this pathway can lead to chronic inflammation, contributing to insulin resistance and type 2 diabetes(72,73). This highlights the crucial role of the vagus nerve in modulating immune responses and its potential as a target for treating metabolic disorders. The gut microbiota, a complex and diverse community of microorganisms residing in the human GI tract, is closely linked to numerous diseases, including those affecting the brain. Researchers have increasingly recognized the gut microbiota-brain axis as a critical pathway through which the gut and brain communicate. This interaction occurs through various mechanisms, such as the vagus nerve, the hypothalamic-pituitary-adrenal (HPA) axis, and microbial metabolites, as well as through cytokine signalling(74). The vagus nerve, one of the longest cranial nerves, serves as the main conduit for gut-to-brain communication, influencing brain functions and behaviour. This bidirectional signalling between the gut and brain can affect mood, stress responses, and even neurodegenerative diseases. For instance, the stimulation of vagal afferent fibers has been shown to influence monoaminergic brain systems, which are implicated in psychiatric conditions like mood and anxiety disorders. Interestingly, vagus nerve stimulation (VNS) has emerged as a promising therapeutic approach for treatment-refractory depression, post-traumatic stress disorder (PTSD), and inflammatory bowel disease. VNS has been shown to increase vagal tone, reduce cytokine production, and enhance resilience to stress(75,76).

3.3. Enteric nervous system (ENS)

The Enteric Nervous System (ENS), often called the "second brain," contains 200-600 million neurons governing gastrointestinal (GI) functions independently of the central nervous system (CNS). The ENS coordinates digestion through reflexes, peristalsis, enzyme secretion, and blood flow regulation while enabling bidirectional communication with the CNS via vagal and spinal pathways. This interaction underscores the ENS's role in modulating sensations and digestive health. Aging correlates with an increase in neurological disorders. A study revealed that the ENS expresses risk genes for diseases beyond the GI system, implicating its role in neuropathic and inflammatory disorders(77). The microbiota-gut-brain (MGB) axis offers insights into such diseases, but research is limited by a lack of causative evidence. The GI tract hosts diverse microorganisms, including bacteria from Bacteroidetes, Firmicutes, Actinobacteria, and Proteobacteria phyla, which influence ENS function through direct or metabolite-mediated interactions. The ENS, part of the autonomic nervous system (ANS), spans the GI tract through the submucosal (Meissner's) and myenteric (Auerbach's) plexuses, housing neurons like nitrergic and cholinergic types(78,79). It forms a sensorimotor reflex circuit responsible for motility and immunity. Microbes impact ENS development and function through signalling molecules like short-chain fatty acids (SCFAs) and lipopolysaccharides (LPSs). The vagus nerve serves as a key conduit between the ENS and CNS, transmitting sensory data to brain areas like the nucleus tractus solitarius (NTS) while receiving CNS-mediated motor signals that influence GI motility and secretion(80). The ENS and microbiota form an integral bidirectional link between the GI system and host physiology. Bacterial molecules traverse epithelial barriers to interact with enteric plexuses, while non-neuronal intermediary cells contribute to enteric neuron activation(81). Future research should emphasize longitudinal, mechanistic studies to elucidate the causal pathways in gut microbe-ENS interactions, paving the way for novel therapeutic strategies against neurological disorders.

4. IMPACT OF STRESS ON GUT MOTILITY

Stress significantly impacts gut motility, disrupting normal gastrointestinal (GI) functions through the gut-brain axis, a bidirectional communication system between the central nervous system and the GI tract. Stress-induced changes in peristalsis, the coordinated muscular contractions of the digestive tract, may lead to symptoms such as diarrhoea (due to hypermotility) or constipation (due to hypomotility)(82). Psychological stress has been implicated in functional GI disorders like irritable bowel syndrome (IBS) and functional dyspepsia, both considered classical psychosomatic conditions influenced by stressors. Psychological stressors can alter motility by influencing neuroendocrine pathways, including the hypothalamic-pituitary-adrenal (HPA) axis, and affecting gut microbiota composition(83). Animal models provide valuable insights into stress-induced gut motility changes. Housing mice with a hungry cat in a two-layer cage demonstrated how acute psychological stress affects small intestinal motility, gut bacteria, and mucosal integrity(84). These findings emphasize that psychological stress is not only a modulator of GI symptoms but also contributes to the pathophysiology of stress-related GI disorders and potential systemic effects.

4.1. Peristalsis and stress: a complex interplay

Peristalsis, the coordinated wave-like contractions of the gastrointestinal (GI) tract, is essential for propelling food and waste through the digestive system. This reflexive activity is mediated by the enteric nervous system (ENS) and influenced by mechanical and chemical stimuli in the gut lumen. Stress, a key disruptor of homeostasis, significantly impacts peristalsis and overall gut motility, often leading to gastrointestinal disorders such as constipation, diarrhoea, and bloating. Peristalsis is initiated by the detection of luminal stimuli by intrinsic primary afferent neurons, which activate interneurons and motor neurons in the ENS. The resulting contraction of circular and longitudinal muscles on the oral side of the bolus and simultaneous relaxation on the aboral side propel contents forward(85). Serotonin (5-HT) plays a critical role in triggering this reflex by stimulating sensory afferents and facilitating neurotransmission(86). While peristalsis is typically anterograde, reverse peristalsis can occur under certain conditions, such as luminal toxicity, indicating its adaptability. Stress triggers activation of the HPA axis and the sympathetic nervous system, resulting in the secretion of cortisol and catecholamines that influence the activity of the ENS. Acute stress can inhibit gastric emptying and intestinal transit while increasing colonic motility and defecation(87). Studies in animal models have demonstrated varied effects of stress on small intestinal motility. For example, restraint stress can either enhance or inhibit transit depending on the stressor type, duration, and individual biological factors such as species, gender, and circadian rhythms(88). Acute stress typically induces delayed gastric emptying and reduced intestinal transit. In contrast, chronic stress can lead to persistent dysregulation of peristalsis, contributing to conditions like irritable bowel syndrome (IBS). Studies using rodent models have shown that psychological stressors such as restraint or exposure to predators impair the migrating motor complex (MMC), a pattern of motility essential for intestinal clearance during fasting(89). CRF serves as a central mediator of stress-related alterations in gastrointestinal motility. CRF acts on the brain and gut via CRF receptors, leading to delayed gastric emptying and altered peristalsis(90). CRF receptor antagonists have shown promise in mitigating stress-related GI symptoms by blocking these pathways, highlighting the central role of the neuroendocrine-immune axis in stress-induced gut dysfunction. The modulation of peristalsis by stress underscores the importance of addressing psychological factors in managing functional GI disorders. Therapies targeting the gut-brain axis, including stress management, dietary interventions, and pharmacological agents such as serotonin modulators and CRF antagonists, have shown efficacy in improving symptoms(91). Additionally, understanding individual variability in stress responses can guide personalized treatment approaches. Stress profoundly affects peristalsis through complex interactions involving the ENS, HPA axis, and

neuroimmune pathways. Acute stress typically inhibits gastric and small intestinal motility while enhancing colonic activity, whereas chronic stress leads to persistent dysregulation, contributing to functional GI disorders(91). Ongoing research into the mechanisms of stress-induced changes in gut motility will further inform therapeutic strategies to improve patient outcomes.

4.2. Stress and constipation: understanding the connection

Constipation, defined by infrequent bowel movements or difficulty in stool passage, is a common gastrointestinal issue that can result from various factors, including dietary habits, hydration levels, physical activity, and stress. Recent studies highlight the strong link between psychological stress and constipation, affecting both children and adults. Stress triggers the release of hormones like epinephrine and cortisol, redirecting blood flow away from the intestines and slowing motility, which predisposes individuals to constipation(92). Additionally, stress-induced activation of corticotropin-releasing factor (CRF) in the gastrointestinal (GI) tract disrupts gut motility, increases intestinal permeability, and promotes inflammation(93). Stress also negatively impacts gut microbiota, reducing healthy bacteria essential for digestion and motility, though further research is needed to confirm this mechanism(94). Research highlights the prevalence of stress-induced constipation in children, showing that stressful life events, such as academic failures or family disruptions, significantly raise the odds of constipation (odds ratio 2.52, $p < 0.0001$)(95). Studies also link emotional and behavioural issues to constipation, with ADHD prevalence higher in children with functional constipation(96). Addressing stress through dietary changes, hydration, exercise, and psychological support, including cognitive-behavioral therapy, can help alleviate constipation and improve overall GI health. Further research is necessary to explore chronic stress's long-term effects on gut function and develop targeted interventions for vulnerable populations.

4.3. Stress response and diarrhoea

Stress significantly contributes to diarrhoea; a condition often linked to the gut-brain axis and the body's "fight-or-flight" response. During stress, neurotransmitters and hormones like serotonin (5-HT) alter gut motility, increasing bowel movements and expelling water and electrolytes too rapidly, leading to loose stools(97). Acute stress accelerates intestinal transit, while chronic stress may alter gastric emptying patterns, highlighting the dual impact of stress on gastrointestinal (GI) function. Stress-induced diarrhoea is linked to heightened visceral sensitivity and immune system disruptions, as observed in weaning mice, where elevated 5-HT levels correlated with immune dysregulation and severe diarrhoea(98). Treatment with para-chlorophenylalanine (PCPA) alleviated symptoms by reducing 5-HT and normalizing immune responses. Stress causes increased colon activity while slowing other digestive functions, resulting in diarrhoea during acute episodes. Persistent stress-related diarrhoea warrants medical evaluation to rule out underlying conditions. Lifestyle factors, such as disrupted eating habits, dehydration, and insufficient sleep, often exacerbate stress-induced diarrhoea.

5. MICROBIOME ALTERATIONS: INFLUENCE OF STRESS ON GUT MICROBIOTA DIVERSITY AND COMPOSITION

Stress significantly impacts gut microbiota, leading to decreased diversity, dysbiosis, and functional changes that affect intestinal permeability, inflammation, and neurotransmitter regulation. This intricate gut-brain connection highlights the profound influence of stress on health(99,100). Psychological stress disrupts the balance of gut microbial communities, often reducing the abundance of beneficial taxa essential for brain and immune function.

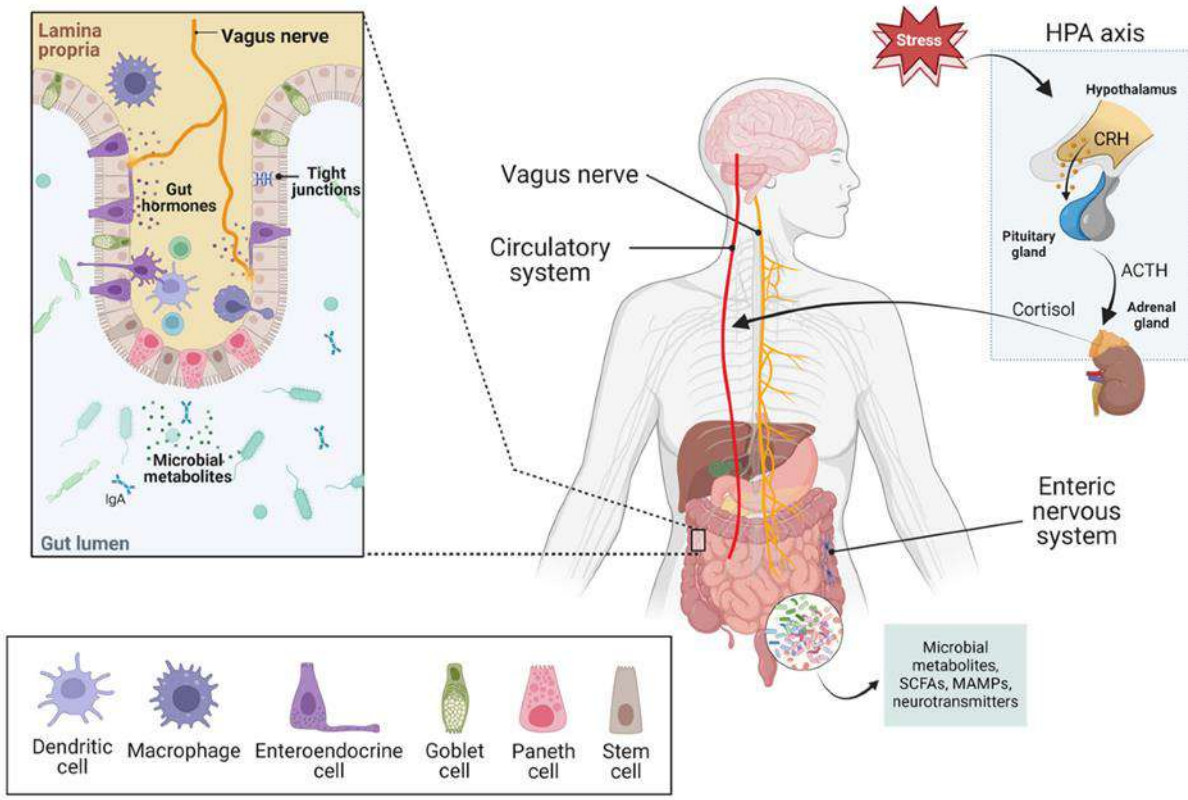

Fig. 5. Schematic overview of the key components of the microbiota-gut-brain axis (MGBA). Gut microbiota influences the intestinal lumen and epithelial surface by releasing various metabolites, such as short-chain fatty acids (SCFAs) and neurotransmitters. These microbial products can traverse the epithelial barrier into the lamina propria and systemic circulation. Some metabolites also act locally on the epithelium, enhancing tight junction integrity and promoting the release of neuroendocrine and immune mediators that affect vagal nerve signalling or enter the bloodstream. Within the lamina propria, immune cells respond to microbial cues detected by dendritic cells by producing anti-inflammatory cytokines. Additionally, stress triggers the activation of the hypothalamic–pituitary–adrenal (HPA) axis, modulating cortisol levels in circulation and influencing gut motility via interactions with the enteric nervous system. This figure is adapted from Binda *et al.* (101).

The microbiota-gut-brain axis (MGBA) operates through a dynamic interplay where microbial metabolites such as short-chain fatty acids (SCFAs) and neurotransmitters influence the intestinal epithelium, enhancing barrier integrity and modulating neuroimmune responses. These metabolites can cross into the lamina propria and systemic circulation, activating immune cells and vagal nerve signalling. Concurrently, stress activates the hypothalamic–pituitary–adrenal (HPA) axis, elevating cortisol levels, which further alter gut motility and microbial composition via enteric nervous system interactions, as described in Fig. 5 (101). Stress-related microbial shifts are linked to reduced resilience against diseases and impaired gastrointestinal health, emphasizing the interplay between mental and gut health(100,102). Chronic stress also disrupts the integrity of critical physiological barriers, such as the intestinal and blood-brain barriers (BBB), allowing microbial products like lipopolysaccharides and short-chain fatty acids to cross into circulation and influence brain function. These disruptions are associated with emotional and behavioral abnormalities(103). Experimental models, such as chronic unpredictable mild stress (CUMS) and social disruption paradigms, reveal that stress-induced microbial alterations are intertwined with changes in cytokines, chemokines, and neurotransmitter levels. However, the lack of models isolating psychological stress limits understanding of its direct effects on the gut microbiome(104). Emerging evidence suggests reduced microbial diversity is linked to anxiety,

stress, and altered social behaviors, underscoring the microbiome-gut-brain axis's critical role in regulating mental and physical health. Targeting stress-induced microbial shifts could provide novel therapeutic strategies for stress-related disorders.

5.1. Impact of stress on gut microbiome composition and diversity

Stress is a significant environmental factor influencing gut microbiota composition and diversity, a phenomenon known as stress-induced dysbiosis. This dysbiosis is characterized by a reduction in beneficial microbial species and an increase in harmful ones, with profound implications for gut health and overall physiological functioning. The interaction between stress and gut microbiota extends beyond the gastrointestinal tract, affecting metabolic, immune, and neurobehavioral functions. This bidirectional relationship underscores the complexity of the gut-brain axis, making it a critical area of investigation. Chronic psychological stress can induce long-lasting alterations in the gut microbiota. Studies have demonstrated that stress significantly decreases the abundance of certain bacterial species associated with mental health resilience, exacerbating conditions like anxiety and depression(105). For instance, alterations at the phylum level often show significant shifts in Bacteroidetes, Firmicutes, and Proteobacteria. While these phyla typically constitute over 98% of the gut microbiota in mammals, stress can disrupt their balance, leading to dysbiosis. In animal studies, researchers have observed that psychological stress reduces microbial diversity and alters microbial composition. Genera such as *Lachnospira*, *Phascolarctobacterium*, and *Sutterella* are often negatively associated with stress, while others, like *Roseburia* and *Methanobrevibacter*, show increased abundance under stress(106). These changes suggest that stress-induced dysbiosis is not merely a reduction in diversity but also an alteration in the functional capabilities of the gut microbiota. The mechanisms through which stress impacts gut microbiota are multifaceted. Stress hormones, such as norepinephrine (NE), influence bacterial gene expression, promoting the growth of specific microbial communities. NE has been shown to alter the gut environment by increasing intestinal motility and mucin secretion, thereby creating conditions that favor the proliferation of certain bacterial species(94). Moreover, stress-induced alterations in gut barrier integrity, mediated by increased production of reactive oxygen species (ROS), can lead to systemic inflammation and metabolic dysfunction. Microbial metabolites also play a significant role in stress responses. Short-chain fatty acids (SCFAs), such as butyrate, produced by beneficial bacteria like *Lachnospiraceae*, are essential for maintaining gut health and modulating immune responses(107). Stress-induced reductions in SCFA-producing bacteria may compromise gut barrier integrity, exacerbate systemic inflammation and promote a maladaptive stress response. The gut-brain axis, a communication network linking the gastrointestinal tract and the central nervous system, plays a pivotal role in mediating the effects of stress on behavior and mental health. Studies in animal models have shown that gut microbiota can influence anxiety-like and depressive-like behaviors. For example, faecal microbiota transplantation from stressed or anxious mice to germ-free mice can induce similar behavioral traits in the recipient animals(108). Some studies report reduced alpha diversity in stressed populations, while others observe increased diversity, influenced by factors such as diet, experimental models, and stress type. Mice exhibiting resistance to stress showed higher levels of *Lactobacillus* and *Akkermansia* in their gut microbiota, while displaying reduced levels of *Bacteroides*, *Alloprevotella*, *Helicobacter*, *Lachnoclostridium*, *Colidextibacter*, and *Lachnospiraceae NK4A136*(109). Interestingly, stress-induced microbial changes are not limited to bacteria but extend to archaea, such as increased Euryarchaeota abundance, which may contribute to adverse health outcomes. Understanding the effects of stress on gut microbiota composition and diversity can inform therapeutic interventions. Probiotics, prebiotics, and dietary modifications show promise in mitigating dysbiosis and improving mental health outcomes(110). Additionally, integrating microbiome research with personalized medicine could enhance treatment efficacy for stress-related disorders. Stress-induced dysbiosis exemplifies the

intricate interplay between psychological stress and gut microbiota(105). Alterations in microbial composition and diversity not only affect gut health but also have far-reaching implications for systemic and mental health. Future research should focus on unravelling the mechanisms driving these changes and developing targeted interventions to alleviate their adverse effects.

5.2. Role of Gut-Brain axis in stress-microbiome interactions

The gut-brain axis is a bidirectional communication network involving the central nervous system (CNS), enteric nervous system (ENS), autonomic nervous system (ANS), and gut microbiota, playing a critical role in stress-related interactions and overall homeostasis. Gut microbiota significantly influences neurophysiology and behaviour through microbial metabolites, such as GABA, serotonin, and tryptophan derivatives, which interact with neural and endocrine pathways(111). For instance, *Lactobacillus rhamnosus* modulates GABA receptor expression in the brain, affecting stress and anxiety responses(112). Studies in maternal separation models of early-life stress reveal alterations in gut microbiota, HPA axis activation, and anxiety-like behaviours, with the microbiota being crucial for these stress-induced effects(113). Similarly, gut dysbiosis caused by a maternal high-fat diet in mice disrupts offspring social behaviour and brain oxytocin levels, which can be ameliorated by restoring microbial balance(114). Evidence from human studies supports these findings, as probiotics like *Bifidobacterium longum* 1714 reduce stress and enhance cognition, although variability in outcomes highlights the influence of diet, lifestyle, and genetics(115). Microbiota also impacts neurodegenerative and developmental disorders, with altered microbial profiles linked to Parkinson's disease and autism spectrum disorders(116). Communication within the gut-brain axis involves the ANS-mediated ENS activity, with microbial signals like indole and serotonin influencing vagal and 5-HT receptor pathways. Stress impacts gut microbiota via the HPA axis, as germ-free mice exhibit hyperactive corticosterone responses, underscoring the regulatory role of gut microbiota(117). Medications, including antibiotics and psychotropics, can further alter gut microbiota and subsequently affect neurophysiology, emphasizing the gut-brain axis's complexity and its therapeutic potential in managing stress and mental health.

6. PSYCHOLOGICAL AND GASTROINTESTINAL DISORDERS LINKED TO STRESS

Early studies established a significant link between psychosocial stress and physiological diseases, emphasizing the critical role of psychological factors in gut dysfunction. This relationship showcases how stress can negatively affect gastrointestinal health, with research indicating that the effects of psychological stress markedly differ from those associated with physical stress(118). For instance, studies utilizing various stress models, including restraint, footshock, and cold exposure, demonstrate these distinctions in stress responses and their impact on gut function(119-121). The dysfunction of the brain-gut axis (BGA) resulting from exposure to stress may lead to the development of numerous gastrointestinal disorders. Conditions such as gastroesophageal reflux disease (GERD), peptic ulcer disease (PUD), inflammatory bowel disease (IBD), irritable bowel syndrome (IBS), and even food allergies have been linked to the compromised functioning of this axis under stress. The impact of stress on these ailments illustrates the need for a comprehensive understanding of both psychological and physiological factors in managing gastrointestinal health.

6.1. Irritable bowel syndrome (IBS)

Irritable bowel syndrome (IBS) is a prevalent functional gastrointestinal disorder affecting 9–23% of the global population, marked by abdominal pain and altered bowel habits without structural

abnormalities(122). Stress plays a crucial role in IBS pathogenesis, with studies revealing comorbid anxiety and depression in over 60% of IBS patients and bidirectional relationships between major depression and IBS symptoms(123). The gut-brain axis, a key mediator, connects the central nervous system (CNS) and the enteric nervous system (ENS), as stress-induced dysregulation of this axis impacts gut motility, permeability, and microbiota composition. Functional MRI studies in IBS patients show increased activation in brain regions like the anterior cingulate cortex, indicating CNS involvement(124). Dysbiosis, characterized by reduced beneficial bacteria like *Lactobacillus* and *Bifidobacterium*, is implicated in IBS and exacerbated by stress and high-fat diets, which induce chronic inflammation and alter gut permeability(125,126). Probiotics targeting gut microbiota have shown promise in relieving symptoms and associated anxiety, suggesting therapeutic potential. At the molecular level, serotonin (5-HT) regulation plays a critical role; IBS subtypes show distinct 5-HT profiles, with decreased levels in constipation-predominant IBS (IBS-C) and increased levels in diarrhoea-predominant IBS (IBS-D), linking sensory dysfunction to symptoms(127,128). Immune activation is another contributing factor, with elevated mast cells, lymphocytes, and cytokine levels observed in IBS patients, as well as increased intestinal permeability. Approximately 10% of IBS cases arise post-infectious gastroenteritis, highlighting inflammation's role in its pathogenesis(129). Stress and psychosocial factors exacerbate symptoms, necessitating psychological interventions like cognitive-behavioural therapy to complement traditional treatments(130). Dietary factors, such as low FODMAP diets, modulate symptoms by influencing gut microbiota and barrier integrity(131). Effective management of IBS includes a combination of dietary modifications, probiotics, and pharmacological interventions like serotonin receptor modulators, rifaximin, and antispasmodics, alongside psychological therapies for stress-related IBS(132). Future research should focus on personalized approaches to optimize treatments for this multifactorial disorder, which exemplifies complex interactions between stress, gut-brain axis dysfunction, and microbiota dynamics.

6.2. Stress and inflammatory bowel disease (IBD)

Inflammatory Bowel Disease (IBD), encompassing ulcerative colitis (UC) and Crohn's disease (CD), is characterized by chronic gastrointestinal inflammation with complex, multifactorial pathogenesis involving immune dysregulation, genetic predisposition, environmental factors, and microbiota alterations(133). Chronic psychological stress has emerged as a key factor in exacerbating IBD, contributing to both disease progression and increased susceptibility to psychiatric comorbidities, such as anxiety and depression(134). Stress-mediated activation of the hypothalamic-pituitary-adrenal (HPA) axis and biogenic amines, including serotonin, plays a critical role in the gut-brain axis, modulating immune responses and the production of pro-inflammatory mediators, as described in Fig. 6 (135).

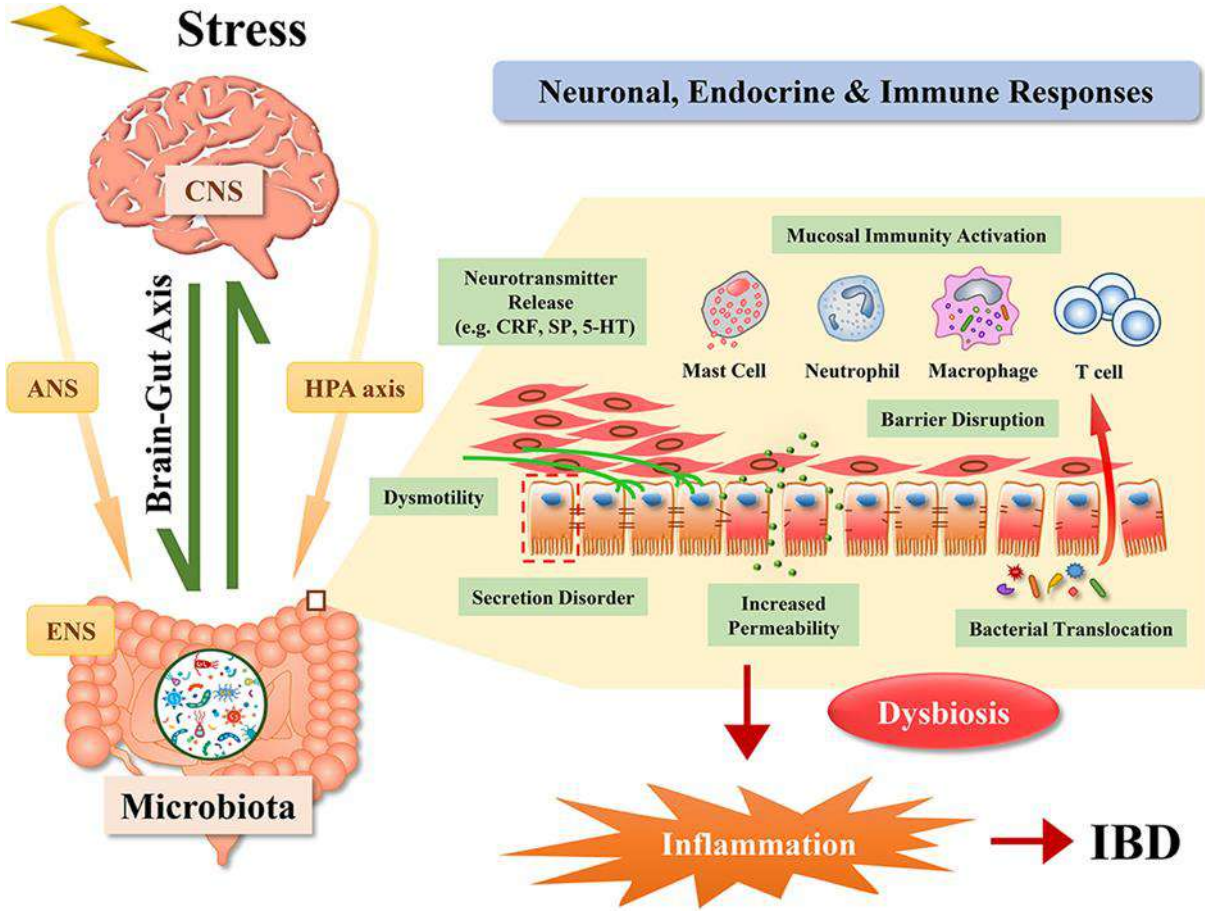

Fig. 6. Pathways through which stress influences the development and progression of inflammatory bowel disease (IBD). Stress exerts multifaceted effects on the gastrointestinal system through coordinated interactions among the nervous, endocrine, and immune systems. It activates the brain-gut axis, including the hypothalamic-pituitary-adrenal (HPA) axis, autonomic nervous system (ANS), and enteric nervous system (ENS). These responses contribute to IBD pathogenesis by inducing gut microbiota imbalances (dysbiosis), impairing gastrointestinal secretion and motility, compromising the integrity of the intestinal barrier, and promoting the release of pro-inflammatory mediators. This figure is adapted from Sun *et al.* (135).

Dysregulated Th17 responses, which produce pro-inflammatory cytokines such as IL-17A and IL-21, contribute to intestinal barrier dysfunction, neuroinflammation, and IBD progression(136). Psychological stress also disrupts the intestinal microbiota, promoting pathogenic colonization, increasing intestinal permeability, and amplifying systemic inflammation, further driving IBD pathology. Studies demonstrate that microbiota dysbiosis, characterized by reduced levels of protective bacteria such as Lactobacillus and Bacteroides, and increased pathogenic bacteria, like adherent-invasive *Escherichia coli*, correlates with IBD severity(137). Moreover, the oral-gut axis has been implicated, as pathobionts from the oral cavity can colonize the intestines, exacerbating inflammation in IBD patients(138). Stress-induced alterations in the gut microbiota and its metabolites, such as serotonin and short-chain fatty acids, affect neuroimmune signalling, highlighting the bidirectional relationship between the brain and gut(139). Therapeutic strategies targeting stress and microbiota, including psychobiotics, antidepressants, and microbiota transplantation, show promise in mitigating IBD symptoms and improving psychological outcomes. Advanced imaging and molecular diagnostic tools are essential for understanding stress-IBD interactions and developing personalized treatments.

6.3. The impact of stress on acid reflux and digestive disturbances

Gastroesophageal reflux disease (GERD), a condition characterized by the backflow of stomach contents into the oesophagus, manifests with symptoms like heartburn and regurgitation, affecting approximately 13.98% of the global population(140). Its prevalence varies significantly worldwide, with higher rates in countries like Sri Lanka (25.3%) compared to global averages, partly due to differences in diagnostic criteria(141). Stress is a recognized risk factor for GERD, exacerbating symptoms and complicating treatment outcomes. Studies reveal that stress amplifies GERD symptoms through mechanisms such as oesophageal hypersensitivity and reduced lower oesophageal sphincter tone(142). Chronic stress may also induce functional dyspepsia or heartburn, mimicking GERD without actual reflux, leading to misdiagnoses and treatment resistance. Stress-related behaviours, including poor dietary choices, smoking, and alcohol consumption, further aggravate GERD symptoms(143). The bidirectional relationship between GERD and stress highlights that while stress can worsen GERD, the chronic discomfort of GERD may itself induce stress, creating a vicious cycle. Stress-induced oesophageal hypersensitivity has been demonstrated in studies where acute stress heightened the perception of oesophageal stimuli without increasing acid exposure, suggesting central sensitization mechanisms(144). Additionally, stressful life events, such as divorce or bereavement, are strongly linked to the exacerbation of GERD symptoms. Notably, patients with higher anxiety levels often report intensified GERD symptoms, particularly chest pain, which is closely associated with stress(145). Despite these insights, the complex interaction between chronic stress, GERD symptoms, and individual susceptibility remains under-researched, especially in regions like South Asia. Future studies focusing on chronic stress models and differentiating between functional and true GERD using advanced diagnostics could refine management strategies and improve outcomes for patients with stress-aggravated GERD.

6.4. Stress-induced gastritis and ulcer

Stress-induced gastritis and ulcers, often a consequence of acute and chronic stress, illustrate the profound interplay between the CNS and the ENS, also known as the "second brain," which consists of approximately 500 million neurons in the gastrointestinal tract(132). Stress-related mucosal disease (SRMD) encompasses a spectrum of conditions from superficial mucosal erosions to stress ulcers, frequently seen in critically ill patients in intensive care units (ICUs)(146). Physiological stress, arising from severe trauma, burns, intracranial injuries, or sepsis, triggers heightened gastric acid secretion mediated by acetylcholine (ACh), gastrin, and histamine, which stimulate parietal cells via complex intracellular pathways, culminating in hydrogen ion secretion and mucosal damage(147). Disrupted gastric mucosal barriers lead to erosions and haemorrhagic lesions, with stress ulcers presenting as shallow but clinically significant features in up to 90% of ICU patients. However, overt bleeding occurs in 0.6–8.5% of cases(148). Mortality rates are markedly higher in patients with stress-induced gastrointestinal bleeding due to underlying conditions or multiorgan failure(149,150). Pathogenesis involves oxidative stress, decreased mucosal blood flow, and reactive oxygen species, countered to some extent by protective factors like nitric oxide(151,152). Calcium channel modulators and dopamine receptor agonists have demonstrated protective effects in experimental models, highlighting the neurochemical underpinnings of stress ulcers(153,154). Esophagogastroduodenoscopy (EGD) often reveals diffuse inflammation, mild erosions, and gastric haemorrhage, with stress-related gastric injuries presenting within days of a significant insult, such as trauma or surgery(155). Clinical manifestations include coffee-ground vomitus, hematemesis, melena, and abdominal pain, often with accompanying nausea or orthostatic symptoms in severe cases(156). Epidemiological studies report declining incidence rates of upper gastrointestinal haemorrhage, attributed to the early use of proton pump inhibitors (PPIs) and histamine blockers, underscoring the importance of prophylactic measures in at-

risk populations(157). Stress-induced gastritis represents a critical area where interprofessional coordination is vital for timely diagnosis, evaluation, and treatment, integrating pharmacological interventions with comprehensive care strategies to mitigate complications and improve patient outcomes.

6.5. Functional gut disorders: The role of psychological factors in conditions like functional dyspepsia

Functional dyspepsia (FD), a prevalent yet poorly understood functional gastrointestinal disorder, exemplifies the complex interplay between psychological and physiological factors, with its pathogenesis attributed to dysregulation within the brain-gut axis (BGA), a bidirectional communication network linking the CNS and ENS(158,159). Research reveals a significant overlap between FD and irritable bowel syndrome (IBS), suggesting potential shared etiologies or manifestations of a single disorder spectrum, with up to 40% of gastroenterological cases displaying overlapping symptoms(160,161). Psychosocial factors, including anxiety, depression, and stress, are closely associated with FD, influencing its onset, symptom severity, and chronicity, potentially through mechanisms such as autonomic hyperarousal, increased visceral hypersensitivity, or unexpressed emotional distress. The biopsychosocial model proposed by Drossman integrates these interactions, emphasizing that FD results from multifactorial influences involving psychological, biological, and social factors, with the BGA serving as the anatomical substrate mediating this complex interaction(162). The BGA's role involves sensory and viscerosensory inputs modulated by cognition and emotion, interacting with neural circuits in the CNS, spinal cord, autonomic nervous system, and ENS, ultimately contributing to dysregulation in intestinal motor and sensory activity. Notably, chronic stress and psychiatric comorbidities, such as depression, are linked to FD, either as precipitating or perpetuating factors, while these conditions also influence healthcare-seeking behaviours(163). Management strategies for FD underscore the importance of addressing psychosocial variables, with psychological therapies and psychotropic medications showing potential benefits, particularly for patients with refractory or chronic symptoms(164). This evolving understanding underscores the importance of the BGA and psychological factors in FD, highlighting the need for integrative management approaches that consider the psychosocial dimensions of the disorder alongside conventional medical treatments.

7. TREATMENT APPROACHES FOR STRESS-INDUCED GUT DISORDERS

7.1. Pharmacological interventions

Treatment approaches for stress-induced gut disorders primarily involve pharmacological interventions targeting the central nervous system (CNS) and gut-brain axis. Antidepressants and anxiolytics, such as selective serotonin reuptake inhibitors (SSRIs) and serotonin-norepinephrine reuptake inhibitors (SNRIs), are commonly used as first-line treatments per the World Federation of Biological Psychiatry (WFSBP) guidelines(165,166). SSRIs, including fluoxetine and citalopram, improve gastrointestinal (GI) motility and alleviate visceral hypersensitivity but may cause agitation, diarrhoea, and sexual dysfunction(167-169). SNRIs like duloxetine and venlafaxine are effective in pain management related to functional gastrointestinal disorders (FGIDs), with side effects such as nausea and dizziness(170,171). Tricyclic antidepressants (TCAs), including amitriptyline and nortriptyline, provide analgesic benefits and improve sleep and diarrhoea but are associated with constipation, dry mouth, and cardiac arrhythmias(172). Novel therapeutic targets include α2-adrenergic agonists (e.g., clonidine) and kappa-opioid antagonists (e.g., CERC-501), which show potential in stress-related

disorders and pain modulation(173,174). Mirtazapine, an atypical antidepressant, enhances gastric accommodation and reduces nausea but can induce sedation and weight gain(175,176). Azapirones such as buspirone improve gastric function by reducing oesophageal contractions, albeit with limited specificity for symptom relief(177).

In intensive care settings, stress ulcer prophylaxis is achieved through proton pump inhibitors (PPIs) and histamine-2-receptor antagonists (H2RAs), though prolonged use may lead to dyspepsia, vitamin B12 deficiency, and alterations in gastric microbiota(178). Emerging pharmacological strategies involve combinatorial approaches with agents targeting complementary CNS pathways, such as glucocorticoid and corticotropin-releasing factor-1 antagonists, for enhanced efficacy in treatment-resistant cases(179,180). The exploration of second-tier candidates, such as metabotropic glutamate receptor (mGluR) modulators and peroxisome proliferator-activated receptor-gamma (PPAR-γ) agonists, holds promise for improving gut sensorimotor function and stress resilience(181). An integrative treatment paradigm that considers the biopsychosocial dimensions of stress-induced gut disorders is crucial for optimizing therapeutic outcomes while mitigating potential adverse effects and withdrawal symptoms linked to chronic pharmacotherapy. Additionally, anxiolytics like benzodiazepines and GABAergic drugs (e.g., pregabalin) provide symptomatic relief in generalized anxiety disorder and related conditions(182). Pharmacological management of stress ulcers primarily involves PPIs and H2RAs, which inhibit gastric acid secretion but carry risks such as parietal cell hyperplasia and gastric cancer in extreme cases(183,184). Understanding drug interactions and contraindications is crucial, particularly in ICU settings where prolonged medication use can exacerbate comorbidities and complicate patient management. Future therapeutic directions emphasize the role of personalized medicine and multidisciplinary approaches to address the complexity of stress-related gut disorders effectively.

7.2. Role of prebiotics and probiotics

Probiotics, defined by the Food and Agriculture Organization and the World Health Organization as live microorganisms that confer health benefits to the gastrointestinal (GI) tract when consumed in sufficient amounts, must withstand harsh gastric conditions to reach the intestines and maintain viability(185). Probiotic efficacy requires a minimum of 10^6–10^8 colony-forming units (cfu) per gram or millilitre, with daily doses exceeding 10^9 cfu necessary for bacterial balance restoration(186). Lactic acid bacteria, such as *Lactobacillus* and *Bifidobacterium* species, and yeasts like *Saccharomyces boulardii* are key probiotics administered through foods, supplements, or pharmaceuticals(187,188). Prebiotics, including fructooligosaccharides (FOSs) and galactooligosaccharides (GOSs), enhance probiotics by selectively promoting beneficial microbial growth, thereby improving GI and mental health(189). Fermentation of prebiotics in the colon produces metabolites that foster gut homeostasis and influence mental health, as the gut microbiota plays a critical role in the gut-brain axis by affecting neurotransmitter production, including gamma-aminobutyric acid (GABA) and short-chain fatty acids(68). Evidence supports the use of probiotics in managing irritable bowel syndrome (IBS) and functional GI disorders diagnosed per Rome IV criteria, often linked to stress-induced microbiota imbalance, depression, and anxiety(190,191). Clinical trials demonstrate that strains such as *Lactobacillus plantarum P-8* alleviate stress, anxiety, and depression by modulating gut microbiota diversity and functionality, reducing pro-inflammatory cytokines, and enhancing neuroactive metabolites(192). Interventions have shown that gut microbial diversity and specific species like *Bifidobacterium longum* and *Faecalibacterium prausnitzii* correlate positively with improved mood and stress resilience, while lower diversity is linked to various disorders(192-194). Additionally, gut microbiota-derived metabolites, such as secondary bile acids and arachidonic acid, support intestinal barrier integrity and cognitive functions(195,196). This integrative approach to gut health underscores the potential of combining probiotics and prebiotics to

mitigate mental and GI disorders, reduce healthcare costs, and improve overall well-being, highlighting the critical interplay between diet, microbiota, and host health.

7.3. Psychological interventions

Cognitive–behavioural therapy (CBT), mindfulness, and relaxation techniques are psychological interventions widely employed to address stress-induced gut disorders and other psychosomatic conditions. CBT, a structured psychotherapy method, focuses on identifying and altering maladaptive thought patterns to foster adaptive behaviours and emotional resilience. Its origins trace back to learning theory principles and subsequent integrations of behavioural and cognitive therapy in the mid-20th century(130). Studies, including randomized controlled trials, demonstrate the effectiveness of CBT in treating mental health conditions such as anxiety, depression, and obsessive-compulsive disorders, as well as physical ailments like irritable bowel syndrome (IBS) and fibromyalgia(130,197). Subtypes such as mindfulness-based cognitive therapy (MBCT) and acceptance and commitment therapy (ACT) extend the scope of CBT by incorporating mindfulness, exposure, and emotional regulation strategies, effectively addressing conditions like post-traumatic stress disorder (PTSD) and chronic pain(198,199). Evidence supports the utility of CBT in managing chronic conditions, improving mental health, and enhancing quality of life, with online and app-based CBT offering cost-effective and scalable solutions(200,201). Relaxation techniques, another adjunct, reduce physiological arousal associated with stress, offering additional benefits for stress-related disorders(202). Despite promising results, further research is needed to assess long-term outcomes and refine biopsychosocial approaches to optimize therapy for diverse populations, ensuring broad applicability and effectiveness.

7.4. Dietary interventions

Stress negatively impacts gut health by disrupting the gut-brain axis, leading to altered gut microbiota composition, increased intestinal permeability, and systemic inflammation. Diet plays a crucial role in mitigating these effects, with anti-inflammatory and fiber-rich diets demonstrating significant benefits. Anti-inflammatory diets, such as the Mediterranean diet, rich in omega-3 fatty acids, polyphenols, and unsaturated fats, have been shown to reduce gut inflammation by promoting a balanced immune response and supporting beneficial gut microbiota(203). Similarly, fiber-rich diets enhance gut health by providing prebiotics, such as inulin and resistant starch, which are metabolized by gut bacteria into short-chain fatty acids (SCFAs) like butyrate. SCFAs play a critical role in strengthening the gut barrier, reducing inflammation, and modulating immune responses(204,205). Conversely, Western diets high in saturated fats and refined carbohydrates are linked to dysbiosis, increased intestinal permeability, and heightened inflammation, exacerbating stress-induced gut dysfunction(206). Interventions like probiotics and fermented foods further support gut health by introducing beneficial microbes and enhancing microbial diversity, which counteract stress-related dysbiosis(188). Overall, adopting a diet rich in anti-inflammatory components and dietary fiber can effectively mitigate stress-induced gut health issues, highlighting the importance of dietary strategies in promoting gastrointestinal and systemic health.

7.5. Gut-specific therapies

Gut-specific therapies, including fecal microbiota transplantation (FMT), targeted probiotics, and gut healing strategies, have emerged as promising interventions for restoring gut microbial balance and treating various gastrointestinal and systemic disorders. FMT, an ancient practice first documented in traditional Chinese medicine 1700 years ago, involves the transfer of fecal microbiota from a healthy donor to a recipient with dysbiosis to restore microbial homeostasis(207). Modern scientific literature has demonstrated FMT's efficacy in treating recurrent Clostridioides difficile infection (CDI), achieving

success rates exceeding 90%, far surpassing traditional antibiotic treatments(208,209). Beyond CDI, FMT is being explored for its potential in managing inflammatory bowel disease (IBD), irritable bowel syndrome (IBS), obesity, metabolic syndrome, and neurological conditions such as Parkinson's disease and autism spectrum disorder, though further clinical validation is required(210). Dysbiosis, characterized by an imbalance in gut microbiota, is implicated in numerous diseases, and the manipulation of the gut microbiome through FMT offers an effective means of addressing these imbalances. While probiotics have been widely used to modulate gut flora, their efficacy is often limited due to the lack of microbial diversity compared to the naturally occurring gut microbiota in healthy individuals. Therefore, FMT provides a more comprehensive microbial restoration by introducing a complete and functional microbial ecosystem. In the context of IBD, including Crohn's disease and ulcerative colitis, studies suggest that FMT can modulate the immune response and promote gut healing by re-establishing a diverse and stable microbiota(211). Gut-specific therapies, including FMT, dietary interventions, and targeted probiotics, offer a holistic approach to managing gut-related disorders by addressing underlying microbial imbalances and promoting gut barrier integrity. However, despite its potential, FMT poses challenges such as donor screening, standardization of procedures, and potential risks of pathogen transmission, which necessitate the establishment of rigorous clinical guidelines(212). The future of gut-specific therapies lies in personalized microbiome-based interventions, leveraging advances in metagenomics and precision medicine to tailor treatments to individual microbiome profiles. As research continues to uncover the intricate relationship between the gut microbiota and human health, gut-specific therapies hold significant promise for revolutionizing the management of both gastrointestinal and systemic diseases through targeted microbiome modulation.

8. CONCLUSION

The intricate relationship between stress and gut health has been increasingly recognized as a pivotal aspect of overall well-being. Stress exerts profound effects on gut physiology through neuroendocrine, autonomic, immune, and metabolic pathways. Central to this relationship is the HPA axis, with glucocorticoids acting as key mediators in the brain-gut axis, shaping gut function and contributing to stress-induced disorders. Advancing our understanding of HPA axis regulation, mitochondrial function, and their roles in stress-related gut pathology opens new avenues for targeted therapeutic interventions. Given the multifaceted effects of stress on gut health, an integrative treatment approach is essential. While traditional pharmacological options like SSRIs and TCAs remain effective, their significant side effects underscore the need for safer, targeted therapies. Natural alternatives, such as phytochemicals with antioxidant properties, offer promising avenues for reducing oxidative stress in the gut. Additionally, lifestyle interventions, including stress management, dietary modifications, and gut microbiome modulation via probiotics and prebiotics, provide complementary strategies to pharmaceutical treatments. Combining pharmacological, natural, and lifestyle interventions into a holistic model may yield the most effective and sustainable outcomes for managing stress-induced gut disorders. Despite recent progress, critical gaps persist in understanding the precise molecular mechanisms linking stress and gut health. Future research should focus on unravelling the interplay between mitochondrial bioenergetics, biogenesis, and energy homeostasis in stress-induced gut pathologies. The emerging concept of the mind-mitochondria-gut axis offers a compelling framework for studying how mental stress translates into physiological responses through mitochondrial dysfunction. Translational research is essential to validate findings from animal models in human populations, ensuring interventions are both effective and safe. Addressing stress-related gut disorders requires a multidisciplinary approach that bridges research, clinical practice, and public health. Collaborative efforts among scientists, clinicians, and healthcare practitioners will be crucial in

developing targeted, innovative strategies to enhance gut health and improve the quality of life for individuals impacted by stress.

9. REFERENCES

1. Lupien, S. J., McEwen, B. S., Gunnar, M. R., and Heim, C. (2009) Effects of stress throughout the lifespan on the brain, behaviour and cognition. *Nature reviews. Neuroscience* **10**, 434-445

2. Yang, L., Zhao, Y., Wang, Y., Liu, L., Zhang, X., Li, B., and Cui, R. (2015) The Effects of Psychological Stress on Depression. *Current neuropharmacology* **13**, 494-504

3. Tsigos, C., Kyrou, I., Kassi, E., and Chrousos, G. P. (2000) Stress: Endocrine Physiology and Pathophysiology. in *Endotext* (Feingold, K. R., Ahmed, S. F., Anawalt, B., Blackman, M. R., Boyce, A., Chrousos, G., Corpas, E., de Herder, W. W., Dhatariya, K., Dungan, K., Hofland, J., Kalra, S., Kaltsas, G., Kapoor, N., Koch, C., Kopp, P., Korbonits, M., Kovacs, C. S., Kuohung, W., Laferrère, B., Levy, M., McGee, E. A., McLachlan, R., Muzumdar, R., Purnell, J., Rey, R., Sahay, R., Shah, A. S., Singer, F., Sperling, M. A., Stratakis, C. A., Trence, D. L., and Wilson, D. P. eds.), MDText.com, Inc. Copyright © 2000-2025, MDText.com, Inc., South Dartmouth (MA). pp

4. Zheng, Y., Bonfili, L., Wei, T., and Eleuteri, A. M. (2023) Understanding the Gut-Brain Axis and Its Therapeutic Implications for Neurodegenerative Disorders. *Nutrients* **15**

5. Zhang, H., Wang, Z., Wang, G., Song, X., Qian, Y., Liao, Z., Sui, L., Ai, L., and Xia, Y. (2023) Understanding the Connection between Gut Homeostasis and Psychological Stress. *The Journal of nutrition* **153**, 924-939

6. Bardou, M., Quenot, J. P., and Barkun, A. (2015) Stress-related mucosal disease in the critically ill patient. *Nature reviews. Gastroenterology & hepatology* **12**, 98-107

7. Vanella, G., Capurso, G., Burti, C., Fanti, L., Ricciardiello, L., Souza Lino, A., Boskoski, I., Bronswijk, M., Tyberg, A., Krishna Kumar Nair, G., Angeletti, S., Mauro, A., Zingone, F., Oppong, K. W., de la Iglesia-Garcia, D., Pouillon, L., Papanikolaou, I. S., Fracasso, P., Ciceri, F., Rovere-Querini, P., Tomba, C., Viale, E., Eusebi, L. H., Riccioni, M. E., van der Merwe, S., Shahid, H., Sarkar, A., Yoo, J. W. G., Dilaghi, E., Speight, R. A., Azzolini, F., Buttitta, F., Porcari, S., Petrone, M. C., Iglesias-Garcia, J., Savarino, E. V., Di Sabatino, A., Di Giulio, E., Farrell, J. J., Kahaleh, M., Roelandt, P., Costamagna, G., Artifon, E. L. A., Bazzoli, F., Testoni, P. A., Greco, S., and Arcidiacono, P. G. (2021) Gastrointestinal mucosal damage in patients with COVID-19 undergoing endoscopy: an international multicentre study. *BMJ open gastroenterology* **8**

8. (2021) Global prevalence and burden of depressive and anxiety disorders in 204 countries and territories in 2020 due to the COVID-19 pandemic. *Lancet (London, England)* **398**, 1700-1712

9. Xiong, J., Lipsitz, O., Nasri, F., Lui, L. M. W., Gill, H., Phan, L., Chen-Li, D., Iacobucci, M., Ho, R., Majeed, A., and McIntyre, R. S. (2020) Impact of COVID-19 pandemic on mental health in the general population: A systematic review. *Journal of affective disorders* **277**, 55-64

10. WHO. (2022) COVID-19 pandemic triggers 25% increase in prevalence of anxiety and depression worldwide. in *WHO*

11. Godoy, L. D., Rossignoli, M. T., Delfino-Pereira, P., Garcia-Cairasco, N., and de Lima Umeoka, E. H. (2018) A Comprehensive Overview on Stress Neurobiology: Basic Concepts and Clinical Implications. *Frontiers in behavioral neuroscience* **12**, 127

12. Selye, H. (1950) Stress and the general adaptation syndrome. *British medical journal* **1**, 1383-1392

13. Sapolsky, R. M. (2005) The influence of social hierarchy on primate health. *Science (New York, N.Y.)* **308**, 648-652

14. Selye, H. (1976) The stress concept. *Canadian Medical Association journal* **115**, 718

15. Chrousos, G. P. (2009) Stress and disorders of the stress system. *Nature reviews. Endocrinology* **5**, 374-381

16. McEwen, B. S. (2007) Physiology and neurobiology of stress and adaptation: central role of the brain. *Physiological reviews* **87**, 873-904

17. Li, R., Ye, J. J., Gan, L., Zhang, M., Sun, D., Li, Y., Wang, T., and Chang, P. (2024) Traumatic inflammatory response: pathophysiological role and clinical value of cytokines. *European journal of trauma and emergency surgery : official publication of the European Trauma Society* **50**, 1313-1330

18. Mahmoud, N. N., Hamad, K., Al Shibitini, A., Juma, S., Sharifi, S., Gould, L., and Mahmoudi, M. (2024) Investigating Inflammatory Markers in Wound Healing: Understanding Implications and Identifying Artifacts. *ACS pharmacology & translational science* **7**, 18-27

19. Knezevic, E., Nenic, K., Milanovic, V., and Knezevic, N. N. (2023) The Role of Cortisol in Chronic Stress, Neurodegenerative Diseases, and Psychological Disorders. *Cells* **12**

20. Akira, S., Uematsu, S., and Takeuchi, O. (2006) Pathogen recognition and innate immunity. *Cell* **124**, 783-801

21. Kenny, G. P., Sigal, R. J., and McGinn, R. (2016) Body temperature regulation in diabetes. *Temperature (Austin, Tex.)* **3**, 119-145

22. Osilla EV, M. J., Shumway KR, et al. (2025) *Physiology, Temperature Regulation.*, Treasure Island (FL): StatPearls

23. Chu B, M. K., Sanvictores T, et al. (2024) *Physiology, Stress Reaction.*, Treasure Island (FL): StatPearls Publishing

24. Stephens, M. A., and Wand, G. (2012) Stress and the HPA axis: role of glucocorticoids in alcohol dependence. *Alcohol research : current reviews* **34**, 468-483

25. Zoccal, D. B., Furuya, W. I., Bassi, M., Colombari, D. S., and Colombari, E. (2014) The nucleus of the solitary tract and the coordination of respiratory and sympathetic activities. *Frontiers in physiology* **5**, 238

26. Herman, J. P., Figueiredo, H., Mueller, N. K., Ulrich-Lai, Y., Ostrander, M. M., Choi, D. C., and Cullinan, W. E. (2003) Central mechanisms of stress integration: hierarchical circuitry controlling hypothalamo-pituitary-adrenocortical responsiveness. *Frontiers in neuroendocrinology* **24**, 151-180

27. McEwen, B. S. (2008) Central effects of stress hormones in health and disease: Understanding the protective and damaging effects of stress and stress mediators. *European journal of pharmacology* **583**, 174-185

28. Heim, C., Ehlert, U., and Hellhammer, D. H. (2000) The potential role of hypocortisolism in the pathophysiology of stress-related bodily disorders. *Psychoneuroendocrinology* **25**, 1-35

29. vonRosenberg, J. (2019) Cognitive Appraisal and Stress Performance: The Threat/Challenge Matrix and Its Implications on Performance. *Air medical journal* **38**, 331-333

30. Ehlers, A., and Clark, D. M. (2000) A cognitive model of posttraumatic stress disorder. *Behaviour research and therapy* **38**, 319-345

31. Ross, R. A., Foster, S. L., and Ionescu, D. F. (2017) The Role of Chronic Stress in Anxious Depression. *Chronic stress (Thousand Oaks, Calif.)* **1**, 2470547016689472

32. Wang, W., Li, J., Sun, G., Cheng, Z., and Zhang, X. A. (2017) Achievement goals and life satisfaction: the mediating role of perception of successful agency and the moderating role of emotion reappraisal. *Psicologia, reflexao e critica : revista semestral do Departamento de Psicologia da UFRGS* **30**, 25

33. Šimić, G., Tkalčić, M., Vukić, V., Mulc, D., Španić, E., Šagud, M., Olucha-Bordonau, F. E., Vukšić, M., and P, R. H. (2021) Understanding Emotions: Origins and Roles of the Amygdala. *Biomolecules* **11**

34. Dvir, Y., Ford, J. D., Hill, M., and Frazier, J. A. (2014) Childhood maltreatment, emotional dysregulation, and psychiatric comorbidities. *Harvard review of psychiatry* **22**, 149-161

35. Ahmed, S. H., Zakai, A., Zahid, M., Jawad, M. Y., Fu, R., and Chaiton, M. (2024) Prevalence of post-traumatic stress disorder and depressive symptoms among civilians residing in armed conflict-affected regions: a systematic review and meta-analysis. *General psychiatry* **37**, e101438

36. Shaw, J. A. (2003) Children exposed to war/terrorism. *Clinical child and family psychology review* **6**, 237-246

37. Green, B. L. (1994) Psychosocial research in traumatic stress: an update. *Journal of traumatic stress* **7**, 341-362

38. Altena, E., Baglioni, C., Espie, C. A., Ellis, J., Gavriloff, D., Holzinger, B., Schlarb, A., Frase, L., Jernelöv, S., and Riemann, D. (2020) Dealing with sleep problems during home confinement due to the COVID-19 outbreak: Practical recommendations from a task force of the European CBT-I Academy. *Journal of sleep research* **29**, e13052

39. Syed, I. U. (2020) Clearing the Smoke Screen: Smoking, Alcohol Consumption, and Stress Management Techniques among Canadian Long-Term Care Workers. *International journal of environmental research and public health* **17**

40. Arnsten, A. F., Raskind, M. A., Taylor, F. B., and Connor, D. F. (2015) The Effects of Stress Exposure on Prefrontal Cortex: Translating Basic Research into Successful Treatments for Post-Traumatic Stress Disorder. *Neurobiology of stress* **1**, 89-99

41. Rutten, B. P., Hammels, C., Geschwind, N., Menne-Lothmann, C., Pishva, E., Schruers, K., van den Hove, D., Kenis, G., van Os, J., and Wichers, M. (2013) Resilience in mental health: linking psychological and neurobiological perspectives. *Acta psychiatrica Scandinavica* **128**, 3-20

42. Akirav, I., and Maroun, M. (2007) The role of the medial prefrontal cortex-amygdala circuit in stress effects on the extinction of fear. *Neural plasticity* **2007**, 30873

43. Pitts, M. W., Todorovic, C., Blank, T., and Takahashi, L. K. (2009) The central nucleus of the amygdala and corticotropin-releasing factor: insights into contextual fear memory. *The Journal of neuroscience : the official journal of the Society for Neuroscience* **29**, 7379-7388

44. Maren, S., Phan, K. L., and Liberzon, I. (2013) The contextual brain: implications for fear conditioning, extinction and psychopathology. *Nature reviews. Neuroscience* **14**, 417-428

45. McEwen, B. S., and Gianaros, P. J. (2010) Central role of the brain in stress and adaptation: links to socioeconomic status, health, and disease. *Annals of the New York Academy of Sciences* **1186**, 190-222

46. Hussain LS, R. V., Maani CV. (2025) *Physiology, Noradrenergic Synapse*, reasure Island (FL): StatPearls Publishing

47. Thau L, G. J., Sharma S. (2023) *Physiology, Cortisol.*, Treasure Island (FL): StatPearls Publishing

48. Kaiser, M., and Jaillardon, L. (2023) Pathogenesis of the crosstalk between reproductive function and stress in animals-part 1: Hypothalamo-pituitary-adrenal axis, sympatho-adrenomedullary system and kisspeptin. *Reproduction in domestic animals = Zuchthygiene* **58 Suppl 2**, 176-183

49. Akirav, I., and Richter-Levin, G. (2006) Factors that determine the non-linear amygdala influence on hippocampus-dependent memory. *Dose-response : a publication of International Hormesis Society* **4**, 22-37

50. Herman, J. P., McKlveen, J. M., Solomon, M. B., Carvalho-Netto, E., and Myers, B. (2012) Neural regulation of the stress response: glucocorticoid feedback mechanisms. *Brazilian journal of medical and biological research = Revista brasileira de pesquisas medicas e biologicas* **45**, 292-298

51. Myers, B., McKlveen, J. M., and Herman, J. P. (2012) Neural Regulation of the Stress Response: The Many Faces of Feedback. *Cellular and molecular neurobiology* **32**, 683-694

52. Herman, J. P., and Tasker, J. G. (2016) Paraventricular Hypothalamic Mechanisms of Chronic Stress Adaptation. *Frontiers in endocrinology* **7**, 137

53. Bartlett, A. A., Lapp, H. E., and Hunter, R. G. (2019) Epigenetic Mechanisms of the Glucocorticoid Receptor. *Trends in endocrinology and metabolism: TEM* **30**, 807-818

54. Hunter, R. G., Seligsohn, M., Rubin, T. G., Griffiths, B. B., Ozdemir, Y., Pfaff, D. W., Datson, N. A., and McEwen, B. S. (2016) Stress and corticosteroids regulate rat hippocampal mitochondrial DNA gene expression via the glucocorticoid receptor. *Proceedings of the National Academy of Sciences of the United States of America* **113**, 9099-9104

55. Khalil B, R. A., Warrington SJ. (2024) *Physiology, Catecholamines.*, Treasure Island (FL): StatPearls Publishing

56. Alotiby, A. (2024) Immunology of Stress: A Review Article. *Journal of clinical medicine* **13**

57. Esler, M. (2000) The sympathetic system and hypertension. *American journal of hypertension* **13**, 99s-105s

58. Balakin, E., Yurku, K., Ivanov, M., Izotov, A., Nakhod, V., and Pustovoyt, V. (2025) Regulation of Stress-Induced Immunosuppression in the Context of Neuroendocrine, Cytokine, and Cellular Processes. *Biology* **14**

59. Dhabhar, F. S. (2008) Enhancing versus Suppressive Effects of Stress on Immune Function: Implications for Immunoprotection versus Immunopathology. *Allergy, asthma, and clinical immunology : official journal of the Canadian Society of Allergy and Clinical Immunology* **4**, 2-11

60. Chen, L., Shao, C., Li, J., and Zhu, F. (2024) Impact of Immunosenescence on Vaccine Immune Responses and Countermeasures. *Vaccines* **12**

61. Govindarajan, A., Rao, B. S., Nair, D., Trinh, M., Mawjee, N., Tonegawa, S., and Chattarji, S. (2006) Transgenic brain-derived neurotrophic factor expression causes both anxiogenic and antidepressant effects. *Proceedings of the National Academy of Sciences of the United States of America* **103**, 13208-13213

62. Sharma, K., Akre, S., Chakole, S., and Wanjari, M. B. (2022) Stress-Induced Diabetes: A Review. *Cureus* **14**, e29142

63. Suganya, K., and Koo, B. S. (2020) Gut-Brain Axis: Role of Gut Microbiota on Neurological Disorders and How Probiotics/Prebiotics Beneficially Modulate Microbial and Immune Pathways to Improve Brain Functions. *International journal of molecular sciences* **21**

64. Carabotti, M., Scirocco, A., Maselli, M. A., and Severi, C. (2015) The gut-brain axis: interactions between enteric microbiota, central and enteric nervous systems. *Annals of gastroenterology* **28**, 203-209

65. Furness, J. B., Callaghan, B. P., Rivera, L. R., and Cho, H. J. (2014) The enteric nervous system and gastrointestinal innervation: integrated local and central control. *Advances in experimental medicine and biology* **817**, 39-71

66. Aziz, M. N. M., Kumar, J., Muhammad Nawawi, K. N., Raja Ali, R. A., and Mokhtar, N. M. (2021) Irritable Bowel Syndrome, Depression, and Neurodegeneration: A Bidirectional Communication from Gut to Brain. *Nutrients* **13**

67. Liu, Y., and Forsythe, P. (2021) Vagotomy and insights into the microbiota-gut-brain axis. *Neuroscience research* **168**, 20-27

68. Silva, Y. P., Bernardi, A., and Frozza, R. L. (2020) The Role of Short-Chain Fatty Acids From Gut Microbiota in Gut-Brain Communication. *Frontiers in endocrinology* **11**, 25

69. Chen, Y., Xu, J., and Chen, Y. (2021) Regulation of Neurotransmitters by the Gut Microbiota and Effects on Cognition in Neurological Disorders. *Nutrients* **13**

70. Nishi, S., Seino, Y., Ishida, H., Seno, M., Taminato, T., Sakurai, H., and Imura, H. (1987) Vagal regulation of insulin, glucagon, and somatostatin secretion in vitro in the rat. *The Journal of clinical investigation* **79**, 1191-1196

71. Peters, J. H., Karpiel, A. B., Ritter, R. C., and Simasko, S. M. (2004) Cooperative activation of cultured vagal afferent neurons by leptin and cholecystokinin. *Endocrinology* **145**, 3652-3657

72. Bastard, J. P., Maachi, M., Lagathu, C., Kim, M. J., Caron, M., Vidal, H., Capeau, J., and Feve, B. (2006) Recent advances in the relationship between obesity, inflammation, and insulin resistance. *European cytokine network* **17**, 4-12

73. Donath, M. Y., and Shoelson, S. E. (2011) Type 2 diabetes as an inflammatory disease. *Nature reviews. Immunology* **11**, 98-107

74. Cruz-Pereira, J. S., Rea, K., Nolan, Y. M., O'Leary, O. F., Dinan, T. G., and Cryan, J. F. (2020) Depression's Unholy Trinity: Dysregulated Stress, Immunity, and the Microbiome. *Annual review of psychology* **71**, 49-78

75. Noble, L. J., Gonzalez, I. J., Meruva, V. B., Callahan, K. A., Belfort, B. D., Ramanathan, K. R., Meyers, E., Kilgard, M. P., Rennaker, R. L., and McIntyre, C. K. (2017) Effects of vagus nerve stimulation on extinction of conditioned fear and post-traumatic stress disorder symptoms in rats. *Translational psychiatry* **7**, e1217

76. Bonaz, B., Sinniger, V., and Pellissier, S. (2021) Therapeutic Potential of Vagus Nerve Stimulation for Inflammatory Bowel Diseases. *Frontiers in neuroscience* **15**, 650971

77. Drokhlyansky, E., Smillie, C. S., Van Wittenberghe, N., Ericsson, M., Griffin, G. K., Eraslan, G., Dionne, D., Cuoco, M. S., Goder-Reiser, M. N., Sharova, T., Kuksenko, O., Aguirre, A. J., Boland, G. M., Graham, D., Rozenblatt-Rosen, O., Xavier, R. J., and Regev, A. (2020) The Human and Mouse Enteric Nervous System at Single-Cell Resolution. *Cell* **182**, 1606-1622.e1623

78. Bayliss, W. M., and Starling, E. H. (1899) The movements and innervation of the small intestine. *The Journal of physiology* **24**, 99-143

79. Furness, J. B. (2012) The enteric nervous system and neurogastroenterology. *Nature reviews. Gastroenterology & hepatology* **9**, 286-294

80. Ma, L., Wang, H. B., and Hashimoto, K. (2025) The vagus nerve: An old but new player in brain-body communication. *Brain, behavior, and immunity* **124**, 28-39

81. Geng, Z. H., Zhu, Y., Li, Q. L., Zhao, C., and Zhou, P. H. (2022) Enteric Nervous System: The Bridge Between the Gut Microbiota and Neurological Disorders. *Frontiers in aging neuroscience* **14**, 810483

82. Konturek, P. C., Brzozowski, T., and Konturek, S. J. (2011) Stress and the gut: pathophysiology, clinical consequences, diagnostic approach and treatment options. *Journal of physiology and pharmacology : an official journal of the Polish Physiological Society* **62**, 591-599

83. Rusch, J. A., Layden, B. T., and Dugas, L. R. (2023) Signalling cognition: the gut microbiota and hypothalamic-pituitary-adrenal axis. *Frontiers in endocrinology* **14**, 1130689

84. Wang, S. X., and Wu, W. C. (2005) Effects of psychological stress on small intestinal motility and bacteria and mucosa in mice. *World journal of gastroenterology* **11**, 2016-2021

85. Patel KS, T. A. (2023) *Physiology, Peristalsis.*, Treasure Island (FL): StatPearls Publishing

86. Guzel, T., and Mirowska-Guzel, D. (2022) The Role of Serotonin Neurotransmission in Gastrointestinal Tract and Pharmacotherapy. *Molecules (Basel, Switzerland)* **27**

87. Stengel, A., and Taché, Y. (2009) Neuroendocrine control of the gut during stress: corticotropin-releasing factor signaling pathways in the spotlight. *Annual review of physiology* **71**, 219-239

88. Williams, C. L., Villar, R. G., Peterson, J. M., and Burks, T. F. (1988) Stress-induced changes in intestinal transit in the rat: a model for irritable bowel syndrome. *Gastroenterology* **94**, 611-621

89. Deloose, E., Janssen, P., Depoortere, I., and Tack, J. (2012) The migrating motor complex: control mechanisms and its role in health and disease. *Nature reviews. Gastroenterology & hepatology* **9**, 271-285

90. Tache, Y., Larauche, M., Yuan, P. Q., and Million, M. (2018) Brain and Gut CRF Signaling: Biological Actions and Role in the Gastrointestinal Tract. *Current molecular pharmacology* **11**, 51-71

91. Khlevner, J., Park, Y., and Margolis, K. G. (2018) Brain-Gut Axis: Clinical Implications. *Gastroenterology clinics of North America* **47**, 727-739

92. Chan, A. O., Cheng, C., Hui, W. M., Hu, W. H., Wong, N. Y., Lam, K. F., Wong, W. M., Lai, K. C., Lam, S. K., and Wong, B. C. (2005) Differing coping mechanisms, stress level and anorectal physiology in patients with functional constipation. *World journal of gastroenterology* **11**, 5362-5366

93. Rodiño-Janeiro, B. K., Alonso-Cotoner, C., Pigrau, M., Lobo, B., Vicario, M., and Santos, J. (2015) Role of Corticotropin-releasing Factor in Gastrointestinal Permeability. *Journal of neurogastroenterology and motility* **21**, 33-50

94. Madison, A., and Kiecolt-Glaser, J. K. (2019) Stress, depression, diet, and the gut microbiota: human-bacteria interactions at the core of psychoneuroimmunology and nutrition. *Current opinion in behavioral sciences* **28**, 105-110

95. Devanarayana, N. M., and Rajindrajith, S. (2010) Association between constipation and stressful life events in a cohort of Sri Lankan children and adolescents. *Journal of tropical pediatrics* **56**, 144-148

96. Dos Santos, I. R., de Abreu, G. E., Dourado, E. R., Martinelli Braga, A. A. N., Lobo, V. A., de Carvalho, I. W. B., Bastos Netto, J. M., and Barroso, U., Jr. (2021) Emotional and behavioural problems in children and adolescents: The role of constipation. *Journal of paediatrics and child health* **57**, 1003-1008

97. Spiller, R. C., Jenkins, D., Thornley, J. P., Hebden, J. M., Wright, T., Skinner, M., and Neal, K. R. (2000) Increased rectal mucosal enteroendocrine cells, T lymphocytes, and increased gut permeability following acute Campylobacter enteritis and in post-dysenteric irritable bowel syndrome. *Gut* **47**, 804-811

98. Dong, Y., Han, Y., Wang, Z., Qin, Z., Yang, C., Cao, J., and Chen, Y. (2017) Role of serotonin on the intestinal mucosal immune response to stress-induced diarrhea in weaning mice. *BMC gastroenterology* **17**, 82

99. Geng, S., Yang, L., Cheng, F., Zhang, Z., Li, J., Liu, W., Li, Y., Chen, Y., Bao, Y., Chen, L., Fei, Z., Li, X., Hou, J., Lin, Y., Liu, Z., Zhang, S., Wang, H., Zhang, Q., Wang, H., Wang, X., and Zhang, J. (2019) Gut Microbiota Are Associated With Psychological Stress-Induced Defections in Intestinal and Blood-Brain Barriers. *Frontiers in microbiology* **10**, 3067

100. Gao, F., Guo, R., Ma, Q., Li, Y., Wang, W., Fan, Y., Ju, Y., Zhao, B., Gao, Y., Qian, L., Yang, Z., He, X., Jin, X., Liu, Y., Peng, Y., Chen, C., Chen, Y., Gao, C., Zhu, F., and Ma, X. (2022) Stressful events induce long-term gut microbiota dysbiosis and associated post-traumatic stress symptoms in healthcare workers fighting against COVID-19. *Journal of affective disorders* **303**, 187-195

101. Binda, S., Tremblay, A., Iqbal, U. H., Kassem, O., Le Barz, M., Thomas, V., Bronner, S., Perrot, T., Ismail, N., and Parker, J. A. (2024) Psychobiotics and the Microbiota-Gut-Brain Axis: Where Do We Go from Here? *Microorganisms* **12**

102. Galley, J. D., Mashburn-Warren, L., Blalock, L. C., Lauber, C. L., Carroll, J. E., Ross, K. M., Hobel, C., Coussons-Read, M., Dunkel Schetter, C., and Gur, T. L. (2023) Maternal anxiety, depression and stress affects offspring gut microbiome diversity and bifidobacterial abundances. *Brain, behavior, and immunity* **107**, 253-264

103. Gwak, M. G., and Chang, S. Y. (2021) Gut-Brain Connection: Microbiome, Gut Barrier, and Environmental Sensors. *Immune network* **21**, e20

104. Luo, Y., Jiang, N., Zhang, Y., Zhao, Y., Chen, F., Li, X., Qiang, M., Zeng, G., He, Q., Liu, X., and Shan, C. (2025) Chronic unpredictable mild stress induces anxiety-like behavior in female C57BL/6N mice, accompanied by alterations in inflammation and the kynurenine pathway of tryptophan metabolism. *Frontiers in neuroscience* **19**, 1556744

105. Clapp, M., Aurora, N., Herrera, L., Bhatia, M., Wilen, E., and Wakefield, S. (2017) Gut microbiota's effect on mental health: The gut-brain axis. *Clinics and practice* **7**, 987

106. Paudel, D., Uehara, O., Giri, S., Yoshida, K., Morikawa, T., Kitagawa, T., Matsuoka, H., Miura, H., Toyofuku, A., Kuramitsu, Y., Ohta, T., Kobayashi, M., and Abiko, Y. (2022) Effect of psychological stress on the oral-gut microbiota and the potential oral-gut-brain axis. *The Japanese dental science review* **58**, 365-375

107. Mostafavi Abdolmaleky, H., and Zhou, J. R. (2024) Gut Microbiota Dysbiosis, Oxidative Stress, Inflammation, and Epigenetic Alterations in Metabolic Diseases. *Antioxidants (Basel, Switzerland)* **13**

108. Li, N., Wang, Q., Wang, Y., Sun, A., Lin, Y., Jin, Y., and Li, X. (2019) Fecal microbiota transplantation from chronic unpredictable mild stress mice donors affects anxiety-like and depression-like behavior in recipient mice via the gut microbiota-inflammation-brain axis. *Stress (Amsterdam, Netherlands)* **22**, 592-602

109. He, H., He, H., Mo, L., Yuan, Q., Xiao, C., Ma, Q., Yi, S., Zhou, T., You, Z., and Zhang, J. (2024) Gut microbiota regulate stress resistance by influencing microglia-neuron interactions in the hippocampus. *Brain, behavior, & immunity - health* **36**, 100729

110. Zhou, P., Chen, C., Patil, S., and Dong, S. (2024) Unveiling the therapeutic symphony of probiotics, prebiotics, and postbiotics in gut-immune harmony. *Frontiers in nutrition* **11**, 1355542

111. Sittipo, P., Choi, J., Lee, S., and Lee, Y. K. (2022) The function of gut microbiota in immune-related neurological disorders: a review. *Journal of neuroinflammation* **19**, 154

112. Bravo, J. A., Forsythe, P., Chew, M. V., Escaravage, E., Savignac, H. M., Dinan, T. G., Bienenstock, J., and Cryan, J. F. (2011) Ingestion of Lactobacillus strain regulates emotional behavior and central GABA receptor expression in a mouse via the vagus nerve. *Proceedings of the National Academy of Sciences of the United States of America* **108**, 16050-16055

113. Park, H. J., Kim, S. A., Kang, W. S., and Kim, J. W. (2021) Early-Life Stress Modulates Gut Microbiota and Peripheral and Central Inflammation in a Sex-Dependent Manner. *International journal of molecular sciences* **22**

114. Ratsika, A., Codagnone, M. G., Bastiaanssen, T. F. S., Hoffmann Sarda, F. A., Lynch, C. M. K., Ventura-Silva, A. P., Rosell-Cardona, C., Caputi, V., Stanton, C., Fülling, C., Clarke, G., and Cryan, J. F. (2024) Maternal high-fat diet-induced microbiota changes are associated with alterations in embryonic brain metabolites and adolescent behaviour. *Brain, behavior, and immunity* **121**, 317-330

115. Wang, H., Braun, C., Murphy, E. F., and Enck, P. (2019) Bifidobacterium longum 1714™ Strain Modulates Brain Activity of Healthy Volunteers During Social Stress. *The American journal of gastroenterology* **114**, 1152-1162

116. Bidaki, R., Hekmati Moghaddam, S. H., and Sadeh, M. (2023) Gut Microbiota and Neuropsychiatric Disorders. *Basic and clinical neuroscience* **14**, 167-170

117. Sudo, N., Chida, Y., Aiba, Y., Sonoda, J., Oyama, N., Yu, X. N., Kubo, C., and Koga, Y. (2004) Postnatal microbial colonization programs the hypothalamic-pituitary-adrenal system for stress response in mice. *The Journal of physiology* **558**, 263-275

118. Levi, L. (1972) Stress and distress in response to psychosocial stimuli. Laboratory and real life studies on sympathoadrenomedullary and related reactions. *Acta medica Scandinavica. Supplementum* **528**, 1-166

119. Koo, M. W., Ogle, C. W., and Cho, C. H. (1985) The effect of cold-restraint stress on gastric emptying in rats. *Pharmacology, biochemistry, and behavior* **23**, 969-972

120. Taché, Y., Martinez, V., Million, M., Wang, L. J. A. J. o. P.-G., and Physiology, L. (2001) III. Stress-related alterations of gut motor function: role of brain corticotropin-releasing factor receptors. **280**, G173-G177

121. Tsukada, F., Sugawara, M., Kohno, H., and Ohkubo, Y. (2001) Evaluation of the effects of restraint and footshock stress on small intestinal motility by an improved method using a radionuclide, 51Cr, in the rat. *Biological & pharmaceutical bulletin* **24**, 488-490

122. Adriani, A., Ribaldone, D. G., Astegiano, M., Durazzo, M., Saracco, G. M., and Pellicano, R. (2018) Irritable bowel syndrome: the clinical approach. *Panminerva medica* **60**, 213-222

123. Fond, G., Loundou, A., Hamdani, N., Boukouaci, W., Dargel, A., Oliveira, J., Roger, M., Tamouza, R., Leboyer, M., and Boyer, L. (2014) Anxiety and depression comorbidities in irritable bowel syndrome (IBS): a systematic review and meta-analysis. *European archives of psychiatry and clinical neuroscience* **264**, 651-660

124. Mertz, H., Morgan, V., Tanner, G., Pickens, D., Price, R., Shyr, Y., and Kessler, R. (2000) Regional cerebral activation in irritable bowel syndrome and control subjects with painful and nonpainful rectal distention. *Gastroenterology* **118**, 842-848

125. Wang, L., Alammar, N., Singh, R., Nanavati, J., Song, Y., Chaudhary, R., and Mullin, G. E. (2020) Gut Microbial Dysbiosis in the Irritable Bowel Syndrome: A Systematic Review and Meta-Analysis of Case-Control Studies. *Journal of the Academy of Nutrition and Dietetics* **120**, 565-586

126. Bahlouli, W., Breton, J., Lelouard, M., L'Huillier, C., Tirelle, P., Salameh, E., Amamou, A., Atmani, K., Goichon, A., Bôle-Feysot, C., Ducrotté, P., Ribet, D., Déchelotte, P., and Coëffier, M. (2020) Stress-induced intestinal barrier dysfunction is exacerbated during diet-induced obesity. *The Journal of nutritional biochemistry* **81**, 108382

127. Longstreth, G. F., Thompson, W. G., Chey, W. D., Houghton, L. A., Mearin, F., and Spiller, R. C. J. G. (2006) Functional bowel disorders. **130**, 1480-1491

128. Gershon, M. D., and Tack, J. J. G. (2007) The serotonin signaling system: from basic understanding to drug development for functional GI disorders. **132**, 397-414

129. Lupu, V. V., Ghiciuc, C. M., Stefanescu, G., Mihai, C. M., Popp, A., Sasaran, M. O., Bozomitu, L., Starcea, I. M., Adam Raileanu, A., and Lupu, A. (2023) Emerging role of the gut microbiome in post-infectious irritable bowel syndrome: A literature review. *World journal of gastroenterology* **29**, 3241-3256

130. Nakao, M., Shirotsuki, K., and Sugaya, N. (2021) Cognitive-behavioral therapy for management of mental health and stress-related disorders: Recent advances in techniques and technologies. *BioPsychoSocial medicine* **15**, 16

131. Zhou, S. Y., Gillilland, M., 3rd, Wu, X., Leelasinjaroen, P., Zhang, G., Zhou, H., Ye, B., Lu, Y., and Owyang, C. (2018) FODMAP diet modulates visceral nociception by lipopolysaccharide-mediated intestinal inflammation and barrier dysfunction. *The Journal of clinical investigation* **128**, 267-280

132. Konturek, P. C., Brzozowski, T., and Konturek, S. J. J. J. P. P. (2011) Stress and the gut: pathophysiology, clinical consequences, diagnostic approach and treatment options. **62**, 591-599

133. McDowell C, F. U., Haseeb M. (2023) *Inflammatory Bowel Disease.*, Treasure Island (FL): StatPearls Publishing

134. Mawdsley, J. E., and Rampton, D. S. (2005) Psychological stress in IBD: new insights into pathogenic and therapeutic implications. *Gut* **54**, 1481-1491

135. Sun, Y., Li, L., Xie, R., Wang, B., Jiang, K., and Cao, H. (2019) Stress Triggers Flare of Inflammatory Bowel Disease in Children and Adults. *Frontiers in pediatrics* **7**, 432

136. Grondin, J. A., and Khan, W. I. (2024) Emerging Roles of Gut Serotonin in Regulation of Immune Response, Microbiota Composition and Intestinal Inflammation. *Journal of the Canadian Association of Gastroenterology* **7**, 88-96

137. Sultan, S., El-Mowafy, M., Elgaml, A., Ahmed, T. A. E., Hassan, H., and Mottawea, W. (2021) Metabolic Influences of Gut Microbiota Dysbiosis on Inflammatory Bowel Disease. *Frontiers in physiology* **12**, 715506

138. Yamazaki, K., and Kamada, N. J. M. i. (2024) Exploring the oral-gut linkage: Interrelationship between oral and systemic diseases. **17**, 147-153

139. Buey, B., Forcén, A., Grasa, L., Layunta, E., Mesonero, J. E., and Latorre, E. (2023) Gut Microbiota-Derived Short-Chain Fatty Acids: Novel Regulators of Intestinal Serotonin Transporter. *Life (Basel, Switzerland)* **13**

140. Nirwan, J. S., Hasan, S. S., Babar, Z. U., Conway, B. R., and Ghori, M. U. (2020) Global Prevalence and Risk Factors of Gastro-oesophageal Reflux Disease (GORD): Systematic Review with Meta-analysis. *Scientific reports* **10**, 5814

141. Wickramasinghe, N., Thuraisingham, A., Jayalath, A., Wickramasinghe, D., Samarasekera, D. N., Yazaki, E., and Devanarayana, N. M. J. P. G. P. H. (2024) Gastroesophageal reflux disease in Sri Lanka: An island-wide epidemiological survey assessing the prevalence and associated factors. **4**, e0003162

142. Lee, H. S., Noh, C. K., and Lee, K. J. (2017) The Effect of Acute Stress on Esophageal Motility and Gastroesophageal Reflux in Healthy Humans. *Journal of neurogastroenterology and motility* **23**, 72-79

143. Zhang, M., Hou, Z. K., Huang, Z. B., Chen, X. L., and Liu, F. B. (2021) Dietary and Lifestyle Factors Related to Gastroesophageal Reflux Disease: A Systematic Review. *Therapeutics and clinical risk management* **17**, 305-323

144. Cho, Y. K. (2017) Can Acute Stress Cause Esophageal Hypersensitivity in Healthy Individuals? *Journal of neurogastroenterology and motility* **23**, 483-484

145. Kessing, B. F., Bredenoord, A. J., Saleh, C. M., and Smout, A. J. (2015) Effects of anxiety and depression in patients with gastroesophageal reflux disease. *Clinical gastroenterology and hepatology : the official clinical practice journal of the American Gastroenterological Association* **13**, 1089-1095.e1081

146. Sesler, J. M. (2007) Stress-related mucosal disease in the intensive care unit: an update on prophylaxis. *AACN advanced critical care* **18**, 119-126; quiz 127-118

147. Kodadek, L. M., and Jones, C. J. S. C. C. T. A. C. O. P. A. (2018) Stress gastritis and stress ulcers: Prevention and treatment. 231-239

148. Quenot, J.-P., Dargent, A., Barkun, A., Bardou, M. J. A. C. C., and Medicine, P. (2019) Prophylaxis for stress related gastrointestinal bleeding in the ICU: Should we adjust to each patient's individual risk? , Elsevier

149. Chait, M. M., Turnbull, A. D., and Winawer, S. J. (1979) Risk factors and mortality in patients with cancer and hemorrhage from stress ulcer. *The American journal of gastroenterology* **72**, 227-233

150. Sostres, C., and Lanas, A. (2011) Epidemiology and demographics of upper gastrointestinal bleeding: prevalence, incidence, and mortality. *Gastrointestinal endoscopy clinics of North America* **21**, 567-581

151. Wang, X., Zhao, Q., Shi, H., Qi, F., Shi, N., Bai, D., Li, X., Yuan, H., and Zuo, X. (2020) Oxidative stress is important in the pathogenesis of stress-related mucosal disease. *Experimental and therapeutic medicine* **20**, 83

152. Elliott, S. N., and Wallace, J. L. (1998) Nitric oxide: a regulator of mucosal defense and injury. *Journal of gastroenterology* **33**, 792-803

153. Katz, A. M. J. T. A. J. o. C. (1985) Basic cellular mechanisms of action of the calcium-channel blockers. **55**, B2-B9

154. Hernandez, D. E., Adcock, J. W., Orlando, R. C., Patrick, K. S., Nemeroff, C. B., and Prange, A. J., Jr. (1984) Prevention of stress-induced gastric ulcers by dopamine agonists in the rat. *Life sciences* **35**, 2453-2458

155. Ahlawat, R., Hoilat, G. J., and Ross, A. B. (2018) Esophagogastroduodenoscopy.

156. Antunes, C., Tian, C., and Copelin II, E. L. (2024) Upper gastrointestinal bleeding. in *StatPearls [internet]*, StatPearls Publishing. pp

157. Ali Khan, M., and Howden, C. W. (2018) The Role of Proton Pump Inhibitors in the Management of Upper Gastrointestinal Disorders. *Gastroenterology & hepatology* **14**, 169-175

158. Sayuk, G. S., and Gyawali, C. P. J. D. (2020) Functional dyspepsia: diagnostic and therapeutic approaches. **80**, 1319-1336

159. Moshiree, B., Talley, N. J. J. N., and Motility. (2021) Functional dyspepsia: A critical appraisal of the European consensus from a global perspective. **33**, e14216

160. Huang, K. Y., Wang, F. Y., Lv, M., Ma, X. X., Tang, X. D., and Lv, L. (2023) Irritable bowel syndrome: Epidemiology, overlap disorders, pathophysiology and treatment. *World journal of gastroenterology* **29**, 4120-4135

161. Gwee, K. A., and Chua, A. S. (2006) Functional dyspepsia and irritable bowel syndrome, are they different entities and does it matter? *World journal of gastroenterology* **12**, 2708-2712

162. Drossman, D. A. (2014) 21 Biopsychosocial Issues in Gastroenterology.

163. Tack, J., Bisschops, R., and Sarnelli, G. J. G. (2004) Pathophysiology and treatment of functional dyspepsia. **127**, 1239-1255

164. Ford, A. C., Luthra, P., Tack, J., Boeckxstaens, G. E., Moayyedi, P., and Talley, N. J. (2017) Efficacy of psychotropic drugs in functional dyspepsia: systematic review and meta-analysis. *Gut* **66**, 411-420

165. Chu, A., and Wadhwa, R. (2023) Selective serotonin reuptake inhibitors. in *StatPearls [internet]*, StatPearls Publishing. pp

166. Drossman, D. A., Tack, J., Ford, A. C., Szigethy, E., Törnblom, H., and Van Oudenhove, L. J. G. (2018) Neuromodulators for functional gastrointestinal disorders (disorders of gut− brain interaction): a Rome foundation working team report. **154**, 1140-1171. e1141

167. Sohel, A. J., Shutter, M. C., Patel, P., and Molla, M. (2024) Fluoxetine. in *StatPearls [Internet]*, StatPearls Publishing. pp

168. Thiwan, S. I., and Drossman, D. A. (2006) Treatment of Functional GI Disorders With Psychotropic Medicines: A Review of Evidence With a Practical Approach. *Gastroenterology & hepatology* **2**, 678-688

169. Ladabaum, U., Sharabidze, A., Levin, T. R., Zhao, W. K., Chung, E., Bacchetti, P., Jin, C., Grimes, B., and Pepin, C. J. (2010) Citalopram provides little or no benefit in nondepressed patients with irritable bowel syndrome. *Clinical gastroenterology and hepatology : the official clinical practice journal of the American Gastroenterological Association* **8**, 42-48.e41

170. Sharbafchi, M. R., Afshar, H., Adhamian, P., Feizi, A., Daghaghzadeh, H., and Adibi, P. (2020) Effects of venlafaxine on gastrointestinal symptoms, depression, anxiety, stress, and quality of life in patients with the moderate-to-severe irritable bowel syndrome. *Journal of research in medical sciences : the official journal of Isfahan University of Medical Sciences* **25**, 115

171. Salehian, R., Mokhtare, M., Ghanbari Jolfaei, A., and Noorian, R. (2021) Investigation the Effectiveness of Duloxetine in Quality of Life and Symptoms of Patients with Irritable Bowel Syndrome. *Advanced biomedical research* **10**, 14

172. Moraczewski, J., Awosika, A. O., and Aedma, K. K. (2023) Tricyclic antidepressants. in *StatPearls [Internet]*, StatPearls Publishing. pp

173. Schiller, L. R., Santa Ana, C. A., Morawski, S. G., and Fordtran, J. S. J. G. (1985) Studies of the antidiarrheal action of clonidine: effects on motility and intestinal absorption. **89**, 982-988

174. Lobe, M. M., Verma, S., Patil, V. M., and Iyer, M. R. J. E. J. o. M. C. (2024) A review of kappa opioid receptor antagonists and their clinical trial landscape. 117205

175. Carbone, F., Vanuytsel, T., and Tack, J. (2017) The effect of mirtazapine on gastric accommodation, gastric sensitivity to distention, and nutrient tolerance in healthy subjects. *Neurogastroenterology and motility* **29**

176. Khalilian, A., Ahmadimoghaddam, D., Saki, S., Mohammadi, Y., and Mehrpooya, M. J. B. m. (2021) A randomized, double-blind, placebo-controlled study to assess efficacy of mirtazapine for the treatment of diarrhea predominant irritable bowel syndrome. **15**, 3

177. Karamanolis, G. P., Panopoulos, S., Denaxas, K., Karlaftis, A., Zorbala, A., Kamberoglou, D., Ladas, S. D., and Sfikakis, P. P. (2016) The 5-HT1A receptor agonist buspirone improves esophageal motor function and symptoms in systemic sclerosis: a 4-week, open-label trial. *Arthritis research & therapy* **18**, 195

178. Zhou, X., Fang, H., Xu, J., Chen, P., Hu, X., Chen, B., Wang, H., Hu, C., and Xu, Z. (2019) Stress ulcer prophylaxis with proton pump inhibitors or histamine 2 receptor antagonists in critically ill adults - a meta-analysis of randomized controlled trials with trial sequential analysis. *BMC gastroenterology* **19**, 193

179. Lockett, J., Inder, W. J., and Clifton, V. L. (2024) The Glucocorticoid Receptor: Isoforms, Functions, and Contribution to Glucocorticoid Sensitivity. *Endocrine reviews* **45**, 593-624

180. Taché, Y., Kiank, C., and Stengel, A. (2009) A role for corticotropin-releasing factor in functional gastrointestinal disorders. *Current gastroenterology reports* **11**, 270-277

181. Hovelsø, N., Sotty, F., Montezinho, L. P., Pinheiro, P. S., Herrik, K. F., and Mørk, A. (2012) Therapeutic potential of metabotropic glutamate receptor modulators. *Current neuropharmacology* **10**, 12-48

182. Garakani, A., Murrough, J. W., Freire, R. C., Thom, R. P., Larkin, K., Buono, F. D., and Iosifescu, D. V. (2020) Pharmacotherapy of Anxiety Disorders: Current and Emerging Treatment Options. *Frontiers in psychiatry* **11**, 595584

183. Pisegna, J. R. (2002) Pharmacology of acid suppression in the hospital setting: focus on proton pump inhibition. *Critical care medicine* **30**, S356-361

184. Spirt, M. J., and Stanley, S. (2006) Update on stress ulcer prophylaxis in critically ill patients. *Critical care nurse* **26**, 18-20, 22-18; quiz 29

185. Moradi Moghaddam, O. (2011) Probiotics in critically ill patients. *Anesthesiology and pain medicine* **1**, 58-60

186. Kechagia, M., Basoulis, D., Konstantopoulou, S., Dimitriadi, D., Gyftopoulou, K., Skarmoutsou, N., and Fakiri, E. M. (2013) Health benefits of probiotics: a review. *ISRN nutrition* **2013**, 481651

187. Williams, N. T. (2010) Probiotics. *American journal of health-system pharmacy : AJHP : official journal of the American Society of Health-System Pharmacists* **67**, 449-458

188. Latif, A., Shehzad, A., Niazi, S., Zahid, A., Ashraf, W., Iqbal, M. W., Rehman, A., Riaz, T., Aadil, R. M., Khan, I. M., Özogul, F., Rocha, J. M., Esatbeyoglu, T., and Korma, S. A. (2023) Probiotics: mechanism of action, health benefits and their application in food industries. *Frontiers in microbiology* **14**, 1216674

189. Davani-Davari, D., Negahdaripour, M., Karimzadeh, I., Seifan, M., Mohkam, M., Masoumi, S. J., Berenjian, A., and Ghasemi, Y. (2019) Prebiotics: Definition, Types, Sources, Mechanisms, and Clinical Applications. *Foods (Basel, Switzerland)* **8**

190. Hanum, A. R. N., Illahika, A. P., Santoso, A. A., and Putra, P. Y. P. J. I. J. o. P. H. (2024) Irritable bowel syndrome following infectious COVID-19: East Java, Indonesia, 2023. **13**, 804-809

191. Distrutti, E., Monaldi, L., Ricci, P., and Fiorucci, S. (2016) Gut microbiota role in irritable bowel syndrome: New therapeutic strategies. *World journal of gastroenterology* **22**, 2219-2241

192. Lew, L.-C., Hor, Y.-Y., Yusoff, N. A. A., Choi, S.-B., Yusoff, M. S., Roslan, N. S., Ahmad, A., Mohammad, J. A., Abdullah, M. F. I., and Zakaria, N. J. C. N. (2019) Probiotic Lactobacillus plantarum P8 alleviated stress and anxiety while enhancing memory and cognition in stressed adults: A randomised, double-blind, placebo-controlled study. **38**, 2053-2064

193. Wong, C. B., Odamaki, T., and Xiao, J.-z. J. J. o. F. F. (2019) Beneficial effects of Bifidobacterium longum subsp. longum BB536 on human health: Modulation of gut microbiome as the principal action. **54**, 506-519

194. Martín, R., Rios-Covian, D., Huillet, E., Auger, S., Khazaal, S., Bermúdez-Humarán, L. G., Sokol, H., Chatel, J. M., and Langella, P. (2023) Faecalibacterium: a bacterial genus with promising human health applications. *FEMS microbiology reviews* **47**

195. Larabi, A. B., Masson, H. L. P., and Bäumler, A. J. (2023) Bile acids as modulators of gut microbiota composition and function. *Gut microbes* **15**, 2172671

196. Swer, N. M., Venkidesh, B. S., Murali, T. S., and Mumbrekar, K. D. (2023) Gut microbiota-derived metabolites and their importance in neurological disorders. *Molecular biology reports* **50**, 1663-1675

197. Sugaya, N., Shirotsuki, K., and Nakao, M. J. B. M. (2021) Cognitive behavioral treatment for irritable bowel syndrome: a recent literature review. **15**, 23

198. Hofmann, S. G., and Gómez, A. F. (2017) Mindfulness-Based Interventions for Anxiety and Depression. *The Psychiatric clinics of North America* **40**, 739-749

199. Francis, S. E., Shawyer, F., Cayoun, B. A., Grabovac, A., and Meadows, G. J. F. i. p. (2024) Differentiating mindfulness-integrated cognitive behavior therapy and mindfulness-based cognitive therapy clinically: the why, how, and what of evidence-based practice. **15**, 1342592

200. Andersson, G., Cuijpers, P., Carlbring, P., Riper, H., and Hedman, E. (2014) Guided Internet-based vs. face-to-face cognitive behavior therapy for psychiatric and somatic disorders: a systematic review and meta-analysis. *World psychiatry : official journal of the World Psychiatric Association (WPA)* **13**, 288-295

201. Hedman-Lagerlöf, E., Carlbring, P., Svärdman, F., Riper, H., Cuijpers, P., and Andersson, G. (2023) Therapist-supported Internet-based cognitive behaviour therapy yields similar effects as face-to-face therapy for psychiatric and somatic disorders: an updated systematic review and meta-analysis. *World psychiatry : official journal of the World Psychiatric Association (WPA)* **22**, 305-314

202. Norelli, S. K., Long, A., and Krepps, J. M. (2018) Relaxation techniques.

203. Theis, B. F., Park, J. S., Kim, J. S. A., Zeydabadinejad, S., Vijay-Kumar, M., Yeoh, B. S., and Saha, P. (2025) Gut Feelings: How Microbes, Diet, and Host Immunity Shape Disease. *Biomedicines* **13**

204. Holscher, H. D. (2017) Dietary fiber and prebiotics and the gastrointestinal microbiota. *Gut microbes* **8**, 172-184

205. Zhang, F., Fan, D., Huang, J.-l., and Zuo, T. J. M. i. M. (2022) The gut microbiome: Linking dietary fiber to inflammatory diseases. **14**, 100070

206. Rohr, M. W., Narasimhulu, C. A., Rudeski-Rohr, T. A., and Parthasarathy, S. J. A. i. N. (2020) Negative effects of a high-fat diet on intestinal permeability: a review. **11**, 77-91

207. Sahle, Z., Engidaye, G., Shenkute Gebreyes, D., Adenew, B., and Abebe, T. A. (2024) Fecal microbiota transplantation and next-generation therapies: A review on targeting dysbiosis in metabolic disorders and beyond. *SAGE open medicine* **12**, 20503121241257486

208. Halkjær, S. I., Christensen, A. H., Lo, B. Z. S., Browne, P. D., Günther, S., Hansen, L. H., and Petersen, A. M. (2018) Faecal microbiota transplantation alters gut microbiota in patients with irritable bowel syndrome: results from a randomised, double-blind placebo-controlled study. *Gut* **67**, 2107-2115

209. Rohlke, F., and Stollman, N. (2012) Fecal microbiota transplantation in relapsing Clostridium difficile infection. *Therapeutic advances in gastroenterology* **5**, 403-420

210. Xu, M. Q., Cao, H. L., Wang, W. Q., Wang, S., Cao, X. C., Yan, F., and Wang, B. M. (2015) Fecal microbiota transplantation broadening its application beyond intestinal disorders. *World journal of gastroenterology* **21**, 102-111

211. Fanizzi, F., D'Amico, F., Zanotelli Bombassaro, I., Zilli, A., Furfaro, F., Parigi, T. L., Cicerone, C., Fiorino, G., Peyrin-Biroulet, L., Danese, S., and Allocca, M. (2024) The Role of Fecal Microbiota Transplantation in IBD. *Microorganisms* **12**

212. Hitch, T. C. A., Hall, L. J., Walsh, S. K., Leventhal, G. E., Slack, E., de Wouters, T., Walter, J., and Clavel, T. (2022) Microbiome-based interventions to modulate gut ecology and the immune system. *Mucosal immunology* **15**, 1095-1113

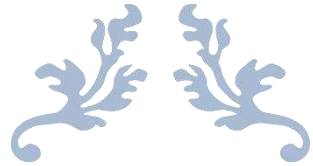

REVIEW CHAPTER 2

Role of Mitochondria in Gut Physiology and Pathology

1. INTRODUCTION

Mitochondria are indispensable organelles in eukaryotic cells, mainly involved in the production of adenosine triphosphate (ATP) through oxidative phosphorylation (OXPHOS)(1). Beyond energy production, they serve as metabolic hubs that coordinate diverse cellular functions, including calcium buffering, apoptotic signalling, redox homeostasis, and biosynthesis of amino acids, lipids, and iron–sulfur (Fe–S) clusters(2). Mitochondria possess their own genome, mitochondrial DNA (mtDNA), a circular double-stranded molecule that encodes 13 critical components of the electron transport chain (ETC) complexes I, III, IV, and V, along with 22 tRNAs and two rRNAs critical for mitochondrial translation(3). However, most mitochondrial proteins are encoded by nuclear DNA and imported into the mitochondria post-translationally, necessitating tightly regulated communication between the nuclear and mitochondrial genomes(4). These organelles are inherently dynamic, undergoing continuous fusion and fission events that adapt mitochondrial morphology in response to cellular metabolic demands and stress stimuli(5,6). Through the concerted activity of ETC complexes I–IV, mitochondria facilitate electron transfer to molecular oxygen, creating a proton gradient across the inner membrane that drives ATP synthesis via complex V (ATP synthase)(7). In parallel, they regulate reactive oxygen species (ROS) generation, autophagic signalling, and innate immune responses, positioning mitochondria as sentinels of cellular integrity(8). Notably, mitochondrial dysfunction is increasingly recognized as an initiating event rather than a consequence—in the etiology of numerous human diseases, including metabolic syndromes, neurodegenerative disorders, and cancer(9). Mitochondrial oxidative stress (MOS), driven by excess ROS and redox imbalance, can disrupt membrane potential, compromise ATP generation, and activate cell death pathways. Moreover, damaged mitochondria release mitochondrial damage-associated molecular patterns (mtDAMPs), including oxidized mitochondrial DNA (mtDNA), cardiolipin, and N-formyl peptides, which are potent activators of inflammasomes and sterile inflammation mechanisms now implicated in gastrointestinal (GI) disorders, such as inflammatory bowel disease (IBD) and peptic ulcer disease(10). Recent studies have illuminated a complex and reciprocal relationship between mitochondrial function and gut homeostasis, extending beyond microbiota composition to include host epithelial integrity and immune surveillance(11). While microbial metabolites such as short-chain fatty acids (SCFAs) are known to influence colonocyte energy supply and mitochondrial gene regulation, current research emphasizes minimizing overreliance on microbial signals to understand intrinsic mitochondrial responses (12). Endogenous mitochondrial signalling via ROS, mtDNA, and metabolic intermediates plays a fundamental role in maintaining epithelial barrier function and modulating mucosal immune responses(13,14). Under pathological conditions, such as dysbiosis or psychological stress, mitochondrial dysfunction manifests as impaired OXPHOS, disrupted dynamics, and compromised redox homeostasis, contributing to gut inflammation and barrier breakdown(15). Additionally, mitochondrial defects influence systemic metabolic balance and immune tolerance, linking local epithelial dysfunction with extraintestinal pathologies. The loss of mitochondrial integrity in the gut epithelium leads to defective mitophagy, excessive ROS production, and activation of pro-inflammatory cascades, hallmarks of diseases such as IBD, irritable bowel syndrome (IBS), and NSAID-induced gastropathy(16-18). While the gut microbiota remains a significant factor in host health, the emerging paradigm underscores mitochondria as both targets and regulators of gut pathophysiology, independent of microbial cues. Thus, elucidating mitochondrial pathways in GI disease offers promising avenues for therapeutic intervention aimed at restoring energy balance, maintaining epithelial homeostasis, and attenuating inflammation.

2. MITOCHONDRIAL FUNCTION AND GUT HEALTH

Mitochondria are central to the maintenance of gastrointestinal (GI) health, especially in intestinal epithelial cells (IECs), which depend on precise mitochondrial control for energy production, redox signalling, organelle dynamics, and regulated cell death(19). This section explores the key mitochondrial processes influencing gut homeostasis and how their dysregulation contributes to gastrointestinal pathologies.

2.1. Mitochondrial bioenergetics and reactive oxygen species (ROS) generation

Mitochondria are central to cellular metabolism, functioning as crucial bioenergetic centres involved in the synthesis of adenosine triphosphate (ATP) through oxidative phosphorylation (OXPHOS)(1). This process involves the oxidation of reduced cofactors nicotinamide adenine dinucleotide (NADH) and flavin adenine dinucleotide ($FADH_2$) derived from core metabolic pathways, including glycolysis, fatty acid β-oxidation, and amino acid catabolism(20). These metabolic routes converge on acetyl-CoA, a pivotal intermediary that enters the tricarboxylic acid (TCA) cycle, where successive oxidative decarboxylation steps yield NADH and $FADH_2$, which subsequently fuel the electron transport chain (ETC). The ETC, composed of five multi-subunit protein complexes (Complexes I–V), facilitates stepwise electron transfer from NADH and $FADH_2$ to molecular oxygen. This electron movement is coupled with proton translocation from the mitochondrial matrix to the intermembrane space, establishing an electrochemical gradient. The return flow of protons through ATP synthase (Complex V) harnesses this gradient to drive the phosphorylation of ADP into ATP, a process foundational to mitochondrial energy output, as described in Fig.1 (21,22).

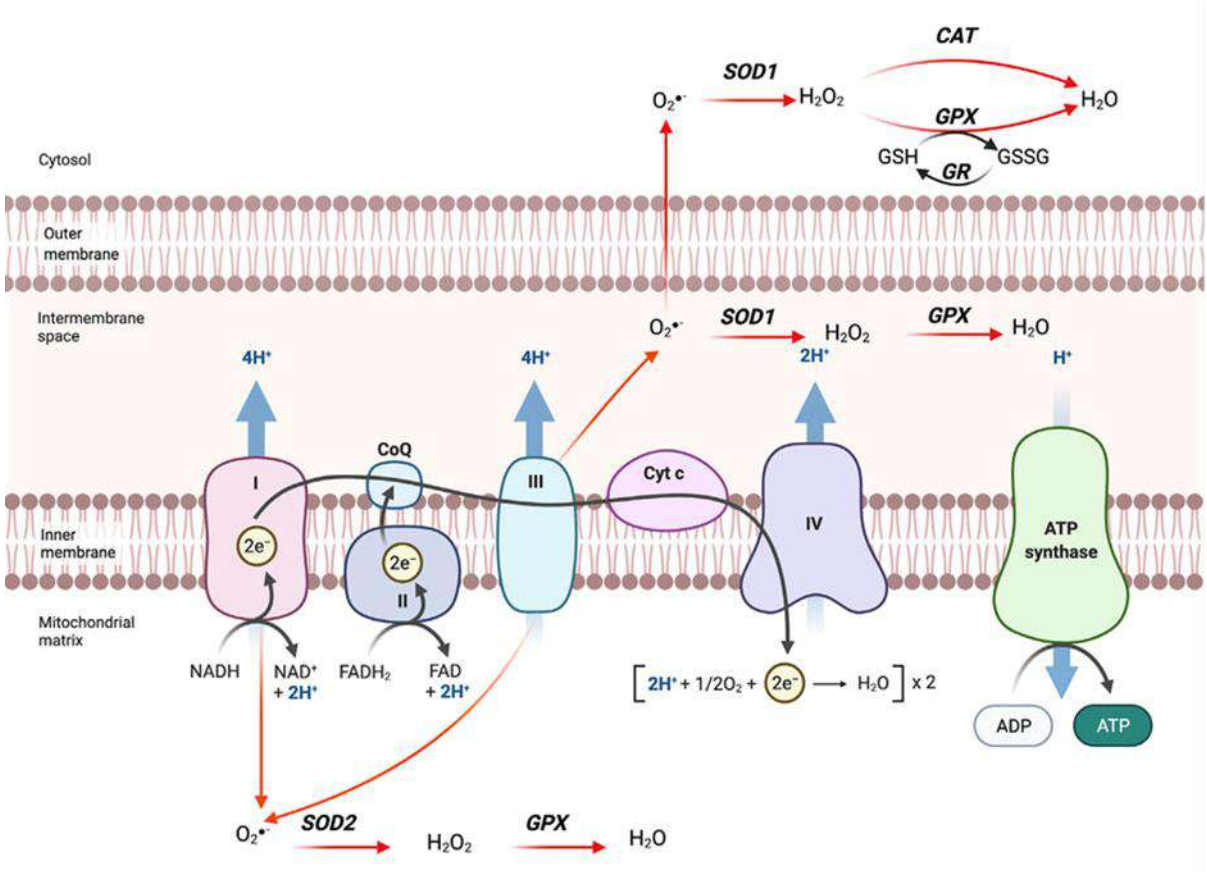

Fig. 1. Electron Transport Chain (ETC) and Reactive Oxygen Species (ROS) Production: The ETC comprises five key enzyme complexes: Complex I (NADH dehydrogenase), Complex II (succinate dehydrogenase), Complex III (ubiquinol-cytochrome c oxidoreductase), Complex IV (cytochrome c oxidase), and Complex V (ATP synthase). NADH and $FADH_2$ donate two electrons each to Complexes I and II, respectively, initiating the electron transfer cascade. These electrons are relayed through iron-sulfur clusters to the lipid-soluble coenzyme Q (CoQ), which then transfers them to Complex III. From there, electrons move to cytochrome c (Cyt c), which delivers them to Complex IV, where the reduction of molecular oxygen (O_2) to water (H_2O) occurs. With the exception of Complex II, each ETC complex uses the energy from electron flow to pump protons from the mitochondrial matrix into the intermembrane space (IMS), creating an electrochemical gradient. This proton gradient powers ATP synthase (Complex V), which converts ADP and inorganic phosphate into ATP through rotational catalysis. However, during this process, electrons can escape from Complexes I and III, reacting with oxygen to form superoxide anions ($O_2^{\bullet -}$). These ROS are subsequently detoxified to hydrogen peroxide (H_2O_2) and water (H_2O) by various antioxidant enzymes, including superoxide dismutase 1 and 2 (SOD1/2), glutathione peroxidase (GPX), catalase (CAT), and glutathione reductase (GR), operating in the mitochondrial matrix, inner membrane, and cytosol. Reduced (GSH) and oxidized (GSSG) glutathione also play critical roles in maintaining redox balance. This figure is adapted from Guerbette *et. al.* (22)

Despite its efficiency, OXPHOS is an inherent source of reactive oxygen species (ROS), predominantly superoxide anions ($O_2^{\bullet -}$), which arise from electron leakage at Complexes I and III. These radicals are further metabolized into downstream species such as hydrogen peroxide (H_2O_2) and hydroxyl radicals(23). In addition to ETC-derived ROS, other mitochondrial enzymes, including pyruvate and α-ketoglutarate dehydrogenases, can generate ROS through flavin-mediated electron transfers(24). Mitochondrial β-oxidation also contributes to ROS production, both indirectly by exacerbating electron leak within the ETC and directly via ROS-generating enzymes like long-chain acyl-CoA dehydrogenase(25).

To counterbalance ROS accumulation and maintain redox homeostasis, cells employ a sophisticated network of antioxidant enzymes, such as superoxide dismutase (SODs), catalase, and glutathione peroxidases-alongside non-enzymatic dietary antioxidants (e.g., vitamins C and E, selenium, zinc)(23,26). However, excessive ROS generation can overwhelm these defences, resulting in oxidative damage to lipids, proteins, nuclear DNA, and particularly mitochondrial DNA (mtDNA), which lacks protective histones and is thus highly susceptible to oxidative lesions(27). Common consequences include strand breaks and base modifications, such as thymine glycol formation(28). ROS-induced injury also compromises TCA cycle enzyme functionality, rendering mitochondria a principal target of oxidative stress and a key node in the regulation of cell fate via apoptosis and ferroptosis(29,30). Importantly, ROS is not solely detrimental. At physiological concentrations, mitochondrial ROS (mtROS) act as signalling molecules participating in the regulation of numerous cellular functions, such as proliferation, differentiation, and immune response modulation(31). They participate in redox-sensitive signalling cascades, notably influencing mitogen-activated protein kinase (MAPK) activity and other intracellular pathways critical for tissue homeostasis. In the intestinal epithelium, a tissue characterized by rapid renewal and high metabolic demand, mitochondria play a particularly crucial role. Intestinal epithelial cells (IECs) depend on mitochondrial ATP to sustain epithelial barrier integrity, facilitate cell turnover, and coordinate immune responses. Metabolic specialization is evident along the crypt–villus axis: proliferative stem cells in the crypts predominantly rely on glycolysis, while differentiated cells in the villi utilize mitochondrial respiration to meet their energy requirements(32). Moreover, mtROS serve essential signalling roles in intestinal homeostasis, governing epithelial regeneration and immune responses(33). Disruption of this finely balanced bioenergetic and redox network contributes to epithelial dysfunction and underpins various gastrointestinal pathologies, including inflammatory bowel disease.

2.2. Mitochondrial functions in intestinal epithelial cells

The intestinal epithelium is a highly dynamic tissue that undergoes constant renewal every 4–5 days, driven by a coordinated interplay of proliferation, differentiation, and cell shedding. In the small intestine, this renewal is organized along the crypt–villus axis, where stem cells residing at the crypt base generate progenitors that proliferate and migrate upward, progressively differentiating into functionally specialized epithelial cell types. These include absorptive enterocytes and colonocytes, as well as secretory lineages such as goblet and enteroendocrine cells(34). At the villus tips or colonic surface, senescent cells detach and are eliminated through anoikis, preserving tissue integrity(35). Paneth cells, essential for maintaining the stem cell niche and microbial defence, remain localized in the small intestinal crypts, while in the colon, $Reg4^+$ cells fulfil a similar supportive role(35). Given the intestinal epithelium's exposure to dietary antigens, microbial metabolites, and pathogens, continuous self-renewal is vital for maintaining barrier function. This regenerative process imposes substantial metabolic demands, largely met by mitochondria, which serve as central regulators of epithelial energy homeostasis(36). Metabolic zonation along the crypt–villus axis underlies functional specialization. As cells transition from proliferative to differentiated states during upward migration, they undergo a metabolic shift that reflects their changing roles and environmental cues. Stem cells and Paneth cells exhibit high glycolytic activity, while $Lgr5^+$ intestinal stem cells (ISCs) rely on both glycolysis and oxidative phosphorylation (OXPHOS), suggesting metabolic flexibility at the crypt base, as shown in Fig.2 (35,37).

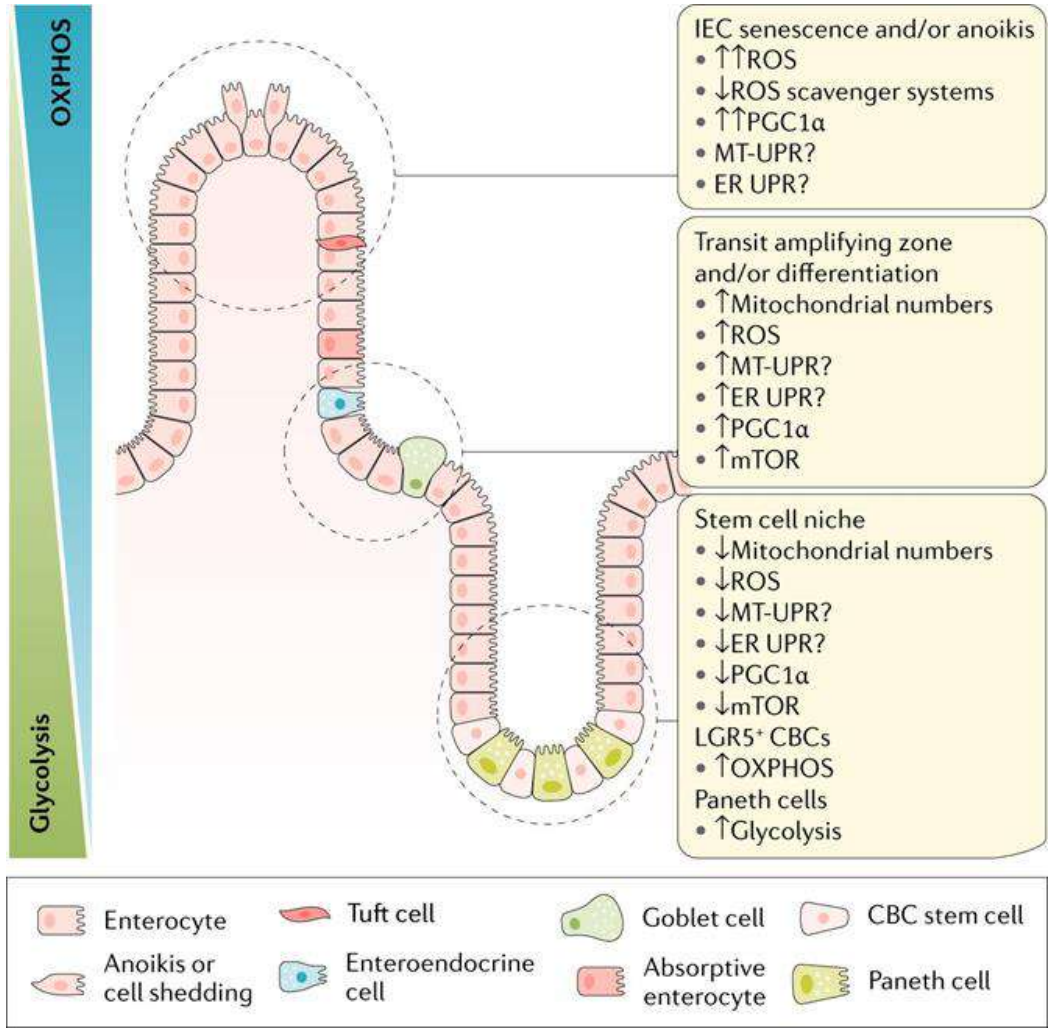

Fig. 2. Metabolic and mitochondrial regulation across the intestinal crypt-villus axis. The crypt-villus axis exhibits a metabolic gradient, with stem cell niches (e.g., LGR5+ CBCs) favouring glycolysis, while differentiated enterocytes increasingly rely on OXPHOS. This shift correlates with elevated mitochondrial content, PGC1α-driven biogenesis, and ROS modulation, which governs IEC fate, including apoptosis in senescent villus cells. PGC1α, mTOR, and UPR pathways (MT/ER-UPR) orchestrate metabolic adaptations during differentiation, with mTOR integrating nutrient signals to regulate mitochondrial biogenesis. Notably, LGR5+ CBCs retain OXPHOS dependence, potentially fuelled by lactate from glycolytic Paneth cells, highlighting niche-specific metabolic interplay. ROS scavenger declines and UPR activation further fine-tune IEC transitions and anoikis susceptibility. This figure is adapted from Rath *et. al.* (37)

In contrast, differentiated enterocytes and colonocytes located at the villus tips or the upper crypt express elevated levels of OXPHOS components and demonstrate increased mitochondrial respiration to sustain their physiological functions(36). This spatial metabolic gradient is mirrored by the distribution and morphology of mitochondria. Studies in rat intestines have shown that villus IECs contain a significantly greater number of mitochondria compared to crypt cells, with larger mitochondrial size indicative of elevated bioenergetic demand(38). Intestinal organoids further support this correlation, demonstrating that IEC differentiation is accompanied by increased mitochondrial biogenesis. The metabolic plasticity of IECs is not only governed by nutrient availability and differentiation signals but also by mitochondrial regulators such as PGC1α and PGC1β. These co-activators orchestrate mitochondrial biogenesis and oxidative metabolism, with PGC1α preferentially expressed in differentiated cells at the epithelial surface and sparsely distributed in proliferative crypt zones(39). Elevated PGC1α levels enhance mitochondrial content and respiratory capacity, as evidenced by increased cytochrome c oxidase activity(40,41). This mitochondrial amplification supports terminal differentiation and is implicated in villus formation during late gestation, where the transition from glycolysis to aerobic respiration is essential for epithelial elongation.

Guanylyl cyclase C (GC-C), a receptor selectively expressed at the apical membrane of enterocytes, has emerged as a key modulator of mitochondrial biogenesis along the crypt–villus axis(42). Mice deficient in GC-C display reduced expression of mitochondrial markers, such as COX protein and mtDNA, coupled with enhanced glycolytic metabolism, underscoring the role of GC-C in epithelial metabolic reprogramming and homeostasis(43). The transcriptional repressor YY1 also contributes to this regulation, promoting genes linked to mitochondrial structure and function, and acting downstream of both mTOR and PGC1α signalling pathways(44). Loss of YY1 leads to impaired villus development and reduced PGC1α expression, further highlighting the interdependence of these regulatory networks(45).

Redox signalling, mediated by mitochondrial ROS, adds another layer of complexity to IEC fate decisions. Mitochondria-derived ROS, primarily superoxide and hydrogen peroxide, play dual roles as signalling molecules facilitating differentiation, and as cytotoxic agents that induce apoptosis when produced in excess. The MAP kinase p38, activated by ROS, is critical for crypt formation and differentiation, particularly during organoid development(46). Disruption of OXPHOS, whether through ETC inhibition or antioxidant treatment, impairs crypt architecture, emphasizing the necessity of redox balance in maintaining epithelial structure and function. Apical enterocytes, which undergo programmed cell death during epithelial turnover, exhibit elevated mitochondrial ROS production. Concomitant low expression of antioxidant defences such as catalase (CAT) and SOD2 may predispose these cells to oxidative stress-induced apoptosis(47). Notably, upregulation of antioxidant systems through PGC1β overexpression reduces ROS accumulation and apoptosis, resulting in epithelial elongation and altered intestinal morphology(48,49). Thus, mitochondrial control of ROS levels is pivotal not only for protecting cellular components from oxidative damage but also for regulating epithelial homeostasis and turnover.

2.3. Mitochondrial-mediated apoptosis and epithelial turnover

Apoptosis, or programmed cell death, is vital for maintaining intestinal epithelial turnover and tissue homeostasis. IECs are continuously renewed; proliferating in the crypts, differentiating during migration up the villi, and eventually undergoing apoptosis at the villus tips(50). This process ensures the removal of aged or damaged cells while maintaining barrier integrity. Mitochondria orchestrate apoptosis via the intrinsic pathway, which is activated in response to metabolic stress, oxidative damage, or cellular injury. Mitochondria-mediated apoptosis begins when stress signals disrupt the permeability of the outer mitochondrial membrane, triggering the release of cytochrome c, activation of caspase-9, and subsequent initiation of the apoptotic pathway(51). ROS act as key regulators of this process, especially when present in excess. Elevated levels of mtROS compromise the integrity of the mitochondrial membrane and facilitate the opening of the mitochondrial permeability transition pore, thereby enhancing apoptotic signalling(52). In IBD, mitochondrial apoptosis becomes dysregulated. Studies have documented increased ROS production and epithelial apoptosis, resulting in loss of barrier integrity, enhanced permeability, and activation of immune responses(53). Excessive epithelial cell death exacerbates inflammation, while insufficient apoptosis can lead to the accumulation of dysfunctional cells, promoting chronic damage and possibly increasing the risk of neoplasia. Mitochondrial dysfunction, by influencing both pro-survival and pro-death signals, is therefore a key determinant of epithelial fate(54). From a therapeutic perspective, strategies aimed at modulating mitochondrial apoptosis, whether by reducing ROS, restoring mitochondrial dynamics, or stabilizing mitochondrial membranes, hold promise in treating gut disorders characterized by epithelial loss and inflammation. By maintaining controlled apoptotic turnover, these interventions may help preserve gut homeostasis and reduce disease severity.

3. MITOCHONDRIAL QUALITY CONTROL IN GUT HOMEOSTASIS

The gastrointestinal (GI) epithelium is one of the most metabolically active tissues in the body, relying heavily on functional mitochondria for energy production, redox balance, and cellular turnover. To maintain this mitochondrial functionality under constant environmental and metabolic stress, intestinal epithelial cells (IECs) depend on an elaborate mitochondrial quality control (MQC) system. MQC encompasses a spectrum of coordinated processes, including biogenesis, redox buffering, mitophagy, and organelle dynamics (fusion and fission). Disruption of these pathways has been implicated in the pathogenesis of intestinal disorders such as inflammatory bowel disease (IBD) and NSAID-induced enteropathy, where impaired mitochondrial clearance and accumulation of damaged organelles contribute to barrier breakdown and chronic inflammation(17,55).

3.1. Mitochondrial biogenesis and the role of PGC-1α in gut health

Mitochondrial biogenesis is a dynamic and highly coordinated process that ensures the renewal and expansion of functional mitochondria to meet cellular energy demands, especially in metabolically active tissues such as the gastrointestinal (GI) epithelium(22). This process entails the replication of mitochondrial DNA (mtDNA), the transcription of both nuclear- and mitochondria-encoded genes, and the assembly of respiratory chain components and structural proteins essential for mitochondrial morphology and function(56). At the centre of this regulatory network is peroxisome proliferator-activated receptor gamma coactivator-1 alpha (PGC-1α), a transcriptional coactivator that orchestrates the expression of genes involved in mitochondrial metabolism, oxidative phosphorylation (OXPHOS), and antioxidant defence. PGC-1α coactivates nuclear respiratory factors NRF1 and NRF2, which regulate the expression of mitochondrial transcription factor A (TFAM), mitochondrial transcription

factor B1/B2 (TFB1M/TFB2M), and various components of the electron transport chain(40,57). These transcription factors are essential for mtDNA replication, mitochondrial gene transcription, and the assembly of OXPHOS complexes. In the intestinal epithelium, PGC-1α plays a vital role in maintaining cellular energy metabolism and epithelial barrier integrity. Its expression is particularly enriched in differentiated villus cells, which rely predominantly on mitochondrial respiration to support energy-intensive processes such as nutrient absorption and tight junction maintenance. Experimental studies have demonstrated that downregulation of PGC-1α, as observed in patients with ulcerative colitis and animal models of colitis, is associated with decreased mitochondrial density, impaired epithelial regeneration, and increased disease severity(58). Conditional deletion of PGC-1α in intestinal epithelial cells renders mice more susceptible to dextran sulphate sodium (DSS)-induced colitis, underscoring its essential role in mucosal defence and metabolic adaptation during inflammatory stress(58). PGC-1α exerts its effects through interaction with various transcriptional regulators. It coactivates estrogen-related receptors (ERRs), particularly ERRα and ERRγ, which control the transcription of genes involved in fatty acid oxidation (FAO), the tricarboxylic acid (TCA) cycle, and mitochondrial respiratory function(59). ERRα also facilitates the induction of intracellular fatty acid transporters and mitochondrial FAO enzymes, enhancing mitochondrial oxidative capacity(60). In contrast, ERRγ has been implicated in regulating ion transport and mitochondrial membrane potential, although its specific roles in gut physiology remain underexplored. The expression and activity of PGC-1α are modulated by several upstream signalling pathways. AMP-activated protein kinase (AMPK), a key energy sensor, phosphorylates and activates PGC-1α in response to cellular energy depletion, thereby promoting mitochondrial biogenesis through the NRF1/2–TFAM axis, shown in Fig.3 (61,62).

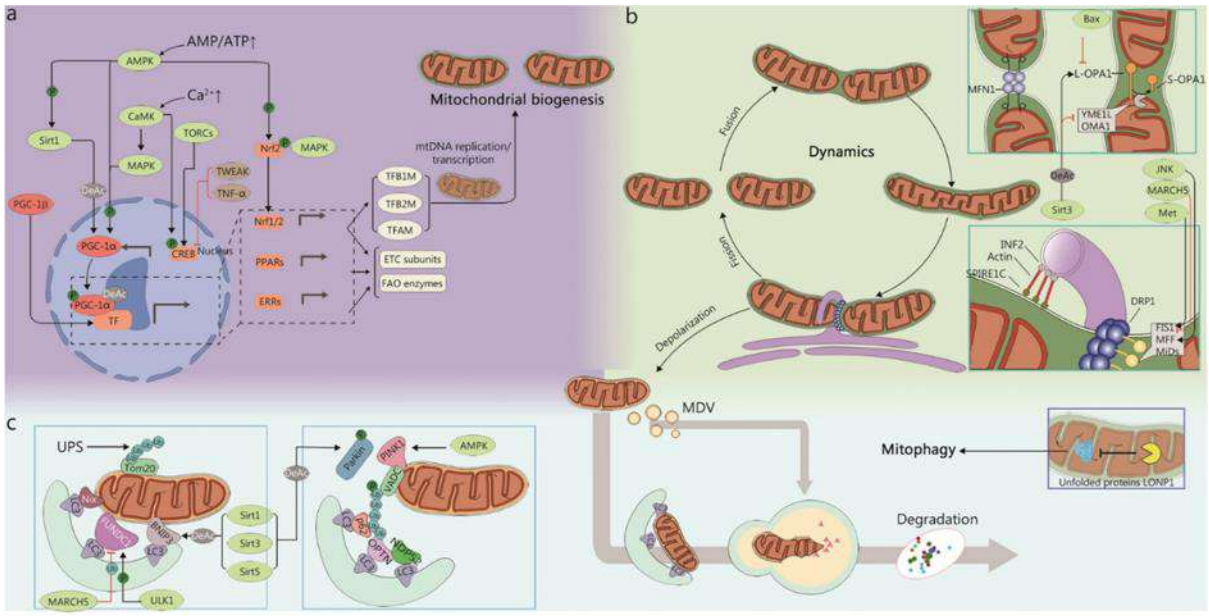

Fig. 3. Molecular regulation of mitochondrial quality control. (a) PGC-1α is central to mitochondrial biogenesis, regulated by AMPK, SIRT1, and Ca^{2+}, with PGC-1β also contributing. (b) Mitochondrial dynamics involve fission (mediated by DRP1, FIS1, and MFF) and fusion (MFNs for outer membrane, OPA1 for inner membrane), both under complex regulation. (c) Mitophagy clears damaged mitochondria via PINK1/Parkin-dependent and -independent pathways, involving autophagosome formation and signal regulation, while mitochondrial protein quality control degrades misfolded proteins, promoting mitophagy when unfolded proteins accumulate. This figure is adapted from Liu *et. al.* (62)

AMPK can also indirectly activate PGC-1α via upstream kinases such as calcium/calmodulin-dependent protein kinase (CaMK), which responds to calcium fluxes and activates transcriptional programs linked to mitochondrial metabolism through CREB and p38 MAPK signalling(63).Sirtuin 1 (SIRT1), a NAD^+-dependent deacetylase, also activates PGC-1α by removing inhibitory acetyl groups, thereby enhancing its transcriptional activity and stabilizing mitochondrial function, especially during fasting or caloric restriction(63). Other modulators of PGC-1α include TORC family coactivators, which amplify CREB-dependent transcription of the PGC-1α gene(64), and post-translational modifications such as histone crotonylation, which has been recently linked to enhanced PGC-1α expression and mitochondrial biogenesis, particularly in models of tissue injury(65). Conversely, inflammatory mediators such as TNF-α and TWEAK can inhibit PGC-1α transcription by activating NF-κB, thus suppressing mitochondrial biogenesis and exacerbating epithelial damage in chronic inflammatory conditions(66). While PGC-1β, a homolog of PGC-1α, also contributes to mitochondrial biogenesis by coactivating NRF1 and ERRs, its expression pattern and inducibility differ. PGC-1β is constitutively expressed in certain tissues and supports basal mitochondrial turnover, especially during cell proliferation and differentiation, such as in M2 macrophages and osteoclasts(67,68). However, unlike PGC-1α, its expression is not significantly upregulated in response to acute metabolic stressors such as exercise or cold exposure, suggesting complementary but non-redundant roles in mitochondrial maintenance. In the context of gastrointestinal health, the PGC-1α axis emerges as a central regulator of epithelial energy metabolism, redox homeostasis, and regenerative capacity. Perturbations in PGC-1α signalling, whether through inflammatory suppression, energy depletion, or transcriptional repression, undermine mitochondrial function and contribute to mucosal barrier dysfunction, as observed in IBD and other enteropathies(17,69). Therapeutic strategies that enhance PGC-1α expression or modulate its upstream regulators, including AMPK and SIRT1, hold promise for restoring mitochondrial integrity and alleviating intestinal inflammation(70).

3.2. Mitochondrial dynamics in gut homeostasis

Mitochondria are highly dynamic organelles that undergo continuous fusion and fission to meet cellular energy demands and respond to stress. This dynamic remodelling is essential for mitochondrial quality control (MQC)(71), maintenance of membrane potential, redistribution of mitochondrial DNA (mtDNA), and adaptation to metabolic fluctuations in intestinal epithelial cells (IECs)(72). In the gut, the equilibrium between fusion and fission ensures mitochondrial integrity and supports epithelial homeostasis. Mitochondrial fusion, regulated by mitofusin 1 and 2 (MFN1/2) and optic atrophy protein 1 (OPA1), promotes the intermixing of mitochondrial contents, allowing functional complementation between damaged and healthy mitochondria. This process is critical for sustaining membrane potential, maintaining respiratory efficiency, and counteracting localized mitochondrial defects. In contrast, mitochondrial fission, primarily driven by dynamin-related protein 1 (DRP1), facilitates the isolation of damaged mitochondria, which are then targeted for degradation via mitophagy, a process essential for preventing the accumulation of dysfunctional organelles(73,74). Under physiological conditions, this dynamic balance maintains cellular and mitochondrial homeostasis. However, during pathological stress, including inflammation and pharmacological injury, this balance becomes disrupted. Excessive fission, driven by hyperactivation of DRP1 (notably through PKCζ-p38-MAPK-mediated phosphorylation at Ser616), results in mitochondrial fragmentation, depolarization, and the initiation of intrinsic apoptotic pathways(55). This mechanism has been implicated in NSAID-induced gastric epithelial injury, where agents like indomethacin and diclofenac induce DRP1-mediated fission and trigger caspase-dependent apoptosis. Similar mitochondrial defects have been observed in models of experimental colitis, where DRP1 inhibition using compounds like Mdivi-1 or the P110 peptide attenuates mitochondrial damage, reduces inflammation, and improves epithelial viability(75). On the

other hand, impaired fusion, due to downregulation of OPA1 or MFN2, leads to fragmented and dysfunctional mitochondria, compromised bioenergetics, and heightened sensitivity to oxidative stress(76). These defects are particularly detrimental in high-turnover tissues like the gut epithelium, where continuous renewal depends on metabolic efficiency and mitochondrial resilience.

3.3. Mitophagy and autophagy pathways in gut integrity

Autophagy, a conserved lysosomal degradation pathway, is indispensable for cellular homeostasis, facilitating the turnover of damaged organelles and misfolded proteins. Macroautophagy, the predominant form, involves the encapsulation of cytoplasmic cargo within double-membraned autophagosomes for lysosomal clearance, a process critical for stress adaptation and organellar quality control(77). Mitophagy, a selective autophagy variant, specifically targets dysfunctional mitochondria, thereby preventing reactive oxygen species (ROS)-mediated damage and maintaining mitochondrial fitness(78). This process is governed by two principal mechanisms: ubiquitin-dependent pathways, orchestrated by PINK1-Parkin signalling, and receptor-mediated pathways, which operate independently of ubiquitination. The PINK1-Parkin axis is activated upon mitochondrial depolarization, wherein PINK1 stabilizes on the outer mitochondrial membrane (OMM) and phosphorylates ubiquitin, recruiting and activating Parkin(79). Subsequent ubiquitination of OMM proteins recruit autophagy adaptors (p62/SQSTM1, NDP52, OPTN) that link damaged mitochondria to LC3-decorated autophagosomes(80). Conversely, receptor-mediated mitophagy employs OMM proteins such as BNIP3, NIX, and FUNDC1, which directly bind LC3 via LIR domains under hypoxia or metabolic stress(81). Phosphorylation of these receptors by kinases like ULK1 and SRC fine-tunes their mitophagic efficiency. Additional players include AMBRA1, which promotes ubiquitin-dependent mitochondrial clearance, and BCL2L13, a functional homolog of yeast Atg32, underscoring the mechanistic diversity of mitophagy(82). Beyond canonical pathways, mitochondrial-derived vesicles (MDVs) export damaged components to lysosomes independently of autophagosome formation, offering an alternative quality-control route. Similarly, mitochondrial spheroids, lysosome-enriched structures, may serve as fail-safe mechanisms during mitophagy impairment. In the intestinal epithelium, mitophagy is pivotal for maintaining barrier function and mitigating inflammation. Dysregulation of this process is implicated in inflammatory bowel disease (IBD), as evidenced by murine models with prohibitin1 (PHB1) deficiency, which exhibit mitochondrial dysfunction and exacerbated colitis(83). Human genetic studies further link IBD susceptibility to polymorphisms in autophagy genes (ATG16L1, IRGM), highlighting the role of mitophagy in epithelial defence. Impaired mitochondrial clearance in intestinal stem cells may also compromise regenerative capacity, perpetuating mucosal damage.(84)

4. MITOCHONDRIAL DYSFUNCTION AND GUT DISORDERS

Mitochondrial dysfunction is increasingly implicated in the pathogenesis of gastrointestinal (GI) disorders, where defects in energy metabolism, redox balance, and mitochondrial quality control contribute to epithelial injury, chronic inflammation, and tumorigenesis. This section reviews the role of mitochondrial impairment in major GI pathologies, including inflammatory bowel disease (IBD), irritable bowel syndrome (IBS), GI cancers, and stress-induced mucosal injury.

4.1. Mitochondrial dysfunction in inflammatory bowel disease (IBD) and irritable bowel syndrome (IBS)

Inflammatory bowel disease (IBD) and irritable bowel syndrome (IBS) represent two prevalent, non-malignant gastrointestinal disorders characterized by chronic inflammation and functional impairment of the gut, often of idiopathic origin. IBD, comprising Crohn's disease and ulcerative colitis, affects over a million individuals in the United States alone, while IBS shows a substantial prevalence of 15–21% in Western and South American populations(85,86). Mitochondrial dysfunction is increasingly recognized as a central pathophysiological mechanism in IBD, where deficiencies in electron transport chain (ETC) complexes II–IV impair OXPHOS, elevate mitochondrial reactive oxygen species (mtROS), and promote epithelial injury, as shown in Fig.4 (17,19). These impairments precede overt histological inflammation in experimental models such as DSS-induced colitis. Genetic evidence underscores this connection through IBD-associated polymorphisms in mitochondrial regulators like SLC22A5, UCP2, SOD2, and HSPA1A/B, as well as mtDNA variants affecting OXPHOS efficiency(87,88). Environmental stressors, including NSAID use, microbial dysbiosis, and psychological stress, exacerbate mitochondrial damage by disrupting tight junction proteins (occludin, ZO-1) and depleting antioxidant defences, thereby compromising intestinal barrier integrity(89-91). The loss of mitochondrial regulators such as PGC-1α and prohibitin 1 further impairs biogenesis, leading to Paneth cell dysfunction and energy failure, while proteomic studies in ulcerative colitis patients reveal reduced levels of mitochondrial chaperones and antioxidant enzymes. Pro-inflammatory cytokines like TNF and IL-1β directly target mitochondria, inhibiting ETC complex I and amplifying mtROS, which in turn activates the NLRP3 inflammasome to drive caspase-1-dependent release of IL-1β/IL-18 and gasdermin D-mediated pyroptosis, processes with context-dependent roles in either exacerbating or mitigating inflammation(92). Mitochondrial dysfunction also promotes necroptosis and the release of mitochondrial DNA (mtDNA), which acts as a damage-associated molecular pattern (DAMP) to activate toll-like receptors, cGAS-STING signalling, and inflammasomes, perpetuating inflammatory cascades(93). Therapeutic strategies targeting mitochondrial pathways, including mitochondria-specific antioxidants (MitoTEMPO, MitoQ), NAD+ supplementation to restore SIRT1-PGC1α-mediated biogenesis, and inhibitors of VDAC1 oligomerization to block mtDNA release, have shown promise in preclinical models by reducing oxidative stress, improving barrier function, and modulating immune responses(94-96). However, the dual roles of mitochondrial signals in both epithelial repair and immune activation highlight the need for cell-type-specific approaches, particularly given the divergent effects of NAD+ modulation on epithelial regeneration versus regulatory T cell induction(97,98). Collectively, these findings position mitochondrial quality control as a critical therapeutic node in IBD, bridging epithelial homeostasis, immune regulation, and microbial interactions, though clinical translation will require careful consideration of the complex, context-dependent roles of mitochondrial pathways in intestinal inflammation.

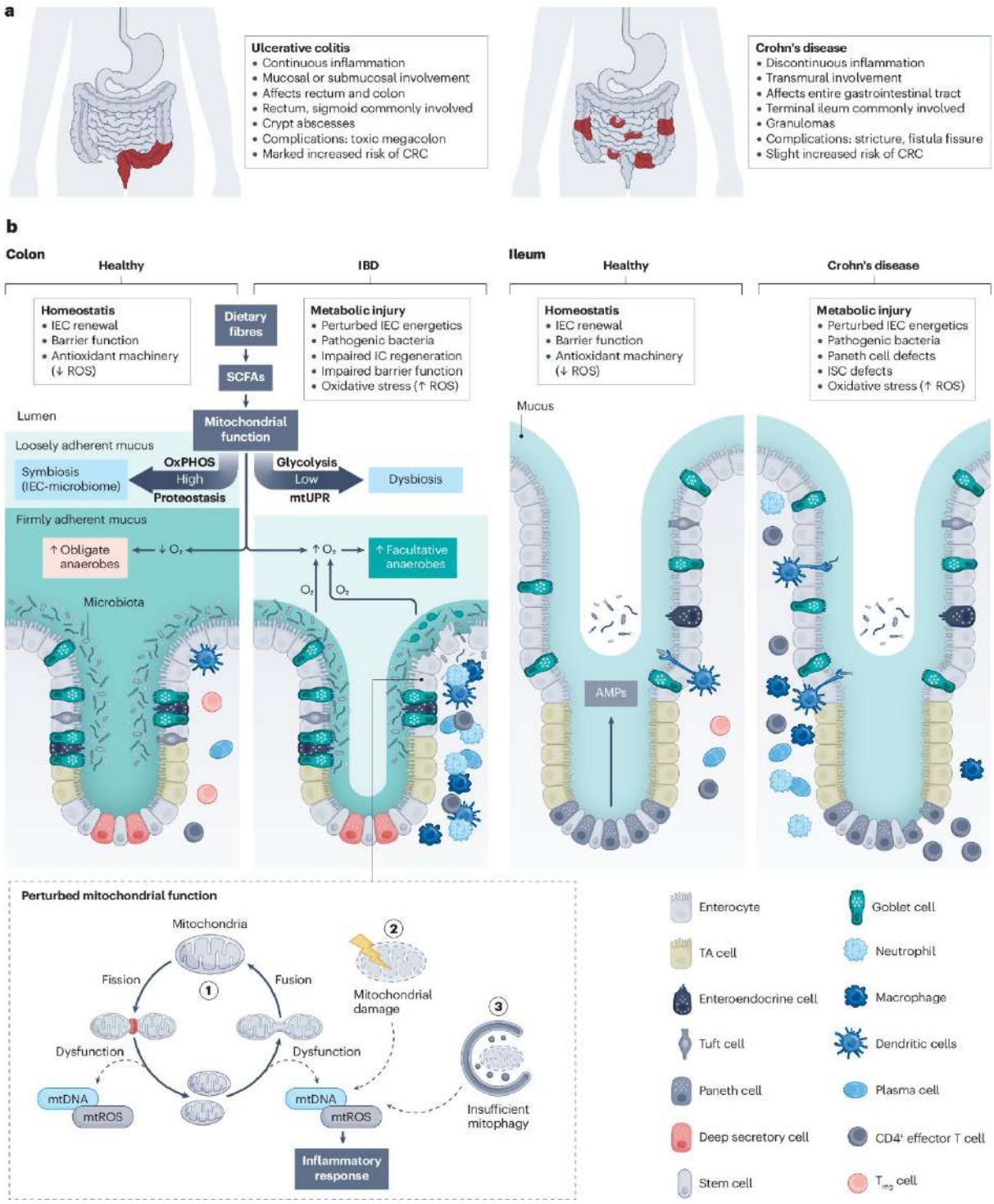
a
Ulcerative colitis
• Continuous inflammation
• Mucosal or submucosal involvement
• Affects rectum and colon
• Rectum, sigmoid commonly involved
• Crypt abscesses
• Complications: toxic megacolon
• Marked increased risk of CRC
Crohn's disease
• Discontinuous inflammation
• Transmural involvement
• Affects entire gastrointestinal tract
• Terminal ileum commonly involved
• Granulomas
• Complications: stricture, fistula fissure
• Slight increased risk of CRC
b
Colon
Healthy
IBD
Homeostatis
• IEC renewal
• Barrier function
• Antioxidant machinery (↓ ROS)
Dietary fibres
SCFAs
Metabolic injury
• Perturbed IEC energetics
• Pathogenic bacteria
• Impaired IC regeneration
• Impaired barrier function
• Oxidative stress (↑ ROS)
Lumen
Mitochondrial function
Loosely adherent mucus
Symbiosis (IEC-microbiome)
OxPHOS
High
Proteostasis
Glycolysis
Low
mtUPR
Dysbiosis
Firmly adherent mucus
↑ Obligate anaerobes
↓ O2
↑ O2
↑ Facultative anaerobes
O2
O2
Microbiota
Ileum
Healthy
Crohn's disease
Homeostatis
• IEC renewal
• Barrier function
• Antioxidant machinery (↓ ROS)
Metabolic injury
• Perturbed IEC energetics
• Pathogenic bacteria
• Paneth cell defects
• ISC defects
• Oxidative stress (↑ ROS)
Mucus
AMPs
Perturbed mitochondrial function
Mitochondria
Fission
Fusion
1
2
Mitochondrial damage
3
Dysfunction
Dysfunction
mtDNA
mtROS
mtDNA
mtROS
Insufficient mitophagy
Inflammatory response
Enterocyte
TA cell
Enteroendocrine cell
Tuft cell
Paneth cell
Deep secretory cell
Stem cell
Goblet cell
Neutrophil
Macrophage
Dendritic cells
Plasma cell
CD4+ effector T cell
Treg cell

Fig. 4. Mitochondrial dysfunction in inflammatory bowel diseases. Ulcerative colitis and Crohn's disease share clinical symptoms like abdominal pain, diarrhoea, and bloody stools but differ in pathological features; ulcerative colitis shows continuous mucosal inflammation limited to the colon, while Crohn's disease involves transmural, patchy inflammation across the gastrointestinal tract, often in the terminal ileum. In a healthy colon, intestinal epithelial cells (IECs) sustain a metabolic gradient with high oxidative phosphorylation (OXPHOS) at the crypt top, creating luminal hypoxia that favours butyrate-producing commensals (e.g., *Bacillota*), forming a symbiotic host-microbiota loop critical for barrier integrity. In IBD, mitochondrial dysfunction disrupts this balance via (1) aberrant fission/fusion dynamics, (2) damage to mitochondrial components (proteins, lipids, mtDNA), and (3) defective mitophagy, leading to mtROS accumulation and mtDNA release that drive inflammation. Impaired IEC OXPHOS shifts metabolism toward glycolysis, increasing luminal oxygen and expanding dysbiotic Proteobacteria. In Crohn's disease, mitochondrial defects specifically impair intestinal stem cells and Paneth cells, exacerbating oxidative stress and microbial imbalance. Key abbreviations: AMPs (antimicrobial peptides), mtUPR (mitochondrial unfolded protein response), TA cell (transit-amplifying cell), Treg cell (regulatory T cell), CRC (colorectal cancer). This figure is adapted from Haque *et. al.* (19)

In contrast, IBS is characterized by visceral hypersensitivity, dysmotility, and disrupted brain-gut interactions. Mitochondrial dysfunction in IBS has been linked to oxidative stress and genetic variants, particularly mtDNA mutations such as the 16519T polymorphism and alterations in *ATP6* and *ATP8,* which are associated with maternally inherited and diarrhoea-predominant IBS(99,100). The overrepresentation of mitochondrial haplogroup H in familial IBS cases suggests a heritable mitochondrial contribution(100). Together, these findings position mitochondrial dysfunction as a converging mechanism in both IBD and IBS, linking genetics, oxidative stress, and environmental triggers to mucosal pathology.

4.2. Mitochondrial dysfunction in gastrointestinal cancers

Mitochondrial dysfunction plays a critical role in the initiation, progression, and prognosis of gastrointestinal (GI) cancers, including colorectal, gastric, and hepatocellular carcinomas. While cancer metabolism is often defined by the Warburg effect, preferential glycolysis even in the presence of oxygen, mitochondria remain essential for biosynthesis, redox balance, and survival signalling in tumour cells(101,102). Disruptions in mitochondrial metabolism, dynamics, and quality control have emerged as key contributors to tumorigenesis and metastasis in GI malignancies. Tumour cells frequently undergo metabolic reprogramming to sustain proliferation. In GI cancers, suppression of the mitochondrial pyruvate carrier (MPC) shifts cellular metabolism from OXPHOS to aerobic glycolysis, enhancing proliferative capacity and resistance to apoptosis(103). The PI3K/Akt/mTOR pathway further drives mitochondrial citrate export for de novo lipid synthesis, supporting membrane biosynthesis and tumour growth(104).

However, mitochondria are not merely passive victims of metabolic shift-they are active participants in oncogenic signalling. In hepatocellular carcinoma (HCC) and colorectal cancer, long non-coding RNAs (lncRNAs) have been found to complex with NRF1 to activate mitochondrial biogenesis, supporting metabolic plasticity and proliferation(105,106). Similarly, in HCC, NRF1 activates E2F1, a key driver of cell cycle progression(107). These findings highlight how mitochondrial transcriptional programs are hijacked during oncogenesis. Mitochondrial dynamics, fusion, and fission are profoundly altered in GI cancers. Increased mitochondrial fission, largely mediated by dynamin-related protein 1 (DRP1), promotes tumour growth, migration, and resistance to apoptosis(108). DRP1 is frequently upregulated in colorectal and gastric cancers and correlates with higher tumour grade and poor prognosis. DRP1 overexpression facilitates cell cycle progression, particularly during the G1/S transition, ensuring sufficient ATP availability for proliferating tumour cells. Pharmacologic or genetic inhibition of DRP1

impairs tumour growth and induces G1 arrest in colorectal cancer cells(108). These findings indicate that disrupted mitochondrial fusion favours oncogenic transformation.

Mitochondrial fission enhances pro-apoptotic signalling in response to stress and chemotherapy. DRP1 activation increases mitochondrial ROS, which in turn triggers the release of cytochrome c and activation of caspase-9, leading to apoptosis(109). In gastric cancer cells, indomethacin-induced DRP1 activation impairs mitochondrial integrity and induces apoptosis(55). Moreover, miR-148a-3p has been shown to sensitize gastric cancer cells to cisplatin by promoting mitochondrial fission and apoptosis(110). Similarly, mitochondrial membrane protein 18 (MTP18) enhances DRP1 accumulation, facilitating chemotherapeutic efficacy via apoptosis(111). Oxidative stress also modulates fusion proteins. Phosphorylation of MFN1 at atypical ERK sites increases mitochondrial membrane permeability, promotes BAK oligomerization, and accelerates cytochrome c release and apoptosis in cells(112). Thus, mitochondrial dynamics are tightly linked to the balance between survival and apoptosis in GI cancers, especially under therapeutic stress. Beyond proliferation and apoptosis, mitochondrial dynamics are integral to tumour cell migration and invasion. Excessive mitochondrial fission increases cytoskeletal remodelling, enhancing cell motility. In gastric cancer, EBV infection promotes DRP1 expression and mitochondrial fragmentation, activating the Notch signalling pathway and promoting metastasis(113). Overexpression of FIS1, another fission regulator, is associated with increased metastatic potential in colorectal cancer(114). Conversely, overexpression of MFN1/2 reduces migratory capacity, induces apoptosis, and impedes PI3K-Akt pathway signalling in gastric cancer cells(115). Targeting mitochondrial dynamics has demonstrated therapeutic potential. For instance, azelastine inhibits the ARF1-IQGAP1-ERK-DRP1 axis, suppressing mitochondrial fission and colon tumour growth(116). Moreover, DRP1 knockdown in HCT116 cells reduces NF-κB activity and downregulates oncogenic targets like cyclin D1 and c-Myc, further implicating mitochondrial fission in colorectal tumorigenesis(117). Aberrant expression of mitochondrial dynamics regulators holds prognostic value. Elevated DRP1 levels are associated with cachexia and advanced-stage gastric cancer(118,119). OMA1, a protease that regulates OPA1 processing, is overexpressed in gastric tumours and correlates with poor survival outcomes(120). Reduced MFN2 expression is linked to higher TNM stage and poorer prognosis in colorectal and gastric cancer cohorts(121). Large-scale transcriptomic and proteomic datasets have further validated these associations. For instance, pan-cancer analyses link high Pink1 expression with reduced survival in breast cancer, while TFAM downregulation is associated with tumour progression in ovarian and head and neck cancers(122,123). Beyond tumour metabolism and dynamics, mitochondrial dysfunction also plays a crucial role in regulating intestinal stem cell (ISC) fate and colorectal cancer (CRC) initiation. Mutations in mitochondrial DNA (mtDNA) and loss of oxidative phosphorylation (OXPHOS) capacity have been observed in early-stage adenomas and aging colonic crypts, contributing to stem cell hyperproliferation and tumorigenesis(124,125). Reduced mitochondrial pyruvate carrier (MPC) expression and altered fatty acid oxidation (FAO) in ISCs further support metabolic reprogramming that favours tumour initiation(126,127). In advanced CRC, elevated mitochondrial biogenesis, mtDNA copy number, and increased reliance on OXPHOS have been associated with aggressive phenotypes, metastasis, and resistance to therapy(128). Mitochondrial metabolism also modulates stemness pathways such as Wnt/β-catenin and Notch Signaling, underscoring the central role of mitochondrial regulation in sustaining cancer cell proliferation, plasticity, and treatment evasion(129,130). Together, these findings reinforce the concept that mitochondrial plasticity is a key determinant of CRC initiation, progression, and therapeutic response.

4.3. Mitochondrial dysfunction in the pathogenesis of peptic ulcer and stress-induced gastric injury

Peptic ulcer disease (PUD) affects approximately 10% of the global population, manifesting as mucosal lesions that penetrate the submucosa or muscularis propria, with clinical presentations ranging from

asymptomatic to life-threatening(131,132). While excessive gastric acid was once believed to be the principal cause, current understanding highlights the central role of oxidative stress–induced mitochondrial dysfunction stemming from *Helicobacter pylori* infection, chronic NSAID use, and psychological stress(133,134). *Helicobacter pylori* infects nearly half the world's population, with virulence factors like CagA and VacA initiating chronic inflammation in gastric epithelial cells. These factors elevate reactive oxygen species (ROS) production, triggering mitochondrial damage and compromising epithelial resilience(135). Host genetic polymorphisms in cytokine genes, notably IL-1β, further amplify this inflammatory cascade and susceptibility to ulcer formation(132).

NSAIDs, particularly drugs like indomethacin, induce ulceration through both cyclooxygenase inhibition and direct mitochondrial toxicity. Indomethacin impairs mitochondrial electron transport chain (ETC) complex I, increasing electron leakage and mitochondrial ROS (mtROS), ultimately inducing apoptosis in both normal and cancerous gastric cells. Key to this damage is the activation of the PKC–p38 MAPK–DRP1 axis, which enhances DRP1-mediated mitochondrial fission. This shift in mitochondrial dynamics, marked by decreased OPA1 and mitofusin expression, leads to mitochondrial fragmentation, cristae disruption, and a bioenergetic crisis characterized by impaired fatty acid oxidation, reduced ETC activity, and ATP depletion(55). The fission inhibitor Mdivi-1 counteracts these effects by restoring mitochondrial integrity, preventing caspase activation, reducing inflammation, and protecting against mucosal injury. A recurring feature in PUD-affected gastric tissue is the Δ4977 mtDNA deletion, a biomarker of oxidative stress and mitochondrial dysfunction(136). Its presence underscores the impact of chronic ROS generation and insufficient DNA repair in ulcer pathology. Together, these findings reveal that mitochondrial hyper-fission and oxidative damage converge as central mechanisms in PUD pathogenesis, promoting epithelial apoptosis and undermining barrier integrity. Therapeutically, this suggests that interventions targeting mitochondrial dynamics, such as DRP1 inhibitors like Mdivi-1, hold promise for mucosal protection and ulcer healing(55). Importantly, psychological stress has emerged as a central, yet underrecognized, contributor to gastropathy, including stress-related mucosal disease (SRMD), particularly in critically ill or chronically stressed individuals. Experimental studies in rodent models have shown that psychological stress induces mitochondrial alterations in the gastric mucosa, including structural fragmentation, impaired energy production, and oxidative damage(137). In the context of escalating societal stress levels and associated stress-related disorders, the incidence of stress-induced gastric injury is projected to rise. These findings underscore the urgent need for mechanistic research to elucidate the precise role of mitochondrial dysfunction in SRMD development, which could reveal novel therapeutic targets for this clinically relevant condition.

5. THE GUT MICROBIOME AND ITS IMPACT ON MITOCHONDRIAL FUNCTION

The gut microbiota exerts a profound influence on host physiology by regulating mitochondrial metabolism, biogenesis, dynamics, and redox balance. By generating microbial metabolites, especially short-chain fatty acids (SCFAs) and bile acids (BAs), the microbiome engages in bidirectional communication with host mitochondria, impacting epithelial health, immune function, and systemic energy metabolism, as shown in Fig.5 (138,139). Short-chain fatty acids (SCFAs), including acetate, propionate, and butyrate, are produced through the fermentation of dietary fibres by commensal gut microbiota(140). Among these, butyrate serves as the principal energy substrate for colonocytes. Beyond bioenergetics, butyrate activates G-protein-coupled receptors (e.g., GPR41/43, GPR109a) and inhibits histone deacetylases (HDACs), influencing gene expression and promoting anti-inflammatory effects(141,142).

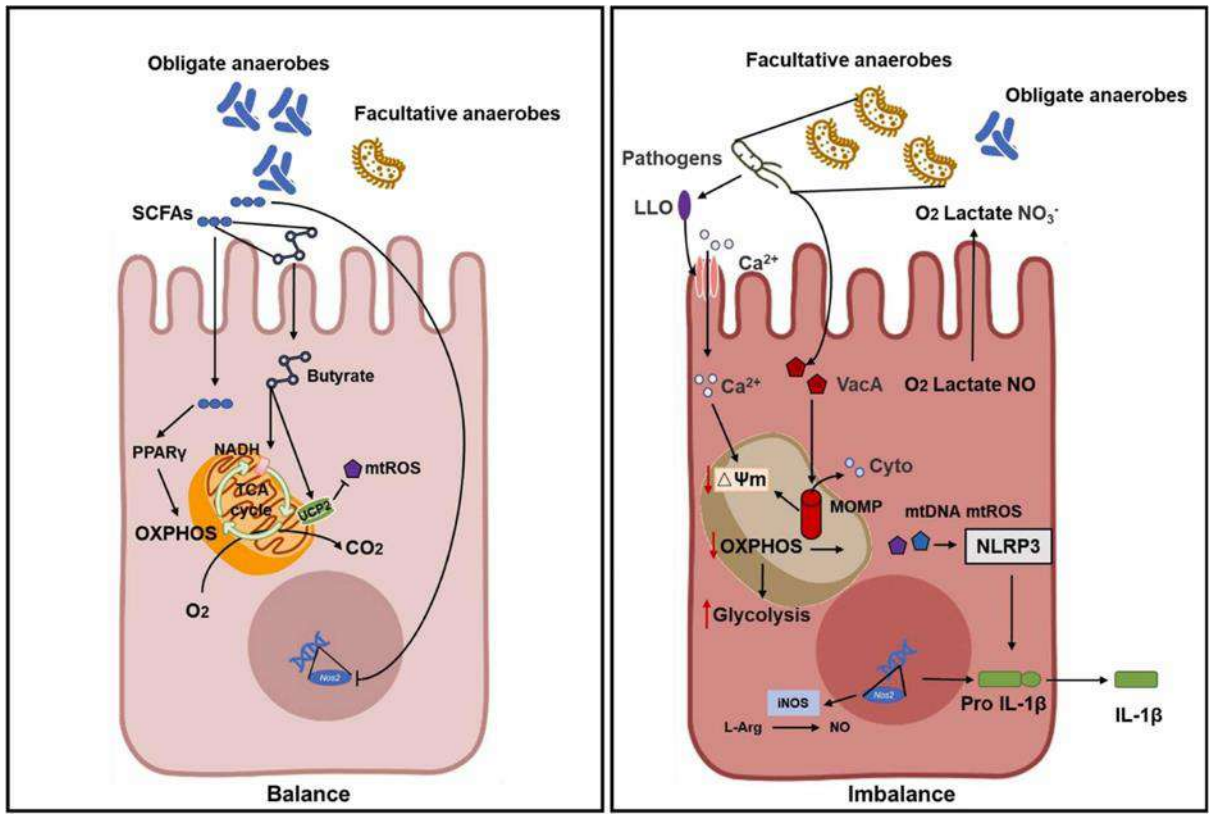

Fig. 5. The model of balance or imbalance interaction between mitochondria and gut microbiota. This figure is adapted from Zhang *et. al.* (139)

Butyrate also regulates mitochondrial function and dynamics(143). It preserves mitochondrial integrity in activated T cells, promotes mitochondria-mediated apoptosis in hyperactive immune cells, and downregulates glycolytic enzymes such as hexokinase 2 via HDAC8 in intestinal epithelial cells(144). Clinical translation of butyrate therapy in IBD has been limited due to formulation challenges and side effects, but its mechanistic relevance remains well supported. Bile acids (BAs), another microbiota-modulated metabolite class, influence mitochondrial signalling through nuclear receptors like FXR and TGR5(145). Microbiota-driven conversion of primary to secondary BAs affects pathways governing oxidative phosphorylation, lipid metabolism, and mitochondrial biogenesis. Hydrophobic BAs such as deoxycholic acid disrupt mitochondrial membranes, induce ROS generation, and trigger apoptosis, mechanisms implicated in colorectal cancer(146). Microbial metabolites directly influence mitochondrial dynamics, particularly fusion-fission balance and mitophagy. Butyrate activates AMPK, which induces mitophagy and reduces oxidative stress in epithelial cells. SCFAs, BAs, and microbial-derived ROS can modulate Drp1 activity, affecting mitochondrial morphology and promoting or inhibiting fission under different conditions(147,148). Drp1 inhibition has been shown to confer neuroprotection and restore microbial balance in disease models. mtDNA variants also affect host-microbiota interactions. Specific mitochondrial haplotypes influence gut microbial diversity by altering redox signalling and ROS production(149). These findings underscore a genetically mediated feedback loop between mitochondrial function and microbial ecology. Mitochondria play a central role in maintaining the rapid turnover of the intestinal epithelium. $Lgr5^+$ intestinal stem cells (ISCs) at the crypt base rely on oxidative phosphorylation to support self-renewal and lineage commitment. Paneth cells contribute to this metabolic niche by supplying lactate from glycolysis, which ISCs utilize via mitochondrial respiration(150). Mitochondrial dysfunction in ISCs due to loss of key chaperones like HSP60 or elevated mtROS impairs proliferation and stemness, effects that are reversible by antioxidant

therapy(151). Microbiota-driven mitochondrial regulation extends beyond the gut, affecting systemic immune function, metabolism, and neurological health. Propionic acid supplementation has improved Treg stability and mitochondrial respiration in multiple sclerosis patients, illustrating the immunometabolic potential of microbial SCFAs(152). In neurodegenerative models, microbiota-induced mitochondrial autophagy defects contribute to diseases such as Parkinson's(153). Gut dysbiosis alters mitochondrial morphology and ROS production in metabolic conditions like diabetes and NAFLD, linking microbial imbalance to mitochondrial dysfunction(154,155). Additionally, microbial metabolites such as trimethylamine and SCFAs modulate mitochondrial DNA (mtDNA) integrity and autophagy in vascular inflammation and atherosclerosis(156). Collectively, these findings underscore mitochondria as integrative hubs for interpreting microbial signals across diverse tissues. Decoding this crosstalk opens up new possibilities for targeted therapies in inflammatory and metabolic diseases.

6. MITOCHONDRIAL METABOLITES AND THEIR ROLE IN GUT PHYSIOLOGY AND PATHOLOGY

Mitochondria generate a range of metabolites that not only fuel bioenergetic processes but also serve as critical regulators of gut homeostasis, immune signalling, epithelial regeneration, and inflammation. These include ATP, reactive oxygen species (ROS), NAD^+-dependent sirtuin effectors, and mitochondrial damage-associated molecular patterns (mtDAMPs). Their roles extend from maintaining gut barrier integrity to shaping host–microbiota interactions and modulating disease pathways.

6.1. ATP and gut barrier integrity

ATP, predominantly produced through mitochondrial oxidative phosphorylation (OXPHOS), is essential for maintaining the structural and functional integrity of the intestinal epithelium. Tight junction proteins, such as occludin, claudins, and ZO-1, require ATP for proper assembly and function, with energy deficits linked to increased epithelial permeability and "leaky gut" phenomena(157,158). AMP-activated protein kinase (AMPK), a metabolic sensor triggered by low ATP levels, reinforces barrier function by enhancing autophagy, suppressing mTOR signalling, and stabilizing apicobasal polarity through adherens junction interactions(159-161). Disruption of mitochondrial ATP synthesis also impairs intestinal stem cell (ISC) renewal and reduces expression of Lgr5 and Olfm4, undermining mucosal repair without directly triggering apoptosis. Furthermore, microbial metabolites such as butyrate, a key energy source for colonocytes, feed directly into the TCA cycle, supporting mitochondrial respiration and reducing ROS production via UCP2 upregulation(162). Loss of SCFA-producing bacteria leads to metabolic reprogramming in colonocytes, luminal oxygenation, and dysbiosis, exacerbating barrier dysfunction. Mitochondria-derived ATP also acts as a danger-associated molecular pattern (DAMP), signalling via purinergic receptors (P2X/P2Y) to activate mast cells, macrophages, and dendritic cells, thereby initiating inflammation(163). Excessive mitochondrial ROS and nitric oxide (NO) contribute further to tight junction destabilization and promote pathogen overgrowth, including *Salmonella* and *Vibrio* species(164,165).

6.2. Reactive oxygen species (ROS): Signalling and stress

Reactive oxygen species (ROS) serve a paradoxical role in gut physiology, acting both as essential signalling molecules and as mediators of oxidative damage. At low-to-moderate levels, ROS, produced primarily by mitochondria and NADPH oxidases, facilitate critical cellular functions such as intestinal stem cell (ISC) proliferation, differentiation, and epithelial regeneration by modulating pathways including Wnt, Notch, and EGFR. However, under pathological conditions such as mitochondrial

oxidative stress (MOS), excessive ROS accumulation disrupts redox homeostasis and impairs vital mitochondrial components like iron-sulfur clusters, leading to compromised electron transport chain (ETC) function, lipid peroxidation, and activation of pro-inflammatory cascades through NF-κB and the unfolded protein response (UPR)(166,167). In the gastrointestinal tract, MOS is a key driver of diseases like inflammatory bowel disease (IBD) and NSAID-induced mucosal injury, where mitochondrial dysfunction, exacerbated by microbial dysbiosis and environmental stressors, triggers epithelial damage and barrier breakdown. NSAIDs, for instance, inhibit ETC complex I, enhancing ROS production and promoting epithelial apoptosis independent of their cyclooxygenase-inhibitory effects(168). The synergistic crosstalk between mitochondrial ROS and endoplasmic reticulum (ER) stress further amplifies mucosal injury and inflammation. Although endogenous antioxidant systems such as superoxide dismutases, glutathione peroxidases, and peroxiredoxins work to neutralize ROS, these defences are frequently overwhelmed in chronic inflammatory states. The NRF2/HO-1 axis provides a compensatory response by upregulating antioxidant and iron-regulating genes, thereby mitigating ferroptosis and limiting inflammatory damage(169). Altogether, mitochondrial redox imbalance constitutes a central mechanism linking environmental stress, immune activation, and epithelial dysfunction in gut pathophysiology.

6.3. NAD^+/Sirtuin axis and mitochondrial resilience

Sirtuins (SIRT1–7), NAD^+-dependent deacetylases, orchestrate mitochondrial function, chromatin remodelling, and inflammatory resolution(170). In the gut, SIRT1 improves barrier integrity and suppresses inflammatory cytokine expression(171). Their activity hinges on intracellular NAD^+ levels, which are shaped by host metabolism and microbial-derived precursors such as nicotinamide, tryptophan, and aspartate(171,172). The gut microbiota modulates NAD^+ metabolism, not only by contributing to precursor synthesis but also by regulating CD38, a key NAD^+-consuming enzyme. CD38 upregulation by LPS contributes to age-related NAD^+ decline and systemic inflammation(173). NAD^+-boosting therapies with NMN or NR improve mitochondrial health and GLP-1 production, though microbial degradation may limit efficacy. Caloric restriction and cold exposure enhance SIRT1-mediated deacetylation of transcription factors such as PGC-1α and FOXO, promoting mitochondrial biogenesis and lipid oxidation(174). Thus, the NAD^+/SIRT axis integrates microbial, dietary, and mitochondrial signals to uphold gut homeostasis and systemic energy balance.

6.4. mtDAMPs and inflammation

Mitochondrial dysfunction, often induced by reactive oxygen species (ROS), membrane depolarization, or metabolic stress, leads to the release of mitochondrial constituents such as mitochondrial DNA (mtDNA), ROS, and cardiolipin. These elements function as mitochondria-derived damage-associated molecular patterns (mtDAMPs), which initiate inflammatory cascades through the activation of pattern recognition receptors, including Toll-like receptor 9 (TLR9), the NLRP3 inflammasome, and the cyclic GMP-AMP synthase-stimulator of interferon genes (cGAS-STING) pathway(175,176). Activation of these receptors ultimately leads to the stimulation of nuclear factor-κB (NF-κB) and interferon regulatory factors (IRFs), thereby promoting pro-inflammatory signalling(175). In the context of inflammatory bowel disease (IBD), both ulcerative colitis (UC) and Crohn's disease (CD) are characterized by increased release of mtDAMPs from epithelial and immune cells, particularly under conditions of mitochondrial injury(177). This release contributes to enhanced inflammasome activation, predominantly mediated by oxidized mtDNA-triggered NLRP3 signalling. The interplay of ROS with reactive nitrogen species (RNS), especially peroxynitrite generated via inducible nitric oxide synthase (iNOS), exacerbates mitochondrial respiratory dysfunction and aggravates mucosal damage(178,179). Among the mtDAMPs, mtDNA has emerged as a pivotal inflammatory mediator in IBD, as shown in

Fig.6 (177). Circulating mtDNA levels are significantly elevated in individuals with UC and CD and positively correlate with clinical severity, blood biomarkers, and endoscopic findings(180). Enhanced mitochondrial damage and increased faecal mtDNA concentrations have been observed in inflamed colonic tissues, indicating that damaged intestinal mucosa constitutes a primary source of mtDNA release. Experimental models, including dextran sulphate sodium (DSS)-induced colitis, have demonstrated that plasma mtDNA levels surge during acute inflammation and are associated with severe disease phenotypes(181). Mechanistically, mtDNA activates multiple innate immune pathways. TLR9, abundantly expressed in the intestinal mucosa, recognizes mtDNA and mediates inflammatory responses(182). Genetic ablation of TLR9 confers protection against colitis, underlining its critical role in mtDNA-induced inflammation. Furthermore, mtDNA acts as a potent activator of the NLRP3 inflammasome, facilitating the maturation and secretion of interleukin-1β (IL-1β)(183). Elevated NLRP3 and IL-1β expression have been documented in inflamed intestinal tissues, and experimental mtDNA administration in DSS-treated wild-type mice amplifies disease severity, reinforcing the contribution of mitochondrial dysfunction to inflammasome-driven pathology(184).

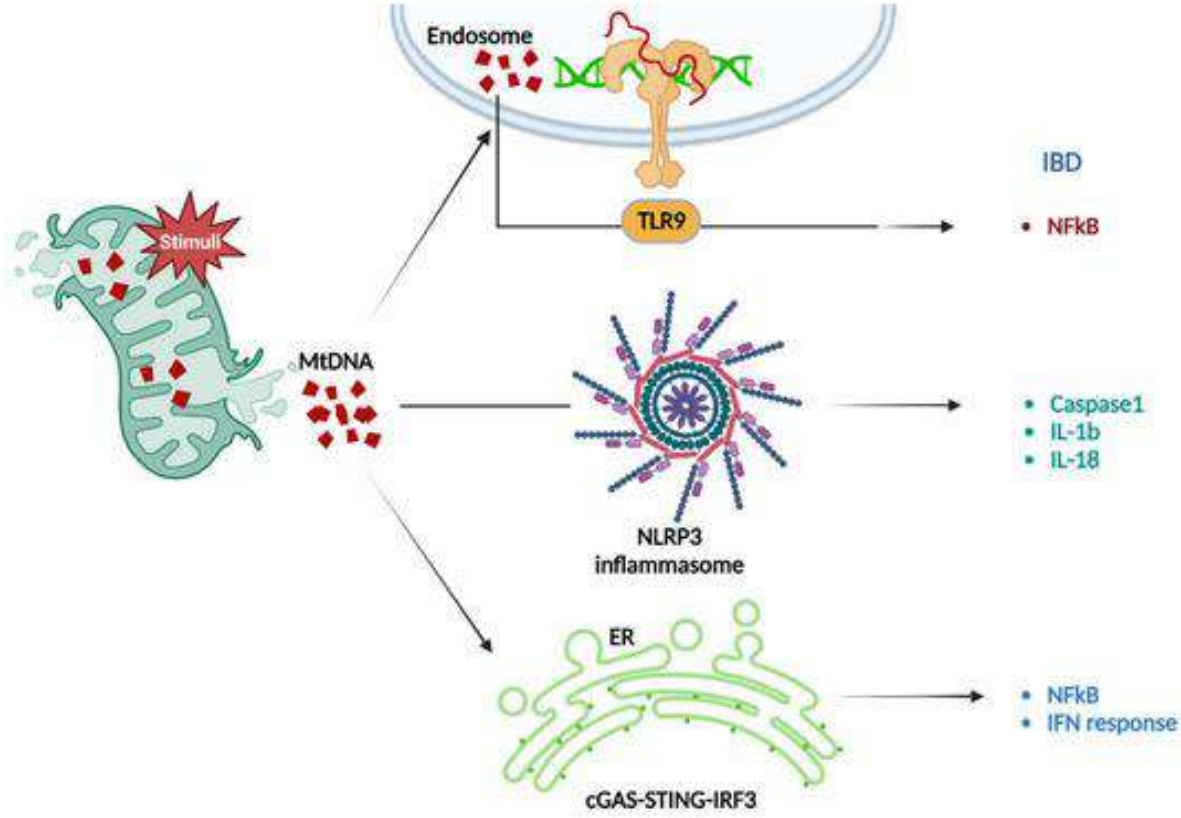

Fig. 6. mtDNA-mediated IBD through different pathways. This figure is adapted from Sui *et. al.* (177)

Ferroptosis, an iron-dependent form of cell death driven by mitochondrial lipid peroxidation, is increasingly implicated in GI inflammation(185). Markers such as ACSL4 and reduced GPX4 activity are elevated in UC and DSS-colitis models. Activation of the NRF2/HO-1 pathway provides protection by limiting iron toxicity and ROS accumulation(186). mtDAMPs are not confined to intracellular compartments. Through mitochondrial-derived vesicles (MDVs) and MPT pores, mtDNA is released into circulation, activating systemic inflammatory responses via TLR9 and cGAS–STING(187,188). This links localized mitochondrial dysfunction to systemic immune activation and disease progression.

7. MITOCHONDRIA AND GUT BARRIER FUNCTION

The intestinal mucosal barrier is a complex, multi-layered defence system comprising the mucus layer, intestinal epithelium, and mucosal immune system. This barrier maintains a delicate balance between allowing the absorption of nutrients and protecting the host from luminal antigens, pathogens, and microbial metabolites. Disruption of this barrier, commonly referred to as "leaky gut" is implicated in a range of gastrointestinal (GI) and systemic diseases(189). Recent advances underscore the critical role of mitochondria as regulators of gut barrier function, linking energy metabolism, redox signalling, and epithelial cell fate decisions to barrier integrity.

7.1. Mitochondrial regulation of tight junction integrity

Tight junctions (TJs), composed of claudins, occludins, and junctional adhesion molecules (JAMs), regulate paracellular permeability and are anchored to the actin cytoskeleton via scaffolding proteins like ZO-1(190). Their integrity is tightly modulated by intracellular energy status and oxidative stress. Mitochondria, as cellular powerhouses, provide the ATP necessary for the assembly and maintenance of TJ complexes and epithelial renewal(191). Mitochondrial dysfunction impairs ATP production and elevates mitochondrial ROS (mtROS), which activates myosin light chain kinase (MLCK), leading to cytoskeletal contraction and TJ disruption(192). In pathological conditions such as IBD or exposure to mycotoxins (e.g., DON, aflatoxin B1), mitochondrial fragmentation and membrane depolarization contribute to the release of pro-apoptotic factors and compromise TJ protein expression(193). These alterations enhance intestinal permeability and microbial translocation, triggering inflammation. In experimental colitis models, antioxidants and mitochondrial protectants (e.g., mitoTEMPO, NAC) restore TJ integrity by suppressing mtROS and stabilizing ZO-1 and occludin(194). Moreover, the mitochondrial-endothelial interface, particularly the glycocalyx composed of proteoglycans like syndecan-1, is also vulnerable to ROS-mediated degradation(195). Heparanase-driven cleavage of glycocalyx components exacerbates vascular permeability and mucosal injury in inflammatory states.

7.2. Mitochondria in intestinal permeability and leaky gut syndrome

Mitochondria play a sentinel role in modulating intestinal permeability under both homeostatic and stress conditions. They regulate cell death pathways, redox balance, and immune signalling, all of which influence epithelial barrier integrity. In IBD and mucosal injury, mitochondrial dysfunction precedes epithelial damage, highlighting its upstream role in pathogenesis. Structural changes such as cristae loss and decreased mitochondrial membrane potential impair OXPHOS and escalate oxidative stress, promoting TJ disassembly(196). Defective mitophagy, particularly in ATG16L1-deficient mice, leads to the accumulation of dysfunctional mitochondria and triggers necroptosis in intestinal epithelial cells. This mitochondrial burden exacerbates inflammation and compromises mucosal defences. Conversely, mitochondrial quality control, via mitophagy and biogenesis, has emerged as a key determinant of barrier preservation. Microbiota-derived metabolites such as butyrate and indole derivatives reinforce mitochondrial function and barrier integrity by activating AMPK and the aryl hydrocarbon receptor (AhR), respectively(197). Vitamin D signaling through the VDR also contributes to mitochondrial fitness and TJ protein expression, with VDR deficiency linked to increased gut permeability(198,199). In this context, mitochondria serve as both effectors and sensors of barrier disruption. Their dynamic responses to stress, immune activation, and microbial cues make them central to the pathophysiology of leaky gut and a promising therapeutic target.

7.3. Dietary regulation of mitochondrial function and barrier integrity

Dietary composition exerts profound effects on both mitochondrial health and intestinal permeability. Nutrients and bioactives modulate mitochondrial biogenesis, antioxidant defenses, and microbiota composition, all of which converge on barrier function. Fermented dairy products, such as yogurt and kefir, contain probiotic strains (e.g., *Lactobacillus plantarum*) that enhance the expression of TJ proteins (ZO-1, occludin, claudin-1) and decrease serum zonulin, a marker of TJ disassembly(200). These effects are mediated via microbial SCFAs and immune modulation. Polyphenols, especially flavonoids such as quercetin and kaempferol, contribute significantly to intestinal health(201). These compounds are abundant in fruits, vegetables, tea, and wine and exhibit potent antioxidant, anti-inflammatory, and mitochondrial-enhancing properties.

Quercetin, a flavonoid abundant in many fruits and vegetables, has been shown to reinforce intestinal barrier integrity by modulating tight junction (TJ) protein expression. In Caco-2 intestinal epithelial cells, quercetin promotes the assembly of TJ components such as ZO-2, occludin, and claudin-1, resulting in enhanced transepithelial electrical resistance (TER), a reliable indicator of barrier function(202). These effects have also been observed in vivo, where quercetin administration in pigs led to increased expression of occludin and ZO-1, alongside a reduction in endotoxemia, suggesting systemic anti-inflammatory benefits(203). Similarly, kaempferol, another dietary flavonoid, improves intestinal barrier integrity by enhancing TER and facilitating the localization of occludin and claudin-3 in epithelial cells(204). These actions are not only barrier-stabilizing but also anti-inflammatory and antioxidative. Quercetin and kaempferol, exert gut-protective effects through three primary mechanisms: (i) upregulation of TJ proteins, (ii) suppression of pro-inflammatory cytokine production (e.g., IL-6, TNF-α), and (iii) enhancement of endogenous antioxidant defences via Nrf2-mediated pathways. Additionally, sulforaphane, a naturally occurring isothiocyanate found in cruciferous vegetables like broccoli activates the Nrf2-Keap1 signalling axis, boosting the transcription of antioxidant enzymes including SOD, catalase, and glutathione peroxidase(205). This not only protects the mucosal epithelium against oxidative injury but also modulates gut microbial composition, favouring the maintenance of an eubiotic state.Conversely, high-fat diets (HFDs) disrupt mitochondrial function, promote ROS generation, and downregulate TJ protein expression. Faecal transplants from HFD-fed mice replicate barrier dysfunction in germ-free animals, implicating microbiota-induced mitochondrial stress in barrier pathology(206). Moreover, caloric restriction (CR) and CR mimetics such as polyphenols and NAD^+ precursors (e.g., NR, NMN) promote mitochondrial resilience by activating SIRT1/AMPK-PGC1α pathways and barrier restoration(207). In conclusion, mitochondria serve as key regulators of gut barrier function by integrating metabolic, oxidative, microbial, and immune signals. Their dysfunction not only precedes epithelial injury but actively drives the pathogenesis of barrier-related disorders.

8. THERAPEUTIC APPROACHES TARGETING MITOCHONDRIA FOR GUT HEALTH

Mitochondria are increasingly recognized as critical regulators of gastrointestinal (GI) homeostasis, with emerging data highlighting the therapeutic potential of targeting mitochondrial dysfunction in the context of gut pathologies. Given the central role of mitochondria in energy metabolism, redox balance, and apoptosis, strategies that preserve or restore mitochondrial function offer promising avenues for preventing and treating gut-related diseases. In this section, key mitochondria-targeted therapies, including mitochondrial antioxidants, probiotics, and small-molecule modulators, are discussed.

8.1. Mitochondrially-targeted antioxidants

Mitochondria possess a unique electrochemical gradient, characterized by a highly negative membrane potential across the inner mitochondrial membrane, which facilitates the selective accumulation of positively charged, lipophilic compounds. This property has been exploited to deliver therapeutic agents directly into mitochondria using triphenylphosphonium (TPP^+) cation conjugation(208). Among the earliest mitochondria-targeted antioxidants was MitoQ, a ubiquinone derivative linked to TPP+, capable of being recycled by the electron transport chain (ETC) to its active form after neutralizing reactive oxygen species (ROS). Other compounds, such as SkQ1, a plastoquinone-conjugated antioxidant, have demonstrated robust efficacy in preclinical models of cardiovascular, renal, and ocular diseases(209). MitoQ has also shown promise in clinical trials for Parkinson's disease and liver pathologies. Despite these advances, the use of TPP-conjugated compounds poses challenges, including off-target effects, membrane destabilization, and disruption of mitochondrial calcium homeostasis due to excessive accumulation. Furthermore, certain TPP-linked antioxidants, such as Mito-Resveratrol and Mito-Curcumin, have paradoxically demonstrated pro-oxidant effects and mitochondrial toxicity in vitro, underlining the need for meticulous safety evaluation(209). To address these limitations, second-generation molecules with shorter alkyl linkers, such as MitoTEMPO (a nitroxide-based superoxide scavenger), have been developed. MitoTEMPO has shown significant protective effects in rodent models of NSAID-induced gastropathy and intestinal barrier dysfunction in inflammatory bowel disease (IBD) (210,211).

8.2. Natural antioxidants and phytochemicals with mitochondrial activity

Natural polyphenols such as resveratrol, curcumin, quercetin, and epigallocatechin-3-gallate are known to confer cytoprotection via modulation of mitochondrial pathways(209,212). While these compounds are not intrinsically mitochondriotropic, their antioxidant and anti-inflammatory effects often converge on mitochondrial protection. For example, curcumin has demonstrated efficacy in clinical trials for ulcerative colitis (ClinicalTrials.gov Identifier: NCT03122613), while other polyphenols such as gallic acid and caffeic acid exhibit metal-chelating and chain-breaking antioxidant activity. Novel derivatives such as AntiOxBENs and AntiOxCINs, created by conjugating TPP^+ to hydroxybenzoic and hydroxycinnamic acids, respectively, have shown encouraging antioxidant effects, although their roles in gastrointestinal protection remain to be fully elucidated(209,213).

8.3. Modulators of mitochondrial dynamics

In addition to antioxidant strategies, targeting mitochondrial dynamics-specifically the balance of fission and fusion, offers a novel therapeutic modality. Excessive mitochondrial fission is a hallmark of epithelial injury in GI disorders. Small-molecule inhibitors such as Mdivi-1, which block the GTPase activity of DRP1, have demonstrated protective effects in models of NSAID-induced and stress-induced gastropathy(55). Despite promising outcomes, Mdivi-1 has been reported to possess non-specific effects, including inhibition of ETC complex I and induction of mitochondrial hyperpolarization(214,215). Thus, while modulation of mitochondrial morphology presents a compelling therapeutic target, the associated risks necessitate further refinement and specificity in drug design.

8.4. Efficacy and safety considerations

The clinical translation of mitochondria-targeted therapies hinges upon resolving several critical challenges: (1) ensuring specificity and bioavailability, (2) minimizing off-target effects, and (3) preserving physiological ROS signalling. It is imperative to acknowledge that excessive scavenging of

ROS may disrupt essential redox signalling pathways, while prolonged suppression of mitochondrial fission may impair mitophagy and promote mitochondrial dysfunction. Moreover, long alkyl linkers used in TPP+ conjugation can exacerbate toxicity by compromising mitochondrial membrane integrity. The rational design of next-generation MTAs must prioritize shorter linkers and implement controlled-release scaffolds to mitigate these effects(208). Combinatorial strategies involving iron chelators such as tiron, which possess dual antioxidant and metal-chelating properties, have also shown superiority over MitoQ in certain oxidative stress models, offering protection against both mitochondrial and nuclear DNA damage(216). These findings support the integration of metal homeostasis modulators into mitochondrial-targeted interventions.

9. CONCLUSION

While significant progress has been made in delineating the central role of mitochondria in gastrointestinal physiology, the precise molecular underpinnings of mitochondrial dysfunction in stress-induced gastric mucosal injury remain inadequately understood. Future research must prioritize the comprehensive mapping of mitochondrial perturbations across spatial and temporal scales, particularly under acute and chronic psychological stress. High-resolution approaches such as high-depth transcriptomic profiling and untargeted metabolomics are essential to capture global changes in gene expression and metabolic flux during disease onset and progression. Focused exploration of the modulation of key mitochondrial regulators, such as PGC-1α, TFAM, and other mitochondrial regulatory proteins, during stress exposure, particularly to corticosterone signalling, is essential. Key gaps remain in defining how mitochondrial processes are regulated in a cell-specific and region-dependent manner along the gastrointestinal tract. The heterogeneity of mitochondrial responses, ranging from hyper-fission and membrane depolarization to inefficient mitophagy, under different stress paradigms demands systematic investigation using advanced in vivo models and single-cell approaches. Following this comprehensive literature review, we hypothesize that mitochondrial dysfunction plays a central role in mediating stress-induced gastric mucosal injury. The subsequent experimental chapter is dedicated to investigating this hypothesis, to delineate the molecular mechanisms through which acute mental stress disrupts mitochondrial homeostasis and contributes to gastropathology. This exploration aims to establish a mechanistic foundation for the development of mitochondria-targeted therapeutic strategies in the context of stress-related gastric injury.

10. REFERENCES

1. Wallace, D. C. (2005) A mitochondrial paradigm of metabolic and degenerative diseases, aging, and cancer: a dawn for evolutionary medicine. *Annual review of genetics* **39**, 359-407

2. Friedman, J. R., and Nunnari, J. (2014) Mitochondrial form and function. *Nature* **505**, 335-343

3. Anderson, S., Bankier, A. T., Barrell, B. G., de Bruijn, M. H., Coulson, A. R., Drouin, J., Eperon, I. C., Nierlich, D. P., Roe, B. A., Sanger, F., Schreier, P. H., Smith, A. J., Staden, R., and Young, I. G. (1981) Sequence and organization of the human mitochondrial genome. *Nature* **290**, 457-465

4. Garesse, R., and Vallejo, C. G. (2001) Animal mitochondrial biogenesis and function: a regulatory cross-talk between two genomes. *Gene* **263**, 1-16

5. Youle, R. J., and van der Bliek, A. M. (2012) Mitochondrial fission, fusion, and stress. *Science (New York, N.Y.)* **337**, 1062-1065

6. Green, A., Hossain, T., and Eckmann, D. M. (2022) Mitochondrial dynamics involves molecular and mechanical events in motility, fusion and fission. *Frontiers in cell and developmental biology* **10**, 1010232

7. Saraste, M. (1999) Oxidative phosphorylation at the fin de siècle. *Science (New York, N.Y.)* **283**, 1488-1493

8. Chandel, N. S. (2015) Evolution of Mitochondria as Signaling Organelles. *Cell metabolism* **22**, 204-206

9. Wallace, D. C. (2012) Mitochondria and cancer. *Nature reviews. Cancer* **12**, 685-698

10. Mazumder, S., Bindu, S., De, R., Debsharma, S., Pramanik, S., and Bandyopadhyay, U. (2022) Emerging role of mitochondrial DAMPs, aberrant mitochondrial dynamics and anomalous mitophagy in gut mucosal pathogenesis. *Life sciences* **305**, 120753

11. Ju, T., Zhang, Y., Liu, L., Zhao, X., Li, X., Liu, C., Sun, S., and Wu, L. A. (2025) The role of gut microbiota-mitochondria crosstalk in neurodegeneration: Underlying mechanisms and potential therapies. *Neural regeneration research*

12. Hu, S., Kuwabara, R., de Haan, B. J., Smink, A. M., and de Vos, P. (2020) Acetate and Butyrate Improve β-cell Metabolism and Mitochondrial Respiration under Oxidative Stress. *International journal of molecular sciences* **21**

13. Sanidad, K. Z., Rager, S. L., Carrow, H. C., Ananthanarayanan, A., Callaghan, R., Hart, L. R., Li, T., Ravisankar, P., Brown, J. A., Amir, M., Jin, J. C., Savage, A. R., Luo, R., Rowdo, F. M., Martin, M. L., Silver, R. B., Guo, C. J., Krumsiek, J., Inohara, N., and Zeng, M. Y. (2024) Gut bacteria-derived serotonin promotes immune tolerance in early life. *Science immunology* **9**, eadj4775

14. Aviello, G., and Knaus, U. G. (2017) ROS in gastrointestinal inflammation: Rescue Or Sabotage? *British journal of pharmacology* **174**, 1704-1718

15. Duboc, H., Rajca, S., Rainteau, D., Benarous, D., Maubert, M. A., Quervain, E., Thomas, G., Barbu, V., Humbert, L., Despras, G., Bridonneau, C., Dumetz, F., Grill, J. P., Masliah, J., Beaugerie, L., Cosnes, J., Chazouillères, O., Poupon, R., Wolf, C., Mallet, J. M., Langella, P., Trugnan, G., Sokol, H., and Seksik, P. (2013) Connecting dysbiosis, bile-acid dysmetabolism and gut inflammation in inflammatory bowel diseases. *Gut* **62**, 531-539

16. Mei, Q., Diao, L., Xu, J.-m., Liu, X.-c., and Jin, J. J. A. P. S. (2011) A protective effect of melatonin on intestinal permeability is induced by diclofenac via regulation of mitochondrial function in mice. **32**, 495-502

17. Novak, E. A., and Mollen, K. P. (2015) Mitochondrial dysfunction in inflammatory bowel disease. *Frontiers in cell and developmental biology* **3**, 62

18. Chimienti, G., Orlando, A., Lezza, A. M. S., D'Attoma, B., Notarnicola, M., Gigante, I., Pesce, V., and Russo, F. (2021) The Ketogenic Diet Reduces the Harmful Effects of Stress on Gut Mitochondrial Biogenesis in a Rat Model of Irritable Bowel Syndrome. *International journal of molecular sciences* **22**

19. Haque, P. S., Kapur, N., Barrett, T. A., and Theiss, A. L. (2024) Mitochondrial function and gastrointestinal diseases. *Nature reviews. Gastroenterology & hepatology* **21**, 537-555

20. Koju, N., Qin, Z. H., and Sheng, R. (2022) Reduced nicotinamide adenine dinucleotide phosphate in redox balance and diseases: a friend or foe? *Acta pharmacologica Sinica* **43**, 1889-1904

21. Jonckheere, A. I., Smeitink, J. A., and Rodenburg, R. J. (2012) Mitochondrial ATP synthase: architecture, function and pathology. *Journal of inherited metabolic disease* **35**, 211-225

22. Guerbette, T., Boudry, G., and Lan, A. (2022) Mitochondrial function in intestinal epithelium homeostasis and modulation in diet-induced obesity. *Molecular metabolism* **63**, 101546

23. Zorov, D. B., Juhaszova, M., and Sollott, S. J. (2014) Mitochondrial reactive oxygen species (ROS) and ROS-induced ROS release. *Physiological reviews* **94**, 909-950

24. Popov, L. D. (2023) Mitochondria as intracellular signalling organelles. An update. *Cellular signalling* **109**, 110794

25. Görlach, A., Dimova, E. Y., Petry, A., Martínez-Ruiz, A., Hernansanz-Agustín, P., Rolo, A. P., Palmeira, C. M., and Kietzmann, T. (2015) Reactive oxygen species, nutrition, hypoxia and diseases: Problems solved? *Redox biology* **6**, 372-385

26. Schieber, M., and Chandel, N. S. (2014) ROS function in redox signaling and oxidative stress. *Current biology : CB* **24**, R453-462

27. Kowalczyk, P., Sulejczak, D., Kleczkowska, P., Bukowska-Ośko, I., Kucia, M., Popiel, M., Wietrak, E., Kramkowski, K., Wrzosek, K., and Kaczyńska, K. (2021) Mitochondrial Oxidative Stress-A Causative Factor and Therapeutic Target in Many Diseases. *International journal of molecular sciences* **22**

28. Andrés, C. M. C., Lastra, J. M. P., Juan, C. A., Plou, F. J., and Pérez-Lebeña, E. (2023) Chemical Insights into Oxidative and Nitrative Modifications of DNA. *International journal of molecular sciences* **24**

29. Napolitano, G., Fasciolo, G., and Venditti, P. (2021) Mitochondrial Management of Reactive Oxygen Species. *Antioxidants (Basel, Switzerland)* **10**

30. Vo, T. T. T., Peng, T. Y., Nguyen, T. H., Bui, T. N. H., Wang, C. S., Lee, W. J., Chen, Y. L., Wu, Y. C., and Lee, I. T. (2024) The crosstalk between copper-induced oxidative stress and cuproptosis: a novel potential anticancer paradigm. *Cell communication and signaling : CCS* **22**, 353

31. Hong, Y., Boiti, A., Vallone, D., and Foulkes, N. S. (2024) Reactive Oxygen Species Signaling and Oxidative Stress: Transcriptional Regulation and Evolution. *Antioxidants (Basel, Switzerland)* **13**

32. Rodríguez-Colman, M. J., Schewe, M., Meerlo, M., Stigter, E., Gerrits, J., Pras-Raves, M., Sacchetti, A., Hornsveld, M., Oost, K. C., Snippert, H. J., Verhoeven-Duif, N., Fodde, R., and Burgering, B. M. (2017) Interplay between metabolic identities in the intestinal crypt supports stem cell function. *Nature* **543**, 424-427

33. Sena, L. A., and Chandel, N. S. (2012) Physiological roles of mitochondrial reactive oxygen species. *Molecular cell* **48**, 158-167

34. Shaker, A., and Rubin, D. C. (2010) Intestinal stem cells and epithelial-mesenchymal interactions in the crypt and stem cell niche. *Translational research : the journal of laboratory and clinical medicine* **156**, 180-187

35. Kai, Y. (2021) Intestinal villus structure contributes to even shedding of epithelial cells. *Biophysical journal* **120**, 699-710

36. Takiishi, T., Fenero, C. I. M., and Câmara, N. O. S. (2017) Intestinal barrier and gut microbiota: Shaping our immune responses throughout life. *Tissue barriers* **5**, e1373208

37. Rath, E., Moschetta, A., and Haller, D. (2018) Mitochondrial function - gatekeeper of intestinal epithelial cell homeostasis. *Nature reviews. Gastroenterology & hepatology* **15**, 497-516

38. Jeynes, B. J., and Altmann, G. G. (1975) A region of mitochondrial division in the epithelium of the small intestine of the rat. *The Anatomical record* **182**, 289-296

39. D'Errico, I., Salvatore, L., Murzilli, S., Lo Sasso, G., Latorre, D., Martelli, N., Egorova, A. V., Polishuck, R., Madeyski-Bengtson, K., Lelliott, C., Vidal-Puig, A. J., Seibel, P., Villani, G., and Moschetta, A. (2011) Peroxisome proliferator-activated receptor-gamma coactivator 1-alpha (PGC1alpha) is a metabolic regulator of intestinal epithelial cell fate. *Proceedings of the National Academy of Sciences of the United States of America* **108**, 6603-6608

40. Wu, Z., Puigserver, P., Andersson, U., Zhang, C., Adelmant, G., Mootha, V., Troy, A., Cinti, S., Lowell, B., Scarpulla, R. C., and Spiegelman, B. M. (1999) Mechanisms controlling mitochondrial biogenesis and respiration through the thermogenic coactivator PGC-1. *Cell* **98**, 115-124

41. Kang, C., and Li Ji, L. (2012) Role of PGC-1α signaling in skeletal muscle health and disease. *Annals of the New York Academy of Sciences* **1271**, 110-117

42. Basu, N., Saha, S., Khan, I., Ramachandra, S. G., and Visweswariah, S. S. (2014) Intestinal cell proliferation and senescence are regulated by receptor guanylyl cyclase C and p21. *The Journal of biological chemistry* **289**, 581-593

43. Prasad, H., Mathew, J. K. K., and Visweswariah, S. S. (2022) Receptor Guanylyl Cyclase C and Cyclic GMP in Health and Disease: Perspectives and Therapeutic Opportunities. *Frontiers in endocrinology* **13**, 911459

44. Cunningham, J. T., Rodgers, J. T., Arlow, D. H., Vazquez, F., Mootha, V. K., and Puigserver, P. (2007) mTOR controls mitochondrial oxidative function through a YY1-PGC-1alpha transcriptional complex. *Nature* **450**, 736-740

45. Perekatt, A. O., Valdez, M. J., Davila, M., Hoffman, A., Bonder, E. M., Gao, N., and Verzi, M. P. J. P. o. t. N. A. o. S. (2014) YY1 is indispensable for Lgr5+ intestinal stem cell renewal. **111**, 7695-7700

46. Roper, J., and Yilmaz Ö, H. (2017) Metabolic Teamwork in the Stem Cell Niche. *Cell metabolism* **25**, 993-994

47. Petrache, I., Medler, T. R., Richter, A. T., Kamocki, K., Chukwueke, U., Zhen, L., Gu, Y., Adamowicz, J., Schweitzer, K. S., Hubbard, W. C., Berdyshev, E. V., Lungarella, G., and Tuder, R. M. (2008) Superoxide dismutase protects against apoptosis and alveolar enlargement

induced by ceramide. *American journal of physiology. Lung cellular and molecular physiology* **295**, L44-53

48. Vianna, C. R., Huntgeburth, M., Coppari, R., Choi, C. S., Lin, J., Krauss, S., Barbatelli, G., Tzameli, I., Kim, Y. B., Cinti, S., Shulman, G. I., Spiegelman, B. M., and Lowell, B. B. (2006) Hypomorphic mutation of PGC-1beta causes mitochondrial dysfunction and liver insulin resistance. *Cell metabolism* **4**, 453-464

49. Bellafante, E., Morgano, A., Salvatore, L., Murzilli, S., Di Tullio, G., D'Orazio, A., Latorre, D., Villani, G., and Moschetta, A. J. P. o. t. N. A. o. S. (2014) PGC-1β promotes enterocyte lifespan and tumorigenesis in the intestine. **111**, E4523-E4531

50. Ramachandran, A., Madesh, M., and Balasubramanian, K. A. (2000) Apoptosis in the intestinal epithelium: its relevance in normal and pathophysiological conditions. *Journal of gastroenterology and hepatology* **15**, 109-120

51. Gupta, S., Kass, G. E., Szegezdi, E., and Joseph, B. (2009) The mitochondrial death pathway: a promising therapeutic target in diseases. *Journal of cellular and molecular medicine* **13**, 1004-1033

52. Kim, Y.-R., Jun, S., Jung, S., Lee, B., Lee, S.-H., Lee, J., Hwang, J.-S., Thoudam, T., Lee, H., Sinam, I. S. J. B., and Pharmacotherapy. (2025) Inhibition of the mitochondrial permeability transition pore as a promising target for protecting auditory function in cisplatin-induced hearing loss. **182**, 117767

53. Muro, P., Zhang, L., Li, S., Zhao, Z., Jin, T., Mao, F., and Mao, Z. (2024) The emerging role of oxidative stress in inflammatory bowel disease. *Frontiers in endocrinology* **15**, 1390351

54. Elmore, S. (2007) Apoptosis: a review of programmed cell death. *Toxicologic pathology* **35**, 495-516

55. Mazumder, S., De, R., Debsharma, S., Bindu, S., Maity, P., Sarkar, S., Saha, S. J., Siddiqui, A. A., Banerjee, C., Nag, S., Saha, D., Pramanik, S., Mitra, K., and Bandyopadhyay, U. (2019) Indomethacin impairs mitochondrial dynamics by activating the PKCζ-p38-DRP1 pathway and inducing apoptosis in gastric cancer and normal mucosal cells. *The Journal of biological chemistry* **294**, 8238-8258

56. Shadel, G. S. (2008) Expression and maintenance of mitochondrial DNA: new insights into human disease pathology. *The American journal of pathology* **172**, 1445-1456

57. Scarpulla, R. C. (2008) Nuclear control of respiratory chain expression by nuclear respiratory factors and PGC-1-related coactivator. *Annals of the New York Academy of Sciences* **1147**, 321-334

58. Cunningham, K. E., Vincent, G., Sodhi, C. P., Novak, E. A., Ranganathan, S., Egan, C. E., Stolz, D. B., Rogers, M. B., Firek, B., Morowitz, M. J., Gittes, G. K., Zuckerbraun, B. S., Hackam, D. J., and Mollen, K. P. (2016) Peroxisome Proliferator-activated Receptor-γ Coactivator 1-α (PGC1α) Protects against Experimental Murine Colitis. *The Journal of biological chemistry* **291**, 10184-10200

59. Vega, R. B., Huss, J. M., and Kelly, D. P. (2000) The coactivator PGC-1 cooperates with peroxisome proliferator-activated receptor alpha in transcriptional control of nuclear genes

encoding mitochondrial fatty acid oxidation enzymes. *Molecular and cellular biology* **20**, 1868-1876

60. Actis Dato, V., Lange, S., and Cho, Y. J. I. j. o. m. s. (2024) Metabolic flexibility of the heart: the role of fatty acid metabolism in health, heart failure, and cardiometabolic diseases. **25**, 1211

61. Jäger, S., Handschin, C., St.-Pierre, J., and Spiegelman, B. M. J. P. o. t. n. a. o. s. (2007) AMP-activated protein kinase (AMPK) action in skeletal muscle via direct phosphorylation of PGC-1α. **104**, 12017-12022

62. Liu, B. H., Xu, C. Z., Liu, Y., Lu, Z. L., Fu, T. L., Li, G. R., Deng, Y., Luo, G. Q., Ding, S., Li, N., and Geng, Q. (2024) Mitochondrial quality control in human health and disease. *Military Medical Research* **11**, 32

63. Lira, V. A., Benton, C. R., Yan, Z., and Bonen, A. (2010) PGC-1alpha regulation by exercise training and its influences on muscle function and insulin sensitivity. *American journal of physiology. Endocrinology and metabolism* **299**, E145-161

64. Wu, Z., Huang, X., Feng, Y., Handschin, C., Feng, Y., Gullicksen, P. S., Bare, O., Labow, M., Spiegelman, B., and Stevenson, S. C. J. P. o. t. N. A. o. S. (2006) Transducer of regulated CREB-binding proteins (TORCs) induce PGC-1α transcription and mitochondrial biogenesis in muscle cells. **103**, 14379-14384

65. Ruiz-Andres, O., Sanchez-Niño, M. D., Cannata-Ortiz, P., Ruiz-Ortega, M., Egido, J., Ortiz, A., and Sanz, A. B. (2016) Histone lysine crotonylation during acute kidney injury in mice. *Disease models & mechanisms* **9**, 633-645

66. Huang, S., Jin, Y., Zhang, L., Zhou, Y., Chen, N., and Wang, W. (2024) PPAR gamma and PGC-1alpha activators protect against diabetic nephropathy by suppressing the inflammation and NF-kappaB activation. *Nephrology (Carlton, Vic.)* **29**, 858-872

67. Galván-Peña, S., and O'Neill, L. A. (2014) Metabolic reprograming in macrophage polarization. *Frontiers in immunology* **5**, 420

68. Park-Min, K. H. (2019) Metabolic reprogramming in osteoclasts. *Seminars in immunopathology* **41**, 565-572

69. Rius-Pérez, S., Torres-Cuevas, I., Millán, I., Ortega Á, L., and Pérez, S. (2020) PGC-1α, Inflammation, and Oxidative Stress: An Integrative View in Metabolism. *Oxidative medicine and cellular longevity* **2020**, 1452696

70. Sun, H., Li, D., Wei, C., Liu, L., Xin, Z., Gao, H., and Gao, R. J. F. i. I. (2024) The relationship between SIRT1 and inflammation: a systematic review and meta-analysis. **15**, 1465849

71. Tilokani, L., Nagashima, S., Paupe, V., and Prudent, J. (2018) Mitochondrial dynamics: overview of molecular mechanisms. *Essays in biochemistry* **62**, 341-360

72. Rath, E., Moschetta, A., Haller, D. J. N. r. G., and hepatology. (2018) Mitochondrial function—gatekeeper of intestinal epithelial cell homeostasis. **15**, 497-516

73. Zerihun, M., Sukumaran, S., and Qvit, N. (2023) The Drp1-Mediated Mitochondrial Fission Protein Interactome as an Emerging Core Player in Mitochondrial Dynamics and Cardiovascular Disease Therapy. *International journal of molecular sciences* **24**

74. Seo, B. J., Yoon, S. H., and Do, J. T. (2018) Mitochondrial Dynamics in Stem Cells and Differentiation. *International journal of molecular sciences* **19**

75. Rahmani, S., Roohbakhsh, A., and Karimi, G. (2023) Inhibition of Drp1-dependent mitochondrial fission by natural compounds as a therapeutic strategy for organ injuries. *Pharmacological research* **188**, 106672

76. Zanfardino, P., Amati, A., Perrone, M., and Petruzzella, V. (2025) The Balance of MFN2 and OPA1 in Mitochondrial Dynamics, Cellular Homeostasis, and Disease. *Biomolecules* **15**

77. Levine, B., and Kroemer, G. (2008) Autophagy in the pathogenesis of disease. *Cell* **132**, 27-42

78. Wang, X. L., Feng, S. T., Wang, Y. T., Yuan, Y. H., Li, Z. P., Chen, N. H., Wang, Z. Z., and Zhang, Y. (2022) Mitophagy, a Form of Selective Autophagy, Plays an Essential Role in Mitochondrial Dynamics of Parkinson's Disease. *Cellular and molecular neurobiology* **42**, 1321-1339

79. Bayne, A. N., and Trempe, J. F. (2019) Mechanisms of PINK1, ubiquitin and Parkin interactions in mitochondrial quality control and beyond. *Cellular and molecular life sciences : CMLS* **76**, 4589-4611

80. Jeong, S. J., Zhang, X., Rodriguez-Velez, A., Evans, T. D., and Razani, B. (2019) p62/SQSTM1 and Selective Autophagy in Cardiometabolic Diseases. *Antioxidants & redox signaling* **31**, 458-471

81. Marinković, M., and Novak, I. (2021) A brief overview of BNIP3L/NIX receptor-mediated mitophagy. *FEBS open bio* **11**, 3230-3236

82. Otsu, K., Murakawa, T., and Yamaguchi, O. (2015) BCL2L13 is a mammalian homolog of the yeast mitophagy receptor Atg32. *Autophagy* **11**, 1932-1933

83. Jackson, D. N., Panopoulos, M., Neumann, W. L., Turner, K., Cantarel, B. L., Thompson-Snipes, L., Dassopoulos, T., Feagins, L. A., Souza, R. F., Mills, J. C., Blumberg, R. S., Venuprasad, K., Thompson, W. E., and Theiss, A. L. (2020) Mitochondrial dysfunction during loss of prohibitin 1 triggers Paneth cell defects and ileitis. *Gut* **69**, 1928-1938

84. Palomino-Morales, R. J., Oliver, J., Gómez-García, M., López-Nevot, M. A., Rodrigo, L., Nieto, A., Alizadeh, B. Z., and Martín, J. (2009) Association of ATG16L1 and IRGM genes polymorphisms with inflammatory bowel disease: a meta-analysis approach. *Genes and immunity* **10**, 356-364

85. Machicado, J. D., Villafuerte-Galvez, J., and Marcos, L. A. (2013) Prevalence of irritable bowel syndrome in South America. *Clinical gastroenterology and hepatology : the official clinical practice journal of the American Gastroenterological Association* **11**, 102

86. Maddineni, G., Choday, S., Morales, A., Aakash, F., Kajal, D., Rehman, O., Karpinska-Leydier, K., Salami, A., Begosh-Mayne, D., and El-Din, M. J. I. B. D. (2024) Shifts in IBD incidence, mortality, and burden: A comprehensive analysis of us and global trends (1990-2019). **30**, S39-S39

87. Wang, Z., He, Z., Chang, X., Xie, L., Song, Y., Wu, H., Zhang, H., Wang, S., Zhang, X., and Bai, Y. (2025) Mitochondrial damage-associated molecular patterns: New perspectives for mitochondria and inflammatory bowel diseases. *Mucosal immunology* **18**, 290-298

88. Serrano León, A., Amir Shaghaghi, M., Yurkova, N., Bernstein, C. N., El-Gabalawy, H., and Eck, P. (2014) Single-nucleotide polymorphisms in SLC22A23 are associated with ulcerative colitis in a Canadian white cohort. *The American journal of clinical nutrition* **100**, 289-294

89. Zhang, M., Xia, S., Feng, L., Han, X., Zhang, Y., Huang, Y., Liu, Y., Zhao, K., Guan, J., Tian, D., Liao, J., and Yu, Y. (2025) Enteric-Coated Aspirin Induces Small Intestinal Injury via the Nrf2/Gpx4 Pathway: A Promising Model for Chronic Enteropathy. *Drug design, development and therapy* **19**, 891-910

90. Wu, S., Liu, H., Yi, J., Xu, M., Jiang, J., Tao, J., and Wu, B. (2024) β-arrestin1 protects intestinal tight junction through promoting mitofusin 2 transcription to drive parkin-dependent mitophagy in colitis. *Gastroenterology report* **12**, goae084

91. Kraimi, N., Lormant, F., Calandreau, L., Kempf, F., Zemb, O., Lemarchand, J., Constantin, P., Parias, C., Germain, K., and Rabot, S. J. P. (2022) Microbiota and stress: a loop that impacts memory. **136**, 105594

92. Cheng, N., Wang, Y., Gu, Z. J. B., and Pharmacotherapy. (2023) Understanding the role of NLRP3-mediated pyroptosis in allergic rhinitis: a review. **165**, 115203

93. Ding, W., Chen, J., Zhao, L., Wu, S., Chen, X., and Chen, H. (2024) Mitochondrial DNA leakage triggers inflammation in age-related cardiovascular diseases. *Frontiers in cell and developmental biology* **12**, 1287447

94. Battogtokh, G., Choi, Y. S., Kang, D. S., Park, S. J., Shim, M. S., Huh, K. M., Cho, Y. Y., Lee, J. Y., Lee, H. S., and Kang, H. C. (2018) Mitochondria-targeting drug conjugates for cytotoxic, anti-oxidizing and sensing purposes: current strategies and future perspectives. *Acta pharmaceutica Sinica. B* **8**, 862-880

95. Buonvicino, D., Ranieri, G., Pittelli, M., Lapucci, A., Bragliola, S., and Chiarugi, A. (2021) SIRT1-dependent restoration of NAD+ homeostasis after increased extracellular NAD+ exposure. *The Journal of biological chemistry* **297**, 100855

96. Ben-Hail, D., Begas-Shvartz, R., Shalev, M., Shteinfer-Kuzmine, A., Gruzman, A., Reina, S., De Pinto, V., and Shoshan-Barmatz, V. (2016) Novel Compounds Targeting the Mitochondrial Protein VDAC1 Inhibit Apoptosis and Protect against Mitochondrial Dysfunction. *The Journal of biological chemistry* **291**, 24986-25003

97. Covarrubias, A. J., Perrone, R., Grozio, A., and Verdin, E. (2021) NAD(+) metabolism and its roles in cellular processes during ageing. *Nature reviews. Molecular cell biology* **22**, 119-141

98. Hubert, S., Rissiek, B., Klages, K., Huehn, J., Sparwasser, T., Haag, F., Koch-Nolte, F., Boyer, O., Seman, M., and Adriouch, S. (2010) Extracellular NAD+ shapes the Foxp3+ regulatory T cell compartment through the ART2-P2X7 pathway. *The Journal of experimental medicine* **207**, 2561-2568

99. Wang, W. F., Li, X., Guo, M. Z., Chen, J. D., Yang, Y. S., Peng, L. H., Wang, Y. H., Zhang, C. Y., and Li, H. H. (2013) Mitochondrial ATP 6 and 8 polymorphisms in irritable bowel syndrome with diarrhea. *World journal of gastroenterology* **19**, 3847-3853

100. van Tilburg, M. A., Zaki, E. A., Venkatesan, T., and Boles, R. G. (2014) Irritable bowel syndrome may be associated with maternal inheritance and mitochondrial DNA control region sequence variants. *Digestive diseases and sciences* **59**, 1392-1397

101. Nath, S., and Balling, R. (2024) The Warburg Effect Reinterpreted 100 yr on: A First-Principles Stoichiometric Analysis and Interpretation from the Perspective of ATP Metabolism in Cancer Cells. *Function (Oxford, England)* **5**, zqae008

102. Tufail, M., Jiang, C.-H., and Li, N. J. M. c. (2024) Altered metabolism in cancer: insights into energy pathways and therapeutic targets. **23**, 203

103. Takaoka, Y., Konno, M., Koseki, J., Colvin, H., Asai, A., Tamari, K., Satoh, T., Mori, M., Doki, Y., Ogawa, K., and Ishii, H. (2019) Mitochondrial pyruvate carrier 1 expression controls cancer epithelial-mesenchymal transition and radioresistance. *Cancer science* **110**, 1331-1339

104. Beloribi-Djefaflia, S., Vasseur, S., and Guillaumond, F. (2016) Lipid metabolic reprogramming in cancer cells. *Oncogenesis* **5**, e189

105. Li, Y., Shi, M., Bie, B., Tian, H., Li, J., Li, Z., and Sun, J. (2025) NRF1-Induced lncRNA DDX11-AS1 Contributes to the Progression of Hepatocellular Carcinoma via Activating CA9 Expression and the MEK/ERK Pathway. *Journal of hepatocellular carcinoma* **12**, 891-908

106. Liu, X., Chen, J., Zhang, S., Liu, X., Long, X., Lan, J., Zhou, M., Zheng, L., and Zhou, J. (2022) LINC00839 promotes colorectal cancer progression by recruiting RUVBL1/Tip60 complexes to activate NRF1. *EMBO reports* **23**, e54128

107. Wang, D., Wan, B., Zhang, X., Sun, P., Lu, S., Liu, C., and Zhu, L. (2022) Nuclear respiratory factor 1 promotes the growth of liver hepatocellular carcinoma cells via E2F1 transcriptional activation. *BMC gastroenterology* **22**, 198

108. Zhan, L., Cao, H., Wang, G., Lyu, Y., Sun, X., An, J., Wu, Z., Huang, Q., Liu, B., and Xing, J. (2016) Drp1-mediated mitochondrial fission promotes cell proliferation through crosstalk of p53 and NF-κB pathways in hepatocellular carcinoma. *Oncotarget* **7**, 65001-65011

109. Hengartner, M. O. (2000) The biochemistry of apoptosis. *Nature* **407**, 770-776

110. Li, B., Wang, W., Li, Z., Chen, Z., Zhi, X., Xu, J., Li, Q., Wang, L., Huang, X., Wang, L., Wei, S., Sun, G., Zhang, X., He, Z., Zhang, L., Zhang, D., Xu, H., El-Rifai, W., and Xu, Z. (2017) MicroRNA-148a-3p enhances cisplatin cytotoxicity in gastric cancer through mitochondrial fission induction and cyto-protective autophagy suppression. *Cancer letters* **410**, 212-227

111. Aung, L. H. H., Li, R., Prabhakar, B. S., Maker, A. V., and Li, P. (2017) Mitochondrial protein 18 (MTP18) plays a pro-apoptotic role in chemotherapy-induced gastric cancer cell apoptosis. *Oncotarget* **8**, 56582-56597

112. Pyakurel, A., Savoia, C., Hess, D., and Scorrano, L. (2015) Extracellular regulated kinase phosphorylates mitofusin 1 to control mitochondrial morphology and apoptosis. *Molecular cell* **58**, 244-254

113. Pal, A. D., Basak, N. P., Banerjee, A. S., and Banerjee, S. J. C. (2014) Epstein–Barr virus latent membrane protein-2A alters mitochondrial dynamics promoting cellular migration mediated by Notch signaling pathway. **35**, 1592-1601

114. Wu, Z., Xiao, C., Li, F., Huang, W., You, F., and Li, X. (2024) Mitochondrial fusion-fission dynamics and its involvement in colorectal cancer. *Molecular oncology* **18**, 1058-1075

115. Zhang, G.-E., Jin, H.-L., Lin, X.-K., Chen, C., Liu, X.-S., Zhang, Q., and Yu, J.-R. J. I. j. o. m. s. (2013) Anti-tumor effects of Mfn2 in gastric cancer. **14**, 13005-13021

116. Hu, H. F., Xu, W. W., Li, Y. J., He, Y., Zhang, W. X., Liao, L., Zhang, Q. H., Han, L., Yin, X. F., Zhao, X. X., Pan, Y. L., Li, B., and He, Q. Y. (2021) Anti-allergic drug azelastine suppresses colon tumorigenesis by directly targeting ARF1 to inhibit IQGAP1-ERK-Drp1-mediated mitochondrial fission. *Theranostics* **11**, 1828-1844

117. Chen, M., Ye, K., Zhang, B., Xin, Q., Li, P., Kong, A. N., Wen, X., and Yang, J. (2019) Paris Saponin II inhibits colorectal carcinogenesis by regulating mitochondrial fission and NF-κB pathway. *Pharmacological research* **139**, 273-285

118. Ni, J., and Zhang, L. (2020) Cancer Cachexia: Definition, Staging, and Emerging Treatments. *Cancer management and research* **12**, 5597-5605

119. Mao, X., Meng, Q., Han, J., Shen, L., Sui, X., Gu, Y., and Wu, G. (2021) Regulation of dynamin-related protein 1 (DRP1) levels modulates myoblast atrophy induced by C26 colon cancer-conditioned medium. *Translational cancer research* **10**, 3020-3032

120. Amini, M. A., Karimi, J., Khodadadi, I., Tavilani, H., Talebi, S. S., and Afshar, B. (2020) Overexpression of ROMO1 and OMA1 are Potentially Biomarkers and Predict Unfavorable Prognosis in Gastric Cancer. *Journal of gastrointestinal cancer* **51**, 939-946

121. Cheng, X., Li, Y., and Liu, F. (2022) Prognostic impact of mitofusin 2 expression in colon cancer. *Translational cancer research* **11**, 3610-3619

122. Wang, M., Luan, S., Fan, X., Wang, J., Huang, J., Gao, X., and Han, D. (2022) The emerging multifaceted role of PINK1 in cancer biology. *Cancer science* **113**, 4037-4047

123. Hsieh, Y. T., Tu, H. F., Yang, M. H., Chen, Y. F., Lan, X. Y., Huang, C. L., Chen, H. M., and Li, W. C. (2021) Mitochondrial genome and its regulator TFAM modulates head and neck tumourigenesis through intracellular metabolic reprogramming and activation of oncogenic effectors. *Cell death & disease* **12**, 961

124. Stamp, C., Whitehall, J. C., Smith, A. L. M., Houghton, D., Bradshaw, C., Stoll, E. A., Blain, A. P., Turnbull, D. M., and Greaves, L. C. (2021) Age-associated mitochondrial complex I deficiency is linked to increased stem cell proliferation rates in the mouse colon. *Aging cell* **20**, e13321

125. Smith, A. L. M., Whitehall, J. C., and Greaves, L. C. (2022) Mitochondrial DNA mutations in ageing and cancer. *Molecular oncology* **16**, 3276-3294

126. Rauckhorst, A. J., and Taylor, E. B. (2016) Mitochondrial pyruvate carrier function and cancer metabolism. *Current opinion in genetics & development* **38**, 102-109

127. Phan, L. M., Yeung, S. C., and Lee, M. H. (2014) Cancer metabolic reprogramming: importance, main features, and potentials for precise targeted anti-cancer therapies. *Cancer biology & medicine* **11**, 1-19

128. Sun, X., Zhan, L., Chen, Y., Wang, G., He, L., Wang, Q., Zhou, F., Yang, F., Wu, J., Wu, Y., Xing, J., He, X., and Huang, Q. (2018) Increased mtDNA copy number promotes cancer progression by enhancing mitochondrial oxidative phosphorylation in microsatellite-stable colorectal cancer. *Signal transduction and targeted therapy* **3**, 8

129. Shi, Q., Xue, C., Zeng, Y., Yuan, X., Chu, Q., Jiang, S., Wang, J., Zhang, Y., Zhu, D., and Li, L. (2024) Notch signaling pathway in cancer: from mechanistic insights to targeted therapies. *Signal transduction and targeted therapy* **9**, 128

130. Han, J., Yuan, Y., Zhang, J., Hou, Y., Xu, H., Nie, X., Zhao, Z., and Hou, J. (2025) Regulatory effect of Wnt signaling on mitochondria in cancer: from mechanism to therapy. *Apoptosis : an international journal on programmed cell death* **30**, 1235-1252

131. Lanas, A., and Chan, F. K. J. T. L. (2017) Peptic ulcer disease. **390**, 613-624

132. Kuna, L., Jakab, J., Smolic, R., Raguz-Lucic, N., Vcev, A., and Smolic, M. (2019) Peptic Ulcer Disease: A Brief Review of Conventional Therapy and Herbal Treatment Options. *Journal of clinical medicine* **8**

133. Han, L., Shu, X., and Wang, J. (2022) Helicobacter pylori-Mediated Oxidative Stress and Gastric Diseases: A Review. *Frontiers in microbiology* **13**, 811258

134. Akash, S. R., Tabassum, A., Aditee, L. M., Rahman, A., Hossain, M. I., Hannan, M. A., Uddin, M. J. J. B., and Pharmacotherapy. (2024) Pharmacological insight of rutin as a potential candidate against peptic ulcer. **177**, 116961

135. Butcher, L. D., den Hartog, G., Ernst, P. B., and Crowe, S. E. (2017) Oxidative Stress Resulting From Helicobacter pylori Infection Contributes to Gastric Carcinogenesis. *Cellular and molecular gastroenterology and hepatology* **3**, 316-322

136. Salehi, Z., Haghighi, A., Haghighi, S., Aminian, K., Asl, S., and Mashayekhi, F. J. M. B. (2017) Mitochondrial DNA deletion Δ4977 in peptic ulcer disease. **51**, 30-33

137. De, R., Mazumder, S., Sarkar, S., Debsharma, S., Siddiqui, A. A., Saha, S. J., Banerjee, C., Nag, S., Saha, D., and Bandyopadhyay, U. (2017) Acute mental stress induces mitochondrial bioenergetic crisis and hyper-fission along with aberrant mitophagy in the gut mucosa in rodent model of stress-related mucosal disease. *Free radical biology & medicine* **113**, 424-438

138. den Besten, G., van Eunen, K., Groen, A. K., Venema, K., Reijngoud, D. J., and Bakker, B. M. (2013) The role of short-chain fatty acids in the interplay between diet, gut microbiota, and host energy metabolism. *Journal of lipid research* **54**, 2325-2340

139. Zhang, Y., Zhang, J., and Duan, L. J. P. r. (2022) The role of microbiota-mitochondria crosstalk in pathogenesis and therapy of intestinal diseases. **186**, 106530

140. O'Riordan, K. J., Collins, M. K., Moloney, G. M., Knox, E. G., Aburto, M. R., Fülling, C., Morley, S. J., Clarke, G., Schellekens, H., and Cryan, J. F. (2022) Short chain fatty acids: Microbial metabolites for gut-brain axis signalling. *Molecular and cellular endocrinology* **546**, 111572

141. Liu, H., Wang, J., He, T., Becker, S., Zhang, G., Li, D., and Ma, X. (2018) Butyrate: A Double-Edged Sword for Health? *Advances in nutrition (Bethesda, Md.)* **9**, 21-29

142. Hodgkinson, K., El Abbar, F., Dobranowski, P., Manoogian, J., Butcher, J., Figeys, D., Mack, D., and Stintzi, A. (2023) Butyrate's role in human health and the current progress towards its clinical application to treat gastrointestinal disease. *Clinical nutrition (Edinburgh, Scotland)* **42**, 61-75

143. Mollica, M. P., Mattace Raso, G., Cavaliere, G., Trinchese, G., De Filippo, C., Aceto, S., Prisco, M., Pirozzi, C., Di Guida, F., Lama, A., Crispino, M., Tronino, D., Di Vaio, P., Berni Canani, R., Calignano, A., and Meli, R. (2017) Butyrate Regulates Liver Mitochondrial Function, Efficiency, and Dynamics in Insulin-Resistant Obese Mice. *Diabetes.*. **66**, 1405-1418

144. Hinrichsen, F., Hamm, J., Westermann, M., Schröder, L., Shima, K., Mishra, N., Walker, A., Sommer, N., Klischies, K., Prasse, D., Zimmermann, J., Kaiser, S., Bordoni, D., Fazio, A., Marinos, G., Laue, G., Imm, S., Tremaroli, V., Basic, M., Häsler, R., Schmitz, R. A., Krautwald, S., Wolf, A., Stecher, B., Schmitt-Kopplin, P., Kaleta, C., Rupp, J., Bäckhed, F., Rosenstiel, P., and Sommer, F. (2021) Microbial regulation of hexokinase 2 links mitochondrial metabolism and cell death in colitis. *Cell metabolism* **33**, 2355-2366.e2358

145. Guan, B., Tong, J., Hao, H., Yang, Z., Chen, K., Xu, H., and Wang, A. (2022) Bile acid coordinates microbiota homeostasis and systemic immunometabolism in cardiometabolic diseases. *Acta pharmaceutica Sinica. B* **12**, 2129-2149

146. Ignacio Barrasa, J., Olmo, N., Pérez-Ramos, P., Santiago-Gómez, A., Lecona, E., Turnay, J., and Antonia Lizarbe, M. (2011) Deoxycholic and chenodeoxycholic bile acids induce apoptosis via oxidative stress in human colon adenocarcinoma cells. *Apoptosis : an international journal on programmed cell death* **16**, 1054-1067

147. Hu, C., Huang, Y., and Li, L. (2017) Drp1-Dependent Mitochondrial Fission Plays Critical Roles in Physiological and Pathological Progresses in Mammals. *International journal of molecular sciences* **18**

148. Sun, Z., Ji, Z., Meng, H., He, W., Li, B., Pan, X., Zhou, Y., and Yu, G. (2024) Lactate facilitated mitochondrial fission-derived ROS to promote pulmonary fibrosis via ERK/DRP-1 signaling. *Journal of translational medicine* **22**, 479

149. Nguyen, H. V. M., Cabello, E., Dyer, D., Fender, C., Garcia-Jaramillo, M., Hord, N. G., Austad, S., Richardson, A., and Unnikrishnan, A. (2025) Age, sex, and mitochondrial-haplotype influence gut microbiome composition and metabolites in a genetically diverse rat model. *Aging* **17**, 524-549

150. Dayton, T. L., and Clevers, H. (2017) Beyond growth signaling: Paneth cells metabolically support ISCs. *Cell research* **27**, 851-852

151. Berger, E., Rath, E., Yuan, D., Waldschmitt, N., Khaloian, S., Allgäuer, M., Staszewski, O., Lobner, E. M., Schöttl, T., Giesbertz, P., Coleman, O. I., Prinz, M., Weber, A., Gerhard, M., Klingenspor, M., Janssen, K. P., Heikenwalder, M., and Haller, D. (2016) Mitochondrial function controls intestinal epithelial stemness and proliferation. *Nature communications* **7**, 13171

152. Duscha, A., Gisevius, B., Hirschberg, S., Yissachar, N., Stangl, G. I., Dawin, E., Bader, V., Haase, S., Kaisler, J., David, C., Schneider, R., Troisi, R., Zent, D., Hegelmaier, T., Dokalis, N., Gerstein, S., Del Mare-Roumani, S., Amidror, S., Staszewski, O., Poschmann, G., Stühler, K., Hirche, F., Balogh, A., Kempa, S., Träger, P., Zaiss, M. M., Holm, J. B., Massa, M. G., Nielsen, H. B., Faissner, A., Lukas, C., Gatermann, S. G., Scholz, M., Przuntek, H., Prinz, M., Forslund, S. K., Winklhofer, K. F., Müller, D. N., Linker, R. A., Gold, R., and Haghikia, A. (2020) Propionic Acid Shapes the Multiple Sclerosis Disease Course by an Immunomodulatory Mechanism. *Cell* **180**, 1067-1080.e1016

153. Liang, Y., Cui, L., Gao, J., Zhu, M., Zhang, Y., and Zhang, H. L. (2021) Gut Microbial Metabolites in Parkinson's Disease: Implications of Mitochondrial Dysfunction in the Pathogenesis and Treatment. *Molecular neurobiology* **58**, 3745-3758

154. Bandopadhyay, P., Ganguly, D. J. P. i. m. b., and science, t. (2022) Gut dysbiosis and metabolic diseases. **191**, 153-174

155. Singh, R., Zogg, H., Wei, L., Bartlett, A., Ghoshal, U. C., Rajender, S., and Ro, S. (2021) Gut Microbial Dysbiosis in the Pathogenesis of Gastrointestinal Dysmotility and Metabolic Disorders. *Journal of neurogastroenterology and motility* **27**, 19-34

156. Li, Y., Yang, S., Jin, X., Li, D., Lu, J., Wang, X., and Wu, M. (2023) Mitochondria as novel mediators linking gut microbiota to atherosclerosis that is ameliorated by herbal medicine: A review. *Frontiers in pharmacology* **14**, 1082817

157. Guo, W., Wang, P., Liu, Z. H., and Ye, P. (2018) Analysis of differential expression of tight junction proteins in cultured oral epithelial cells altered by Porphyromonas gingivalis, Porphyromonas gingivalis lipopolysaccharide, and extracellular adenosine triphosphate. *International journal of oral science* **10**, e8

158. Odenwald, M. A., and Turner, J. R. (2017) The intestinal epithelial barrier: a therapeutic target? *Nature reviews. Gastroenterology & hepatology* **14**, 9-21

159. Towler, M. C., and Hardie, D. G. (2007) AMP-activated protein kinase in metabolic control and insulin signaling. *Circulation research* **100**, 328-341

160. Hardie, D. G. (2011) AMP-activated protein kinase: an energy sensor that regulates all aspects of cell function. *Genes & development* **25**, 1895-1908

161. Rowart, P., Wu, J., Caplan, M. J., and Jouret, F. (2018) Implications of AMPK in the Formation of Epithelial Tight Junctions. *International journal of molecular sciences* **19**

162. Rose, S., Bennuri, S. C., Davis, J. E., Wynne, R., Slattery, J. C., Tippett, M., Delhey, L., Melnyk, S., Kahler, S. G., MacFabe, D. F., and Frye, R. E. (2018) Butyrate enhances mitochondrial function during oxidative stress in cell lines from boys with autism. *Translational psychiatry* **8**, 42

163. Grazioli, S., and Pugin, J. J. F. i. i. (2018) Mitochondrial damage-associated molecular patterns: from inflammatory signaling to human diseases. **9**, 832

164. Singhal, R., and Shah, Y. M. J. J. o. B. C. (2020) Oxygen battle in the gut: Hypoxia and hypoxia-inducible factors in metabolic and inflammatory responses in the intestine. **295**, 10493-10505

165. Leclerc, M., Bedu-Ferrari, C., Etienne-Mesmin, L., Mariadassou, M., Lebreuilly, L., Tran, S.-L., Brazeau, L., Mayeur, C., Delmas, J., and Rué, O. J. M. (2021) Nitric oxide impacts human gut microbiota diversity and functionalities. **6**, 10.1128/msystems. 00558-00521

166. Zhou, D., Shao, L., and Spitz, D. R. (2014) Reactive oxygen species in normal and tumor stem cells. *Advances in cancer research* **122**, 1-67

167. Burtenshaw, D., Hakimjavadi, R., Redmond, E. M., and Cahill, P. A. J. A. (2017) Nox, reactive oxygen species and regulation of vascular cell fate. **6**, 90

168. Bindu, S., Mazumder, S., and Bandyopadhyay, U. (2020) Non-steroidal anti-inflammatory drugs (NSAIDs) and organ damage: A current perspective. *Biochemical pharmacology* **180**, 114147

169. Chen, Y., Jiang, Z., and Li, X. (2024) New insights into crosstalk between Nrf2 pathway and ferroptosis in lung disease. *Cell death & disease* **15**, 841

170. Rajendran, R., Garva, R., Krstic-Demonacos, M., and Demonacos, C. (2011) Sirtuins: molecular traffic lights in the crossroad of oxidative stress, chromatin remodeling, and transcription. *Journal of biomedicine & biotechnology* **2011**, 368276

171. Yang, Y., Liu, Y., Wang, Y., Chao, Y., Zhang, J., Jia, Y., Tie, J., and Hu, D. (2022) Regulation of SIRT1 and Its Roles in Inflammation. *Frontiers in immunology* **13**, 831168

172. Chellappa, K., McReynolds, M. R., Lu, W., Zeng, X., Makarov, M., Hayat, F., Mukherjee, S., Bhat, Y. R., Lingala, S. R., Shima, R. T., Descamps, H. C., Cox, T., Ji, L., Jankowski, C., Chu, Q., Davidson, S. M., Thaiss, C. A., Migaud, M. E., Rabinowitz, J. D., and Baur, J. A. (2022) NAD precursors cycle between host tissues and the gut microbiome. *Cell metabolism* **34**, 1947-1959.e1945

173. Kitada, M., Araki, S. I., and Koya, D. (2023) The Role of CD38 in the Pathogenesis of Cardiorenal Metabolic Disease and Aging, an Approach from Basic Research. *Cells* **12**

174. Lettieri Barbato, D., Baldelli, S., Pagliei, B., Aquilano, K., and Ciriolo, M. R. (2012) Caloric Restriction and the Nutrient-Sensing PGC-1α in Mitochondrial Homeostasis: New Perspectives in Neurodegeneration. *International journal of cell biology* **2012**, 759583

175. Lin, M. M., Liu, N., Qin, Z. H., and Wang, Y. (2022) Mitochondrial-derived damage-associated molecular patterns amplify neuroinflammation in neurodegenerative diseases. *Acta pharmacologica Sinica* **43**, 2439-2447

176. Li, S., Hu, Q., Huang, J., Wu, X., and Ren, J. (2019) Mitochondria-Derived Damage-Associated Molecular Patterns in Sepsis: From Bench to Bedside. *Oxidative medicine and cellular longevity* **2019**, 6914849

177. Sui, G. Y., Wang, F., Lee, J., and Roh, Y. S. (2022) Mitochondrial Control in Inflammatory Gastrointestinal Diseases. *International journal of molecular sciences* **23**

178. Fubini, B., and Hubbard, A. (2003) Reactive oxygen species (ROS) and reactive nitrogen species (RNS) generation by silica in inflammation and fibrosis. *Free radical biology & medicine* **34**, 1507-1516

179. Mittal, M., Siddiqui, M. R., Tran, K., Reddy, S. P., and Malik, A. B. (2014) Reactive oxygen species in inflammation and tissue injury. *Antioxidants & redox signaling* **20**, 1126-1167

180. Boyapati, R. K., Dorward, D. A., Tamborska, A., Kalla, R., Ventham, N. T., Doherty, M. K., Whitfield, P. D., Gray, M., Loane, J., Rossi, A. G., Satsangi, J., and Ho, G. T. (2018) Mitochondrial DNA Is a Pro-Inflammatory Damage-Associated Molecular Pattern Released During Active IBD. *Inflammatory bowel diseases* **24**, 2113-2122

181. Chassaing, B., Aitken, J. D., Malleshappa, M., and Vijay-Kumar, M. (2014) Dextran sulfate sodium (DSS)-induced colitis in mice. *Current protocols in immunology* **104**, 15.25.11-15.25.14

182. Fang, C., Wei, X., and Wei, Y. (2016) Mitochondrial DNA in the regulation of innate immune responses. *Protein & cell* **7**, 11-16

183. Shimada, K., Crother, T. R., Karlin, J., Dagvadorj, J., Chiba, N., Chen, S., Ramanujan, V. K., Wolf, A. J., Vergnes, L., and Ojcius, D. M. J. I. (2012) Oxidized mitochondrial DNA activates the NLRP3 inflammasome during apoptosis. **36**, 401-414

184. Liu, W., Guo, W., Wu, J., Luo, Q., Tao, F., Gu, Y., Shen, Y., Li, J., Tan, R., Xu, Q., and Sun, Y. (2013) A novel benzo[d]imidazole derivate prevents the development of dextran sulfate sodium-induced murine experimental colitis via inhibition of NLRP3 inflammasome. *Biochemical pharmacology* **85**, 1504-1512

185. Tang, D., Chen, X., Kang, R., and Kroemer, G. J. C. r. (2021) Ferroptosis: molecular mechanisms and health implications. **31**, 107-125

186. Chen, Y., Zhang, P., Chen, W., and Chen, G. J. I. l. (2020) Ferroptosis mediated DSS-induced ulcerative colitis associated with Nrf2/HO-1 signaling pathway. **225**, 9-15

187. Giordano, L., Ware, S. A., Lagranha, C. J., and Kaufman, B. A. (2025) Mitochondrial DNA signals driving immune responses: Why, How, Where? *Cell communication and signaling : CCS* **23**, 192

188. Pérez-Treviño, P., Velásquez, M., and García, N. J. B. e. B. A.-M. B. o. D. (2020) Mechanisms of mitochondrial DNA escape and its relationship with different metabolic diseases. **1866**, 165761

189. Neurath, M. F., Artis, D., Becker, C. J. T. L. G., and Hepatology. (2025) The intestinal barrier: a pivotal role in health, inflammation, and cancer.

190. Liang, G. H., and Weber, C. R. J. C. o. i. p. (2014) Molecular aspects of tight junction barrier function. **19**, 84-89

191. Chernyavskij, D., Galkin, I., Pavlyuchenkova, A., Fedorov, A., and Chelombitko, M. J. M. B. (2023) Role of mitochondria in intestinal epithelial barrier dysfunction in inflammatory bowel disease. **57**, 1024-1037

192. Rigor, R. R., Shen, Q., Pivetti, C. D., Wu, M. H., and Yuan, S. Y. (2013) Myosin light chain kinase signaling in endothelial barrier dysfunction. *Medicinal research reviews* **33**, 911-933

193. Gao, Y., Meng, L., Liu, H., Wang, J., and Zheng, N. (2020) The Compromised Intestinal Barrier Induced by Mycotoxins. *Toxins* **12**

194. Fock, E. M., and Parnova, R. G. J. P. (2021) Protective effect of mitochondria-targeted antioxidants against inflammatory response to lipopolysaccharide challenge: a review. **13**, 144

195. Iba, T., Levy, J. J. J. o. t., and haemostasis. (2019) Derangement of the endothelial glycocalyx in sepsis. **17**, 283-294

196. Li, J., Geng, Z., Yin, L., Huang, J., Niu, M., Zhang, K., Song, X., Wang, Y., Zuo, L., and Hu, J. J. A. (2025) Engeletin Targets Mitochondrial Dysfunction to Attenuate Oxidative Stress and Experimental Colitis in Intestinal Epithelial Cells Through AMPK/SIRT1/PGC-1α Signaling. **14**, 524

197. Chen, K., Wang, H., Yang, X., Tang, C., Hu, G., and Gao, Z. J. P. R. (2024) Targeting gut microbiota as a therapeutic target in T2DM: A review of multi-target interactions of probiotics, prebiotics, postbiotics, and synbiotics with the intestinal barrier. **210**, 107483

198. Zhang, Y. G., Wu, S., Lu, R., Zhou, D., Zhou, J., Carmeliet, G., Petrof, E., Claud, E. C., and Sun, J. (2015) Tight junction CLDN2 gene is a direct target of the vitamin D receptor. *Scientific reports* **5**, 10642

199. Wang, J., Mei, L., Hao, Y., Xu, Y., Yang, Q., Dai, Z., Yang, Y., Wu, Z., and Ji, Y. (2024) Contemporary Perspectives on the Role of Vitamin D in Enhancing Gut Health and Its Implications for Preventing and Managing Intestinal Diseases. *Nutrients* **16**

200. Putt, K. K., Pei, R., White, H. M., and Bolling, B. W. (2017) Yogurt inhibits intestinal barrier dysfunction in Caco-2 cells by increasing tight junctions. *Food & function* **8**, 406-414

201. Cardona, F., Andrés-Lacueva, C., Tulipani, S., Tinahones, F. J., and Queipo-Ortuño, M. I. J. T. J. o. n. b. (2013) Benefits of polyphenols on gut microbiota and implications in human health. **24**, 1415-1422

202. Suzuki, T., and Hara, H. (2009) Quercetin enhances intestinal barrier function through the assembly of zonula [corrected] occludens-2, occludin, and claudin-1 and the expression of claudin-4 in Caco-2 cells. *The Journal of nutrition* **139**, 965-974

203. Ho, G. T., and Theiss, A. L. (2022) Mitochondria and Inflammatory Bowel Diseases: Toward a Stratified Therapeutic Intervention. *Annual review of physiology* **84**, 435-459

204. Suzuki, T., Tanabe, S., and Hara, H. (2011) Kaempferol enhances intestinal barrier function through the cytoskeletal association and expression of tight junction proteins in Caco-2 cells. *The Journal of nutrition* **141**, 87-94

205. Zhang, Y., Wu, Q., Liu, J., Zhang, Z., Ma, X., Zhang, Y., Zhu, J., Thring, R. W., Wu, M., Gao, Y. J. B., and Pharmacotherapy. (2022) Sulforaphane alleviates high fat diet-induced insulin resistance via AMPK/Nrf2/GPx4 axis. **152**, 113273

206. Porras, D., Nistal, E., Martínez-Flórez, S., Olcoz, J. L., Jover, R., Jorquera, F., González-Gallego, J., García-Mediavilla, M. V., Sánchez-Campos, S. J. M. N., and Research, F. (2019) Functional interactions between gut microbiota transplantation, quercetin, and high-fat diet determine non-alcoholic fatty liver disease development in germ-free mice. **63**, 1800930

207. Gillespie, Z. E., Pickering, J., and Eskiw, C. H. J. F. i. G. (2016) Better living through chemistry: caloric restriction (CR) and CR mimetics alter genome function to promote increased health and lifespan. **7**, 142

208. Zielonka, J., Joseph, J., Sikora, A., Hardy, M., Ouari, O., Vasquez-Vivar, J., Cheng, G., Lopez, M., and Kalyanaraman, B. (2017) Mitochondria-Targeted Triphenylphosphonium-Based Compounds: Syntheses, Mechanisms of Action, and Therapeutic and Diagnostic Applications. *Chemical reviews* **117**, 10043-10120

209. Teixeira, J., Deus, C. M., Borges, F., Oliveira, P. J. J. T. i. j. o. b., and biology, c. (2018) Mitochondria: Targeting mitochondrial reactive oxygen species with mitochondriotropic polyphenolic-based antioxidants. **97**, 98-103

210. Mazumder, S., De, R., Sarkar, S., Siddiqui, A. A., Saha, S. J., Banerjee, C., Iqbal, M. S., Nag, S., Debsharma, S., and Bandyopadhyay, U. (2016) Selective scavenging of intra-mitochondrial superoxide corrects diclofenac-induced mitochondrial dysfunction and gastric injury: A novel gastroprotective mechanism independent of gastric acid suppression. *Biochemical pharmacology* **121**, 33-51

211. Chernyavskij, D. A., Galkin, II, Pavlyuchenkova, A. N., Fedorov, A. V., and Chelombitko, M. A. (2023) [Role of Mitochondria in Intestinal Epithelial Barrier Dysfunction in Inflammatory Bowel Disease]. *Molekuliarnaia biologiia* **57**, 1028-1042

212. Sharifi-Rad, M., Fokou, P. V. T., Sharopov, F., Martorell, M., Ademiluyi, A. O., Rajkovic, J., Salehi, B., Martins, N., Iriti, M., and Sharifi-Rad, J. J. M. (2018) Antiulcer agents: From plant extracts to phytochemicals in healing promotion. **23**, 1751

213. Mousavi, T., Hadizadeh, N., Nikfar, S., and Abdollahi, M. J. E. O. o. D. D. (2020) Drug discovery strategies for modulating oxidative stress in gastrointestinal disorders. **15**, 1309-1341

214. Smith, G., and Gallo, G. (2017) To mdivi-1 or not to mdivi-1: Is that the question? *Developmental neurobiology* **77**, 1260-1268

215. Bordt, E. A., Clerc, P., Roelofs, B. A., Saladino, A. J., Tretter, L., Adam-Vizi, V., Cherok, E., Khalil, A., Yadava, N., Ge, S. X., Francis, T. C., Kennedy, N. W., Picton, L. K., Kumar, T., Uppuluri, S., Miller, A. M., Itoh, K., Karbowski, M., Sesaki, H., Hill, R. B., and Polster, B. M. (2017) The Putative Drp1 Inhibitor mdivi-1 Is a Reversible Mitochondrial Complex I Inhibitor that Modulates Reactive Oxygen Species. *Developmental cell* **40**, 583-594.e586

216. Oyewole, A. O., Wilmot, M. C., Fowler, M., and Birch-Machin, M. A. (2014) Comparing the effects of mitochondrial targeted and localized antioxidants with cellular antioxidants in human skin cells exposed to UVA and hydrogen peroxide. *FASEB journal : official publication of the Federation of American Societies for Experimental Biology* **28**, 485-494

EXPERIMENTAL CHAPTER

Acute mental stress impairs mitochondrial biogenesis in the gastric mucosa and activates GR signaling to induce gastric mucosal injury

1. INTRODUCTION

Mental and gastric health are deeply interconnected through the gut-brain axis, a complex bidirectional communication system regulated by millions of nerves and biochemical signals. Psychological stress has been linked to various gastrointestinal disorders, including peptic ulcers. Stress-induced gastric mucosal damage is frequently observed in critically ill patients requiring mechanical ventilation, individuals with septic shock, and those suffering from severe burns covering more than 35% of their body surface area (1). Emerging evidence suggests that acute psychological stress plays a critical role in the pathophysiology of various gastrointestinal disorders, including peptic ulcers and inflammatory bowel disease (IBD) (2-5). The impact of stress on the gastrointestinal system extends beyond functional disturbances, often leading to structural damage such as stress-related mucosal disease (SRMD) and gastric ulcers (6,7). One of the most striking demonstrations of this relationship comes from natural disasters, which expose individuals to extreme psychological distress. Studies conducted after the Great East Japan Earthquake (2011) and the Hanshin-Awaji Earthquake (1995) have highlighted a significant increase in the incidence of stress-induced gastric ulcers and IBD exacerbations among affected populations (8-10). A retrospective cohort study found that ulcerative colitis (UC) patients experienced nearly twice the relapse rate after the earthquake compared to the same period the previous year. In contrast, Crohn's disease (CD) remained largely unaffected. These findings emphasize the differential impact of stress on the gastrointestinal tract, with UC being more stress-sensitive than CD (10). A Danish study tracking 3,379 adults over 11–12 years found that individuals with high stress scores had a significantly higher ulcer incidence (3.5% vs. 1.6%, $P < .01$) (10). Stress remained an independent ulcer risk factor, even after adjusting for *H. pylori*, alcohol use, sleep patterns, and NSAID use (11). Beyond its epidemiological significance, psychological stress is increasingly recognized as a key contributor to gastric mucosal injury at the cellular level. In this study, a representative animal model of acute mental stress was used (12). It was observed that cold-restraint stress in rats caused severe impairment of mitochondrial biogenesis, leading to a bioenergetic crisis in gastric mucosal tissues. This impairment arises from the disruption of mitochondrial biogenesis, compounded by stress-induced elevation of serum corticosterone levels. Specifically, stress-mediated proteasomal degradation of PGC-1α, coupled with dysregulated fatty acid metabolism and electron transport chain (ETC) dysfunction, results in mitochondrial impairment, oxidative stress, and compromised energy homeostasis.

In this rat model of SRMD, cold-restraint stress triggered significant mitochondrial dysfunction, characterized by downregulation of mitochondria-encoded ETC genes, reflecting bioenergetic failure. Interestingly, while PGC-1α gene expression paradoxically increased, its protein levels declined, probably due to ubiquitination-mediated degradation. Furthermore, the main transcriptional regulator NRF1, the direct target of PGC-1α, was significantly downregulated at both gene and protein levels, leading to a substantial reduction in TFAM, a critical factor for mitochondrial DNA replication and transcription (13,14). Mechanistic study further revealed that stress-induced elevation of serum corticosterone activates the glucocorticoid receptor (GR), facilitating its translocation to the nucleus and initiating transcriptional reprogramming that enhances ubiquitin-mediated proteasomal degradation, thereby contributing to mitochondrial dysfunction. Notably, this study is the first to identify and elucidate the activation of the GR–KLF15–FBXO32 signalling axis in stress-induced gastric injury. It was demonstrated that acute psychological stress impairs the electron transport chain (ETC) within gastric mucosal cells, resulting in electron leakage and excessive production of reactive oxygen species (ROS). This oxidative milieu, in synergy with GR activation, induces the upregulation of KLF15 and FBXO32, accelerating the proteasomal degradation of essential mitochondrial regulatory proteins and ultimately compromising mitochondrial biogenesis and function. To counteract this, three

mechanistically distinct therapeutic strategies were employed. First, pre-treatment with quercetin-3-glucoside (Q3G), a natural antioxidant polyphenolic derivative, preserved mitochondrial gene expression, reduced oxidative stress, and stabilized mitochondrial biogenesis regulators such as PGC-1α and TFAM. Second, olanzapine, an antipsychotic agent, attenuated systemic corticosterone elevation and downregulated GR-responsive catabolic genes, partially restoring mitochondrial bioenergetics. Third, RU486, a competitive GR antagonist, most effectively blocked GR-mediated transcriptional activation of the KLF15–FBXO32 pathway, resulting in preserved mitochondrial integrity and ATP production despite elevated corticosterone levels. These findings underscore the central role of ETC dysfunction and GR-driven proteostatic imbalance in the pathogenesis of stress-induced mitochondrial injury. Targeting these mechanisms, either by inhibiting GR signaling, modulating central stress perception, or enhancing antioxidant defences, offers a multifaceted and promising therapeutic strategy. Collectively, the protective effects of RU486, olanzapine, and Q3G highlight the potential of mitochondria-targeted interventions in mitigating acute stress-induced gastric pathology and lay the groundwork for future therapies aimed at preserving gastric mucosal health under psychological stress.

2. MATERIALS AND METHODS

2.1. Materials

Sodium azide, fatty acid-free BSA, quercetin 3-glucoside, RU486, along with HRP-conjugated secondary antibodies targeting rabbit and mouse, were obtained from Sigma (St. Louis, MO, USA). The TRIzol, RevertAid H Minus First Strand cDNA Synthesis kit, PureLink RNA Mini Kit, Nuclease-free water, PCR Master Mix, PBS (HyClone), Alexa Fluor 647 antibody, and Hoechst 33342 were procured from Thermo Fisher Scientific (Waltham, MA, USA). Mitochondria Isolation Kit was procured from BioChain. 5,5,'6,6'-tetrachloro1,1',3,3'-tetraethylbenzimidazol-carbocyanine iodide (JC-1) was procured from Invitrogen. Protease inhibitor cocktail (Set V) was purchased from Calbiochem. Sulfosalicylic acid was obtained from SRL (Mumbai, India). Fatty acid oxidation enzyme activity assay kits (Catalogue No E-141L and E-141M) were procured from the Biomedical Research Service Center, State University of New York (Buffalo, NY). Serum corticosterone ELISA kit was procured from Abcam (Boston, MA, USA). Luminata Forte HRP substrate, for ECL-based chemiluminescence, was obtained from Mark-Millipore. Nitrocellulose transfer membrane (BioTrace NT) was purchased from Pall Corporation (Port Washington, NY, USA). All additional reagents used were of analytical grade quality.

2.2. Animal model of stress-induced gastric mucosal damage and pharmacological interventions

All *in vivo* experiments were conducted in strict compliance with the guidelines of the Institutional Animal Ethics Committee (IAEC) of CSIR-IICB, which is registered under CPCSEA, India (Permit Number: 147/1999/CPCSEA). Every effort was made to ensure humane treatment of the animals and to minimize discomfort, distress, or pain during all stages of experimental handling. Sprague-Dawley rats weighing between 200-250 g were maintained under standardized environmental conditions (24 ± 2 °C, 12-hour light/dark cycle) with unrestricted access to water. To eliminate dietary influences on gastric acid secretion and mucosal sensitivity, animals were fasted for 24 hours prior to experimentation. Acute gastric mucosal injury was induced using a cold-restraint stress (CRS) model, in which rats were immobilized in a dorsal supine position on a wooden platform under light ether anaesthesia and exposed to a cold environment (4 ± 1 °C) for 3.5 hours, as previously described(12,15). Age-matched, fasted control animals were maintained at room temperature in normothermic, non-stressed conditions for the same duration. Pharmacological agents were administered according to

established protocols. Quercetin-3-glucoside (10 mg/kg, b.w.) was administered intraperitoneally 60 minutes before CRS exposure, with this dose previously identified in this study as optimal based on dose–response analysis. RU486 (20 mg/kg body weight), suspended in 0.5% carboxymethyl cellulose (CMC) with 0.05% Tween-20, was administered via oral gavage 40 minutes before stress induction. Olanzapine (10 mg/kg, b.w.) was administered by intraperitoneal injection in sterile 0.9% saline, one hour before stress exposure. The dosages of the aforementioned molecules were determined based on previous studies (16,17). Appropriate vehicle controls were included to account for potential solvent effects. Each experimental group included five rats (n = 5). Gastric mucosal injury was evaluated by calculating the Injury Index (II), defined as the percentage of mucosal surface area exhibiting lesions such as haemorrhagic erosions, blood clots, and hyperaemia, scored in a blinded manner to prevent observer bias, as described earlier (18). Tissues intended for gene expression analysis were preserved in RNAlater (Sigma-Aldrich), whereas those designated for metabolomic and protein analyses were rapidly snap-frozen in liquid nitrogen. Mitochondrial fractions were subsequently isolated using a commercial mitochondria isolation kit, as described in the corresponding methods section below.

2.3. Histological evaluation of gastric mucosa

Gastric mucosal tissues were fixed in 10% neutral-buffered formalin, followed by paraffin embedding. Semi-thin sections measuring 5 μm were prepared using a microtome and mounted onto glass slides. Xylene was used for the deparaffinization of these sections, and then rehydrated through a graded ethanol series, and stained with hematoxylin and eosin (H&E) to assess cellular and tissue architecture. Histopathological evaluation was conducted using a Leica DM-2500 light microscope (Leica Microsystems, Wetzlar, Germany), enabling detailed visualization of morphological changes across the experimental groups.

2.4. Next-generation sequencing-based transcriptomic analysis

Transcriptomic analysis was performed through total RNA sequencing using the TruSeq Stranded Total RNA Library Preparation Kit (Illumina). Total RNA was isolated from approximately 45 mg of tissue using the PureLink RNA Mini Kit (Thermo Fisher Scientific), adhering strictly to the manufacturer's protocols. The quality and concentration of RNA were evaluated using the NanoDrop 2000 spectrophotometer (Thermo Fisher Scientific) and the Agilent 2100 Bioanalyzer. Only RNA samples with an RNA Integrity Number (RIN) ≥ 7.0 were included in the library preparation. For each sample, 200 ng of high-quality RNA was processed through ribosomal RNA depletion using the Ribo-Zero Human/Mouse/Rat module. The remaining RNA was fragmented by divalent cation treatment, purified, and then used for first-strand cDNA synthesis, A-tailing, and ligation of dual-index adapters. The libraries were subsequently purified, amplified via PCR, and quality-checked using the Agilent 2200 TapeStation (Agilent Technologies). Following quantification and normalization, the libraries were pooled at equimolar concentrations and sequenced using paired-end reads (100 bp) on the Illumina NovaSeq 6000 platform. The raw output Bcl files were converted to Fastq format and assessed for quality using FastQC v0.11.7 (19). Adapter sequences were trimmed using Cutadapt v1.16 (20). High-quality reads were aligned to the Rat Rnor6 reference genome using Hisat2 v2.1.0 (21), and the resulting BAM files were sorted with SAMtools v1.19 (22). Read counts were obtained using FeatureCounts (23), and differential gene expression analysis was conducted using DESeq2 (24). Genes with a fold-change ≥1.5 or ≤1.5, P-value ≤ 0.05, and false discovery rate (FDR) ≤ 0.05 were considered differentially expressed (DEGs). For rat gastric mucosal samples, an additional filtering criterion (≥1.2 or ≤1.2 fold-change, P-value ≤ 0.05, and FDR ≤ 0.05) was applied to specifically identify genes implicated in mitochondrial metabolism and function. Enrichment and pathway analyses of the DEGs were performed using Ingenuity Pathway Analysis (IPA). The transcriptomic data generated from rat

samples have been submitted to the Gene Expression Omnibus (GEO) with the accession number GSE299825.

2.5. LC-MS-based metabolomics

The tissue sample was frozen with liquid nitrogen and pulverized using a mortar and pestle. 10 ml of acetonitrile (90%) was added to the powdered tissue and incubated on a gel rocker for 2-3 hours at room temperature. The sample was then centrifuged at 12,000 g for 20 minutes at 4 °C. To the supernatant, 3 volumes of chilled methanol were added, mixed well by inversion, and then incubated at -20 °C for 2 hours. The sample was centrifuged at 4 °C for 20 min at 12000g, and the supernatant was collected. The collected supernatant was dried under Speed Vac and redissolved with 0.1% formic acid in methanol/water (80:20 v/v) solution. For LC-MS analysis, each methanolic extract was filtered through a 0.22 µm hydrophilic polyether sulfone (PES) membrane filter (Merck), and 8 µl of the filtrate was subsequently injected into a Waters Xevo G2-XS QT of an LC-MS system. The extract components were separated through an ACQUITY UPLC BEH C18 column (2.1×150 mm, particle size 1.7 µm). Gradient concentrations of mobile phase A, viz. water (with 0.1% formic acid), and B, viz. acetonitrile (with 0.1% formic acid), were 95% A and 5% B for 3 min, 55% A and 45% B for next 42 min, 0% A and 100% B in next 7 min and kept at same gradient flow for next 3 min. Thereafter, the gradient flow was changed to 98% A and 2% B at 55.10 min and kept at the same gradient for the next 5 min. The total run time was 60 minutes. The flow rate was set at 0.3 ml/min, and the column temperature was maintained at 40 °C. The eluent was alternatively connected to a Q-TOF analyzer (Thermo, USA), with positive ionization mode and 30 eV collision energy. Source temperature was maintained at 100°C, and mass acquisition range was set to 50–3000 Da. The LC–MS data were processed using ProteinLynx Global Server (PLGS) software (Waters). Metabolites were putatively identified by their MS1 patterns and pseudo molecular masses (either protonated or non-protonated) derived by MS1 (within permissible mass error<0.005 Da). Post-processing and further analysis of raw data obtained from LC-MS were performed in Metaboanalyst 5.0. For statistical significance, a fold change between -1 and 1 between the control and treatment groups and an FDR value of < 0.05 (in case of pathway impact and enrichment analysis) were considered.

2.6. Mitochondria isolation

The mitochondria isolation kit was used for mitochondria isolation from gastric mucosal tissues, following the manufacturer's instructions. The isolation procedure is based on sequential differential centrifugation, enabling enrichment of intact and functionally active mitochondria. In brief, approximately 200 mg of gastric mucosa from each experimental group was homogenized on ice in hypotonic lysis buffer supplemented with protease inhibitors using a Dounce homogenizer. The homogenate underwent initial low-speed centrifugation at 600 × g for 10 minutes to remove nuclei, unbroken cells, and cellular debris. The resulting supernatant was subjected to high-speed centrifugation at 12,000 × g for 15 minutes to pellet the mitochondrial fraction. The mitochondrial pellets were washed three times with isolation buffer to enhance purity.

2.7. Assessment of mitochondrial membrane potential (ΔΨm)

The mitochondrial transmembrane potential (ΔΨm) was evaluated using the potentiometric dye JC-1, a lipophilic cationic fluorochrome that differentially fluoresces depending on mitochondrial polarization status. In energized mitochondria, JC-1 accumulates within the matrix due to the negative inner membrane potential and forms red fluorescent J-aggregates (excitation/emission ∼590 nm). In contrast, depolarized or dysfunctional mitochondria fail to support JC-1 aggregation, resulting in the retention of its monomeric, green-fluorescent form (excitation/emission ∼530 nm). In the current study,

mitochondrial membrane potential (ΔΨm) was assessed using mitochondria isolated from gastric mucosal tissues of both control and stress-exposed rats, employing an F-7000 Fluorescence Spectrophotometer (Hitachi High-Technologies Corporation). Equal quantities of mucosal tissue were used for mitochondrial isolation, and protein concentrations were measured to standardize mitochondrial input across all samples for accurate ΔΨm assessment. The isolated mitochondria were incubated in the dark for 15 minutes in 500 µL of JC-1 assay buffer supplemented with ATP and containing 300 nM JC-1 dye. JC-1 monomers and aggregates were detected using a single-excitation, dual-emission protocol at 530 nm and 590 nm, respectively. The mitochondrial membrane potential was quantified as the fluorescence intensity ratio of 590 nm to 530 nm, following the method as described earlier (25).

2.8. Quantification of gastric mucosal ATP content

To assess the bioenergetic status of gastric mucosal cells following exposure to stress, tissue adenosine triphosphate (ATP) levels were measured. As ATP synthesis predominantly occurs within structurally intact and functionally competent mitochondria, any reduction in ATP levels is indicative of mitochondrial impairment and associated energy deficits in the tissue. ATP quantification was performed using a commercially available bioluminescent assay kit (ATP Determination Kit, A22066; Thermo Fisher Scientific), following the manufacturer's protocol. This assay is based on the ATP-dependent bioluminescent reaction catalyzed by recombinant firefly luciferase, which oxidizes the substrate D-luciferin in the presence of oxygen and magnesium ions, yielding oxyluciferin, AMP, pyrophosphate, carbon dioxide, and visible light. The emitted light, with a peak at 560 nm under physiological pH (7.8), is directly proportional to the ATP concentration in the sample.

For experimental analysis, 50 mg of gastric mucosa was harvested from control and cold restraint stress-exposed rats. The tissue was minced and homogenized in 5% sulfosalicylic acid. Following centrifugation at 12,000 × g, the supernatants were collected, and ATP levels were measured using a luminometer (BioTek). The luminescence readings were normalized to total protein concentrations in each sample, as described earlier (15,26), ensuring accurate comparison across experimental groups. This method provides a sensitive and specific measure of mitochondrial bioenergetic function and allows for the detection of stress-induced alterations in cellular energy metabolism.

2.9. RNA extraction and quantitative real-time PCR analysis

Total RNA was isolated from gastric mucosal tissues of all experimental groups using TRIzol reagent (Invitrogen, Carlsbad, CA), following the manufacturer's guidelines. RNA concentration was measured using a MaestroNano Micro-Volume Spectrophotometer (Life Teb Gen Co., Tehran, Iran). To remove any residual genomic DNA, the extracted RNA was treated with recombinant DNase (rDNase). Subsequently, 2 µg of RNA was reverse-transcribed into complementary DNA (cDNA) using oligo(dT)$_{18}$ primers and the RevertAid First Strand cDNA Synthesis Kit (Thermo Fisher Scientific). Quantitative real-time PCR (qRT-PCR) was then carried out with SYBR Green Master Mix (Roche) on a Roche LightCycler 96 platform. Gene-specific primers (listed in Table 1) were synthesized by Integrated DNA Technologies (San Diego, CA, USA). PCR reactions were run with the following thermal profile: an initial denaturation at 95 °C for 10 minutes, followed by 40 amplification cycles consisting of 15 seconds at 95 °C for denaturation, 30 seconds at gene-specific annealing temperatures (Table 1), and 25 seconds at 72 °C for extension. The housekeeping gene Gapdh was used as an internal reference, and relative expression levels were calculated using the $2^{\wedge -\Delta\Delta Cq}$ method, with results expressed as fold changes relative to the control group (15,26,27).

Table 1: List of primer sequences used in q-RT-PCR reaction

Genes	Primer sequence (Rat)		Annealing temperature
mt-Nd1	FP	5'-CACCCCCTTATCAACCTCAA-3'	59˚C
	RP	5'-ATTTGTTTCTGCGAGGGTTG-3'	
mt-Nd3	FP	5'-GAAATTGCGAGAATGGTGGT-3'	60˚C
	RP	5'-GGCAGTTGCTATTATTGTAGTGG-3'	
mt-Nd4	FP	5'-TCCCACTCTTAATTGCCCTC-3'	60˚C
	RP	5'-GAGGATGATGAATGGGTAGG-3'	
Mt-Nd5	FP	5'-TTCTCCAACAACAACGACAATC -3'	60˚C
	RP	5'-TCCGAGGCAAAGTATAGTTGTT-3'	
mt-Co 1	FP	5'-GACACCCGAGCCTACTTTAC-3'	60˚C
	RP	5'-GCTATGATGGCGAATACTGC-3'	
mt-Co 2	FP	5'-GCTTACAAGACGCCACATCACC-3'	60˚C
	RP	5'-CGTAGGGAGGGAAGGGCAAT-3'	
mt-Co 3	FP	5'-ACCTACCAAGGCCACCACACT CC-3'	60˚C
	RP	5'-CAGCC TCC TAG ATC ATG TGTTGG-3'	
mt-Cyt B	FP	5'-CGGCTGACTAATCCGATACC-3'	60˚C
	RP	5'-TGGGAGTACATAGCCCATGA-3'	
mt-Atp 6	FP	5'-CGAACCTGAGCCCTAATA-3'	60˚C
	RP	5'-GTAGCTCCTCCGATTAGA-3'	
mt-Atp 8	FP	5'-TGCCACAACTAGACACATCCA-3'	60˚C
	RP	5'-TGTGGGGGTAATGAAAGAGG-3'	
Ppargc1a	FP	5'-GCACCAGAAAACAGCTCCAA-3'	60˚C
	RP	5'-TTGCCATCCCGTAGTTCACT-3'	
Nrf1	FP	TACAAGGCGGGGGACAGATA	60˚C
	RP	ACTCCATCTGGGCCATTAGC	
Tfam	FP	5'-ATCAAGACTGTGCGTGCATC-3'	60˚C
	RP	5'-AGAACTTCACAAACCCGCAC-3'	
Cpt1a	FP	5'-GCACCAAGATCTGGATGGCTATGG-3'	62˚C
	RP	5'-TACCTGCTCACAGTATCTTTGAC-3'	
Acadm	FP	5'-TTAGCTTCTGCCCTGTGGTG-3'	60˚C
	RP	5'-ACTCTTTCTGCTGCTCCGTC-3'	
Nrf2	FP	5'-CTCTCTGGAGACGGCCATGACT-3'	60˚C
	RP	5'-CTGGGCTGGGGACAGTGGTAGT-3'	
Fbxo32	FP	5'-CACTCTACACTGGCAACAGCA-3'	60˚C
	RP	5'-GGTGATCGTGAGACCTTTGAA-3'	
Klf15	FP	5'-CTGCAGCAAGATGTACACCAA-3'	62˚C
	RP	5'-TCATCTGAGCGTGAAAACCTC-3'	
Klf9	FP	5'-GTCACGACCAGAGTGCTTCA-3'	62˚C
	RP	5'-GGTGTGCTCTTGCTTGCATA-3'	
Hmox1	FP	5'-TGCACATCCGTGCAGAGAAT-3'	60˚C
	RP	5'-AGGGAAGTAGAGTGGGGCAT-3'	
Gapdh	FP	5'-AGTATGACTCTACCCACGGC-3'	60˚C
	RP	5'-TGAAGACGCCAGTAGACTCC-3'	

2.10. Enzyme-linked immunosorbent assay (ELISA)

Serum corticosterone concentrations were measured using a commercial ELISA kit (Abcam, ab108821) following the manufacturer's protocol. In brief, blood samples were obtained from euthanized rats and left to clot at room temperature for 30 minutes. The serum was separated by centrifuging the samples at 600 × g for 5 minutes and then diluted 1:100 before analysis. Absorbance was recorded at 450 nm using a BioTek microplate reader. Corticosterone levels were determined by comparing the absorbance readings to a standard curve generated from known concentrations, and results were expressed as fold changes relative to the control group.

2.11. Confocal immunofluorescence imaging of tissue sections

To investigate the nuclear translocation of the glucocorticoid receptor (GR) in gastric mucosal tissues of control and stress-exposed rats, immunofluorescence-based confocal microscopy was employed. Paraffin-embedded, formalin-fixed tissue sections were first deparaffinized and rehydrated through graded ethanol, followed by heat-mediated antigen retrieval using sodium citrate buffer. Non-specific binding was minimized by blocking the sections with 10% goat serum and 1% bovine serum albumin (BSA) in Tris-buffered saline (TBS) for two hours at room temperature. Subsequently, the sections were incubated overnight at 4°C with a primary antibody targeting the glucocorticoid receptor alpha (GRα), as detailed in Table 02. After incubation with the primary antibody, the sections were rinsed and subsequently incubated with an Alexa Fluor 647-conjugated anti-rabbit secondary antibody. 4′,6-diamidino-2-phenylindole (DAPI) was used for nuclear counterstaining, and the slides were mounted in 30% glycerol prepared in phosphate-buffered saline (PBS). A Leica TCS-SP8 confocal laser scanning microscope (Leica Microsystems, Wetzlar, Germany) was used for imaging, with acquisition managed via the Leica Application Suite X (LAS X) software. Each experiment was independently replicated thrice, and representative regions from the gastric mucosal sections were selected at random for image documentation. Post-acquisition processing, including uniform brightness and contrast adjustments, was performed using Adobe Photoshop, and figure assembly was completed in CorelDraw X7, as previously described (15,25).

2.12. Assay of Fatty acid oxidation (FAO)

Enzyme activity for fatty acid oxidation was quantitatively assessed using specialized assay kits procured from the Biomedical Research Service Center, State University of New York (Buffalo, NY), following the manufacturer's protocol. Gastric mucosal tissues were first homogenized and processed for total protein extraction, and the resulting lysates were quantified using the Lowry method. Protein concentrations were normalized to 1 mg/ml across all samples to ensure consistency. For the enzymatic assay (Catalogue No E-141L and E-141M), a volume of 10 µl from the normalized protein lysate was combined with 50 µl of the fatty acid oxidation (FAO) assay solution or the corresponding control solution in a 96-well plate. The samples were incubated at 37 °C for 60 minutes in a non-CO_2 humidified incubator to allow for optimal enzyme-substrate interaction. The reactions were subsequently terminated by the addition of 50 µl of 3% (v/v) acetic acid to each well. Absorbance was measured at 492 nm using a spectrophotometric plate reader. To determine the enzymatic activity, the absorbance reading from the blank was subtracted from that of the test sample. The resulting differential absorbance (ΔOD_{492}) was taken as a direct measure of fatty acid oxidation, as previously described (27). Data were expressed as fold changes relative to the control group.

2.13. Western blotting

Immunoblotting was performed following previously established protocols (15,25). In summary, extraction of total protein was done from homogenized gastric mucosal tissues using RIPA lysis buffer (composed of 150 mM NaCl, 1.0% NP-40 or Triton X-100, 0.5% sodium deoxycholate, 0.1% SDS, and 50 mM Tris, pH 8.0), supplemented with a protease inhibitor cocktail (Set V, Calbiochem). Protein concentration was assessed using the Lowry method. The protein samples were denatured using Laemmli buffer, and equal amounts were loaded into the wells of 10% SDS–polyacrylamide gels. Electrophoresis was carried out at 100 V in running buffer containing 25 mM Tris, 190 mM glycine, and 0.1% SDS. Proteins were then transferred onto nitrocellulose membranes at 45 V for 2 hours using transfer buffer (190 mM glycine, 20 mM Tris, pH 8.3). Membranes were blocked for 1 hour at room temperature with TBS (25 mM Tris, 150 mM NaCl, 2 mM KCl, pH 7.4) containing 5% non-fat dry milk, followed by overnight incubation at 4 °C with primary antibodies prepared according to the manufacturer's recommended dilutions. After a brief rinse, membranes were thoroughly washed with TBS containing 0.1% Tween-20 and subsequently incubated for 2 hours with HRP-conjugated secondary antibodies in the same buffer. A complete list of primary antibodies used is provided in Table 2. Immunoreactive bands were visualized using the Bio-Rad ChemiDoc imaging system or by DAB and hydrogen peroxide staining. Band intensities were quantified using ImageJ software, normalized to control levels, and expressed as fold changes.

Table 2: List of antibodies used for immunoblotting and immunofluorescent studies

Antibodies	Supplier	Species	Catalogue number
PGC1α	Abcam	Rabbit	Ab54481
Glucocorticoid Receptor	Invitrogen	Rabbit	PA1-516
NRF1	Cell Signaling Technology	Rabbit	46743
TFAM	Abcam	Rabbit	ab131607
KLF15	Santa Cruz Biotechnology	Mouse	sc-271675
FBXO32	Abcam	Rabbit	ab74023
Bax	Santa Cruz Biotechnology	Mouse	sc-7480
Bcl-xL	Cell Signaling Technology	Rabbit	2764
Actin	Cell Signaling Technology	Mouse	3700
Anti-rabbit IgG	Sigma	Goat	A0545
Anti-mouse IgG	Sigma	Rabbit	A9044
Alexa Fluor 647	Invitrogen	Goat	A-21245

2.14. Data and statistical analysis

All data and statistical analyses were conducted following established guidelines for randomized, blinded experimental design to ensure balanced group sizes and reduced bias. *In vivo* experiments were performed using randomly assigned rats, with each experimental group consisting of five animals (n = 5). *In vitro* experiments were conducted in triplicate, and all experiments were independently repeated a minimum of three times to ensure reproducibility. Data are presented as mean ± standard deviation (SD). Statistical comparisons between two groups were performed using an unpaired t-test with Welch's

correction. For comparisons involving more than two groups, one-way analysis of variance (ANOVA) was conducted, followed by Bonferroni's post hoc test for multiple comparisons. A p-value less than 0.05 was considered indicative of statistical significance in all analyses. Group sizes refer to the number of independent biological replicates, and statistical tests were performed using these independent values. GraphPad Prism 8 and Microsoft Excel 2019 were used for data analysis. For metabolomics data, raw LC-MS files were processed and analyzed using MetaboAnalyst 5.0, and Origin software was used to generate principal component analysis (PCA) plots.

3. RESULTS

3.1 Transcriptomic profiling of rat gastric mucosa under acute mental stress

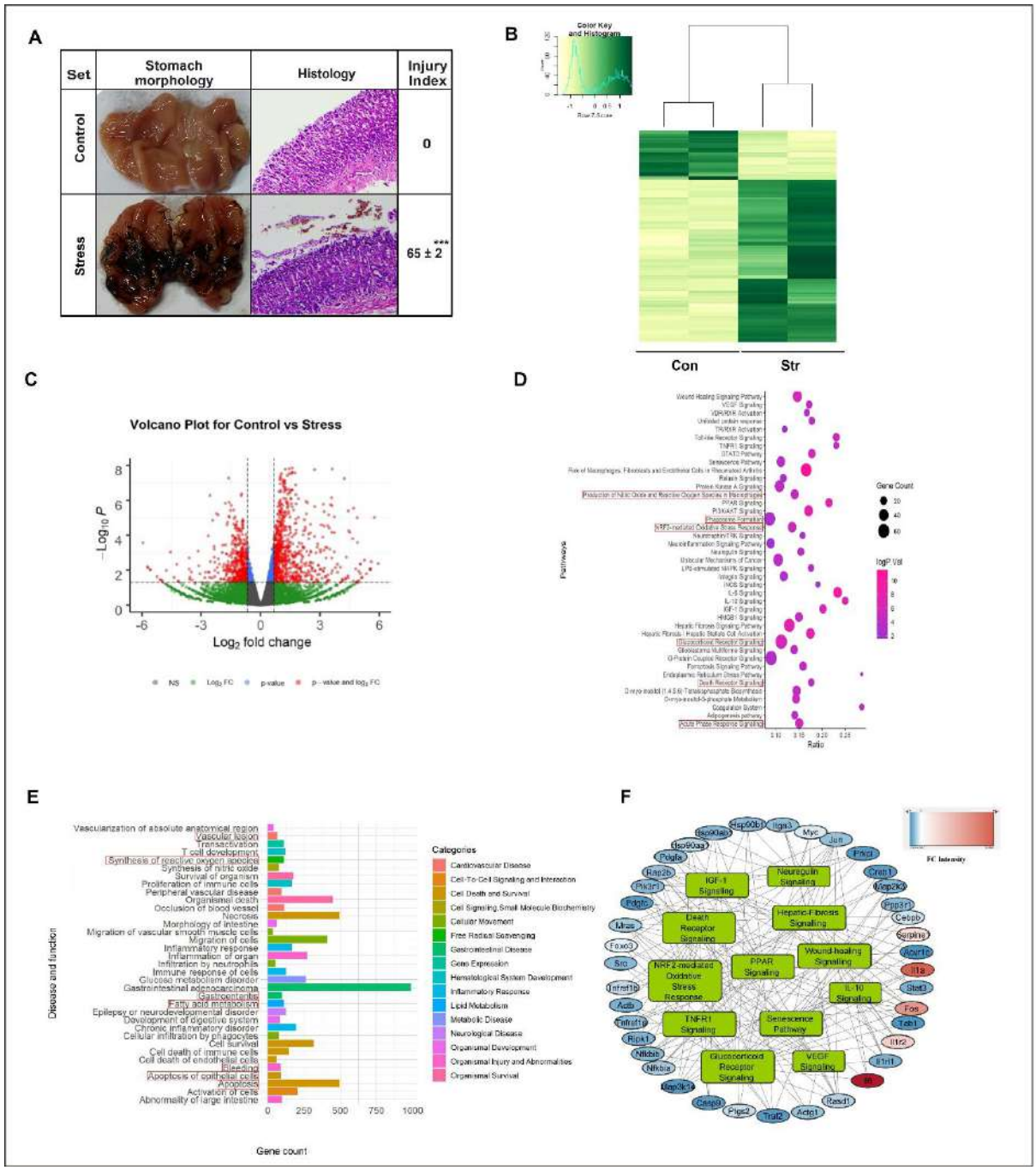

Fig.1. Acute stress induces gastric mucosal injury and alters gene expression profiles. (A) Representative histopathological images of the gastric mucosa of rats exposed to acute stress and control showed different gastric mucosal morphology and tissue architecture when stained with haematoxylin and eosin (n = 5). (B) Heatmap showing differentially expressed genes (DEGs) between the control (Con) and stress (Str) (false discovery rate [FDR] ≤ 0.05). The gene expression data was clustered using the Euclidean distance metric. Genes were analyzed with a fold change cut off of 1.5, and their expression levels were represented using a colour gradient, ranging from light green (indicating strong down-regulation) to dark green (representing strong up-regulation). (C) Volcano plot depicting DEGs between the control and stress groups. The x-axis represents the Log_2 fold change, while the y-axis indicates the Log_{10}P-value. Red dots highlight significantly upregulated or downregulated genes, whereas non-significant genes are in black. Green dots represent genes with significant fold change but not p-value, and blue dots indicate genes with significant p-value but not fold change. (D) Dot plot illustrating enriched biological pathways associated with DEGs. Pathways are categorized based on their functional significance, with dot size indicating gene count, and the ratio represents the number of genes in the fraction for the total number of genes that map to the same pathway. The range of colour indicates Bonferroni corrected P values (log transformed). (E) Bar graph showing disease and function enrichment analysis for genes affected by stress. Gene counts are plotted for each category, with colour coding representing different biological functions and disease pathways. (F) Gene network diagram, created using Cytoscape, depicting interactions between key stress-related genes, gene names represented in oval shapes, whereas associated functions are represented by rectangular boxes. Genes are categorized based on functional roles. Colour code represents fold change in gene expression. The connections indicate known relationships between the indicated genes. GEO accession number GSE299825

Psychological stress exerts deleterious effects on gastric mucosal integrity, contributing to the pathogenesis of stress-related gastropathy. However, the precise molecular mechanisms underlying this phenomenon remain incompletely elucidated. To investigate the molecular perturbations associated with stress-induced gastric mucosal injury, a well-established rat model of acute mental stress was employed (15). Comprehensive transcriptomic analysis was first conducted to delineate stress-mediated alterations in gastric mucosal gene expression. In this study, experimental animals were exposed to cold-restraint stress (CRS), after which tissues were collected for transcriptome sequencing from both control and stress-exposed groups exhibiting severe mucosal injury. In contrast, control group animals exhibited no evidence of gastric mucosal bleeding or pathological alterations (Fig. 1A). Through high-throughput transcriptomic profiling, the differential gene expression patterns were systematically characterized in stressed gastric mucosal tissues. After applying a fold change (FC) cut-off of 1.5, along with a p-value of ≤ 0.05, the heat map revealed a differentially expressed gene (DEG) set comprising 1057 upregulated genes and 623 down-regulated genes in “CRS” (“CRS” is marked as “Str” in Fig. 1B) compared to the “control” group. Gene enrichment analysis conducted with 'Ingenuity Pathway Analysis' identified the main pathways and 'disease and function' associated with gastric mucosal injury induced by CRS (Fig. 1D-E). The volcano plot illustrates the differential gene expression profile between control (Con) and stress (Str) gastric mucosa samples. The red-colored region in the volcano plot represents genes that meet both the fold change and p-value cutoffs, indicating significantly differentially expressed genes. Significantly upregulated genes (red, right side) show high fold change (FC > 1.2) with strong statistical significance ($p < 0.05$), while significantly downregulated genes (red, left side) exhibit reduced expression (FC < -1.2, $p < 0.05$). From pathway analysis, the following pathways were identified: ‘production of nitric oxide and reactive oxygen species in macrophages’, ‘NRF2-mediated oxidative stress response’, ‘phagosome formation’, ‘glucocorticoid receptor signalling’, ‘ferroptosis signalling pathway’, ‘death receptor signalling’, and ‘acute phase response signalling’ (Fig. 1D). Concurrently, ‘vascular lesion’, ‘synthesis of reactive oxygen species’, ‘synthesis of nitric oxide’, ‘peripheral vascular disease’, ‘occlusion of the blood vessel’, ‘necrosis’, ‘inflammatory response’, ‘gastroenteritis’, ‘fatty acid metabolism’, ‘cell death of endothelial cells’, ‘bleeding’, and ‘apoptosis of epithelial cells’ emerged as the most enriched "disease and function" categories, significantly influencing the differentially expressed gene (DEG) profiles (Fig. 1E). In the Cytoscape

network, gene names are depicted in oval shapes, while their associated functions are represented by rectangular boxes. Prominent pathways, including 'NRF2-mediated oxidative stress response' and 'Glucocorticoid receptor signaling,' were identified as critically implicated and subsequently subjected to rigorous mechanistic investigation. Based on the profound transcriptomic perturbations observed in key metabolic pathways, complementary untargeted metabolomic profiling was conducted to elucidate the functional metabolic consequences of acute stress exposure. By integrating metabolomic signatures from gastric mucosal tissue with transcriptomic findings, the mechanistic interplay between stress-induced gene expression dysregulation and subsequent metabolic network disturbances was further explored.

3.2. Metabolomic analysis reveals mitochondrial dysfunction in gastric tissue in acute stress.

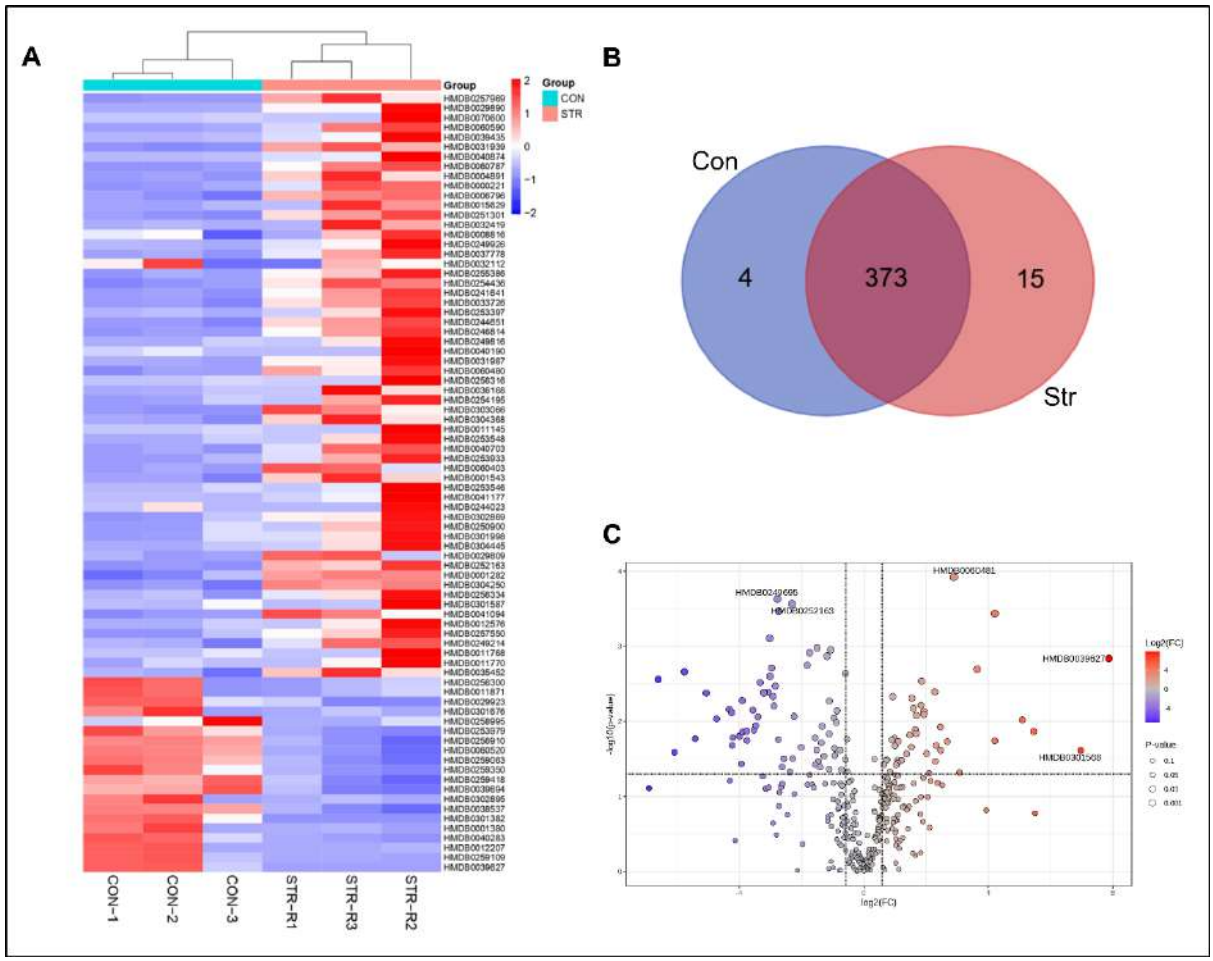

Figure 2. Acute stress induces metabolic alterations in the gastric mucosa. (A) Heatmap illustrating the differential relative abundance of metabolites between control (CON-1, CON-2, CON-3) and stress (STR-R1, STR-R2, STR-R3) groups. Rows represent metabolites, and columns represent individual samples. The colour gradient indicates relative abundance, with red representing upregulation and blue representing downregulation (FDR < 0.05 and fold change cutoff <-1 and >1). Hierarchical clustering was performed using the maximum likelihood algorithm to group samples based on metabolic similarity. (B) Venn diagram showing the shared and unique metabolites identified in control (Con) and stress (Str). A total of 373 metabolites are shared between both groups, while 4 are unique to the control group and 15 are specific to the stress. (C) Volcano plot depicting differentially expressed metabolites between the 'control' and 'stress'. The x-axis represents the $\log_2$ fold change, and the y-axis represents the $-\log_{10}$ p-value. Coloured dots highlight significantly altered metabolites, with upregulated and downregulated metabolites represented in red and blue, respectively. Raw data access-Appendix

To validate the transcriptomic alterations in genes associated with various metabolic pathways, untargeted metabolomic profiling was performed on gastric mucosal tissues from control (CON) and cold-restraint stress-exposed (STR) rats. Liquid chromatography–mass spectrometry (LC-MS) analysis revealed significant metabolic perturbations, with a total of 373 metabolites detected across both groups. Among the 373 identified metabolites, 109 demonstrated an upward trend, whereas 111 displayed a marked decline under stress conditions. Furthermore, 4 metabolites were uniquely detected in the control group, while 15 were exclusively present in the stress-exposed group, collectively indicating profound stress-induced metabolic reprogramming. Of the differentially expressed metabolites (DEMs), 79 were significantly upregulated (log_2 FC >1) and 73 were downregulated (log_2 FC <-1). The volcano plot illustrates the differential abundance of metabolites between the control and stress-exposed group (Fig. 2B). Significantly upregulated metabolites (right side, red dots) indicate stress-induced metabolic alterations. Significantly downregulated metabolites (left side, blue dots) represent metabolites that are depleted under stress conditions. The combination of the Venn diagram and Volcano plot suggests major metabolic reprogramming in the gastric tissue under stress exposure, with specific metabolites showing significant changes. Stress-induced metabolic shifts altered key pathways, including lipid, steroid, sphingolipid, and nicotinate/nicotinamide metabolism. Notably, NADH (HMDB0001487) and NADPH (HMDB0000221) were upregulated, indicating increased energy demand and antioxidant defence. upregulated phosphatidic acid (PA(O-16:0/18:0) HMDB0011145, ceramides (d18:0/25:0), ganglioside GA2 (d18:1/18:0), and phosphatidylcholine (PC 24:1(15Z)/24:1(15Z)) HMDB0008816 suggest enhanced lipid signalling, apoptosis, and membrane remodelling in stress-exposed gastric tissues.

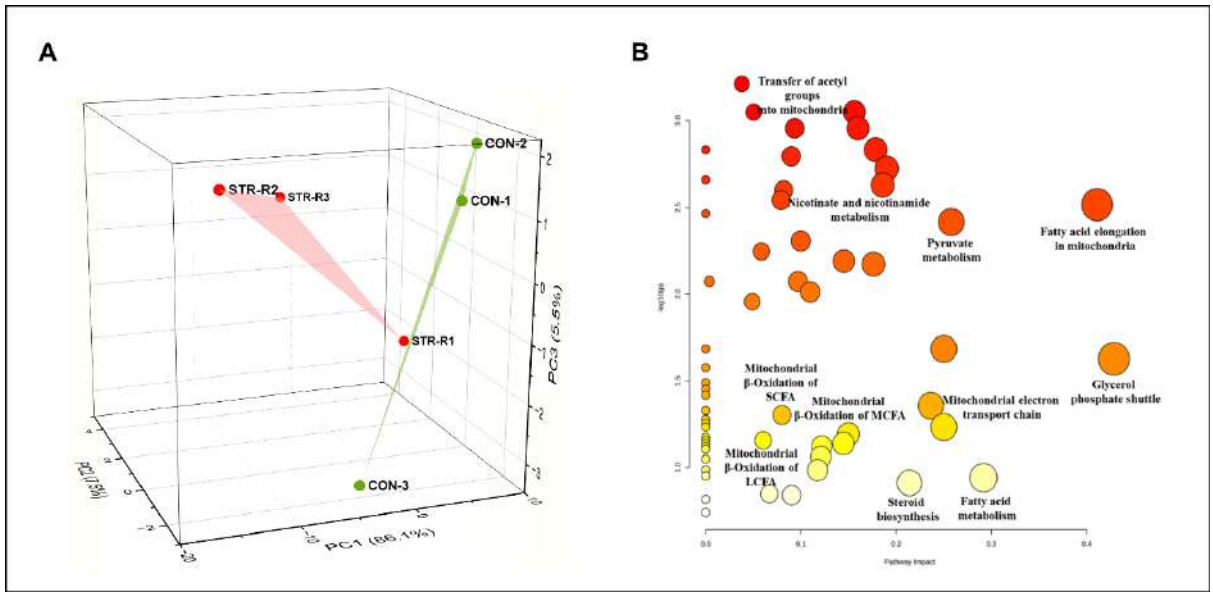

Figure 3. Multivariate and pathway enrichment analysis of metabolic profiles under stress. (A) 3D Principal Component Analysis (PCA) score plot showing clear separation between metabolomic profiles of stress-treated (STR) and control (CON) samples. Each point represents a biological replicate (n = 3 per group), with STR-R1 to STR-R3 (red) and CON-1 to CON-3 (green) indicating 'stress' and 'control' samples, respectively. (B) Metabolic pathway impact analysis (bubble plot) based on significantly altered metabolites between stress-treated and control conditions. The x-axis denotes the pathway impact score derived from pathway topology analysis, while the y-axis shows the significance of pathway enrichment as $-log_{10}$(p-value). The size of each bubble corresponds to the pathway impact, and the colour gradient from yellow to red represents increasing statistical significance.

Principal Component Analysis (PCA) using covariance matrix was performed to segregate samples based on their metabolomic profiles and to explain variations between groups (Fig. 3A). The first principal component (PC1) accounted for the majority of the variation (86.1%; eigenvalue: 68.571), followed by PC2 (7.5%; eigenvalue: 5.963) and PC3 (5.5%; eigenvalue: 4.44). Control (CON) and stress-exposed (STR) groups formed distinct clusters, with the CON group positioned along the positive PC1 axis, while the STR group was shifted along the negative PC1 axis. The control group exhibited significant loadings of lipids containing long-chain fatty acids, such as Cer (d18:0/20:4), Cer (d18:0/25:0), PS (24:0/24:0), TG (22:0/18:2/22:2), Ganglioside GA2 (d18:1/18:0), and nicotinamide metabolites like NADH and NADPH. In contrast, stress-exposed samples showed an enrichment of lipid classes containing small- to mid-chain fatty acids, including CE (15D5), Ceramide AP, DG (18:2n6/0:0/20:2n6), SM(d18:0/16:0), Cer(d18:0/12:0), and Ganglioside GD3 (d18:1/14:0). These metabolic shifts indicate a fundamental alteration in lipid metabolism under stress conditions. The pathway impact analysis reveals significant metabolic disruptions in stress-exposed gastric tissue, particularly in mitochondrial and lipid metabolism (Fig. 3B). The most affected pathways include the transfer of acetyl groups into mitochondria and nicotinate/nicotinamide metabolism, indicating disruptions in energy metabolism and redox balance. Alterations in pyruvate metabolism and fatty acid elongation in mitochondria further suggest impaired mitochondrial energy processing. Changes in mitochondrial β-oxidation of fatty acids reflect alterations in lipid catabolic processes, whereas impairments in the mitochondrial electron transport chain suggest a reduction in ATP synthesis efficiency. Changes in the glycerol phosphate shuttle and fatty acid metabolism suggest altered lipid utilization and oxidative stress adaptation, whereas variations in steroid biosynthesis may reflect stress-induced hormonal imbalances. Collectively, these findings suggest that stress exposure leads to mitochondrial dysfunction, disrupting energy metabolism and lipid signaling pathways.

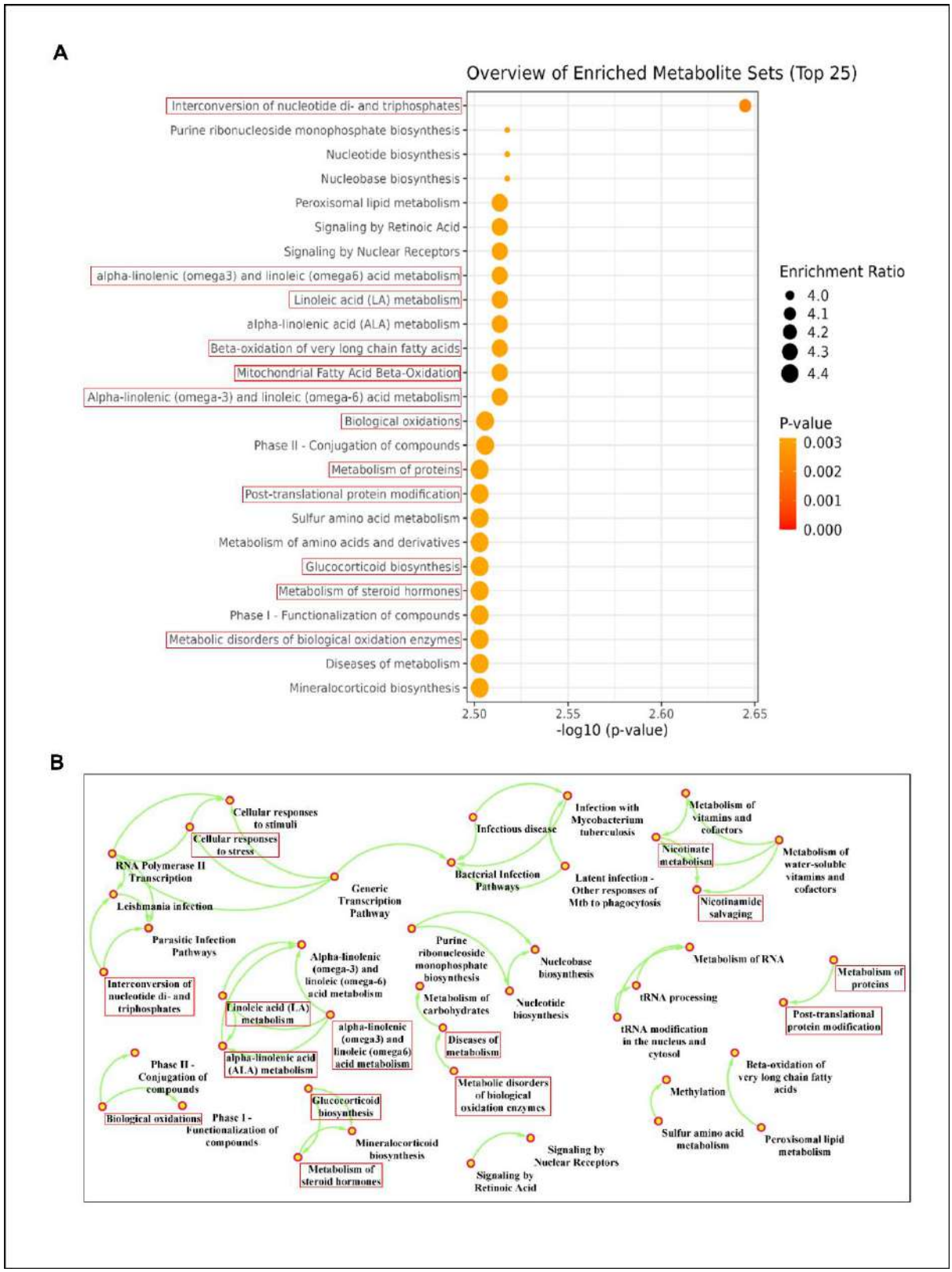
A
Overview of Enriched Metabolite Sets (Top 25)
Interconversion of nucleotide di- and triphosphates
Purine ribonucleoside monophosphate biosynthesis
Nucleotide biosynthesis
Nucleobase biosynthesis
Peroxisomal lipid metabolism
Signaling by Retinoic Acid
Signaling by Nuclear Receptors
alpha-linolenic (omega3) and linoleic (omega6) acid metabolism
Linoleic acid (LA) metabolism
alpha-linolenic acid (ALA) metabolism
Beta-oxidation of very long chain fatty acids
Mitochondrial Fatty Acid Beta-Oxidation
Alpha-linolenic (omega-3) and linoleic (omega-6) acid metabolism
Biological oxidations
Phase II - Conjugation of compounds
Metabolism of proteins
Post-translational protein modification
Sulfur amino acid metabolism
Metabolism of amino acids and derivatives
Glucocorticoid biosynthesis
Metabolism of steroid hormones
Phase I - Functionalization of compounds
Metabolic disorders of biological oxidation enzymes
Diseases of metabolism
Mineralocorticoid biosynthesis
2.50
2.55
2.60
2.65
-log10 (p-value)
Enrichment Ratio
4.0
4.1
4.2
4.3
4.4
P-value
0.003
0.002
0.001
0.000
B
Cellular responses to stimuli
Cellular responses to stress
RNA Polymerase II Transcription
Leishmania infection
Parasitic Infection Pathways
Generic Transcription Pathway
Infectious disease
Bacterial Infection Pathways
Infection with Mycobacterium tuberculosis
Latent infection - Other responses of Mtb to phagocytosis
Metabolism of vitamins and cofactors
Nicotinate metabolism
Nicotinamide salvaging
Metabolism of water-soluble vitamins and cofactors
Interconversion of nucleotide di- and triphosphates
Alpha-linolenic (omega-3) and linoleic (omega-6) acid metabolism
Linoleic acid (LA) metabolism
alpha-linolenic (omega3) and linoleic (omega6) acid metabolism
alpha-linolenic acid (ALA) metabolism
Phase II - Conjugation of compounds
Biological oxidations
Phase I - Functionalization of compounds
Glucocorticoid biosynthesis
Mineralocorticoid biosynthesis
Metabolism of steroid hormones
Purine ribonucleoside monophosphate biosynthesis
Metabolism of carbohydrates
Diseases of metabolism
Metabolic disorders of biological oxidation enzymes
Nucleobase biosynthesis
Nucleotide biosynthesis
Signaling by Nuclear Receptors
Signaling by Retinoic Acid
Metabolism of RNA
tRNA processing
tRNA modification in the nucleus and cytosol
Metabolism of proteins
Post-translational protein modification
Beta-oxidation of very long chain fatty acids
Methylation
Sulfur amino acid metabolism
Peroxisomal lipid metabolism

Figure 4. Acute stress triggers activation of stress-associated pathways in the gastric mucosa. (A) Enrichment plot displaying the top 25 enriched metabolite sets from KEGG pathway analysis. The x-axis represents the -log10 (p-value), indicating the statistical significance of enrichment, while the y-axis lists the enriched pathways. The size of the dots corresponds to the enrichment ratio, and the colour gradient represents different p-value ranges. (B) Disease network analysis and metabolic pathway-disease interaction networks created using MetaboAnalyst 5.0, showing the relationship between altered metabolic pathways and associated diseases. Red boxes highlight significantly affected pathways, while green lines indicate interconnections between pathways. Raw data access-Appendix

KEGG enrichment analysis was conducted to explore the impact of stress exposure on biological processes and identify differentially expressed metabolites associated with specific metabolic functions. Among over 400 significantly enriched biological processes ($p<0.05$), the top 25 were highlighted (Fig. 4A). Notably, pathways such as mitochondrial fatty acid beta-oxidation and metabolic disorders of biological oxidation enzymes were enriched, indicating mitochondrial involvement in the stress response, which aligns with our findings from transcriptome analysis. A network-based view of metabolic pathway-disease interactions highlights metabolic perturbations under stress exposure (Fig. 4B). The interconnected pathways further highlight mitochondrial dysfunction, particularly through mitochondrial fatty acid β-oxidation and metabolic disorders of biological oxidation enzymes. These disruptions suggest impaired mitochondrial energy metabolism and oxidative stress responses. Additionally, the clustering of biological oxidations, glucocorticoid biosynthesis, and alpha-linolenic (omega-3) and linoleic (omega-6) metabolism indicates that stress exposure significantly alters lipid metabolism and steroid hormone biosynthesis processes closely linked to mitochondrial function. The presence of post-translational protein modification and metabolism of proteins in the network suggests potential mitochondrial protein dysregulation, which may contribute to mitochondrial dysfunction. Overall, the metabolomics data collectively point toward mitochondrial impairment as a central factor in stress-induced metabolic alterations.

3.3. Transcriptomic insights into the alterations of mitochondrial gene expression under stress

Metabolomic data provided compelling evidence of redox imbalance and disruptions in energy metabolism, strongly implicating mitochondrial dysfunction as a central feature of stress-induced gastric injury. These findings suggest potential impairment of the electron transport chain (ETC), either through functional deficits or altered expression of its component genes within the mitochondria. Notably, the initial transcriptomic analysis, conducted using a stringent fold change (FC) threshold of ≥1.5, did not reveal significant differential expression of genes encoding ETC components. However, upon refining the analysis parameters by lowering the FC threshold to ≥1.2, additional mitochondrial regulatory genes, including those associated with the ETC, were identified as differentially expressed. Hierarchical clustering heatmap analysis revealed distinct transcriptional differences between control and stress groups, with stress-exposed samples showing significant alterations in gene expression patterns (Fig. 5A). Pathway enrichment analysis identified key biological processes impacted by stress, including oxidative stress responses (NRF2-mediated oxidative stress response), inflammatory signaling (LPS-mediated, PI3K/AKT, and Toll-like receptor pathways), and mitochondrial dysfunction (Endoplasmic reticulum stress and necroptosis signaling pathways) (Fig. 5B). Functional classification of differentially expressed genes highlighted several biological functions associated with metabolic disease, inflammation of organ, bleeding, apoptosis, and synthesis of reactive oxygen species (Fig. 5C). A specific focus on mitochondrial electron transport chain (ETC) gene expression revealed a notable downregulation of genes encoding Complex I (Mt-nd1, Mt-nd2, Mt-nd3, Mt-nd4, Mt-nd4l, Mt-nd6), Complex III (Mt-cyb), and Complex V (Mt-atp6, Mt-atp8) (Fig. 5D). Transcriptomic analysis also

revealed significant dysregulation of mitochondrial-related genes (both mitochondrial and nuclear encoded) in gastric mucosal tissues. The heatmaps visualize differential gene expression patterns, with

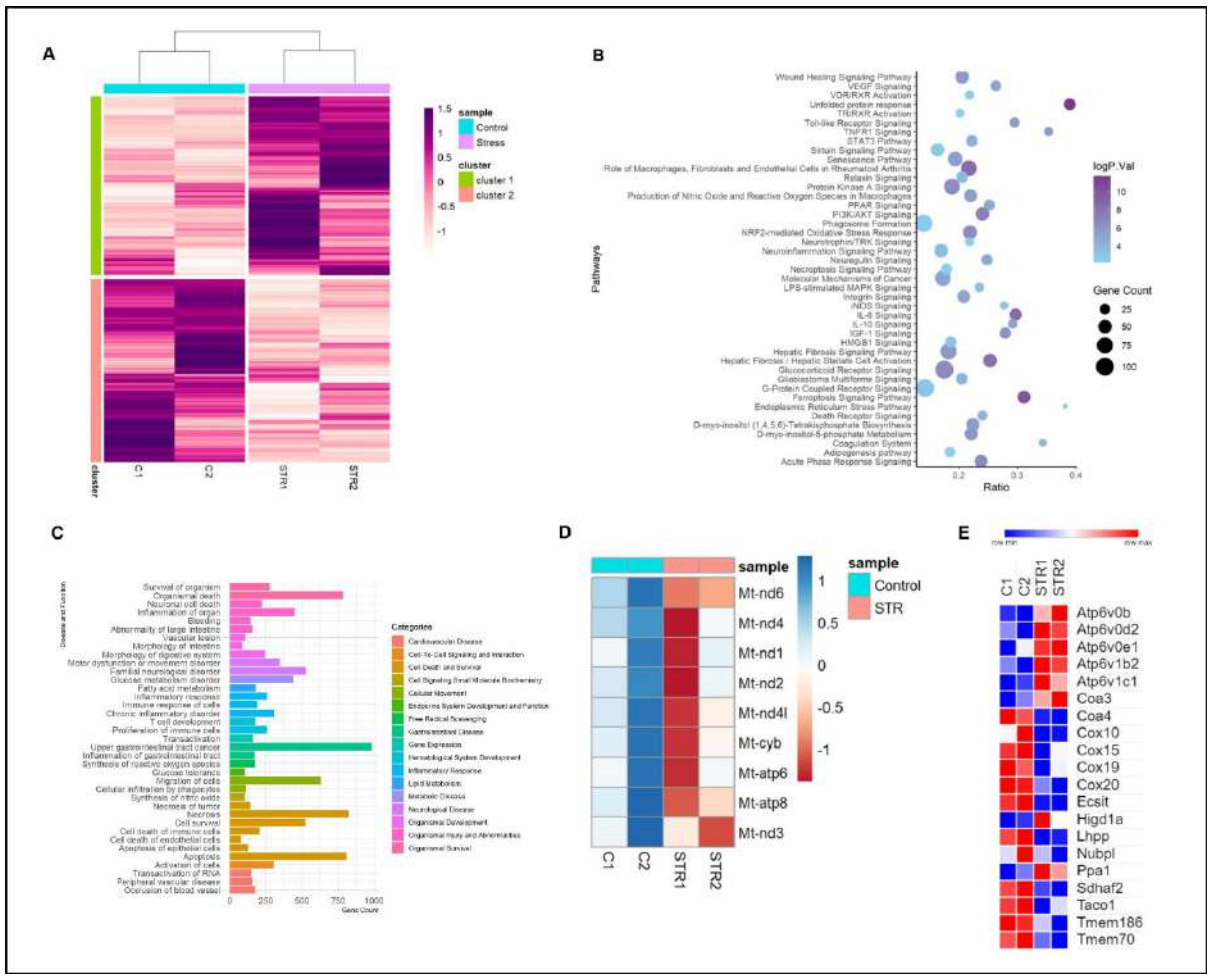

Figure 5. Acute stress triggers transcriptomic alterations in the gastric mucosa linked with aberrant mitochondrial signalling. (A) Heatmap reveals distinct clustering of samples representing both control (Con) and stress-exposed (Str) rats. The gene expression data for the differentially expressed genes (DEGs) was clustered using the Euclidean distance metric. The genes' expression values were analyzed with a fold change cutoff of 1.2. A colour gradient scale was applied, ranging from white for significant down-regulation to dark purple for significant up-regulation. (B) The dot plot visualizes enriched canonical pathways. Dot size reflects the proportion of genes associated with each signalling pathway, while the colour range indicates Bonferroni-corrected p-values (log-transformed). The ratio denotes the fraction of genes relative to the total number of genes mapped to the pathway. (C) The bar graph illustrates the diseases and functions that are enriched in the tissue set exposed to stress. (D) Mitochondrial gene expression heatmap based on the values analyzed with a fold change cutoff of 1.2. A colour gradient scale was applied, ranging from red for down-regulation to blue for up-regulation. (E) Heatmap representation of a subset of differentially expressed mitochondrial and mitochondria-associated genes between control (C1, C2) and stress (STR1, STR2) groups as checked using next-generation transcriptome sequencing and analysed using a fold change cut-off of 1.2. The colour scale represents row-wise normalized expression values, with red indicating upregulation and blue indicating downregulation.

red indicating upregulation and blue indicating downregulation. Several mitochondrial genes involved in ATP synthesis (Atp6v0b, Atp6v0d2, Atp6v0e1, Atp6v1b2, Atp6v1c1) and oxidative phosphorylation (Coa3, Coa4, Cox10, Cox15, Cox19, Cox20) are with altered expression as depicted in the heatmap along with marked expression changes in genes critical for mitochondrial maintenance, such as

Tmem70, Taco1, and Nubpl (Fig. 5E). This decrease in ETC and mitochondrial maintenance gene expression suggests impaired oxidative phosphorylation that may lead to reduced ATP production, increased ROS generation, and heightened cellular stress, exacerbating gastric tissue damage. Overall, these transcriptomic findings strongly reinforce the metabolomics data, confirming that stress-induced mitochondrial dysfunction plays a central role in energy metabolism disruption and oxidative stress-related gastric injury.

3.4. Stress-induced loss of mitochondrial integrity and function

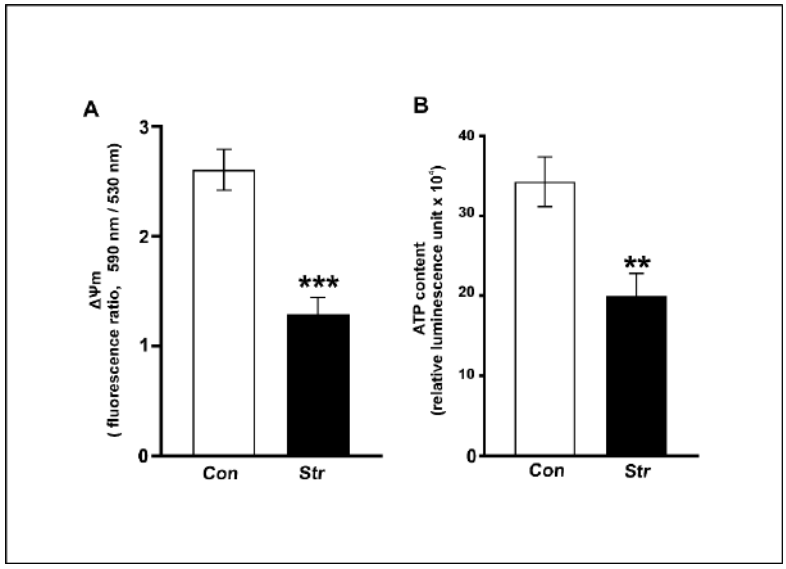

Figure 6. Acute stress triggers mitochondrial dysfunction and bioenergetic crisis. (A) Mitochondrial transmembrane potential (ΔΨm) in the gastric mucosal mitochondrial fractions from control (Con) and stress (Str) exposed rats (n = 5). (B) Gastric mucosal ATP content. Data are presented as mean ± SD, n = 5. $^{**}P < 0.01$ and $^{***}P < 0.001$ compared to the control; unpaired Student's t test with Welch's correction. The number of independent experiments is 3.

The mitochondrial membrane potential (ΔΨm), established by proton pumps of Complexes I, III, and IV during oxidative phosphorylation, is vital for cellular energy storage. Alongside the proton gradient (ΔpH), ΔΨm constitutes the electrochemical potential across the inner mitochondrial membrane, which drives ATP synthesis. Under normal physiological conditions, both ΔΨm and intracellular ATP levels are tightly regulated, with only minor fluctuations reflecting metabolic activity. However, persistent alterations in ΔΨm can disrupt respiratory chain function, leading to impaired ATP production, energy depletion, and ultimately, cell death (28,29). To further validate mitochondrial dysfunction, we assessed mitochondrial membrane potential (ΔΨm) using JC-1 staining and ATP levels via a luminescence-based assay. JC-1 staining revealed a significant reduction in the fluorescence ratio (590 nm/530 nm) in stress-exposed tissues, indicating mitochondrial depolarization and loss of membrane integrity (Fig. 6A). Concurrently, ATP levels were significantly lower, suggesting impaired mitochondrial energy production (Fig. 6B). Since ATP synthesis depends on an intact electron transport chain (ETC) and efficient oxidative phosphorylation, its decline underscores functional mitochondrial impairment. These findings align with transcriptomic and metabolomic data, reinforcing that stress disrupts mitochondrial function at multiple levels. Mitochondrial depolarization, a hallmark of dysfunction, often precedes apoptosis and increased reactive oxygen species (ROS) production, while reduced ATP levels indicate an energy metabolism shift, exacerbating gastric tissue damage. Overall, these findings confirm that stress exposure leads to mitochondrial dysfunction, characterized by membrane depolarization and reduced ATP production, ultimately contributing to gastric injury.

3.5. Stress-induced downregulation of genes and proteins of mitochondrial electron transport chain

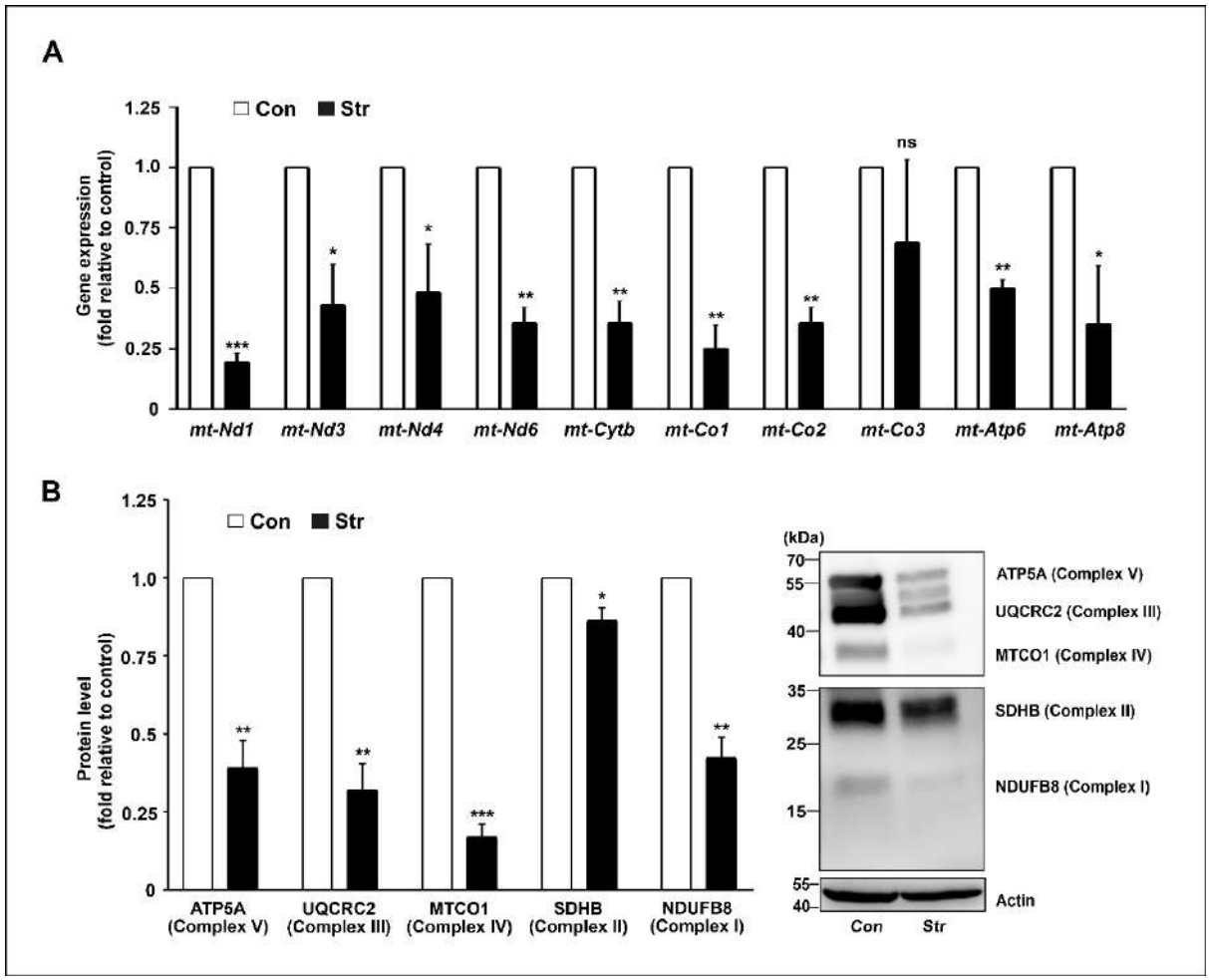

Figure 7. Acute stress alters mitochondrial gene and protein expression. (A) Quantitative PCR (qPCR) analysis of mitochondrial DNA-encoded genes in control (Con) and stress (Str) conditions. The expression levels of mitochondrial genes (mt-Nd1, mt-Nd3, mt-Nd4, mt-Nd6, mt-Cytb, mt-Co1, mt-Co2, mt-Atp6, and mt-Atp8) are shown as fold change relative to control. (B) Immunoblot analysis of oxidative phosphorylation (OXPHOS) complex proteins of tissues from control and stress. Representative immunoblots show the expression of ATP5A (Complex V), UQCRC2 (Complex III), MTCO1 (Complex IV), SDHB (Complex II), and NDUFB8 (Complex I) alongside the bar graphs. Actin was used as a loading control. Data are presented as mean ± SD, n = 5. $^{**}P < 0.01$ and $^{***}P < 0.001$ compared to the control; calculated using unpaired Student's t test with Welch's correction. Relative expression values are presented as fold change relative to control, wherein expression values corresponding to control are considered as 1-fold. The number of independent experiments is 3. ns = not significant

Based on prior transcriptomic evidence demonstrating dysregulation of mitochondrial electron transport chain (ETC) gene expression in stress-induced gastric injury, these findings were further substantiated through quantitative PCR (qPCR) and immunoblot analyses, thereby confirming alterations at both the transcriptional and protein levels. Quantitative gene expression analysis revealed a significant downregulation of key mitochondrial ETC-related genes in the stress group compared to controls, indicating impaired oxidative phosphorylation (Fig. 7A). Specifically, genes encoding complex I components (mt-Nd1, mt-Nd3, mt-Nd4, mt-Nd6) were significantly reduced, complex III (mt-Cytb) and complex IV (mt-Co1, mt-Co2) exhibited notable downregulation. Additionally, complex V (ATP Synthase) genes (mt-Atp6, mt-Atp8) also showed a significant decline, reinforcing mitochondrial ETC dysfunction under stress conditions. Immunoblot analysis further confirmed reduced expression of key

ETC proteins, with ATP5A (Complex V) and UQCRC2 (Complex III) showing significant decreases, while MTCO1 (Complex IV) and SDHB (Complex II) were also downregulated, aligning with transcriptomic data (Fig. 7B). Additionally, NDUFB8 (Complex I) levels were markedly decreased, indicating defects in the initial phase of oxidative phosphorylation. These findings strongly support the hypothesis that stress exposure disrupts mitochondrial electron transport chain (ETC) function, leading to diminished ATP synthesis and enhanced electron leakage, thereby increasing reactive oxygen species (ROS) generation and exacerbating gastric tissue injury.

3.6. Stress-induced disruption of fatty acid oxidation and mitochondrial maintenance via PGC1α-associated networks

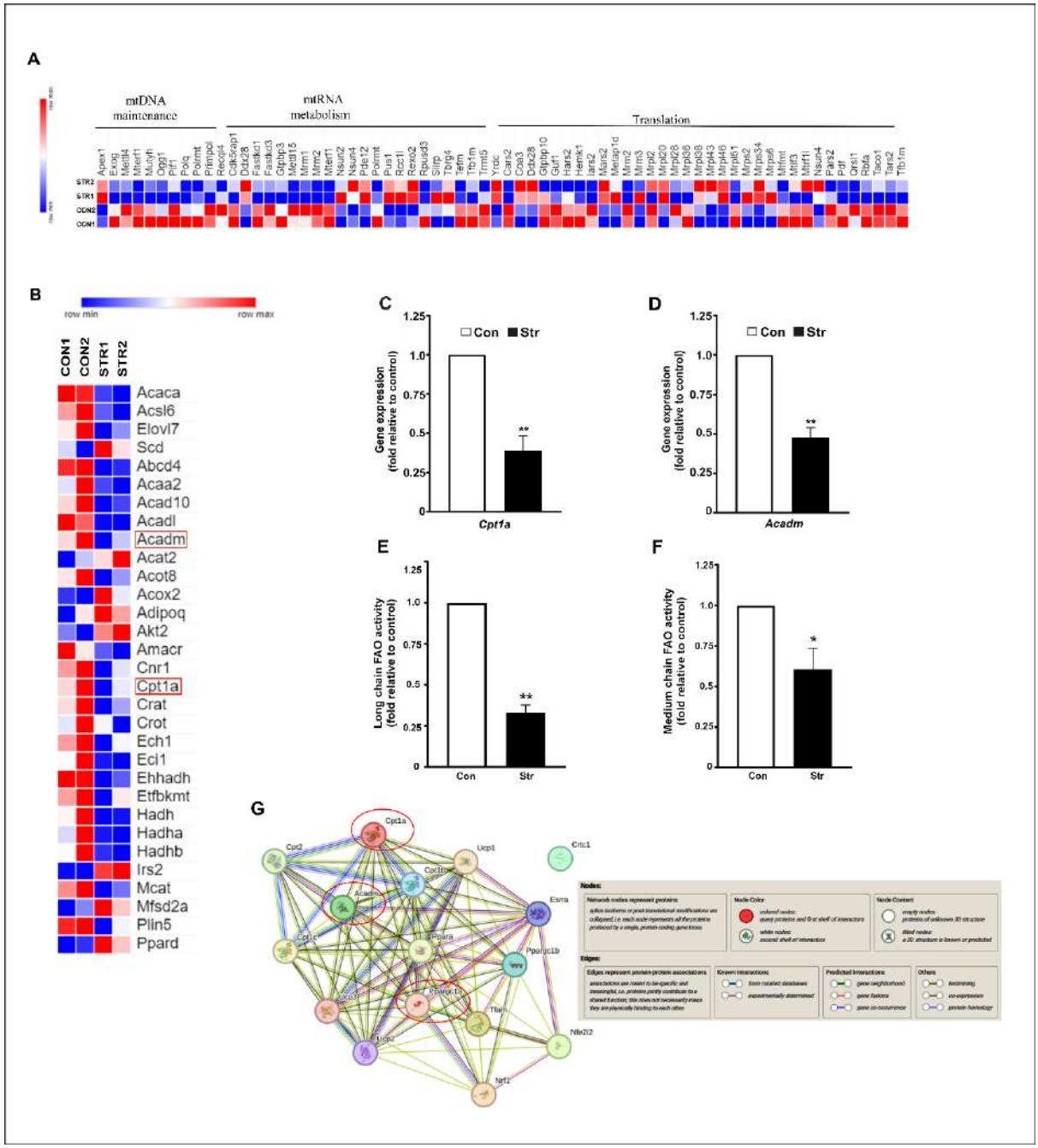

Figure 8. Acute stress affected mitochondrial maintenance, fatty acid oxidation, and PGC-1α-associated networks. (A) Heatmap depicts the differential expression of genes involved in mitochondrial central dogma including 'mtDNA maintenance', 'mtRNA metabolism' and 'mitochondrial translation' between 'Con' and 'Str' as checked by NGS-based transcriptomics and analysed using a fold change cut off of 1.2. The colour gradient represents relative expression levels, with red indicating upregulation and blue indicating downregulation. (B) Heatmap shows a subset of DEGs associated with fatty acid β-oxidation in control (C1, C2) and stress (STR1, STR2) as checked by NGS-based transcriptomics and analysed using a fold change cut off of 1.2. The colour gradient represents relative expression levels, with red indicating upregulation and blue indicating downregulation. (C, D) Quantitative PCR (qPCR) analysis of Cpt1a (carnitine palmitoyl transferase 1A) and Acadm (acyl-CoA dehydrogenase medium chain) genes. The results are depicted as fold change in gene expression compared to the control after normalizing by Gapdh. (E, F) Enzyme activity assays measuring Cpt1a and Acadm functional activity (represented as long chain and medium chain fatty acid oxidation, respectively) in control (Con) and stress (Str). Data are represented as fold change relative to the control. (G) Protein-protein interaction (PPI) network analysis by STRING (https://string-db.org/) highlighting the regulatory role of Ppargc1a (PGC-1α) in mitochondrial function and fatty acid oxidation. The STRING network visualization shows interactions among key metabolic regulators, including Cpt1a, Acadm, and other mitochondrial-associated proteins. The red circle emphasizes PGC-1α as a central regulator in this network. Data (C-F) are presented as mean ± SD, n = 5. $^{*}P < 0.05$ and $^{**}P < 0.01$ compared to the control, calculated using unpaired Student's t test with Welch's correction. Relative values for gene expressions and enzyme activities are presented as fold change relative to control wherein expression or activity values corresponding to control are considered as 1-fold. The number of independent experiments is 3. ns = not significant.

Transcriptome analysis revealed a significant downregulation of genes associated with mtDNA maintenance, mRNA metabolism, and mitochondrial translation, indicating impaired mitochondrial maintenance under stress conditions (Fig. 8A). Additionally, genes involved in lipid metabolism and mitochondrial fatty acid β-oxidation were markedly downregulated in stress-exposed samples (Fig. 8B). In particular, Cpt1a (carnitine palmitoyltransferase IA) and Acadm (acyl-CoA dehydrogenase medium chain), which are the key mitochondrial β-oxidation genes, showed substantial transcriptomic repression, indicating impaired fatty acid entry into mitochondria and disrupted β-oxidation. Other notably downregulated genes included Acadl, Acaa2, Acad10, Acox2, Hadha, Hadhb, Ehhadh, Crat, and Mcat, collectively reflecting widespread suppression of mitochondrial lipid catabolic pathways under acute stress conditions. Quantitative PCR and assay of enzyme activity further confirmed these transcriptomic findings (Fig. 8C-F). Expression of Cpt1a, the rate-limiting enzyme in mitochondrial long-chain fatty acid β-oxidation, was significantly lower in the stress group, alongside a marked downregulation of Acadm, responsible for medium-chain fatty acid β-oxidation (Fig. 8C and D). The data indicated a significant reduction in the oxidation of both long-chain and medium-chain fatty acids, as evident from the reduced enzymatic activity of CPT1A and ACADM (Fig. 8E and F). This metabolic disruption likely contributes to compromised energy production and overall mitochondrial dysfunction in stressed tissues. Protein–protein interaction (PPI) network analysis using STRING revealed that Cpt1a and Acadm are closely linked to Ppargc1a (PGC-1α), which emerged as a central hub interacting with numerous regulators of mitochondrial function and lipid metabolism (Fig. 8G). The transcriptional coactivator PGC1α serves as a master regulator of cellular energy metabolism, exerting its control over fatty acid catabolism, mitochondrial gene expression, and mitochondrial biogenesis. PGC1α controls the expression of key β-oxidation genes, Cpt1a and Acadm (30,31) while synchronously coordinating mitochondrial DNA (mtDNA) transcription, replication, and maintenance through the PGC1α–NRF1–TFAM axis. Given its central regulatory role, it was imperative to assess the expression of PGC1α under acute stress conditions to determine its potential contribution to the observed suppression of lipid catabolism and the dysregulation of the mitochondrial electron transport chain (ETC). Accordingly, the expression profile of PGC1α was investigated.

3.7. Stress-induced impairment of mitochondrial biogenesis and increased ubiquitination

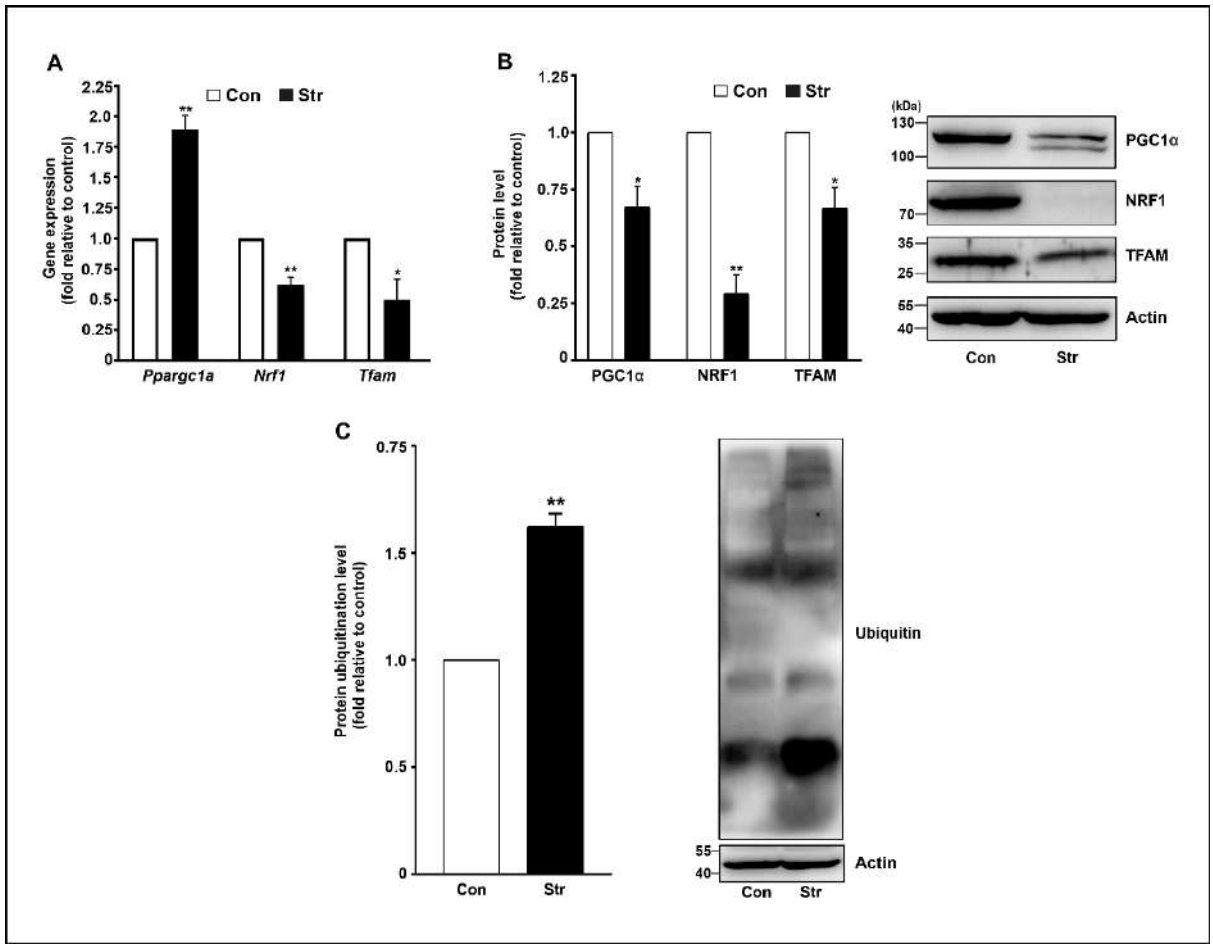

Figure 9. Effects of acute stress on PGC-1α expression, mitochondrial biogenesis regulators, and protein ubiquitination. (A) Gene expression analysis of Ppargc1a and its target genes involved in mitochondrial biogenesis (Nrf1 and Tfam,), measured by qPCR. The results are depicted as a bar graph showing the fold change in gene expression compared to the control after normalizing by Gapdh. (B) Immunoblot analysis of PGC-1α, NRF1, and TFAM proteins in gastric mucosal tissues from the 'Con' and 'Str' rats. Representative blots are shown beside the bar graph. Actin was used as a loading control. (C) Immunoblot showing gastric mucosal total proteome ubiquitination in 'Con' and 'Str' samples. Actin was used as the loading control. Representative blot provided alongside the bar graph. Data are presented as mean ± SD, n = 5. $^{*}P < 0.05$ and $^{**}P < 0.01$ compared to the control and calculated using unpaired Student's t test with Welch's correction. Relative expression values are presented as fold change relative to control, wherein expression values corresponding to control are considered as 1-fold. The number of independent experiments is 3. ns = not significant.

Transcriptomic analyses revealed a paradoxical increase in the expression of Ppargc1a (PGC-1α), a master regulator of mitochondrial biogenesis and energy metabolism, in response to acute stress. To validate this observation and further elucidate downstream effects, the expression profiles of PGC-1α and its key effectors were checked at both the transcript and protein levels. Quantitative RT-PCR confirmed a significant upregulation of Ppargc1a mRNA in stressed gastric tissues, substantiating the transcriptomic findings (Fig. 9A). However, this transcriptional upregulation of PGC1α did not correspond to functional activation of its downstream effectors. Notably, the mRNA levels of Nrf1 (nuclear respiratory factor 1) and Tfam (mitochondrial transcription factor A), both integral components of the mitochondrial biogenesis axis, were significantly downregulated under stress (Fig. 9A). Immunoblot analysis revealed a substantial reduction in PGC1-α in stress-exposed gastric tissues,

despite its upregulation at the mRNA level (Fig. 9B). This paradoxical discrepancy between gene and protein expression suggests increased post-translational degradation of PGC1-α, potentially due to ubiquitin-mediated proteasomal degradation. To investigate this, total protein ubiquitination was assessed. Further immunoblot analysis revealed a significant increase in total protein ubiquitination, supporting the hypothesis that stress-induced abnormal protein turnover contributes to PGC1-α depletion (Fig. 9C). In addition, NRF1 and TFAM protein levels were markedly reduced, reinforcing the evidence of compromised mitochondrial biogenesis at both the transcriptional and translational levels. These findings strongly suggest that stress exposure leads to impaired mitochondrial biogenesis, primarily due to ubiquitination-mediated degradation of PGC1-α and downregulation of its downstream transcription factors. The disruption of the PGC1α–NRF1–TFAM axis further exacerbates mitochondrial dysfunction, leading to reduced mitochondrial biogenesis, energy deficits, and increased oxidative stress.

3.8. Stress-induced activation of glucocorticoid signalling and its role in ubiquitin-mediated proteasomal degradation

Following the observation of increased protein ubiquitination in stress-induced gastric injury, transcriptomic analysis was conducted to assess the expression profile of E3 ubiquitin ligase genes. The analysis revealed a significant upregulation of several E3 ligases, notably including established glucocorticoid receptor (GR) target genes such as Fbxo32, Smurf1, Traf6, and Trim63, indicating transcriptional activation of the ubiquitination machinery under stress (Fig. 10A). To further elucidate the regulatory framework underlying these transcriptional alterations, a hub gene network was constructed using Molecular Complex Detection (MCODE) (32) plugin in Cytoscape (33). This analysis identified GR signalling as a central regulatory node influencing a broad array of cellular processes. The interactome revealed extensive crosstalk between GR signalling and critical biological pathways, including apoptosis, necrosis, immune modulation, glucose metabolism, and inflammation mechanisms closely linked to gastric mucosal pathology (Fig. 10B). Furthermore, GR target genes such as Klf15 and Fbxo32 exhibited pronounced transcriptional modulation in response to stress exposure, reinforcing the role of GR as a master regulator in this context. To substantiate the involvement of glucocorticoid receptor signalling in stress-induced gastric pathology, serum corticosterone concentrations were quantified. The nuclear translocation and activation status of the glucocorticoid receptor (GR) were evaluated. A significant elevation in serum corticosterone levels was observed in stress-exposed rats (Fig. 10C), indicative of the activation hypothalamic-pituitary-adrenal (HPA) axis and systemic upregulation of glucocorticoids. Immunoblot analysis further demonstrated an increase in GR nuclear localization in stress-exposed tissues, as confirmed by its enrichment in nuclear fraction (Fig. 10D). Immunoconfocal microscopy revealed enhanced nuclear translocation of GR, with a significant increase in colocalization with stained nuclei from 31.5% (control) to 51.5% (stress-exposed), indicating GR activation under stress conditions (Fig. 10E). These findings collectively indicate that stress-induced activation of the glucocorticoid receptor (GR) initiates a transcriptional program that upregulates E3 ubiquitin ligases, thereby promoting ubiquitin-mediated proteasomal degradation. This aligns with previous findings of PGC1-α depletion at the protein level (Fig. 9B) despite transcriptional upregulation (Fig. 9A), supporting the hypothesis that GR activation promotes protein turnover and mitochondrial dysfunction.

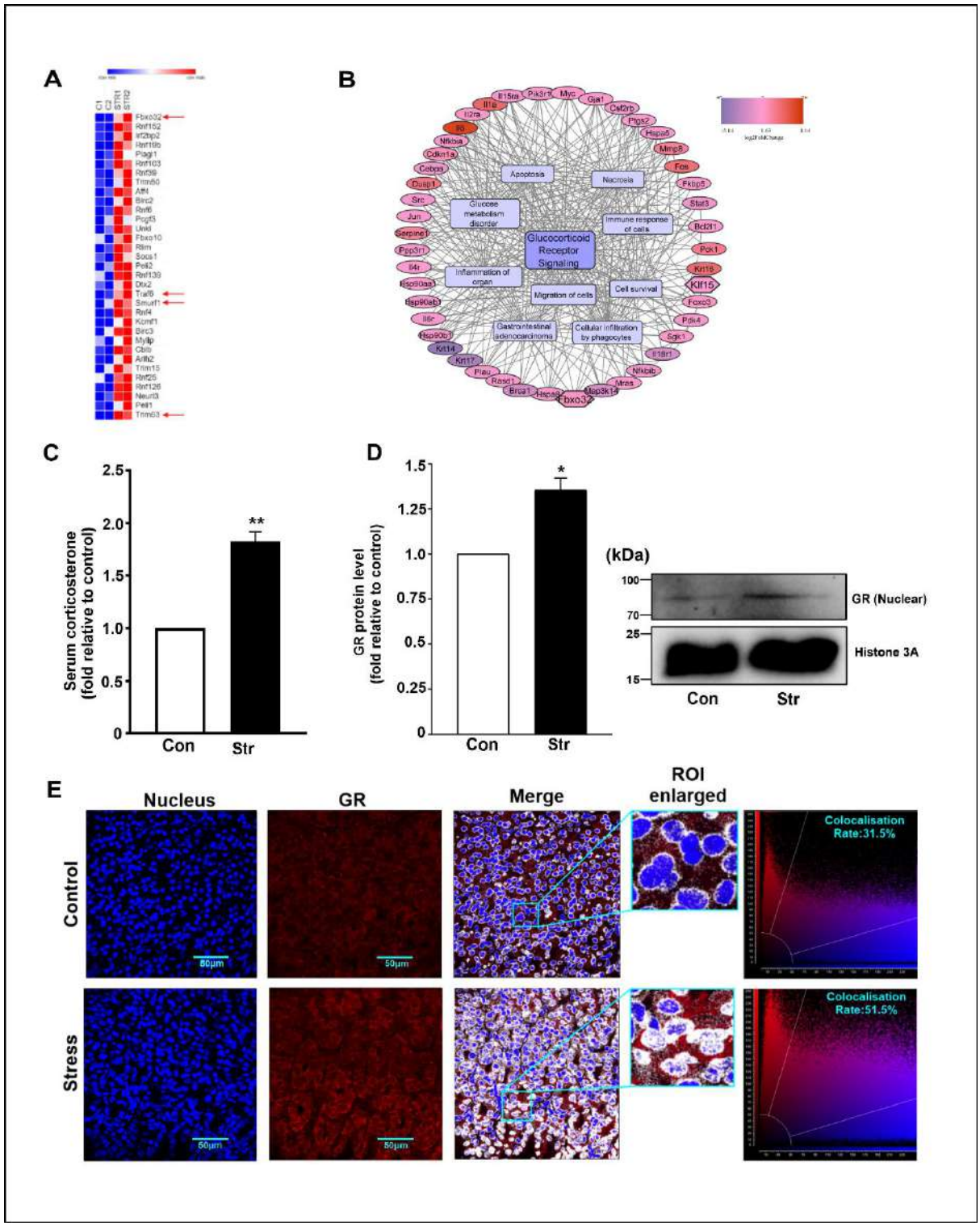
A
B
Glucocorticoid Receptor Signaling
Apoptosis
Necrosis
Glucose mesabolism disorder
Immune response of cells
Inflammation of organ
Cell survival
Migration of cells
Gastrointestinal adenocarcinoma
Cellular infiltration by phagocytes
C
Serum corticosterone (fold relative to control)
Con
Str
D
GR protein level (fold relative to control)
(kDa)
GR (Nuclear)
Histone 3A
E
Nucleus
GR
Merge
ROI enlarged
Control
Stress
Colocalisation Rate:31.5%
Colocalisation Rate:51.5%

Figure 10. Acute stress induces the expression of E3 ubiquitin ligase genes and activates the glucocorticoid receptor. (A) Heatmap depicting a subset of DEGs comprising of E3 ubiquitin ligase genes in control (C1, C2) and stress (STR1, STR2). Stress upregulated several GR target genes, including Fbxo32, Smurf1, Traf6, and Trim63 genes are marked with red arrows. (B) Interactome network created using Cytoscape to represent the association of DEGs, and glucocorticoid receptor signalling pathway as well as other major cellular events and functions via commonly shared genes, including Fbxo32 and Klf15. Expression values of genes, in terms of $\log_2$ fold change, are represented using a colour gradient scale with light-purple being highly downregulated to red being highly upregulated. (C) Serum corticosterone levels were measured by ELISA in gastric mucosal tissues from the 'Con' and 'Str' rats. (D) Immunoblot of glucocorticoid receptor (GR) protein level in the nuclear fraction of the 'Con' and 'Str' samples. Histone 3A is used as the loading control. Representative blots are provided alongside the bar graph in the panel. (E) Confocal immunohistochemical staining showing nuclear translocation of GR in the gastric mucosa of rats in control and during stress exposure. DAPI (blue) stains nuclei, while GR (red) represents glucocorticoid receptor localization. The merged images show increased nuclear GR localization under stress. Enlarged regions of interest (ROI) and colocalization analysis confirm a higher percentage of GR nuclear translocation in stress conditions. Data are presented (C, D) as mean ± SD, n = 5. $^{*}P < 0.05$ and $^{**}P < 0.01$ compared to the

3.9. Stress-induced upregulation of KLF15 and its target FBXO32

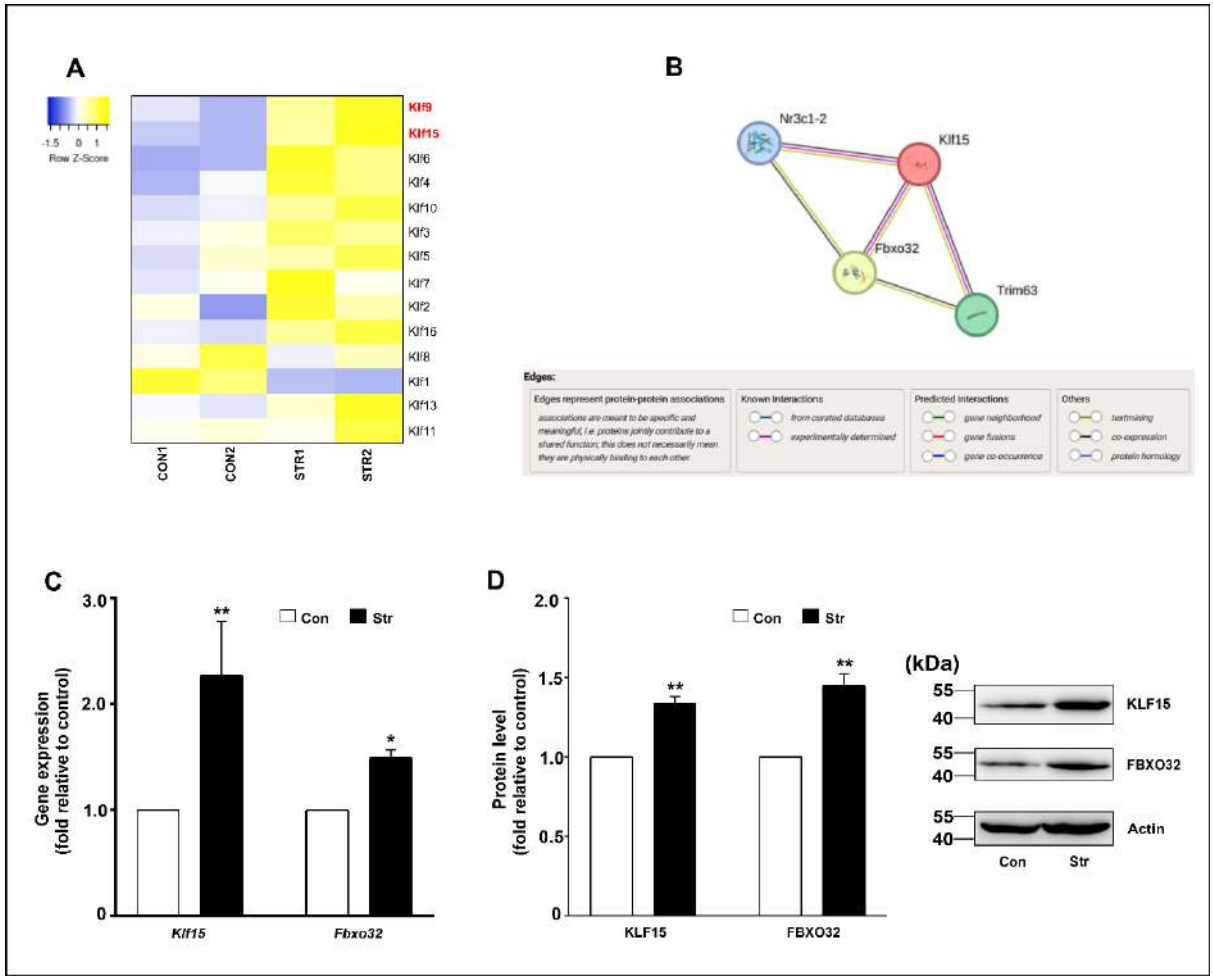

Figure 11. Acute stress induces the expression of glucocorticoid receptor (GR) target genes. (A) Heatmap showing a subset of DEGs checked using transcriptome sequencing to indicate the differential expression of Klf family genes in control (Con1, Con2) and stress (Str1, Str2). Klf15 and Klf9 are the target genes of GR showing upregulation under stress are marked in red. (B) Protein-protein interaction (PPI) network analysis by STRING (https://string-db.org/) highlighting GR(Nr3c1-2) and KLF15 interactions with Fbxo32 and Trim63. (C) Quantitative PCR (qPCR) analysis of Klf15 and its downstream target Fbxo32 expression in gastric mucosal tissues of control (Con) and stress (Str) exposed rats. Expression levels are shown as fold change relative to control. (D) Immunoblot analysis of KLF15 and FBXO32 proteins in gastric mucosal tissues from the 'Con' and 'Str' rats. Representative blots are shown alongside the bar graph. Actin was used as a loading control. Data are presented (C, D) as mean ± SD, n = 5. $^{*}P < 0.05$ and $^{**}P < 0.01$ compared to the control, and calculated using unpaired Student's t test with Welch's correction. Relative expression values (C-D) are presented as fold change relative to control, wherein expression values corresponding to control are considered as 1-fold. The number of independent experiments is 3.

Since KLF15 is a direct target of the activated glucocorticoid receptor (GR) (34,35) and functions as a transcriptional activator of Fbxo32 (35), we explored the transcriptional regulation of FBXO32, an E3 ubiquitin ligase involved in proteasomal degradation. To this end, the expression profile of the Krüppel-like factor (KLF) gene family was first analyzed using transcriptomic data, and the expression of KLF15, a key transcription factor regulating FBXO32, was further validated (Fig. 11A and C). Transcriptomic data revealed a significant upregulation of KLF15 under stress conditions, along with other KLF family members. Notably, Klf15 and Klf9, known target genes of activated GR (36), were among the most highly upregulated under stress, as depicted in the heatmap. Protein-protein interaction (PPI) analysis using the STRING network highlighted strong predicted interactions among GR (Nr3c1), KLF15, FBXO32, and Trim63, emphasizing their role in proteasomal degradation pathways (Fig. 11B). Further qPCR validation confirmed the significant upregulation of KLF15, and FBXO32 at the mRNA level in stress-exposed gastric tissues compared to controls (Fig. 11C). At the protein level, immunoblot analysis demonstrated an increase in KLF15 and FBXO32 expression under stress conditions, further supporting their transcriptional upregulation (Fig. 11D). These findings strongly suggest that stress-mediated activated GR further activates KLF15, which subsequently enhances the expression of FBXO32, leading to increased protein ubiquitination and proteasomal degradation. This GR-KLF15-FBXO32 axis may play a crucial role in stress-induced mitochondrial dysfunction and contribute to metabolic imbalances and impaired cellular homeostasis in gastric tissues. The identification of this pathway provides novel insights into the molecular mechanisms underlying stress-induced protein dysregulation leading to gastropathy.

3.10. Stress-induced ROS, phospholipase activation, and phosphatidic acid accumulation cause gastric mucosal injury

Mitochondrial electron transport chain (ETC) dysfunction plays a central role in driving ROS overproduction under acute stress conditions. In earlier stages of this study, proteasomal degradation and substantial depletion of critical mitochondrial regulatory proteins, such as PGC1-α and TFAM, were observed (Fig. 9B). Additionally, several mitochondrial ETC genes were significantly downregulated (Fig. 7). These alterations disrupt normal electron flow, leading to increased electron leakage and subsequent accumulation of ROS, thereby initiating a state of severe oxidative stress. Integrative transcriptomic and metabolomic analyses further confirmed oxidative stress as a principal mediator of stress-induced gastric mucosal injury. Based on these findings, the present investigation explored the downstream consequences of this redox imbalance, particularly its impact on lipid metabolism and membrane remodelling processes.

Oxidative stress plays a critical role in cellular dysfunction, primarily by triggering the peroxidation of membrane phospholipids, which leads to the accumulation of lipid peroxides. These peroxides activate phospholipase enzymes, including phospholipase D (PLD), which hydrolyses membrane lipids to

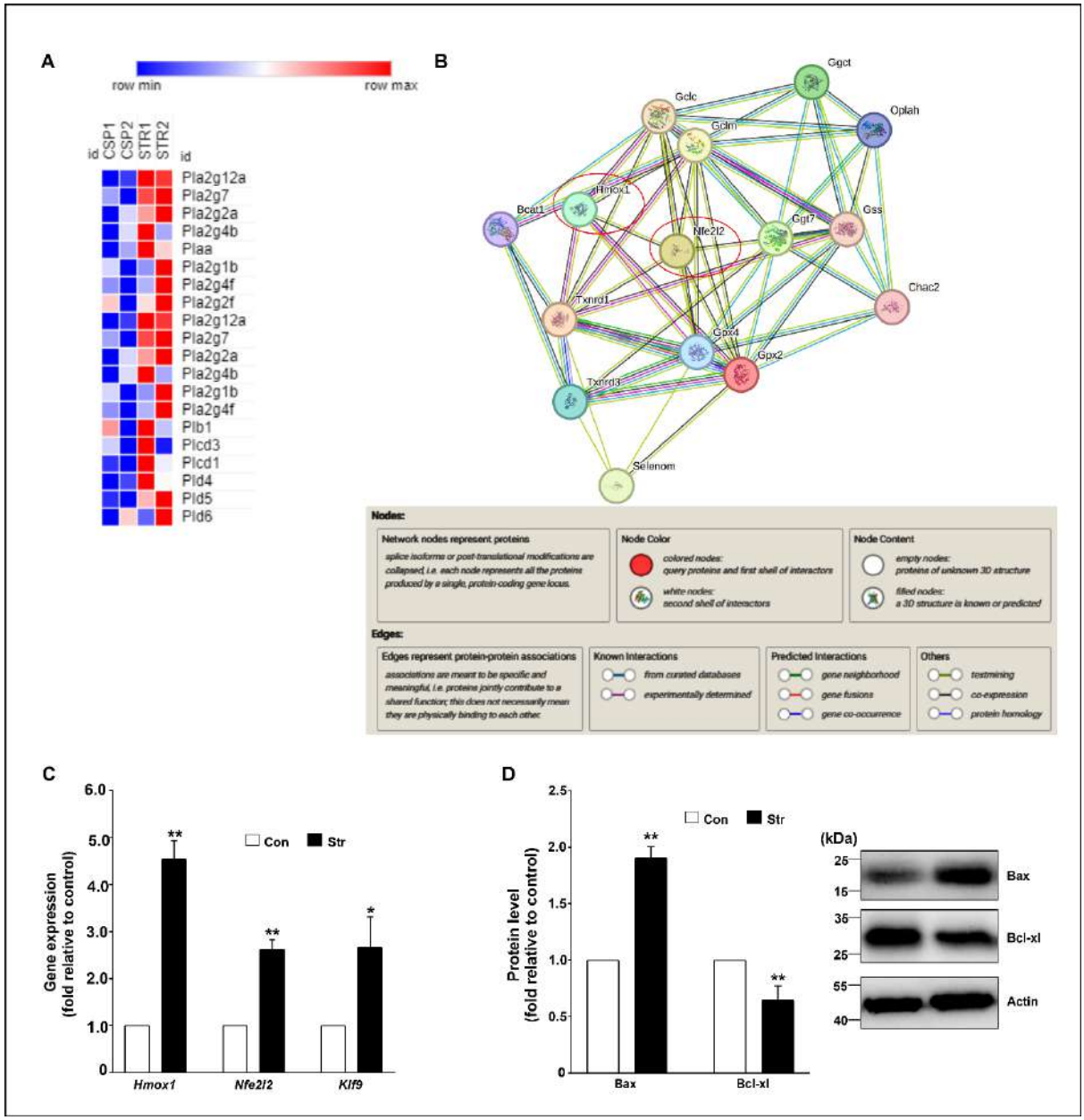

Figure 12. Acute stress induces transcriptional activation of phospholipase, antioxidant pathways, and apoptosis. (A) Heatmap of a subset of DEGs showing differential expression of phospholipase genes between 'Con' and 'Str' checked using transcriptome sequencing and analysed with a fold change cut off of 1.2. The colour gradient represents relative expression levels, with red indicating upregulation and blue indicating downregulation. (B) Protein-protein interaction (PPI) network analysis of redox-related genes by STRING (https://string-db.org/) highlighting key interactions between oxidative stress regulators such as Nfe2l2 (Nrf2), Hmox1, and other antioxidant defence genes. (C) Quantitative PCR (qPCR) analysis of Hmox1, Nfe2l2 (Nrf2), and Klf9 expression in gastric mucosal tissues of control (Con) and stress (Str) samples. The results are depicted as fold change in gene expression compared to the control (controls are considered as 1-fold) after normalizing by Gapdh. (D) Immunoblot analysis of Bax and Bcl-xl proteins in gastric mucosal tissues from the 'Con' and 'Str' rats. Representative blots are alongside the bar graphs. Protein expression levels were normalized to actin as a loading control and shown as fold change relative to the control. Data are presented (C-D) as mean ± SD, n = 5. $^{*}P < 0.05$ and $^{**}P < 0.01$ compared to the control; calculated using unpaired Student's t test with Welch's correction. The number of independent experiments is 3.

produce phosphatidic acid (PA), a crucial lipid signalling molecule involved in stress responses. Additionally, phospholipase A2 (PLA2) plays a key role in oxidative stress conditions, breaking down plasma membrane components, including peroxidized fatty acids, thereby exacerbating cellular damage (37,38). Metabolomic study revealed a significant upregulation of phosphatidic acid (PA) levels in stress-exposed groups compared to controls. Since PA is primarily generated through phospholipase activation, transcriptomic data were analyzed to assess phospholipase gene expression. Transcriptome analysis revealed the upregulation of multiple phospholipase genes under stress conditions, indicating an enhanced capacity for PA synthesis (Fig. 12A). Increased PLD activity and PA production further stimulate reactive oxygen species (ROS) generation by activating NADPH oxidases, creating a self-perpetuating cycle that amplifies oxidative stress. The accumulation of oxidized phospholipids further enhances phospholipase activity, triggering inflammatory pathways and promoting cellular injury. In stress-exposed gastric mucosa, the activation of PLA2, PLC, and PLD genes led to a detectable rise in PA production. This suggests a stress-induced lipid remodeling process, leading to an excess of bioactive lipid mediators involved in oxidative stress signaling. To further assess oxidative stress levels due to mitochondrial ETC dysfunction, a STRING network analysis was performed, revealing key interactions between oxidative stress regulators such as Nrf2, HMOX1, and other antioxidant defence genes (Fig.12 B). To elucidate the dynamics of redox signalling under stress conditions, we performed real-time PCR analysis of key oxidative stress-responsive genes, including Hmox1, Nfe2l2 (Nrf2), and Klf9 (Fig. 12C). A significant upregulation of these genes was observed, indicative of an activated NRF2-mediated antioxidant response.

The marked increase in Hmox1, a pivotal cytoprotective enzyme, further suggests a compensatory cellular effort to counteract oxidative damage induced by stress. Interestingly, we detected a significant upregulation of Klf9 in transcriptomics data (Fig. 11A) and also validated using qPCR (Fig. 12C). Klf9 is a transcription factor known to amplify oxidative stress, despite being a downstream target of Nrf2 and the glucocorticoid receptor (GR)(39-41). Nrf2 activation initially upregulates antioxidant defences but paradoxically induces Klf9, which transcriptionally represses key antioxidant genes, thereby perpetuating oxidative stress, disrupting redox homeostasis, and exacerbating cellular injury (39). This ROS amplification cascade ultimately drives gastric mucosal cell apoptosis and exacerbates severe mucosal injury in stress-exposed rats. To further investigate the impact of oxidative stress on cell survival and apoptosis, immunoblot analysis was performed to assess the expression of BAX (pro-apoptotic) and Bcl-xL (anti-apoptotic) proteins in stress-exposed gastric mucosa. A significant increase in BAX levels was observed, indicating enhanced apoptotic signalling under stress conditions, while Bcl-xL expression was markedly reduced, suggesting a weakened cellular survival response (Fig. 12D).

This shift in the BAX/Bcl-xL ratio toward apoptosis underscores a stress-induced pro-apoptotic environment, aligning with the previously observed oxidative stress and glucocorticoid receptor (GR) activation. These changes collectively indicate that mitochondrial impairment, oxidative stress, and apoptosis contribute to stress-induced gastric mucosal injury.

3.11. Quercetin-3-glucoside (Q3G), olanzapine, and RU486 attenuate stress-induced acute gastric mucosal injury

Based on the above findings, three mechanistically distinct intervention strategies were systematically evaluated to prevent stress-induced gastric mucosal injury: (1) antioxidant supplementation to counter oxidative damage, (2) central modulation of stress perception to interrupt upstream neuroendocrine signalling, and (3) direct antagonism of glucocorticoid receptor (GR) signalling to block downstream molecular mediators of tissue injury. Quercetin, a widely studied flavonoid, exhibits potent antioxidant properties, making it a promising therapeutic candidate in conditions characterized by oxidative stress and cellular injury, such as stress-induced gastric mucosal damage. However, its clinical translation has been limited by poor bioavailability, particularly in its aglycone form. In this context, quercetin-3-glucoside (isoquercetin) emerges as a superior alternative due to its enhanced absorption and pharmacokinetic profile. Pretreatment with Q3G significantly attenuated gastric injury in rats subjected to cold restraint stress.

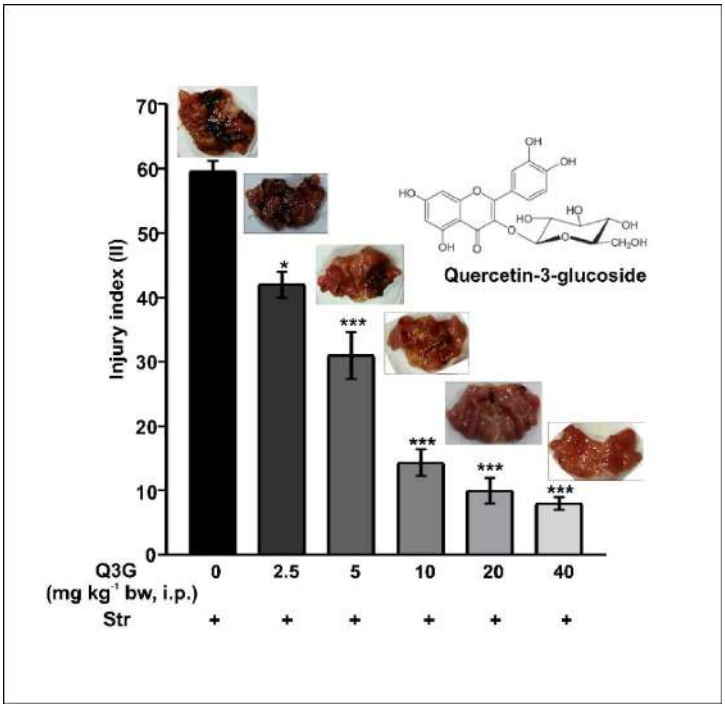

Figure 13. Dose-dependent effect of quercetin-3-glucoside (Q3G) on acute stress-induced gastric mucosal injury. The bar graph shows the dose response of quercetin-3-glucoside (Q3G) pre-treatment on acute stress-induced gastric mucosal injury. The inset image displays representative morphology of the gastric mucosa corresponding to different doses of Q3G. The chemical structure of Q3G is also presented. Data are presented as mean ± SD, n = 5. $^{*}P < 0.05$, $^{***}P < 0.001$, and $^{****}P < 0.0001$; significantly different from Q3G 0 mg.kg $^{-1}$, one-way ANOVA followed by Bonferroni's post hoc test. Number of independent experiments: 3

A dose–response analysis identified 10 mg/kg (intraperitoneal) as the optimal gastroprotective dose, as higher doses offered no additional benefit (Fig. 13). At this dose, Q3G reduced the gastric injury index by approximately 70% compared to the stress group (18 ± 4 vs. 60 ± 5; $P < 0.001$), demonstrating robust mucosal protection (Fig. 14). To intervene upstream in the stress signalling cascade, olanzapine, a centrally acting antipsychotic known to suppress stress perception, was administered. Pretreatment with olanzapine similarly reduced gastric injury (Injury Index: 14 ± 4; $P < 0.001$ vs. stress), suggesting that central modulation of stress perception can effectively alleviate gastric pathology (Fig. 14). However, due to its sedative properties and long-term side effect profile, its clinical application may be limited. Acute stress elevates serum corticosterone levels, leading to GR activation and triggering the GR–KLF15–FBXO32 signalling axis implicated in proteasomal degradation and mucosal injury. Recognizing the central role of glucocorticoid signalling in mediating stress responses, the GR pathway was then directly

targeted. To counteract this mechanism, mifepristone (RU486), a competitive GR antagonist, was administered. RU486 pretreatment conferred the most substantial cytoprotection, significantly reducing the Injury Index (12 ± 2; $P < 0.001$ vs. stress). Macroscopic examination revealed preserved gastric morphology, and histological analysis of haematoxylin-eosin-stained sections confirmed marked protection against mucosal disintegration (Fig. 14). These findings collectively demonstrate that stress-induced gastric injury can be effectively attenuated through interventions targeting oxidative stress, neuropsychological stress perception, or GR signalling. In particular, direct inhibition of the GR–KLF15–FBXO32 axis emerged as a potent strategy for preserving gastric mucosal integrity under acute stress conditions. These findings also emphasize the critical role of mitochondrial biogenesis and metabolic homeostasis in gastric mucosal protection and provide a foundation for developing mitochondria-targeted therapies to counteract stress-induced gastric injury.

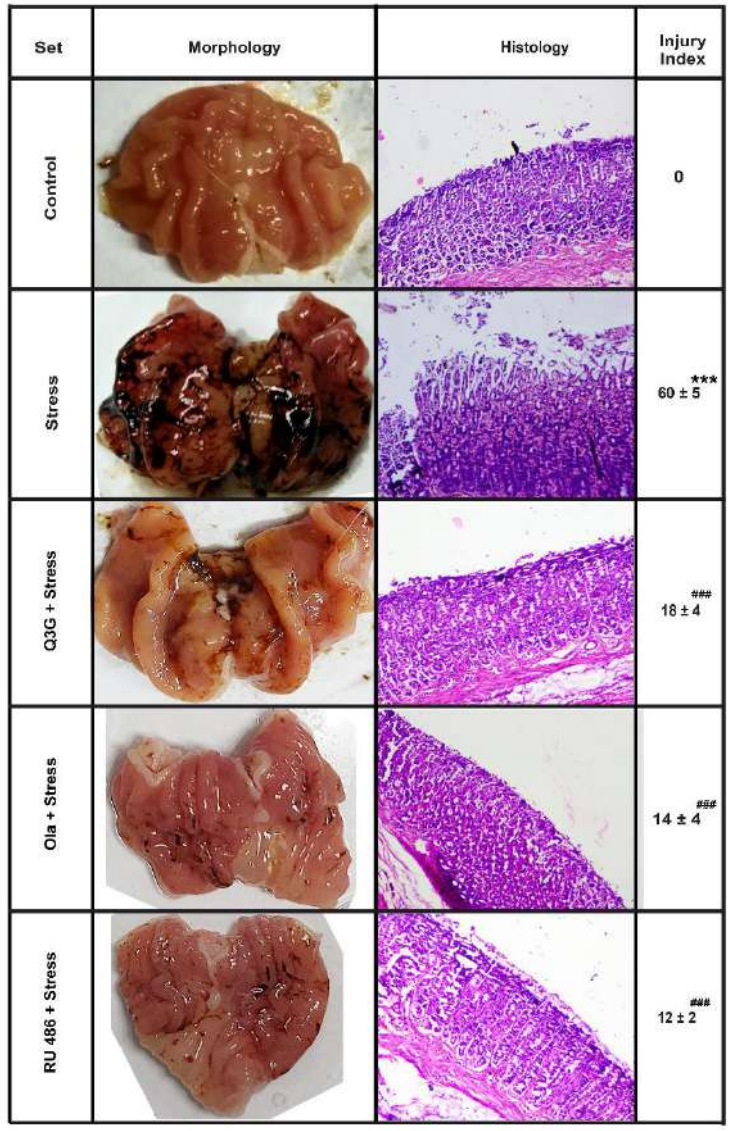

Figure 14. Effects of quercetin-3-glucoside (Q3G), olanzapine, and RU486 on acute stress-induced gastric mucosal injury. Gastric mucosal morphology and histology (haematoxylin-eosin stained) of rats subjected to different experimental conditions: Control, Stress, "Quercetin-3-glucoside (Q3G) + Stress", "Olanzapine (Ola) + Stress", and "RU486 + Stress". The injury index quantifies the severity of mucosal damage under each condition. Data are presented as mean ± SD. $^{***}P < 0.001$ compared to the control; $^{###}P < 0.001$ compared to stress, calculated using one-way ANOVA followed by Bonferroni's post hoc test.

3.12. Quercetin-3-glucoside preserves mitochondrial function and restores redox and metabolic homeostasis by modulating stress-responsive gene expression

As a first-line intervention strategy targeting oxidative stress, the therapeutic efficacy of quercetin-3-glucoside (Q3G), a bioavailable flavonoid with potent antioxidant activity, was investigated in a rat model of cold restraint stress-induced gastric mucosal injury. This approach aimed to assess whether antioxidant supplementation could mitigate the deleterious effects of acute psychological stress on mitochondrial function, redox balance, and metabolic homeostasis within the gastric mucosa. Pre-treatment with Q3G significantly alleviated stress-induced gastric mucosal injury in rats exposed to cold restraint stress. Transcriptomic analysis revealed a distinct clustering of gene expression profiles between stress-exposed (STR) and Q3G-treated stress (SQG) groups, as shown in the heatmap, suggesting significant transcriptomic alterations induced by Q3G treatment (Fig. 15A). Venn diagram analysis using a 1.5-fold change cutoff showed that stress upregulated 882 genes and downregulated 602 genes, while Q3G reversed 824 stress-induced genes (protection down) and upregulated 739 genes

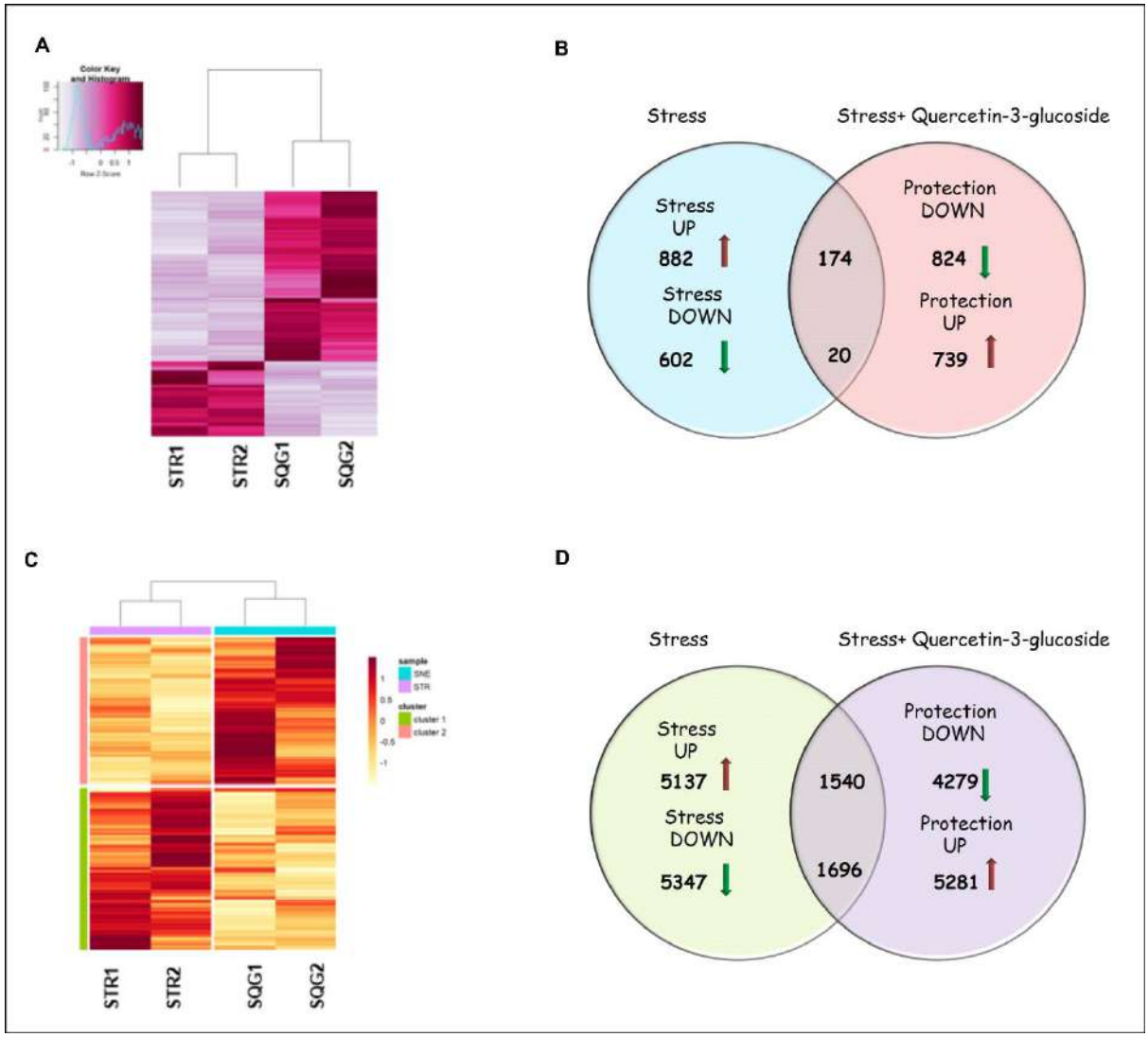

Figure 15. Transcriptomic analysis of the protective effects of quercetin-3-glucoside against stress-induced damage. (A) Heatmap showing differentially expressed genes (DEGs) obtained from separate clustering of samples from stress (STR) and quercetin-3-glucoside+stress (SQG) rats (false discovery rate [FDR] ≤ 0.05). The Euclidean distance metric was used while clustering the gene expression data. Expression value of genes analysed with FC cut-off of 1.5; colour gradient scale with red being highly up-regulated to white being highly down-regulated. (B) The Venn diagram compares the number of upregulated and downregulated genes in stress versus stress+quercetin-3-glucoside treatment. Quercetin-3-glucoside reversed the expression of 824 stress-induced genes (Protection DOWN) and upregulated 739 genes (Protection UP). (C-D) Heatmap and Venn diagram analysis using a 1.2-fold change (FC) cutoff. The broader analysis reveals a larger number of differentially expressed genes, with quercetin-3-glucoside reversing 4,279 stress-induced genes and upregulating 5,281 genes. GEO accession number GSE299825

(protection up), demonstrating its regulatory role in stress-related pathways (Fig. 15B). A broader analysis with a 1.2-fold change cutoff revealed that stress led to the upregulation of 5,137 genes and downregulation of 5,347 genes, whereas Q3G reversed 4,279 stress-induced genes and upregulated 5,281 genes, highlighting its widespread impact on gene expression (Fig. 15D). These findings suggest that Q3G effectively modulates gene expression patterns associated with stress responses.

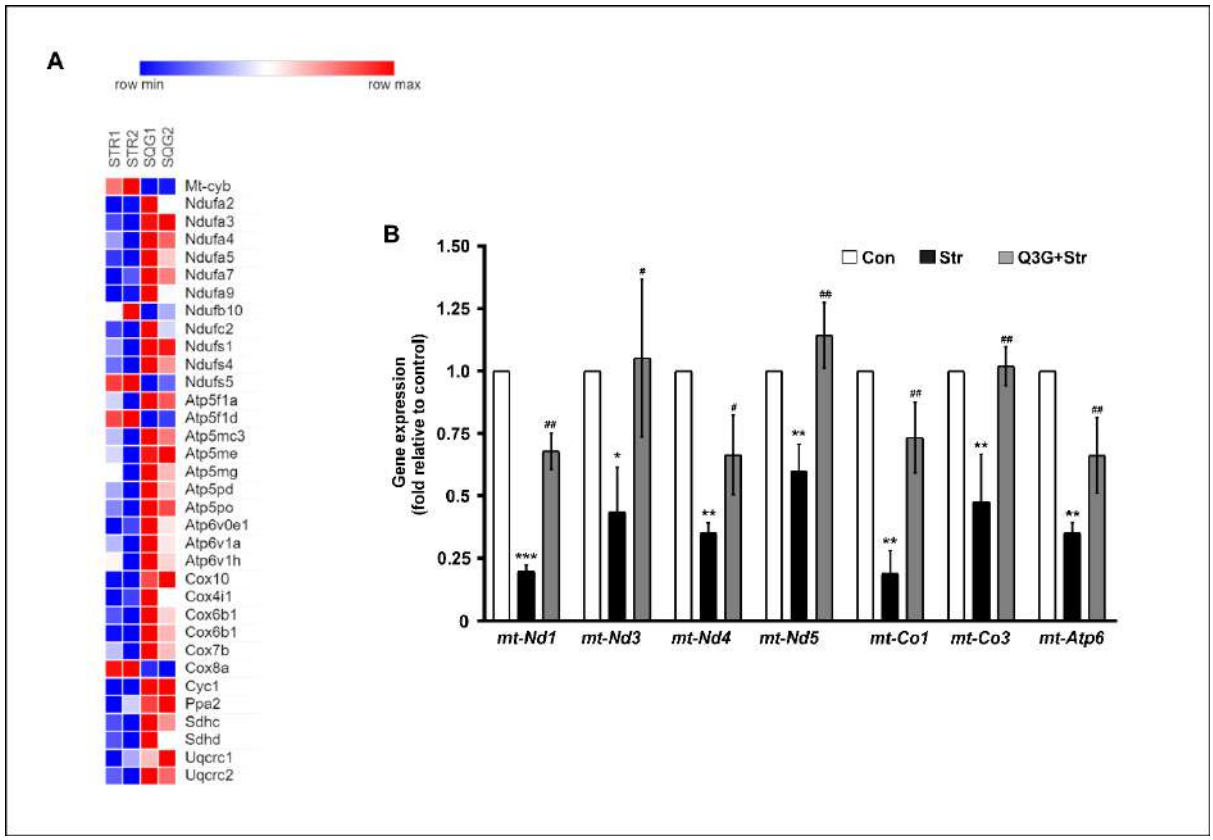

Figure 16. Quercetin-3-glucoside pretreatment reverses stress-induced alteration of mitochondrial gene expression. (A) Heatmaps represent differentially expressed mitochondrial electron transport chain and oxidative phosphorylation-related genes across stress-exposed (STR) and quercetin-3-glucoside-treated stressed (SQG) rats, checked by transcriptome sequencing and analysed with a fold change cut off of 1.2. DEGs colour gradient scale, with red being highly up-regulated and blue representing highly down-regulated. Gene expression analysis for mt-Nd1, mt-Nd3, mt-Nd4, mt-Nd5, mt-Co1, mt-Co3, and mt-Atp6 by qPCR in control (Con), stress (STR), and quercetin-3-glucoside+stress (SQG) samples. Bar graphs indicate fold change in gene expression relative to control (after normalization by Gapdh). Data presented as mean ± SD, n = 5. $^{*}P < 0.05$, $^{**}P < 0.01$, $^{***}P < 0.001$ compared to control; $^{\#}P < 0.05$, $^{\#\#}P < 0.01$ compared to stress and calculated using one-way ANOVA followed by Bonferroni's post hoc test. The number of independent experiments is 3.

Based on transcriptomic and other experimental findings that highlighted stress-induced mitochondrial dysfunction, redox imbalance, and metabolic dysregulation, the protective effects of Q3G in alleviating these impairments were investigated. Analysis of mitochondrial and mitochondria-associated nuclear gene expression revealed that Q3G treatment counteracts stress-induced mitochondrial dysfunction. Heatmaps demonstrated a significant downregulation of key mitochondrial genes and nuclear-encoded mitochondrial genes under stress conditions. However, Q3G treatment restored their expression, shifting them toward control levels (Fig. 16A). Additionally, quantitative RT-PCR analysis confirmed that stress significantly reduced mitochondrial electron transport chain (ETC) gene expression (ND1, ND3, ND4, ND5, Cox1, Cox3 and ATP6), whereas Q3G treatment effectively rescued their expression (Fig. 16B). Transcriptomic analysis revealed Q3G treatment alters the expression of major antioxidant genes, including Nfe2l2 (Nrf2), Sod2, Glrx3, Txrnd1, and various glutathione peroxidases (Gpx1, Gpx2, Gpx8) along with Hmox1, in the gastric mucosa of rats (Fig. 17A). The protein–protein interaction (PPI) analysis using STRING highlights strong functional connectivity among redox regulators such as Nfe2l2 (Nrf2), Txrnd1, Gpx1/2/8, Sod2, Glrx3, and Hmox1, indicating their coordinated role in maintaining oxidative homeostasis (Fig. 17B). These findings suggest that Q3G alleviates stress-induced mitochondrial dysfunction by preserving mitochondrial gene expression, supporting energy metabolism, and reducing oxidative damage. Stress significantly downregulated

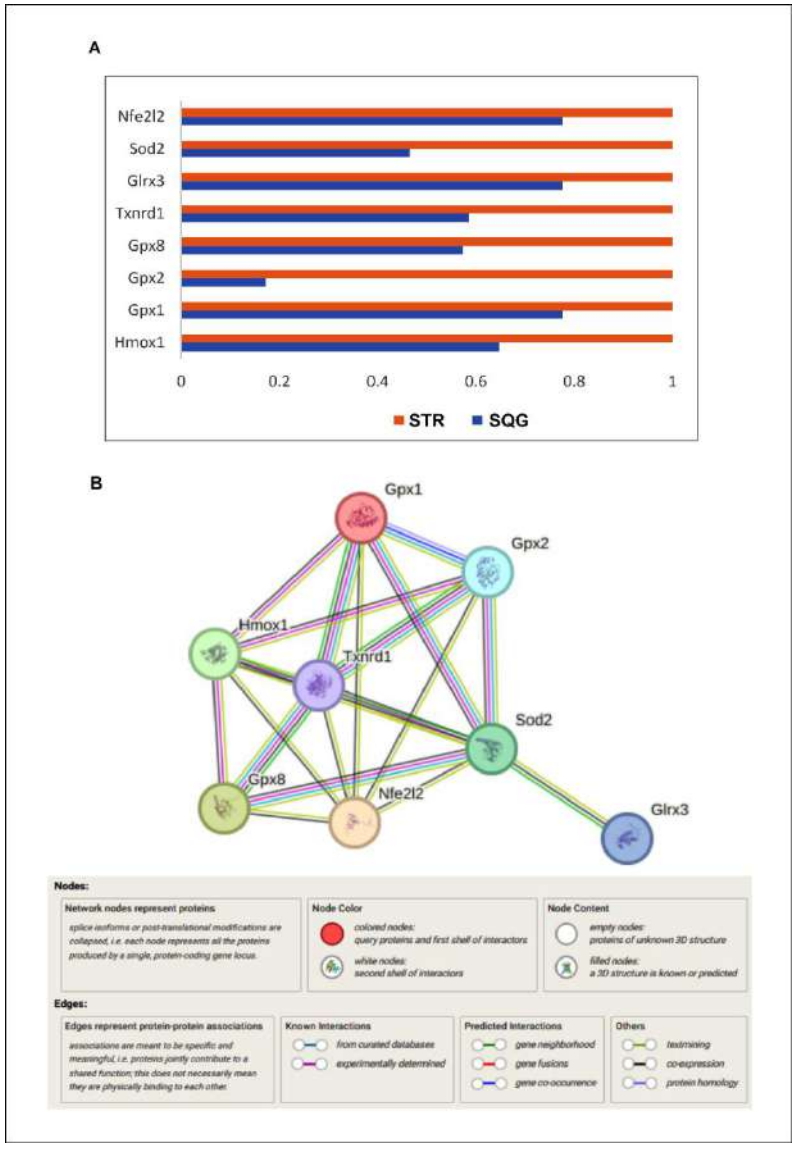

Figure 17. Quercetin-3-glucoside pretreatment reverses stress-induced alteration of antioxidant gene expression. (A) Transcriptomic analysis (fold change cut off of 1.2) showing relative mRNA expression levels of key antioxidant and redox-regulatory genes in gastric tissues from stress-exposed (STR) and quercetin-3-glucoside-treated stressed (SQG) rats. (B) Protein-protein interaction (PPI) network of antioxidant defence proteins derived from the STRING database (https://string-db.org/).

genes involved in mitochondrial DNA maintenance (Mgme1, Polq, Tfam), RNA metabolism (Mterf1, Tfb1m, Tfb2m, Trmt10c), and translation (Mrpl35, Mrps16, Mrps18c), as revealed by heatmap analysis. However, Q3G treatment restored their expression toward control levels (Fig. 18A). To further explore the role of Q3G in mitochondrial function, we analyzed its impact on mitochondrial biogenesis. Immunoblot analysis further confirmed that stress exposure significantly reduced the expression of key mitochondrial biogenesis regulators PGC1α, NRF1, and TFAM, all of which were markedly restored following Quercetin 3-glucoside (Q3G) treatment (Fig. 18B).

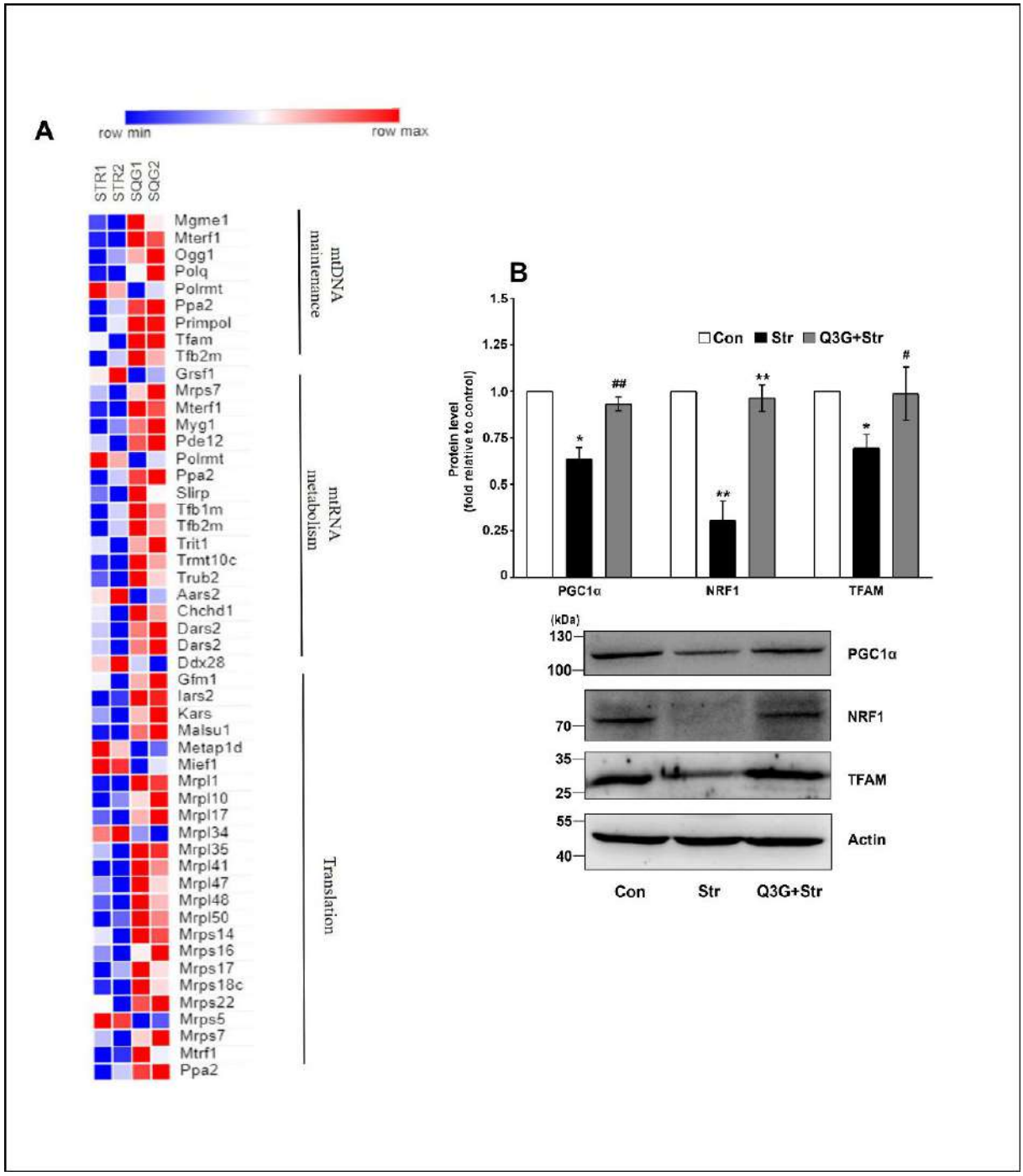

Figure 18. Protective effects of quercetin-3-glucoside (Q3G) against stress-induced mitochondrial dyshomeostasis. (A) Heatmap of a subset of DEGs showing differentially expressed genes involved in mitochondrial DNA maintenance, mRNA metabolism, and translation in stress (STR) and Q3G + stress (SQG) conditions, as checked by transcriptome sequencing and analysed using an FC cut-off of 1.2. (B) Immunoblots of mitochondrial biogenesis markers PGC1α, NRF1, and TFAM. Actin was used as the loading control; representative blots are presented below the bar graph. Data are presented as mean ± SD, n = 5. Relative expression values are presented as fold change relative to control wherein expression value corresponding to control are considered as 1-fold. $^{*}P < 0.05$, $^{**}P < 0.01$ compared to control; $^{\#}P < 0.05$ $^{\#\#}P < 0.01$ compared to stress and calculated using one-way ANOVA followed by Bonferroni's post hoc test. The number of independent experiments is 3

Stress-induced mitochondrial dysfunction severely impaired fatty acid β-oxidation and overall metabolic homeostasis. Heatmaps revealed that stress downregulated key genes involved in fatty acid-CoA synthesis (Acaca, Acacb) and fatty acid oxidation (Cpt1a, Cpt2, Hadha, Hadb), whereas Q3G treatment upregulated these genes, promoting efficient fatty acid metabolism (Fig. 19A). Similarly, Q3G restored amino acid metabolism (Aass, Acat1, Aldh5a1) (Fig. 19C) and glucose metabolism (Aldoa, Pck2, Pgm2) (Fig. 19D), as shown in heatmap analysis. Furthermore, ATP production, which was significantly reduced under stress conditions, was effectively restored by Q3G pre-treatment (Fig. 19B).

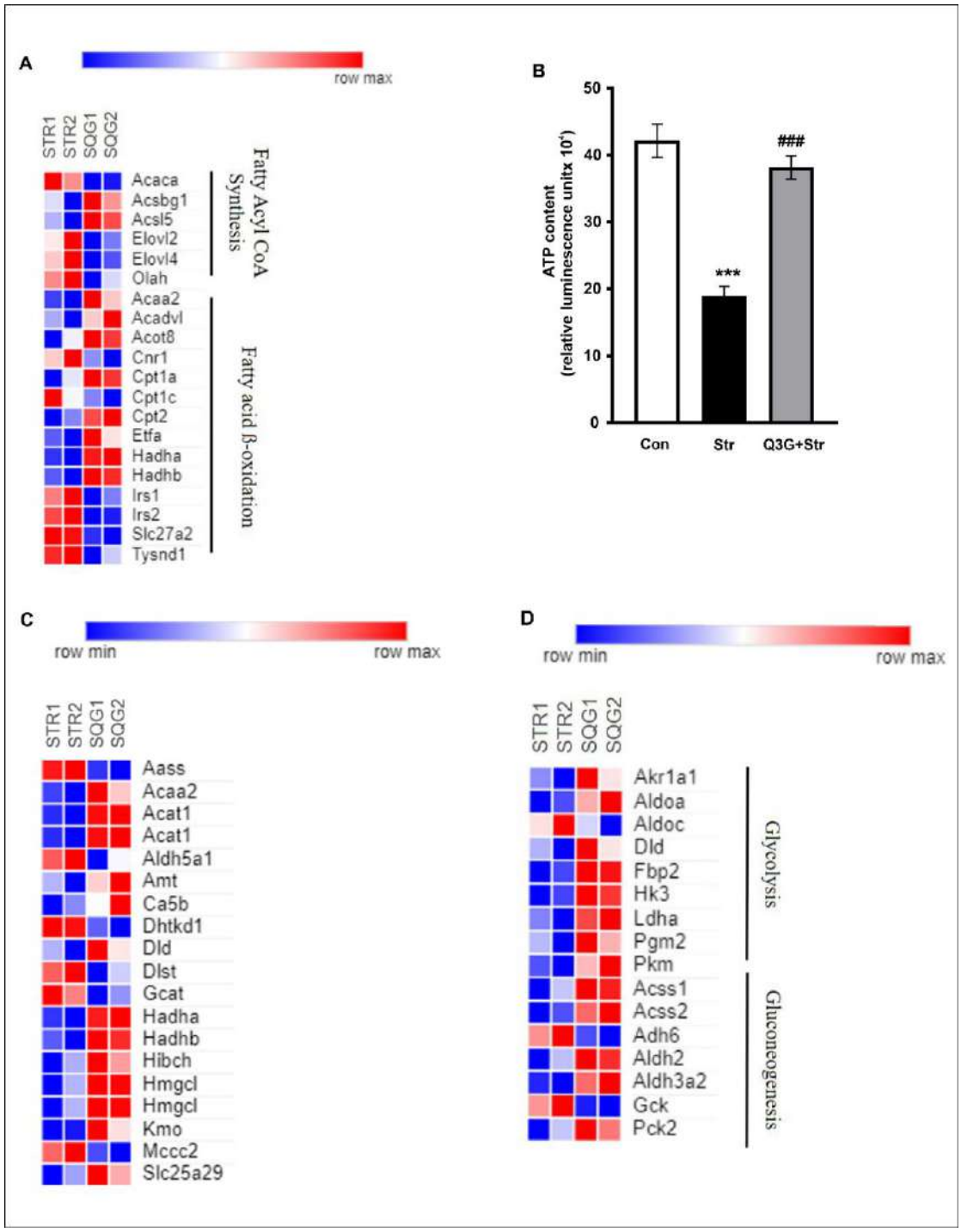

Figure 19. Quercetin-3-glucoside (Q3G) pre-treatment prevents detrimental alteration in gene expression profiles associated with metabolic pathways and bioenergetic crisis (A) Heatmap showing a subset of differential expression of genes involved in fatty acyl CoA synthesis and fatty acid oxidation in stress (STR) and Q3G + stress (SQG)samples as checked by transcriptome sequencing and analysed using a fold change cut off of 1.2. Differential gene expression is represented using a colour gradient with red indicating upregulation and blue indicating downregulation. (B) Gastric mucosal ATP content. (C) Heatmap of a subset of differential expression of genes illustrating the restoration of amino acid metabolism by Q3G pre-treatment in stress-exposed rats. (D) Heatmap of a subset of differential expression of genes showing the effect of Q3G pre-treatment on glucose metabolism, including glycolysis and gluconeogenesis, in the stress sample. Data (B) presented as mean ± SD, n = 5. $^{***}P < 0.001$ compared to control; $^{###}P < 0.001$; compared to stress; one-way ANOVA followed by Bonferroni's post hoc test. The number of independent experiments is 3

3.13. Olanzapine pretreatment protects against stress-induced gastric injury and mitochondrial dysfunction by restoring biogenesis and ATP production

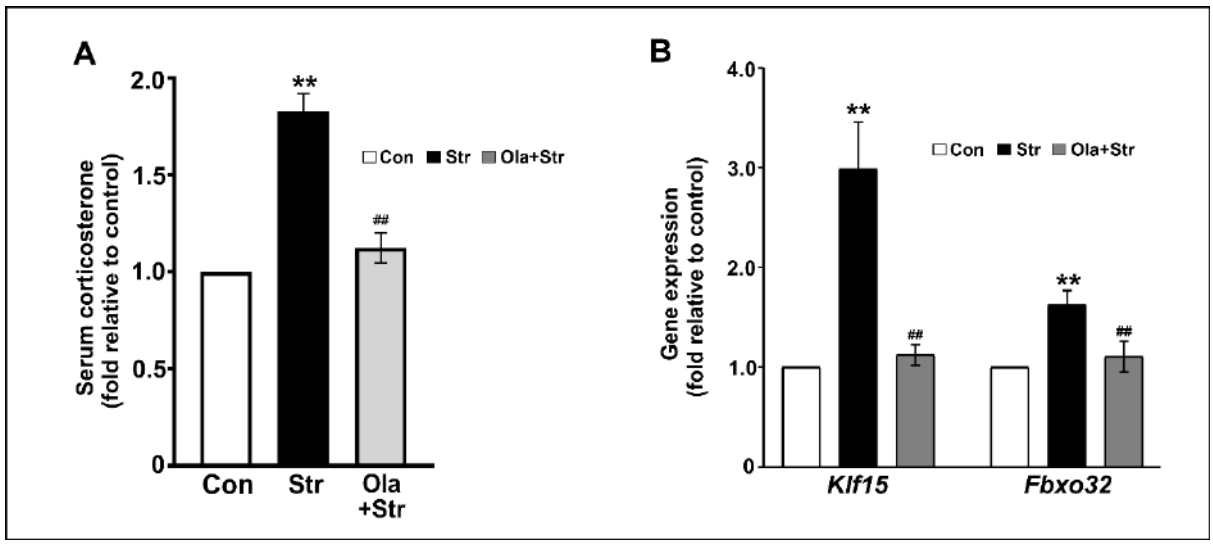

Figure 20. Olanzapine reduces stress-induced elevation of corticosterone and glucocorticoid receptor target gene expression. (A) Serum corticosterone levels (fold relative to control) in control (Con), stress (Str), and olanzapine-treated stress (Ola + Str) groups. (B) Gene expression analysis of Klf15 and Fbxo32 in gastric mucosal tissues from (Con), (Str), and (Ola + Str) by qPCR. Bar graphs indicate fold change in gene expression relative to control (after normalization with Gapdh). Data presented as mean ± SD, n = 5. Relative expression values are presented as fold change relative to control, wherein the expression value corresponding to control is considered as 1-fold. $^{**}P < 0.01$ compared to control; $^{\#\#}P < 0.01$; compared to stress; one-way ANOVA followed by Bonferroni's post hoc test. The number of independent experiments is 3.

As a second therapeutic strategy, central modulation of stress perception was explored to target upstream neuroendocrine signalling. Olanzapine, a centrally acting atypical antipsychotic, was employed to suppress stress-induced activation of the hypothalamic-pituitary-adrenal (HPA) axis and mitigate downstream molecular and mitochondrial dysfunction associated with gastric mucosal injury. Olanzapine effectively mitigates stress-induced corticosterone elevation, gene expression changes, and mitochondrial dysfunction. Stress (Str) significantly increased serum corticosterone levels compared to the control (Con) group, while olanzapine treatment (Ola + Str) significantly reduced corticosterone levels, indicating its protective effect against stress-induced hormonal dysregulation (Fig. 20A). Additionally, stress markedly upregulated Klf15 and Fbxo32, genes associated with GR-activated protein degradation, whereas olanzapine treatment significantly reduced the expression of both genes, suggesting its role in preventing stress-induced molecular changes (Fig. 20B). Furthermore, immunoblot analysis demonstrates that stress significantly reduced the expression of PGC1α and TFAM, key regulators of mitochondrial biogenesis, while olanzapine treatment restored their levels, indicating its role in maintaining mitochondrial integrity (Fig. 21A). Functionally, ATP content, a marker of mitochondrial activity, was significantly reduced under stress conditions, but olanzapine treatment significantly restored ATP levels (Fig. 21B), suggesting its ability to improve mitochondrial function under stress. These findings highlight the potential of olanzapine in alleviating stress-induced physiological and molecular alterations.

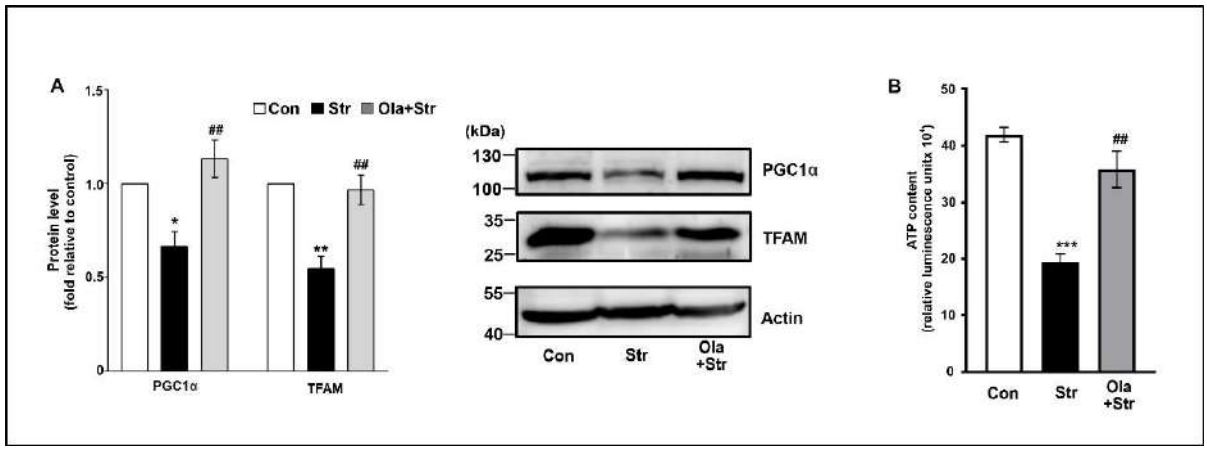

Figure 21. Olanzapine restores mitochondrial biogenesis and prevents stress-induced mitochondrial dysfunction. (A) Immunoblot analysis of mitochondrial biogenesis markers PGC1α and TFAM in control (Con), stress-exposed (Str), and olanzapine-treated stress (Ola+Str) groups. Actin was used as a loading control. Relative expression values are presented as fold change relative to control wherein the expression value corresponding to control is considered as 1-fold. (B) ATP content in gastric mucosal tissue. Data presented as mean ± SD, n = 5. $^{*}P < 0.05$, $^{**}P < 0.01$, $^{***}P < 0.001$ compared to control; $^{\#\#}P < 0.01$; compared to stress; one-way ANOVA followed by Bonferroni's post hoc test. The number of independent experiments is 3.

3.14. RU486 alleviates stress-induced catabolic gene expression and restores mitochondrial function

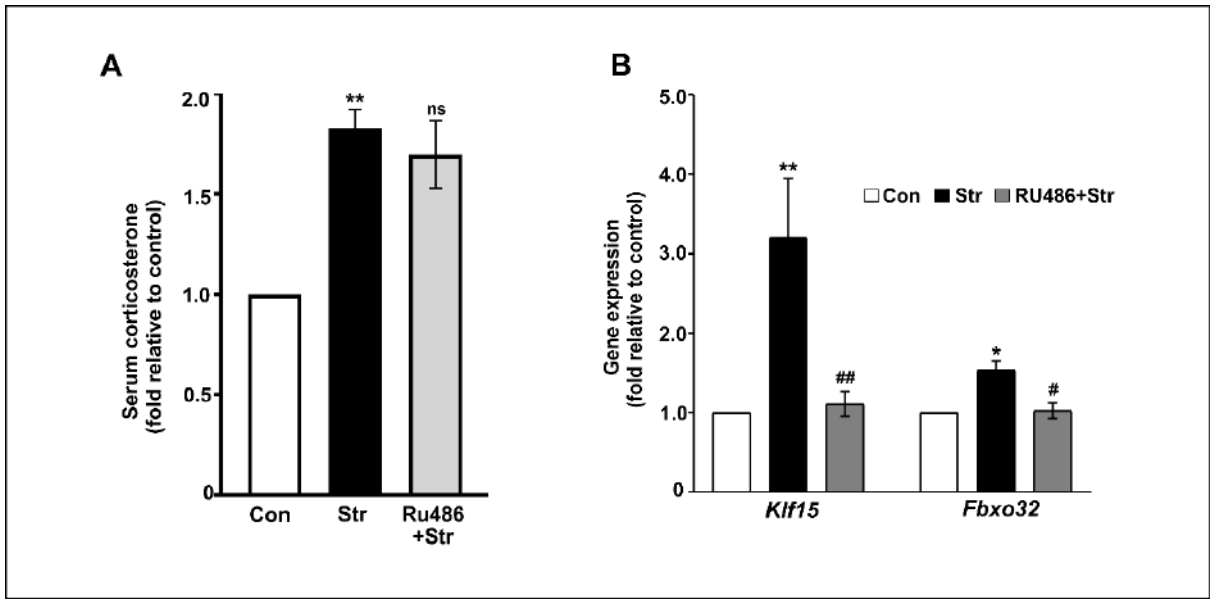

Figure 22. RU486 prevents stress-induced upregulation of Klf15 and Fbxo32 without affecting serum corticosterone levels. (A) Serum corticosterone levels (fold relative to control) in Control (Con), Stress (Str), and RU486 + Stress (RU486 + Str) groups. (B) Gene expression analysis of Klf15 and Fbxo32 in gastric mucosal tissues from (Con), (Str), and (RU486 + Str) by qPCR. Bar graphs indicate fold change in gene expression relative to control (after normalization with Gapdh). Data presented as mean ± SD, n = 5. Relative values are presented as fold change relative to control wherein expression values corresponding to control are considered as 1-fold. $^{*}P < 0.05$, $^{**}P < 0.01$ compared to control; $^{\#}P < 0.05$, $^{\#\#}P < 0.01$; compared to stress; one-way ANOVA followed by Bonferroni's post hoc test. ns: non-significant. The number of independent experiments is 3.

As the third therapeutic approach, direct antagonism of glucocorticoid receptor (GR) signalling was employed to block downstream molecular mediators of stress-induced gastric injury. RU486

(mifepristone), a competitive GR antagonist, was used to inhibit the GR–KLF15–FBXO32 axis, aiming to prevent proteolytic degradation of mitochondrial regulatory proteins and restore mitochondrial biogenesis and function under acute stress conditions. RU486 was used to treat rats 30 min before the stress exposure. Serum corticosterone levels were markedly increased in the stress (Str) group compared to the control. However, RU486 treatment (Ru486 + Str) did not significantly reduce corticosterone levels (Fig. 22A), indicating that the glucocorticoid receptor antagonist did not alter systemic corticosterone secretion under stress conditions rather chemically modulated the GR activation. Despite this, RU486 effectively suppressed the stress-induced upregulation of Klf15 and Fbxo32, two key genes involved in protein degradation (Fig. 22B) by chemically blocking glucocorticoid receptor activation. Klf15 expression was significantly elevated in the stress group but markedly reduced with RU486 treatment. Similarly, Fbxo32 expression was markedly reduced in the RU486-treated rats compared to stress.

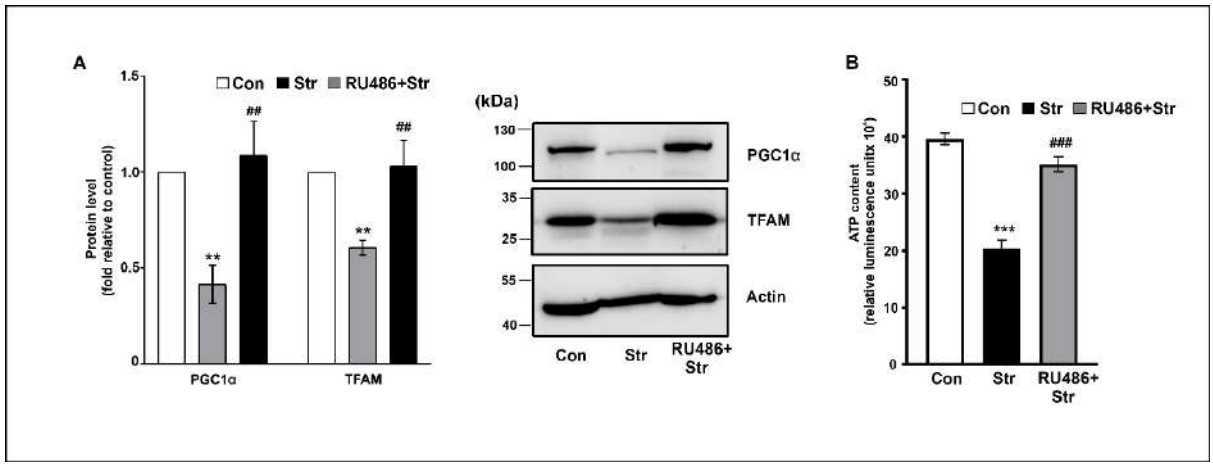

Figure 23. RU486 prevents stress-induced mitochondrial dysfunction and restores mitochondrial biogenesis. (A) Immunoblots of PGC1α and TFAM in tissues from Control (Con), Stress (Str), and RU486 + Stress (RU486 + Str) samples. Actin was used as a loading control. Relative expression values are presented as fold change relative to control, wherein the expression value corresponding to control is considered as 1-fold. (B) Tissue ATP content. Data presented as mean ± SD, n = 5. $^{*}P < 0.05$, $^{**}P < 0.01$, $^{***}P < 0.001$ compared to control; $^{\#}P < 0.05$, $^{\#\#\#}P < 0.001$ compared to stress; and calculated using one-way ANOVA followed by Bonferroni's post hoc test. ns: non-significant. The number of independent experiments is 3.

These findings suggest that RU486 prevents the activation of stress-induced catabolic pathways at the transcriptional level, independent of circulating corticosterone levels, through direct inhibition of glucocorticoid receptor signalling. Stress (Str) significantly reduced the expression of PGC1α and TFAM, key regulators of mitochondrial biogenesis, compared to the control (Con) group. However, RU486 treatment (Ru486 + STR) restored PGC1α and TFAM levels, indicating its protective effect against stress-induced impairment of mitochondrial biogenesis (Fig. 23A). Significant decrease in ATP content was observed in the gastric mucosa of stressed rats, indicating mitochondrial impairment, while RU486 treatment significantly restored ATP levels, suggesting its protective role in preserving mitochondrial function under stress conditions.

4. DISCUSSION

This study elucidates the complex interplay between acute psychological stress and gastric mitochondrial dysfunction, emphasizing the pivotal role of the PGC1α-NRF1-TFAM axis in maintaining mitochondrial biogenesis and oxidative metabolism. PGC1α (peroxisome proliferator-

activated receptor gamma coactivator 1-alpha) regulates mitochondrial biogenesis by activating nuclear respiratory factor 1 (NRF1), which in turn induces the expression of mitochondrial transcription factor A (TFAM) (42). TFAM is a critical regulator of mitochondrial DNA transcription, replication, and overall mitochondrial function(43,44). Under stress conditions, the observed suppression of PGC1α correlates with reduced NRF1 and TFAM expression, leading to impaired mitochondrial biogenesis and bioenergetic failure. Our integrative approach, encompassing transcriptomics, metabolomics, mitochondrial function assays, and pharmacological interventions, systematically demonstrates that stress disrupts mitochondrial homeostasis, leading to bioenergetic failure, oxidative stress amplification, and cellular damage in the gastric mucosa. Transcriptome analysis and qPCR studies revealed significant downregulation of genes encoding electron transport chain (ETC) components, including those of complexes I-IV, along with suppressed expression of mitochondrial biogenesis regulators such as NRF1 and TFAM. These transcriptomic alterations were accompanied by metabolic perturbations, including ATP depletion, impaired lipid metabolism, and energy homeostasis disruption, as identified by metabolomics profiling. Mitochondrial functional assays, including JC-1 and ATP measurements, confirmed a loss of mitochondrial integrity and reduced bioenergetic capacity in stress-exposed gastric tissues. Disruption of the electron transport chain (ETC) function was demonstrated by reduced ATP synthesis and downregulation of core oxidative phosphorylation (OXPHOS) genes, reflecting impaired mitochondrial energy metabolism and elevated reactive oxygen species (ROS) generation. A significant aspect of this study was the role of glucocorticoid receptor (GR) signalling in stress-induced gastric mucosal injury. Acute mental stress triggers GR-induced upregulation of KLF15 and FBXO32, which are involved in ubiquitin-mediated proteasomal degradation. This accelerates the turnover of mitochondrial regulatory proteins, directly impairing mitochondrial function, elevating reactive oxygen species (ROS) production, and reducing ATP synthesis. This study also demonstrates that stress-induced reactive oxygen species (ROS) accumulation and phosphatidic acid (PA) buildup act as key mediators of oxidative damage and apoptosis in gastric mucosal epithelial cells. Mitochondrial energy metabolism impairment was further amplified by excessive oxidative stress, as indicated by the upregulation of Hmox1 and Nrf2, redox-sensitive genes that mediate oxidative stress responses. While NRF2 activation is often a protective mechanism, its failure to alleviate oxidative stress in this study suggests that prolonged stress exposure overwhelms mitochondrial antioxidant defences. Upregulation of Klf9, a common target of glucocorticoid receptor and NRF2, further amplified oxidative stress, reinforcing redox imbalance and exacerbating mitochondrial dysfunction. The sustained oxidative stress, coupled with mitochondrial bioenergetic deficits, contributed to increased apoptotic signalling, as indicated by BAX upregulation and Bcl-xL downregulation in stressed tissues. Pathway analysis and disease-function further highlighted significant enrichment in 'NRF2-mediated oxidative stress response,' 'death receptor signalling,' 'glucocorticoid receptor signalling,' pathways, and 'apoptosis' as associated functions, reinforcing the role of mitochondrial oxidative damage in stress-induced gastric injury. Lipid peroxidation likely contributed to phosphatidic acid accumulation, further exacerbating mitochondrial dysfunction through ROS amplification. Due to the overwhelming accumulation of dysfunctional mitochondria and the resultant excessive oxidative stress, the capacity for cellular rescue is critically impaired, rendering the recovery of damaged gastric mucosal cells unfeasible. Consequently, programmed cell death pathways, particularly apoptosis, are activated, culminating in severe gastric tissue injury.

To explore potential gastroprotective strategies, the potential gastroprotective effects of quercetin-3-glucoside (Q3G), olanzapine, and RU486 against stress-induced gastric mucosal injury were evaluated. Quercetin-3-glucoside (Q3G), a glycosylated derivative of the flavonoid quercetin, was evaluated for its potent antioxidant and mitochondrial-protective properties. Q3G exhibited strong gastroprotective effects, showing antioxidant effects, restoring mitochondrial functions, and preserving mitochondrial

integrity. Mechanistically, Q3G preserved mitochondrial membrane potential, restored both nuclear and mitochondrial-encoded gene expression involved in oxidative phosphorylation and biogenesis, and reduced oxidative stress markers such as Hmox1 and Klf9. Its strong gastroprotective efficacy and favorable safety profile support its potential as an antioxidant-based therapeutic agent for stress-related gastrointestinal disorders. Olanzapine, a centrally acting atypical antipsychotic, was administered to attenuate the upstream perception of psychological stress. Olanzapine pretreatment significantly reduced stress-induced serum corticosterone elevation and ameliorated transcriptional dysregulation of stress-responsive pathways. This intervention led to partial restoration of mitochondrial function, including stabilization of membrane potential and ATP production. Notably, olanzapine reduced the gastric injury index to 14 ± 4 ($P < 0.001$ vs. stress), indicating a substantial protective effect. However, the clinical application of olanzapine is constrained by its sedative properties and long-term metabolic side effects. Despite these limitations, its efficacy in this model highlights the therapeutic potential of targeting central stress circuits to achieve peripheral cytoprotection. RU486 (mifepristone), a competitive antagonist of the glucocorticoid receptor, emerged as the most effective intervention in mitigating stress-induced mucosal pathology. Acute psychological stress elevates systemic corticosterone levels, leading to GR activation and transcriptional upregulation of KLF15 and FBXO32, components of a proteasomal degradation axis implicated in mitochondrial destabilization and tissue injury. RU486 pretreatment significantly suppressed this GR–KLF15–FBXO32 signaling cascade, thereby preserving mitochondrial regulatory proteins and preventing bioenergetic collapse. Functionally, RU486 restored mitochondrial biogenesis, normalized ATP levels, and maintained epithelial integrity. Histological and macroscopic assessments confirmed substantial protection, with a marked reduction in gastric injury index (12 ± 2; $P < 0.001$ vs. stress) and preserved gastric architecture. These findings underscore the pivotal role of GR signaling in mediating stress responses and validate GR antagonism as a potent therapeutic strategy for preventing stress-induced gastric mucosal injury.

These results collectively highlight the potential of a multifaceted therapeutic approach for stress-induced gastric mucosal injury. Quercetin-3-glucoside (Q3G) demonstrated strong antioxidant efficacy, while RU486 effectively blocked stress-activated glucocorticoid signaling pathways implicated in mitochondrial dysfunction and proteasomal degradation. The promising protective effects observed for each agent suggest that a combination therapy, or a novel hybrid molecule integrating the antioxidant capacity of Q3G with the glucocorticoid receptor antagonism of RU486, could serve as an innovative mitochondrial-targeted intervention for stress-related gastropathies. This approach promotes the development of next-generation cytoprotective treatments that integrate metabolic, mitochondrial, and neuroendocrine regulation.

5. CONCLUSION

This study delineates a comprehensive mechanistic framework underlying acute mental stress-induced gastric injury, with a central emphasis on mitochondrial dysfunction mediated through the disruption of the PGC1α-NRF1-TFAM signalling axis. Integrative multi-omics and functional analyses reveal that stress-induced suppression of mitochondrial biogenesis and oxidative phosphorylation leads to significant bioenergetic deficits, increased oxidative stress, and activation of apoptotic signalling in gastric mucosal cells. The critical involvement of glucocorticoid receptor (GR) signalling, particularly via the GR–KLF15–FBXO32 axis, further underscores the nexus between neuroendocrine stress responses and mitochondrial destabilization. The convergence of impaired mitochondrial biogenesis, dysregulated mitochondrial gene expression, and persistent redox imbalance drives progressive cellular dysfunction, ultimately leading to irreversible epithelial injury and the loss of gastric mucosal integrity.

Therapeutic intervention studies elucidate distinct modes of cytoprotection. Quercetin-3-glucoside (Q3G) alleviates oxidative damage through robust antioxidant and mitochondrial-stabilizing actions, while olanzapine attenuates upstream neuroendocrine activation, partially restoring mitochondrial functionality. Notably, RU486 emerges as the most potent agent, effectively abrogating GR-mediated transcriptional cascades and preserving mitochondrial bioenergetics and tissue architecture. These findings collectively establish mitochondrial quality control as a critical determinant of gastric mucosal resilience under stress and substantiate GR antagonism as a compelling therapeutic avenue. Importantly, the translational implications of this work extend beyond monotherapies. The potential synergy between antioxidant strategies and GR antagonism suggests that combinatorial or hybrid therapeutic platforms, such as a molecule integrating the antioxidant efficacy of Q3G with the receptor specificity of RU486, may offer a paradigm shift in the management of stress-induced gastropathies. This study thus provides a foundational basis for future research aimed at developing mitochondria-centered, neuroendocrine-modulating cytoprotective therapies for stress-related gastrointestinal disorders.

6. REFERENCES

1. Doenyas, C., Clarke, G., and Cserjési, R. (2025) Gut-brain axis and neuropsychiatric health: recent advances. *Scientific reports* **15**, 3415

2. Ge, L., Liu, S., Li, S., Yang, J., Hu, G., Xu, C., and Song, W. (2022) Psychological stress in inflammatory bowel disease: Psychoneuroimmunological insights into bidirectional gut-brain communications. *Frontiers in immunology* **13**, 1016578

3. Saeed, M., Bass, S., and Chaisson, N. F. (2022) Which ICU patients need stress ulcer prophylaxis? *Cleveland Clinic journal of medicine* **89**, 363-367

4. Carabotti, M., Scirocco, A., Maselli, M. A., and Severi, C. (2015) The gut-brain axis: interactions between enteric microbiota, central and enteric nervous systems. *Annals of gastroenterology* **28**, 203-209

5. Peppas, S., Pansieri, C., Piovani, D., Danese, S., Peyrin-Biroulet, L., Tsantes, A. G., Brunetta, E., Tsantes, A. E., and Bonovas, S. (2021) The Brain-Gut Axis: Psychological Functioning and Inflammatory Bowel Diseases. *Journal of clinical medicine* **10**

6. Plummer, M. P., Blaser, A. R., and Deane, A. M. (2014) Stress ulceration: prevalence, pathology and association with adverse outcomes. *Critical care (London, England)* **18**, 213

7. Metz, D. C. (2005) Preventing the gastrointestinal consequences of stress-related mucosal disease. *Current medical research and opinion* **21**, 11-18

8. Aoyama, N., Kinoshita, Y., Fujimoto, S., Himeno, S., Todo, A., Kasuga, M., and Chiba, T. (1998) Peptic ulcers after the Hanshin-Awaji earthquake: increased incidence of bleeding gastric ulcers. *The American journal of gastroenterology* **93**, 311-316

9. Shiga, H., Miyazawa, T., Kinouchi, Y., Takahashi, S., Tominaga, G., Takahashi, H., Takagi, S., Obana, N., Kikuchi, T., Oomori, S., Nomura, E., Shiraki, M., Sato, Y., Takahashi, S., Umemura, K., Yokoyama, H., Endo, K., Kakuta, Y., Aizawa, H., Matsuura, M., Kimura, T., Kuroha, M., and Shimosegawa, T. (2013) Life-event stress induced by the Great East Japan Earthquake was associated with relapse in ulcerative colitis but not Crohn's disease: a retrospective cohort study. *BMJ open* **3**

10. Yamanaka, K., Miyatani, H., Yoshida, Y., Asabe, S., Yoshida, T., Nakano, M., Obara, S., and Endo, H. (2013) Hemorrhagic gastric and duodenal ulcers after the Great East Japan Earthquake Disaster. *World journal of gastroenterology* **19**, 7426-7432

11. Mazumder, S., Bindu, S., De, R., Debsharma, S., Pramanik, S., and Bandyopadhyay, U. (2022) Emerging role of mitochondrial DAMPs, aberrant mitochondrial dynamics and anomalous mitophagy in gut mucosal pathogenesis. *Life sciences* **305**, 120753

12. Rigalli, A., & Di Loreto, V. (2009) *Experimental Surgical Models in the Laboratory Rat (1st ed.).* CRC Press

13. Taherzadeh-Fard, E., Saft, C., Akkad, D. A., Wieczorek, S., Haghikia, A., Chan, A., Epplen, J. T., and Arning, L. (2011) PGC-1alpha downstream transcription factors NRF-1 and TFAM are genetic modifiers of Huntington disease. *Molecular neurodegeneration* **6**, 32

14. Bremer, K., Kocha, K. M., Snider, T., and Moyes, C. D. (2016) Sensing and responding to energetic stress: The role of the AMPK-PGC1α-NRF1 axis in control of mitochondrial biogenesis in fish. *Comparative biochemistry and physiology. Part B, Biochemistry & molecular biology* **199**, 4-12

15. De, R., Mazumder, S., Sarkar, S., Debsharma, S., Siddiqui, A. A., Saha, S. J., Banerjee, C., Nag, S., Saha, D., and Bandyopadhyay, U. (2017) Acute mental stress induces mitochondrial bioenergetic crisis and hyper-fission along with aberrant mitophagy in the gut mucosa in rodent model of stress-related mucosal disease. *Free radical biology & medicine* **113**, 424-438

16. Leung, J. Y., Pang, C. C., Procyshyn, R. M., and Barr, A. M. (2014) Cardiovascular effects of acute treatment with the antipsychotic drug olanzapine in rats. *Vascular pharmacology* **62**, 143-149

17. Gay, M. S., Li, Y., Xiong, F., Lin, T., and Zhang, L. (2015) Dexamethasone Treatment of Newborn Rats Decreases Cardiomyocyte Endowment in the Developing Heart through Epigenetic Modifications. *PloS one* **10**, e0125033

18. Chattopadhyay, I., Nandi, B., Chatterjee, R., Biswas, K., Bandyopadhyay, U., and Banerjee, R. K. (2004) Mechanism of antiulcer effect of Neem (Azadirachta indica) leaf extract: effect on H+-K+-ATPase, oxidative damage and apoptosis. *Inflammopharmacology* **12**, 153-176

19. Andrews, S. (2010) FastQC: A quality control tool for high throughput sequence data (Andrews, S. ed., online

20. Martin, M. (2011) Cutadapt removes adapter sequences from high throughput sequencing reads. *EMBnet Journal* **17**, 10-12

21. Pertea, M., Kim, D., Pertea, G. M., Leek, J. T., and Salzberg, S. L. (2016) Transcript-level expression analysis of RNA-seq experiments with HISAT, StringTie and Ballgown. *Nature protocols* **11**, 1650-1667

22. Li, H., Handsaker, B., Wysoker, A., Fennell, T., Ruan, J., Homer, N., Marth, G., Abecasis, G., and Durbin, R. (2009) The Sequence Alignment/Map format and SAMtools. *Bioinformatics (Oxford, England)* **25**, 2078-2079

23. Liao, Y., Smyth, G. K., and Shi, W. (2014) featureCounts: an efficient general purpose program for assigning sequence reads to genomic features. *Bioinformatics (Oxford, England)* **30**, 923-930

24. Love, M. I., Huber, W., and Anders, S. (2014) Moderated estimation of fold change and dispersion for RNA-seq data with DESeq2. *Genome biology* **15**, 550

25. Mazumder, S., De, R., Debsharma, S., Bindu, S., Maity, P., Sarkar, S., Saha, S. J., Siddiqui, A. A., Banerjee, C., Nag, S., Saha, D., Pramanik, S., Mitra, K., and Bandyopadhyay, U. (2019) Indomethacin impairs mitochondrial dynamics by activating the PKCζ-p38-DRP1 pathway and inducing apoptosis in gastric cancer and normal mucosal cells. *The Journal of biological chemistry* **294**, 8238-8258

26. Mazumder, S., De, R., Sarkar, S., Siddiqui, A. A., Saha, S. J., Banerjee, C., Iqbal, M. S., Nag, S., Debsharma, S., and Bandyopadhyay, U. (2016) Selective scavenging of intra-mitochondrial superoxide corrects diclofenac-induced mitochondrial dysfunction and gastric injury: A novel gastroprotective mechanism independent of gastric acid suppression. *Biochemical pharmacology* **121**, 33-51

27. Kwong, S. C., Jamil, A. H. A., Rhodes, A., Taib, N. A., and Chung, I. (2019) Metabolic role of fatty acid binding protein 7 in mediating triple-negative breast cancer cell death via PPAR-α signaling. *Journal of lipid research* **60**, 1807-1817

28. Joshi, D. C., and Bakowska, J. C. (2011) Determination of mitochondrial membrane potential and reactive oxygen species in live rat cortical neurons. *Journal of visualized experiments : JoVE*

29. Zorova, L. D., Popkov, V. A., Plotnikov, E. Y., Silachev, D. N., Pevzner, I. B., Jankauskas, S. S., Babenko, V. A., Zorov, S. D., Balakireva, A. V., Juhaszova, M., Sollott, S. J., and Zorov, D. B. (2018) Mitochondrial membrane potential. *Analytical biochemistry* **552**, 50-59

30. Song, S., Attia, R. R., Connaughton, S., Niesen, M. I., Ness, G. C., Elam, M. B., Hori, R. T., Cook, G. A., and Park, E. A. (2010) Peroxisome proliferator activated receptor alpha (PPARalpha) and PPAR gamma coactivator (PGC-1alpha) induce carnitine palmitoyltransferase IA (CPT-1A) via independent gene elements. *Molecular and cellular endocrinology* **325**, 54-63

31. Huss, J. M., Torra, I. P., Staels, B., Giguère, V., and Kelly, D. P. (2004) Estrogen-related receptor alpha directs peroxisome proliferator-activated receptor alpha signaling in the transcriptional control of energy metabolism in cardiac and skeletal muscle. *Molecular and cellular biology* **24**, 9079-9091

32. Bader, G. D., and Hogue, C. W. (2003) An automated method for finding molecular complexes in large protein interaction networks. *BMC bioinformatics* **4**, 2

33. Shannon, P., Markiel, A., Ozier, O., Baliga, N. S., Wang, J. T., Ramage, D., Amin, N., Schwikowski, B., and Ideker, T. (2003) Cytoscape: a software environment for integrated models of biomolecular interaction networks. *Genome research* **13**, 2498-2504

34. Sasse, S. K., Kadiyala, V., Danhorn, T., Panettieri, R. A., Jr., Phang, T. L., and Gerber, A. N. (2017) Glucocorticoid Receptor ChIP-Seq Identifies PLCD1 as a KLF15 Target that Represses

Airway Smooth Muscle Hypertrophy. *American journal of respiratory cell and molecular biology* **57**, 226-237

35. Shimizu, N., Yoshikawa, N., Ito, N., Maruyama, T., Suzuki, Y., Takeda, S., Nakae, J., Tagata, Y., Nishitani, S., Takehana, K., Sano, M., Fukuda, K., Suematsu, M., Morimoto, C., and Tanaka, H. (2011) Crosstalk between glucocorticoid receptor and nutritional sensor mTOR in skeletal muscle. *Cell metabolism* **13**, 170-182

36. Bonett, R. M., Hu, F., Bagamasbad, P., and Denver, R. J. (2009) Stressor and glucocorticoid-dependent induction of the immediate early gene kruppel-like factor 9: implications for neural development and plasticity. *Endocrinology* **150**, 1757-1765

37. Beaulieu, E., Ioffe, J., Watson, S. N., Hermann, P. M., and Wildering, W. C. (2014) Oxidative-stress induced increase in circulating fatty acids does not contribute to phospholipase A2-dependent appetitive long-term memory failure in the pond snail Lymnaea stagnalis. *BMC neuroscience* **15**, 56

38. Adibhatla, R. M., and Hatcher, J. F. (2008) Phospholipase A(2), reactive oxygen species, and lipid peroxidation in CNS pathologies. *BMB reports* **41**, 560-567

39. Zucker, S. N., Fink, E. E., Bagati, A., Mannava, S., Bianchi-Smiraglia, A., Bogner, P. N., Wawrzyniak, J. A., Foley, C., Leonova, K. I., Grimm, M. J., Moparthy, K., Ionov, Y., Wang, J., Liu, S., Sexton, S., Kandel, E. S., Bakin, A. V., Zhang, Y., Kaminski, N., Segal, B. H., and Nikiforov, M. A. (2014) Nrf2 amplifies oxidative stress via induction of Klf9. *Molecular cell* **53**, 916-928

40. Shewade, L. H., Schneider, K. A., Brown, A. C., and Buchholz, D. R. (2017) In-vivo regulation of Krüppel-like factor 9 by corticosteroids and their receptors across tissues in tadpoles of Xenopus tropicalis. *General and comparative endocrinology* **248**, 79-86

41. Thakkar, C., Alikunju, S., Niranjan, N., Rizvi, W., Abbas, A., Abdellatif, M., and Sayed, D. (2023) Klf9 plays a critical role in GR -dependent metabolic adaptations in cardiomyocytes. *Cellular signalling* **111**, 110886

42. Li, L., Pan, R., Li, R., Niemann, B., Aurich, A. C., Chen, Y., and Rohrbach, S. (2011) Mitochondrial biogenesis and peroxisome proliferator-activated receptor-γ coactivator-1α (PGC-1α) deacetylation by physical activity: intact adipocytokine signaling is required. *Diabetes* **60**, 157-167

43. Kang, D., Kim, S. H., and Hamasaki, N. (2007) Mitochondrial transcription factor A (TFAM): roles in maintenance of mtDNA and cellular functions. *Mitochondrion* **7**, 39-44

44. Yu, S., Lu, X., Li, C., Han, Z., Li, Y., Zhang, X., and Guo, D. (2024) TFAM and Mitochondrial Protection in Diabetic Kidney Disease. *Diabetes, metabolic syndrome and obesity : targets and therapy* **17**, 4355-4365

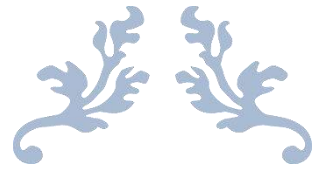

SUMMARY OF THE WORK

SUMMARY OF THE WORK

Mental stress has a profound impact on gastric health, which includes gastric mucosal ulceration, hyperacidity, and associated gastric complications, collectively called gastropathy. However, the molecular mechanisms of how mental stress imparts gastropathy are not very clear. This work investigated the molecular and subcellular events in acute stress-induced gastropathy using a rat model of acute stress. This study identified that mental stress impairs the electron transport chain (ETC) and mitochondrial biogenesis in the gastric mucosa, leading to disruption in ATP production and mitochondrial homeostasis. Impaired ETC function further led to excessive production of reactive oxygen species (ROS), exacerbating oxidative stress and contributing to mitochondrial damage. Induction of cold-restraint stress on rats led to downregulation of mitochondrial biogenesis regulators, including PGC-1α, NRF1, and TFAM, resulting in bioenergetic failure and associated gastric mucosal damage. The study also revealed that stress-induced activation of the glucocorticoid receptor (GR) pathway led to ubiquitination-mediated degradation of PGC-1α, resulting in compromised mitochondrial function, impaired mitochondrial biogenesis, and disrupted lipid metabolism. Elevated corticosterone levels and altered expression of key catabolic genes, such as Klf15 and Fbxo32, contributed to mitochondrial dysfunction, reinforcing the connection between stress and impaired gastric energy metabolism. To counteract the mitochondrial and metabolic dysfunction induced by acute psychological stress, this study systematically evaluated three mechanistically distinct therapeutic strategies: (1) antioxidant supplementation using quercetin-3-glucoside (Q3G), (2) central modulation of stress perception through the administration of olanzapine, and (3) direct antagonism of glucocorticoid receptor (GR) signalling via RU486. Q3G, a bioavailable antioxidant flavonoid, significantly restored the expression of genes involved in oxidative phosphorylation, fatty acid oxidation, and glucose metabolism, as confirmed by transcriptomic and qRT-PCR analyses. It preserved mitochondrial function by stabilizing key regulatory proteins such as PGC-1α and TFAM. Olanzapine effectively attenuated systemic corticosterone elevation and suppressed GR-driven catabolic gene expression (Klf15, Fbxo32), partially restoring mitochondrial biogenesis and ATP production. RU486, a competitive GR antagonist, offered the most robust protection by directly blocking GR-mediated transcriptional pathways, thereby preserving mitochondrial bioenergetic function despite elevated corticosterone levels. Collectively, these interventions highlight the therapeutic potential of targeting mitochondrial integrity, redox homeostasis, and neuroendocrine stress pathways in the prevention of stress-induced gastric mucosal injury.

In conclusion, this study provides novel insights into the molecular mechanisms underlying stress-induced gastropathy while emphasizing mitochondrial dysfunction as a central contributor of gastric injury. By demonstrating that stress disrupts mitochondrial biogenesis, ETC function, and metabolic homeostasis, the findings reinforce the importance of targeting mitochondrial pathways in stress-related gastric disorders. Importantly, the study highlights the therapeutic promise of three targeted intervention strategies: antioxidant supplementation with Q3G, central modulation of stress perception via olanzapine, and direct inhibition of GR signalling using RU486. This research work paves the way for innovative strategies to combat stress-induced gastric disorders. By shedding light on mitochondria-targeted therapies, it opens new avenues for the development of cutting-edge interventions that could revolutionize the treatment of stress-related gastrointestinal diseases.

APPENDIX

Complete list of metabolites identified through Liquid Chromatography-Mass Spectrometry (LC-MS) analysis of rat gastric tissue samples.

Accepted Description	m/z	HMDB ID	CON-1	CON-2	CON-3	STR-R1	STR-R2	STR-R3
NADPH	768.069	HMDB0000221	549.9	552.7	515.8	873.1	1366.9	1336.8
trans-zeatin riboside triphosphate	606.009	HMDB0304509	0	0	0	85.9	168.2	103.2
PS(24:0/24:0)	998.735	HMDB0112908	0	0	0	23.4	853.2	177.8
2-[4-(4-Hydroxyphenoxy)-2-iodophenyl]-2,2-diiodoacetic acid	639.748	HMDB0257662	1146.9	1298.8	422.5	409.1	554	257.1
Casokefamide	671.265	HMDB0249695	0	0	0	175.5	318.2	252.2
C.I. Food Black 2	759.911	HMDB0033393	197.9	1970.3	1529.7	985.6	4373.9	376
2-Mesatp	575.934	HMDB0245197	269.1	253.9	301.3	466.6	577.5	503
NADH	704.098	HMDB0001487	0	0	0	149.7	463.9	139.9
Colistin A	1169.766	HMDB0250405	0	0	0	188.5	1898	264.4
Danoprevir	754.243	HMDB0250844	0	0	0	101.6	236.8	179.4
Alilusem	395.045	HMDB0248137	0	0	0	0	147.9	71.1
Dtgammae	1695.812	HMDB0251631	0	0	0	101.9	181	444.2
Violaxanthin linoleate linolenate	1161.805	HMDB0303015	0	0	0	473.5	2946.6	2262.8
4'-Iododoxorubicinol	656.111	HMDB0246636	6074.9	4814.8	12551.3	4892.7	11937.5	4603.8
Emblicanin B	818.997	HMDB0030436	375.2	304.1	263.7	258	469.4	304.3
Zaragozic acid A	708.318	HMDB0259988	0	0	0	57	378	72.4
Iodoquinol	419.853	HMDB0253533	0	0	0	9991.3	147.6	265.1
Deltorphin	955.397	HMDB0250986	0	0	0	113.8	105.9	236.7
(R)-Benzylsuccinyl-CoA	980.147	HMDB0012129	0	0	0	235.9	704.7	189.4
Calicheamicin	1406.315	HMDB0249553	0	0	0	156.6	109	418.9
UDP-3-O-(3-hydroxymyristoyl)-alpha-D-glucosamine	829.225	HMDB0304525	0	0	0	330.7	203.8	422.8
Sorbitan tristearate	980.898	HMDB0029890	0	0	8.5	250.4	895.4	203.1
[(2S,3R,5S,6S)-2,3,4,5,6-Pentaphosphonooxycyclohexyl] phosphanyl hydrogen phosphate	690.806	HMDB0257969	16.4	44.2	79.7	2427.7	1621.7	3921
6-Methoxy-2-naphthylacetic acid	750.188	HMDB0060787	0	0	9.7	90.4	231.9	188.1
Roflumilast N-oxide	456.995	HMDB0060590	3.3	0	19.4	118.7	579.1	460.6

2-(4-Methyl-5-thiazolyl)ethyl decanoate	315.212	HMDB0032419	208	242.3	242.1	173.4	374	729.1
TG(a-25:0/a-25:0/a-25:0)[rac]	1186.174	HMDB0070600	0	0	14.1	0	550.1	0
Guavin C	1169.192	HMDB0039435	62.6	61.4	182.3	659.1	4849.8	994.5
Ganglioside GA2 (d18:1/18:0)	1131.686	HMDB0004891	25.1	69.8	0	626.4	554.9	1297.6
Sitaxentan	492.974	HMDB0015629	11.1	0	282.1	312	2576.4	3903.9
PA(O-16:0/18:0)	685.508	HMDB0011145	0	0	312.9	4.9	7119.1	40.6
P1,P4-Bis(5'-uridyl) tetraphosphate	828.964	HMDB0006796	906.8	834.5	1599.8	1666.7	1948.7	1884.3
Glycine, L-gamma-glutamyl-2-(1-methyl-4-(nitrosothio)-4-piperidinyl)glycyl-	458.113	HMDB0253933	0	0	17	43.3	206.1	117.6
Dihydrocyclosporin	1242.856	HMDB0251301	59.3	29.3	0	417.5	844.8	615.8
Arachisprenol 11	784.745	HMDB0031939	1877.7	1670.5	989.4	1603	1021	1368.2
CXCR3 Antagonist 6c	654.121	HMDB0249926	14.6	13.6	0	59.8	346.5	97.9
Quinquenoside R1	1168.637	HMDB0040874	77.2	82.1	91.8	440.8	3392.5	578.5
2-Hexadecyloctadec-9-enal	491.526	HMDB0255386	0	15.3	6.7	70.9	209	102.5
1,2,4-Nonadecanetriol	334.34	HMDB0032112	2402	3556.9	1561.9	1665.5	1568.2	2051.7
Menaquinone-7	666.518	HMDB0254436	0	23	41.7	234.9	396.6	470.4
Pulcherosine	540.202	HMDB0040703	305.3	436.2	309.8	1217.2	3565.5	3376.4
Ile-Ile-Ala-Glu-Lys	573.359	HMDB0253397	21.9	54.7	0	89.8	845.7	309.9
Endotoxin inhibitor	1241.726	HMDB0244651	99.9	83.1	0	687.9	1309.2	956.8
oxalyl-CoA	873.011	HMDB0304445	0	0	216.6	239.8	2290.5	825.7
Guanosine 3'-diphosphate 5'-triphosphate	683.87	HMDB0060480	879.9	874.1	390.2	660.5	652.9	708.2
13E-Tetranor-16-oxo-16-CoA-LTE4	1163.245	HMDB0012576	0	0	371.2	295.7	3700.7	1126.8
PC(24:1(15Z)/24:1(15Z))	976.782	HMDB0008816	1667	1832.5	821.1	1239.6	3149.1	2256.7
gentiodelphin	1131.309	HMDB0304368	212.6	168.4	0	1138	1012.5	2412.6
Ganoderiol I	541.333	HMDB0037778	109.8	146.2	55.5	373.8	1204.2	763.1
(17Z)-Hexacos-17-enoylcarnitine	560.46	HMDB0241641	500.1	767.3	244.7	2793.6	7343.6	5115.5
Cyanidin 3-O-[[4-Hydroxy-3,5-dimethoxycinnamoyl-(->2)-b-D-glucopyranosyl-(1->2)]-[4-hydroxy-3-methoxycinnamoyl-(->6)]-b-D-glucopyranoside] 5-O-(6-O-malonyl-b-D-glucopyranoside)	1242.293	HMDB0033726	148.5	184.8	24.5	870.6	1771.8	1254.1
5-Iodoacetamidofluorescein	537.939	HMDB0246814	745.6	685.9	1458.5	1027.4	2606.7	1431.2

Ceramide trihexosides	1162.868	HMDB0249816	104.4	66.5	787.7	654.8	6688.6	2203
Chlorpyrifos-methyl	321.893	HMDB0250138	0	0	40.5	63.8	246.7	92.6
Diguanosine hexaphosphate	1130.934	HMDB0001543	3092	3082.4	1924.8	2682.2	1874.6	4088.2
Sulforhodamine B	576.188	HMDB0031987	33.4	30.2	13.9	148.7	438.9	153.8
6-Hydroxy-5-[(4-sulfophenyl)azo]-2-naphthalenesulfonic acid	446.937	HMDB0034022	0	0	79.9	32.7	542.8	163.5
Permetin A	1118.761	HMDB0030527	0	0	381.9	13.9	3317	156.6
Perfluorodecane	556.001	HMDB0256316	58.4	66.3	223.3	171.2	2815.8	152.5
Cer(d18:0/24:0)	669.746	HMDB0011768	1110.4	1118.7	1105.8	983.2	1700.1	1481
Bis(2-methyl-3-furanyl)tetrasulfide	312.943	HMDB0036168	1294.9	1382.6	1417.5	1359.8	2077	4995.1
Lufenuron	510.967	HMDB0254195	5979.5	6228.1	19956.7	4718.2	32292.6	5623.9
Malvidin 3-chlorogenic acid glucoside	846.241	HMDB0303066	119.1	93.6	112.4	1165.4	546.7	937.4
AR-C67085MX	685.898	HMDB0248544	36.5	0	0	26.1	157.2	110.7
Pelargonidin 3-O-[2-O-(6-(E)-caffeoyl-beta-D-glucopyranosyl)-6-O-(E)-p-coumaroyl-beta-D-glucopyranoside] 5-O-(beta-D-glucopyranoside)	1083.328	HMDB0301998	0	12.4	230.2	232.1	1231.3	461.7
Valolaginic acid	988.057	HMDB0302895	4402.2	4474.8	2639.7	2789	2034.3	2356.3
Perfluorotetradecanoic acid	714.942	HMDB0256334	502.8	532.8	503.3	494.1	464.5	548.8
Iosimide	871.88	HMDB0253548	197.2	182.2	834.5	734.8	5886.6	2222
5,6,7,8-Tetrahydromethanopterin	777.282	HMDB0060403	30	51.8	34.7	340.6	107.2	319
Bimosiamose	880.396	HMDB0249214	45.7	41.7	0	85.8	243.9	231
Cer(d18:0/25:0)	683.669	HMDB0011770	0	53.1	25.4	26.7	364.2	101.9
Pelargonidin 3-O-[b-D-Glucopyranosyl-(1->2)-[4-hydroxycinnamoyl-(->6)]-b-D-glucopyranoside](E-) 5-O-(6-O-malonyl-b-D-glucopyranoside)	990.267	HMDB0035452	770.5	627.2	268.6	851.9	1113.3	1268.9
Iophenoxic acid	589.787	HMDB0253546	132093.3	129188.6	298457.6	139500.9	365897.4	150224
Panaxynol linoleate	524.437	HMDB0041177	259.7	247.4	340.4	478.4	2169.1	607.3
4-Methyltritriacontane	479.562	HMDB0302869	61.8	77.1	227	428.2	1130.4	444.9
2',3'-Dideoxythymidine triphosphate	484.029	HMDB0250900	478.6	344.3	2926.5	2133.8	12258.4	6105.4
Phytosulfokine a	864.277	HMDB0029809	125.2	71	88.8	627.7	173.6	661.1
Fam-vad-fmk	845.15	HMDB0252163	65.5	83.4	69	326.5	499.8	290.2

Diadenosine hexaphosphate	997.046	HMDB0001282	266.9	236.3	226.5	478.4	520.8	550
8-oxo-GTP	573.938	HMDB0304250	554.8	601.9	481.9	979.9	1614.1	1219.7
15-(3,4-dimethyl-5-pentylfuran-2-yl)pentadecanoyl-CoA	1178.429	HMDB0301587	228.4	146.4	9412.4	463.3	46156.4	2305.3
1-Bromo-3-iodoacetone	284.821	HMDB0040190	85	212.9	0	0	1438.6	0
Gingerglycolipid B	696.419	HMDB0041094	280.2	377.9	402.7	2164.5	1050.1	1838.2
N-(3,5-Dichloro-1-oxido-4-pyridinyl)-8-methoxy-2-(trifluoromethyl)-5-quinoline carboxamide	449.042	HMDB0257550	41.5	42.2	95.1	166	412.7	212.7
2,4,5-Trichlorophenyl acetate	276.896	HMDB0245476	528.9	450.8	635.8	1199.2	678.7	1050.8
Ganglioside GD3 (d18:1/14:0)	1416.743	HMDB0011871	5076.3	4620.1	192	411.6	3306.5	1177.4
Echinacoside	825.233	HMDB0251686	836.6	862.6	189.1	117.3	564.7	264.3
Relcovaptan (SR-49059)	620.103	HMDB0258455	86.9	90.7	82.7	256	470.1	236.5
1,1-Diiodoethane	320.818	HMDB0244023	9496.9	15783	1280.5	583.6	12077.3	926.4
Heptacarboxyporphyrin	619.06	HMDB0253093	9611.7	8666.2	24540.8	10033.6	36407.4	12986.5
P1,P4-Bis(5'-xanthosyl) tetraphosphate	871.011	HMDB0003834	594.9	620.3	550.7	788	1090.7	860.4
bisorganyltrisulfane	683.08	HMDB0304276	599.9	755.4	1005.5	514.7	200.9	406.9
Pepsinogen (1-12)	1417.871	HMDB0256300	2747.3	2456.5	127.7	186.7	1689.9	658.2
Physalin K	576.206	HMDB0034347	87.9	59.3	66	243	234.2	248.8
Biotinyl-5'-AMP	591.184	HMDB0004220	275.9	303.6	336.9	435.4	1922.2	659.5
Pentacarboxyl porphyrinogen III	723.269	HMDB0001957	241.9	207.3	50.9	384.9	494.6	740.1
Filfiline	407.409	HMDB0030953	118.8	72.8	140.5	306.2	477.1	261.8
Fumonisin B4	690.408	HMDB0040968	177.3	54.5	18.6	209.6	299.8	267.6
Guanosine pentaphosphate adenosine	955.017	HMDB0001472	168.3	127.6	207.6	496.4	319.2	691
Nb-Pentacosanoyltryptamine	542.506	HMDB0040820	34312.9	34175.6	75304.4	24719.4	79258.6	19008.3
2-(alpha-hydroxyethyl)thiamine diphosphate	467.056	HMDB0304055	72.5	61.9	70.9	202.5	193.4	199
p-Coumaroyl vitisin A	708.167	HMDB0029239	176.5	146.9	76.4	288	319.6	254.4
N-Acetylsphinganine	361.333	HMDB0249513	816.3	1569	99.1	88.7	4933.7	158
5-Hexatriacontanone	543.562	HMDB0030937	833.2	777.2	605.3	906.5	664.1	731.7
Bn-NCC-2	815.293	HMDB0038230	218.7	159.7	67.8	374.6	385.7	490.3
(8S)-8-amino-7-oxononanoyl-CoA	954.263	HMDB0301611	1173.6	1107.2	1279.1	3169.3	2083.6	4595.1

Cer(d18:0/20:4)	605.561	HMDB0240729	367.3	295.8	1264.1	187.5	3421.6	268.6
Cephamycin A	682.113	HMDB0249811	167.4	182.7	904.5	108.7	3098.8	131.5
Inarigivir soproxil	726.16	HMDB0253441	99.2	97.8	95.9	163.3	374	238.7
SM(d18:2(4E,14Z)/23:1(9Z))	819.636	HMDB0240668	81.3	39.5	42.2	152.4	177.6	100.7
2-Fluoro-araatp	543.024	HMDB0245128	106.6	120.9	38.3	169.4	224.8	297
Trestatin B	1008.296	HMDB0259124	62.2	0	209.8	295.6	202.5	202.9
Propyliodone	447.932	HMDB0256841	124.8	134.5	110.2	176.6	262	264.9
Polyoxyethylene sorbitan monooleate	622.452	HMDB0256687	297	302.4	1220.6	256.3	3921.2	330
Glunicate	722.223	HMDB0252800	67.4	85.8	123.6	196	158.7	320.7
Flavidulol D	542.458	HMDB0040736	289.4	275.4	132.3	418.9	511	738.8
3(S)-Hydroxy-2(S),6-dimethyl-heptanoyl-CoA	962.193	HMDB0060157	0	162.4	82.5	122.2	172.7	288.4
1,7-Pentatriacontadien-11-ol	522.547	HMDB0041033	211.8	248	326.7	438.4	923.1	456.9
Iopanoic acid	571.767	HMDB0253545	61743.7	62110.3	90895.2	86528	58071.9	61999.4
Pralmorelin	856.389	HMDB0256731	488.2	472.5	326.5	439.6	719.7	541.5
Degalloyltheaflavonin	802.183	HMDB0040548	66.3	90.6	57	129.8	262	91.5
Ppads	533.978	HMDB0256715	96.1	104.7	139.5	110.9	439.4	212.7
Lipoyl-GMP	590.049	HMDB0013617	0	0	3202.9	50.6	6349	679.9
N-[[(2S,3S,4R,5R)-5-[2-Chloro-6-[(3-iodophenyl)methylamino]purin-9-yl]-3,4-dihydroxyoxolan-2-yl]-hydroxymethyl]-N-methylformamide	592.054	HMDB0257746	2804	2536.6	9525.8	3247.4	12415.3	4239.1
6-Mercaptopurine ribonucleoside 5'-diphosphate	482.951	HMDB0060660	471	682.1	1598.5	1940.1	2116.7	1808.5
1,26-Hexacosanediol	416.465	HMDB0036581	223.9	220.9	535.4	295.1	618.8	935.7
TTF-1	574.033	HMDB0259312	116.6	91.2	298.8	66.2	917.2	47.7
Jubanine C	666.35	HMDB0037300	356.3	273.2	1559.4	358.4	2804	397.8
Isopropyl 4-(1-(2-fluoro-4-(methylsulfonyl)phenyl)-1H-pyrazolo[3,4-d]pyrimidin-4-yloxy)piperidine-1-carboxylate	495.18	HMDB0248507	110.1	109.7	131.8	168.9	323.3	211.7
Dox-ga3	900.273	HMDB0251599	359.4	249.9	278.1	418.3	739.7	596.8
Hexasodium metaphosphate (P6O186(-))	634.712	HMDB0303419	126.7	106.2	94.8	178	210.6	254
Perfluorododecanoic acid	636.945	HMDB0256318	157.9	172.3	398.7	354.4	514.1	495.9
Bisdiphosphoinositol tetrakisphosphate	842.864	HMDB0006230	60.8	98.8	155	161.1	173.6	249.9

Heptacarboxylporphyrin III	801.278	HMDB0001956	376.7	474.1	479.9	559.5	555.4	505
2-Cl-IB-Meca	582.943	HMDB0245083	1857.1	1889.6	1150.3	2751.9	1748.9	1935.7
Lyciumin A	874.373	HMDB0038672	317.1	317.6	211.1	578.3	463.9	509.7
CE(12:0)	569.543	HMDB0002262	14493.8	15084.5	22286.1	22160.3	12888.8	13055.2
Closantel	662.83	HMDB0250369	211.7	212.6	239.3	297.5	492.9	382.6
Reticulatamone	533.489	HMDB0031396	1160.1	1336.6	765.3	713.6	3434.8	1470.2
Cyclanilide	295.983	HMDB0250621	235	198.7	375.3	430.7	504.6	471.1
Asp-Tyr-Met-Gly-Trp-Met-Asp-Phe-NH2	1101.364	HMDB0248663	629.7	627.2	1242.2	1071	2145.6	1119.9
Nicomol	663.203	HMDB0255582	78.9	142.8	121	200.1	177.7	207.2
C.I. Food Black 1	801.956	HMDB0033389	172.6	218.9	251.4	345	483.7	266.6
Pelargonidin 3-O-[4-Hydroxy-3-methoxy-E-cinnamoyl-(->4)-a-L-rhamnopyranosyl-(1->6)-b-D-glucopyranoside] 5-O-b-D-glucopyranoside	918.266	HMDB0033021	501.6	414.3	354.9	761.6	569.6	758.2
Crustacean Cardioactive Peptide	973.402	HMDB0250548	520.6	502.6	340.1	640	660.5	691.5
Methyl helicterate	650.446	HMDB0254592	71.2	101	172.2	176.8	186.5	187
5-(Acetylamino)-N,N'-bis(2,3-dihydroxypropyl)-2,4,6-triiodo-1,3-benzenedicarboxamide	747.798	HMDB0246133	71.7	95.9	65.6	131.7	161.9	78
Diiodomethane	285.86	HMDB0251350	57	167.5	72.8	73	212.1	186.2
GDP-mannuronate	617.016	HMDB0304366	154.4	155.7	106.7	134.5	172.7	175.9
1-Tritriacontanol	498.564	HMDB0041478	157	169.7	152.7	190.7	333.4	226.1
Caged insp3	591.983	HMDB0249534	178.7	96.9	447.1	147.8	799.6	180.2
p-coumaroyl hexose	693.594	HMDB0304590	150.9	246.2	0	67.5	407.7	144.2
Epimedin B	826.315	HMDB0251854	1117.6	1127.2	2083	1789.1	3049.8	1893.2
Calcium citrate	526.927	HMDB0303432	47.9	57	79.8	99.4	91.9	96
(2R)-2-[[(2R)-2-amino-3-(1-methoxycarbonylindol-3-yl)propanoyl]-[(2S)-2-[[(2R,6S)-2,6-dimethylpiperidine-1-carbonyl]amino]-4,4-dimethylpentanoyl]amino]hexanoic acid	664.363	HMDB0260055	505.2	498.4	192.1	393.2	691.6	768.2
Diepomuricanin A	569.456	HMDB0040921	153.7	142.3	120.5	211.6	157.2	273.4
Direct Blue 1	943.008	HMDB0259652	896.1	942.5	754.9	864.8	1090.1	1293
GDP-alpha-D-glucose	642.033	HMDB0304367	421	431.6	366.3	439.8	746.9	635.2

PE-NMe2(24:1(15Z)/24:1(15Z))	940.788	HMDB0114659	205.5	124.4	161.8	218	234	282
Dihydroergocornine	586.301	HMDB0251308	604.1	479.8	1236.6	1454	794.7	1205.8
Flumethrin	548.064	HMDB0252337	151.2	174.8	185	236.4	252.9	270.2
Malonyl-CoA	854.133	HMDB0001175	123.1	155.8	191.9	194.2	246.4	254.7
Arachidyl alcohol	316.351	HMDB0011619	3523.7	6338.4	78	126.3	2708.6	402.7
Pentosan Polysulfate	640.863	HMDB0014824	1012.8	1299.8	384.6	986.7	1109.2	1839.8
Oolongtheanin	755.124	HMDB0038858	97.6	62	79	99.7	129.8	117.4
Phenylacetyl-CoA	908.137	HMDB0006503	755.4	677.1	646.2	727.3	969.4	916.8
Thiopeptin	1568.434	HMDB0259022	459.1	205.3	787	166.9	1424.9	475.6
2,4-Dichlorophenyl-p-nitrophenyl ether	586.911	HMDB0257558	161	174.9	267.6	162.9	531	164
Adenosine tetraphosphate	609.943	HMDB0001364	302.9	360.1	385.5	374.2	310.5	393.3
Acetyl-arginyl-glycyl-aspartyl-serinamide	513.182	HMDB0247924	316.3	363.8	253.9	367.8	424.3	512.9
2,3-DI-Phytanyl-glycerol	670.731	HMDB0245415	174.9	185.8	299.2	234.9	235.7	282.6
Mulberrofuran M	629.085	HMDB0033261	2404.5	2356.3	2549.3	2795	3989	3211.7
Physagulin E	724.354	HMDB0039693	274.9	268.8	629.7	359.6	911.5	318.5
N-Nervonoyl Methionine	515.423	HMDB0242096	132.2	152.8	155.3	160.6	233.9	200.6
Niaziminin A	837.249	HMDB0303175	154.4	175.8	166.3	179.7	213.6	276.4
3',5'-Diiodo-L-thyronine-beta-D-glucuronoside	701.907	HMDB0060110	127.1	181.4	246.5	394.2	149	205.2
Isothiocyanates	536.82	HMDB0302328	96.8	111.7	127.2	148.8	149.6	152.3
3,3',5-Triiodothyroacetic acid sulfate	724.72	HMDB0246013	165.9	181.3	162.4	204.7	266.3	212.2
Pelargonidin 3-O-[2-O-(6-(E)-feruloyl-beta-D-glucopyranosyl)-6-O-(E)-p-coumaroyl-beta-D-glucopyranoside] 5-O-(beta-D-glucopyranoside)	1080.306	HMDB0302000	160.1	120.3	286.6	265.7	241.1	248
Volixibat	828.264	HMDB0259870	476.3	656.7	189.2	419.9	649.9	684.6
Nodulisporic acid	702.382	HMDB0255694	36.8	254.9	0	0	385.3	0
Adtepp	638.107	HMDB0248031	229.6	247.1	368.8	308.5	298	331
Gly-Pro-Gly-Arg-Ala-Phe	604.32	HMDB0252833	540	595.8	589.8	636.4	778.7	824.4
CE(14:0)	597.566	HMDB0006725	261.1	327.6	188.1	278.4	212.6	201.8
Anhydrosafflor Yellow B	1083.156	HMDB0031914	380.1	395.3	453.7	526.6	468.2	588.9
Tripalmitoyl-s-glyceryl-cysteinyl-seryl-serine	1084.776	HMDB0256067	1232.4	1481.8	0	486.8	1288.9	1702.1

3-[(2-oxoacetyl)oxy]-4-(trimethylazaniumyl)butanoate-CoA	862.006	HMDB0301541	3982.7	3635	3897.8	2707.4	1966.8	2301.1
Perfluorotridecanoic acid	681.981	HMDB0256336	130.2	139	109.2	143.2	146.5	190.1
Chakaflavonoside A	1089.327	HMDB0302043	203.7	136.2	95.4	209.3	141.6	200.5
Pemptoporphyrin	575.204	HMDB0256216	2431.6	2337.3	5110.8	5131.1	3843.9	3370.4
retinyl stearate	570.579	HMDB0257181	247.6	253.3	269.2	283.6	329.8	333
Phaeophorbide b	645.217	HMDB0031149	71	63.7	83.7	83.8	108.5	75
Erucoylacetone	379.359	HMDB0035951	132.7	136.4	284.1	123	316.7	234.4
Inositol nicotinate	828.248	HMDB0253495	1685.3	2047.2	1991.8	2038.9	1056.6	983.9
(10R,13R,17R)-3-Hexadecoxy-10,13-dimethyl-17-[(2R)-6-methylheptan-2-yl]-2,3,4,7,8,9,11,12,14,15,16,17-dodecahydro-1H-cyclopenta[a]phenanthrene	633.581	HMDB0260062	2451.6	2642.2	2913.3	2778.4	3537.5	3060.6
Avagacestat	521.063	HMDB0248734	167.6	176.8	96	156.9	164.5	205.8
inosine pyruvate	377.052	HMDB0253490	130.9	199.2	32.9	16.7	207.8	205
p-coumaroyl pentose	658.655	HMDB0304588	110	153.2	110.7	168.1	123.7	149.5
delphinidin 3-O-glucosyl-5-O-caffeoylglucoside	827.136	HMDB0304328	428.5	442.7	322.9	543.2	197.4	615
TG(22:4(7Z,10Z,13Z,16Z)/18:2(9Z,12Z)/22:5(7Z,10Z,13Z,16Z,19Z))	1012.811	HMDB0054781	2759.9	2621.3	1630.8	1902.5	3195.3	2028.1
N1,N5,N10-Tris-trans-p-coumaroylspermine	658.356	HMDB0039962	580.3	587.9	529.5	667	578.2	662
Thiamine monophosphate	368.071	HMDB0002666	107.2	247.6	0	0	396.4	0
15-(3-Methyl-5-pentylfuran-2-yl)pentadecanoylcarnitine	558.409	HMDB0241842	251.2	212.3	414.9	249.5	337.3	382.8
1,2,2'-Trisinapoylgentiobioside	999.225	HMDB0041127	2144.8	2365.6	711.9	1910.2	1948.6	1891.3
1,4-dihydroxy-2-naphthoyl-CoA	971.186	HMDB0304010	1344.4	1184.8	717.6	990.5	1581.1	996.6
arachidyl amido cholanoic acid	702.599	HMDB0248560	169.7	127.4	314.1	193.6	325.5	152.4
Emblicanin A	800.115	HMDB0030437	228.4	219.8	308.4	241.7	284	299.3
3a,7a,12a-Trihydroxy-5b-24-oxocholestanoyl-CoA	1252.464	HMDB0006891	652.6	596.2	200.7	115.3	1060	376.6
Potassium citrate	347.878	HMDB0303753	260.3	273	454.6	312.6	336.4	407.6
(S)-3-hydroxy-isobutanoyl-CoA	867.147	HMDB0303996	102.5	57.3	833	125.6	665.7	267.8
Tricin 7-[feruloyl-(->2)-glucuronyl-(1->2)-[glucuronyl-(1->3)]-glucuronide]	1073.191	HMDB0039908	18.7	63.5	521.3	295.7	39	306.1
TG(22:0/18:2(9Z,12Z)/22:2(13Z,16Z))	1047.872	HMDB0046646	1181.3	943.3	2561.7	1953	2594.7	413.7
3-hydroxypropanoyl-CoA	836.123	HMDB0304134	203.1	250.4	114.3	159.7	159.1	277.3

carlliiionaln	488.999	HMDB0249679	26859.8	34822.1	15683.2	18498.6	13172.5	10897.9
APC	657.233	HMDB0060661	583.9	462.8	1249.2	451.9	1522.1	420.7
(5Z)-7-{2-[(1E)-3,3-difluoro-4-phenoxybut-1-en-1-yl]-3,5-dihydroxycyclopentyl}hept-5-enoyl-CoA	1160.2	HMDB0301648	533	527.2	577.2	757.8	469.9	439
Phyllanthusol B	810.265	HMDB0035904	175.4	120.9	228.8	187.9	178.1	169
A6 Peptide	928.384	HMDB0247728	393.5	415.9	226.5	357.4	337.4	355.9
Avenestergenin A1	676.36	HMDB0035264	2712.8	2192.5	6238.6	2288.7	6782.2	2210.4
4-[[2-[[(5Z)-5-(2,6-Dioxo-1,3-dipropylpurin-8-ylidene)-1-methyl-2H-pyrazol-3-yl]oxy]acetyl]amino]benzoic acid	527.235	HMDB0248640	150.8	118.9	7.9	67.5	128.7	83.4
TY-51469	564.934	HMDB0259332	139.2	160.6	117.2	119.5	144.5	155.7
Hydroxyethyl myristyl oxyhydroxypropyl decanamide	508.42	HMDB0244501	144.6	167.8	85.9	104.5	124.4	171.8
Nitrocellulose	1038.065	HMDB0255645	1434	1291.5	566	1014.3	1568	722.7
Promin	737.113	HMDB0252790	1353	1164	1456.4	1439.3	1484.2	1054.7
Heparan sulfate	661.996	HMDB0000693	93.7	71.2	201	89.4	136.5	137.6
Nb-Tricosanoyltryptamine	497.447	HMDB0040818	2052.9	1795.7	2553.4	2492.2	2250.8	1615.4
Brassilexin	197.014	HMDB0039638	120	121.9	149.3	153.5	112.7	121.3
4-Hydroxy duloxetine glucuronide	528.113	HMDB0060763	64.4	59.1	0	26.7	42.1	52.3
DG(24:0/0:0/18:2n6)	736.735	HMDB0056120	2042.2	1741.6	2208.5	2158.1	2150.4	1517.1
S-Trichlorovinyl-N-acetylcysteine	329.888	HMDB0244383	546.1	544.4	794.1	684.9	541.4	601.9
Basellasaponin A	1009.399	HMDB0039399	496	457	496.3	527.1	435.8	438.9
Perfluorotributylamine	689.012	HMDB0256335	217.5	223.2	76.7	226.4	74	199
Tetragastrin	619.22	HMDB0005775	14.3	0	116.6	0	25.4	100.1
Ellagitannin	1015.027	HMDB0251750	1243.8	1172.1	758.6	556.8	289.9	606.6
BENSULFURON-METHYL	449.052	HMDB0248961	227	227.8	149.4	222	154	195.2
Peonidin 3-(6"-p-coumaroyl-glucoside) 5-glucoside	792.229	HMDB0038092	11217.6	11757.9	10933.6	11191.7	11450.5	9411.3
Citbismine C	702.223	HMDB0041435	496.4	507	530.1	557.2	475.2	401.2
2",3",6"-Trigalloyliriflophenone 3-C-glucoside	903.102	HMDB0029630	154	121.4	232.4	147.7	241.8	81.4
3,3',4,4'-Tetrachloroazoxybenzene	356.906	HMDB0246008	384.6	313.9	772.9	484.9	467.6	405.9
pppGpp	694.904	HMDB0304469	4649.9	4879.5	4271	5513.4	2866.6	4112.2
NAADPH	764.112	HMDB0255413	226.4	148.4	110.8	163	137.1	147.1

4-(2'-carboxyphenyl)-4-oxobutyryl-CoA	989.111	HMDB0304165	1529.7	1349.9	409.9	638.6	1574.5	780.3
5-Iodo-2'-deoxyuridine triphosphate	632.829	HMDB0251498	1812.7	1779.7	2887.7	1824.5	2252.5	1757.1
(-)-Epigallocatechin 3-gallate 7-glucoside 4”-glucuronide	#N/A	#N/A	364.9	345.5	532	439.6	305.4	333.1
Cer(d17:1/16:0)	524.519	HMDB0240685	78751.7	80303.8	99813.1	83127.8	61911.3	40112.9
25-Methyl-21-tritriacontene-1,9,11-triol	542.546	HMDB0041032	64934.2	65287.6	82600.8	78493.7	42207.5	60939.8
C.I. Acid Green 50	593.069	HMDB0033390	251.2	337.5	125.2	185.3	180.6	242.6
Rifamycins	734.256	HMDB0257226	362	412.5	340.6	294	356.6	297.2
2,2,2-Trichloroethyl chloroformate	248.843	HMDB0245336	128.5	110.3	151.5	140.1	83.1	107
alpha-Amyrin tetratriacontanoate	917.912	HMDB0036743	8770.7	8255.5	2736.4	7809.6	2527.5	6302.5
2,4,6-Tribromophenol	328.783	HMDB0029642	106.1	115.8	151.1	158.5	97.5	56.3
N-Acetyl-L-phenylalanyl-3,5-diiodo-L-tyrosine	660.959	HMDB0255059	636.1	768.5	739.5	669.3	583.1	467.6
1-Octadec-9-enoxyoctadec-9-ene	536.616	HMDB0255338	111.7	130.3	243.2	152.1	71.8	181.9
Sambacolignoside	945.278	HMDB0038933	1029.9	1108.6	959.4	805.3	292.5	526.7
Liriodendrin	743.274	HMDB0036410	264.9	231.9	291.7	268.6	218.4	169.9
Alisertib	557.077	HMDB0248139	565.4	547.2	578.2	464.9	414	488.8
2-Hexadecanoyloctadec-9-enal	522.537	HMDB0255385	545.3	535.9	525.8	389.2	472.1	438.5
Ipodate	615.823	HMDB0253566	969.2	874.2	1192.7	1006.7	676.2	769.8
Iodipamide ethyl ester	1234.51	HMDB0253515	704.7	796.8	1193.9	557.7	1074.7	529.2
18(R)-Hydroxy-20-oxo-20-CoA-LTE4	1235.27	HMDB0012605	101.2	124.6	232.4	65	182.4	115.8
o-Cresolphthalein complexone	637.209	HMDB0255845	992.1	827.7	1113.8	975.3	579.7	762.4
Sodium copper chlorophyllin	696.137	HMDB0303293	1934	1987.1	2375.9	2580.6	1141.6	1231.2
Potassium metaphosphate	472.67	HMDB0303423	309.8	302	365.3	321.9	177.8	173.7
2-phospho-4-(cytidine 5'-diphospho)-2-C-methyl-D-erythritol	624.022	HMDB0304084	415.1	398.6	289.4	285	268.8	309.7
Amino (methoxysulfinyl) pentasulfide	293.826	HMDB0031980	1091.6	1737.7	406.9	416.6	895.4	257.8
propanoyl-CoA	842.12	HMDB0304472	985.7	1011.5	422.5	873.8	433.3	560.6
Trifucosyllacto-N-hexaose	1511.566	HMDB0006621	1002.6	968.5	1469.1	937.9	1084	618.4
Alatanin A	1510.436	HMDB0041165	1193.8	1206.8	1725.6	1133	1266.3	711
Trioctylamine	371.465	HMDB0259251	982.6	1049.7	1609.4	1497.8	805.4	394.6

Cucurbituril	1035.279	HMDB0250585	530.2	462.4	774.1	457.9	285.2	562.6
2,2'-Dithiodiethanesulfonic acid	320.88	HMDB0246681	722.3	681.1	822.5	647.2	412.6	405.1
Cer(d18:0/23:0)	638.632	HMDB0011767	228.4	232.4	181.2	170.4	92.3	209
Phomopsin B	772.35	HMDB0038884	264.5	246.6	295.9	211.6	189.3	188
Aluminum myristate	726.632	HMDB0303189	462.8	401.9	222	337.6	179	270.6
Ethylene glycol distearate	595.568	HMDB0032260	242.5	267.5	310.4	250.6	156.3	184.4
Apigenin 7-di-O-xyloside	589.12	HMDB0302800	280.4	282	133.5	210.8	136.4	149.6
Docosanal	325.355	HMDB0251560	102.2	97.9	116.5	78.9	72.2	72.8
Surugatoxin	701.085	HMDB0030173	7221.4	8119.9	3709.5	4615.1	4082.1	4711.2
Peonidin acetyl 3,5-diglucoside	690.122	HMDB0301895	83.2	104	50.1	67	32	66.9
p-Iodoclonidine	393.88	HMDB0256047	193.9	177.8	157.8	190.2	122.3	56.8
N-(4-Methoxybenzyl)-N'-(5-nitro-1,3-thiazol-2-YL)urea	331.05	HMDB0248543	209.4	178.5	252.8	197.9	169	78.3
UDP-alpha-D-sulfoquinovopyranose	665.936	HMDB0304528	467.7	491.1	244.3	372.1	262.9	195.2
Iohexol	859.908	HMDB0015449	1320.7	1411.1	1425.8	1266.2	764.6	837.1
(6-Aminopurin-9-yl) [hydroxy(phosphonooxy)phosphoryl] hydrogen phosphate	429.902	HMDB0258010	308.1	314.4	299.9	261	160	201.9
Cer(d18:1/25:0)	686.661	HMDB0004957	304	269	457.6	338.1	213.1	138.2
Tritriacontyl octacosanoate	925.894	HMDB0041479	4323.6	4402.3	6173.8	3299.9	4098.7	2524.3
Haloprogin	382.825	HMDB0014931	552.2	724.4	572.5	442.1	399.6	216
2-(Thiocyanomethylthio)benzothiazole	276.935	HMDB0245617	8919.7	9548.9	7722.9	7971.6	3790.7	5440.5
Eltenac	339.941	HMDB0251756	231.3	270.5	276.7	209	155.7	97.7
Lyciumoside IX	739.346	HMDB0033502	275.5	295.2	299.6	199.8	164.9	202.9
2,2,2-Trichloroacetamide	161.935	HMDB0245334	361.1	406.2	359.1	346.6	171.6	216.4
1-Nitro-3,5-dinitroso-1,3,5-triazinane	208.079	HMDB0253137	78.2	97	90	74.6	40.1	57.7
2-Oxothiazolidine-4-carboxylic acid	169.991	HMDB0245287	217.3	211.2	180.1	177.8	93.3	118.5
2'-Deoxyinosine triphosphate	492.987	HMDB0003537	179126.9	187468.6	206461.6	172968.8	101871.4	91171.4
Torvoside D	765.376	HMDB0029624	9609.1	10227.4	10617.8	8723.1	5085.1	5486
Sodium magnesium aluminosilicate	302.827	HMDB0303736	3541.7	3497.9	4671.3	3543.9	2171.8	1699.9
(S)-4-(2-(N-Methylisoquinoline-5-sulfonamido)-3-oxo-3-(4-phenylpiperazin-1-yl)propyl)phenyl isoquinoline-5-sulfonate	760.169	HMDB0253809	480.7	499.6	55.1	264.8	202.8	182

m-Methyl acetophenone	303.958	HMDB0302879	258.5	247.6	325.2	245.2	158.1	113.5
CE(22:4(7Z,10Z,13Z,16Z))	723.621	HMDB0006729	552	499.8	535	390.9	288	307.5
Eujambin	697.02	HMDB0038286	584.1	594.2	424.2	446	222.9	319.4
Solanesol	631.598	HMDB0258363	142.3	150.9	368.6	140.2	4.6	258.3
Decamethonium	281.3	HMDB0015375	3326.3	3813.5	3184.8	2899.5	1447.3	1880.2
neuronostatin	1453.77	HMDB0255560	6821.7	8020.9	9048.9	7223	2112.4	5066.3
SM(d18:0/16:0)	722.617	HMDB0010168	1159.1	1254.1	1396.4	902.1	367.1	1026.7
Xyloglucan Heptasaccharide	1085.333	HMDB0253105	888	1122.1	0	84.8	421.1	697.6
Nbd-phallicidin	1069.41	HMDB0255018	4830.2	4992.9	4085	3720.3	2016.3	2578.6
Perfluorodichlorooctane	508.879	HMDB0256317	909.9	940.5	762.9	721.6	348.2	484.7
Folcepri	746.226	HMDB0251680	27281.5	30920.3	28359.5	23262.2	13419.5	14737.8
N(4)-Octadecyl-1-arabinofuranosylcytosine	496.378	HMDB0248147	207.7	186.3	241	192.5	93.1	90.1
mepitiostane	405.285	HMDB0254455	565.3	865.9	623.4	610.1	289.8	300.6
Gly-arg-gly-glu-ser-pro	619.309	HMDB0252941	442.3	468.2	138.4	270.6	176.2	155.2
Bis(sulfanyl)carbamic acid	125.963	HMDB0257766	1041.5	1123.4	898.6	839.9	383.8	520.2
2,3,4,4-Tetramethylpentane-2,3-diamine	181.167	HMDB0258064	973.2	1174.6	893.8	832.6	389.3	498.6
Diloxanide	349.998	HMDB0015684	2606.1	3592.3	2546.8	2330	1078.4	1504.5
2-Heptadecylfuran	307.327	HMDB0033608	416.8	514.3	418.7	358.2	173.3	226
L-AMP	645.96	HMDB0253868	654.6	725.7	581.8	420.6	280.2	348.3
2,3-Bis-[2-methoxy-4-nitro-5-sulfophenyl]-2h-tetrazole-5-carboxanilide	675.978	HMDB0258115	2024	1963	1403.6	1058.1	874.8	901.8
Sodium Zirconium Cyclosilicate	364.761	HMDB0304889	379.7	311.5	1341.4	513.5	408	130.9
Celosianin	893.165	HMDB0302989	567.8	543.8	667.1	385	162.9	372.5
Xanthosine 5-triphosphate	546.973	HMDB0000293	355	339.2	97.3	254.4	78.3	70
Glycinoprenol 10	722.78	HMDB0038537	2264.2	2344.4	2252.2	914.3	161.7	719.1
Polyoxyethylene dioleate	613.52	HMDB0032475	400.1	404.2	326	246.7	154.7	170.7
Perfluorodecane sulfonic acid	622.913	HMDB0246166	638.6	684.4	626.9	398	246.5	334.6
Cefazedone	564.994	HMDB0249753	1166.6	1080.2	367.8	868.8	228	209
Lorazepam glucuronide	519.032	HMDB0041917	376.8	353.6	156.7	169.8	100.4	168

Legumin	543.011	HMDB0302886	592.7	588.6	269.7	289.3	181.8	243.2
Fenoprop	285.982	HMDB0252208	1517.9	1722.2	659.9	1463.9	249.4	206.4
Cer(d18:1/22:1(13Z))	620.641	HMDB0011775	678.5	572.7	922.8	378.3	245.7	446
16-oxo-palmitate	270.218	HMDB0304028	246.8	286.4	230.6	187.5	82.4	105.7
2,3,5-Triiodobenzoic acid	517.715	HMDB0245436	136.2	160.8	115.8	100.5	54.6	45.8
Gallocatechin-(4alpha->8)-gallocatechin-(4alpha->8)-gallocatechin	953.163	HMDB0040378	522.6	810	194.9	338.2	267.1	127.8
DG(18:2n6/0:0/20:2n6)	676.575	HMDB0056284	1028.1	984.9	803.4	652	310.2	362.2
Fipronil sulfone	474.92	HMDB0252267	737.2	956.1	195.9	387.3	175.2	321.5
Chymosin preparation, escherichia coli k-12	708.104	HMDB0032199	1042.5	736.7	580	478.1	277	344.7
Ceftaroline fosamil	706.974	HMDB0249777	5790.3	4260.8	3582.7	2630.1	1699.9	2003.4
Savoury taste-enhancing peptide	1314.323	HMDB0303439	316.4	288	0	26.1	183.4	70.3
precorrin-1	843.236	HMDB0304470	932.9	1072.5	980.6	648.3	107.5	611.1
4-(4-Hydroxy-3-isopropylphenoxy)-3,5-diiodophenylacetic acid	555.925	HMDB0246055	378	492.2	231.8	275.3	125.1	89.3
Bentonite	143.943	HMDB0303391	84.3	82.5	58.3	48	25.1	26.2
Mii-coa	1034.157	HMDB0254716	372.4	446.6	368	231.5	105.7	173.8
ADP-Ribosyl-L-arginine	754.118	HMDB0001260	120.4	282.4	29.9	53.9	125.4	0
Dichlorphenamide	321.947	HMDB0015275	776	1706.2	0	0	1015.8	0
Betavulgaroside VI	1011.423	HMDB0033426	1375.3	1414	1578.7	828.7	155.3	793.3
Dieckol	781.024	HMDB0251228	83.3	297.5	0	0	152.6	0
Pectolinarin	623.197	HMDB0256193	737.4	827.7	667.5	405.9	169.3	281.1
Jubanine B	752.342	HMDB0030206	147	159.6	123.7	73.1	0	89.3
Valorphin	931.393	HMDB0059789	145.2	196.8	668	303.7	0	76.1
Lifitegrast	653.033	HMDB0254086	2828	3224.5	1038.9	1421.4	245.6	907
Guanine polynucleotide	1076.113	HMDB0256676	812.8	742.1	638.7	391.4	185.5	211.5
(2S)-2-Amino-3-[(2S,3R)-2-amino-3-[(2S)-2-amino-3-(4-hydroxyphenyl)propanoyl]oxybutanoyl]oxypropanoic acid	387.187	HMDB0257991	280.3	571	0	0	302.2	0
Palmitoylcholine	343.345	HMDB0240592	138.8	298.4	0	0	150.7	2.8
Cer(d18:0/12:0)	522.434	HMDB0011758	1760.2	2091.6	671.6	850.5	148.3	562.3
ADP-ribose 1"-2" cyclic phosphate	660.01	HMDB0011671	2326.3	2649.5	1723.7	1025.2	660.4	600.5

TRYPSINOGEN	960.314	HMDB0259306	1083.3	965.7	536.9	445.4	225.4	211.3
Methyclothiazide	376.993	HMDB0014377	3596.6	3343.5	2743.7	1487.5	817.5	892.7
Bisnorbadioquinone A	651.017	HMDB0033267	1148.1	1044.8	965.9	518.2	235	252.9
2,5,7-trihydroxy-4'-methoxyisoflavanone	340.033	HMDB0304042	13310.3	18115.9	8688	8972	1896.3	1878.1
Torvoside G	647.354	HMDB0030337	3134.8	3105.9	3297.4	1472.5	639.9	890.8
Bromocriptine	692.186	HMDB0015331	1685.7	1457.7	1106	627	321.1	366.5
3-Piperidinecarboxamide, N-((2-chloro-5-(2-methoxyethyl)phenyl)methyl)-N-cyclopropyl-4-(6-(2-(2,6-dichloro-4-methylphenoxy)ethox	#N/A	#N/A	280.8	319.8	254.4	166.6	12.7	82.2
CE(15D5)	792.798	HMDB0112210	1077.7	1216.5	12	21.6	612.3	46
Phosphoribosyl-ATP	741.952	HMDB0003665	198.2	190.5	194.3	67.8	41.6	53.7
Amlaic acid	691.056	HMDB0036349	4093.8	3559.8	2792.8	1400.5	717.4	800.6
Phosphothiophosphoric acid-adenylate ester	561.922	HMDB0252625	480.7	625.9	544.9	236.2	5.7	213.5
(2,6-dihydroxy-4-{7-methyl-11-oxo-4-[(3,4,5-trihydroxy-6-{[(3,4,5-trihydroxy-6-methyloxan-2-yl)oxy]methyl}oxan-2-yl)oxy]-2,8-dio	#N/A	#N/A	2258.2	1918	1570.1	777.1	360	374.3
Procion blue MX-R	674.94	HMDB0257125	285.8	406.9	369.8	213.5	0	65.7
Nifursol	403.987	HMDB0031764	6064.8	5402.9	4361	2137.7	1034.4	971
Cer(d16:1/LTE4)	710.534	HMDB0289854	343.2	368.9	1084.7	312.2	48.1	90.1
Xanthan	1051.237	HMDB0029923	575	573.8	229.4	192.3	75.3	64
Cep-1347	633.216	HMDB0249804	301.3	416	47.3	102	0	77.2
Epicatechin-(2alpha->7,4alpha->8)-epicatechin 3-galactoside	729.178	HMDB0301676	1483.3	2046.4	134.1	211.1	209.2	378.2
Thio-NAD	680.088	HMDB0258995	28.2	54.9	186.6	12.3	35.4	9.4
Lapaquistat acetate	683.218	HMDB0253979	914.5	694.3	501.6	201.2	101.6	127.5
Luteolin 7-O-[beta-D-glucuronosyl-(1->2)-beta-D-glucuronide]-4'-O-beta-D-glucuronide	815.106	HMDB0060296	225.3	271.7	145.7	85	0	44.9
Phosphatidylinositol 3,4,5-trisphosphate	1117.387	HMDB0256910	1378.3	1418.2	1288.5	468.6	76.1	272.5
Trypanothione	741.333	HMDB0060520	3473.4	3307.7	2914.6	972.1	229	695.8
thyroxine iodide	909.572	HMDB0259063	656.6	616.9	488.8	191.7	32.7	87.9
Tyropanoic acid	658.901	HMDB0259350	2020.7	1616	825.3	414.2	145.2	230.7
Myo-inositol trispyrophosphate	606.78	HMDB0259418	427.3	402.1	546.8	173.8	7.6	56.9

Ceramide AP	622.533	HMDB0249815	602.1	722.3	219.7	170.3	0	93.2
ent-Epiafzelechin(2a->7,4a->8)epiafzelechin 3-(4-hydroxybenzoic acid)	687.154	HMDB0032793	119.2	182.9	243.3	92.6	0	0
(4Z,7Z,10Z,13Z,16Z)-19,20-dihydroxydocosa-4,7,10,13,16-pentaenoyl-CoA	1134.331	HMDB0301382	3476.2	3758	1681	175.6	120	175
Physagulin G	745.318	HMDB0039694	191.1	200.3	275.6	66.6	0	10.3
Ethylene diamine tetra (methylene phosphonic acid)	773.943	HMDB0257939	459.2	515	300.3	138.4	0	0
Diguanosine pentaphosphate	966.022	HMDB0001380	897.4	1128.2	28.5	46.6	0	69.7
(8R,8'R)-Secoisolariciresinol 9,9'-bis-[4-carboxy-3-hydroxy-3-methylbutanoyl-(->6)-glucoside]	1013.348	HMDB0040283	950.3	906.9	225.9	63.8	0	34.6
Transfectam	824.861	HMDB0259109	719.4	742	88.5	15.7	8.1	19
Cyclohex-1,5-diene-1-carboxyl-CoA	912.098	HMDB0012207	714.5	736.6	0	0	23.2	0
Psiguavin	1213.045	HMDB0039627	989.5	1009	174.5	0	6.8	0
(5Z)-7-[(1R,2R,3R)-3-hydroxy-2-[(1E,3S)-3-hydroxy-5-phenylpent-1-en-1-yl]-5-oxocyclopentyl]hept-5-enoyl-CoA	1158.282	HMDB0301568	762.6	847.4	20.7	0	0	0
heparan sulfate alpha-D-glucosaminide	756.992	HMDB0060481	481.4	582	306.8	0	0	0
Mannosyl-inositol-phosphorylceramide	1133.767	HMDB0012257	2716.8	3107.6	871.1	0	0	0
Starch, hydrogen phosphate, 2-hydroxypropyl ether	1237.265	HMDB0258485	1119.5	1059	82.2	0	0	0

List of Publications

1. **Honokiol, an inducer of Sirtuin 3, protects against NSAID-induced gastric mucosal mitochondrial pathology, apoptosis and inflammatory tissue injury**. Subhashis Debsharma, **Saikat Pramanik**, Samik Bindu, Somnath Mazumder, Troyee Das, Debanjan Saha, Rudranil De, Shiladitya Nag, Chinmoy Banerjee, Asim Azhar Siddiqui, Zhumur Ghosh, Uday Bandyopadhyay. ***British Journal of Pharmacology, PMID: 36914615, 2023***

2. **SIRT3, a target of non-steroidal anti-inflammatory drug to trigger mitochondrial dysfunction and gastric cancer cell death.** Subhashis Debsharma, **Saikat Pramanik**, Samik Bindu, Somnath Mazumder, Troyee Das, Uttam Pal, Rudranil De, Shiladitya Nag, Chinmoy Banerjee, Nakul Chandra Maiti, Zhumur Ghosh, Uday Bandyopadhyay. ***iScience, PMID: 38550981, 2024***

3. **Indomethacin impairs mitochondrial dynamics by activating the PKCζ-p38-DRP1 pathway and inducing apoptosis in gastric cancer and normal mucosal cells.** Somnath Mazumder, Rudranil De, Subhashis Debsharma, Samik Bindu, Pallab Maity, Souvik Sarkar, Shubhra Jyoti Saha, Asim Azhar Siddiqui, Chinmoy Banerjee, Shiladitya Nag, Debanjan Saha, **Saikat Pramanik**, Kalyan Mitra, Uday Bandyopadhyay. ***J Biol Chem; PMID: 30940726, 2019***

4. **Emerging role of mitochondrial DAMPs, aberrant mitochondrial dynamics and anomalous mitophagy in gut mucosal pathogenesis.** Somnath Mazumder, Samik Bindu, Rudranil De, Subhashis Debsharma, **Saikat Pramanik**, Uday Bandyopadhyay, ***Life Sci. PMID: 35787999, 2022***

5. **Hydrazonophenol, a Food Vacuole-Targeted and Ferriprotoporphyrin IX-Interacting Chemotype Prevents Drug-Resistant Malaria.** Shubhra Jyoti Saha, Asim Azhar Siddiqui, **Saikat Pramanik**, Debanjan Saha, Rudranil De, Somnath Mazumder, Subhashis Debsharma, Shiladitya Nag, Chinmoy Banerjee, and Uday Bandyopadhyay ***ACS Infect Dis. PMID: 30472841, 2019***

6. **Macrophage migration inhibitory factor regulates mitochondrial dynamics and cell growth of human cancer cell lines through CD74-NF-κB signaling.** Rudranil De, Souvik Sarkar, Somnath Mazumder, Subhashis Debsharma, Asim Azhar Siddiqui, Shubhra Jyoti Saha, Chinmoy Banerjee, Shiladitya Nag, Debanjan Saha, **Saikat Pramanik**, Uday Bandyopadhyay ***J Biol Chem, PMID: 30366984, 2018***

7. **Rab7 of Plasmodium falciparum is involved in its retromer complex assembly near the digestive vacuole.** Asim Azhar Siddiqui, Debanjan Saha, Mohd Shameel Iqbal, Shubhra Jyoti Saha, Souvik Sarkar, Chinmoy Banerjee, Shiladitya Nag, Somnath Mazumder, Rudranil De, **Saikat Pramanik**, Subhashis Debsharma, Uday Bandyopadhyay. ***Biochim Biophys Acta Gen Subj, PMID: 32512169, 2020***

8. **Nuclease activity of Plasmodium falciparum Alba family protein PfAlba3**. Chinmoy Banerjee, Shiladitya Nag, Manish Goyal, Debanjan Saha, Asim Azhar Siddiqui, Somnath Mazumder, Subhashis Debsharma, **Saikat Pramanik**, Uday Bandyopadhyay. ***Cell Reports, PMID: 36947546, 2023***

9. **Structure-function analysis of nucleotide housekeeping protein HAM1 from human malaria parasite Plasmodium falciparum.** Debanjan Saha, Atanu Pramanik, Aline Freville, Asim Azhar Siddiqui, Uttam Pal, Chinmoy Banerjee, Shiladitya Nag, Subhashis Debsharma, **Saikat Pramanik**, Somnath Mazumder, Nakul C Maiti, Saumen Datta, Christiaan van Ooij, Uday Bandyopadhyay. ***FEBS J*, *PMID: 39003571, 2024***

10. **Plasmodium falciparum Alba6 exhibits DNase activity and participates in stress response.** Shiladitya Nag; Chinmoy Banerjee; Manish Goyal; Asim Azhar Siddiqui; Debanjan Saha; Somnath Mazumder; Subhashis Debsharma; **Saikat Pramanik**; Shubhra Jyoti Saha; Rudranil De; Uday Bandyopadhyay. ***iScience, PMID: 38558939***

Conference

ORAL PRESENTATION

1. **Title: Impact of acute mental stress on gastropathy and gut-mitochondrial biogenesis: role of GR signalling.**

   Conference: Zoospectra 2022; 5-6th December 2022, Dept. of Zoology, University of Calcutta, India.

2. **Title: Impaired mitochondrial biogenesis and functionality contributes to gastropathy in Stress related Mucosal Disease (SRMD); A mechanistic study.**

   Conference: Mechanistic and Therapeutic Approaches in Human and Animal Health, 2021; 6-8th December 2021, Dept. of Zoology, Cooch Behar Panchanan Barma University, India

Received: 1 August 2022 | Revised: 22 December 2022 | Accepted: 8 March 2023

DOI: 10.1111/bph.16070

RESEARCH ARTICLE

Honokiol, an inducer of sirtuin-3, protects against non-steroidal anti-inflammatory drug-induced gastric mucosal mitochondrial pathology, apoptosis and inflammatory tissue injury

Subhashis Debsharma[1] | Saikat Pramanik[1] | Samik Bindu[2] | Somnath Mazumder[3] | Troyee Das[4] | Debanjan Saha[1] | Rudranil De[5] | Shiladitya Nag[1] | Chinmoy Banerjee[1] | Asim Azhar Siddiqui[1] | Zhumur Ghosh[4] | Uday Bandyopadhyay[1,6]

[1]Division of Infectious Diseases and Immunology, CSIR-Indian Institute of Chemical Biology, Kolkata, West Bengal, India

[2]Department of Zoology, Cooch Behar Panchanan Barma University, Cooch Behar, West Bengal, India

[3]Department of Zoology, Raja Peary Mohan College, Uttarpara, West Bengal, India

[4]Division of Bioinformatics, Bose Institute, Kolkata, West Bengal, India

[5]Amity Institute of Biotechnology, Amity University, Kolkata, Kolkata, West Bengal, India

[6]Division of Molecular Medicine, Bose Institute, Kolkata, West Bengal, India

Correspondence
Dr Uday Bandyopadhyay, Division of Molecular Medicine, Bose Institute, EN 80, Sector V, Bidhan Nagar, Kolkata, West Bengal 700091, India.
Email: ubandyo_1964@yahoo.com; udayb@jcbose.ac.in

Funding information
Department of Biotechnology, Ministry of Science and Technology, India; Science and Engineering Research Board, Grant/Award Number: SB/S2/JCB-54/2014

Background and Purpose: Mitochondrial oxidative stress, inflammation and apoptosis primarily underlie gastric mucosal injury caused by the widely used non-steroidal anti-inflammatory drugs (NSAIDs). Alternative gastroprotective strategies are therefore needed. Sirtuin-3 pivotally maintains mitochondrial structural integrity and metabolism while preventing oxidative stress; however, its relevance to gastric injury was never explored. Here, we have investigated whether and how sirtuin-3 stimulation by the phytochemical, honokiol, could rescue NSAID-induced gastric injury.

Experimental Approach: Gastric injury in rats induced by indomethacin was used to assess the effects of honokiol. Next-generation sequencing-based transcriptomics followed by functional validation identified the gastroprotective function of sirtuin-3. Flow cytometry, immunoblotting, qRT-PCR and immunohistochemistry were used measure effects on oxidative stress, mitochondrial dynamics, electron transport chain function, and markers of inflammation and apoptosis. Sirtuin-3 deacetylase activity was also estimated and gastric luminal pH was measured.

Key Results: Indomethacin down-regulated sirtuin-3 to induce oxidative stress, mitochondrial hyperacetylation, 8-oxoguanine DNA glycosylase 1 depletion, mitochondrial DNA damage, respiratory chain defect and mitochondrial fragmentation leading to severe mucosal injury. Indomethacin dose-dependently inhibited sirtuin-3 deacetylase activity. Honokiol prevented mitochondrial oxidative damage and inflammatory tissue injury by attenuating indomethacin-induced depletion of both sirtuin-3 and its transcriptional regulators PGC1α and ERRα. Honokiol also accelerated gastric wound healing but did not alter gastric acid secretion, unlike lansoprazole.

Conclusions and Implications: Sirtuin-3 stimulation by honokiol prevented and reversed NSAID-induced gastric injury through maintaining mitochondrial integrity.

Abbreviations: 8-oxo-dG, 8-oxo-7,8-dihydro-2′-deoxyguanosine; DEG, differentially expressed gene; ERRα, oestrogen-related receptor α; ETC, electron transport chain; i.g., intragastric; II, injury index; MFN, mitofusin; MOS, mitochondrial oxidative stress; NRF2, nuclear factor erythroid 2-related factor 2; NSAIDs, non-steroidal anti-inflammatory drugs; OGG1, 8-oxoguanine DNA glycosylase 1; OPA1, optic atrophy 1; PGC1α, peroxisome proliferator-activated receptor-gamma coactivator 1-alpha; PPI, proton pump inhibitor; RIN, RNA integrity number; Sirt3, sirtuin-3; SOD2, superoxide dismutase; TBS, Tris-buffered saline; ΔΨm, mitochondrial transmembrane potential.

Honokiol did not affect gastric acid secretion. Sirtuin-3 stimulation by honokiol may be utilized as a mitochondria-based, acid-independent novel gastroprotective strategy against NSAIDs.

KEYWORDS
apoptosis, gastric injury, honokiol, mitochondria, non-steroidal anti-inflammatory drugs, Sirtuin-3

1 | INTRODUCTION

Non-steroidal anti-inflammatory drugs (NSAIDs) are widely used for managing diverse inflammatory disorders (Crofford, 2013; Ong et al., 2007). Furthermore, drug repurposing studies have shown NSAIDs to exhibit potent anticancer activities, as long-term NSAID users have a relatively lower risk of developing cancers in the GI tract, breast, prostate and lung (Cuzick et al., 2009; Kazberuk et al., 2020; Khoo et al., 2019). In spite of such a wide spectrum of therapeutic utility, prolonged usage of NSAIDs appears risky owing to their toxic effects on multiple organs, with the GI tract being the most severely affected (Bindu et al., 2020; Sostres et al., 2013). Therefore, precise knowledge about the subcellular target(s) of NSAIDs is crucial for optimizing their clinical usage while rationally avoiding their toxicity. NSAIDs are standard **cyclooxygenase 1/2** (COX1/2) inhibitors (Bindu et al., 2020; Whittle, 2000), although COX-independent effects are equally shown (Gurpinar et al., 2013; Gurpinar et al., 2014; Kolawole & Kashfi, 2022; Liggett et al., 2014). In this regard, mitochondrial oxidative stress (MOS) and intrinsic apoptosis constitute the major COX-independent NSAID actions, accounting for gut mucosal injury (Matsui et al., 2011). NSAIDs directly target mitochondria to jeopardize mitochondrial metabolism (Aminzadeh-Gohari et al., 2020; Bindu et al., 2020; Krause et al., 2003; Mazumder et al., 2022; Sandoval-Acuna et al., 2012; Suzuki et al., 2010). Therefore, it is logical that endogenous cytoprotective factors would promptly respond to combat the stress.

Mitochondrial antioxidants such as superoxide dismutase (SOD2) and the base excision repair enzyme, **8-oxoguanine DNA glycosylase 1 (OGG1)**, as well as mitochondrial electron transport chain (ETC) complex proteins and mitochondria-resident key enzymes in metabolic pathways, are regulated by deacetylation (Mazumder et al., 2020; Murugasamy et al., 2022; Zhang et al., 2020). Moreover, mitochondrial structural dynamics regulating outer membrane fusion GTPase, optic atrophy 1 (OPA1) and the master regulator of mitochondrial biogenesis, **PPAR-γ coactivator 1α (PGC1α)** are also stabilized by deacetylation. Such deacetylation is carried out by the NAD^+-dependent class III histone deacetylase **sirtuin-3 (Sirt3)**, functioning as a gatekeeper of mitochondrial integrity against stress (H. S. Kim et al., 2010; Mazumder et al., 2020). Thus, in Sirt3 knockout (KO) mice, there is a marked increase in acetylated mitochondrial proteins (Murugasamy et al., 2022). Further, Sirt3 depletion has been observed in several organ pathologies (Mao et al., 2022; Morigi et al., 2015; Pillai et al., 2015; Sun et al., 2020). However, there is no report about any involvement of Sirt3 in NSAID-induced GI pathology or whether Sirt3 can be targeted as a possible gastroprotective strategy.

We therefore used an unbiased forward approach of target mining by next-generation sequencing of the gastric transcriptome in NSAID-treated rats. Interestingly, Sirt3 appeared as a prominent lead, and specific stimulation of Sirt3, by the phyto-polyphenol **honokiol** clearly prevented NSAID-induced mitochondrial damage and gastropathy without affecting basal gastric acid secretion, unlike existing anti-ulcer compounds. We compared the efficacy of intraperitoneal (i.p.) with that of intragastric (i.g.) administration of honokiol and found that a much lower dose was sufficient to provide significant

What is already known

- Despite their gastrodamaging side-effects, NSAIDs appear unavoidable owing to their anti-inflammatory effects in diverse pathologies.
- NSAIDs target mitochondria, COX-independently, inducing apoptosis. However, precise sub-mitochondrial target(s) of NSAIDs are not known.

What does this study add

- Sirt3 is a new target of NSAIDs which is down-regulated during development of gastric injury.
- Honokiol-induced Sirt3 stimulation prevents indomethacin-induced mitochondrial pathology and inflammatory gastric injury without affecting acid secretion.

Clinical significance

- Sirt3 is a non-canonical COX-independent target of NSAIDs to induce gastric mucosal injury.
- Sirt3 stimulation represents a promising gastroprotective strategy that may benefit NSAIDs usage bypassing their side-effects.

gastroprotection when administered i.p. Further, we extensively investigated the specific mitoprotective mode of action of honokiol in the gastric mucosa of NSAID-treated rats. Our findings identify Sirt3 as a hitherto unreported, dominant gastroprotective target, while revealing the potency of honokiol as a new generation gastroprotective agent. These findings will certainly provide novel therapeutic insights into NSAID-based treatment modalities, in which targeted stimulation of Sirt3 may help to avoid the toxic effects of NSAIDs, while strategically optimizing the benefits.

2 | METHODS

2.1 | In vivo model of NSAID-induced gastric mucosal damage

All animal care and experimental procedures were carried out with strict adherence to the approved guidelines of ARRIVE and the institutional animal ethics committee, registered with the Committee for the Purpose of Control and Supervision of Experiments on Animals (CPCSEA), India (Permit No. 147/1999/CPCSEA). Utmost care was taken to minimize the pain and suffering of the rats during experimental handling. Animal studies are reported in compliance with the ARRIVE guidelines (Percie du Sert et al., 2020) and with the recommendations made by the *British Journal of Pharmacology* (Lilley et al., 2020).

Sprague–Dawley rats (180–220 g) were provided by the institutional animal facility of CSIR-Indian Institute of Chemical Biology. Animals were maintained at 24 ± 2°C with 12-h light–dark cycles and provided with standard rat chow and ad libitum access to water. Before the experiments, the rats were subjected to fasting for 24 h with free access to water. Rats of either sex were used for all in vivo experiments. However, in any specific experiment, rats from only a single sex have been used.

Gastric mucosal injury was induced by NSAIDs given by oral administration. Indomethacin (48 $mg{\cdot}kg^{-1}$) was dissolved in distilled water supplemented with minimal volumes of alkali (Na_2CO_3), as mentioned previously (Bindu et al., 2013; Mazumder et al., 2019). The pH of the resultant solution was checked before administration. Diclofenac (75 $mg{\cdot}kg^{-1}$) and ibuprofen (400 $mg{\cdot}kg^{-1}$) were obtained as sodium salts and hence dissolved in distilled water; aspirin (400 $mg{\cdot}kg^{-1}$) was administered as suspension in 1% carboxymethylcellulose, as mentioned previously (Ghori et al., 2016; Maharani, 2022; Mazumder et al., 2016; Raghavendran et al., 2011). A separate group of rats (n = 5) were also treated with vehicles (1% carboxymethylcellulose or alkaline water). No detectable gastric mucosal injury was observed. The gastric injury was allowed to develop, and after 4 h, the rats were humanely killed (asphyxiation with >90% CO_2 followed by cervical dislocation) and gastric mucosal samples were collected for subsequent experiments. For the honokiol-induced protection set (HKL + Indo), rats were pre-treated with honokiol i.p. (40 $mg{\cdot}kg^{-1}$), followed by oral administration of indomethacin after 30 min. For i.p. administration, honokiol was dissolved in peanut oil and injected as described previously (Pillai et al., 2015). The ED_{50} of honokiol was derived from a dose–response study ranging from 5 to 60 $mg{\cdot}kg^{-1}$. A separate group of rats (n = 5) were also treated with the vehicle (peanut oil) followed by oral administration of indomethacin. No detectable protection was observed in the vehicle-treated group, and the extent of mucosal injury was comparable with that after indomethacin treatment. Honokiol, at different doses (20, 40, 60 and 80 $mg{\cdot}kg^{-1}$ bw), was also given i.g. in a separate group of rats 30 min prior to indomethacin administration as mentioned above, to compare the efficacy of i.p. with that of i.g. administration. For i.g. administration, honokiol was suspended in a solution of carboxymethylcellulose sodium salt (0.5%), as described previously (Wang, Zhai, & Chen, 2018). Gastric injury was allowed to develop. After 4 h, the rats were humanely killed and the gastric mucosa examined to determine the injury index (II) scores and comparison of efficacy between ip and ig administration of honokiol. A separate group of rats (n = 5) were treated i.g. with 0.5% carboxymethylcellulose solution followed by oral administration of indomethacin. No detectable protection was observed in the vehicle-treated group.

For gastric mucosal wound healing studies, 2 sets of rats (20 rats per set) were treated with indomethacin and mucosal injury was allowed to develop for 4 h. After 4 h, 1 set of rats (n = 20) was treated once with honokiol and samples were collected, after humane killing, at different time points, namely, 0, 8, 12 and 20 h following honokiol injection. Thus, 0 h of healing corresponds to 4 h of indomethacin treatment when the injury is at the peak. A parallel set of rats (n = 20) were treated with the vehicle (instead of honokiol) and maintained in the same way to compare the efficacy of honokiol-induced healing and spontaneous healing. Vehicle-treated rats were also used for sample collection at identical time points to that of honokiol-treated rats. In every group, the number of rats was maintained at n = 5.

Scores of mucosal injury (II) were generated by an individual unaware of the treatment condition, to avoid bias. The II was calculated as the percentage of the injured area in the stomach formed by bleeding lesions, blood clots and visible hyperaemia. Mean II was calculated as the sum of the total scores in each group of rats divided by the number of rats in that respective group. Tissue samples for next-generation sequencing and PCR-based gene expression profiling were preserved by storing in RNAlater (Cat# R0901, Sigma-Aldrich), whereas tissues for protein expression profiling were snap-frozen and stored until further use. For mitochondrial preparation, tissue samples were subjected to subcellular fractionation using a commercially available mitochondria isolation kit, as described below.

2.2 | Histological study of gastric mucosa

Semi-thin (5 μm) sections were prepared from buffered formalin-fixed and paraffin-embedded gastric mucosal tissues. The semi-thin sections were collected on a glass slide, deparaffinized and passed through

graded solutions of ethanol for double staining with haematoxylin and eosin. The stained sections were examined under a microscope (Leica DM-2500, Leica Microsystems, Wetzlar, Germany).

2.3 | Next-generation sequencing-based transcriptomics

Total RNA sequencing library preparations were generated, using TruSeq Stranded Total RNA Library preparation kit from Illumina. Briefly, total RNA was isolated from the tissue or cell samples using PureLink RNA Mini Kit (Thermo Fisher Scientific) following the manufacturer's guidelines. The starting material was 45 mg of tissue. The quality and concentration of the isolated RNA samples were checked in Nanodrop 2000 (Thermo Fisher Scientific) and Agilent 2100 Bioanalyzer. Samples with RNA integrity number (RIN) ≥ 7.0 were subsequently used for library preparation. An equal amount (200 ng) of RNA from each sample was first subjected to ribosomal RNA depletion using the Ribo-Zero Human/Mouse/Rat depletion module of the kit followed by purification and divalent cation-based fragmentation. The resulting fragments were purified and subjected to cDNA synthesis, A-tailing and dual index adapter ligation. The products were subsequently purified and PCR enriched. The resulting RNA libraries were checked in Agilent 2200 TapeStation (Agilent Technologies), quantified, normalized and subjected to equimolar pooling. The pooled libraries were finally loaded on a sequencing run flow cell (Illumina) and subjected to 100-bp paired-end massively parallel sequencing in NovaSeq 6000 sequencer (Illumina). Resulting Bcl files were converted to Fastq files and the data were subjected to a quality check using FastQC v0.11.7 (Andrews, 2010). This was followed by adapter trimming with Cutadapt v1.16 (Martin, 2011) using Illumina Universal Adapter. Hisat2 v2.1.0 (Pertea et al., 2016) was used to align the trimmed reads with Rat Rno6 reference genome (for rat samples). Sorting of Bam files was performed with SAMtools v1.19 (H. Li et al., 2009) Next, gene count was performed with FeatureCounts (Liao et al., 2014) followed by differential analysis using DESeq2 (Love et al., 2014). Differentially expressed genes (DEGs) with ≥1.5- or ≤1.5-fold expression change and *P* value ≤ 0.05 and false discovery rate (FDR) ≤ 0.05 were filtered. Finally, gene-enrichment and pathway analyses were performed with IPA (Ingenuity Pathway Analysis) software. For rat gastric mucosal samples, data were also filtered with ≥1.2- or ≤1.2-fold expression change and *P* value ≤ 0.05 and FDR cut-off ≤ 0.05 to include genes regulating mitochondrial metabolism and functions. The Gene Expression Omnibus (GEO) accession number for rat transcriptomic data is GSE201565.

2.4 | Isolation of mitochondria

Mitochondria were isolated from tissue samples using the Mitochondria Isolation Kit (Cat# KC010100, purchased from BioChain) following the manufacturer's guidelines. Mitochondrial isolation used here, in principle, depends on two-step differential centrifugations. The tissue after mechanical disruption (in hypotonic lysis buffer supplemented with protease inhibitors) by homogenization is subjected to low-speed centrifugation for removal of precipitated debris, unfragmented cells and large cellular organelles. Subsequently, high-speed centrifugation of the supernatant (of the first step) is performed to isolate viable and enzymatically active mitochondria. A pure mitochondrial fraction is obtained by repeated washing of the final pellet. In the present study, an equal amount of gastric mucosal tissues (200 mg) from each experimental set was subjected to mitochondria isolation. Mild homogenization of the samples was carried out with a Dounce homogenizer, on ice. Nuclei and cell debris were removed by centrifugation at 600 x g for 10 min and the supernatant was collected, which was further centrifuged at 12,000 x g for 15 min to obtain the mitochondrial fraction. The mitochondrial pellets were washed three times in mitochondria isolation buffer, and the resultant pellets (approximately 99% pure) were either used for respiratory chain complex and dehydrogenase assays or lysed for immunoblotting, as described earlier (Mazumder et al., 2019).

2.5 | Immunoblot analysis

For immunoblot analysis, total protein was extracted from gastric mucosal tissues by homogenization of samples in pre-chilled mammalian cell lysis buffer (supplemented with protease and phosphatase inhibitors), as described previously (Mazumder et al., 2019). Mitochondrial extracts were prepared by subcellular fractionation of tissue samples as mentioned above. For analysis of mitochondrial protein acetylation, mitochondria isolation and lysis buffers were supplemented with nicotinamide (50 mM) and trichostatin A (10 μM). Protein was quantified by Lowry's method, and an equal amount of protein was loaded in each well of the 10% polyacrylamide–SDS gels and subjected to electrophoresis followed by wet transfer-based immunoblotting using nitrocellulose membrane. Blots were blocked in 5% skimmed milk or 5% BSA solution followed by incubation in primary antibodies (Table S1) overnight as per the manufacturer's guidelines. The blots were washed in Tris-buffered saline (TBS) solution supplemented with 0.1% Tween 20 and subsequently incubated in HRP-conjugated secondary antibody for 2 h at room temperature. The blots were finally washed in TBS solution supplemented with 0.1% Tween 20, and immuno-reactive bands were developed in Bio-Rad ChemiDoc system. Actin and TOM20 were used as the loading controls for total protein and mitochondrial protein, respectively. Densitometric analyses were carried out using ImageJ software, and data are represented as fold change (FC) relative to control. The experimental procedures provided here conform with the *BJP* guidelines (Alexander et al., 2018).

2.6 | Analysis of mitochondrial transmembrane potential (ΔΨm)

ΔΨm was measured using JC-1. In principle, JC-1 is a cationic lipophilic dye (naturally showing green fluorescence) that enters

mitochondria, accumulates there in a concentration-dependent manner and starts forming reversible complexes, known as J aggregates (exhibiting excitation and emission in the red spectrum, maximum at ~590 nm). Thus, in a healthy cells with mitochondria having normal ΔΨm, JC-1 enters in mitochondria (negatively charged) and accumulates there forming red fluorescent J aggregates. On the contrary, in unhealthy cells or mitochondria, the JC-1 entry is greatly reduced owing to the loss of mitochondrial transmembrane electrochemical potential, which renders the mitochondrial inner membrane less negative. Under this condition, JC-1 fails to reach its threshold level for the formation of J aggregates, resulting in the maintenance of its monomeric, green fluorescent state. In the present study, ΔΨm was measured in the mitochondria isolated from control and treated stomachs, using a F-7000 Fluorescence Spectrophotometer (Hitachi High-Technologies Corporation). Equal amounts of mucosal tissue from each sample were used for mitochondria isolation followed by protein estimation to use equal amounts of mitochondria for ΔΨm analysis. Mitochondria were incubated in darkness for 15 min in 500 μl of ATP-supplemented JC-1 assay buffer containing 300 nM of JC-1. A single-excitation–dual-emission format was used for analysing JC-1 monomers and aggregates at 530 and 590 nm, respectively. ΔΨm was expressed as fluorescence ratio of 590 nm/530 nm, as described previously (Mazumder et al., 2019).

2.7 | Measurement of ATP content

ATP content of gastric mucosal tissue was measured to follow the bioenergetic state of the mucosal cells upon treatment with indomethacin. Because tissue ATP production is mostly attributed to functional mitochondria with integrity, depletion in ATP would reflect mitochondrial dysfunction and resultant bioenergetic deficit of the affected tissue. ATP determination kit (A22066; Thermo Fisher Scientific) was used to measure gastric mucosal ATP level in control and treated rats by following the manufacturer's instructions. This is a bioluminescence-based assay kit and it contains recombinant firefly luciferase and its substrate D-luciferin. The principle of the assay is based upon the ATP requirement of luciferase enzyme for the production of the light (emission maximum of ~560 nm at pH 7.8). The greater the amount of ATP present in the tissue extract, the greater the amount of light emitted from the reaction, as follows.

$$\text{Luciferin} + \text{ATP} + \text{O}_2 \xrightarrow{\text{Mg}^{2+}\text{ and luciferase}} \text{Oxyluciferin} + \text{AMP} + \text{Pyrophosphate} + \text{CO}_2 + \text{Light}$$

Briefly, an equal amount of tissue (50 mg) from each sample was minced and lysed in 5% sulfosalicylic acid solution (for sample deproteinization). The lysates were centrifuged at 12,000 x g and the supernatants were used for ATP measurement in a luminometer (BioTek). The values were normalized by protein concentrations of the respective samples, as described previously (De et al., 2017; Mazumder et al., 2016).

2.8 | RNA isolation and quantitative real-time PCR (qRT-PCR)

Total RNA was isolated by using TRIzol (Thermo Fisher Scientific), following the manufacturer's protocol, and estimated using Maestrogen Spectrophotometer (MaestroGen Inc., Taiwan). The obtained total RNA (2 μg) was reverse transcribed with oligo-dT18 primer using RevertAid H Minus First Strand cDNA Synthesis Kit (Thermo Fisher Scientific) followed by rDNAse treatment. The resultant cDNAs were used for qPCR after proper dilution by using primers (Table S2) obtained from Integrated DNA Technologies Inc. (San Diego, CA, USA). The Roche LightCycler 96 qPCR system was used for performing the qPCR by using SYBR green mastermix (Roche) in following the as-mentioned cycle conditions: initial denaturation temperature at 95°C/10 min followed by 40 cycles of denaturation at 95°C/15 s, annealing (at indicated annealing temperatures; Table S2) for 30 s and extension at 72°C/25 s. Relative gene expression was calculated using $2^{-\Delta\Delta Cq}$ method and the data were represented as FC relative to control, as described previously (De et al., 2017; Dey et al., 2014; Mazumder et al., 2019). *Gapdh* was used as the internal control.

2.9 | Determination of Sirt3 deacetylase activity

Sirt3 fluorometric activity assay kit (Abcam, ab156067) was used to measure deacetylase activity of Sirt3, with or without indomethacin. The experiment was performed as per the manufacturer's protocol. Briefly, in presence of increasing concentrations of indomethacin (100–500 μM), the activity of purified human recombinant Sirt3 was assessed, taking the kinetic measurement at 2-min intervals till 45 min, in a BioTek Synergy H1 Hybrid Multi-Mode Reader with excitation at 350 nm and emission at 450 nm.

2.10 | Mitochondrial dehydrogenase assay

Mitochondrial metabolic integrity in tissue samples was measured by analysing mitochondrial dehydrogenase activity, which can reduce MTT into a purple-coloured formazan that can be solubilized and quantified spectrophotometrically at 570 nm. An equal amount of gastric tissue (200 mg) from different experimental sets was used for mitochondria isolation, and the resultant fractions were incubated in MTT solution (1 mg·ml^{-1} in PBS) for 3.5 h at 37°C/5% CO_2. Samples were centrifuged and pellets were solubilized in equal volumes of anhydrous DMSO. The absorbance of the purple solution was measured spectrophotometrically at 570 nm, as described previously (De et al., 2017; Mazumder et al., 2019). Mitochondrial protein from every fraction was estimated and used for normalization of the ODs corresponding to the respective samples.

2.11 | Isolation of mtDNA and measurement of 8-oxo-7,8-dihydro-2′-deoxyguanosine by ELISA

DNA from the isolated mitochondrial pellets was extracted by the phenol-chloroform method. Briefly, the mitochondrial pellet was resuspended in 100 µl of Proteinase K-supplemented lysis buffer and incubated at 50°C for 3 h, following which 200 µl of phenol-chloroform was added and mixed thoroughly. The contents were centrifuged at 11,000 x g for 10 minutes at 25^{0}C to separate the phases. The aqueous phase was collected and 200 µl of 7.5-M ammonium acetate and 500 µl of ethanol were added. The tubes were kept at −20°C for 2 h. The samples were next centrifuged at 10,000 x g for 30 min. The pellets were washed with 500 µl of 70% ethanol and, finally, the DNA pellets were dissolved in 30 µl of Tris-EDTA buffer. The mtDNA was spectrophotometrically estimated. An equal amount of mtDNA from each experimental set was then taken for assay of OGG1 activity, by measuring levels of 8-oxo-7,8-dihydro-2′-deoxyguanosine (8-oxo- dG) with a commercially available HT 8-oxo-dG ELISA Kit II from Trevigen, as described by Bindu et al. (2017).

2.12 | Confocal immunohistochemical analysis

The accumulation of 8-oxo-dG content in gastric mucosal tissue of Con, Indo and HKL + Indo rats was followed by confocal fluorescent immunohistochemical analyses. Formalin-fixed and paraffinized tissue sections were deparaffinized, rehydrated and subjected to antigen retrieval by heating in sodium citrate buffer. Next, the tissue sections were blocked with 10% goat serum and 1% BSA in TBS for 2 h. The tissue sections were incubated overnight in primary antibody solution containing 8-oxo-dG (anti-DNA/RNA damage antibody) (Table S1). The slides were washed and incubated in Alexa Fluor 647-tagged anti-mouse secondary antibody. The slides were again washed. 4′,6-Diamidino-2-phenylindole (DAPI) was used for nuclear staining. The washed slides were mounted in 30% glycerol in PBS and observed under a microscope. Confocal images were taken in the Leica TCS-SP8 confocal microscope (Leica Microsystems, Wetzlar, Germany) using Leica Application Suite X (LAS X) software. All experiments were repeated three times and the confocal images presented are randomly picked up portions of the gastric mucosal sections. Image cropping and global adjustments for brightness/contrast were done in Adobe Photoshop and assembled in CorelDraw X7, as mentioned previously (De et al., 2017; Mazumder et al., 2019). The experimental procedure provided herein duly conforms with the *BJP* guidelines (Alexander et al., 2018).

2.13 | Detection of mitochondrial superoxide anion ($O_2^{\bullet -}$)

MitoSox staining was used to detect the presence of mitochondrial $O_2^{\bullet -}$ in isolated gastric mucosal cells, as described by De et al., (2017). Briefly, gastric mucosal scrapings were washed in pre-warmed Hanks Balanced Salt Solution (HBSS) and incubated in a pre-aerated solution containing 100 units·ml^{-1} penicillin and 100 µg·ml^{-1} streptomycin supplemented with 0.05% hyaluronidase and 0.1% collagenase for 80 min, with shaking, at 37°C/5% CO_2. The cell suspension was aseptically filtered using 50-µm cell strainers. The filtered cells were washed thrice in pre-warmed HBSS and resuspended in PBS. The cells were next checked for viability (using the Trypan blue exclusion method). Viable cells were counted and 10^6 cells from each set were incubated with MitoSox Red (Thermo Fisher Scientific) at 37°C for 30 min. Next, the cells were washed three times and analysed by flow cytometry in FACS, LSRFortessa, BD. Data were analysed in FACS DIVA software under standard parameters; 10^4 cells were evaluated per set and experiments were repeated three times.

2.14 | Assay of mitochondrial ETC complex I and III activities

Mitochondrial ETC complex I (NADH:ubiquinone oxidoreductase) and complex III (decylubiquinol cytochrome c oxidoreductase) activities were spectrophotometrically quantified through the rate of oxidation of NADH (measured as change in $OD_{340\ nm}$) and reduction of cytochrome c (measured as change in $OD_{550\ nm}$), as described elsewhere (Carrasco-Pozo et al., 2011; Spinazzi et al., 2012). Briefly, an equal amount of isolated mitochondria (15 µg of protein) was lysed in a hypotonic buffer before using for enzymatic assays. For complex I assay, NADH and ubiquinone were used as substrates. Specific complex I activity was derived by estimating the rotenone-sensitive NADH–ubiquinone oxidoreductase action of the mitochondrial extract from control and treated samples. For the complex III assay, oxidized cytochrome c and ubiquinol were used as substrates. The specific complex III activity was derived by estimating the antimycin A-sensitive decylubiquinol cytochrome c oxidoreductase action of the mitochondrial extract. In either case, the rate of enzymatic activity was recorded for 2 min.

2.15 | Measurement of gastric luminal pH

Rats were fasted for 24 h with free access to water. On the day of the experiment, rats were injected with **lansoprazole** (20 mg·kg^{-1}, i.p.) or honokiol (40 mg·kg^{-1}, i.p.) 30 min prior to administration of 2-mercapto-1-methylimidazole (MMI) (40 mg·kg^{-1}, i.p.), as described previously (Mazumder et al., 2016). This set was indicated as 'stimulated' because MMI stimulates acid secretion. The second set of starved rats was treated with lansoprazole or honokiol without MMI injection. This set was denoted as 'unstimulated (basal)'. At 4 h after treatment, rats were humanely killed, the abdomen opened and the oesophageal and pyloric ends of the stomach were tied with a thread to prevent the escape of gastric secretions. A small incision was made at the cardiac end of the stomach and the contents were flushed with 2 ml of 0.9% saline and the clear supernatant was collected after centrifugation (5000 x *g* for 10 minutes at 25^{0}C).

The pH of the fluid was then measured with a hand-held pH meter.

2.16 | Data and statistical analysis

The data and statistical analysis comply with the recommendations of the *British Journal of Pharmacology* on experimental design and analysis, and experiments have been designed to generate groups of equal size, using randomization and blinded analysis (Curtis et al., 2022). All animal studies were done with randomly segregated rats. For every set, the animal number was maintained at 5 ($n = 5$), as standardized and reported previously (Bindu et al., 2013; Mazumder et al., 2016; Mazumder et al., 2019). The in vitro experiments were done in triplicate. All experiments were repeated at least three times. Experimental data are shown as means ± SD. When comparing two experimental groups, unpaired *t* test (with Welch's correction) was done to calculate the level of significance, whereas one-way analysis of variance (ANOVA) followed by Bonferroni's multiple-comparison test was done for comparing more than two groups. For all data, P value < 0.05 was considered statistically significant. The group size mentioned here is the number of independent values, and that statistical analysis was done using these independent values. Statistical analysis of data was done using GraphPad Prism 8 and Microsoft Office Excel 2019 software.

2.17 | Materials

Indomethacin (Cat# I7378), **ibuprofen** (Cat# I1892), **diclofenac** (Cat# D6899), **aspirin** (Cat# A5376), honokiol (Cat# 384620), 2-mercapto-1-methylimidazole (MMI, Cat#301507), lansoprazole (Cat# L8533), RNase ZAP 3-(4,5-dimethylthiazol-2-yl)-2,5-diphenyltetrazolium bromide (MTT) (Cat# CT01-5), carboxymethylcellulose sodium salt (Cat# C5678), bovine serum albumin (BSA) (Cat# A7906) and DMSO were procured from Sigma (St. Louis, MO, USA). TRIzol (Cat# 15596026), PureLink RNA Mini Kit (Cat# 12183018A), RevertAid H Minus First Strand cDNA Synthesis Kit (Cat# 18091050), ATP Determination Kit (Cat# A22066), PowerUp™ SYBR™ Green Master Mix (Cat# A25742), 5,5′,6,6′-tetrachloro-1,1′,3,3′-tetraethylbenzimi-dazoylcarbocyanineiodide (JC-1) dye (Cat# T3168), MitoSOX™ mitochondrial superoxide indicator (Cat# M36008), nuclease-free water (Cat# AM9937), Hoechst 33342 (Cat# H3570) and phosphate-buffered saline (PBS) (Cat# 10010031) were purchased from Thermo Fisher Scientific (Waltham, MA USA). Mitochondria Isolation Kit (Cat# KC010100) was purchased from BioChain (Newark, CA, USA). HT 8-oxo-dG enzyme-linked immunosorbent assay (ELISA) Kit II (Cat# 4380-096-K) was procured from Trevigen (Bio-Techne, Minneapolis, USA). Luminata Forte Western horseradish peroxidase (HRP) substrate (Cat# WBLUF0500) for electrochemiluminescence (ECL)-based chemiluminescence was procured from Merck Millipore (Burlington, MA, USA). Sirt3 activity assay kit (Fluorometric) (Cat# ab156067) and Mitochondrial DNA (mtDNA) Isolation Kit (Cat# ab65321) were purchased from Abcam (Boston, MA, USA). BioTrace NT nitrocellulose transfer membrane (Cat# 66485) was procured from Pall Corporation (Port Washington, NY, USA). Blotting-Grade Blocker (Cat# 1706404) was procured from Bio-Rad Laboratories, Inc. (Hercules, CA, USA). All other reagents were of analytical grade purity.

2.18 | Nomenclature of targets and ligands

Key protein targets and ligands in this article are hyperlinked to corresponding entries in http://www.guidetopharmacology.org and are permanently archived in the Concise Guide to PHARMACOLOGY 2021/2022 (Alexander, Cidlowski et al., 2021; Alexander, Fabbro, Kelly, Mathie, Peters, Veale, Armstrong, Faccenda, Harding, Pawson, Southan, Davies, Beuve et al., 2021; Alexander, Fabbro, Kelly, Mathie, Peters, Veale, Armstrong, Faccenda, Harding, Pawson, Southan, Davies, Boison et al., 2021; Alexander, Kelly et al., 2021).

3 | RESULTS

3.1 | Transcriptome analysis revealed the association of Sirt3 in NSAID-induced gastric mucosal injury

As the stomach is the organ most severely affected by the toxic effects of NSAIDs, we undertook high-depth transcriptome sequencing of control and indomethacin-treated rat gastric mucosa to comprehensively explore the alterations in gene expression, during gastropathy. Indomethacin was used as a prototype COX non-selective NSAID. Tissues for transcriptome sequencing were collected from control and indomethacin-treated samples with high-grade mucosal injury (Figure 1a). Heat map analysis revealed the DEG set with 885 up-regulated and 211 down-regulated genes in 'indomethacin' compared with 'control' when filtered with log FC cut-off of 1.5, P value ≤ 0.05 and FDR ≤ 0.05 (Figure 1b and File S1a–c) (GSE201565). Gene-enrichment analysis using 'ingenuity pathway analysis' revealed the prominent pathways and 'disease and function' involved in indomethacin-induced gastric cytotoxicity (Figure 1c,d). 'Apoptosis and death receptor signalling', 'TNFR signalling', 'p38 MAPK signalling', 'interferon signalling', 'granulocyte and agranulocyte adhesion and diapedesis', 'acute phase signalling' and 'NRF2-mediated oxidative stress response' appeared as prominently highlighted pathways (Figure 1c), whereas 'gastroenteritis', 'synthesis, production and metabolism of reactive oxygen species', 'cell cycle progression', 'apoptosis', 'bleeding', 'inflammation of gastrointestinal tract', 'inflammatory bowel disease', 'fibrosis', 'colitis' and 'phagocyte and macrophage activation' appeared as predominant class of 'disease and function', significantly contributing to the DEG counts (Figure 1d). Because mitochondria are associated with a wide array of pathways and functions identified in the transcriptome data, we checked **caspase 9** and **caspase 3**, as well as cytochrome c, as terminal markers of intrinsic apoptosis due to mitochondrial dysfunction. We also measured $\Delta\Psi m$ and ATP content. Data indicated significant

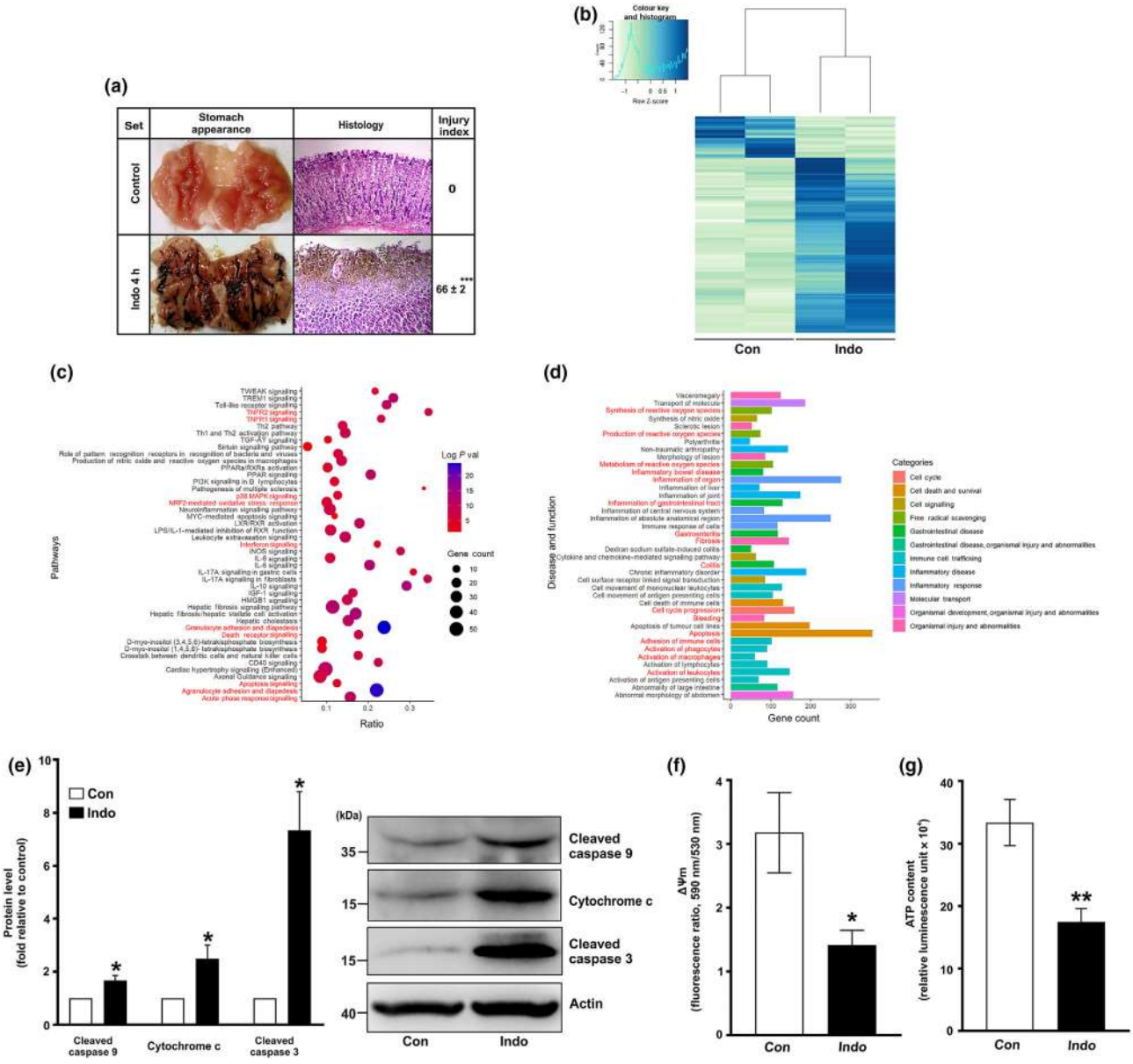

FIGURE 1 Indomethacin induces transcriptome alteration, intrinsic apoptosis and mitochondrial dysfunction in gastric mucosa. (a) Gastric mucosal morphology and haematoxylin/eosin-stained histology of control (Con) and indomethacin-treated (Indo) rats (n = 5). Representative images are provided. (b) Heatmap shows separate clustering of samples corresponding to control 'Con' and indomethacin 'Indo' (false discovery rate [FDR] ≤ 0.05). Euclidean distance metric was used while clustering the gene expression data of the differentially expressed genes (DEGs). Euclidean distance metric was used while clustering the gene expression data. The expression value of genes analysed with fold change cut-off of 1.5; colour gradient scale with white being highly down-regulated to blue being highly up-regulated. (c) Dot plot showing enriched canonical pathways. The size of dots represents the proportion of genes involved in the particular signalling pathway, whereas the range of colour indicates Bonferroni corrected *P* values (−log transformed). The ratio represents the number of genes in fraction with respect to the total number of genes that map to the same pathway. (d) Bar graph showing the disease and functions enriched in the 'indomethacin' set. (e) Immunoblots of cleaved caspase 9, cytochrome c and cleaved caspase 3 in gastric mucosal tissues from control and indomethacin-treated rats (n = 5). Actin was used as the loading control. Representative blots are shown on the right. (f) Mitochondrial transmembrane potential (ΔΨm) in gastric mucosal tissues from control and indomethacin-treated rats (n = 5). (g) ATP content in gastric mucosal tissues from control and indomethacin-treated rats. Indomethacin treatment: 48 mg·kg^{-1} for 4 h. Data (a, e–g) are mean ± SD, n = 5. *P < 0.05, significantly different from control; unpaired Student's *t* test with Welch's correction. The number of independent experiments is 3.

elevation of cleaved caspase 9 and 3 as well as cytochrome c along with drastic mitochondrial depolarization and ATP depletion in the indomethacin-treated tissues (Figure 1e–g).

As immunoblotting indicated mitochondrial dysfunction, we delved deeper into the transcriptome data to check for crucial genes regulating ETC and mitochondrial metabolism (Figure 2). ETC

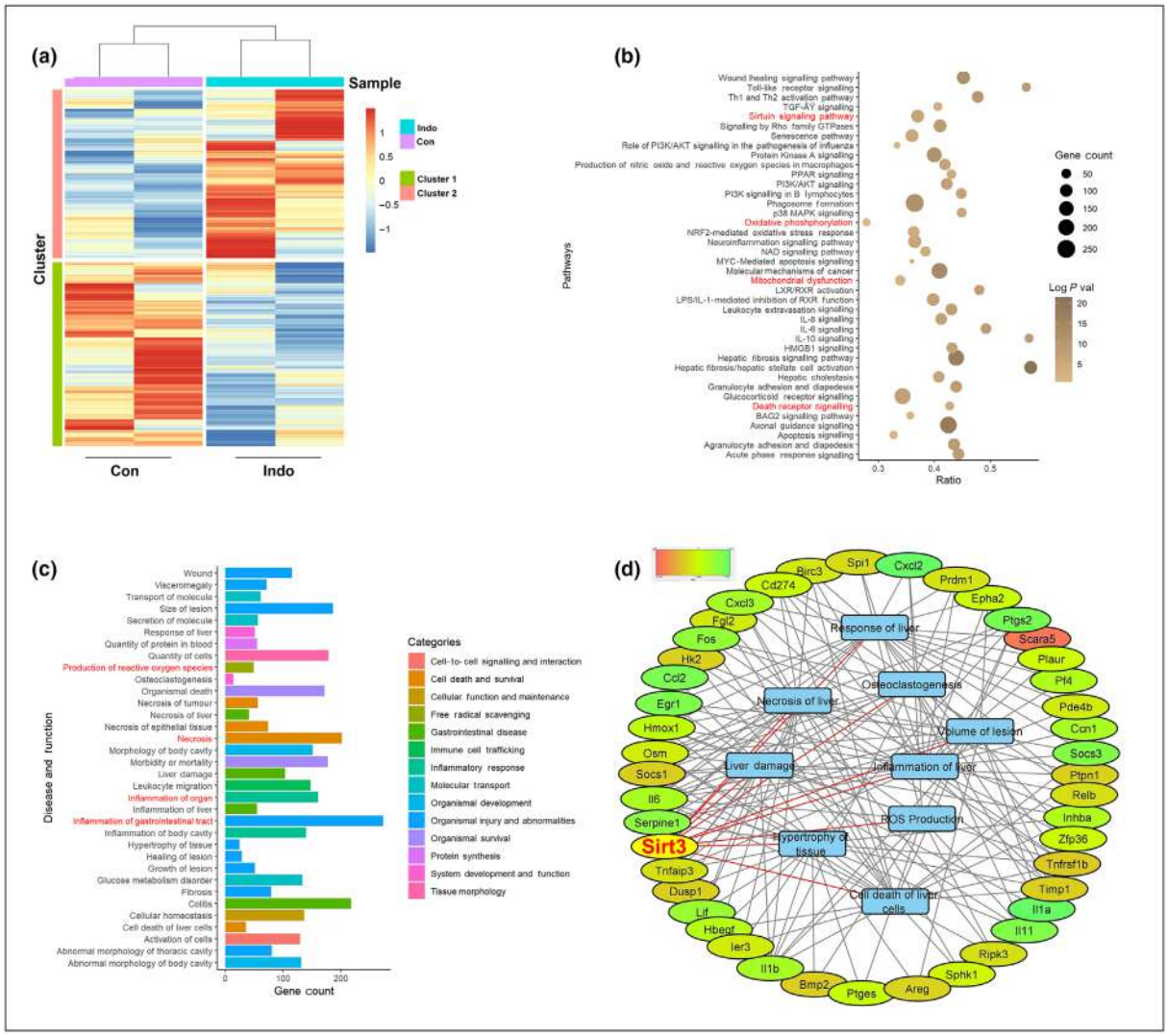

FIGURE 2 Indomethacin alters gene expression programmes that regulate mitochondrial functions and sirtuin signalling. (a) Heatmap shows separate clustering of samples corresponding to control (Con) and indomethacin –treated (Indo) rats. Euclidean distance metric was used while clustering the gene expression data of the differentially expressed genes (DEGs). The expression value of genes analysed with fold change cut-off of 1.2; colour gradient scale with blue being highly down-regulated to red being highly up-regulated. (b) The dot plot shows enriched canonical pathways. The size of dots represents the proportion of genes involved in the particular signalling/pathway, whereas the range of colour indicates Bonferroni corrected *P* values (−log transformed). Ratio represents the number of genes in fraction with respect to the total number of genes that map to the same pathway. (c) The bar graph shows the disease and functions enriched in the indomethacin-treated set. (d) Hub gene network; gene names represented in oval shapes whereas associated functions are represented by rectangular boxes. The expression value of genes represented with colour gradient scale with red being highly down-regulated to green being highly up-regulated. Grey lines indicate the association of genes with associated functions, whereas red lines indicate the association of sirtuin-3 (Sirt3), the hub gene, with respective associated functions.

complex genes however did not show up in the transcriptome data when analysed with an FC cut-off of 1.5, even with evident mito-pathology and ATP depletion in the indomethacin-treated tissues. Therefore, we rationally relaxed the standard FC cut-off (of 1.5) slightly to 1.2 to check for DEGs regulating mitochondrial functions (Figure 2a and File S1d). Interestingly, 'mitochondrial dysfunction' and 'oxidative phosphorylation' were significantly reflected as important pathways (Figure 2b and File S1e). ETC complex-related gene expression was severely compromised along with elevation of proapoptotic and down-regulation of antioxidant and anti-apoptotic markers (File S1e). Functional enrichment analysis revealed the association of 272 DEGs with GI inflammation, 160 DEGs with organ inflammation, 147 DEGs with leukocyte migration, 74 DEGs with epithelial tissue necrosis and 49 DEGs with reactive oxygen species (ROS) production (File S1e). Interestingly, the 'sirtuin signalling pathway' was highlighted with Sirt3, turning out as a common gene associated with several categories of disease and functions including 'gastrointestinal disease', 'free radical scavenging', 'inflammatory response', 'cell death and survival', 'cellular function and maintenance', 'cell-to-cell signalling and interaction', 'molecular

transport', 'protein synthesis', 'tissue morphology', 'organismal development' and 'injury and abnormalities' (Figure 2c and File S1f). We subsequently used Molecular Complex Detection (MCODE) (Bader & Hogue, 2003) plugin in Cytoscape (Shannon et al., 2003) to build the gene interaction network and screened the hub gene(s) regulating mitochondrial metabolism and cellular integrity. *Sirt3* appeared as a top hub gene controlling myriad signalling processes, regulating mitochondrial metabolism and cellular integrity (Figure 2d). Because there are no reports linking Sirt3 with NSAID-induced bioenergetic crisis and gastric injury, we explored the functional correlation of this protein in NSAID-induced gastric injury in our model.

3.2 | NSAID impairs Sirt3 expression, thereby inducing gastric mucosal cell injury, and inhibits deacetylase activity of purified Sirt3

Sirt3 down-regulation directed us to follow its mechanistic aspects. Validation of the transcriptome data by qRT-PCR and immunoblotting revealed significant depletion of Sirt3 during maximum tissue injury (Figure 3a,b). Functional relevance of Sirt3 was evident from depletion of OGG1 in the injured mucosa (Figure 3b). To understand the pattern of Sirt3 expression in the course of injury induction followed by spontaneous resolution, we checked the kinetics of Sirt3 expression. Both Sirt3 and OGG1 followed a concerted temporal depletion with the progression of mucosal damage from 0 to 4 h of indomethacin treatment followed by gradual restoration by 72 h when the lesions spontaneously healed, as evident from tissue restitution (Figure 3c,d). To check whether indomethacin has any direct effect on the deacetylase activity of Sirt3, we evaluated the deacetylase activity of Sirt3 in presence of increasing concentration of indomethacin. Data indicated that indomethacin dose-dependently inhibited the deacetylase activity of purified Sirt3 (Figure 3e). In addition, we observed that indomethacin treatment significantly elevated mitochondrial proteome acetylation (Figure 3f) along with profound 8-oxo-dG accumulation in mtDNA, implying oxidative damage to mtDNA (Figure 3g). Even in the transcriptome sequencing data, it was clear that several Sirt3 targets, including *Ogg1*, *Xrcc6*, *Pdha1*, *Aco1*, *Idh1*, *Sdhb*, *Mdh1*, *Ndufa9*, *Glud1* and *Acadl* exhibited prominent down-regulation (File S1d). Further, we observed a concurrent reduction in mitochondrial dehydrogenase activity (Figure 3h) and elevation of mitochondrial proteome ubiquitination (Figure 3i), suggesting mitochondrial dysfunction due to Sirt3 depletion followed by increased clearance of damaged mitochondria.

So far, we documented how Sirt3 deficiency could account for indomethacin-induced mitopathology and cell death. But how did the NSAID actually cause Sirt3 down-regulation? As indomethacin depleted Sirt3 gene expression, we asked whether indomethacin targets any upstream transcriptional regulator/s. Surprisingly, we found significant depletion of both PGC1α and the **oestrogen-related receptor α (ERRα)** in the injured mucosa, thereby revealing the basis of transcriptional depletion of Sirt3 (Figure 3j).

3.3 | Sirt3 induction by honokiol prevents NSAID-induced transcriptome alteration and mitochondrial pathology to avert mucosal cell death and attenuate gastric mucosal injury

We next asked whether Sirt3 stimulation can prevent NSAID-induced gastric cell death and mucosal injury. Rats were pre-treated with honokiol, a specific pharmacological Sirt3 inducer (Pillai et al., 2015), given i.p.. The dose–response study indicated 40 $mg{\cdot}kg^{-1}$ as the optimum gastroprotective dose, against indomethacin, with an ED_{50} of 12.32 $mg{\cdot}kg^{-1}$ (Figure 4a,b). Following these data, we next asked whether i.g. administration of honokiol would exhibit any gastroprotective effect against indomethacin. This might also reflect any better clinical relevance as such a non-invasive route of administration is certainly more advantageous in terms of drug delivery. To compare the different effects of i.p. and i.g. routes of honokiol administration, four doses of honokiol (20, 40, 60 and 80 $mg{\cdot}kg^{-1}$) were selected, based on the data obtained after i.p. administration. The dose–response study (Figure 4c) clearly indicated that i.g. administration of honokiol at 80 $mg{\cdot}kg^{-1}$ offered gastroprotection, comparable to that after i.p. administration of honokiol at 40 $mg{\cdot}kg^{-1}$. To avoid administration of the higher doses of honokiol to the rats, we opted for the i.p. route in the subsequent experiments.

Next, we checked the gastric transcriptome profiles of honokiol-pre-treated indomethacin-treated (HKL + Indo) rats. Sequencing data revealed that gene expression pattern in HKL + Indo group was largely similar to that in the control group and significantly opposed to the pattern in the Indo only group (Figure 4d–g). DEG analysis (at FC cut-off of 1.5) revealed 417 up-regulated and 815 down-regulated genes in HKL + Indo, compared with Indo, out of which 505 up-regulated and 85 down-regulated genes found in Indo group showed reversed expression relative to those in the HKL + Indo group, suggesting a protective effect of honokiol-induced Sirt3 stimulation (Figure 4e). At FC cut-off of 1.2, 4215 up-regulated and 3176 down-regulated genes in the Indo group showed reversed expression relative to those in the HKL + Indo group (Figure 4f,g). Significant DEGs mostly constituted genes controlling mitochondrial functions and those implicated in gastric injury, inflammatory and apoptotic pathways (File S2a,b). *Hmox1*, *Txnrd1*, *Sod1*, *Mmp13*, *Mmp3*, *Tnf1b*, *Ccl2*, *Cxcl2*, *Icam1*, *Vcam1*, *Hif1a*, *Cxcl3*, *Il6*, *Il1b*, *Il1a*, *Nfkb2*, *Nfkb1*, *Nlrp3*, *Fas*, *Bcl2* and *Tlr9* were prominently observed, thereby indicating that honokiol treatment decreased MOS and inflammation. Notably, the expression of *Sirt3* in the HKL + Indo group was comparable to that in the control group. The protective effect of honokiol against indomethacin was clearly evident from the restoration of Sirt3 expression (Figure 4h,i). Further, we could also show a stimulatory action of honokiol on the expression of tricarboxylic acid (TCA) cycle enzymes, such as like *Aco1* and *Idh1*, which are important targets of Sirt3 (File S2b).

To understand the mechanistic basis of honokiol-dependent Sirt3 stimulation and prevention of NSAID-induced gastropathy, we checked the status of Sirt3 targets and acetylation status of the mitochondrial proteome. We found that honokiol pre-treatment prevented indomethacin-induced OGG1 depletion (Figure 4i) and rescued Sirt3

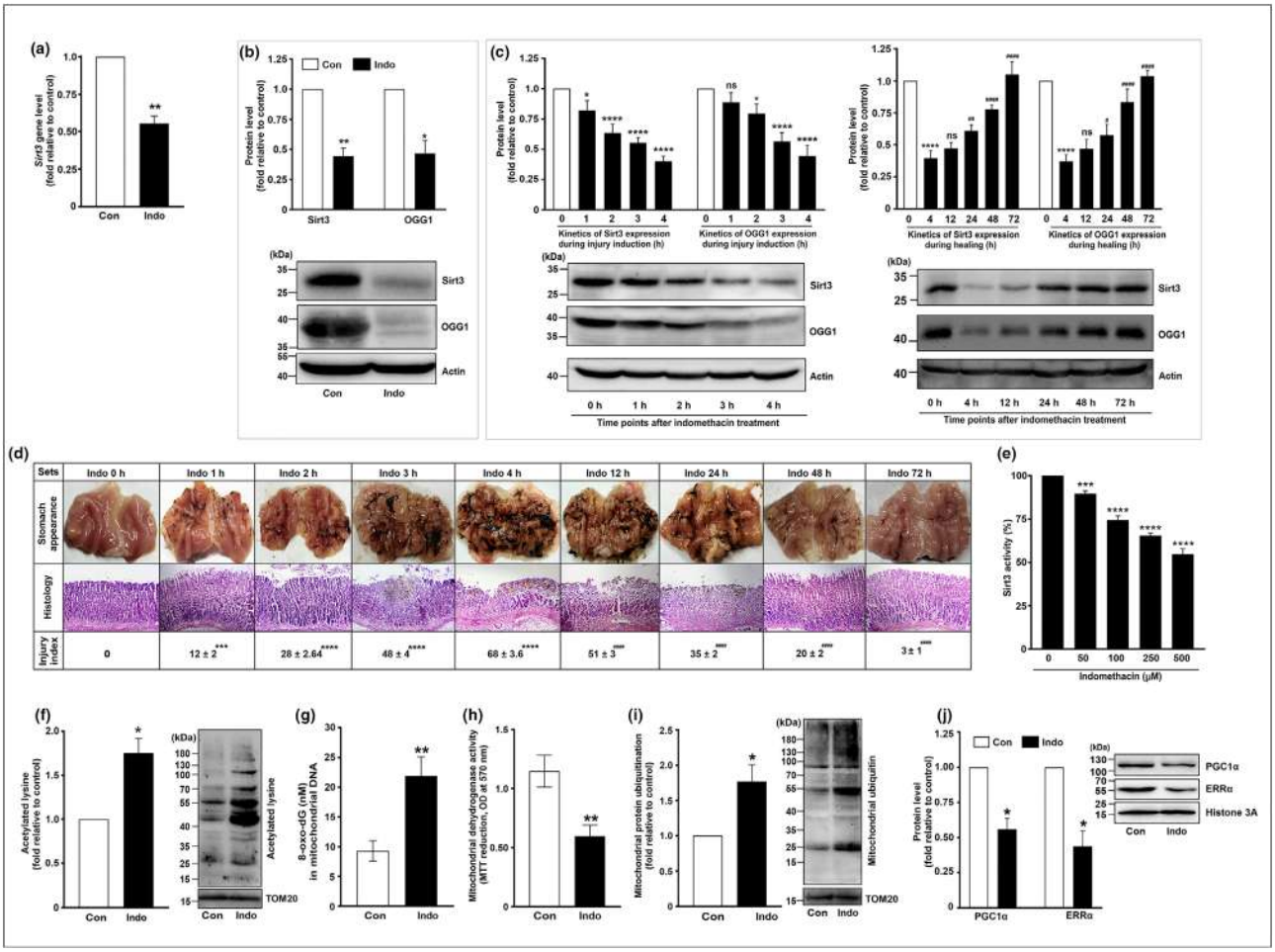

FIGURE 3 Impaired sirtuin-3 (Sirt3) expression and activity are associated with indomethacin-induced gastric mucosal cell damage. (a) *Sirt3* gene expression analysis in gastric mucosal tissues from control (Con) and indomethacin –treated (Indo) rats by qPCR; bar graph indicates fold change in gene expression relative to control (after normalization by *Gapdh*). (b) Immunoblots of Sirt3 and 8-oxoguanine DNA glycosylase 1 (OGG1) in gastric mucosal tissues from control and indomethacin –treated rats. Representative blots are shown below the bar graph. (c) Immunoblots of Sirt3 and OGG1 in indomethacin –treated rats at indicated time points. Representative blots are below the bar graphs. Actin: loading control (b, c). (d) Gastric mucosal morphology and haematoxylin/eosin-stained histology from indomethacin –treated rats (n = 5) at indicated time points; representative images and micrographs are shown. (e) Deacetylase activity of purified Sirt3 measured in presence of increasing concentrations of indomethacin. (f) Immunoblot of acetylated lysine in the mitochondrial fraction of gastric mucosal tissues from control and indomethacin –treated rats. TOM20: loading control. (g) Mitochondrial DNA (mtDNA) damage measured by 8-oxo-dG enzyme-linked immunosorbent assay (ELISA) in gastric mucosal tissues from control and indomethacin –treated rats. (h) Mitochondrial dehydrogenase activity, measured by MTT reduction assay, in the mitochondrial fraction of gastric mucosal tissues from control and indomethacin –treated rats. (i) Immunoblot of ubiquitination in the mitochondrial fraction from control and indomethacin –treated rats. TOM20: loading control. (j) Immunoblot of PGC1α and ERRα in the nuclear fraction from control and indomethacin –treated rats. Histone 3A: loading control. Representative blots are presented alongside the bar graphs (f, i, j). Data (c, d) are mean ± SD, n = 5. $^{*}P < 0.05$, significantly different from Indo 0 h; $^{\#}P < 0.05$, significantly different from Indo 4 h; one-way ANOVA followed by Bonferroni's post hoc test. Data (e) are mean ± SD, n = 5. $^{*}P < 0.05$, significantly different from Indo 0 μM; one-way ANOVA followed by Bonferroni's post hoc test. Unpaired Student's *t* test with Welch's correction (for comparing two groups) was used for analysing the data in (a, b, f–j). ns, non-significant. The number of independent experiments is 3.

activity as evident from attenuation of mitochondrial proteome hyper-acetylation (Figure 4j) and specific acetylation of OGG1 and SOD2 (Figure 4k). Prevention of OGG1 deactivation was further reflected through reduction of indomethacin-induced 8-oxo-dG accumulation in mtDNA, as shown by ELISA (Figure 4l) and immunohistochemical analysis (Figure 4m) of tissue levels of 8-oxo-dG in situ. Because 8-oxo-dG accumulation is a direct consequence of mtDNA oxidation, we checked the level of the progenitor ROS molecule, superoxide ($O_2^{\bullet -}$), in the gastric mucosal cells isolated from rats treated with indomethacin, with and without honokiol, through MitoSox-based flow cytometry. Pre-treatment with honokiol blocked NSAID-induced intracellular $O_2^{\bullet -}$ accumulation (Figure 4n) coupled with restoration of $\Delta\Psi m$, preservation of mitochondrial dehydrogenase activity and prevention of bioenergetic crisis (Figure 4o–q). In The honokiol-

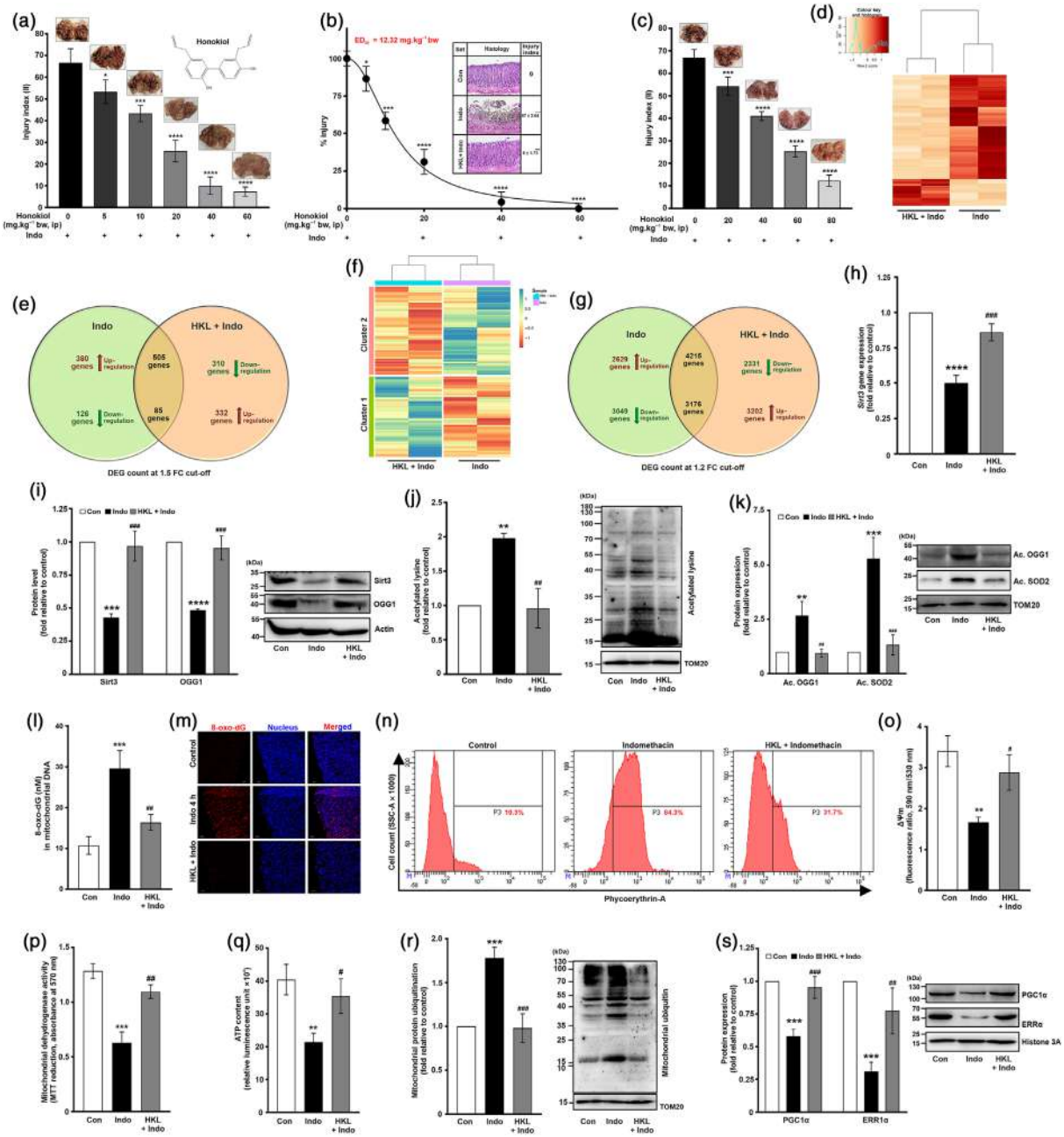

FIGURE 4 Legend on next page.

dependent Sirt3 stimulation also significantly prevented indomethacin-induced mitochondrial ubiquitination (Figure 4r). From a mechanistic perspective, we observed that endogenous Sirt3 stimulation by honokiol significantly reversed the down-regulation of PGC1α and ERRα induced by indomethacin (Figure 4s), revealing a feedback regulation.

3.4 | Sirt3 induction prevents NSAID-induced altered expression of mtDNA-encoded ETC complex, aberrant mitochondrial quality control, mucosal inflammasome activation and apoptosis

Because Sirt3 depletion by indomethacin involved down-regulation of OGG1, reduction of mitochondrial dehydrogenase activity and associated ATP depletion, we checked the effect of Sirt3 stimulation on mtDNA-encoded ETC complex subunits controlling bioenergy production. qRT-PCR and immunoblotting revealed that Sirt3 stimulation by pre-treatment with honokiol, significantly prevented indomethacin-induced down-regulation of *mt-Nd1*, *mt-Nd3*, *mt-Nd4* and NDUFB8 (complex I), *mt-Cytb* and UQCRC2 (complex III), *mt-Co1*, *mt-Co2* and MTCO1 (complex IV) and *mt-Atp6*, *mt-Atp8* and ATP5A (complex V) (Figure 5a,b). Direct measurement of ETC complex I and III activities also indicated that honokiol prevented indomethacin-induced deterioration of both complexes, thereby ensuring proper electron flow during OXPHOS (Figure 5c,d). Because mitochondrial functions critically depend on the homeostasis of mitochondrial dynamics, we next checked the mitochondrial structure under the indomethacin-induced, Sirt3 depleted state and during honokiol-induced Sirt3 stimulation (Figure 5e). Interestingly, honokiol pre-treatment also prevented indomethacin-induced depletion of **mitofusin (MFN)1**, **MFN2** and OPA1 and increase of DRP1 activation (through reducing phospho-DRP1-Ser616), thereby indicating stabilization of mitochondrial dynamics (Figure 5e). We also checked mitochondrial quality control by following two key mitophagy regulators, Parkin and **PINK1**. Data revealed that Parkin and PINK1 were highly elevated during indomethacin treatment whereas honokiol pre-treatment restored aberrant PINK1–Parkin expression (Figure 5f). In addition, honokiol also prevented the decrease in the mitochondrial biogenesis master-regulator PGC1α and TOM20 (Figure 5f) to maintain mitochondrial biogenesis, which is jeopardized by NSAID treatment.

As mitochondrial pathology affects the inflammatory status of the tissue, we checked the effect of honokiol on gastric inflammation and inflammasome activation. We found that the indomethacin-induced elevation of pro-inflammatory cytokines (***Il1a***, ***Il1b*** and ***Il6***), chemokines (***Cxcl3*** and ***Mcp1***) and intercellular adhesion molecules (***Icam1*** and ***Vcam1***) was prevented by honokiol pre-treatment (Figure 5g). Moreover, we also observed that indomethacin triggered inflammasome activation in the gastric mucosa, shown by raised levels of **NLRP3** and IL-1β, along with **caspase 1** cleavage (Figure 5h).

FIGURE 4 Stimulation of sirtuin-3 (Sirt3) prevents indomethacin-induced gastric transcriptome alteration, mitochondrial dysfunctions and tissue injury. (a) Bar graph showing the dose-response of honokiol (HKL; given i.p.) pre-treatment on indomethacin-induced (Indo) gastric mucosal injury. Representative image of the gastric mucosal morphology corresponding to indicated dose of honokiol is shown as inset (on respective bars). Chemical structure of honokiol is shown as inset. (b) Dose–response curve of honokiol showing effective dose (ED_{50}) and haematoxylin/eosin-stained gastric mucosal histology from control (Con), indomethacin (Indo) and HKL + Indo treated rats; representative micrographs presented. (c) Bar graph showing the intragastric (ig) dose response of honokiol pre-treatment on indomethacin-induced gastric mucosal injury. Representative image of the gastric mucosal morphology corresponding to indicated dose of honokiol has been shown as inset (on respective bars). (d) Heatmap shows separate clustering of samples from HKL + Indo and Indo treated rats (false discovery rate [FDR] ≤ 0.05). Euclidean distance metric was used while clustering gene expression data. The expression value of genes analysed with fold change (FC) cut-off of 1.5; colour gradient scale: white being highly down-regulated to brown being highly up-regulated. (e) Venn diagram of differentially expressed gene (DEG) count in Indo (compared with control) and HKL + Indo (compared with Indo) when analysed with an FC cut-off of 1.5. (f) Heatmap for samples from HKL + Indo'and Indo treated rats after analysis with FC cut-off of 1.2; colour gradient scale: red being highly down-regulated to blue being highly up-regulated. (g) Venn diagram of DEG count in Indo (compared with control) and HKL + Indo (compared with Indo) treated rats, when analysed with an FC cut-off of 1.2 for better resolution of genes controlling mitochondrial functions. Brown upward and green downward arrows (along with corresponding DEG counts) indicate up-regulation and down-regulation of gene expression, respectively, DEG counts in the intersection regions of the Venn diagrams indicate common genes that were up-regulated/down-regulated with Indo treatment (compared with control) whereas their expression was reversed with HKL + Indo treatment (when compared with Indo). (h) *Sirt3* gene expression analysis in gastric mucosal tissues from Con, Indo and HKL + Indo by qPCR; bar graph indicates FC in gene expression relative to control (after normalization to *Gapdh*). (i) Immunoblots of Sirt3 and 8-oxoguanine DNA glycosylase 1 (OGG1) in tissues from Con, Indo and HKL + Indo treated rats. Actin: loading control. (j, k) Immunoblots of acetylated lysine (j), acetylated OGG1 and acetylated superoxide dismutase (SOD2) (k) in the mitochondrial fraction of tissues from Con, Indo and HKL + Indo treated rats. TOM20: loading control. (l) mtDNA damage as measured by 8-oxo-dG levels, with ELISA. (m) Confocal immunohistochemical staining showing 8-oxo-dG (green) and nucleus (blue) in Con, Indo and HKL + Indo treated rats. (n) Flow cytometry for mitochondrial superoxide accumulation in Con, Indo and HKL + Indo treated rats. (o) Mitochondrial transmembrane potential (ΔΨm). (p) Mitochondrial dehydrogenase activity. (q) ATP content. (r) Immunoblot of ubiquitination in the mitochondrial fraction of tissues from Con, Indo and HKL + Indo treated rats. TOM20: loading control. (s) Immunoblot of PGC1α and ERRα in the nuclear fraction of tissues from Con, Indo and HKL + Indo treated rats. Histone 3A: loading control. Representative blots are presented alongside the bar graphs (i–k, r, s). Data are mean ± SD, n = 5. $^{*}P < 0.05$, significantly different from HKL 0 $mg{\cdot}kg^{-1}$; one-way ANOVA followed by Bonferroni's post hoc test. Number of independent experiments: 3 (a–c). Data are mean ± SD, n = 5. $^{*}P < 0.05$, significantly different from Con; $^{\#}P < 0.05$, significantly different from Indo; one-way ANOVA followed by Bonferroni's post hoc test (b, h–l, o–s). The number of independent experiments is 3.

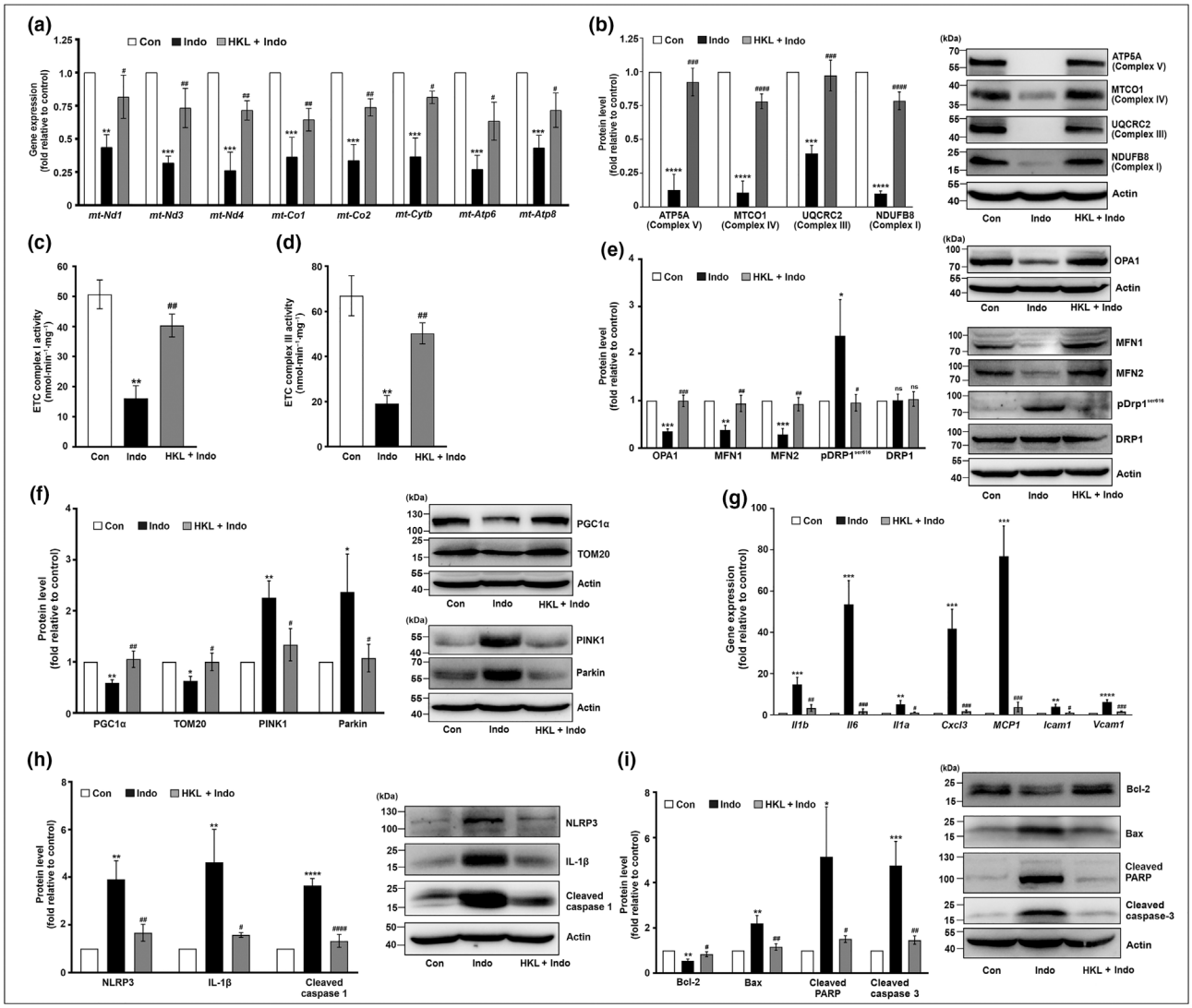

FIGURE 5 Stimulation of sirtuin-3 (Sirt3) prevents indomethacin-induced block of electron transport chain (ETC) complex gene expression, aberrant mitochondrial dynamics, mucosal inflammation and apoptosis. (a) Gene expression analysis for *mt-Nd1*, *mt-Nd3*, *mt-Nd4*, *mt-Cytb*, *mt-Co1*, *mt-Co2*, *mt-Atp6* and *mt-Atp8* by qRT-PCR) in control (Con), indomethacin (Indo) and honokiol+indomethacin (HKL + Indo) treated rats. Bar graphs indicate fold change in gene expression relative to control (after normalization by *Gapdh*). (b) Immunoblots of ATP5A, MTCO1, UQCRC2 and NDUFB8 in tissues from Con, Indo and HKL + Indo treated rats. (c) ETC complex I activity and (d) ETC complex III activity in the mitochondrial fraction of tissues from Con, Indo and HKL + Indo treated rats. (e) Immunoblots of MFN1, MFN2 OPA1, pDRP1^{ser616} and DRP1 in tissues from Con, Indo and HKL + Indo treated rats. (f) Immunoblots of PGC1α, TOM20, PINK1 and Parkin in tissues from Con, Indo and HKL + Indo treated rats. (g) Gene expression analysis for *Il1b*, *Il6*, *Il1a*, *Cxcl3*, *Mcp1*, *Icam1* and *Vcam1* by qRT-PCR in samples from Con, Indo and HKL + Indo treated rats. Bar graphs indicate fold change in gene expression relative to control (after normalization by *Gapdh*). (h) Immunoblots of NLRP3, IL-1β and cleaved caspase 1 in tissues from Con, Indo and HKL + Indo treated rats. (i) Immunoblots of Bcl-2, Bax, cleaved PARP and cleaved caspase 3 in tissues from Con, Indo and HKL + Indo treated rats. Actin was used as the loading control; representative blots are presented alongside the bar graphs (b, e, f, h, i). Data are mean ± SD, n = 5. $^{*}P < 0.05$, significantly different from control; $^{\#}P < 0.05$, significantly different from Indo-treated rats; one-way ANOVA followed by Bonferroni's post hoc test. The number of independent experiments is 3.

However, honokiol significantly prevented indomethacin-induced up-regulation of inflammasome markers (Figure 5h). Because inflammatory tissue damage is often associated with cell death (Rock & Kono, 2008), we finally checked the expression profiles of typical pro-apoptotic and anti-apoptotic markers and found that honokiol significantly attenuated indomethacin-induced mucosal cell apoptosis through blocking the depletion of **Bcl-2** while preventing **PARP** and caspase 3 cleavage, as well as the up-regulation of **Bax** (Figure 5i).

3.5 | Honokiol accelerates the healing of pre-formed gastric lesions and offers gastroprotection against indomethacin without affecting gastric acid secretion

After documenting the prophylactic potency of honokiol against NSAID gastropathy, we checked whether Sirt3 stimulation could be used as a therapeutic strategy to accelerate the healing of pre-formed

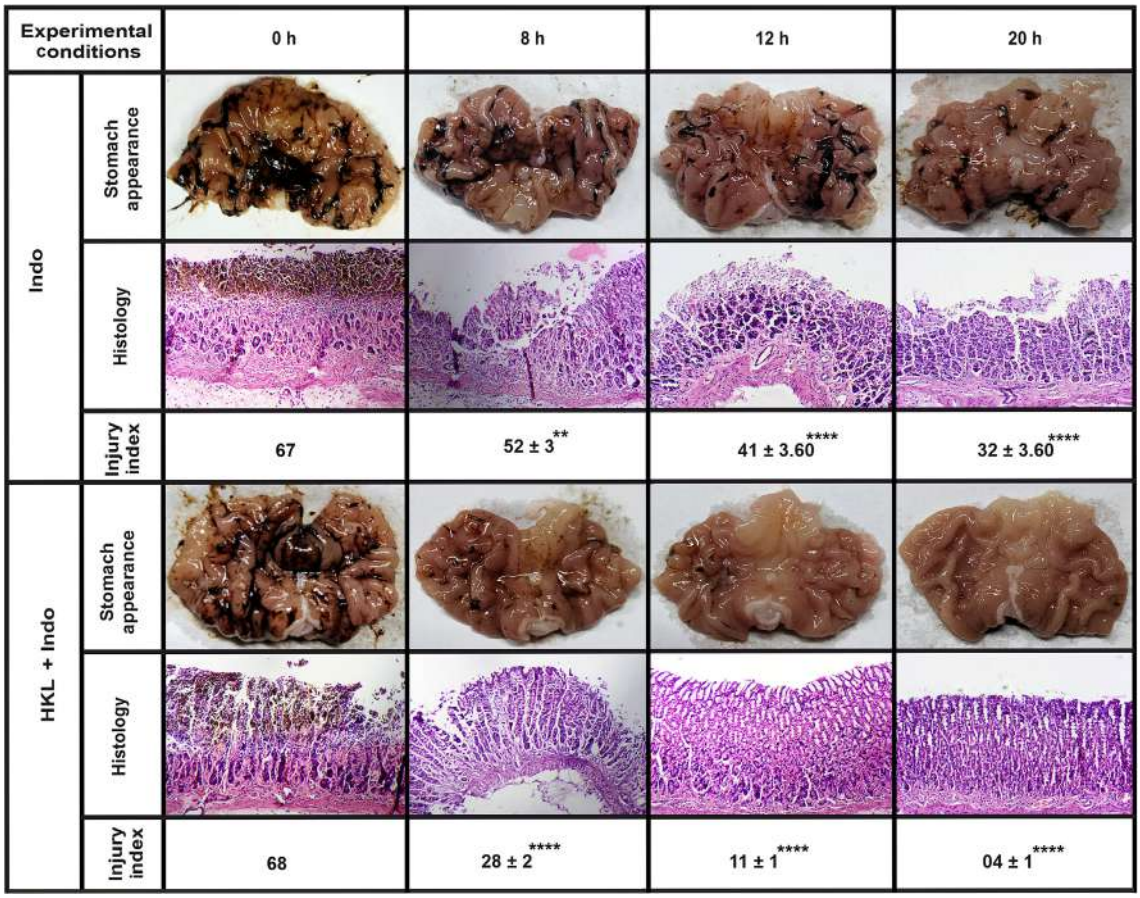

FIGURE 6 Honokiol (HKL) accelerates the healing of pre-formed gastric lesions induced by indomethacin. Stomach morphology and histology of indomethacin (Indo)–treated rats (upper panel) and HKL + Indo-treated rats (lower panel).

gastric lesions. Rats were treated with indomethacin and allowed to develop gastric injury for 4 h after which one set of rats was treated with honokiol and the other set was left untreated. At 0, 8, 12 and 20 h after treatment with honokiol, the extent of wound resolution was compared with that in rats treated with indomethacin only, at the same time point (Figure 6). We observed that honokiol significantly accelerated the healing of pre-formed gastric lesions.

We next checked whether honokiol treatment affected gastric acid production by measuring luminal pH under states of basal (unstimulated) and elevated (MMI-stimulated) acid secretion. Interestingly, honokiol treatment did not change gastric luminal pH significantly, unlike lansoprazole, which drastically elevated the pH (Table 1). Thus, the gastroprotection provided by honokiol was not mediated by altered gastric acid production.

TABLE 1 pH of gastric luminal secretion of different experimental groups of rats.

Experimental set	Stomach luminal pH
Control	2.73 ± 0.45
Control + honokiol	2.48 ± 0.17^{ns}
Control + lansoprazole	7.09 ± 0.26****
MMI	1.63 ± 0.15*
MMI + honokiol	1.83 ± 0.35*
MMI + Lansoprazole	6.61 ± 0.52****

Note: Data shown represent gastric luminal pH in control, control + honokiol', control + lansoprazole, 2-mercapto-1-methylimidazole (MMI), MMI + honokiol and MMI + lansoprazole-treated rats (n = 5). Data are mean ± SD. The number of independent experiments is 3. *P < 0.05, significantly different from control, ns, non-significant; one-way ANOVA followed by Bonferroni's post hoc test.

3.6 | Sirt3 depletion is a generalized response elicited by common NSAIDs to trigger gastric mucosal injury

Finally, we checked whether Sirt3 depletion was specific to indomethacin or common to NSAIDs such as diclofenac, ibuprofen and aspirin, frequently found as principal components in typical anti-inflammatory formulations for humans. Aspirin was particularly selected because of its cardioprotective and anti-neoplastic effects. We observed that all these NSAIDs significantly down-regulated Sirt3 and OGG1, similar to the effects of indomethacin. Sirt3 depletion led to significantly compromised mitochondrial dehydrogenase activity and severe mucosal injury (Figure 7a–c). Hence, Sirt3 depletion appeared a common

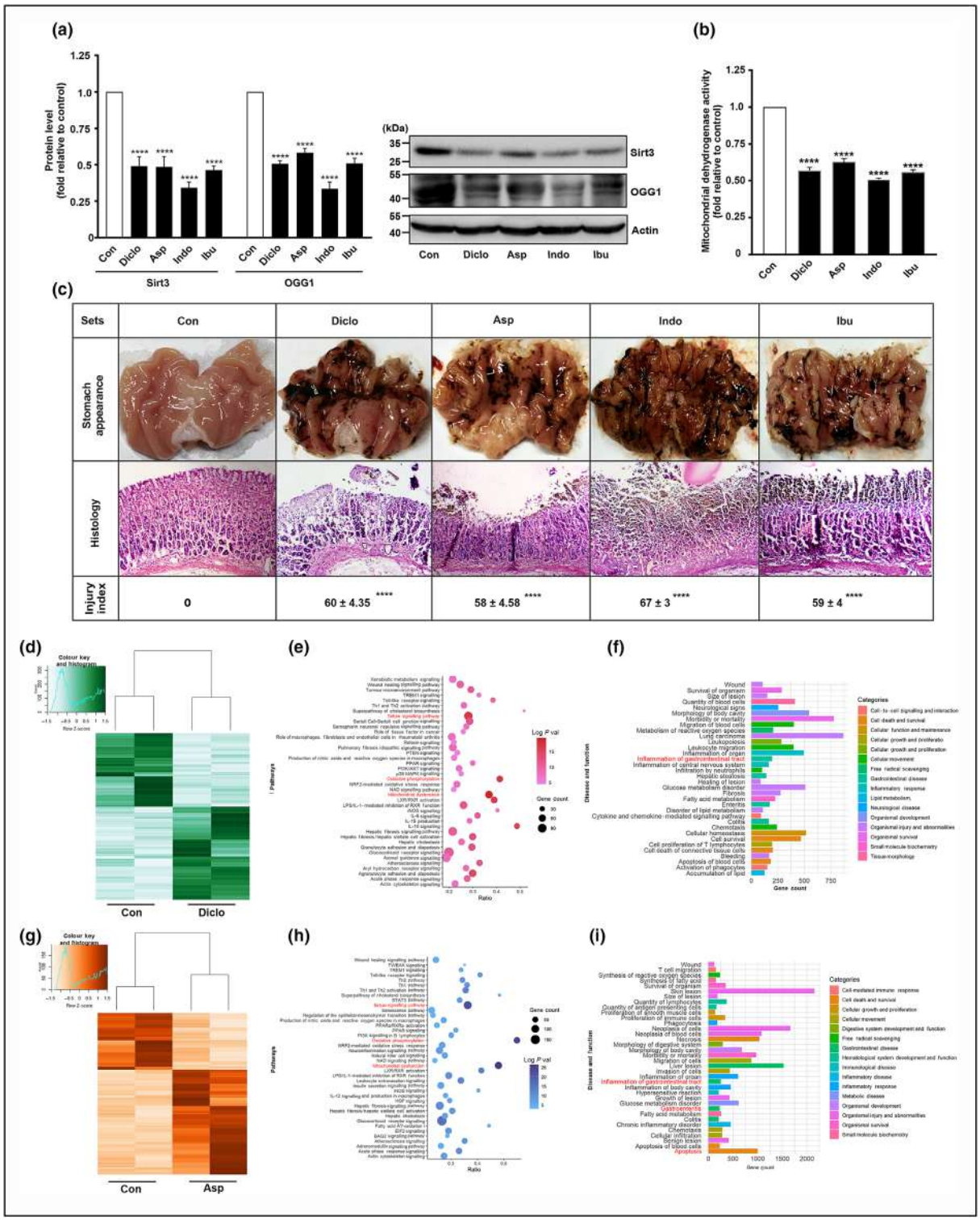

FIGURE 7 Legend on next page.

pathway targeted by NSAIDs. Further, gastric transcriptomics of diclofenac (Figures 7d–f and 8a–c) and aspirin (Figures 7g–i and 8d–f)-treated rats revealed patterns of DEGs and associated gene expression programmes, similar to those in rats treated with indomethacin (Files S3a–f and S4a–f).

4 | DISCUSSION

Here, we have identified Sirt3 as a novel gastroprotective target, which is severely down-regulated by NSAIDs to activate mitochondrial oxidative damage and a consequent cellular bioenergetic crisis, in gastric mucosal cells, leading to apoptosis and inflammatory tissue injury. We showed that NSAID directly inhibited Sirt3 deacetylase activity and suppressed its transcriptional regulators PGC1α and ERRα to exert a top-down suppression. Most notably, Sirt3 stimulation by honokiol markedly blocked NSAID-induced mitochondrial fragmentation, the exacerbated redox perturbation, inflammasome activation and apoptosis to prevent mucosal injury, besides accelerating the healing of pre-formed gastric lesions without affecting basal gastric acid secretion.

Despite their toxic side-effects, NSAIDs are still widely used as the first-line medicines against pain and inflammation. Emerging reports on drug repurposing of NSAIDs, which revealed their anti-neoplastic potential, have further expanded their clinical utility (Kumar, 2016; L. Li et al., 2019). Interestingly, supplementation with prostaglandins actually fails to completely ameliorate the toxic effects of NSAIDs, thereby indicating towards the involvement of extra-COX actions (Gurpinar et al., 2013). Therefore, we were keen to explore newer, COX-independent, target(s) of NSAIDs, which may be utilized for neutralizing their toxic effects while optimizing their safer usage. We used indomethacin as a prototype NSAID with negligible COX selectivity to rule out potential COX1/COX2 bias. A gastric mucosal injury model in rats was used because the gut is most severely affected by NSAIDs.

Sequencing-based target prediction was used for unbiased gene expression profiling upon NSAID treatment. Sirt3 was identified as a hub gene associated with diverse metabolic effects elicited by NSAIDs including redox homeostasis, bioenergy production, inflammation and cell death. As the mitochondrial guardian, Sirt3 controls mitochondrial protein stability to regulate antioxidant defence, structural dynamics, biogenesis, mtDNA repair and metabolism primarily through the deacetylation of target proteins including FOXO3a, OGG1, OPA1, SOD2, pyruvate dehydrogenase, citrate synthase, aconitase, isocitrate dehydrogenase, succinate dehydrogenase, malate dehydrogenase, succinate dehydrogenase, Ku70, GSK3β, mitochondrial trifunctional protein and phosphofructokinase (Murugasamy et al., 2022; Zhang et al., 2020). Loss of Sirt3 has been critically implicated in diverse pathologies involving mitochondrial structural and functional defects, leading to metabolic and bioenergetic problems (Peng et al., 2022; Sherin et al., 2021; Wu et al., 2019; Zhang et al., 2020). As a result, metabolically active tissues are susceptible to Sirt3 deficiency (Dittenhafer-Reed et al., 2015; Zhang et al., 2020). However, there is no report citing the role of Sirt3 in maintaining gastric mucosal integrity, in spite of gut mucosa having a rapid cellular turnover (Timmons et al., 2012). NSAIDs directly target the ETC complex I to cause electron leakage. These leaked electrons trigger partial reduction of oxygen to produce $O_2^{\bullet -}$, which subsequently transforms into other ROS species such as H_2O_2 and •OH. In this context, SOD2 and OGG1 are major mitochondrial antioxidant arsenals controlling oxidative stress through neutralizing intra-mitochondrial $O_2^{\bullet -}$ and excising 8-oxo-dG in mtDNA (J. Liu et al., 2017). Coincidentally, both OGG1 and SOD2 are deacetylation targets of Sirt3. Moreover, 8-oxo-dG also serves as a biomarker for endogenous oxidative stress and redox-associated pathologies including cancer (Valavanidis et al., 2009). Indomethacin-induced Sirt3 down-regulation along with direct inhibition of Sirt3 deacetylase activity and elevation of OGG1–SOD2 acetylation explained the basis of MOS induction and cell death. Sirt3 serves as a cellular longevity promoting factor by boosting the antioxidant defences (Kincaid & Bossy-Wetzel, 2013; Merksamer et al., 2013). Sirt3-deficient cardiomyocytes produce double the amount of ROS (Sundaresan et al., 2009), whereas Sirt3 overexpression significantly increased glutathione (GSH) levels (J. Liu et al., 2017). Here, we show that indomethacin-induced Sirt3 depletion resulted in a severe bioenergetic crisis through attenuated mitochondrial dehydrogenase activity, ETC complex I and III dysfunction and ATP depletion. Ubiquitination-dependent mitochondrial elimination further potentiated the damage. Moreover, it is noteworthy that Sirt3 depletion-

FIGURE 7 Popular NSAIDs deplete Sirtuin-3 (Sirt3) to induce gastric mucosal injury and transcriptomic alteration. (a) Immunoblots of Sirt3 and 8-oxoguanine DNA glycosylase 1 (OGG1) in tissues from samples from control (Con), diclofenac (Diclo), aspirin (Asp), indomethacin (Indo) and ibuprofen (Ibu) treated rats. Actin: loading control; representative blots alongside the bar graphs. (b) Dehydrogenase activities in the mitochondrial extracts from control and indicated NSAIDs-treated rats. (c) Gastric mucosal morphology and haematoxylin/eosin-stained histology; representative images provided with injury index. Data shown in (a, b) are means ± SD; n = 5. *$P < 0.05$ significantly different from control; one-way ANOVA, followed by Bonferroni's post hoc test. The number of independent experiments is 3. (d) Heatmap of samples from control (Con) and diclofenac (Diclo) treated rats (false discovery rate [FDR] ≤ 0.05). Euclidean distance metric was used while clustering the gene expression data. The expression value of genes analysed with fold change (FC) cut-off of 1.5; colour gradient scale: white being highly down-regulated to green being highly up-regulated. (e) Dot plot showing enriched canonical pathways. Dot size: proportion of genes involved in a particular signalling pathway; colour range: Bonferroni corrected *P* values (−log transformed). Ratio: number of genes in fraction with respect to the total number of genes that map to the same pathway. (f) Bar graph showing 'disease and functions' enriched in diclofenac- treated rats. (g) Heatmap of from control (Con) and aspirin (Asp) treated rats (FDR ≤ 0.05). The expression value of genes analysed with FC cut-off of 1.5; colour gradient scale with white being highly down-regulated to brown being highly up-regulated. (h) The dot plot shows enriched canonical pathways. (i) Bar graph showing 'disease and functions' enriched in aspirin-treated rats.

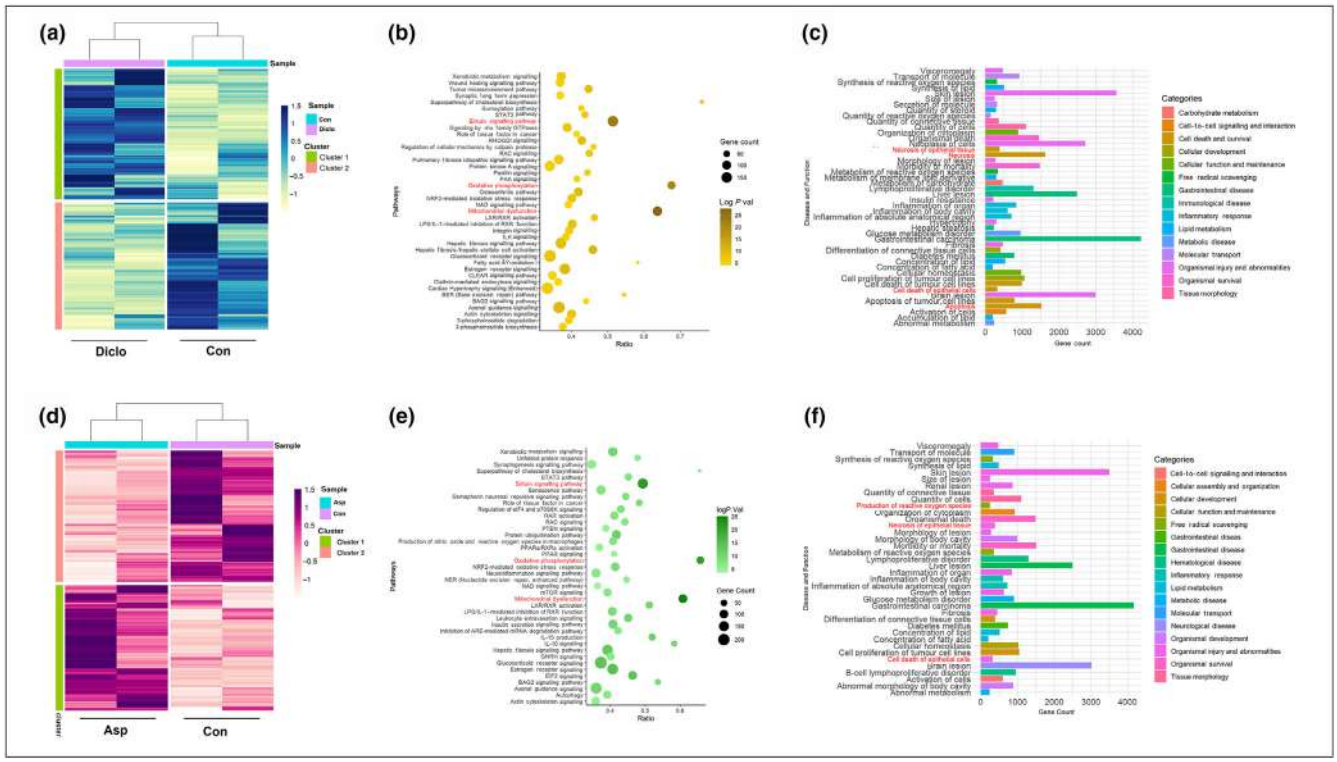

FIGURE 8 Gastric mucosal transcriptome alteration by diclofenac and aspirin after analysis at 1.2 fold change (FC) cut-off. (a) Heatmap shows separate clustering of samples from control (Con) and diclofenac (Diclo) treated rats (false discovery rate [FDR] ≤ 0.05). Euclidean distance metric was used while clustering the gene expression data. Expression value of genes analysed with FC cut-off of 1.2; colour gradient scale with blue being highly up-regulated to white being highly down-regulated. (b) Dot plot shows enriched canonical pathways. Size of dots: proportion of genes involved in particular signalling/pathway; colour range: Bonferroni corrected *P* values (−log transformed). Ratio represents the number of genes in fraction with respect to the total number of genes that map to the same pathway. (c) Bar graph showing 'disease and functions' enriched in diclofenac-treated rats. (d) Heatmap shows separate clustering of samples from control (Con) and aspirin (Asp) treated rats (FDR ≤ 0.05). Euclidean distance metric was used while clustering the gene expression data. Expression value of genes analysed with FC cut-off of 1.2; colour gradient scale with magenta being highly up-regulated to white being highly down-regulated. (e) Dot plot shows enriched canonical pathways. Size of dots: proportion of genes involved in particular signalling/pathway; colour range: Bonferroni corrected *P* values (−log transformed). Ratio represents the number of genes in fraction with respect to the total number of genes that map to the same pathway. (f) Bar graph showing 'disease and functions' enriched in aspirin-treated rats.

associated mitochondrial toxicity and cell death appeared to be a common side-effect of popular NSAIDs. This information is crucial while devising novel approaches to avoid NSAID toxicity.

From a mechanistic perspective, it was imperative to explore how NSAIDs down-regulate Sirt3. Therefore, we checked the upstream events controlling Sirt3 expression, and found that indomethacin induced the down-regulation of PGC1α and ERRα. The action of Sirt3 in regulating the PGC1α–ERRα duo has recently emerged as a pivotal nuclear transcriptional axis, orchestrating several gene expressions controlling mitochondrial bioenergetics (Y. Kim & Park, 2019; Kincaid & Bossy-Wetzel, 2013). Coincidentally, PGC1α also regulates mitochondrial biogenesis (Austin & St-Pierre, 2012), which justified mitochondrial depletion during Sirt3 down-regulation by indomethacin. Upon indomethacin treatment, we observed prominent depletion of PGC1α in both nuclear and mitochondrial fractions. This clearly suggested that NSAID blocks both nuclear and mitochondrial transcriptional activities of PGC1α to exert a comprehensive detrimental effect on gastric cell metabolism. Moreover, indomethacin-induced Sirt3 and PGC1α depletion also implied a mutual feedback regulation. Existing reports suggest that Sirt3-dependent FOXO3 deacetylation induces its nuclear translocation to up-regulate PGC1α expression as a cytoprotective response (Fasano et al., 2019; Olmos et al., 2009) that is blunted by Sirt3 depletion. This is likely to involve direct PGC1α–FOXO3 interaction to activate *Sod2* transcription (Olmos et al., 2009). Sirt3 is noted for regulating diverse mitochondrial functions including mitosis, biogenesis, transcription, translation, OXPHOS, TCA cycle, and lipid, glycoside and amino acid metabolism (Zhang et al., 2020). Around 20% of mitochondrial proteins are highly acetylated and Sirt3 directly interacts with about 84 mitochondrial proteins to control metabolism and bioenergetics (Zhang et al., 2020). Sirt3 also controls mitochondrial dynamics and mitophagy through deacetylation-dependent regulation of OPA1, AMPK, Lon protease and FOXO3 (Meng et al., 2019). Sirt3 indirectly and/or directly (through FOXO3a deacetylation) regulates the expression of mediators of mitochondrial dynamics, such as MFN2, DRP1 and FIS1, and key mitophagy players, such as Bnip3/Nix and LC3 (Meng

et al., 2019). In this regard, indomethacin-induced MOS, mitochondrial hyperfission and aberrant mitophagy appear as direct attributes of Sirt3 depletion and intra-mitochondrial pro-oxidant accumulation to trigger ETC dysfunction.

Functional validation of the cytoprotective action of Sirt3 against indomethacin specifically relied on pharmacological Sirt3 stimulation by honokiol, a specific inducer (Pillai et al., 2015; Pillai et al., 2017; Wang, Nisar, et al., 2018). It is worth mentioning that, at present, there is apparently no commercially available synthetic Sirt3 peptide suitable for use in vivo, which would exhibit resistance against pepsin/other proteases (to protect it during systemic delivery) and be cell-permeable and mito-targeting, to allow intra-mitochondrial localization and retention for expressing the deacetylase activity. Therefore, honokiol-induced stimulation of endogenous Sirt3 levels served as the most suitable and specific pharmacological strategy to check the putative gastroprotective action of Sirt3. This approach also had the benefit of providing a novel gastroprotective strategy, specifically relying on pharmacological Sirt3 stimulation, because of the ease of this mode of intervention strategy, compared with the more precise but elaborate and highly expensive genetic manipulation-based intervention strategies while considering from a real-life therapeutic point of view. Interestingly, honokiol-induced Sirt3 stimulation corrected indomethacin-induced mitochondrial metabolic crisis and cellular damage through salvaging MOS and preserving ETC function as a consequence of attenuating mitochondrial proteome hyperacetylation and ubiquitination. honokiol pre-treatment significantly diminished transcriptome alteration by indomethacin while blocking intra-mitochondrial $O_2^{\bullet -}$ accumulation to prevent oxidative mtDNA damage. In fact, it was remarkable to find that the protective actions of honokiol extended to almost all the ETC complexes, as shown from the expressions of representative components corresponding to complex I, II, IV and V as well as direct enzymatic activities of complex I and III, which serve as major sources of mitochondrial electron leakage during ETC dysfunction. If a compound safeguards mitochondria, it seems imperative to offer protection and stability to mitochondrial structural dynamics. It was clear that the excess mitochondrial fission, aberrant mitophagy and inhibited biogenesis, induced by indomethacin, were markedly prevented by honokiol. Recently, mitochondria have been considered as epicentre of NLRP3 inflammasome activation because several mtDAMPs, including mtROS, oxidized mtDNA and oxidized cardiolipin (released during tissue injury), potently trigger NLRP3 activation (Q. Liu et al., 2018; Mazumder et al., 2022). So far, there is negligible evidence of NSAID-induced gastric mtDAMP release leading to inflammasome activation during gastric mucosal injury. Here, we clearly observed for the first time that honokiol-induced Sirt3 stimulation significantly prevented indomethacin-mediated NLRP3 activation and caspase 1 cleavage to block IL-1β upregulation in the gastric mucosa. This was concurrent with honokiol-induced prevention of canonical inflammation and apoptosis, triggered by indomethacin. Therefore, we provide evidence that indomethacin down-regulated Sirt3 expression along with directly inhibiting Sirt3 deacetylase activity to inflict mitochondrial structural and functional damage for triggering gastric mucosal inflammatory and apoptotic tissue damage. Honokiol, by stimulating Sirt3 expression, prevented indomethacin-induced gastropathy. It is worth mentioning that in addition to its direct Sirt3-stimulating effect, honokiol is also credited with partial agonism or activation of non-adipogenic PPARγ (Atanasov et al., 2013). Moreover, PPARγ activation has also been reported to offer gastroprotection and hasten ulcer healing in rodent models (Saha, 2015). Therefore, possible PPARγ agonism by honokiol may also contribute to or synergize its collective gastroprotective response. However, it is also noteworthy that the PPARγ–PGC1α couple has already been shown to crucially regulate energy metabolism (Kosgei et al., 2020), in a process where PGC1α is likely to be positively regulated by Sirt3 through a feedback loop. Therefore, although honokiol might have multiple responses, specificity of honokiol for Sirt3, as a defined target amongst many other off-targets, is supposedly good enough to prevent NSAID-induced gastric injury, as observed here. The observations in the present study are in direct agreement with several other studies where Sirt3 stimulation by honokiol has been found to preserve and maintain mitochondrial integrity, leading to protection against diverse pathologies (Pillai et al., 2017; Quan et al., 2020; Ramesh et al., 2018; Yi et al., 2019).

So far, we have considered the prophylactic effects of honokiol-induced Sirt3 stimulation, against NSAID gastropathy. However, a comprehensive efficacy of a cytoprotective compound stands incomplete without assessment of its therapeutic potency. In this context, honokiol also qualified as a potent gastroprotective compound because of its remarkable ability to accelerate the healing of preformed gastric lesions by indomethacin. Whereas untreated rats took 72 h after indomethacin treatment for complete resolution of mucosal injury, rats given honokiol treatment after developing profuse mucosal injury, had a shorter time (20 h) to complete wound resolution, thereby revealing its potent therapeutic efficacy. We also checked the comparative efficacy of i.p. and i.g. routes of honokiol administration, in an attempt to address the applied biomedical relevance of considering honokiol as a potential gastroprotective compound. It was clear, in the present study, that i.p. administration of honokiol required a much lower dose compared with i.g. administration, in order to provide protection against NSAIDs, at least in terms of the indomethacin-induced gastric mucosal injury in rodents. This certainly warrants further exploratory studies, specifically focused on formulating newer strategies to enhance oral bioavailability of honokiol, for ensuring its optimal utilization as a future gastroprotective drug available in oral formulations. Finally, it is imperative to state that most of the existing anti-ulcer gastroprotective compounds rely on gastric acid suppression, because acid aggravates injury. Although this logic definitely has a merit, however, it is undeniable that gastric acid is not a physiological evil. Rather, acid safeguards the GI tract from opportunist pathobiont attack besides maintaining normal gut microbiota balance, facilitating the absorption of various drug and minerals and, most notably, mediating protein digestion (Martinsen et al., 2005). Extensive usage of anti-ulcer formulations such as the proton pump inhibitors (PPIs) or histamine receptor antagonists, are often associated with several health hazards (Histamine Type-2 Receptor Antagonists (H2 Blockers), 2018; Maffei et al., 2007). Although a direct relation

between PPI intake and disease occurrence is not absolutely certain in every case and demands extensive randomized control trials (Eusebi et al., 2017), the over-usage of acid-suppressing drugs is not encouraged due to the need for physiological levels of acid. Therefore, it would be beneficial if a novel gastroprotective formulation directly targeted only the cytotoxic events (causing mucosal injury) while avoiding effects on acid secretion. Interestingly, the anti-apoptotic and cytoprotective action of honokiol did not affect basal acid secretion. This is an advantage because the harmful effects of acid suppression (such as gut dysbiosis, malabsorption of certain medicines, protein indigestion, vitamin B12 deficiency, osteoporosis, rebound acid secretion, gastrinemia and parietal cell hyperplasia) can be avoided using this gastroprotective strategy. Indeed, a recent report suggests that honokiol is apparently safe for human consumption as a natural antioxidant supplement (Sarrica et al., 2018). Further, it is also worth mentioning that several studies on cancers have projected Sirt3 as a double-edged sword, reflecting its cancer and/or context-specific oncogenic or tumour-suppressive attributes, depending on the nature and metabolic requirements of the tumours and their unique microenvironment (Ouyang et al., 2022). However, in regard to non-malignant pathologies, Sirt3 stimulation is mostly beneficial and offers protection against a range of pathologies associated with inflammation, oxidative stress, mitochondrial dysfunction and energy dyshomeostasis (Bugga et al., 2022; Dikalova et al., 2020; Zhang et al., 2020). The excess level of ROS accumulated in course of the pathogenesis is neutralized by Sirt3 stimulation by honokiol, leading to protection from the disease.

Taken together, our data showed Sirt3 to be a non-canonical, COX-independent, target of NSAIDs, which is severely downregulated leading to mitochondrial structural and functional disorder during gastric mucosal injury. The phyto-polyphenol, honokiol, acting as a Sirt3 inducer, offers strong gastroprotection while not affecting gastric acid secretion. Precisely exploiting this knowledge may lead to the design of novel gastroprotective compounds, specifically targeting mitochondria. Furthermore, NSAID treatment, coupled with endogenous Sirt3 stimulation by honokiol, may definitely help to optimize the therapeutic usage of these 'wonder drugs', while avoiding their side effects.

AUTHOR CONTRIBUTIONS

Subhashis Debsharma: Conceptualization (lead); data curation (lead); formal analysis (equal); funding acquisition (equal); investigation (equal); methodology (equal); validation (lead); visualization (lead); writing—original draft (lead); writing—review and editing (lead). **Saikat Pramanik:** Formal analysis (supporting); investigation (equal); methodology (supporting); writing—original draft (supporting). **Samik Bindu:** Conceptualization (lead); writing—original draft (equal); writing—review and editing (equal). **Somnath Mazumder:** Conceptualization (lead); formal analysis (equal); investigation (equal); methodology (equal); visualization (equal); writing—original draft (lead); writing—review and editing (lead). **Troyee Das:** Formal analysis (equal); investigation (supporting). **Debanjan Saha:** Investigation (supporting). **Rudranil De:** Investigation (supporting). **Shiladitya Nag:** Investigation (supporting). **Chinmoy Banerjee:** Investigation (supporting). **Asim Azhar Siddiqui:** Investigation (supporting). **Zhumur Ghosh:** Data curation (supporting); formal analysis (supporting); methodology (supporting); resources (supporting); software (lead); supervision (supporting); validation (supporting); visualization (supporting); writing—original draft (supporting); writing—review and editing (supporting). **Uday Bandyopadhyay:** Conceptualization (lead); data curation (lead); formal analysis (lead); funding acquisition (lead); investigation (equal); methodology (equal); project administration (lead); resources (lead); software (equal); supervision (lead); validation (equal); visualization (equal); writing—original draft (lead); writing—review and editing (lead).

ACKNOWLEDGEMENTS

UB acknowledges the Science and Engineering Research Board, Department of Science and Technology, Ministry of Science and Technology, India, for providing support through J.C. Bose National Fellowship (Grant No. SB/S2/JCB-54/2014) to perform this work. SD acknowledges the Department of Biotechnology, Ministry of Science and Technology, India, for doctoral research fellowship.

The authors thankfully acknowledge the DBT-National Genomics Core and Core Technologies Research Initiative, National Institute of Biomedical Genomics, India, for helping with next-generation sequencing.

CONFLICT OF INTEREST STATEMENT

The authors declare no competing interests with any part of the manuscript.

DECLARATION OF TRANSPARENCY AND SCIENTIFIC RIGOUR

This Declaration acknowledges that this paper adheres to the principles for transparent reporting and scientific rigour of preclinical research as stated in the *BJP* guidelines for Design & Analysis, Immunoblotting and Immunochemistry, and Animal Experimentation, and as recommended by funding agencies, publishers and other organizations engaged with supporting research.

DATA AVAILABILITY STATEMENT

Processed and raw RNA-seq data generated in this study are available in the GEO with accession number GSE201565 for rat transcriptomics data. All data pertaining to this study are provided in the manuscript and supporting information.

ORCID

Uday Bandyopadhyay https://orcid.org/0000-0002-5928-6790

REFERENCES

Alexander, S. P., Cidlowski, J. A., Kelly, E., Mathie, A., Peters, J. A., Veale, E. L., Armstrong, J. F., Faccenda, E., Harding, S. D., Pawson, A. J., Southan, C., Davies, J. A., Coons, L., Fuller, P. J., Korach, K. S., & Young, M. J. (2021). THE CONCISE GUIDE TO PHARMACOLOGY 2021/22: Nuclear hormone receptors. *British Journal of Pharmacology*, *178*(S1), S246–S263. https://doi.org/10.1111/bph.15540

Alexander, S. P., Fabbro, D., Kelly, E., Mathie, A., Peters, J. A., Veale, E. L., Armstrong, J. F., Faccenda, E., Harding, S. D., Pawson, A. J., Southan, C., Davies, J. A., Beuve, A., Brouckaert, P., Bryant, C., Burnett, J. C., Farndale, R. W., Friebe, A., Garthwaite, J., … Waldman, S. A. (2021). THE CONCISE GUIDE TO PHARMACOLOGY 2021/22: Catalytic receptors. *British Journal of Pharmacology*, *178*(S1), S264–S312. https://doi.org/10.1111/bph.15541

Alexander, S. P., Fabbro, D., Kelly, E., Mathie, A., Peters, J. A., Veale, E. L., Armstrong, J. F., Faccenda, E., Harding, S. D., Pawson, A. J., Southan, C., Davies, J. A., Boison, D., Burns, K. E., Dessauer, C., Gertsch, J., Helsby, N. A., Izzo, A. A., Koesling, D., … Wong, S. S. (2021). THE CONCISE GUIDE TO PHARMACOLOGY 2021/22: Enzymes. *British Journal of Pharmacology*, *178*(S1), S313–S411. https://doi.org/10.1111/bph.15542

Alexander, S. P., Kelly, E., Mathie, A., Peters, J. A., Veale, E. L., Armstrong, J. F., Faccenda, E., Harding, S. D., Pawson, A. J., Southan, C., Buneman, O. P., Cidlowski, J. A., Christopoulos, A., Davenport, A. P., Fabbro, D., Spedding, M., Striessnig, J., Davies, J. A., Ahlers-Dannen, K. E., … Zolghadri, Y. (2021). THE CONCISE GUIDE TO PHARMACOLOGY 2021/22: Other Protein Targets. *British Journal of Pharmacology*, *178*(S1), S1–S26. https://doi.org/10.1111/bph.15537

Alexander, S. P. H., Roberts, R. E., Broughton, B. R. S., Sobey, C. G., George, C. H., Stanford, S. C., Cirino, G., Docherty, J. R., Giembycz, M. A., Hoyer, D., Insel, P. A., Izzo, A. A., Ji, Y., MacEwan, D. J., Mangum, J., Wonnacott, S., & Ahluwalia, A. (2018). Goals and practicalities of immunoblotting and immunohistochemistry: A guide for submission to the *British Journal of Pharmacology*. *British Journal of Pharmacology*, *175*, 407–411. https://doi.org/10.1111/bph.14112

Aminzadeh-Gohari, S., Weber, D. D., Vidali, S., Catalano, L., Kofler, B., & Feichtinger, R. G. (2020). From old to new—Repurposing drugs to target mitochondrial energy metabolism in cancer. *Seminars in Cell & Developmental Biology*, *98*, 211–223. https://doi.org/10.1016/j.semcdb.2019.05.025

Andrews, S. (2010). FastQC: A quality control tool for high throughput sequence data [Online]. Available online at: http://www.bioinformatics.babraham.ac.uk/projects/fastqc/

Atanasov, A. G., Wang, J. N., Gu, S. P., Bu, J., Kramer, M. P., Baumgartner, L., Fakhrudin, N., Ladurner, A., Malainer, C., Vuorinen, A., Noha, S. M., Schwaiger, S., Rollinger, J. M., Schuster, D., Stuppner, H., Dirsch, V. M., & Heiss, E. H. (2013). Honokiol: A non-adipogenic PPARγ agonist from nature. *Biochimica et Biophysica Acta*, *1830*, 4813–4819. https://doi.org/10.1016/j.bbagen.2013.06.021

Austin, S., & St-Pierre, J. (2012). PGC1α and mitochondrial metabolism—Emerging concepts and relevance in ageing and neurodegenerative disorders. *Journal of Cell Science*, *125*, 4963–4971. https://doi.org/10.1242/jcs.113662

Bader, G. D., & Hogue, C. W. (2003). An automated method for finding molecular complexes in large protein interaction networks. *BMC Bioinformatics*, *4*, 2. https://doi.org/10.1186/1471-2105-4-2

Bindu, S., Mazumder, S., & Bandyopadhyay, U. (2020). Non-steroidal anti-inflammatory drugs (NSAIDs) and organ damage: A current perspective. *Biochemical Pharmacology*, *180*, 114147. https://doi.org/10.1016/j.bcp.2020.114147

Bindu, S., Mazumder, S., Dey, S., Pal, C., Goyal, M., Alam, A., Iqbal, M. S., Sarkar, S., Azhar Siddiqui, A., Banerjee, C., & Bandyopadhyay, U. (2013). Nonsteroidal anti-inflammatory drug induces proinflammatory damage in gastric mucosa through NF-κB activation and neutrophil infiltration: Anti-inflammatory role of heme oxygenase-1 against non-steroidal anti-inflammatory drug. *Free Radical Biology & Medicine*, *65*, 456–467. https://doi.org/10.1016/j.freeradbiomed.2013.07.027

Bindu, S., Pillai, V. B., Kanwal, A., Samant, S., Mutlu, G. M., Verdin, E., Dulin, N., & Gupta, M. P. (2017). SIRT3 blocks myofibroblast differentiation and pulmonary fibrosis by preventing mitochondrial DNA damage. *American Journal of Physiology. Lung Cellular and Molecular Physiology*, *312*, L68–L78. https://doi.org/10.1152/ajplung.00188.2016

Bugga, P., Alam, M. J., Kumar, R., Pal, S., Chattopadyay, N., & Banerjee, S. K. (2022). Sirt3 ameliorates mitochondrial dysfunction and oxidative stress through regulating mitochondrial biogenesis and dynamics in cardiomyoblast. *Cellular Signalling*, *94*, 110309. https://doi.org/10.1016/j.cellsig.2022.110309

Carrasco-Pozo, C., Gotteland, M., & Speisky, H. (2011). Apple peel polyphenol extract protects against indomethacin-induced damage in Caco-2 cells by preventing mitochondrial complex I inhibition. *Journal of Agricultural and Food Chemistry*, *59*, 11501–11508. https://doi.org/10.1021/jf202621d

Crofford, L. J. (2013). Use of NSAIDs in treating patients with arthritis. *Arthritis Research & Therapy*, *15*(Suppl 3), S2. https://doi.org/10.1186/ar4174

Curtis, M. J., Alexander, S. P. H., Cirino, G., George, C. H., Kendall, D. A., Insel, P. A., Izzo, A. A., Ji, Y., Panettieri, R. A., Patel, H. H., Sobey, C. G., Stanford, S. C., Stanley, P., Stefanska, B., Stephens, G. J., Teixeira, M. M., Vergnolle, N., & Ahluwalia, A. (2022). Planning experiments: Updated guidance on experimental design and analysis and their reporting III. *British Journal of Pharmacology*, *179*, 3907–3913. https://doi.org/10.1111/bph.15868

Cuzick, J., Otto, F., Baron, J. A., Brown, P. H., Burn, J., Greenwald, P., Jankowski, J., La Vecchia, C., Meyskens, F., Senn, H. J., & Thun, M. (2009). Aspirin and non-steroidal anti-inflammatory drugs for cancer prevention: An international consensus statement. *The Lancet Oncology*, *10*, 501–507. https://doi.org/10.1016/S1470-2045(09)70035-X

De, R., Mazumder, S., Sarkar, S., Debsharma, S., Siddiqui, A. A., Saha, S. J., Banerjee, C., Nag, S., Saha, D., & Bandyopadhyay, U. (2017). Acute mental stress induces mitochondrial bioenergetic crisis and hyperfission along with aberrant mitophagy in the gut mucosa in rodent model of stress-related mucosal disease. *Free Radical Biology & Medicine*, *113*, 424–438. https://doi.org/10.1016/j.freeradbiomed.2017.10.009

Dey, S., Mazumder, S., Siddiqui, A. A., Iqbal, M. S., Banerjee, C., Sarkar, S., De, R., Goyal, M., Bindu, S., & Bandyopadhyay, U. (2014). Association of heme oxygenase 1 with the restoration of liver function after damage in murine malaria by *Plasmodium yoelii*. *Infection and Immunity*, *82*, 3113–3126. https://doi.org/10.1128/IAI.01598-14

Dikalova, A. E., Pandey, A., Xiao, L., Arslanbaeva, L., Sidorova, T., Lopez, M. G., Billings, F. T., Verdin, E., Auwerx, J., Harrison, D. G., & Dikalov, S. I. (2020). Mitochondrial deacetylase Sirt3 reduces vascular dysfunction and hypertension while Sirt3 depletion in essential hypertension is linked to vascular inflammation and oxidative stress. *Circulation Research*, *126*, 439–452. https://doi.org/10.1161/CIRCRESAHA.119.315767

Dittenhafer-Reed, K. E., Richards, A. L., Fan, J., Smallegan, M. J., Fotuhi Siahpirani, A., Kemmerer, Z. A., Prolla, T. A., Roy, S., Coon, J. J., & Denu, J. M. (2015). SIRT3 mediates multi-tissue coupling for metabolic fuel switching. *Cell Metabolism*, *21*, 637–646. https://doi.org/10.1016/j.cmet.2015.03.007

Eusebi, L. H., Rabitti, S., Artesiani, M. L., Gelli, D., Montagnani, M., Zagari, R. M., & Bazzoli, F. (2017). Proton pump inhibitors: Risks of long-term use. *Journal of Gastroenterology and Hepatology*, *32*, 1295–1302. https://doi.org/10.1111/jgh.13737

Fasano, C., Disciglio, V., Bertora, S., Lepore Signorile, M., & Simone, C. (2019). FOXO3a from the nucleus to the mitochondria: A round trip in cellular stress response. *Cell*, *8*(9), 1110.

Ghori, S. S., Amer, M. F., & Siddiqa, S. (2016). Antiulcer potential of *Ficus dalhousiae* stem bark methanolic extract in albino rats. *Indo American Journal of Pharmaceutical Sciences*, *3*(10), 1096–1101.

Gurpinar, E., Grizzle, W. E., & Piazza, G. A. (2013). COX-independent mechanisms of cancer chemoprevention by anti-inflammatory drugs.

Frontiers in Oncology, *3*, 181. https://doi.org/10.3389/fonc.2013.00181

Gurpinar, E., Grizzle, W. E., & Piazza, G. A. (2014). NSAIDs inhibit tumorigenesis, but how? *Clinical Cancer Research*, *20*, 1104–1113. https://doi.org/10.1158/1078-0432.CCR-13-1573

Histamine type-2 receptor antagonists (H2 blockers). (2018). In *LiverTox: Clinical and research information on drug-induced liver injury*. National Institute of Diabetes and Digestive and Kidney Diseases.

Kazberuk, A., Zareba, I., Palka, J., & Surazynski, A. (2020). A novel plausible mechanism of NSAIDs-induced apoptosis in cancer cells: The implication of proline oxidase and peroxisome proliferator-activated receptor. *Pharmacological Reports*, *72*, 1152–1160. https://doi.org/10.1007/s43440-020-00140-z

Khoo, B. L., Grenci, G., Lim, J. S. Y., Lim, Y. P., Fong, J., Yeap, W. H., Bin Lim, S., Chua, S. L., Wong, S. C., Yap, Y. S., Lee, S. C., Lim, C. T., & Han, J. (2019). Low-dose anti-inflammatory combinatorial therapy reduced cancer stem cell formation in patient-derived preclinical models for tumour relapse prevention. *British Journal of Cancer*, *120*, 407–423. https://doi.org/10.1038/s41416-018-0301-9

Kim, H. S., Patel, K., Muldoon-Jacobs, K., Bisht, K. S., Aykin-Burns, N., Pennington, J. D., van der Meer, R., Nguyen, P., Savage, J., Owens, K. M., Vassilopoulos, A., Ozden, O., Park, S. H., Singh, K. K., Abdulkadir, S. A., Spitz, D. R., Deng, C. X., & Gius, D. (2010). SIRT3 is a mitochondria-localized tumor suppressor required for maintenance of mitochondrial integrity and metabolism during stress. *Cancer Cell*, *17*, 41–52. https://doi.org/10.1016/j.ccr.2009.11.023

Kim, Y., & Park, C. W. (2019). Mechanisms of adiponectin action: Implication of adiponectin receptor agonism in diabetic kidney disease. *International Journal of Molecular Sciences*, *20*, 1782. https://doi.org/10.3390/ijms20071782

Kincaid, B., & Bossy-Wetzel, E. (2013). Forever young: SIRT3 a shield against mitochondrial meltdown, aging, and neurodegeneration. *Frontiers in Aging Neuroscience*, *5*, 48. https://doi.org/10.3389/fnagi.2013.00048

Kolawole, O. R., & Kashfi, K. (2022). NSAIDs and cancer resolution: New paradigms beyond cyclooxygenase. *International Journal of Molecular Sciences*, *23*, 1432. https://doi.org/10.3390/ijms23031432

Kosgei, V. J., Coelho, D., Gueant-Rodriguez, R. M., & Gueant, J. L. (2020). Sirt1-PPARS cross-talk in complex metabolic diseases and inherited disorders of the one carbon metabolism. *Cell*, *9*, 1882. https://doi.org/10.3390/cells9081882

Krause, M. M., Brand, M. D., Krauss, S., Meisel, C., Vergin, H., Burmester, G. R., & Buttgereit, F. (2003). Nonsteroidal antiinflammatory drugs and a selective cyclooxygenase 2 inhibitor uncouple mitochondria in intact cells. *Arthritis and Rheumatism*, *48*, 1438–1444. https://doi.org/10.1002/art.10969

Kumar, R. (2016). Repositioning of non-steroidal anti inflammatory drug (NSAIDs) for cancer treatment: Promises and challenges. *Journal of Nanomedicine & Nanotechnology*, *7*, 1000e140. https://doi.org/10.4172/2157-7439.1000e140

Li, H., Handsaker, B., Wysoker, A., Fennell, T., Ruan, J., Homer, N., Marth, G., Abecasis, G., Durbin, R., & Subgroup, G. P. D. P. (2009). The sequence alignment/map format and SAMtools. *Bioinformatics*, *25*, 2078–2079. https://doi.org/10.1093/bioinformatics/btp352

Li, L., Hu, M., Wang, T., Chen, H., & Xu, L. (2019). Repositioning aspirin to treat lung and breast cancers and overcome acquired resistance to targeted therapy. *Frontiers in Oncology*, *9*, 1503. https://doi.org/10.3389/fonc.2019.01503

Liao, Y., Smyth, G. K., & Shi, W. (2014). featureCounts: An efficient general purpose program for assigning sequence reads to genomic features. *Bioinformatics*, *30*, 923–930. https://doi.org/10.1093/bioinformatics/btt656

Liggett, J. L., Zhang, X., Eling, T. E., & Baek, S. J. (2014). Anti-tumor activity of non-steroidal anti-inflammatory drugs: Cyclooxygenase-independent targets. *Cancer Letters*, *346*, 217–224. https://doi.org/10.1016/j.canlet.2014.01.021

Lilley, E., Stanford, S. C., Kendall, D. E., Alexander, S. P. H., Cirino, G., Docherty, J. R., George, C. H., Insel, P. A., Izzo, A. A., Ji, Y., Panettieri, R. A., Sobey, C. G., Stefanska, B., Stephens, G., Teixeira, M. M., & Ahluwalia, A. (2020). ARRIVE 2.0 and the British Journal of Pharmacology: Updated guidance for 2020. *British Journal of Pharmacology*, *177*, 3611–3616. https://doi.org/10.1111/bph.15178

Liu, J., Li, D., Zhang, T., Tong, Q., Ye, R. D., & Lin, L. (2017). SIRT3 protects hepatocytes from oxidative injury by enhancing ROS scavenging and mitochondrial integrity. *Cell Death & Disease*, *8*, e3158. https://doi.org/10.1038/cddis.2017.564

Liu, Q., Zhang, D., Hu, D., Zhou, X., & Zhou, Y. (2018). The role of mitochondria in NLRP3 inflammasome activation. *Molecular Immunology*, *103*, 115–124. https://doi.org/10.1016/j.molimm.2018.09.010

Love, M. I., Huber, W., & Anders, S. (2014). Moderated estimation of fold change and dispersion for RNA-seq data with DESeq2. *Genome Biology*, *15*, 550. https://doi.org/10.1186/s13059-014-0550-8

Maffei, M., Desmeules, J., Cereda, J. M., & Hadengue, A. (2007, 1938). Side effects of proton pump inhibitors (PPIs). *Revue Médicale Suisse*, *3*, 1934–1936.

Maharani, B. (2022). Screening methods for the evaluation of antiulcer drugs. In D. G. S. Mageshwaran Lakshmanan & G. M. Raj (Eds.), *Introduction to basics of pharmacology and toxicology* (pp. 371–382). Springer Nature.

Mao, R. W., He, S. P., Lan, J. G., & Zhu, W. Z. (2022). Honokiol ameliorates cisplatin-induced acute kidney injury via inhibition of mitochondrial fission. *British Journal of Pharmacology*, *179*, 3886–3904. https://doi.org/10.1111/bph.15837

Martin, M. (2011). Cutadapt removes adapter sequences from high-throughput sequencing reads. *EMBnet Journal*, *17*, 10–12. https://doi.org/10.14806/ej.17.1.200

Martinsen, T. C., Bergh, K., & Waldum, H. L. (2005). Gastric juice: A barrier against infectious diseases. *Basic & Clinical Pharmacology & Toxicology*, *96*, 94–102. https://doi.org/10.1111/j.1742-7843.2005.pto960202.x

Matsui, H., Shimokawa, O., Kaneko, T., Nagano, Y., Rai, K., & Hyodo, I. (2011). The pathophysiology of non-steroidal anti-inflammatory drug (NSAID)-induced mucosal injuries in stomach and small intestine. *Journal of Clinical Biochemistry and Nutrition*, *48*, 107–111. https://doi.org/10.3164/jcbn.10-79

Mazumder, S., Barman, M., Bandyopadhyay, U., & Bindu, S. (2020). Sirtuins as endogenous regulators of lung fibrosis: A current perspective. *Life Sciences*, *258*, 118201. https://doi.org/10.1016/j.lfs.2020.118201

Mazumder, S., Bindu, S., De, R., Debsharma, S., Pramanik, S., & Bandyopadhyay, U. (2022). Emerging role of mitochondrial DAMPs, aberrant mitochondrial dynamics and anomalous mitophagy in gut mucosal pathogenesis. *Life Sciences*, *305*, 120753. https://doi.org/10.1016/j.lfs.2022.120753

Mazumder, S., De, R., Debsharma, S., Bindu, S., Maity, P., Sarkar, S., Saha, S. J., Siddiqui, A. A., Banerjee, C., Nag, S., Saha, D., Pramanik, S., Mitra, K., & Bandyopadhyay, U. (2019). Indomethacin impairs mitochondrial dynamics by activating the PKCζ-p38-DRP1 pathway and inducing apoptosis in gastric cancer and normal mucosal cells. *The Journal of Biological Chemistry*, *294*, 8238–8258. https://doi.org/10.1074/jbc.RA118.004415

Mazumder, S., De, R., Sarkar, S., Siddiqui, A. A., Saha, S. J., Banerjee, C., Iqbal, M. S., Nag, S., Debsharma, S., & Bandyopadhyay, U. (2016). Selective scavenging of intra-mitochondrial superoxide corrects diclofenac-induced mitochondrial dysfunction and gastric injury: A novel gastroprotective mechanism independent of gastric acid

suppression. *Biochemical Pharmacology*, *121*, 33–51. https://doi.org/10.1016/j.bcp.2016.09.027

Meng, H., Yan, W. Y., Lei, Y. H., Wan, Z., Hou, Y. Y., Sun, L. K., & Zhou, J. P. (2019). SIRT3 regulation of mitochondrial quality control in neurodegenerative diseases. *Frontiers in Aging Neuroscience*, *11*, 313. https://doi.org/10.3389/fnagi.2019.00313

Merksamer, P. I., Liu, Y., He, W., Hirschey, M. D., Chen, D., & Verdin, E. (2013). The sirtuins, oxidative stress and aging: An emerging link. *Aging (Albany NY)*, *5*, 144–150. https://doi.org/10.18632/aging.100544

Morigi, M., Perico, L., Rota, C., Longaretti, L., Conti, S., Rottoli, D., Novelli, R., Remuzzi, G., & Benigni, A. (2015). Sirtuin 3-dependent mitochondrial dynamic improvements protect against acute kidney injury. *The Journal of Clinical Investigation*, *125*, 715–726. https://doi.org/10.1172/JCI77632

Murugasamy, K., Munjal, A., & Sundaresan, N. R. (2022). Emerging roles of SIRT3 in cardiac metabolism. *Frontiers in Cardiovascular Medicine*, *9*, 850340. https://doi.org/10.3389/fcvm.2022.850340

Olmos, Y., Valle, I., Borniquel, S., Tierrez, A., Soria, E., Lamas, S., & Monsalve, M. (2009). Mutual dependence of Foxo3a and PGC-1α in the induction of oxidative stress genes. *The Journal of Biological Chemistry*, *284*, 14476–14484. https://doi.org/10.1074/jbc.M807397200

Ong, C. K., Lirk, P., Tan, C. H., & Seymour, R. A. (2007). An evidence-based update on nonsteroidal anti-inflammatory drugs. *Clinical Medicine & Research*, *5*, 19–34. https://doi.org/10.3121/cmr.2007.698

Ouyang, S., Zhang, Q., Lou, L., Zhu, K., Li, Z., Liu, P., & Zhang, X. (2022). The double-edged sword of SIRT3 in cancer and its therapeutic applications. *Frontiers in Pharmacology*, *13*, 871560. https://doi.org/10.3389/fphar.2022.871560

Peng, M. L., Fu, Y., Wu, C. W., Zhang, Y., Ren, H., & Zhou, S. S. (2022). Signaling pathways related to oxidative stress in diabetic cardiomyopathy. *Frontiers in Endocrinology (Lausanne)*, *13*, 907757. https://doi.org/10.3389/fendo.2022.907757

Percie du Sert, N., Hurst, V., Ahluwalia, A., Alam, S., Avey, M. T., Baker, M., Browne, W. J., Clark, A., Cuthill, I. C., Dirnagl, U., Emerson, M., Garner, P., Holgate, S. T., Howells, D. W., Karp, N. A., Lazic, S. E., Lidster, K., MacCallum, C. J., Macleod, M., … Würbel, H. (2020). The ARRIVE guidelines 2.0: updated guidelines for reporting animal research. *PLoS Biology*, *18*, e3000410.

Pertea, M., Kim, D., Pertea, G. M., Leek, J. T., & Salzberg, S. L. (2016). Transcript-level expression analysis of RNA-seq experiments with HISAT, StringTie and Ballgown. *Nature Protocols*, *11*, 1650–1667. https://doi.org/10.1038/nprot.2016.095

Pillai, V. B., Kanwal, A., Fang, Y. H., Sharp, W. W., Samant, S., Arbiser, J., & Gupta, M. P. (2017). Honokiol, an activator of Sirtuin-3 (SIRT3) preserves mitochondria and protects the heart from doxorubicin-induced cardiomyopathy in mice. *Oncotarget*, *8*, 34082–34098. https://doi.org/10.18632/oncotarget.16133

Pillai, V. B., Samant, S., Sundaresan, N. R., Raghuraman, H., Kim, G., Bonner, M. Y., Arbiser, J. L., Walker, D. I., Jones, D. P., Gius, D., & Gupta, M. P. (2015). Honokiol blocks and reverses cardiac hypertrophy in mice by activating mitochondrial Sirt3. *Nature Communications*, *6*, 6656. https://doi.org/10.1038/ncomms7656

Quan, Y., Park, W., Jin, J., Kim, W., Park, S. K., & Kang, K. P. (2020). Sirtuin 3 activation by honokiol decreases unilateral ureteral obstruction-induced renal inflammation and fibrosis via regulation of mitochondrial dynamics and the renal NF-κB-TGF-β1/Smad signaling pathway. *International Journal of Molecular Sciences*, *21*, 402. https://doi.org/10.3390/ijms21020402

Raghavendran, H. R., Srinivasan, P., & Rekha, S. (2011). Immunomodulatory activity of fucoidan against aspirin-induced gastric mucosal damage in rats. *International Immunopharmacology*, *11*, 157–163. https://doi.org/10.1016/j.intimp.2010.11.002

Ramesh, S., Govindarajulu, M., Lynd, T., Briggs, G., Adamek, D., Jones, E., Heiner, J., Majrashi, M., Moore, T., Amin, R., Suppiramaniam, V., & Dhanasekaran, M. (2018). SIRT3 activator Honokiol attenuates β-Amyloid by modulating amyloidogenic pathway. *PLoS ONE*, *13*, e0190350. https://doi.org/10.1371/journal.pone.0190350

Rock, K. L., & Kono, H. (2008). The inflammatory response to cell death. *Annual Review of Pathology*, *3*, 99–126. https://doi.org/10.1146/annurev.pathmechdis.3.121806.151456

Saha, L. (2015). Role of peroxisome proliferator-activated receptors alpha and gamma in gastric ulcer: An overview of experimental evidences. *World Journal of Gastrointestinal Pharmacology and Therapeutics*, *6*, 120–126. https://doi.org/10.4292/wjgpt.v6.i4.120

Sandoval-Acuna, C., Lopez-Alarcon, C., Aliaga, M. E., & Speisky, H. (2012). Inhibition of mitochondrial complex I by various non-steroidal anti-inflammatory drugs and its protection by quercetin via a coenzyme Q-like action. *Chemico-Biological Interactions*, *199*, 18–28. https://doi.org/10.1016/j.cbi.2012.05.006

Sarrica, A., Kirika, N., Romeo, M., Salmona, M., & Diomede, L. (2018). Safety and toxicology of magnolol and honokiol. *Planta Medica*, *84*, 1151–1164. https://doi.org/10.1055/a-0642-1966

Shannon, P., Markiel, A., Ozier, O., Baliga, N. S., Wang, J. T., Ramage, D., Amin, N., Schwikowski, B., & Ideker, T. (2003). Cytoscape: A software environment for integrated models of biomolecular interaction networks. *Genome Research*, *13*, 2498–2504. https://doi.org/10.1101/gr.1239303

Sherin, F., Gomathy, S., & Antony, S. (2021). Sirtuin3 in neurological disorders. *Current Drug Research Reviews*, *13*, 140–147. https://doi.org/10.2174/2589977512666201207200626

Sostres, C., Gargallo, C. J., & Lanas, A. (2013). Nonsteroidal anti-inflammatory drugs and upper and lower gastrointestinal mucosal damage. *Arthritis Research & Therapy*, *15*(Suppl 3), S3. https://doi.org/10.1186/ar4175

Spinazzi, M., Casarin, A., Pertegato, V., Salviati, L., & Angelini, C. (2012). Assessment of mitochondrial respiratory chain enzymatic activities on tissues and cultured cells. *Nature Protocols*, *7*, 1235–1246. https://doi.org/10.1038/nprot.2012.058

Sun, R., Kang, X., Zhao, Y., Wang, Z., Wang, R., Fu, R., Li, Y., Hu, Y., Wang, Z., Shan, W., Zhou, J., Tian, X., & Yao, J. (2020). Sirtuin 3-mediated deacetylation of acyl-CoA synthetase family member 3 by protocatechuic acid attenuates non-alcoholic fatty liver disease. *British Journal of Pharmacology*, *177*, 4166–4180. https://doi.org/10.1111/bph.15159

Sundaresan, N. R., Gupta, M., Kim, G., Rajamohan, S. B., Isbatan, A., & Gupta, M. P. (2009). Sirt3 blocks the cardiac hypertrophic response by augmenting Foxo3a-dependent antioxidant defense mechanisms in mice. *The Journal of Clinical Investigation*, *119*, 2758–2771. https://doi.org/10.1172/JCI39162

Suzuki, Y., Inoue, T., & Ra, C. (2010). NSAIDs, mitochondria and calcium signaling: Special focus on aspirin/salicylates. *Pharmaceuticals (Basel)*, *3*, 1594–1613. https://doi.org/10.3390/ph3051594

Timmons, J., Chang, E. T., Wang, J. Y., & Rao, J. N. (2012). Polyamines and gut mucosal homeostasis. *Journal of Gastrointestinal & Digestive System*, *2*, 001. https://doi.org/10.4172/2161-069X.S7-001

Valavanidis, A., Vlachogianni, T., & Fiotakis, C. (2009). 8-hydroxy-2′-deoxyguanosine (8-OHdG): A critical biomarker of oxidative stress and carcinogenesis. *Journal of Environmental Science and Health. Part C, Environmental Carcinogenesis & Ecotoxicology Reviews*, *27*, 120–139. https://doi.org/10.1080/10590500902885684

Wang, J., Nisar, M., Huang, C., Pan, X., Lin, D., Zheng, G., Jin, H., Chen, D., Tian, N., Huang, Q., Duan, Y., Yan, Y., Wang, K., Wu, C., Hu, J., Zhang, X., & Wang, X. (2018). Small molecule natural compound agonist of SIRT3 as a therapeutic target for the treatment of intervertebral disc degeneration. *Experimental & Molecular Medicine*, *50*, 1–14. https://doi.org/10.1038/s12276-018-0173-3

Wang, J., Zhai, T., & Chen, Y. (2018). Effects of honokiol on CYP450 activity and transporter mRNA expression in type 2 diabetic rats.

International Journal of Molecular Sciences, *19*, 815. https://doi.org/10.3390/ijms19030815

Whittle, B. J. (2000). COX-1 and COX-2 products in the gut: Therapeutic impact of COX-2 inhibitors. *Gut*, *47*, 320–325. https://doi.org/10.1136/gut.47.3.320

Wu, J., Zeng, Z., Zhang, W., Deng, Z., Wan, Y., Zhang, Y., An, S., Huang, Q., & Chen, Z. (2019). Emerging role of SIRT3 in mitochondrial dysfunction and cardiovascular diseases. *Free Radical Research*, *53*, 139–149. https://doi.org/10.1080/10715762.2018.1549732

Yi, X., Guo, W., Shi, Q., Yang, Y., Zhang, W., Chen, X., Kang, P., Chen, J., Cui, T., Ma, J., Wang, H., Guo, S., Chang, Y., Liu, L., Jian, Z., Wang, L., Xiao, Q., Li, S., Gao, T., & Li, C. (2019). SIRT3-dependent mitochondrial dynamics remodeling contributes to oxidative stress-induced melanocyte degeneration in vitiligo. *Theranostics*, *9*, 1614–1633. https://doi.org/10.7150/thno.30398

Zhang, J., Xiang, H., Liu, J., Chen, Y., He, R. R., & Liu, B. (2020). Mitochondrial Sirtuin 3: New emerging biological function and therapeutic target. *Theranostics*, *10*, 8315–8342. https://doi.org/10.7150/thno.45922

SUPPORTING INFORMATION

Additional supporting information can be found online in the Supporting Information section at the end of this article.

How to cite this article: Debsharma, S., Pramanik, S., Bindu, S., Mazumder, S., Das, T., Saha, D., De, R., Nag, S., Banerjee, C., Siddiqui, A. A., Ghosh, Z., & Bandyopadhyay, U. (2023). Honokiol, an inducer of sirtuin-3, protects against non-steroidal anti-inflammatory drug-induced gastric mucosal mitochondrial pathology, apoptosis and inflammatory tissue injury. *British Journal of Pharmacology*, *180*(18), 2317–2340. https://doi.org/10.1111/bph.16070

iScience

CellPress
OPEN ACCESS

Article

NSAID targets SIRT3 to trigger mitochondrial dysfunction and gastric cancer cell death

Subhashis Debsharma,[1] Saikat Pramanik,[1] Samik Bindu,[2] Somnath Mazumder,[3] Troyee Das,[4] Uttam Pal,[5] Debanjan Saha,[1] Rudranil De,[6] Shiladitya Nag,[1] Chinmoy Banerjee,[1] Nakul Chandra Maiti,[5] Zhumur Ghosh,[4] and Uday Bandyopadhyay[1,7,8,*]

SUMMARY

Gastric cancer (GC) is a deadly malignancy that demands effective therapeutic intervention capitalizing unique drug target/s. Here, we report that indomethacin, a cyclooxygenase non-selective non-steroidal anti-inflammatory drug, arrests GC cell growth by targeting mitochondrial deacetylase Sirtuin 3 (SIRT3). Interaction study revealed that indomethacin competitively inhibited SIRT3 by binding to nicotinamide adenine dinucleotide (NAD)-binding site. The Cancer Genome Atlas data meta-analysis indicated poor prognosis associated with high SIRT3 expression in GC. Further, transcriptome sequencing data of human gastric adenocarcinoma cells revealed that indomethacin treatment severely downregulated SIRT3. Indomethacin-induced SIRT3 downregulation augmented SOD2 and OGG1 acetylation, leading to mitochondrial redox dyshomeostasis, mtDNA damage, respiratory chain failure, bioenergetic crisis, mitochondrial fragmentation, and apoptosis via blocking the AMPK/PGC1α/SIRT3 axis. Indomethacin also downregulated SIRT3 regulators ERRα and PGC1α. Further, SIRT3 knockdown aggravated indomethacin-induced mitochondrial dysfunction as well as blocked cell-cycle progression to increase cell death. Thus, we reveal how indomethacin induces GC cell death by disrupting SIRT3 signaling.

INTRODUCTION

Gastric cancer (GC) is the 5th most commonly (5.6%) diagnosed cancer and 4th most leading (7.7%) cause of cancer deaths[1] with a low 5-year overall survival (OS) rate.[2] Despite much advances in experimental and clinical anti-cancer research, treatment options for advanced-stage GC are still inadequate owing to the molecular heterogeneity and complex pathogenesis.[3] Thus, precisely understanding the pathological basis along with identifying potential anti-GC strategies is warranted. Further, rampantly escalating anti-neoplastic drug resistance in gastric malignancies alarmingly underscores the urgency for identifying convenient druggable targets as well as associated low-cost therapeutic options/drugs which can also tame down the financial burden of expensive immunotherapy modalities. Repurposing of already Food and Drug Administration (FDA)-approved drugs as effective neo-adjuvant anti-cancer agents is therefore increasingly exploited to overcome anti-cancer multidrug resistance as well as in cancer stem cell therapeutics. Contextually, non-steroidal anti-inflammatory drugs (NSAIDs) have emerged, of late, as promising anti-neoplastic agents against diverse high-risk malignancies.[4–7]

Mitochondrial DNAs (mtDNAs) in cancer cells are highly susceptible to oxidative genotoxic stress by anti-cancer drugs.[8] Contextually, 8-oxoguanine DNA glycosylase (OGG1) and superoxide dismutase 2 (SOD2), the major mitochondrial proteins mitigating oxidative damage, are regulated by deacetylation-dependent stabilization.[9] Further, diverse proteins involved in glycolysis, tricarboxylic acid (TCA) cycle, lipid and amino acid metabolism, and redox homeostasis as well as regulators of mitochondrial biogenesis, dynamics, mitochondrial permeability transition pore opening, and components of electron transport chain (ETC) are also regulated by deacetylation.[10] This highlights the importance of deacetylation as a crucial regulator of cellular pathophysiology. In this regard, longevity-promoting NAD^+-dependent mitochondrial deacetylase sirtuin 3 (SIRT3), popularly referred to as the "*guardian of mitochondria*," is critically implicated in myriad diseases including cancer.[11] Although toxic effects of NSAIDs in cancer cells were suggested,[5,7] it is yet unexplored whether SIRT3 deacetylase is targeted by these age-old wonder drugs in GC cells as a part of their cytotoxic effect, if at all.

[1]Division of Infectious Diseases and Immunology, CSIR-Indian Institute of Chemical Biology, 4 Raja S.C. Mullick Road, Kolkata 700032, India
[2]Department of Zoology, Cooch Behar Panchanan Barma University, Cooch Behar, West Bengal 736101, India
[3]Department of Zoology, Raja Peary Mohan College, 1 Acharya Dhruba Pal Road, Uttarpara, West Bengal 712258, India
[4]Division of Bioinformatics, Bose Institute, EN 80, Sector V, Bidhan Nagar, Kolkata 700091, India
[5]Structural Biology and Bioinformatics, CSIR-Indian Institute of Chemical Biology, 4 Raja S.C. Mullick Road, Kolkata 700032, India
[6]Amity Institute of Biotechnology, Amity University, Kolkata, Plot No: 36, 37 & 38, Major Arterial Road, Action Area II, Kadampukur Village, Newtown, Kolkata 700135, India
[7]Department of Biological Sciences, Bose Institute, Unified Academic Campus, EN 80, Sector V, Bidhan Nagar, Kolkata 700091, West Bengal, India
[8]Lead contact
*Correspondence: ubandyo_1964@yahoo.com
https://doi.org/10.1016/j.isci.2024.109384

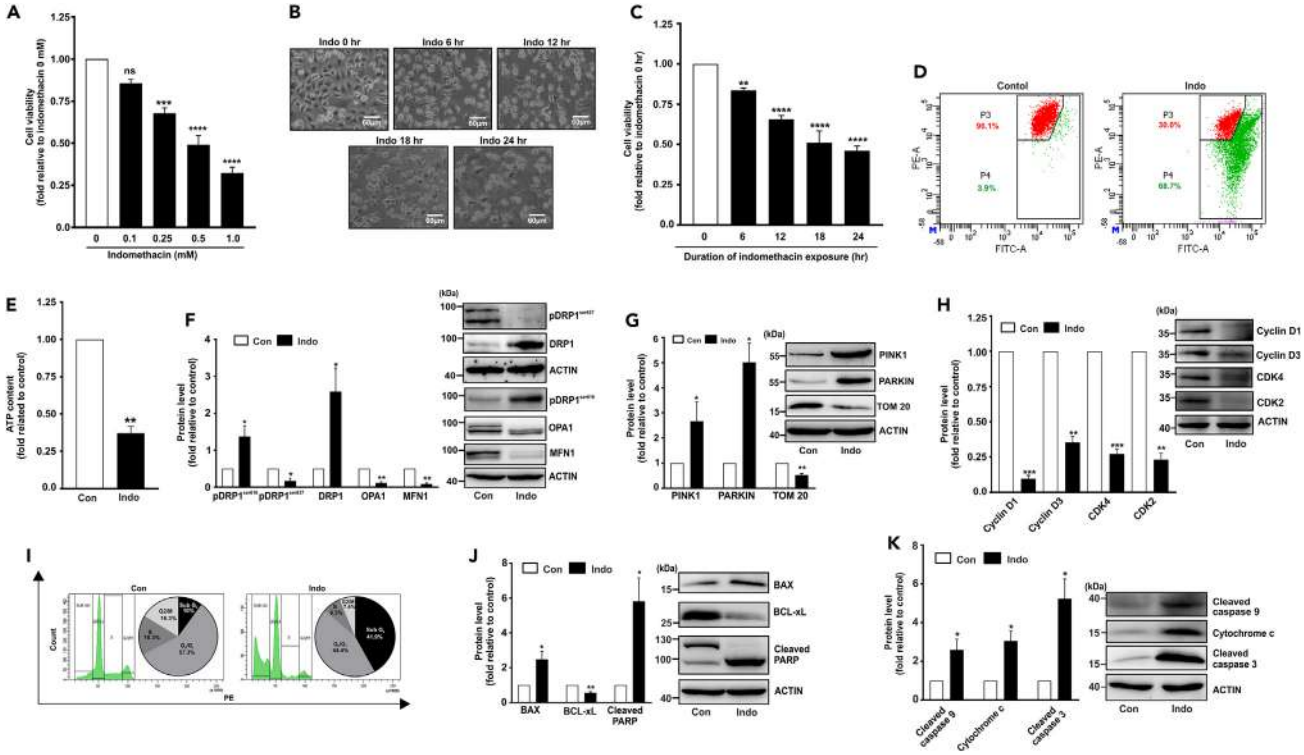

Figure 1. Indomethacin detrimentally affects gastric cancer (AGS) cell viability by inducing mitochondrial dysfunction and cell death

(A) Bar graph showing dose response pattern of indomethacin, checked as AGS cell viability by following MTT reduction.

(B) Phase-contrast micrographs (representative images) of AGS cells treated with indicated indomethacin for the indicated duration (in hours).

(C) Kinetic evaluation of AGS cell viability as measured by MTT reduction assay in indomethacin-treated cells.

(D) Flow cytometric detection of mitochondrial transmembrane potential change ($\Delta\Psi$m) in AGS cells upon indomethacin treatment. 10,000 cells were checked per set and numerical values within the quadrants indicate the percentage of cells therein.

(E) Bar graph showing ATP content in "Con"- and "Indo"-treated AGS cells for 24 h.

(F–H) Immunoblots of pDRP1^{ser637}, DRP1, pDRP1^{ser616}, OPA1, and MFN1 (F), PINK1, PARKIN, and TOM 20 (G), Cyclin D1, Cyclin D3, CDK4, CDK2 (H).

(I) Flow cytometry analysis of cell cycle in "Con"- and "Indo"-treated cells. 10,000 cells were checked per set; pie charts are presented as insets of the respective histograms.

(J and K) Immunoblots of BAX, BCL-xL and cleaved PARP (J), cleaved caspase-9, cytochrome *c*, and cleaved caspase-3 (K) in "con"- and "indo"-treated AGS cells with 0.5 mM indomethacin for 24 h. ACTIN was used as the loading control for all the immunoblots. Representative blot alongside of bar graph (F–H, J–K). (A, C) Data are mean ± SD. **p < 0.01; ***p < 0.001; ****p < 0.0001 versus "indomethacin 0 h" calculated by one-way ANOVA followed by Bonferroni's *post hoc* test. (E–H, J–K), Data are mean ± SD. *p < 0.05; **p < 0.01 versus control calculated by unpaired Student's *t* test with Welch correction. ns: non-significant. The number of independently repeated experiments is 3 in every experiment.

Here, we report with mechanistic details that indomethacin, a known cyclooxygenase (COX) non-selective anti-inflammatory drug, induces human gastric adenocarcinoma (AGS) cell death by negatively targeting both the activity and expression of SIRT3 thereby causing mitochondrial pathology. Moreover, indomethacin was also found to directly suppress SIRT3 regulators, PGC1α and ERRα, as well as affect AMP-activated protein kinase (AMPK) activation to block the AMPK-PGC1α-SIRT3 signaling axis. This study certainly provides novel therapeutic insights into indomethacin-based anti-neoplastic treatment modalities wherein targeted SIRT3 inhibition can be strategically exploited to optimize the benefits toward anti-cancer therapeutics.

RESULTS

Indomethacin triggers GC cell death by inflicting mitochondrial pathology

Indomethacin was found to induce GC cell death in both dose- and time-dependent manner (Figures 1A–1C). We subsequently ventured to explore the detailed mechanism through which it induces GC cell death. As mitochondrial integrity is essential for maintaining cellular health, we immediately checked mitochondrial functional parameters. Contextually, mitochondrial dysfunction was clearly evident from significant mitochondrial depolarization (Figure 1D) and ATP depletion in indomethacin-treated AGS cells (Figure 1E). Next, we checked mitochondrial dynamics and quality control as mitochondrial fission-fusion homeostasis is essential for maintaining cellular metabolic integrity. Interestingly, upon indomethacin treatment significant upregulation of fissogenic regulators such as phospho-DRP1^{ser616} and total DRP1 and depletion of fusogenic mediators including OPA1 and MFN1 as well as phospho-DRP1^{ser637} were observed indicating that mitochondrial dynamics

trajected more toward fission (Figure 1F). To check whether this hyperfission is associated with mitophagy, we followed the protein expression profiles of key mitophagy regulators like PINK1 and PARKIN. To this extent, upregulation of PINK1 and PARKIN clearly indicated elevation of mitophagy upon indomethacin treatment (Figure 1G). Moreover, reduction of TOM20 expression also validated the depletion of mitochondrial copy number as a logical consequence of elevated mitophagy (Figure 1G). Further, we evaluated cell-cycle parameters to understand the impact of mitochondrial dysfunction on cell proliferation. In this regard, indomethacin-induced mitochondrial dysfunction was found to be associated with altered expression of crucial components of cell cycle (Figure 1H). Indomethacin treatment drastically reduced the expression of CDK4, CDK2, cyclin D1, and cyclin D3 implying the suppressive effect of indomethacin on AGS cell-cycle progression. Flow cytometry analysis further revealed the overall impact of indomethacin on the different stages of cell cycle wherein it was clearly evident that there was a significant elevation in the sub-G_0 population along with a considerable reduction in the S and G_2/M phase population in the indomethacin-treated cells (Figure 1I). Finally, it was observed that indomethacin triggered the activation of apoptosis as evident from the elevation of Bcl-2 associated X-protein (BAX) and poly (ADP-ribose) polymerase (PARP) cleavage but depletion of BCL-xL (Figure 1J). Direct mitochondrial involvement, via activation of intrinsic apoptosis, was reflected as elevation of cleaved caspase-9 and caspase-3 as well as cytochrome *c* (Figure 1K).

Indomethacin inhibited mitochondrial deacetylase SIRT3 and interacted with the NAD-binding site

As indomethacin induces mitochondrial dysfunction and it has myriad COX-independent effects, we zoomed into the intricacies of mitochondrial metabolism and checked whether indomethacin affects the function of SIRT3, the guardian of mitochondria that regulates several aspects of mitochondrial functions by virtue of its deacetylase activity. By *in silico* screening, we primarily checked whether indomethacin at all interacts with SIRT3 using accurate molecular docking. Thermodynamic stability of SIRT3-indomethacin complex and binding free energy of indomethacin were obtained by screening against SIRT3 conformers using molecular docking studies using a stochastic algorithm (randomly screening through several possible configurations and repeating the process until convergence is achieved). 31 crystal structures (retrieved 1 Sept 2022) of SIRT3 (UniProtKB: SIR3_HUMAN) were obtained (Table S1) from the Protein Data Bank (PDB) or the PDB-REDO repositories.[12] Based on the model qualities (according to the Worldwide Protein Data Bank [wwPDB] validation report available at the PDB website), 22 crystal structures with good geometries and electron density map fitting were selected for docking studies with indomethacin (Table S2). Indomethacin indeed appeared to be a potent ligand with fairly low binding energy (−10.06 kcal/mol) with SIRT3 (Figure S1; Table S2). Mean binding energy of indomethacin across different conformers of SIRT3 was found to be -8.43 ± 0.89 kcal/mol, indicating a strong interaction with a binding dissociation constant of 1.77 ± 2.8 μM. Computed binding energy for the control ligands, 5-bromo resveratrol (PDB ID: BVB in 4C7B) and (S)-selisistat (PDB ID: OCZ in 4BV3), was found to be −6.21 kcal/mol and −9.23 kcal/mol, respectively. Thus, indomethacin binding with SIRT3 is better than BVB and comparable to OCZ. However, the binding site of indomethacin does not overlap with that of BVB or OCZ (Figure S2). Based on the clustering of binding patterns, most probable binding modes for indomethacin are presented (Figure S1). When compared with NAD binding (Figure S2), indomethacin binding indicates competitive mode of interaction with NAD because of binding-site overlap. Binding energies for NAD and ADP-D-ribose are −10.14 kcal/mol and −9.07 kcal/mol, respectively, which are similar to binding energy of indomethacin suggesting plausible competition for binding site between indomethacin and NAD.

Molecular dynamics simulation was further performed with four low-energy/high-frequency-bound conformers (Figure S1) of indomethacin as obtained by docking to probe the stability of the binding modes and understand the specific interactions involved. Apo- and NAD-bound holo-conformations of SIRT3 were studied as controls. Snapshots of protein/protein-ligand complex structures at 2.4 ns intervals and superimposed for comparison are presented (Figures 2A–2F) for qualitative understanding of the stability of apo-, holo-, and indomethacin-bound complexes. Further, quantitative depiction is presented (Figures 2G–2I) in terms of time-correlated or time-averaged standard deviations (root-mean-square deviation [RMSD] and root-mean-square fluctuation [RMSF], respectively). Apoprotein as well as the NAD-bound holoprotein shows impeccable structural integrity in water. Initial 2–3 Å increase in RMSD is observed due to the relaxation of crystal structure in solvent environment (Figure 2G). Once equilibrated, both the apoprotein and holoprotein maintained a stable conformation throughout the simulation timescale. Out of the four probable complexes of indomethacin, 5z94 complex was the most stable followed by 3glt complex. In the case of the 4bvf complex, the ligand moved to the distal end of the NAD-binding tunnel and attained a stable conformation. However, in 4jt8, the ligand dissociated from the binding site (marked by sudden increase in RMSD at around 80 ns [Figure 2H]). No stable interaction could be observed in the rest of the simulation trajectory although the ligand remained bound to the surface of the enzyme. Ligand binding in all the cases was found to induce perturbations in the helical module in the zinc-binding domain (Figure S3). This is also reflected in the increased C_α RMSF (Figure 2I).

Further, interacting amino acid residues and the important functional groups of indomethacin were identified by analyzing the protein ligand contacts over the simulation trajectory (Figures S4 and S5). Significant SIRT3-ligand contacts were observed at least 20% of times during the simulation for three most stable conformers (5z94, 3glt, and 4bvf) (Figures 2J–2L). In 5z94 and 3glt, binding occurs near the catalytic His248 residue with similar interactions. His248 can form a hydrogen bond with the amide carbonyl (57%) or a pi-stacking interaction (42%) with the chlorobenzene moiety of indomethacin. Phe180 and Phe294 are also involved in pi-stacking interaction with the indole ring (44%) or chlorobenzene (29%) of indomethacin. Arg158 is an important NAD-binding residue that was found to form a salt bridge (24%) with the carboxylate group of indomethacin. It can also form a cation-pi interaction (23%) with the chlorobenzene group. The carboxylate group of indomethacin was found to interact with Glu177 of the protein via two water bridges (36%). Gly295 can stabilize the methoxy group by donating a hydrogen bond (38%). Apart from these specific interactions, Phe157, Phe294, and Ile230 formed hydrophobic contacts with chlorobenzene,

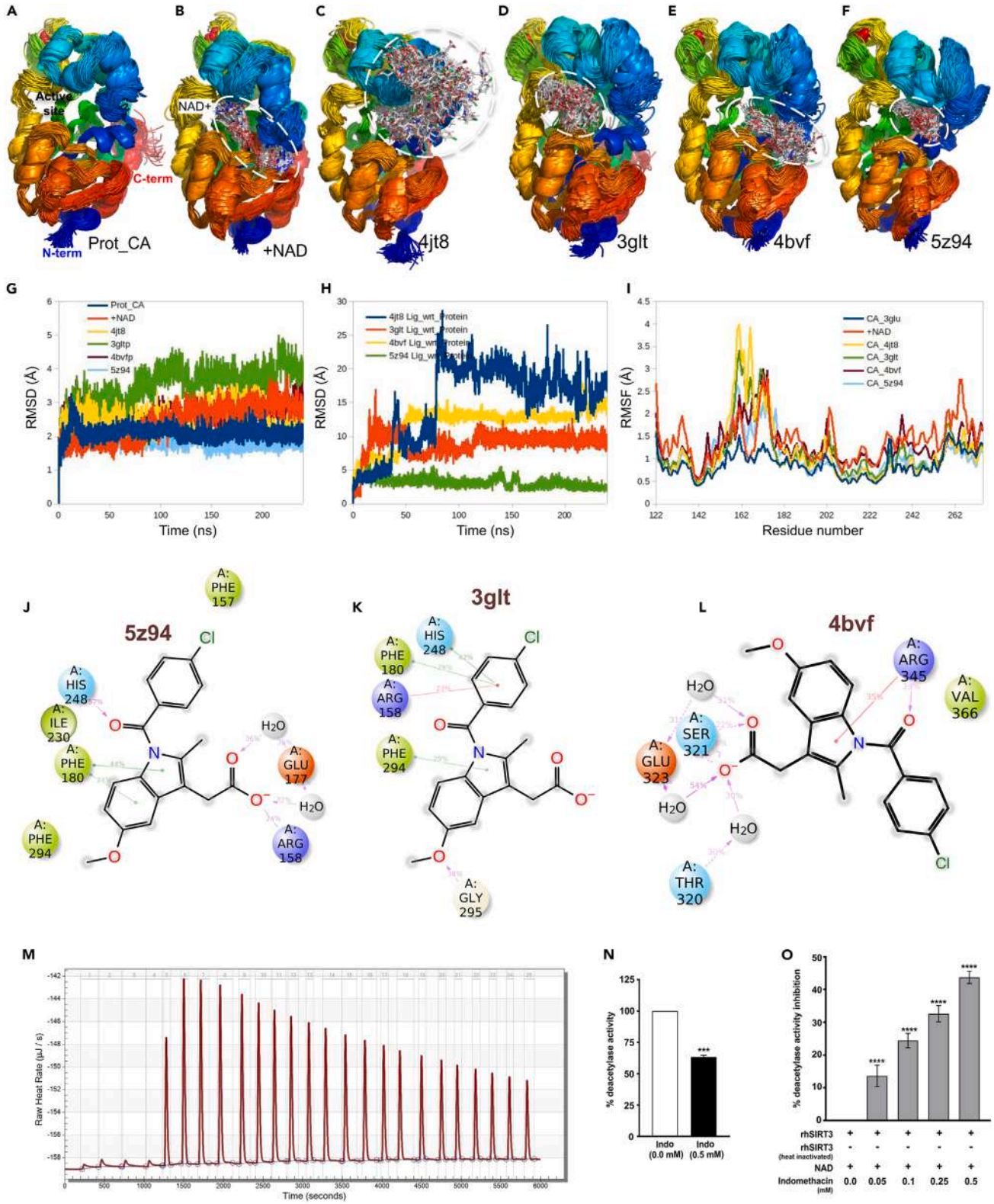

Figure 2. Indomethacin inhibits deacetylase activity of SIRT3 and shows competitive inhibition by binding to NAD-binding site

(A) Apoenzyme (PDB: 3glu) control in SPC water under OPLS-AA force field for 240 ns. 100 snapshots at 2.4 ns intervals are superimposed. Protein is shown in ribbon representation and N-terminal to C-terminal is colored in rainbow (blue to red). Active site is labeled.

Figure 2. *Continued*

(B) NAD^+-bound holoenzyme (PDB: 4bv3) control. NAD^+ in white stick model is labeled, and the binding region is encircled with white dashed line.

(C) 4jt8 indomethacin complex. Indomethacin is shown in white stick model, and the binding region is encircled with white dashed line.

(D) 3glt indomethacin complex.

(E) 4bvf indomethacin complex.

(F) 5z94 indomethacin complex.

(G) Protein backbone C_α RMSD for apoenzyme, holoenzyme, and all the indomethacin-bound complexes of apoenzyme with respect to the initial conformations.

(H) RMSD of indomethacin in all the four bound complexes with respect to the initial conformation of the complexes.

(I) Residue-wise fluctuations (RMSFs) in protein backbone for apo, holo, and indomethacin-bound conditions.

(J–L) Time average interaction of indomethacin with sirtuin 3 (5z94, 3glt. 5bvf) as obtained from molecular dynamics simulations. Three possible conformations are shown. 5z94 and 3glt show binding near the active site. His248. 4bvf shows binding in the distal part of NAD^+ binding channel. (J) In 5z94, catalytic His248 forms a hydrogen bond (pink arrow from H donor to acceptor) with the amide carbonyl moiety of indomethacin. Phe180 showed pi-stacking interaction (green lines) with the indole ring of indomethacin. Carboxylate group of indomethacin formed two water bridges through H bonds (pink arrows) with Glu177 and a salt bridge (red/blue line) with the positively charged Arg158. Phe157, Phe294, and Ile230 formed hydrophobic contacts with chlorobenzene, indole, and methoxy moieties, respectively. (K) 3glt shows another stable bound conformation of indomethacin within the active site of the enzyme. In this conformation catalytic His248 forms pi-stacking with chlorobenzene moiety of indomethacin along with Phe180 (green lines). Positively charged Arg158 forms cation-pi interaction (red line) with chlorobenzene. Phe294 forms pi-pi stacking (green line) with the indole moiety of indomethacin. Gly295 forms a hydrogen bond (pink arrow from H donor to acceptor). (L) 4bvf shows yet another stable bound conformation in the distal part of NAD^+ binding tunnel. In this conformation, the carboxylate group of indomethacin forms water bridges with Thr320 and Glu323 and a direct hydrogen bond (pink arrows) with Ser321. Arg345 forms a cation-pi interaction with the indole and an H bond with the amide carbonyl of indomethacin. Val366 forms hydrophobic contacts with chlorobenzene moiety.

(M) Isothermal titration plot for rhSIRT3-indomethacin interaction.

(N) SIRT3 deacetylase activity in mitochondrial extract treated with 0.5 mM indomethacin. Data are mean ± SD. ***$p < 0.001$ versus indomethacin 0 mM calculated by unpaired Student's *t* test with Welch correction.

(O) Dose-dependent inhibition of rhSIRT3 deacetylase activity by indomethacin. Data are mean ± SD. ****$p < 0.0001$ versus indomethacin 0 mM calculated using one-way ANOVA with Bonferroni's *post hoc* test. See also Figures S1–S5.

indole, and methoxy moieties, respectively (Figures 2J and 2K). On the other hand, 4bvf shows a stable bound conformation of indomethacin in the distal part of NAD-binding tunnel (Figure 2L). In this conformation, the carboxylate group of indomethacin forms water bridges with Thr320 and Glu323 and a direct hydrogen bond with Ser321. Arg345 forms a cation-pi interaction with the indole and a hydrogen bond with the amide carbonyl of indomethacin. Val366 forms hydrophobic contacts with chlorobenzene moiety. Thus, the amide carbonyl, indole, carboxylate, chlorobenzene, and the methoxy moiety of indomethacin were found to play significant roles in the interaction with SIRT3. SIRT3-indomethacin interaction, observed *in silico*, was next validated using isothermal calorimetry (ITC). Recombinant human SIRT3 (rhSIRT3) was gradually titrated with indomethacin, and the detectable heat changes were measured using a sensitive micro-calorimeter (Figure 2M). A series of initial indomethacin injections were made wherein the micro-calorimeter measured the heat release. The quantity of heat measured, as depicted in the isotherm, was found to be directly proportional to the amount of rhSIRT3-indomethacin binding (measured in μJ/s). The molar ratio between indomethacin and rhSIRT3 was gradually increased through a series of indomethacin injections whereupon rhSIRT3 got more and more saturated, thereby resulting less binding of indomethacin. Consequently, the heat change (enthalpy) started to decrease which was documented (Figure 2M). Finally, to explore the fate of SIRT3-indomethacin interaction, we measured the deacetylase activity of SIRT3 in the mitochondrial extract from AGS cells treated with indomethacin (used at a dose that triggered mitochondrial pathology and cell death mentioned in the precious data). It was clearly observed that indomethacin significantly reduced the deacetylase activity of SIRT3 (Figure 2N). Further, to check whether indomethacin per se or any of its metabolic by-product causes this SIRT3 inhibition, we directly measured the activity of rhSIRT3 deacetylase in presence/absence of different concentrations of indomethacin. Fluorescence, generated by rhSIRT3 deacetylase-dependent modification of the fluorescent-labeled acetylated substrate peptide, indicated that indomethacin significantly inhibited the deacetylase activity of rhSIRT3 (Figure 2O).

Human dataset mining revealed the prognostic relevance of SIRT3 in GC

Before delving deeper into further exploring the mechanistic basis of indomethacin-SIRT3 interaction and its effect on AGS cells, we checked whether SIRT3 abundance has any direct clinical impact on GC. The Cancer Genome Atlas (TCGA) data for normal and patient-derived stomach adenocarcinom (STAD) samples were analyzed. Difference in SIRT3 expression between primary gastric tumor (n = 415) and normal tissues (n = 34) was followed (Figure 3A). The University of Alabama at Birmingham Cancer data analysis portal (UALCAN) analysis revealed that tumor samples have significantly higher median (40.549 transcript per million) SIRT3 transcripts compared to normal (19.018 transcript per million). Further, we checked the concordance of the gene expression pattern with SIRT3 protein expression. Immunohistochemical archives of representative normal and GC samples in the Human Protein Atlas database (stained with the antibody CAB037142) revealed high expression of SIRT3 in the tumor cells compared to medium expression in the glandular cells (Figure 3B). The representative image of the patient sample, in the figure, indicates intestinal-type GC. Next, UALCAN analysis of SIRT3 expression based on pathological staging of GC revealed that SIRT3 expression is higher in the late-stage tumors implying its plausible association with tumor progression and invasion (Figure 3C). Moreover, high SIRT3 expression was also documented in the various histological subtypes of GC as evident in the TCGA patient data (Figure 3D). Because the predominance of GC varies in the different races, we checked SIRT3 expression in the patient data from Caucasian, African American, and Asian samples and found that, while there is significant difference in SIRT3 expression between normal and tumor

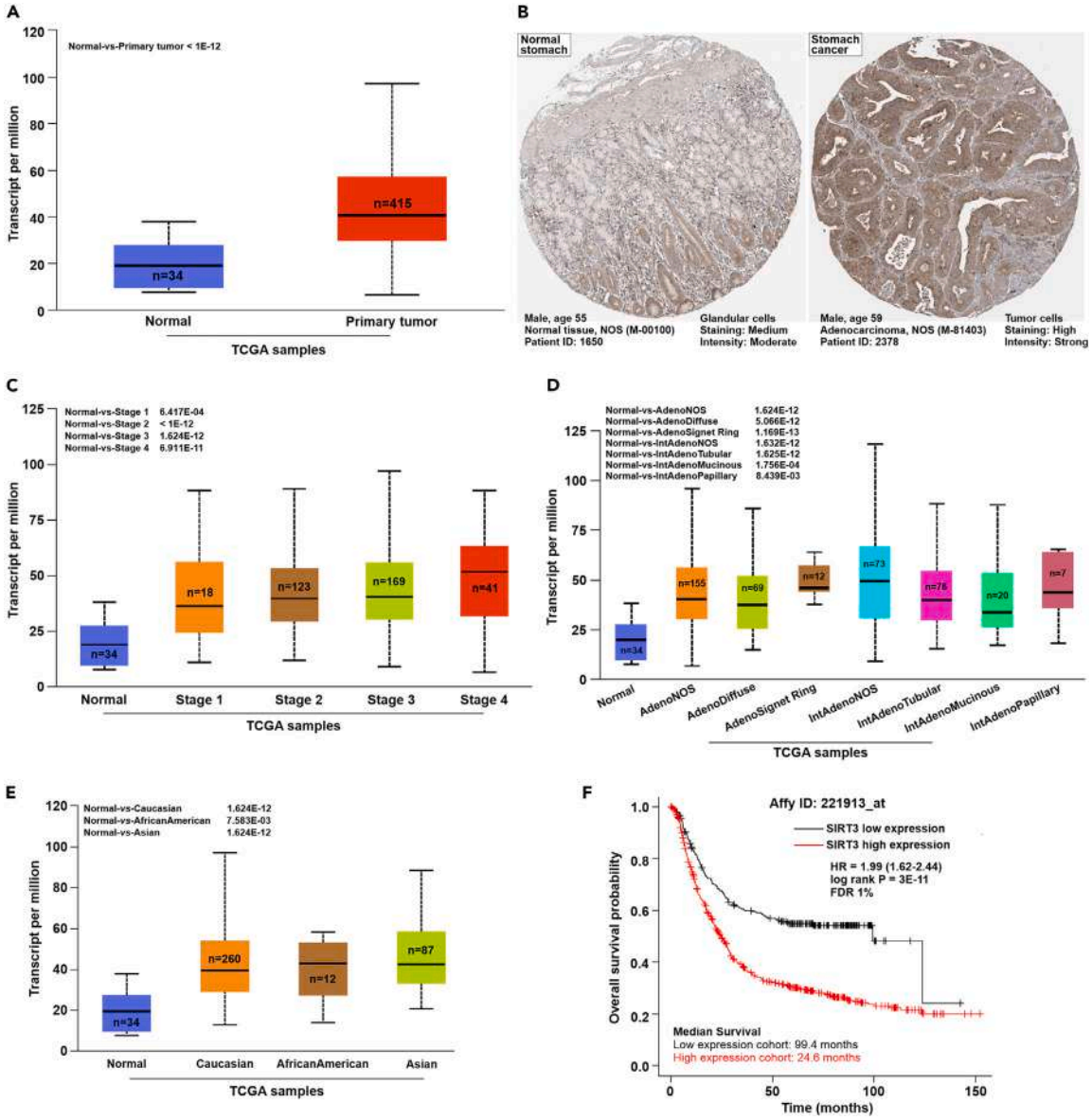

Figure 3. High SIRT3 expression is associated with poor prognosis of GC

(A) UALCAN analysis for the correlation between SIRT3 mRNA expression and human gastric adenocarcinoma; p < 1E-12 for Normal-vs-Primary tumor.

(B) SIRT3 expression in gastric cancer and normal tissues from the Human Protein Atlas (HPA) database. Immunohistochemical staining done with antibody CAB037142.

(C) UALCAN analysis for the correlation between SIRT3 mRNA expression and pathological stages of human gastric adenocarcinoma; N-vs-S1 6.417E-04, N-vs-S2 <1E-12, N-vs-S3 1.624E-12, N-vs-S4 6.911E-11.

(D) UALCAN analysis for the correlation between *Sirt3* mRNA expression and histological subtypes (Adenocarcinoma NOS, Adenocarcinoma Diffuse, Adenocarcinoma SignetRing, Intestinal Adenocarcinoma NOS, Intestinal Adenocarcinoma Tubular, Intestinal Adenocarcinoma Mucinous, Intestinal Adenocarcinoma Papillary) of human gastric adenocarcinoma; *p* 1.62458935193399E-12 for Normal-vs-Adenocarcinoma (NOS), 5.06639175057444E-12 for Normal-vs-Adenocarcinoma (Diffuse), 1.16906484493029E-13 for Normal-vs-Adenocarcinoma (Signet Ring), 1.632471935408 83E-12 for Normal-vs-Intestinal Adenocarcinoma (NOS), 1.6251444634463E-12 for Normal-vs-Intestinal Adenocarcinoma(Tubular), 1.756760E-04 for Normal-vs-Intestinal Adenocarcinoma(Mucinous), 8.439600E-03 for Normal-vs-Intestinal Adenocarcinoma(Papillary).

(E) UALCAN analysis for the correlation between SIRT3 mRNA expression and human races (Caucasian, African American, and Asian); *p* 1.62436730732907E-12 for Normal-vs-Caucasian, 7.583800E-03 for Normal-vs-African American, 1.62447832963153E-12 for Normal-vs-Asian.

(F) Kaplan-Meier survival curve comparing the high and low expressions of SIRT3 (n = 875) in overall survival (OS) checked with mRNA gene chip Affy ID: 221913_at; HR: 1.99 (1.62–2.44), log rank P: 3.0E-11, FDR: 1%.

samples, there was no apparent significant difference between the races implying elevated SIRT3 expression as a general property of gastric malignancies (Figure 3E). All these associations logically warranted to explore the prognostic relevance of elevated SIRT3 transcripts. Kaplan-Meier survival curves indeed revealed that high SIRT3 expression is associated with low median OS of 24.6 months, compared to 99.4 months in low SIRT3 expression (hazard ratio [HR] = 1.99, log rank P = 3e-11) (Figure 3F), thereby suggesting bad prognosis. Cumulatively, TCGA data indicate that SIRT3 expression can be a prognostic indicator of mortality risk in GC.

Transcriptome analysis revealed SIRT3 as a major hub gene targeted by indomethacin to detrimentally affect multiple metabolic pathways in AGS cells

So far, it was found that indomethacin directly inhibited the deacetylated activity of SIRT3. Now we were interested to know whether it only inhibits the activity or it has any effect on the expression of SIRT3 in human GC cells. To check the status of SIRT3 upon indomethacin treatment, high-depth next-generation transcriptome sequencing of control and indomethacin-treated AGS cells was performed for an overall probing of SIRT3 and associated genes as well as signaling pathways/gene expression programs affected by indomethacin. Heatmap (Figure 4A) showing the differentially expressed genes (DEGs), analyzed with a log fold change (FC) cutoff of 1.5 (false discovery rate [FDR] $\leq$0.05), revealed clear separate sample clustering, with 3,984 upregulated and 4,474 downregulated genes in indomethacin-treated cells compared to "control" (File S1A–S1C) (GSE202140). Gene enrichment analysis with IPA (ingenuity pathway analysis) identified gene expression programs among which "Sirtuin signaling pathway" and associated DEGs drew special attention owing to their association with myriad cellular events (Figures 4B and 4C). We subsequently used MCODE[13] plugin in Cytoscape[14] to build the gene interaction network and screened the hub gene/s regulating mitochondrial metabolism and cellular integrity. Notably, SIRT3 appeared as one of the top hub genes controlling myriad signaling pathways. Other crucial regulators of mitochondrial metabolism including ETC complex subunits, SOD, FOXO3/1, voltage-dependent anion channel 1 (VDAC1), mammalian target of rapamycin (MTOR), and nuclear factor κB (NF-κB) subunits were also observed (Figure 4D). IPA-based interactome analysis further indicated that SIRT3 is intricately connected with most of these players. The putative association of SIRT3 with indomethacin-associated GC cell death, as reflected in transcriptome data, fascinated us to delve deeper into the functional aspects of SIRT3. We further zoomed into the heatmaps for checking specific gene expression profiles altered by indomethacin including "mitochondrial central dogma" (Figure 4E), oxidative phosphorylation ("OXPHOS") (Figures 4F–4H), and major arms of cancer metabolism including carbohydrate (Figures 4I and 4J) and fatty acid (Figure 4K) metabolism. Incidentally, majority of the DEGs reflected a significant gross downregulation upon indomethacin treatment thereby reiterating the multidimensional damage caused by indomethacin. Further the data also implied that, being a dominant regulator of cellular metabolism and longevity, loss of SIRT3 during indomethacin treatment was logically associated with activation of myriad subcellular factors and signaling pathways underlying metabolic crisis and cell death.

Downregulation of indomethacin-induced SIRT3 underlies the reduction of ETC complex gene expression, mitochondrial fragmentation, aberrant mitophagy, and cell death via PGC1α/AMPK-dependent signaling

Downregulation of SIRT3, as indicated in sequencing, was validated by RT-qPCR (Figure 5A) followed by evaluation at the protein level to inquire the effect of indomethacin on SIRT3 protein expression. It was found that indomethacin treatment dose-dependently triggered SIRT3 protein depletion (Figure 5B). Before proceeding further, we compared basal SIRT3 expression profile between GC cells and non-malignant gastric cells (Figure 5C). Immunoblot data clearly indicated that SIRT3 expression was significantly higher in the AGS cells compared to human normal cell line Hs738. Further, it was also observed that a much higher concentration of indomethacin was required for reducing the viability of Hs738 cells as well as downregulating SIRT3 expression, thereby substantiating the fact that indomethacin-induced cell death is strongly associated with inherently upregulated SIRT3 levels in GC cells (Figures S6A–S6C) and that indomethacin-induced cytotoxicity is more pronounced and attainable at a much lower concentration in AGS cells compared to normal cells. Moving forward, we observed that, in AGS cells, indomethacin time-dependently reduced the expression of SIRT3 in concurrence with downregulating OGG1, a prime SIRT3 target as well as the principal base excision repair protein correcting mtDNA damage (Figure 5D). Because SIRT3 is a deacetylase, we next checked the functional consequence of SIRT3 depletion on the acetylation status of mitochondrial proteome and specifically its major targets OGG1 and SOD2. Acetylation of mitochondrial proteome (Figure 5E) and specifically that of OGG1 and SOD2 (Figure 5F) were significantly elevated along with profound increase of 8-oxo-dG content in mtDNA (Figure 5G). This was found concurrently with significant reduction of SOD2 enzymatic activity (Figure 5H), thereby suggesting mtDNA damage and concerted downregulation of mitochondrial antioxidant defense. Contextually, it is worth mentioning that Kaplan-Meier survival curves for OGG1-high-expressing groups also indicated a lower median OS of 23.2 months (HR = 1.87, log rank p = 6.7e-12) compared to OGG1-low-expressing groups with 77.2 months (Figure S7), thereby reiterating the prognostic relevance of SIRT3-OGG1 duo in GC.

Because indomethacin-dependent SIRT3 reduction accompanied OGG1 downregulation, ATP depletion, and compromised cell viability, we therefore checked the status of mtDNA-encoded ETC subunits and found downregulation of MT-ND1, MT-ND6, MT-ATP6, MT-CYTB, and MT-CO1 corresponding to complex I, V, III, and IV, respectively, after indomethacin treatment (Table S3). To understand the mechanistic basis of indomethacin-induced SIRT3 depletion, we next checked whether indomethacin targets the upstream transcriptional control on SIRT3 expression as induced by peroxisome proliferator-activated receptor gamma coactivator 1 alpha (PGC1α) and estrogen receptor related receptor α (ERRα). We observed that indomethacin drastically reduced PGC1α and ERRα expression (Figure 5I). The data further indicated that indomethacin also suppressed AMPK activation (Figure 5J), thereby affecting the AMPK/PGC-1α/SIRT3 signaling axis which plausibly operates in a feedback loop.[15]

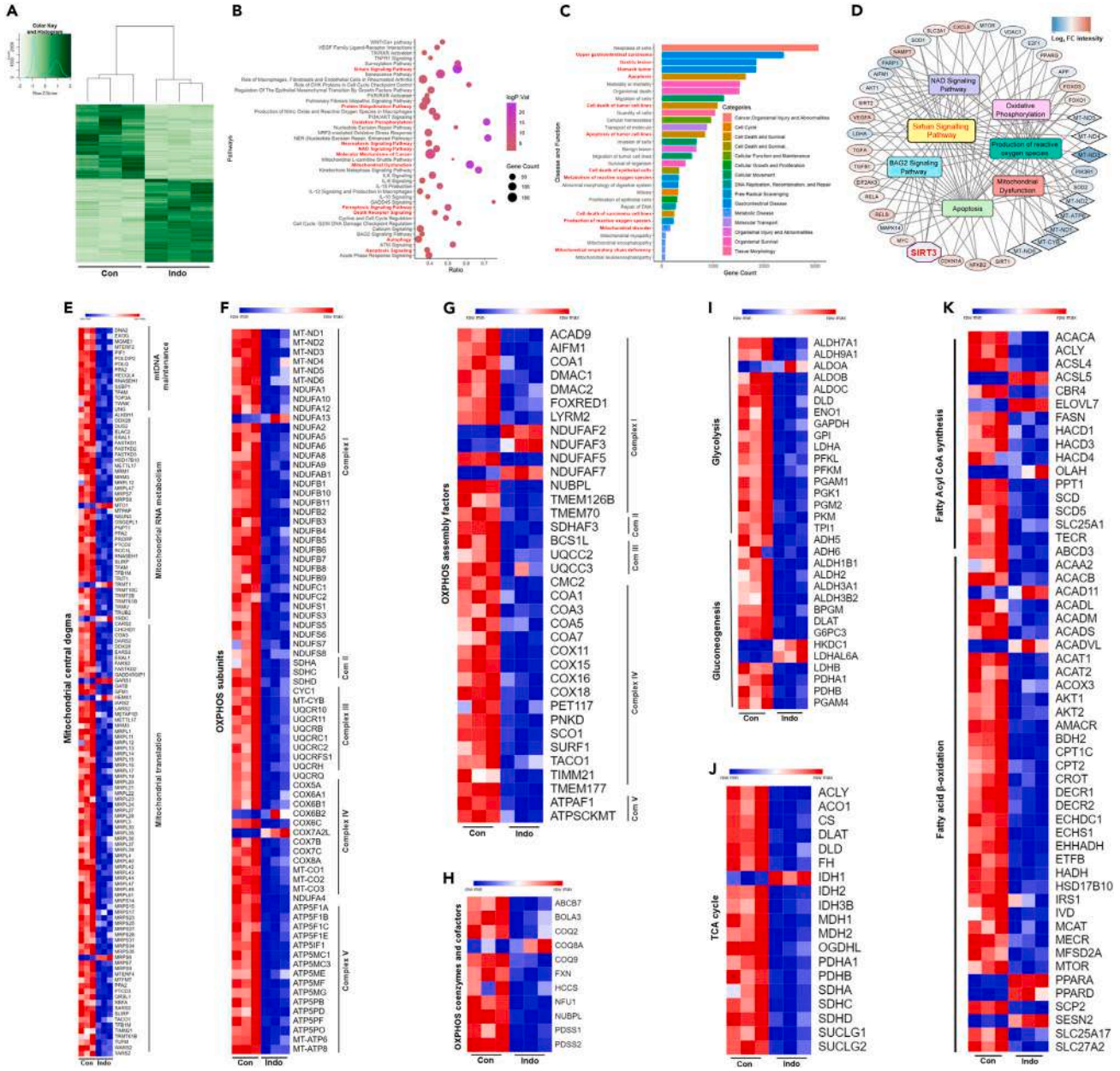

Figure 4. Transcriptome data indicating cellular metabolic crisis and mitochondrial dysfunction by indomethacin in gastric cancer cells

(A) Heatmap shows separate clustering of "Con" and "Indo" (FDR ≤ 0.05). Euclidean distance metric was used while clustering the gene expression data. The expression value of genes analyzed with fold change cutoff of 1.5; color gradient scale with white being highly downregulated to green being highly upregulated.

(B) Dot plot showing enriched canonical pathways. The size of dots represents the proportion of genes involved in the particular signaling/pathway while the range of color indicates Bonferroni corrected p values (-log transformed). The ratio represents the number of genes in fraction with respect to the total number of genes that map to the same pathway.

(C) Bar graph showing the disease and functions enriched in the "Indo" set.

(D) Hub gene network. The expression values of genes are represented with color gradient scale with blue being highly downregulated to red being highly upregulated.

(E–K) Heatmap shows the association of a subset of DEGs with mitochondrial central dogma including "mtDNA maintenance," "mtRNA metabolism." and "mitochondrial translation" (E), OXPHOS subunits including genes for complex I (CI), complex II (CII), complex III (CIII), complex IV (CIV), and complex V (CV) (F), OXPHOS assembly factors including genes for complex I (CI), complex II (CII), complex III (CIII), complex IV (CIV), and complex V (CV) (G), OXPHOS enzymes and cofactors (H), "glycolysis" and "gluconeogenesis" (I), "TCA cycle" (J), "fatty acyl CoA synthesis" and "fatty acid β-oxidation" (K) between "Con" and "Indo" (FDR ≤ 0.05). The expression value of genes analyzed with fold change cutoff of 1.5; color gradient scale with blue: downregulated to red: upregulated (E–K). All sequencing experiments were done in triplicates.

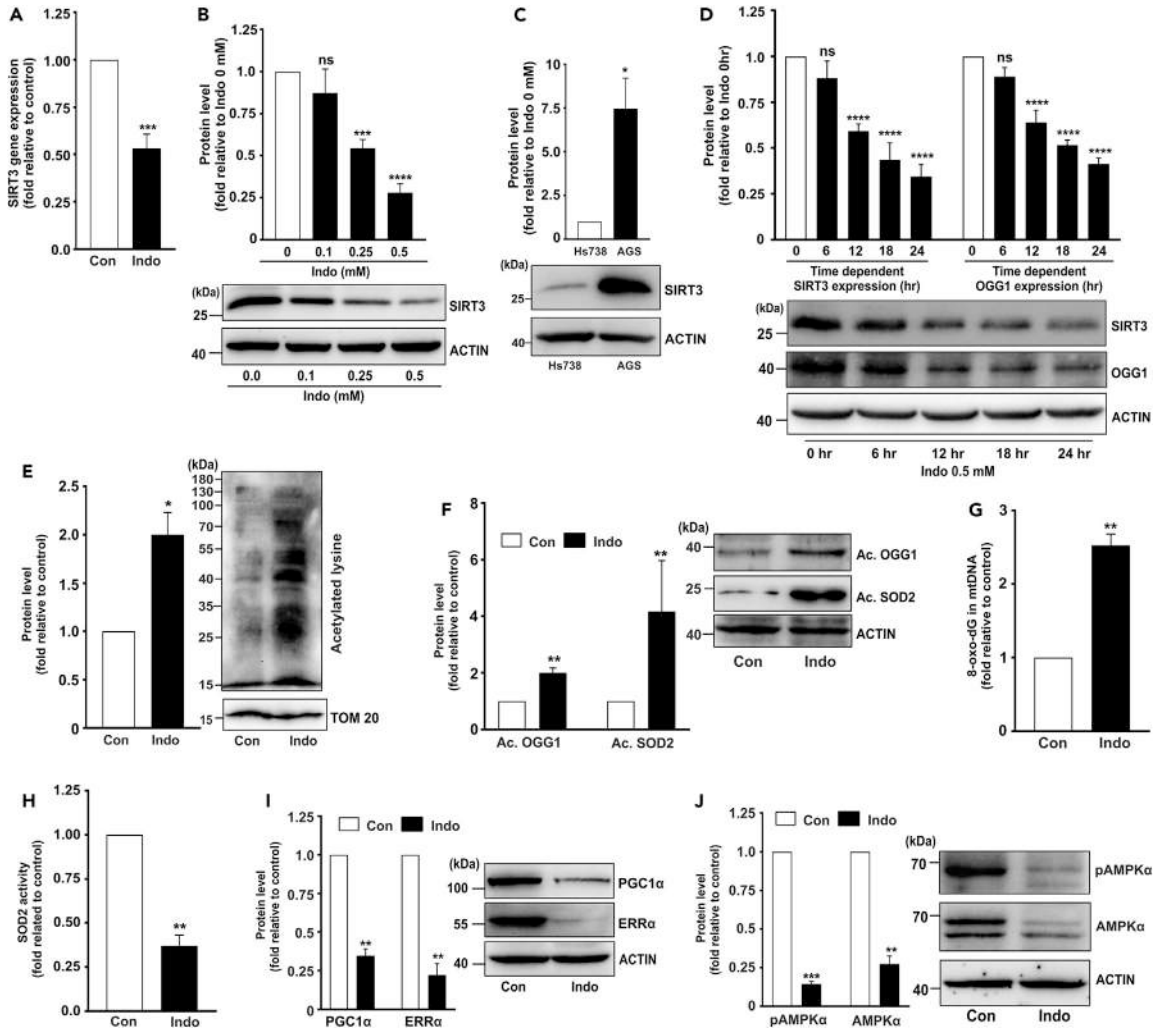

Figure 5. Indomethacin by downregulating SIRT3 reduces mtDNA-encoded ETC complex gene expression and induces mitochondrial hyperfission and cell death

(A) Quantitative RT-PCR for SIRT3 gene expression in control and indomethacin-treated cells; bar graph indicates fold change in gene expression relative to control (after normalization by GAPDH).

(B) Immunoblot of SIRT3 in AGS cells treated with indomethacin at indicated concentrations for 24 h.

(C) Immunoblot of SIRT3 in Hs738 and AGS cells.

(D) Immunoblots of SIRT3 and OGG1 in AGS cells treated with 0.5 mM indomethacin for the indicated duration. ACTIN was used as the loading control (B–D).

(E) Immunoblot of acetylated lysine in the mitochondrial fraction of AGS cells treated with 0.5 mM indomethacin for 24 h. TOM20 was used as the loading control.

(F) Immunoblots of acetylated OGG1 and acetylated SOD2 in AGS cells treated with 0.5 mM indomethacin for 24 h. ACTIN was used as the loading control.

(G) mtDNA damage as measured by 8-oxo-dG ELISA in AGS cells treated with 0.5 mM indomethacin for 24 h.

(H) Mitochondrial SOD2 activity in AGS cells treated with 0.5 mM indomethacin for 24 h.

(I and J) Immunoblots for PGC1α, ERRα (I), pAMPKα and AMPKα (J) in "'Con"- and "Indo"-treated AGS cells. ACTIN was used as the loading control. The number of independent experiments is 3 (A–J). Representative blot below the bar graph (B–D) and alongside the bar graph (E and F; I and J). (A, C, E–J), Data are mean ± SD. *$p < 0.05$; **$p < 0.01$; ***$p < 0.001$ versus control calculated by unpaired Student's *t* test with Welch correction. (B, D) Data are mean ± SD. ***$p < 0.001$; ****$p < 0.0001$ versus "Indo 0 mM (B) or Indo 0 h" (D) calculated by one-way ANOVA followed by Bonferroni's *post hoc* test. ns: non-significant. The number of independently repeated experiments is 3 in every experiment. See also Figures S6 and S7.

SIRT3 knockdown aggravates indomethacin-induced mitochondrial damage and cytopathology

If SIRT3 is so essential for regulating cellular and mitochondrial metabolism, we asked what would be the fate of indomethacin treatment in SIRT3-silenced cells. Further, it would also functionally validate the data so far. Phase-contrast images indicated that SIRT3 knockdown amplified indomethacin-induced cytoarchitectural damage (Figure S8). SIRT3 knockdown intensified indomethacin-induced SIRT3 and OGG1 downregulation (Figure 6A) along with aggravating OGG1 and SOD2 acetylation (Figure 6B). Functional impact of SIRT3 knockdown was observed in flow cytometric data indicating intra-mitochondrial superoxide ion ($O_2^{\cdot-}$) elevation (Figure 6C). Intra-cellular 8-oxo-dG

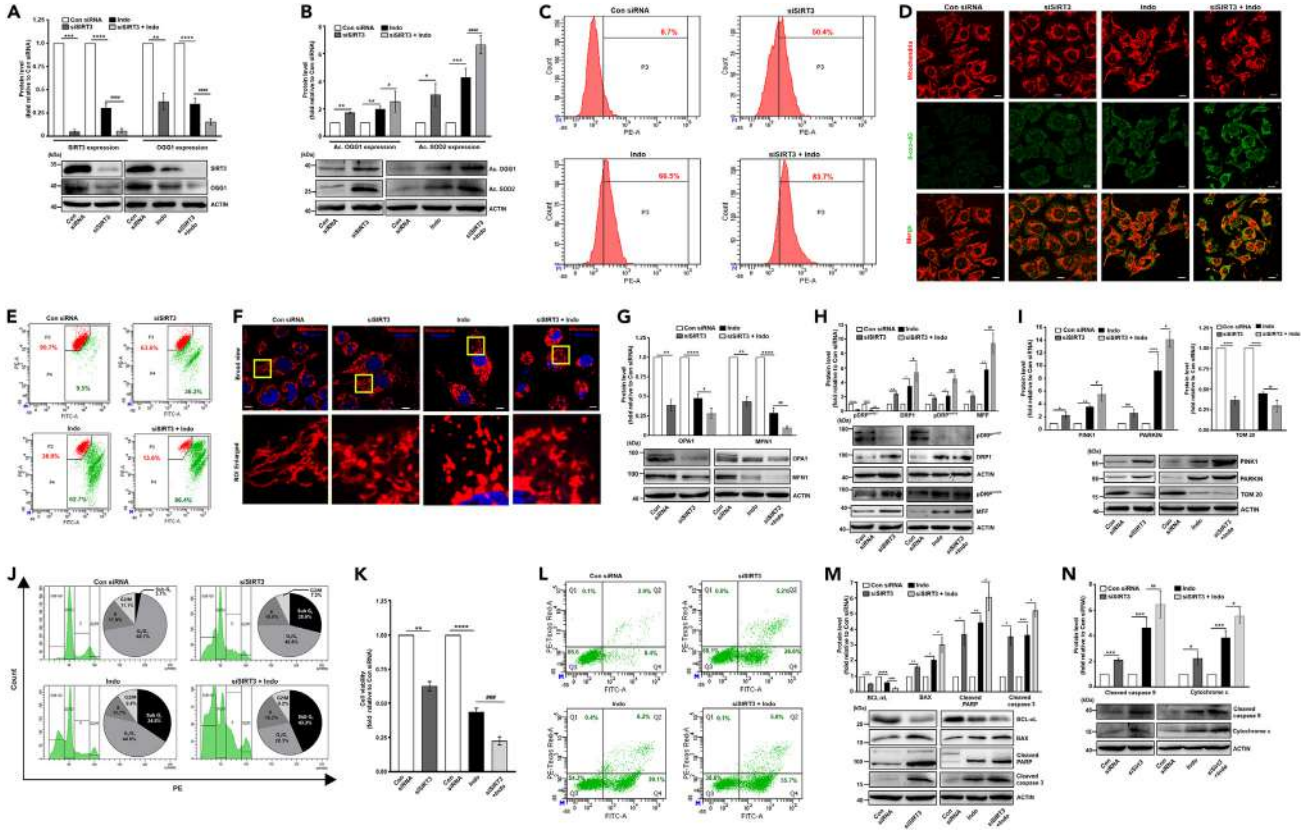

Figure 6. SIRT3 silencing aggravates indomethacin-induced mitochondrial dysfunction and associated cytotoxic responses in AGS cells

(A) Immunoblot of SIRT3 and OGG1 in SIRT3-silenced AGS cells treated with indomethacin for 24 h.

(B) Immunoblot of acetylated OGG1 and SOD2 in SIRT3-silenced AGS cells treated with indomethacin for 24 h.

(C) Flow cytometric detection of mitochondrial superoxide ion (O_2^-) accumulation in SIRT3-silenced AGS cells treated with indomethacin (0.5 mM) for 24 h.

(D) Confocal immunofluorescent micrographs showing 8-oxo-dG (green) and TOM20 (red) in SIRT3-silenced AGS cells treated with indomethacin (0.5 mM) for 24 h.

(E) Flow cytometric detection of $\Delta\Psi$m (mitochondrial membrane potential change) in SIRT3-silenced AGS cells treated with indomethacin (0.5 mM) for 24 h; 10,000 cells were checked per set and numerical values within the quadrants indicate the percentage of cells therein.

(F) Live-cell confocal immunofluorescent micrographs showing MitoTracker red-stained mitochondria and Hoechst 33342-stained nuclei for depicting mitochondrial structural dynamics. The size bar indicates 10 μm. At least 3 randomly selected fields were captured and representative micrographs are presented.

(G–I) Immunoblots of OPA1, MFN1 (G), pDRP1^{ser637}, total DRP1, pDRP1^{ser616}, mitochondrial fission factor (MFF) (H), and PINK1, PARKIN, and TOM20 (i) in SIRT3-silenced AGS cells treated with indomethacin (0.5 mM) for 24 h. ACTIN was used as the loading control.

(J) Flow cytometry analysis of cell cycle in SIRT3-silenced AGS cells treated with indomethacin for 24 h 10,000 cell were checked per set; pie charts are presented as insets of the respective histograms.

(K) Cell viability measured by MTT reduction assay in SIRT3-silenced cells treated with indomethacin (0.5 mM) for 24 h.

(L) Flow cytometric detection of Annexin V/PI (propidium iodide)-stained cells for measuring apoptosis in SIRT3-silenced AGS cells treated with indomethacin; 10,000 cells were checked per set. Numerical values within the quadrants indicate the percentage of cells therein.

(M and N) Immunoblots of BCL-xL, BAX, cleaved PARP and cleaved caspase-3 (M) and cleaved caspase-9, and cytochrome *c* (N) in SIRT3-silenced AGS cells treated with indomethacin (0.5 mM) for 24 h. For immunoblots (A,B, G–I, M,N) ACTIN was used as the loading control and representative blots presented below the bar graphs. Data are mean ± SD. *p < 0.05; **p < 0.01; ***p < 0.001; ****p < 0.0001 versus "Con siRNA" and $^{\#}$p < 0.05; $^{\#\#}$p < 0.01; $^{\#\#\#}$p < 0.001 versus "Indo." Unpaired Student's *t* test with Welch correction was used to compare "siSIRT3" versus "Con siRNA" while one-way ANOVA followed by Bonferroni's *post hoc* test was used to compare "Indo" and "siSIRT3+Indo" versus "Con siRNA." ns: non-significant. For confocal microscopy, at least 3 randomly selected fields were captured and a representative image has been provided. The number of independently repeated experiments is 3 in every case. Also see Figure S8.

accumulation, as observed in confocal micrographs, further validated the consequence of OGG1 downregulation (Figure 6D). Aggravated mitochondrial oxidative stress further translated into loss of mitochondrial integrity as evident from exacerbated mitochondrial depolarization in SIRT3-silenced cells supplemented with indomethacin compared to small interfering RNA against SIRT3 (siSIRT3) or indomethacin treatment alone (Figure 6E).

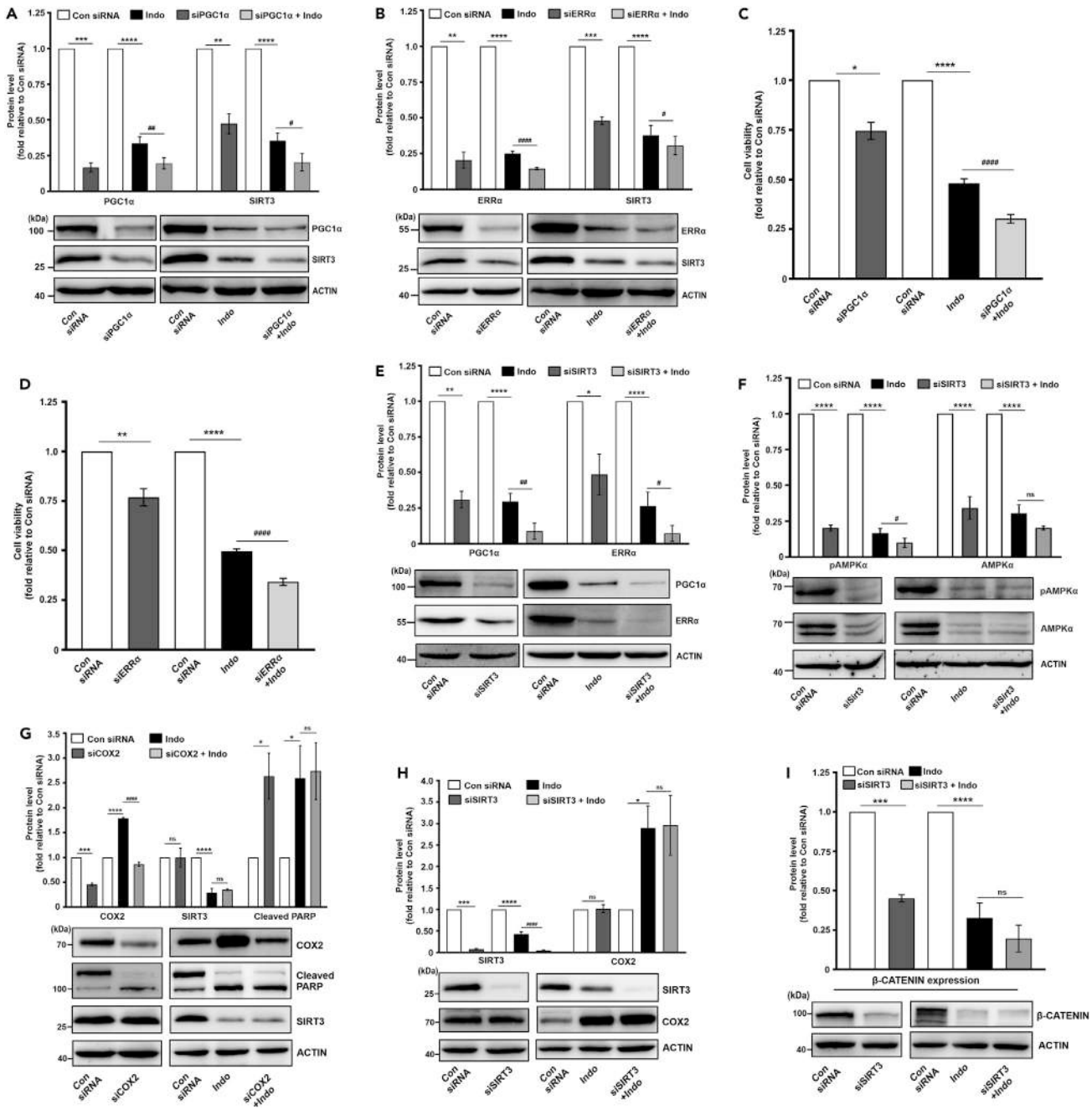

Figure 7. Indomethacin downregulates transcriptional regulators of SIRT3 and reduces AMPK phosphorylation

(A) Immunoblots of PGC1α and SIRT3 in PGC1α-silenced AGS cells treated with 0.5 mM indomethacin.

(B) Immunoblots of ERRα and SIRT3 in ERRα-silenced AGS cells treated with indomethacin. ACTIN was used as the loading control; representative blots are shown below the bar graphs (A-B).

(C and D) Cell viability was measured by MTT reduction assay in PGC1α-silenced (C) and ERRα-silenced (D) AGS cells treated with 0.5 mM indomethacin for 24 h.

(E and F) Immunoblots of PGC1α and ERRα (E) and pAMPKα and AMPKα (F) in SIRT3-silenced AGS cells treated with indomethacin (0.5 mM).

(G and H) Immunoblots of COX2, cleaved PARP, SIRT3 in COX2-silenced cells treated with indomethacin (0.5 mM) (G) and in SIRT3-silenced AGS cells treated with indomethacin (0.5 mM) (H).

(I) Immunoblot for β-catenin expression in AGS cells treated with siSIRT3, indomethacin or siSIRT3+indomethacin. ACTIN was used as the loading control; representative blots are shown below the bar graphs. Data are mean ± SD. *p < 0.05; **p < 0.01; ***p < 0.001; ****p < 0.0001 versus "Con siRNA" and $^{\#}$p < 0.05; $^{\#\#}$p < 0.01; $^{\#\#\#\#}$p < 0.0001 versus "Indo." ns: non-significant. Unpaired Student's *t* test with Welch correction was used to compare "siPGC1α" versus "Con siRNA" (A, C), "siERRα" versus "Con siRNA" (B, D), "siSIRT3" versus "Con siRNA" (E, F, H, I) and "siCOX2" versus "Con siRNA" (G) One-way

Figure 7. *Continued*

ANOVA followed by Bonferroni's *post hoc* test was used to compare "Indo" and "siPGC1α+Indo" versus "Con siRNA" (A, C), "Indo" and "siERRα+Indo" versus "Con siRNA" (B, D), "Indo" and "siSIRT3+Indo" versus "Con siRNA" (E, F, H, I) and "Indo" and "siCOX2+Indo" versus "Con siRNA" (G). The number of independently repeated experiments is 3 in every case. See also Figures S8 and S9.

Loss of mitochondrial functional integrity got clearly reflected in mitochondrial structure which indicated profuse hyperfission as evident from high-resolution confocal micrographs. Mitochondria displayed highly fragmented and perinuclearly clustered punctate state in indomethacin-treated cells compared to filamentous mitochondria in control-small interfering RNA (siRNA)-treated cells. Moreover, SIRT3 silencing further intensified shrinkage, clustering, and fragmentation of mitochondria (Figure 6F). Mitochondrial fragmentation was also confirmed from OPA1, MFN1, and phospho-DRP1^{ser637} reduction and MFF, phospho-DRP1^{ser616}, and DRP1 elevation (Figures 6G and 6H). In fact, mitochondrial depletion and aberrant mitophagy also synchronously progressed with hyperfission (in absence of any compensatory rescuing effect of mitochondrial biogenesis) as evident from the concerted elevation of key mitophagy regulators PINK1 and PARKIN and reduction of TOM20 (Figure 6I). The cumulative impact of mitochondrial dysfunction due to indomethacin treatment under SIRT3-silenced state ultimately reflected in drastic deterioration in cell cycle (as evident from significant increase in sub-G_0 population) (Figure 6J) coupled with exacerbated reduction of cell viability (Figure 6K) and increase in cell death (Figures 6L and 6M). Precisely, contribution of intrinsic apoptosis was clearly evident from elevation of caspase-9 and cytochrome *c* (Figure 6N). Collectively, detrimental impact of 'siSIRT3 + indomethacin' was clearly much higher compared to either siSIRT3 or indomethacin treatment alone.

Indomethacin downregulates transcriptional regulators of SIRT3 and blocks the feedback loop of AMPK/PGC1α/SIRT3 signaling

So far, we observed that indomethacin-induced mitochondrial pathology and AGS cell death involved suppression of AMPK/PGC-1α/SIRT3 signaling axis. For further validation, we checked whether suppression of SIRT3 transcriptional regulators, per se, exerts any effect on indomethacin treatment. We observed that silencing PGC1α or ERRα significantly reduces SIRT3 expression. In addition, indomethacin treatment actually aggravated the SIRT3-downregulating effect of PGC1α or ERRα knockdown (Figures 7A and 7B) to further worsen the cytoarchitectural damage (Figure S8) and intensify the deterioration of cell viability (Figures 7C and 7D). Moreover, SIRT3 silencing also aggravated the direct inhibitory effect of indomethacin on PGC1α and ERRα as well as activation of AMPKα (Figures 7E and 7F) to confirm the inhibitory effect on the feedback loop of AMPK/PGC-1α/SIRT3 signaling.

Indomethacin-mediated SIRT3 inhibition during AGS cell death is independent of its COX2-modulating action

Being the rate-limiting factor controlling prostaglandin biosynthesis, COX2 expression contributes to cancer cell viability, metabolic integrity, and proliferation.[16,17] To check whether SIRT3 inhibition-dependent anti-cancer action of indomethacin involves COX2 or operates independently, we specifically followed the effect of COX2 silencing on SIRT3 expression and cell viability. We observed that AGS cell cytoarchitecture, viability, and death are only slightly affected by COX2 silencing (Figures S9A and S9B). Moreover, COX2 silencing also did not affect SIRT3 expression as evident from the immunoblots (Figure 7G). On the contrary, indomethacin treatment upregulated COX2 expression along with increasing PARP cleavage and compromising cell viability. Interestingly, COX2 silencing did not produce much aggravating effect on indomethacin-mediated SIRT3 reduction and cell death. We also checked the effect of SIRT3 silencing on COX2 expression and found that siSIRT3 treatment did not affect COX2 expression. In fact, the COX2 modulating effect of indomethacin was also found unaffected in the SIRT3-silenced state (Figure 7H). Therefore, it was evident that SIRT3 inhibition by indomethacin operates exclusively of COX2 expression alteration by this NSAID. Further, we also checked β-catenin protein expression under "SIRT3-silenced" as well as "SIRT3-silenced + indomethacin-treated" conditions and found that β-catenin expression gets reduced by both SIRT3 silencing and indomethacin treatment. However, SIRT3 silencing did not aggravate indomethacin-mediated β-catenin reduction (Figure 7I).

SIRT3 reduction is a common cytotoxic action triggered by popular NSAIDs to induce cancer cell death

Finally, we checked whether SIRT3 downregulation was specific to indomethacin or general to popular NSAIDS like diclofenac, aspirin, and ibuprofen also exhibiting anti-neoplastic action as well as being used as medicines for treating inflammatory disorders. Data indicated that all these three NSAIDs significantly reduced SIRT3 expression (Figure 8A) concurrently with depleting cell viability and damaging the cytoarchitecture (Figures 8B and 8C). The effects were largely comparable to indomethacin, thereby suggesting SIRT3 depletion as a common event underlying the toxic effects of NSAIDs.

DISCUSSION

The present work reports mitochondrial deacetylase SIRT3 as a direct target of indomethacin to induce COX-independent anti-proliferative effect leading to mitochondrial pathology and GC cell death. We provide evidence that indomethacin causes competitive inhibition of SIRT3 deacetylase activity along with severely downregulating both the gene as well as protein expressions of SIRT3 to induce a comprehensive blockage in SIRT3 signaling pathway. This SIRT3-inhibiting action of NSAIDs can be strategically used for designing novel and safer NSAID-based strategies which can bypass the COX-dependent side effects while still retaining the cytotoxic action against cancer cells.

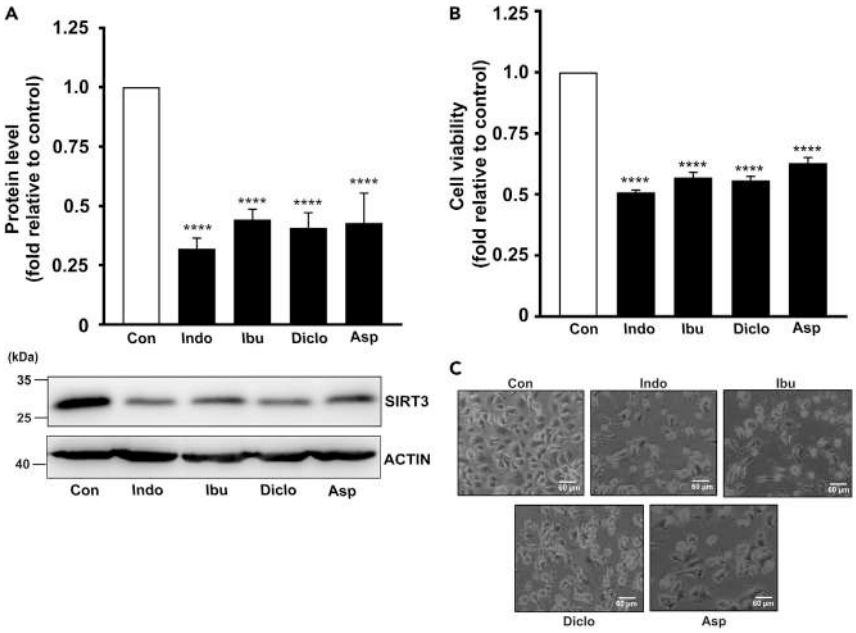

Figure 8. Downregulation of SIRT3 is associated with the anti-cancer property of popular NSAIDs including diclofenac, aspirin, and ibuprofen

(A) Immunoblot of SIRT3 in AGS cells treated with Indo (0.5 mM), Ibu (2.5 mM), Diclo (0.5 mM), and Asp (8 mM) for 24 h. ACTIN was used as the loading control; representative blots below the bar graph.

(B) Cell viability measured by dehydrogenase activity (MTT reduction assay) in the control and NSAID-treated cells.

(C) Phase-contrast micrographs of AGS cells treated with indicated NSAIDs. At least 3 randomly selected fields were captured and representative micrographs are presented. Data (A,B), are mean ± SD ****$p < 0.0001$ versus "control" calculated by one-way ANOVA followed by Bonferroni's *post hoc* test. The number of independently repeated experiments is 3 in every case.

GC is a highly aggressive malignancy with complex pathogenesis, molecular heterogeneity, and dearth of effective treatment options especially for advance-stage tumors and multiple metastases cases.[18] Notably, GC is almost always diagnosed in the advanced stages thereby further worsening the prognosis. Precise knowledge about gastric tumor biology and risk factors is therefore crucial while strategizing treatment regimen.

Repurposing of already FDA-approved non-anti-cancer drugs for exploring their potent anti-neoplastic effects is coming to the limelight in order to fight increasing chemoresistance and resist aggressive tumors as well as cancer stem cells. Contextually, emerging reports on drug repurposing of NSAIDs in cancer have highlighted their anti-neoplastic potential in GCs.[19–21] Although NSAIDs have side effects which are mostly experienced in long-term users, these age-old anti-inflammatory compounds are found to exhibit remarkable anti-cancer properties.[22] Moreover, when compared with conventional anti-cancer compounds, NSAIDs appear less toxic and safer.[23,24] COX-independent oncosuppressor effects of NSAIDs predominantly involve induction of severe mitochondrial damage.[25] However, precise sub-mitochondrial targets of NSAIDs, specifically in the aggressive-phenotype GC cells, remain yet to be identified. Because cancer cell mitochondria undergo metabolic remodeling to enable survival of malignant cells in a hypoxic tumor microenvironment with high energy reequipments for rapid proliferation, metastasis, and immune evasion, therefore we zoomed into major mitochondrial proteins acting as metabolic gatekeepers and pivotal regulators of mitochondrial structural and functional integrity. Contextually, SIRT3 appeared as a common factor linking diverse metabolic pathways, mitochondrial antioxidant defense, and cellular bioenergetic integrity. Often referred to as the "guardian of mitochondria," SIRT3 (via its deacetylase activity) regulates diverse mitochondrial proteins ranging in action from TCA cycle and mitochondrial biogenesis to mitochondrial dynamics.[26] These effects of SIRT3 may also be largely attributed to its cofactor NAD^+ which has been rightly addressed as a golden nucleotide sitting on a crown of thorns.[27] By virtue of its interplay with NADH, NAD^+ crucially regulates myriad cellular processes including fatty acid oxidation, energy metabolism, glycolysis, OXPHOS, and TCA cycle.[28] NAD^+ is also implicated in oxidative stress, immune activation, cell viability, regulation of DNA repair, cellular stress resistance, and apoptosis.[27] Interestingly, these cellular processes are also regulated by SIRT3 in diverse diseases including cancer.[28] SIRT3 also regulates gene expression through deacetylation-dependent regulation of transcriptional regulators like FOXO3 and LKB1. To this end, NSAIDs have been often observed to negatively regulate vital cellular processes thereby compromising cell viability and triggering cell death by affecting mitochondrial integrity and cellular redox homeostasis. Recently in a rodent model of gastropathy, indomethacin has been found to induce acute non-malignant gastric mucosal injury via inhibiting SIRT3.[29] However, there are no studies, as of now, exploring the effect of NSAIDs on SIRT3 in GC. Therefore, we attempted for assessing a plausible direct association of indomethacin and SIRT3 in inflicting GC cell death. Because indomethacin is a typical NSAID with reversible negligible COX selectivity, we rationally used it in the present study to rule out COX1/COX2 bias. The mitotoxic effects of indomethacin on AGS cells were confirmed at the outset wherein severe bioenergetic crisis, mitochondrial depolarization, hyperfission, and consequent activation of intrinsic

pathway of apoptosis were distinctly observed. Loss of mitochondrial integrity by indomethacin rationally paved the way to check the effect of this highly potent oncosuppressor NSAID on mitochondrial metabolic guardian, SIRT3. Notably, molecular simulation studies clearly revealed direct SIRT3-indomethacin interaction with thermodynamically favorable binding score along with conceivable binding-site overlap with NAD. This suggested that indomethacin plausibly exerts competitive inhibition of SIRT3 deacetylase activity. Subsequently, indomethacin was found to actually compete with NAD for stably binding with SIRT3 with minimal conformational distortion. Further, in depth structural analysis relied on molecular dynamics simulation followed by validation through ITC-based direct evaluation of SIRT3-indomethacin interaction. ITC enables to directly measure bimolecular interactions, without the need of any label/s in a single experiment. Whenever a binding event occurs, heat is either absorbed or released. This was measured by the sensitive micro-calorimeter during the gradual titration of indomethacin into the sample cell containing rhSIRT3. The amide carbonyl, indole, carboxylate, chlorobenzene, and methoxy moieties of indomethacin participate significantly during binding with SIRT3 wherein His248, Phe180, Phe294, Arg158, Glu177, Gly295, Phe157, Phe294, Ile 230, Thr320, Glu323, Ser 321, Arg345, and Val366 residues participate through different degrees of interactions in the form of hydrogen bonds, pi-stacking, salt bridges, water bridges, cation-pi interactions, and hydrophobic contacts. Biophysical studies were further succeeded by direct estimation of SIRT3 deacetylase activity to understand the impact of indomethacin-SIRT3 binding. Usage of recombinant protein as well as direct mitochondrial extract enabled the confirmation of a direct inhibitory action of indomethacin (and not any metabolic by-product) on SIRT3 enzymatic activity. Together, it proved that indomethacin is a potential SIRT3 inhibitor which can be capitalized in NSAID-based anti-cancer drug development against GC specifically targeting SIRT3.

Based on indomethacin-SIRT3 interaction and SIRT3 deacetylase inhibition data, we moved ahead to check whether indomethacin at all exerts any effect on SIRT3 expression. To this end, we primarily undertook deep transcriptomic sequencing of treated AGS cells for unbiased identification of any novel actionable sub-mitochondrial target. It is worth mentioning at this point that indomethacin is also used against human malignancies besides treating pain/inflammation.[30,31] AGS cells provided the ease for mechanistic exploration and functional validation of the direct cytotoxic effects of indomethacin on a pure gastric carcinoma cell line, while bypassing plausible interfering metabolic effect/s as expected *in vivo*. A relatively low (half-maximal inhibitory concentration [IC_{50}]) dose of indomethacin used in this study enabled to monitor the subtle subcellular events which might have been difficult to track at a higher toxic dose. Distinct separation of gene sets was noticed in the transcriptome data from control and indomethacin-treated cells. Pathway analysis and network clustering indicated toward concerted activation of gene expression programs pertaining to cell death, protein ubiquitination, reactive prooxidant metabolism, and overall downregulation of metabolic pathways concerning carbohydrate, amino acid, and fatty acid metabolism as well as mitochondrial central dogma and specifically OXPHOS.

Of the various highlighted DEGs, SIRT3 was found to be significantly downregulated thereby providing support to our speculation of plausible targeting of SIRT3 expression by NSAIDs in GC cells. Before delving into the intricate functional aspects of SIRT3 inhibition by indomethacin, we first compared basal SIRT3 expression between gastric normal and cancer cells to ascertain the prognostic relevance of SIRT3 in GC. A significantly low basal SIRT3 level in Hs738 cells, compared to AGS cells, supported the tumorigenic action of this protein in the present study as well as GC per se. In fact, this observation is also in concordance with the TCGA data which also indicate that both SIRT3 and SOD2 are highly expressed in GC. Kaplan-Meier survival curves also indicate that SIRT3- and OGG1-high-expressing groups/patients have a lower median OS. In addition, TCGA datasets also indicated that, although GC has a differential racial incidence, significantly high SIRT3 expression is common to GCs from different races like Caucasian, African American, and Asian. Thus, SIRT3 appears as an important mitochondrial target associated with poor prognosis in GC. Concerning the antioxidant defense of SIRT3, SOD2 and OGG1 implicated in diverse pathologies including cancer are the predominant deacetylation targets of SIRT3.[32] In this context, indomethacin was found to target SIRT3 at multiple levels; blocking SIRT3 deacetylase activity, depleting SIRT3 gene and protein expressions, and increasing mitochondrial protein acetylation and specific acetylation of OGG1 and SOD2. Regarding the differences in the extent of indomethacin-induced SIRT3 reduction and cell death in cancer versus normal cells, a much higher concentration of indomethacin is required to exert these detrimental effects in the Hs738 normal cell line compared to AGS cells. Therefore, it appears that, although indomethacin-induced SIRT3 reduction is toxic even to normal cells, the damaging effects are realized at a much lower concentration in the cancer cells thereby further justifying its merit as a potent SIRT3-based anti-cancer compound worth of investment for SIRT3-based anti-neoplastic purposes. In regards to the mechanistic basis underlying SIRT3 reduction, indomethacin was found to downregulate SIRT3 transcriptional regulators ERRα and PGC1α to exert a comprehensive suppressive effect on SIRT3 gene expression. Further indomethacin also blocked the AMPK-PGC1α-SIRT3 signaling axis. Indomethacin treatment in AGS cells actually reduced total AMPK and phosphorylated AMPK levels concerted with ATP depletion and SIRT3 as well as PGC1α downregulation. This is in congruence with the studies which suggest that SIRT3 indirectly regulates PGC1α expression (via FOXO3A deacetylation) and AMPK activation,[33] and AMPK-PGC1α signaling stimulates SIRT3 expression along with preserving mitochondrial structural and functional integrity.[34] Further, it also justifies mitochondrial depletion triggered by indomethacin because PGC1α is a potent regulator of mitochondrial biogenesis. Loss of SIRT3 upon indomethacin treatment is therefore associated with elevated mitochondrial fission and clearance of damaged mitochondria with high superoxide burden. In fact, SIRT3 knockdown aggravated this effect. This is in corroboration with previous reports where loss of SIRT3 has been associated with mtDNA damage in diseases.[35] In this context, we specifically found that intra-mitochondrial superoxide burden and 8-oxo-dG accumulation severely increased when indomethacin was applied to SIRT3-silenced cells thereby proving the direct detrimental effect of acetylated SOD2 and OGG1 as immediate effect of SIRT3 depletion. All these effects are translated into loss of AGS cell viability wherein depleted SIRT3 accounted for severe mitochondrial depolarization and consequent apoptosis. Further, indomethacin-induced depletion of ERRα and PGC1α also resulted in both SIRT3 downregulation and depression of cell viability, thereby clarifying the basis of SIRT3 depression by indomethacin at the gene level. Here, SIRT3 reduction has

been found to be a major factor contributing to indomethacin-induced cancer cell death. However, COX modulation being one of the dominant effects of NSAIDs in mediating their biological/cytotoxic actions, we also checked whether SIRT3 downregulation-dependent AGS cell death involved COX pathway. Interestingly, no significant change in COX2 expression was found upon SIRT3 silencing. Moreover, it was also found that COX2 silencing did not affect indomethacin-induced SIRT3 downregulation or aggravated cell death. Apparently, it turns out that in the present model SIRT3 reduction and cancer cell death by indomethacin operate independent of COX modulation, although we cannot absolutely rule out the possibility that the parallelly acting COX modulation and SIRT3 reduction pathways triggered by indomethacin would exert any synergistic anti-neoplastic effect in the systemic context.

In regards to cancer, although SIRT3 is known to favor OXPHOS over glycolysis,[26] tumor-specific roles of SIRT3 cannot be ignored owing to its elevated expression and glycolysis-enhancing effects which ensure cell proliferation.[36] This implies a context-dependent oncogenic role of SIRT3 even in glycolysis-dependent tumors that are less addicted to OXPHOS. In fact, cancer cells dynamically adapt to changing environments by switching between glycolysis and OXPHOS to meet energy requirements for ensuring maximal survival within compromised tumor microenvironment.[37–39] Ample evidence supports both tumor-suppressing and oncogenic role of SIRT3 in different malignancies.[26] However, we clearly observed that SIRT3 downregulation significantly aggravated indomethacin-induced AGS cell death. We also found that SIRT3 silencing moderately affected cell viability owing to its importance in cellular integrity under basal conditions.[36] Similar to SIRT3 silencing, ectopic SIRT3 overexpression might also prove risky for cancer cells owing to the fact that hyperactivated SIRT3 would deacetylate CypD leading to its dissociation from VDAC complex. Released CypD in turn would impede hexokinase II (HK2) binding to VDAC, thereby causing its dissociation from mitochondrial inner membrane. Mitochondrial membrane-bound HK2 exerts anti-neoplastic cytoprotective effect by decreasing mitochondrial BAX accumulation.[40] In fact, HK2 has been found to resist indomethacin-induced cytochrome *c* release and caspase-3 activation.[41] Further, SIRT3 overexpression might also affect the redox homeostasis in cancer cells by over-suppression of reactive prooxidants level (owing to its multidimensional antioxidant effects), which could be also detrimental. Therefore, we rationally avoided SIRT3 overexpression as a validation approach in this study because optimum SIRT3 level is quintessential for maintaining cancer cell integrity and extremely difficult to attain in ectopic overexpression system. Finally, it is imperative to consider the putative efficacy of indomethacin in blocking SIRT3, *in vivo*, which is actually necessary for eliciting the anti-tumor effect. Contextually, while the present study comprehensively emphasizes on the multidimensional mechanistic aspects of indomethacin-dependent blocking of SIRT3 signaling in the GC cells *in vitro*, recently it has been reported that mitochondrial extracts isolated from indomethacin-treated injured rat gastric mucosa exhibit highly reduced SIRT3 deacetylase activity along with significantly downregulated SIRT3 expression.[29] Further, *in vivo* anti-tumor action of indomethacin has already been observed.[5,42] In fact, indomethacin is also ventured in combinatorial anti-cancer strategies against human malignancies in clinical trials (ClinicalTrials.gov ID NCT02935205). Therefore, indomethacin-induced SIRT3 downregulation, *in vivo*, in tumors may also be logically expected. However, further *in vivo* studies to directly validate indomethacin-induced SIRT3 downregulation and inhibition specifically in the gastric tumors are advocated. In specific regards to the importance of SIRT3 inhibition as a potent effect of NSAIDs compared to their other anti-neoplastic actions, it is worth reiterating that, being the central regulator of mitochondrial metabolism, SIRT3 is crucial for cellular integrity and indomethacin strikes at this very base of it thereby triggering cancer cell death. An optimum SIRT3 level is essential for redox homeostasis and mitochondrial metabolic integrity of cancer cells. SIRT3 downregulation as well as direct inhibition of its deacetylase activity by indomethacin severely impacts cancer cell viability thereby proving its immense relevance as a potent anti-neoplastic effect.

Thus, we conclude that SIRT3 is a novel target of indomethacin in GC cells whose downregulation actually underlies its COX-independent anti-cancer effect. This knowledge holds immense translational relevance where SIRT3 silencing coupled with indomethacin treatment may be exploited as an effective anti-neoplastic strategy against drug-resistant tumors with poor prognosis.

Limitations of the study

- The present study reports the effect of indomethacin on SIRT3 as validated exclusively in the AGS cells which is a human gastric adenocarcinoma cell line. Additional validation in other GC cell lines would further substantiate the effect in the context of GC per se.
- The present study comprehensively reports mechanistic aspects of indomethacin-dependent inhibition of SIRT3 signaling in the GC cells. Further direct *in vivo* studies to validate indomethacin-induced SIRT3 downregulation and inhibition specifically in the gastric tumors would confirm the efficacy of indomethacin in blocking SIRT3 *in vivo*.

STAR★METHODS

Detailed methods are provided in the online version of this paper and include the following:

- KEY RESOURCES TABLE
- RESOURCE AVAILABILITY
  - Lead contact
  - Materials availability
  - Data and code availability
- EXPERIMENTAL MODEL AND STUDY PARTICIPANT DETAILS
  - Cell culture and indomethacin treatment
- METHOD DETAILS

- Cell viability assay and phase contrast microscopy for detecting cytoarchitecture
- Analysis of mitochondrial transmembrane potential ($\Delta\Psi m$)
- Measurement of ATP content
- Immunoblot analysis
- Cell cycle analysis
- Molecular simulation to explore SIRT3-indomethacin interaction
- Isothermal calorimetry for SIRT3-indomethacin interaction
- Determination of SIRT3 deacetylase activity
- SIRT3 expression analysis in human samples
- Next-generation sequencing based transcriptomics
- RNA isolation and real-time RT-PCR
- Isolation of mitochondria
- Isolation of mitochondrial DNA and measurement of 8-oxo-dG by ELISA
- Superoxide dismutase-2 (SOD2) activity assay
- Small interfering RNA (siRNA) transfection
- Confocal microscopy for mitochondrial structure analysis and immunocytochemistry
- Measurement of mitochondrial superoxide
- FITC-annexin V staining for cell death determination

- QUANTIFICATION AND STATISTICAL ANALYSIS

SUPPLEMENTAL INFORMATION

Supplemental information can be found online at https://doi.org/10.1016/j.isci.2024.109384.

ACKNOWLEDGMENTS

The authors thankfully acknowledge DBT-National Genomics Core and Core Technologies Research Initiative (CoTeRI), National Institute of Biomedical Genomics, India, for helping with next-generation sequencing. The authors also thank Dr. Ankita Chatterjee, National Institute of Biomedical Genomics, India, for helping with TCGA data analysis.

This work was supported by Science and Engineering Research Board, Department of Science and Technology, Ministry of Science and Technology, Govt. of India, through the J.C. Bose National Fellowship (grant no: SB/S2/JCB-54/2014) to U.B. for performing this work. S.D. acknowledges the Department of Biotechnology, Govt. of India, for doctoral research fellowship.

AUTHOR CONTRIBUTIONS

S.D., S.B., S.M., and U.B. conceived the study. S.D., S.B., S.M., U.P., Z.G., and U.B. wrote the manuscript. S.D., S.M., and S.P. conducted majority of the experiments. S.D., S.B., S.M., and U.B. analyzed the data. U.P. and N.C.M. performed molecular docking and simulation studies. T.D. and Z.G. performed NGS data analysis. D.S. and S.D. performed ITC experiments. R.D., S.N., and C.B. assisted in experiments. U.B. obtained funding and performed overall supervision of the project.

DECLARATION OF INTERESTS

The authors declare no competing interests.

Received: April 10, 2023
Revised: December 4, 2023
Accepted: January 23, 2024
Published: March 1, 2024

REFERENCES

1. Sung, H., Ferlay, J., Siegel, R.L., Laversanne, M., Soerjomataram, I., Jemal, A., and Bray, F. (2021). Global Cancer Statistics 2020: GLOBOCAN Estimates of Incidence and Mortality Worldwide for 36 Cancers in 185 Countries. CA. Cancer J. Clin. *71*, 209–249. https://doi.org/10.3322/caac.21660.
2. Li, Y., Feng, A., Zheng, S., Chen, C., and Lyu, J. (2022). Recent Estimates and Predictions of 5-Year Survival in Patients with Gastric Cancer: A Model-Based Period Analysis. Cancer Control *29*, 10732748221099227. https://doi.org/10.1177/10732748221099227.
3. Kumar, V., Soni, P., Garg, M., Kamholz, S., and Chandra, A.B. (2018). Emerging Therapies in the Management of Advanced-Stage Gastric Cancer. Front. Pharmacol. *9*, 404. https://doi.org/10.3389/fphar.2018.00404.
4. Guo, Y.C., Chang, C.M., Hsu, W.L., Chiu, S.J., Tsai, Y.T., Chou, Y.H., Hou, M.F., Wang, J.Y., Lee, M.H., Tsai, K.L., and Chang, W.C. (2013). Indomethacin inhibits cancer cell migration via attenuation of cellular calcium mobilization. Molecules *18*, 6584–6596. https://doi.org/10.3390/molecules18066584.
5. Wang, H.M., and Zhang, G.Y. (2005). Indomethacin suppresses growth of colon cancer via inhibition of angiogenesis *in vivo*. World J. Gastroenterol. *11*, 340–343. https://doi.org/10.3748/wjg.v11.i3.340.
6. Vallecillo-Hernández, J., Barrachina, M.D., Ortiz-Masiá, D., Coll, S., Esplugues, J.V., Calatayud, S., and Hernández, C. (2018). Indomethacin Disrupts Autophagic Flux by Inducing Lysosomal Dysfunction in Gastric

Cancer Cells and Increases Their Sensitivity to Cytotoxic Drugs. Sci. Rep. *8*, 3593. https://doi.org/10.1038/s41598-018-21455-1.

7. Kassab, S.E. (2018). Indomethacin from Anti-Inflammatory to Anticancer Agent. In Medicinal Chemistry, J.V.a.L. Vaško, ed. (IntechOpen). https://doi.org/10.5772/intechopen.79677.
8. Huang, M., Myers, C.R., Wang, Y., and You, M. (2021). Mitochondria as a Novel Target for Cancer Chemoprevention: Emergence of Mitochondrial-targeting Agents. Cancer Prev. Res. *14*, 285–306. https://doi.org/10.1158/1940-6207.CAPR-20-0425.
9. Ansari, A., Rahman, M.S., Saha, S.K., Saikot, F.K., Deep, A., and Kim, K.H. (2017). Function of the SIRT3 mitochondrial deacetylase in cellular physiology, cancer, and neurodegenerative disease. Aging Cell *16*, 4–16. https://doi.org/10.1111/acel.12538.
10. Kumar, S., and Lombard, D.B. (2015). Mitochondrial sirtuins and their relationships with metabolic disease and cancer. Antioxid. Redox Signal. *22*, 1060–1077. https://doi.org/10.1089/ars.2014.6213.
11. Carafa, V., Rotili, D., Forgione, M., Cuomo, F., Serretiello, E., Hailu, G.S., Jarho, E., Lahtela-Kakkonen, M., Mai, A., and Altucci, L. (2016). Sirtuin functions and modulation: from chemistry to the clinic. Clin. Epigenet. *8*, 61. https://doi.org/10.1186/s13148-016-0224-3.
12. Joosten, R.P., Womack, T., Vriend, G., and Bricogne, G. (2009). Re-refinement from deposited X-ray data can deliver improved models for most PDB entries. Acta Crystallogr. D Biol. Crystallogr. *65*, 176–185. https://doi.org/10.1107/S0907444908037591.
13. Bader, G.D., and Hogue, C.W.V. (2003). An automated method for finding molecular complexes in large protein interaction networks. BMC Bioinf. *4*, 2. https://doi.org/10.1186/1471-2105-4-2.
14. Shannon, P., Markiel, A., Ozier, O., Baliga, N.S., Wang, J.T., Ramage, D., Amin, N., Schwikowski, B., and Ideker, T. (2003). Cytoscape: a software environment for integrated models of biomolecular interaction networks. Genome Res. *13*, 2498–2504. https://doi.org/10.1101/gr.1239303.
15. Wang, Y., Li, X., and Zhao, F. (2021). MCU-Dependent mROS Generation Regulates Cell Metabolism and Cell Death Modulated by the AMPK/PGC-1alpha/SIRT3 Signaling Pathway. Front. Med. *8*, 674986. https://doi.org/10.3389/fmed.2021.674986.
16. Menter, D.G., Schilsky, R.L., and DuBois, R.N. (2010). Cyclooxygenase-2 and cancer treatment: understanding the risk should be worth the reward. Clin. Cancer Res. *16*, 1384–1390. https://doi.org/10.1158/1078-0432.CCR-09-0788.
17. Hashemi Goradel, N., Najafi, M., Salehi, E., Farhood, B., and Mortezaee, K. (2019). Cyclooxygenase-2 in cancer: A review. J. Cell. Physiol. *234*, 5683–5699. https://doi.org/10.1002/jcp.27411.
18. Selim, J.H., Shaheen, S., Sheu, W.C., and Hsueh, C.T. (2019). Targeted and novel therapy in advanced gastric cancer. Exp. Hematol. Oncol. *8*, 25. https://doi.org/10.1186/s40164-019-0149-6.
19. Brusselaers, N., and Lagergren, J. (2018). Maintenance use of non-steroidal anti-inflammatory drugs and risk of gastrointestinal cancer in a nationwide population-based cohort study in Sweden. BMJ Open *8*, e021869. https://doi.org/10.1136/bmjopen-2018-021869.
20. Li, L., Hu, M., Wang, T., Chen, H., and Xu, L. (2019). Repositioning Aspirin to Treat Lung and Breast Cancers and Overcome Acquired Resistance to Targeted Therapy. Front. Oncol. *9*, 1503. https://doi.org/10.3389/fonc.2019.01503.
21. Kumar, R. (2016). Repositioning of Non-Steroidal Anti Inflammatory Drug (NSAIDs) for Cancer Treatment: Promises and Challenges. J. Nanomed. Nanotechnol. *7*. https://doi.org/10.4172/2157-7439.1000e140.
22. Bindu, S., Mazumder, S., and Bandyopadhyay, U. (2020). Non-steroidal anti-inflammatory drugs (NSAIDs) and organ damage: A current perspective. Biochem. Pharmacol. *180*, 114147. https://doi.org/10.1016/j.bcp.2020.114147.
23. Würth, R., Thellung, S., Bajetto, A., Mazzanti, M., Florio, T., and Barbieri, F. (2016). Drug-repositioning opportunities for cancer therapy: novel molecular targets for known compounds. Drug Discov. Today *21*, 190–199. https://doi.org/10.1016/j.drudis.2015.09.017.
24. Sousa, S.M., Xavier, C.P.R., Vasconcelos, M.H., and Palmeira, A. (2023). Repurposing some of the Well-known Non-steroid Anti-inflammatory Drugs (NSAIDs) for Cancer Treatment. Curr. Top. Med. Chem. *23*, 1171–1195. https://doi.org/10.2174/1568026623666230130150029.
25. Brandolini, L., Antonosante, A., Giorgio, C., Bagnasco, M., d'Angelo, M., Castelli, V., Benedetti, E., Cimini, A., and Allegretti, M. (2020). NSAIDs-dependent adaption of the mitochondria-proteasome system in immortalized human cardiomyocytes. Sci. Rep. *10*, 18337. https://doi.org/10.1038/s41598-020-75394-x.
26. Zhang, J., Xiang, H., Liu, J., Chen, Y., He, R.R., and Liu, B. (2020). Mitochondrial Sirtuin 3: New emerging biological function and therapeutic target. Theranostics *10*, 8315–8342. https://doi.org/10.7150/thno.45922.
27. Massudi, H., Grant, R., Guillemin, G.J., and Braidy, N. (2012). NAD+ metabolism and oxidative stress: the golden nucleotide on a crown of thorns. Redox Rep. *17*, 28–46. https://doi.org/10.1179/1351000212Y.0000000001.
28. Navas, L.E., and Carnero, A. (2021). NAD(+) metabolism, stemness, the immune response, and cancer. Signal Transduct. Target. Ther. *6*, 2. https://doi.org/10.1038/s41392-020-00354-w.
29. Debsharma, S., Pramanik, S., Bindu, S., Mazumder, S., Das, T., Saha, D., De, R., Nag, S., Banerjee, C., Siddiqui, A.A., et al. (2023). Honokiol, an inducer of Sirtuin 3, protects against NSAID-induced gastric mucosal mitochondrial pathology, apoptosis and inflammatory tissue injury. Br. J. Pharmacol. *180*, 2317–2340. https://doi.org/10.1111/bph.16070.
30. Woo, J.K., Kang, J.H., Jang, Y.S., Ro, S., Cho, J.M., Kim, H.M., Lee, S.J., and Oh, S.H. (2015). Evaluation of preventive and therapeutic activity of novel non-steroidal anti-inflammatory drug, CG100649, in colon cancer: Increased expression of TNF-related apoptosis-inducing ligand receptors enhance the apoptotic response to combination treatment with TRAIL. Oncol. Rep. *33*, 1947–1955. https://doi.org/10.3892/or.2015.3793.
31. Lai, S.W., and Liao, K.F. (2013). Aspirin use after diagnosis improves survival in older adults with colon cancer. J. Am. Geriatr. Soc. *61*, 843–844. https://doi.org/10.1111/jgs.12236.
32. Torrens-Mas, M., Oliver, J., Roca, P., and Sastre-Serra, J. (2017). SIRT3: Oncogene and Tumor Suppressor in Cancer. Cancers *9*, 90. https://doi.org/10.3390/cancers9070090.
33. Li, Y., Wang, Q., Li, J., Shi, B., Liu, Y., and Wang, P. (2021). SIRT3 affects mitochondrial metabolic reprogramming via the AMPK-PGC-1alpha axis in the development of benign prostatic hyperplasia. Prostate *81*, 1135–1148. https://doi.org/10.1002/pros.24208.
34. Yu, L., Gong, B., Duan, W., Fan, C., Zhang, J., Li, Z., Xue, X., Xu, Y., Meng, D., Li, B., et al. (2017). Melatonin ameliorates myocardial ischemia/reperfusion injury in type 1 diabetic rats by preserving mitochondrial function: role of AMPK-PGC-1alpha-SIRT3 signaling. Sci. Rep. *7*, 41337. https://doi.org/10.1038/srep41337.
35. Pillai, V.B., Bindu, S., Sharp, W., Fang, Y.H., Kim, G., Gupta, M., Samant, S., and Gupta, M.P. (2016). Sirt3 protects mitochondrial DNA damage and blocks the development of doxorubicin-induced cardiomyopathy in mice. Am. J. Physiol. Heart Circ. Physiol. *310*, H962–H972. https://doi.org/10.1152/ajpheart.00832.2015.
36. Cui, Y., Qin, L., Wu, J., Qu, X., Hou, C., Sun, W., Li, S., Vaughan, A.T.M., Li, J.J., and Liu, J. (2015). SIRT3 Enhances Glycolysis and Proliferation in SIRT3-Expressing Gastric Cancer Cells. PLoS One *10*, e0129834. https://doi.org/10.1371/journal.pone.0129834.
37. Shiratori, R., Furuichi, K., Yamaguchi, M., Miyazaki, N., Aoki, H., Chibana, H., Ito, K., and Aoki, S. (2019). Glycolytic suppression dramatically changes the intracellular metabolic profile of multiple cancer cell lines in a mitochondrial metabolism-dependent manner. Sci. Rep. *9*, 18699. https://doi.org/10.1038/s41598-019-55296-3.
38. Läsche, M., Emons, G., and Gründker, C. (2020). Shedding New Light on Cancer Metabolism: A Metabolic Tightrope Between Life and Death. Front. Oncol. *10*, 409. https://doi.org/10.3389/fonc.2020.00409.
39. Jose, C., Bellance, N., and Rossignol, R. (2011). Choosing between glycolysis and oxidative phosphorylation: a tumor's dilemma? Biochim. Biophys. Acta *1807*, 552–561. https://doi.org/10.1016/j.bbabio.2010.10.012.
40. Schoeniger, A., Wolf, P., and Edlich, F. (2022). How Do Hexokinases Inhibit Receptor-Mediated Apoptosis? Biology *11*, 412. https://doi.org/10.3390/biology11030412.
41. Pastorino, J.G., Shulga, N., and Hoek, J.B. (2002). Mitochondrial binding of hexokinase II inhibits Bax-induced cytochrome c release and apoptosis. J. Biol. Chem. *277*, 7610–7618. https://doi.org/10.1074/jbc.M109950200.
42. Quidville, V., Segond, N., Pidoux, E., Cohen, R., Jullienne, A., and Lausson, S. (2004). Tumor growth inhibition by indomethacin in a mouse model of human medullary thyroid cancer: implication of cyclooxygenases and 15-hydroxyprostaglandin dehydrogenase. Endocrinology *145*, 2561–2571. https://doi.org/10.1210/en.2003-0915.
43. Wang, B., Chen, H., and Zhang, Y. (2019). Involvement of GASL1 in postoperative distant recurrence of gastric adenocarcinoma after gastrectomy distal resection and the possible mechanism. J. Cell. Biochem. *120*, 11454–11461. https://doi.org/10.1002/jcb.28423.

44. De, R., Sarkar, S., Mazumder, S., Debsharma, S., Siddiqui, A.A., Saha, S.J., Banerjee, C., Nag, S., Saha, D., Pramanik, S., and Bandyopadhyay, U. (2018). Macrophage migration inhibitory factor regulates mitochondrial dynamics and cell growth of human cancer cell lines through CD74-NF-kappaB signaling. J. Biol. Chem. *293*, 19740–19760. https://doi.org/10.1074/jbc.RA118.003935.
45. Mazumder, S., De, R., Debsharma, S., Bindu, S., Maity, P., Sarkar, S., Saha, S.J., Siddiqui, A.A., Banerjee, C., Nag, S., et al. (2019). Indomethacin impairs mitochondrial dynamics by activating the PKCzeta-p38-DRP1 pathway and inducing apoptosis in gastric cancer and normal mucosal cells. J. Biol. Chem. *294*, 8238–8258. https://doi.org/10.1074/jbc.RA118.004415.
46. Trott, O., and Olson, A.J. (2010). AutoDock Vina: improving the speed and accuracy of docking with a new scoring function, efficient optimization, and multithreading. J. Comput. Chem. *31*, 455–461. https://doi.org/10.1002/jcc.21334.
47. Azuara, C., Lindahl, E., Koehl, P., Orland, H., and Delarue, M. (2006). PDB_Hydro: incorporating dipolar solvents with variable density in the Poisson-Boltzmann treatment of macromolecule electrostatics. Nucleic Acids Res. *34*, W38–W42. https://doi.org/10.1093/nar/gkl072.
48. Morris, G.M., Huey, R., Lindstrom, W., Sanner, M.F., Belew, R.K., Goodsell, D.S., and Olson, A.J. (2009). AutoDock4 and AutoDockTools4: Automated docking with selective receptor flexibility. J. Comput. Chem. *30*, 2785–2791. https://doi.org/10.1002/jcc.21256.
49. Pal, U., Pramanik, S.K., Bhattacharya, B., Banerji, B., and C Maiti, N. (2016). Binding interaction of a gamma-aminobutyric acid derivative with serum albumin: an insight by fluorescence and molecular modeling analysis. SpringerPlus *5*, 1121. https://doi.org/10.1186/s40064-016-2752-x.
50. Biswas, S., Adhikari, A., Mukherjee, A., Das, S., and Adak, S. (2020). Regulation of Leishmania major PAS domain-containing phosphoglycerate kinase by cofactor Mg(2+) ion at neutral pH. FEBS J. *287*, 5183–5195. https://doi.org/10.1111/febs.15305.
51. Huo, Q., Li, Z., Cheng, L., Yang, F., and Xie, N. (2020). SIRT7 Is a Prognostic Biomarker Associated With Immune Infiltration in Luminal Breast Cancer. Front. Oncol. *10*, 621. https://doi.org/10.3389/fonc.2020.00621.
52. Szász, A.M., Lánczky, A., Nagy, Á., Förster, S., Hark, K., Green, J.E., Boussioutas, A., Busuttil, R., Szabó, A., and Győrffy, B. (2016). Cross-validation of survival associated biomarkers in gastric cancer using transcriptomic data of 1,065 patients. Oncotarget *7*, 49322–49333. https://doi.org/10.18632/oncotarget.10337.
53. Andrews, S. (2010). FastQC: A Quality Control Tool for High Throughput Sequence Data. http://www.bioinformatics.babraham.ac.uk/projects/fastqc/.
54. Martin, M. (2011). Cutadapt Removes Adapter Sequences from High-Throughput Sequencing Reads. EMBnet. j. *17*, 10–12. https://doi.org/10.14806/ej.17.1.200.
55. Pertea, M., Kim, D., Pertea, G.M., Leek, J.T., and Salzberg, S.L. (2016). Transcript-level expression analysis of RNA-seq experiments with HISAT, StringTie and Ballgown. Nat. Protoc. *11*, 1650–1667. https://doi.org/10.1038/nprot.2016.095.
56. Li, H., Handsaker, B., Wysoker, A., Fennell, T., Ruan, J., Homer, N., Marth, G., Abecasis, G., and Durbin, R.; 1000 Genome Project Data Processing Subgroup (2009). The Sequence Alignment/Map format and SAMtools. Bioinformatics *25*, 2078–2079. https://doi.org/10.1093/bioinformatics/btp352.
57. Liao, Y., Smyth, G.K., and Shi, W. (2014). featureCounts: an efficient general purpose program for assigning sequence reads to genomic features. Bioinformatics *30*, 923–930. https://doi.org/10.1093/bioinformatics/btt656.
58. Love, M.I., Huber, W., and Anders, S. (2014). Moderated estimation of fold change and dispersion for RNA-seq data with DESeq2. Genome Biol. *15*, 550. https://doi.org/10.1186/s13059-014-0550-8.

STAR★METHODS

KEY RESOURCES TABLE

REAGENT or RESOURCE	SOURCE	IDENTIFIER
Antibodies		
SIRT3	Cell Signaling Technology	Cat# 2627; RRID: AB_2188622
OGG1	Novus Biologicals	Cat# NB100-106; RRID: AB_10104097
PGC1α	Abcam	Cat# Ab54481; RRID: AB_881987
ERRα	Cell Signaling Technology	Cat# 13826; RRID: AB_2750873
Acetylated lysine	Cell Signaling Technology	Cat# 9814; RRID: AB_10544700
Acetylated OGG1	Abcam	Cat# ab93670; RRID: AB_10562267
Acetylated SOD2	Abcam	Cat# Ab137037; RRID: AB_2784527
Phospho-DRP1 (Ser637)	Cell Signaling Technology	Cat# 4867; RRID: AB_10622027
pAMPKα	Abcam	Cat# ab133448; RRID: AB_2923300
AMPK	Abcam	Cat# ab32047; RRID: AB_722764
Parkin	Sigma-Aldrich	Cat# P6248; RRID: AB_477384
PINK1	Novus Biologicals	Cat# BC100-494; RRID: AB_10127658
TOM20	Santa Cruz Biotechnology	Cat# sc-11415; RRID: AB_2207533
Cleaved Caspase 9	Cell Signaling Technology	Cat# 9505; RRID: AB_2290727
Bax	Santa Cruz Biotechnology	Cat# sc-7480; RRID: AB_626729
Cytochrome C	Abcam	Cat# ab53056; RRID: AB_869315
Bcl-xL	Cell Signaling Technology	Cat# 2764; RRID: AB_2228008
Cleaved caspase 3	Cell Signaling Technology	Cat# 9664; RRID: AB_2070042
Cleaved PARP	Cell Signaling Technology	Cat# 5625; RRID: AB_10699459
Anti-DNA/RNA Damage antibody [15A3]	Abcam	Cat# ab62623; RRID: AB_940049
Actin	Cell Signaling Technology	Cat# 3700; RRID: AB_2242334
OPA1	Abcam	Cat# ab42364; RRID: AB_944549
MFN1	Abcam	Cat# ab104585; RRID: AB_10712602
MFF	Abcam	Cat# ab81127; RRID: AB_1860496
DRP1	Abcam	Cat# ab184247; RRID: AB_2895215
Phospho-DRP1 (Ser616)	Cell Signaling Technology	Cat# 4494; RRID: AB_11178659
COX2	Abcam	Cat# ab15191; RRID: AB_2085144
β-catenin (H-102)	Santa Cruz Biotechnology	Cat# sc-7199; RRID: AB_634603
Rabbit anti-mouse IgG	Sigma-Aldrich	Cat# A9044; RRID: AB_258431
Goat anti-mouse IgG	Sigma-Aldrich	Cat# A0545; RRID: AB_257896
Goat anti-Mouse IgG (H+L) Cross-Adsorbed Secondary Antibody, Alexa Fluor 647	Thermo Fisher Scientific	Cat# A-21235; RRID: AB_2535804
Goat anti-Rabbit IgG (H+L) Highly Cross-Adsorbed Secondary Antibody, Alexa Fluor™ 488	Thermo Fisher Scientific	Cat# A-11034; RRID: AB_2576217
Chemicals, peptides, and recombinant proteins		
Indomethacin	Sigma-Aldrich	Cat# I7378
Diclofenac	Sigma-Aldrich	Cat# D6899
Ibuprofen	Sigma-Aldrich	Cat# I1892
Aspirin	Sigma-Aldrich	Cat# A2093
RNase ZAP	Sigma-Aldrich	Cat# 83930
MTT	Sigma-Aldrich	Cat# CT01-5

(*Continued on next page*)

Continued

REAGENT or RESOURCE	SOURCE	IDENTIFIER
Nicotinamide	Sigma-Aldrich	Cat# 72340
Trichostatin A, Ready Made Solution	Sigma-Aldrich	Cat#T1952
DMSO	Thermo Fisher Scientific	Cat# 276855
TRIzol	Thermo Fisher Scientific	Cat# 276855
Nuclease-free water	Thermo Fisher Scientific	Cat# AM9937
PBS	Thermo Fisher Scientific	Cat# 10010031
Lipofectamine 2000	Thermo Fisher Scientific	Cat# 11668019
Halt™ Protease and Phosphatase Inhibitor Cocktail (100X)	Thermo Fisher Scientific	Cat# 78440
Western BLoT Stripping Buffer	TaKaRa	Cat#T7135A
JC-1 Dye	Thermo Fisher Scientific	Cat# T3168
MitoSOX™ mitochondrial superoxide indicator	Thermo Fisher Scientific	Cat# M36008
MitoTracker™ Red CMXRos	Thermo Fisher Scientific	Cat# M7512
Luminata forte western HRP substrate	Millipore	Cat# WBLUF0500
Nutrient Mixture F-12 Ham, Kaighn's Modification	HiMedia Laboratories	Cat# AL106A
Dulbecco's Modified Eagle Medium, High glucose	HiMedia Laboratories	Cat# AL066A
Opti-MEM™ Reduced Serum Medium	Gibco, Sigma-Aldrich	Cat# 31985070
Recombinant Human Sirtuin 3	R&D system	Cat# 7488-DA
Critical commercial assays		
PureLink RNA Mini Kit	Thermo Fisher Scientific	Cat# 12183018A
RevertAid H Minus First Strand cDNA Synthesis kit	Thermo Fisher Scientific	Cat# 18091050
ATP Determination Kit	Thermo Fisher Scientific	Cat#A22066
Mitochondria Isolation Kit	BioChain	Cat# KC010100
HT 8-oxo-dG ELISA Kit II	Trevigen	Cat# 4380 KC010100
SIRT3 activity assay kit	Abcam	Cat# ab156067
Superoxide Dismutase Activity Assay Kit	Abcam	Cat# ab65354
Propidium Iodide Flow Cytometry Kit	Abcam	Cat# ab139418
Deposited data		
RNA-seq raw and analyzed data	This paper	GEO: GSE202140
Experimental models: Cell lines		
AGS	ATCC	Cat# CRL-1739
Hs 738.St/Int	ATCC	Cat# CRL-7869
Oligonucleotides		
SIRT3 siRNA	Santa Cruz Biotechnology	Cat# sc-61555
PGC1α siRNA	Santa Cruz Biotechnology	Cat# sc-38884
ERRα siRNA	Santa Cruz Biotechnology	Cat# sc-44706
COX2 siRNA	Santa Cruz Biotechnology	Cat# sc-29279
Scrambled siRNA	Santa Cruz Biotechnology	Cat# Sc-37007
Primers for mt-ND1, mt-ND6, mt-CO1, mt-ATP6, mt-CYT-B, SIRT3 and GAPDH, see Table S4	Integrated DNA Technologies	N/A
Software and algorithms		
ImageJ software	ImageJ	RRID: SCR_003070
LAS X software	LAS X	RRID: SCR_013673
GraphPad Prism-8	GraphPad	RRID: SCR_002798

RESOURCE AVAILABILITY

Lead contact

Further information and requests for resources should be sent to and fulfilled by the lead contact, Dr. Uday Bandyopadhyay (ubandyo_1964@yahoo.com and udayb@jcbose.ac.in).

Materials availability

This study did not generate new unique reagents.

Data and code availability

- The data presented in this study are available in the article and supplemental information. Processed and raw RNA-seq data generated in this study are deposited in the Gene Expression Omnibus (GEO) with accession number GSE202140 available online at the GEO repository.
- This paper does not report any original code.
- Any additional information necessary to reanalyze the data given in this paper can be obtained from the lead contact upon request.

EXPERIMENTAL MODEL AND STUDY PARTICIPANT DETAILS

Cell culture and indomethacin treatment

AGS cells (human gastric carcinoma cells, ATCC-CRL-1739) and Hs738.St/Int (human normal cell line of gastrointestinal origin, ATCC-CRL-7869) were procured from American Type Culture Collection (Manassas, USA). Cells were cultured as described earlier.[43,44] Briefly, AGS cells were maintained in F-12 Ham-Kaighn's modification medium whereas Hs738 cells were maintained in Dulbecco's Modified Eagle's Medium. The respective culture media were supplemented with 10% fetal bovine serum. The cells were kept at 37°C in 5% CO_2 incubator. Trypsinization was employed for splitting the cells once every 3 days. For experiments, cells were plated at a density of $1X10^6$ and allowed to grow overnight after which fresh media was replenished for treatment. Cells were treated with increasing concentrations of NSAIDs to check the effect on cell viability by dehydrogenase activity assay. A sublethal dose of 0.5 mM (obtained from viability assay) for indomethacin has been used to treat cells for transcriptome analysis and protein expression profiling to capture the subtle effects on cellular metabolism. Indomethacin was dissolved in alkaline distilled water. Ibuprofen and diclofenac were dissolved in distilled water. Aspirin was dissolved in DMSO. The final concentration of DMSO was maintained at 0.1% during treatment of cells. Diclofenac (0.5 mM), ibuprofen (2.5 mM) and aspirin (8 mM) were used to treat cells for SIRT3 expression profiling and cell viability assays. In every case the experiments were repeated thrice.

METHOD DETAILS

Cell viability assay and phase contrast microscopy for detecting cytoarchitecture

Cellular dehydrogenase activity was measured for the evaluation of cell viability, based on 3-(4,5-dimethylthiazol-2-yl)-2,5- diphenyl tetrazolium bromide (MTT) reduction assay as mentioned earlier.[44] In brief, 48 well culture plates were plated with cells were plated at equal density and allowed to grow till 60-70% confluency, followed by indomethacin treatment. After completion of the treatment, MTT (1 mg/mL) in PBS added to the cells for an incubation period of 3.5 hr under 37°C/5% CO_2 and finally the purple formazan was solubilized in anhydrous DMSO. The optical density was spectrophotometrically measured at 570 nm. For live cell phase contrast imaging, cells after treatment were washed with pre-warmed PBS and viewed under inverted phase contrast microscope (Leica Microsystems). At least 5 independent fields were randomly captured and representative images have been provided. All experiments were repeated thrice.

Analysis of mitochondrial transmembrane potential ($\Delta\Psi m$)

For $\Delta\Psi m$ analysis in AGS cells, $3x10^6$ cells were used for JC-1 staining followed by flow cytometry as mentioned earlier.[45] In brief, after indomethacin treatment, the cells were washed in pre-warmed media (37°C) and incubated with JC-1 (5 μg/mL) diluted in cell culture media, for 15 min at 37°C/5% CO_2 in darkness. After the incubation, the cells were detached by trypsinization and diluted in PBS to a density of 10^6 cells/mL and analysed in FACS-LSR Fortessa, BD, using FACS DIVA software under standard parameters. 10^4 cells were evaluated per set and experiments were repeated thrice.

Measurement of ATP content

ATP content from AGS cells was measured using an ATP determination kit (Invitrogen Corp., Carlsbad, CA, USA) as mentioned earlier following the manufacturer's instructions.[45] In short, an equal number of cells (10^7 cells per experimental set) were lysed in chilled cell lysis buffer (supplemented with Triton X-100). The lysates were centrifuged and the clear supernatants were used. ATP content was measured in a luminometer (BioTek). The ATP content of each sample was normalized by their respective protein concentration. In every case the experiments were repeated thrice.

Immunoblot analysis

For immunoblot analysis, total protein was isolated from AGS cells by using pre-chilled mammalian cell lysis buffer (supplemented with protease and phosphatase inhibitors, Halt™ Protease and Phosphatase Inhibitor Cocktail (100X), Thermo). Mitochondria were isolated from AGS cells using a commercially available kit from Biochain. For the study of mitochondrial protein acetylation, isolated mitochondria were lysed in the cell lysis buffer supplemented with nicotinamide (50 mM) and trichostatin A (10 μM). Quantification of protein was performed by Lowry's method and equal quantity of proteins were mixed in SDS loading buffer and resolved in 10% polyacrylamide-SDS gels. The resolved proteins were then transferred to a nitrocellulose membrane (0.22 μM) by electroblotting. 5% skimmed milk or 5% BSA solution were used to block the membrane and followed by incubation in primary antibodies (key resources table, STAR Methods) overnight. The blots were washed in TBS solution supplemented with 0.1% Tween 20 and subsequently incubated in HRP-conjμgated secondary antibody for 2 hr at room temperature. The blots were finally washed and immuno-reactive bands were developed in Bio-Rad Chemidoc system. Each blot was stripped with stripping buffer (Cat#T7135A, TAKARA) and re-probed for checking ACTIN and TOM20 used as the loading controls for total protein and mitochondrial protein respectively. Densitometric analyses were done using ImageJ software and data were represented as fold change relative to control. In every case the experiments were repeated thrice.

Cell cycle analysis

Flow cytometric technique was used to analyse the cell cycle as per standard procedure.[44] Propidium Iodide Flow Cytometry Kit (Abcam, Cat# ab139418) was used for this assay. Briefly, AGS cells were grown in 6 well plate and after the treatment was over cells were harvested and fixed in chilled ethanol (70% v/v) with gentle vortexing and the cells were kept overnight at 4°C. Next day the fixed cells were washed in PBS and stained using Propidium Iodide Flow Cytometry Kit (Abcam, Cat# ab139418) suggested in the manufacturer's protocol followed by flowcytometric screening. The analysis was done in BD LSR Fortessa using BD FACS Diva 6.2 software. 10^4 cells were evaluated per set and experiments were repeated thrice.

Molecular simulation to explore SIRT3-indomethacin interaction

Chemical structure of indomethacin has been obtained from PubChem (PubChem CID: 3715). 31 crystal structures (retrieved 1 Sept 2022) of Sirtuin 3 (UniProtKB: SIR3_HUMAN) were obtained from the protein data bank (PDB) or the PDB-REDO repositories.[12] Based on the model qualities (according to the wwPDB validation report available at PDB website), 22 crystal structures with good geometries and electron density map fitting were selected for docking studies (Table S1). Molecular docking simulation was performed with AutoDock Vina.[46] Any bound ligands and crystallographic water molecules were removed from the protein crystal structures. Any missing side chains of the protein were filled using PDB_Hydro.[47] Alternate atom positions were removed. Polar hydrogens were added using AutoDockTools.[48] AutoDock4 atom types were assigned. Ligand structures were prepared similarly. All the rotatable bonds in the ligands were set free. Binding dissociation constant, K_D, was calculated from binding free energies using the equation $\Delta G = -RT \ln K_{eq}$ where $K_{eq} = 1/K_D$.

Molecular dynamics (MD) was run under OPLS (optimized potentials for liquid simulations) force field in SPC (simple point-charge) water environment using Desmond molecular dynamics software implemented in Schrodinger Maestro (Academic release 2020-4).[49] MD simulations were performed on the free, NAD^+-bound and indomethacin-bound SIRT3 under defined temperature and pressure for a certain length of time (300 K, 1 bar and 240 ns, respectively, in this study). In MD simulation, the atomic model of protein or the protein ligand complex is placed in an explicit water environment and the whole system is incubated at a defined temperature and pressure for a certain length of time. Temperature gives motions to the atoms and the molecules can move freely in water as per Brownian motions. Thus, it considers the effects of solvents and receptor flexibility on the ligand interactions. Any structural changes in the protein induced by the ligand binding can also be observed. Low energy and higher frequency bound conformations were chosen for the MD simulation. Structural changes in terms of root mean square deviations (RMSD), residue-wise fluctuations in terms of root mean square fluctuations (RMSF), secondary structural properties, time correlated interactions, and interaction energies were obtained from the simulation trajectories using Schrodinger Maestro (Academic Release 2020-4).

Isothermal calorimetry for SIRT3-indomethacin interaction

To identify the binding response of recombinant human SIRT3 (rhSIRT3) with indomethacin, isothermal calorimetry (ITC) and titration experiments were conducted using an Affinity-ITC (TA Instruments). Standard procedure, as mentioned earlier, was followed[50] with minor modifications as required. The experiments were performed at 25°C, and all samples were thoroughly vacuum-degassed before loading. The protein (rhSIRT3) and indomethacin were present in the same buffer of 25 mM Tris-HCl and 50 mM NaCl of pH 7.5. In the sample cell, 0.1 μM indomethacin solution was loaded, and the syringe was filled with 1.0 μM of rhSIRT3 solution. Indomethacin solution was injected in volumes of 5 μL up to 25 injections with a stirring RPM of 75. This experiment allowed us to plot the heat rate (μJ/sec) with respect to time (sec).

Determination of SIRT3 deacetylase activity

SIRT3 fluorometric activity assay kit (Abcam, ab156067) was used to measure deacetylase activity of SIRT3 in absence/presence of indomethacin. The experiment was performed as per manufactures protocol. Briefly, in presence of increasing concentrations of indomethacin (0.1-0.5 mM) the activity of purified recombinant human SIRT3 (rhSIRT3) was assessed taking the kinetic measurement at 2 min intervals till 45 min in BioTek Synergy H1 Hybrid Multi-Mode Reader with excitation at 350 nm and emission at 450 nm. For measuring mitochondrial

SIRT3 activity within cells, mitochondrial extract was incubated with 0.5 mM indomethacin and then fluorescence was measured. Each reaction was performed in duplicates as mentioned in the kit and the experiment was repeated thrice.

SIRT3 expression analysis in human samples

SIRT3 expression in stomach adenocarcinoma (STAD) patient and normal individual stomach samples were evaluated using UALCAN, HPA and KM plotter database analysis tools as mentioned previously.[51] UALCAN (http://ualcan.path.uab.edu/) analysis was undertaken for mining SIRT3 expression data across TCGA normal and STAD primary tumors. Data were represented as transcripts per million. Differential SIRT3 expression was evaluated from multiple dimensions, viz. sample types (normal, n = 34 and primary tumor, n = 415), individual cancer stages (stage 1, n = 18; stage 2, n = 123; stage 3, n = 169 and stage 4, n = 41), histological subtypes (Adenocarcinoma NOS, n = 155; Adenocarcinoma Diffuse, n=69; Adenocarcinoma SignetRing, n = 12; Intestinal Adenocarcinoma NOS, n = 73; Intestinal Adenocarcinoma Tubular, n = 76; Intestinal Adenocarcinoma Mucinous, n = 20 and Intestinal Adenocarcinoma Papillary, n = 7) and patient's race (Caucasian, n = 260; AfricanAmerican, n = 12 and Asian, n = 87). Statistical significance has been mentioned as inset in the respective boxplot data.

In situ SIRT3 protein expression between healthy stomach tissue and STAD tumor samples was evaluated in Human Protein Atlas (https://www.Proteinatlas.org/). SIRT3 expression was checked in the tissue and pathology modules of HPA by selecting stomach as the target organ. Representative images of a normal stomach section (patient id: 1650) and an intestinal type stomach cancer section (patient id: 2378) has been shown. Immunohistochemistry in these two sections were done using the antibody CAB037142. Glandular cells in the normal stomach and tumor cells in the STAD sections displayed medium and high staining respectively.

Prognostic relevance of SIRT3 in regards to GC survival was calculated using Kaplan-Meier Plotter Database Analysis (http://kmplot.com/analysis/).[52] KM plotter for Gastric Cancer module was used to calculate overall survival (OS) probability associated with low and high SIRT3 expressions. Hazard ratio (HR) for 95% confidence interval and $p < 0.05$ have been considered statistically significant. The Affy id/Gene symbol for SIRT3 was 221913_at and the analysis was run on 875 patient samples data. Median survival values for low and high SIRT3 expression cohorts were shown in the survival plot in the figure as inset. For OS analysis of OGG1 low and high expression cohorts using, Kaplan-Meier Plotter, same parameters were followed with the OGG1 Affy ID/Gene symbol being 205760_s_at.

Next-generation sequencing based transcriptomics

Total RNA sequencing library preparation using TruSeq Stranded Total RNA Library preparation kit from Illumina. Briefly, total RNA was isolated from AGS cells using PureLink RNA Mini Kit (Thermo) following the manufacturer's guidelines. 10^7 cells per sample were used as the starting material. The quality and concentration of the isolated RNA samples were checked in Nanodrop 2000 (Thermo) and Agilent 2100 Bioanalyzer. Samples with RIN $\geq$ 7.0 were subsequently used for library preparation. An equal amount (200 ng) of RNA from each sample was first subjected to ribosomal RNA depletion using the Ribo-Zero Human/Mouse/Rat depletion module of the kit followed by purification and divalent cation-based fragmentation. The resulting fragments were purified and subjected to cDNA synthesis, A-tailing and dual index adapter ligation. The products were subsequently purified and PCR enriched. The resulting RNA libraries were checked in Agilent 2200 TapeStation (Agilent Technologies), quantified, normalized and subjected to equimolar pooling. The pooled libraries were finally loaded on a sequencing run flow cell (Illumina) and subjected to 100 bp paired-end massively parallel sequencing in Novaseq 6000 sequencer (Illumina). Resulting Bcl files were converted to Fastq files and the data were subjected to a quality check using FastQC v.0.11.7.[53] This was followed by adapter trimming with Cutadapt v1.16[54] using Illumina Universal Adapter. Hisat2 2.1.0.[55] was used to align the trimmed reads with Rat Rno6 reference genome (for rat samples) and Homo sapiens (human) genome assembly GRCh38 (hg38 for AGS cells). Sorting of Bam files was performed with Samtools v1.19[56] Next, gene count was performed with Feature Counts[57] followed by differential analysis using DESeq2.[58] Differentially expressed genes with $\geq$ or $\leq$ 1.5-fold expression change and p value $\leq$ 0.05 and FDR $\leq$ 0.05 were filtered. Finally, gene enrichment and pathway analysis were performed with IPA (Ingenuity Pathway Analysis) software. For rat gastric mucosal samples data were also filtered with $\geq$ or $\leq$ 1.2-fold expression change and p value and FDR cut off of $\leq$ 0.05 to include genes regulating mitochondrial metabolism and functions. Sequencing was performed in triplicate. The GEO accession number for transcriptomic data is GSE202140.

RNA isolation and real-time RT-PCR

TRIzol (Invitrogen, Carlsbad, CA) was used to isolate total RNA from AGS cells following the manufacturer's instructions. Isolated RNA was then and estimated using Maestrogen nano Spectrophotometer (Life Teb Gen co, Tehran-Iran). Obtained total RNA (2 μg) was reverse transcribed with oligo-dT18 primer using RevertAid H Minus first strand cDNA synthesis kit (Thermo) followed by rDNAse treatment. The resultant cDNAs were used for qPCR after proper dilution by using Primers (Table S4) obtained from Integrated DNA Technologies Inc. (San Diego, California, USA). Roche LightCycler 96 qPCR system was used for performing the qPCR by using SYBR green master mix (Roche) in following the as mentioned cycle conditions: initial denaturation temperature at 95°C/10 min followed by 40 cycles of denaturation at 95°C/15 sec, annealing (at indicated annealing temperatures, Table S4) for 30 sec and extension at 72°C/25 sec. Relative gene expression was calculated using $2^{-\Delta\Delta Cq}$ method and the data represented as a fold relative to control. GAPDH was used as the internal control. In every case the experiments were repeated thrice.

Isolation of mitochondria

Mitochondria were using BioChain's mitochondria isolation kit following the manufacturer's procedures. In short, an equal amount of AGS cells ($2x10^8$) from separate experimental sets were taken for mitochondria isolation. Gentle homogenization for each sample was performed in Dounce homogenizer on ice. Next the samples were centrifuged at 600 g for 10 min to remove the nuclei and cell debris. The supernatant was collected and again centrifuged at 12,000 g for 15 min to get the mitochondrial fraction. The mitochondrial pellets were washed thrice in mitochondria isolation buffer and resultant pellets (approximately 99% pure) were used for either respiratory chain complex and dehydrogenase assays or lysed for immunoblotting as required. In every case the experiments were repeated thrice.

Isolation of mitochondrial DNA and measurement of 8-oxo-dG by ELISA

DNA from the isolated mitochondrial pellets from AGS cells were extracted by the phenol-chloroform method. In short, the mitochondrial pellet was resuspended in 100 μL of Proteinase K-supplemented lysis buffer and incubated at 50°C for 3 hrs following which 200 μL of phenol-chloroform was added and mixed thoroughly. The contents were centrifuged at 10,000 g to separate the phases. The aqueous phase was collected and 200 μL of 7.5 M ammonium acetate and 500 μL of ethanol were added. The tubes were kept at -20°C for 2 hrs. The samples were next centrifuged at 10,000 g for 30 mins. The pellets were washed with 500 μL of 70% ethanol and finally, the DNA pellets were dissolved in 30 μL of TB buffer. The mtDNA was spectrophotometrically estimated. An equal amount of mtDNA from each experimental set was then taken for 8-oxo-dG measurement using ELISA using a commercially available HT 8-oxo-dG ELISA Kit II from Trevigen. In every case the experiments were repeated thrice.

Superoxide dismutase-2 (SOD2) activity assay

Commercially available superoxide dismutase (SOD) activity assay kit ab65354 (Abcam) was used to measure the mitochondrial superoxide dismutase (SOD) activity. Briefly, mitochondria were isolated from control and indomethacin-treated cells. The mitochondrial pellets were then lysed in ice cold 0.1M Tris/HCl, pH 7.4 containing 0.5% Triton X-100, 5mM β-ME, 0.1 mg/ml PMSF and the superoxide dismutase (SOD) activity from the mitochondrial fraction was measured following the manufacturer's protocol. The data is presented as ratio to 100% which is the SOD activity of control mitochondrial fraction. The relative SOD activity was normalized by estimating the protein amount in their respective mitochondrial fraction. In every case the experiments were repeated thrice.

Small interfering RNA (siRNA) transfection

siRNA-based reverse transfection was undertaken for silencing the expressions of SIRT3, ERRα, PGC1α, COX1 and COX2 following standard protocol for transfection.[44] Briefly, lyophilized siRNA duplexes were reconstituted in the nuclease-free resuspension buffer (10 μM Tris-HCl, 20 mM NaCl, 1 mM EDTA, pH 8.0) to a final concentration of 10 μM. Cells at a confluency of 50-60% were exposed to respective siRNAs or scrambled siRNA (control siRNA). 75 pmol of siRNA and Lipofectamine RNAiMAX (Thermo) were independently diluted in OptiMEM, tap-mixed, combined and finally added to the OptiMEM pre-acclimatized cells. Transfections with scrambled siRNAs (control siRNA) were performed each time. The cells were maintained in the transfection medium for 16-18 hr following which the media was replaced with complete growth media. The transfected cells were treated with 0.5 mM indomethacin for 24 hr. In every case the experiments were repeated thrice.

Confocal microscopy for mitochondrial structure analysis and immunocytochemistry

For live-cell confocal imaging to evaluate the mitochondrial structure, cells (after treatment) were washed with pre-warmed media and stained with MitoTracker Red CMX ROS (100 nM) for 20 minutes. Nuclei were stained with Hoechst 33342. After staining, the cells were washed in pre-warmed media and observed under 63X oil immersion lens of the Leica TCS-SP8 confocal microscope (Leica Microsystems, Wetzlar, Germany) provided with a thermo-regulated stage in 5% CO_2 environment. Laser intensity was maintained below 2% to avoid laser-induced toxicity to the cells. Next the immunofluorescence staining of 8-oxo-dG was performed by following the protocol mentioned previously.[45] In brief, indomethacin treated AGS cells (on glass coverslips) were fixed (2% paraformaldehyde), permeabilized in 0.15% Triton X-100, and blocked in 2% BSA solution in PBS.[44] Primary antibodies against TOM20 (for detecting mitochondria, 1:250) and 8-oxo-dG (anti DNA/RNA damage antibody, 1:250) were diluted in the blocking solution and incubated overnight. The next day the cells were washed and incubated with secondary antibodies against TOM20 (Alexa fluor 647-conjμgated anti-rabbit IgG, 1:1000) and 8-oxo-dG (Alexa fluor 488-conjμgated anti-mouse IgG, 1:500). The coverslips were washed and mounted on glass slides for visualizing under 63X oil immersion lens. Digital zooming was performed as required and at least 100 cells were screened per experimental set. At least 5 independent fields were randomly captured and representative images have been provided. The images are representatives of independently replicated experiments. In every case the experiments were repeated thrice.

Measurement of mitochondrial superoxide

MitoSox staining was performed to measure the accumulation of mitochondrial reactive pro-oxidants in AGS cells. After treatment, the cells were washed with pre-warmed PBS and dissociated. Next, the cells were stained with MitoSox following the manufacturer's instructions. Cells were washed thrice with pre-warmed PBS and analyzed in FACS LSR Fortessa, BD. Data were analyzed in FACS DIVA software under standard parameters. 10^4 cells were evaluated per set and experiments were repeated thrice.

FITC-annexin V staining for cell death determination

Apoptosis in the AGS cells was determined by annexin V/propidium iodide (PI) dual staining as described elsewhere.[44] Briefly, after treatment, the cells were dissociated. The cells were subsequently taken in annexin V binding buffer (Abcam) and stained with FITC-annexin V and PI (propidium iodide) following the manufacturer's protocol. Cells were subsequently analysed in FACS LSR Fortessa, BD. Data were analyzed in FACS DIVA software under standard parameters. 10^4 cells were evaluated per set and experiments were repeated thrice.

QUANTIFICATION AND STATISTICAL ANALYSIS

All experiments were repeated at least thrice. Data acquired from experiments were represented as mean $\pm$ standard deviation. When comparing two experimental groups, unpaired t-test (with Welch correction) was done to calculate the level of significance while one-way ANOVA followed by Bonferroni's Multiple-Comparison test was done for comparing more than two groups. For statistical significance a P value less than 0.05 ($P<0.05$) was considered. Statistical analysis of data was done using GraphPad Prism 8 and Microsoft Office Excel 2019 software.

Indomethacin impairs mitochondrial dynamics by activating the PKCζ–p38–DRP1 pathway and inducing apoptosis in gastric cancer and normal mucosal cells

Received for publication, June 12, 2018, and in revised form, March 27, 2019 Published, Papers in Press, April 2, 2019, DOI 10.1074/jbc.RA118.004415

Somnath Mazumder[‡1], Rudranil De[‡1], Subhashis Debsharma[‡], Samik Bindu[§], Pallab Maity[‡], Souvik Sarkar[‡], Shubhra Jyoti Saha[‡], Asim Azhar Siddiqui[‡], Chinmoy Banerjee[‡], Shiladitya Nag[‡], Debanjan Saha[‡], Saikat Pramanik[‡], Kalyan Mitra[¶], and Uday Bandyopadhyay[‡2]

From the [‡]Division of Infectious Diseases and Immunology, CSIR-Indian Institute of Chemical Biology, Kolkata, West Bengal 700032, the [§]Department of Zoology, Cooch Behar Panchanan Barma University, Cooch Behar, West Bengal 736101, and the [¶]Sophisticated Analytical Instrument Facility, CSIR-Central Drug Research Institute, Sector 10, Jankipuram Extension, Sitapur Road, Lucknow 226031, Uttar Pradesh, India

Edited by Luke O'Neill

The subcellular mechanism by which nonsteroidal anti-inflammatory drugs (NSAIDs) induce apoptosis in gastric cancer and normal mucosal cells is elusive because of the diverse cyclooxygenase-independent effects of these drugs. Using human gastric carcinoma cells (AGSs) and a rat gastric injury model, here we report that the NSAID indomethacin activates the protein kinase Cζ (PKCζ)–p38 MAPK (p38)– dynamin-related protein 1 (DRP1) pathway and thereby disrupts the physiological balance of mitochondrial dynamics by promoting mitochondrial hyper-fission and dysfunction leading to apoptosis. Notably, DRP1 knockdown or SB203580-induced p38 inhibition reduced indomethacin-induced damage to AGSs. Indomethacin impaired mitochondrial dynamics by promoting fissogenic activation and mitochondrial recruitment of DRP1 and down-regulating fusogenic optic atrophy 1 (OPA1) and mitofusins in rat gastric mucosa. Consistent with OPA1 maintaining cristae architecture, its down-regulation resulted in EM-detectable cristae deformity. Deregulated mitochondrial dynamics resulting in defective mitochondria were evident from enhanced Parkin expression and mitochondrial proteome ubiquitination. Indomethacin ultimately induced mitochondrial metabolic and bioenergetic crises in the rat stomach, indicated by compromised fatty acid oxidation, reduced complex I–associated electron transport chain activity, and ATP depletion. Interestingly, Mdivi-1, a fission-preventing mito-protective drug, reversed indomethacin-induced DRP1 phosphorylation on Ser-616, mitochondrial proteome ubiquitination, and mitochondrial metabolic crisis. Mdivi-1 also prevented indomethacin-induced mitochondrial macromolecular damage, caspase activation, mucosal inflammation, and gastric mucosal injury. Our results identify mitochondrial hyper-fission as a critical and common subcellular event triggered by indomethacin that promotes apoptosis in both gastric cancer and normal mucosal cells, thereby contributing to mucosal injury.

Nonsteroidal anti-inflammatory drugs (NSAIDs)[3] are the most effective medicines for treating pain and inflammation (1, 2). In addition to their anti-nociceptive action, NSAIDs are also gaining significant importance because of their anti-neoplastic effects against a wide spectrum of cancers. In fact, prolonged NSAID users are at lower risk of developing cancers (3, 4), and these noncanonical anti-cancer drugs are now included in a combination– chemotherapy regimen as they potentiate chemotherapy and radiotherapy (5). Although prostaglandin depletion due to cyclooxygenase (COX) inhibition is primarily responsible for both anti-inflammatory as well as cytotoxic anti-cancer action of NSAIDs (6), COX-independent targets, including cGMP phosphodiesterase, peroxisome proliferator-activated receptors, retinoid X receptor, IKKβ, AMP kinase, and other targets of these drugs as well as their metabolites (7), help to trigger cell death by apoptosis while blocking proliferation. Hence, NSAIDs are gaining immense importance and have been under exploration in various diseases, including cancer (7–10). Despite their multidimensional health benefits, the toxic actions of NSAIDs are observed against various normal cells of the body that compromise metabolic homeostasis and tissue integrity (6, 11, 12). Of the several organs affected by long-term NSAID usage (13–16), the gastrointestinal system

This work was supported by a Council of Scientific and Industrial Research, New Delhi, India, fellowship (to S. M. and R. D.), Research Grants BEnD, BSC 0206, and DST (J. C. Bose Fellowship) Grant SB/S2/JCB-54/2014. The authors declare that they have no conflicts of interest with the contents of this article.

[1] Both authors contributed equally to this work.

[2] To whom correspondence should be addressed: Division of Infectious Diseases and Immunology, CSIR-Indian Institute of Chemical Biology, 4 Raja S.C. Mullick Rd., Kolkata 700032, West Bengal, India. Tel.: 91-33-2499-5735 or 91-33-2473-5197; Fax: 91-33-2473-0492 or 91-33-2472-3967; E-mail: ubandyo_1964@yahoo.com.

[3] The abbreviations used are: NSAID, nonsteroidal anti-inflammatory drug; MFF, mitochondrial fission factor; MTT, 3-(4,5-dimethylthiazol-2-yl)-2,5-diphenyltetrazolium bromide; STED, stimulated emission depletion microscopy; ETC, electron transport chain; ROS, reactive oxygen species; OCR, oxygen consumption ratio; ANOVA, analysis of variance; TEM, transmission EM; COX, cyclooxygenase; IMM, inner mitochondrial membrane; MOS, mitochondrial oxidative stress; RCR, respiratory control ratio; qPCR, quantitative PCR; NAO, nonyl acridine orange; AGS, human gastric epithelial cell; PSI, pseudo-substrate inhibitor; FCCP, carbonyl cyanide *p*-trifluoromethoxyphenylhydrazone; II, injury index; ROI, region of interest; MAPK, mitogen-activated protein kinase; ERK, extracellular signal-regulated kinase; JNK, c-Jun N-terminal kinase; PG, prostaglandin; FtMt, mitochondrial ferritin; DAPI, 4′,6-diamidino-2-phenylindole; DAB, 3,3′-diaminobenzidine.

Life Sciences 305 (2022) 120753

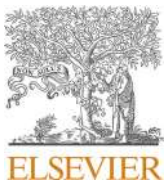

Contents lists available at ScienceDirect

Life Sciences

journal homepage: www.elsevier.com/locate/lifescie

Review article

Emerging role of mitochondrial DAMPs, aberrant mitochondrial dynamics and anomalous mitophagy in gut mucosal pathogenesis

Somnath Mazumder [a,1], Samik Bindu [b,1], Rudranil De [c], Subhashis Debsharma [d], Saikat Pramanik [d], Uday Bandyopadhyay [d,e,*]

[a] Department of Zoology, Raja Peary Mohan College, 1 Acharya Dhruba Pal Road, Uttarpara, West Bengal 712258, India
[b] Department of Zoology, Cooch Behar Panchanan Barma University, Cooch Behar, West Bengal 736101, India
[c] Amity Institute of Biotechnology, Amity University, Kolkata, Plot No: 36, 37 & 38, Major Arterial Road, Action Area II, Kadampukur Village, Newtown, Kolkata, West Bengal 700135, India
[d] Division of Infectious Diseases and Immunology, CSIR-Indian Institute of Chemical Biology, 4 Raja S.C. Mullick Road, Kolkata, West Bengal 700032, India
[e] Division of Molecular Medicine, Bose Institute, EN 80, Sector V, Bidhan Nagar, Kolkata, West Bengal 700091, India

ARTICLE INFO

Keywords:
Mitochondrial oxidative stress
Inflammation
Peptic ulcer
Inflammatory bowel disease
COVID-19
Mitochondria targeted antioxidants

ABSTRACT

Gastroduodenal inflammation and ulcerative injuries are increasing due to expanding socio-economic stress, unhealthy food habits-lifestyle, smoking, alcoholism and usage of medicines like non-steroidal anti-inflammatory drugs. In fact, gastrointestinal (GI) complications, associated with the prevailing COVID-19 pandemic, further, poses a challenge to global healthcare towards safeguarding the GI tract. Emerging evidences have discretely identified mitochondrial dysfunctions as common etiological denominators in diseases. However, it is worth realizing that mitochondrial dysfunctions are not just consequences of diseases. Rather, damaged mitochondria severely aggravate the pathogenesis thereby qualifying as perpetrable factors worth of prophylactic and therapeutic targeting. Oxidative and nitrosative stress due to endogenous and exogenous stimuli triggers mitochondrial injury causing production of mitochondrial damage associated molecular patterns (mtDAMPs), which, in a feed-forward loop, inflicts inflammatory tissue damage. Mitochondrial structural dynamics and mitophagy are crucial quality control parameters determining the extent of mitopathology and disease outcomes. Interestingly, apart from endogenous factors, mitochondria also crosstalk and in turn get detrimentally affected by gut pathobionts colonized during luminal dysbiosis. Although mitopathology is documented in various pre-clinical/clinical studies, a comprehensive account appreciating the mitochondrial basis of GI mucosal pathogenesis is largely lacking. Here we critically discuss the molecular events impinging on mitochondria along with the interplay of mitochondria-derived factors in fueling mucosal damage. We specifically emphasize on the potential role of aberrant mitochondrial dynamics, anomalous mitophagy, mitochondrial lipoxidation and ferroptosis as emerging regulators of GI mucosal pathogenesis. We finally discuss about the prospect of mitochondrial targeting for next-generation drug discovery against GI disorders.

1. Introduction

Gastrointestinal (GI) disorders are escalating worldwide owing to multiple factors including stress, trauma, excess cigarette smoking, alcohol abuse, increasing inclination towards painkiller (non-steroidal anti-inflammatory drugs, NSAIDs) usage, *Helicobacter pylori* infection and of course increasing influence of gluten-enriched diet (which significantly alters the normal gut microbiota composition to instate a chronic basal inflammation) [1,2]. Mucosal inflammation, a central denominator in major GI pathologies, is a multifactorial phenomenon where mitochondrial structural and functional aberrance critically compromises the tissue integrity besides triggering a maladaptive immunological regulation of the pathogenesis [3–5]. Owing to the high energy requirement for maintaining intestinal barrier functions as well as cellular turnover, to replenish the constantly denuding GI mucosal surface, mitochondrial health is quintessential for maintaining GI integrity. Mitopathology is therefore likely to fuel the occurrence and/or recurrence of GI disorders. Clinical manifestations of mitochondrial

* Corresponding author at: Division of Molecular Medicine, Bose Institute, EN 80, Sector V, Bidhan Nagar, Kolkata 700091, India.
E-mail address: udayb@jcbose.ac.in (U. Bandyopadhyay).
[1] These authors contributed equally to this work.

https://doi.org/10.1016/j.lfs.2022.120753
Received 11 May 2022; Received in revised form 13 June 2022; Accepted 27 June 2022
Available online 3 July 2022

ACS Infectious Diseases

Article

Cite This: ACS Infect. Dis. 2019, 5, 63−73

pubs.acs.org/journal/aidcbc

Hydrazonophenol, a Food Vacuole-Targeted and Ferriprotoporphyrin IX-Interacting Chemotype Prevents Drug-Resistant Malaria

Shubhra Jyoti Saha, Asim Azhar Siddiqui, Saikat Pramanik, Debanjan Saha, Rudranil De, Somnath Mazumder, Subhashis Debsharma, Shiladitya Nag, Chinmoy Banerjee, and Uday Bandyopadhyay*

Division of Infectious Diseases and Immunology, CSIR - Indian Institute of Chemical Biology, 4 Raja S. C. Mullick Road, Jadavpur, Kolkata 700032, West Bengal, India

Supporting Information

ABSTRACT: The rapid emergence of resistance against frontline antimalarial drugs essentially warrants the identification of new-generation antimalarials. Here, we describe the synthesis of (*E*)-2-isopropyl-5-methyl-4-((2-(pyridin-4-yl)hydrazono)methyl)phenol (**18**), which binds ferriprotoporphyrin-IX (Fe^{III}-PPIX) (K_d = 33 nM) and offers antimalarial activity against chloroquine-resistant and sensitive strains of *Plasmodium falciparum* in vitro. Structure−function analysis reveals that compound **18** binds Fe^{III}-PPIX through the −C═N−NH− moiety and 2-pyridyl substitution at the hydrazine counterpart plays a critical role in antimalarial efficacy. Live cell confocal imaging using a fluorophore-tagged compound confirms its accumulation inside the acidic food vacuole (FV) of *P. falciparum*. Furthermore, this compound concentration-dependently elevates the pH in FV, implicating a plausible interference with Fe^{III}-PPIX crystallization (hemozoin formation) by a dual function: increasing the pH and binding free Fe^{III}-PPIX. Different off-target bioassays reduce the possibility of the promiscuous nature of compound **18**. Compound **18** also exhibits potent in vivo antimalarial activity against chloroquine-resistant *P. yoelii* and *P. berghei* ANKA (causing cerebral malaria) in mice with negligible toxicity.

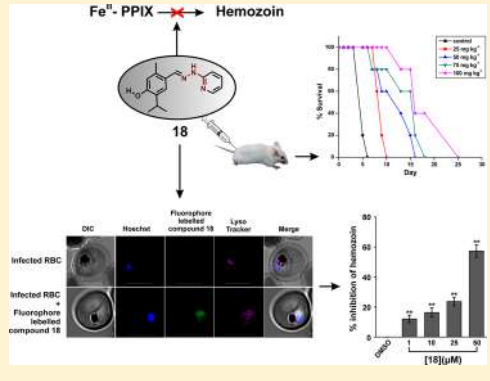

KEYWORDS: *Plasmodium, malaria, hemozoin, food vacuole, parasite metabolism*

The adverse effect of malaria across the globe demands serious attention due to the increasing number of reports of multi-drug-resistant (MDR) strains posing a severe threat to human life and productivity.[1,2] Reports of 216 million cases with 445 000 deaths in 2016 repeatedly accentuate the desideratum of new antimalarial chemotherapeutics against MDR strains.[3] Moreover, the emergence of drug resistance against artemisinin partner drugs such as piperaquine and mefloquine has resulted in a significant failure of artemisinin combination therapy (ACT) on the Thai−Cambodian border, where chloroquine (CQ) resistance was developed almost 50 years ago.[4] The spread of resistance therefore needs to be dealt with in the identification of new antimalarial chemotypes that are efficacious against MDR malaria in the most unfortified regions.[1,5]

Intraerythrocytic stages of *P. falciparum* are responsible for its clinical symptoms, and during these stages, the parasite digests hemoglobin in the acidic food vacuole (FV) and thereby releases heme (Fe^{III}-PPIX), a nonprotein constituent of hemoglobin as a byproduct.[6,7] This free Fe^{III}-PPIX, a well-known pro-oxidant, may cause severe oxidative damage to the lipid bilayers of the parasitic cell membrane, leading to membrane lesion.[8−10] In order to evade the detrimental consequences of free Fe^{III}-PPIX accumulation, *Plasmodium* crystallizes it into nontoxic inert hemozoin (Hz).[11,12] It was found that the development of CQ resistance in parasites was mainly due to multiple mutations in the *P. falciparum* CQ resistance transporter (*Pf*CRT) that results in structure-specific efflux of the drug from FV.[13] Despite this resistance, the Hz crystallization pathway within the parasite is still essential, and thus it may be used as a sustainable drug target.[14] Thus, scaffolds which bind to free Fe^{III}-PPIX and inhibit Hz crystallization can be detrimental to parasites due to free Fe^{III}-PPIX accumulation within the FV and have merit as potent antimalarials.

In the search for new antimalarial chemotypes, we focused our study on Fe^{III}-PPIX binding moieties that are capable of interacting with high affinity. A novel class of chiral gallium(III) complexes of amine-phenol ligand and schiff-base phenol ligand were reported to possess decent efficacy against CQ-sensitive and -resistant strains.[15] These cationic

Received: July 23, 2018
Published: November 25, 2018

DOI: 10.1021/acsinfecdis.8b00178
ACS Infect. Dis. 2019, 5, 63−73

Macrophage migration inhibitory factor regulates mitochondrial dynamics and cell growth of human cancer cell lines through CD74–NF-κB signaling

Received for publication, May 11, 2018, and in revised form, September 25, 2018 Published, Papers in Press, October 26, 2018, DOI 10.1074/jbc.RA118.003935

Rudranil De[1], **Souvik Sarkar**[1], **Somnath Mazumder, Subhashis Debsharma, Asim Azhar Siddiqui, Shubhra Jyoti Saha, Chinmoy Banerjee, Shiladitya Nag, Debanjan Saha, Saikat Pramanik, and Uday Bandyopadhyay**[2]

From the Division of Infectious Diseases and Immunology, CSIR-Indian Institute of Chemical Biology, Jadavpur, Kolkata 700032, West Bengal, India

Edited by Luke O'Neill

The indispensable role of macrophage migration inhibitory factor (MIF) in cancer cell proliferation is unambiguous, although which specific roles the cytokine plays to block apoptosis by preserving cell growth is still obscure. Using different cancer cell lines (AGS, HepG2, HCT116, and HeLa), here we report that the silencing of MIF severely deregulated mitochondrial structural dynamics by shifting the balance toward excess fission, besides inducing apoptosis with increasing sub-G_0 cells. Furthermore, enhanced mitochondrial Bax translocation along with cytochrome *c* release, down-regulation of Bcl-xL, and Bcl-2 as well as up-regulation of Bad, Bax, and p53 indicated the activation of a mitochondrial pathway of apoptosis upon MIF silencing. The data also indicate a concerted down-regulation of Opa1 and Mfn1 along with a significant elevation of Drp1, cumulatively causing mitochondrial fragmentation upon MIF silencing. Up-regulation of Drp1 was found to be further coupled with fissogenic serine 616 phosphorylation and serine 637 dephosphorylation, thus ensuring enhanced mitochondrial translocation. Interestingly, MIF silencing was found to be associated with decreased NF-κB activation. In fact, NF-κB knockdown in turn increased mitochondrial fission and cell death. In addition, the silencing of CD74, the cognate receptor of MIF, remarkably increased mitochondrial fragmentation in addition to preventing cell proliferation, inducing mitochondrial depolarization, and increasing apoptotic cell death. This indicates the active operation of a MIF-regulated CD74–NF-κB signaling axis for maintaining mitochondrial stability and cell growth. Thus, we propose that MIF, through CD74, constitutively activates NF-κB to control mitochondrial dynamics and stability for promoting carcinogenesis via averting apoptosis.

Macrophage migration inhibitory factor (MIF)[3] is a pluripotent inflammatory marker, which is widely known for its proinflammatory role in generating immune response by activating macrophages and T cells (1). MIF has been shown to promote tumorigenesis in many models of colorectal adenomas, intestinal tumors, ovarian cancer, and hepatocellular carcinoma (2, 3). MIF is high in both serum and epithelial cells of gastric cancer patients (4, 5). The intricate association of up-regulated MIF expression in gastrointestinal tract malignancies makes MIF a biomarker for gastric cancer as well as a potential target in anti-cancer therapies. Despite its significance in cancer, the precise role of MIF in carcinogenesis is still elusive, although some critical MIF-mediated pathways including P115 (6), inactivation of p53 (7), and stimulation of angiogenesis (2) have been investigated. The literature also suggests that CD74, the cognate receptor of MIF, upon stimulation activates NF-κB, a key molecular player in cancer and inflammation, which triggers the entry of stimulated cells into the S-phase, elevates DNA synthesis and cell division and augments BCL-X_L expression (8). CD74-MIF signaling is suspected to play a vital prognostic role in many malignancies (9). Notably, clinical immunotherapies are also being conducted targeting CD74 by milatuzumab, the monoclonal anti-CD74 antibody, in malignancies like B-cell lymphomas (10) and multiple myeloma (11).

Mitochondria are organelles that provide the majority of the energy in most cells by synthesizing ATP (12). As mitochondria are dynamic organelles that continuously undergo fission and fusion (12), mitochondrial structural integrity plays a critical role in metabolic functions (13). Severe defects in either mitochondrial fusion or fission lead to mitochondrial dysfunction (14). The Warburg effect proposes redundancy of mitochondrial oxidative phosphorylation as a major source of cellular bioenergy production; however the heterogeneity of cancer

This work was supported by a fellowship (to R. D.) and Research Grants BEnD and BSC 0206 from the Council of Scientific and Industrial Research, New Delhi. This work also was supported by J. C. Bose Fellowship SB/S2/JCB-54/2014 from the Department of Science and Technology, Ministry of Science and Technology (DST). The authors declare that they have no conflicts of interest with the contents of this article.

[1] Both authors contributed equally to this work.

[2] To whom correspondence should be addressed: Division of Infectious Diseases and Immunology, CSIR-Indian Institute of Chemical Biology, 4 Raja S. C. Mullick Rd., Jadavpur, Kolkata 700032, West Bengal, India. Tel.: 91-33-24995735; Fax: 91-33-4730284; E-mail: ubandyo_1964@yahoo.com or udayb@iicb.res.in.

[3] The abbreviations used are: MIF, macrophage migration inhibitory factor; MTT, 3-(4,5-dimethylthiazol-2-yl)-2,5-diphenyl tetrazolium bromide; PI, propidium iodide; AGS, human gastric adenocarcinoma (cells); DMEM, Dulbecco's modified Eagle's medium; JC-1, 5,5′,6,6′-tetrachloro-1,1′,3,3′-tetraethylbenzimidazolylcarbocyanine iodide; RLU, relative light unit; STED, stimulated emission depletion (microscopy); qPCR, real-time quantitative PCR; ANOVA, analysis of variance; ROI, region of interest; KD, knock down; L-DOPA, L-Dopachrome methyl ester.

BBA - General Subjects 1864 (2020) 129656

Contents lists available at ScienceDirect

BBA - General Subjects

journal homepage: www.elsevier.com/locate/bbagen

Rab7 of *Plasmodium falciparum* is involved in its retromer complex assembly near the digestive vacuole

Asim Azhar Siddiqui, Debanjan Saha, Mohd Shameel Iqbal, Shubhra Jyoti Saha, Souvik Sarkar, Chinmoy Banerjee, Shiladitya Nag, Somnath Mazumder, Rudranil De, Saikat Pramanik, Subhashis Debsharma, Uday Bandyopadhyay*

Division of Infectious Diseases and Immunology, CSIR-Indian Institute of Chemical Biology, 4, Raja S. C. Mullick Road, Jadavpur, Kolkata 700032, West Bengal, India

ARTICLE INFO

Keywords:
Plasmodium falciparum
Rab7
GTPase
Digestive vacuole
Retromer complex

ABSTRACT

Background:

Intracellular protein trafficking is crucial for survival of cell and proper functioning of the organelles; however, these pathways are not well studied in the malaria parasite. Its unique cellular architecture and organellar composition raise an interesting question to investigate.

Methods:

The interaction of *Plasmodium falciparum* Rab7 (*Pf*Rab7) with vacuolar protein sorting-associated protein 26 (*Pf*VPS26) of retromer complex was shown by coimmunoprecipitation (co-IP). Confocal microscopy was used to show the localization of the complex in the parasite with respect to different organelles. Further chemical tools were employed to explore the role of digestive vacuole (DV) in retromer trafficking in parasite and GTPase activity of *Pf*Rab7 was examined.

Results:

*Pf*Rab7 was found to be interacting with retromer complex that assembled mostly near DV and the Golgi in trophozoites. Chemical disruption of DV by chloroquine (CQ) led to its disassembly that was further validated by using compound 5f, a heme polymerization inhibitor in the DV. *Pf*Rab7 exhibited Mg^{2+} dependent weak GTPase activity that was inhibited by a specific Rab7 GTPase inhibitor, CID 1067700, which prevented the assembly of retromer complex in *P. falciparum* and inhibited its growth suggesting the role of GTPase activity of *Pf*Rab7 in retromer assembly.

Conclusion:

Retromer complex was found to be interacting with *Pf*Rab7 and the functional integrity of the DV was found to be important for retromer assembly in *P. falciparum*.

General significance:

This study explores the retromer trafficking in *P. falciparum* and describes amechanism to validate DV targeting antiplasmodial molecules.

1. Introduction

Plasmodium falciparum is an intracellular parasite that infects the erythrocytes of its host. The intraerythrocytic stages of the parasite are responsible for its pathogenesis when it digests host hemoglobin in its DV that is a temporary organelle formed only during intraerythrocytic stages of the parasite [1]. DV is often regarded as the metabolic headquarter of the parasite and a known target for several antiplasmodial compounds [2]. The parasite thrives in the host erythrocyte and depends on its hemoglobin for nutrition and growth. It has a specialized machinery of various proteases to digest host hemoglobin inside DV [3]. Hemoglobin digestion in DV results in the release of free heme that is highly toxic to the cell. The DV of the parasite utilizes a unique mechanism where it converts free heme into an insoluble and non-toxic crystalline pigment called hemozoin [4]. Because of these factors, DV is one of the most potential targets of antiplasmodial molecules. Organellar architecture of *Plasmodium* is highly dissimilar from other eukaryotes. It has a very unusual single mitochondrion per cell [5], its endoplasmic reticulum is not well defined [6], Golgi bodies in *Plasmodium* are primitive [7]. This peculiar organization of organelles

* Corresponding author.
E-mail address: udayb@iicb.res.in (U. Bandyopadhyay).

https://doi.org/10.1016/j.bbagen.2020.129656
Received 24 January 2020; Received in revised form 22 April 2020; Accepted 2 June 2020
Available online 05 June 2020

Cell Reports

CellPress
OPEN ACCESS

Article

Nuclease activity of *Plasmodium falciparum* Alba family protein PfAlba3

Chinmoy Banerjee,[1] Shiladitya Nag,[1] Manish Goyal,[1] Debanjan Saha,[1] Asim Azhar Siddiqui,[1] Somnath Mazumder,[1] Subhashis Debsharma,[1] Saikat Pramanik,[1] and Uday Bandyopadhyay[1,2,3,*]

[1]Division of Infectious Diseases and Immunology, CSIR-Indian Institute of Chemical Biology, 4, Raja S. C. Mullick Road, Jadavpur, Kolkata, West Bengal 700032, India

[2]Division of Molecular Medicine, Bose Institute, EN 80, Sector V, Bidhan Nagar Kolkata, 700091, West Bengal, India

[3]Lead contact

*Correspondence: ubandyo_1964@yahoo.com

https://doi.org/10.1016/j.celrep.2023.112292

SUMMARY

Plasmodium falciparum Alba domain-containing protein Alba3 (PfAlba3) is ubiquitously expressed in intra-erythrocytic stages of *Plasmodium falciparum*, but the function of this protein is not yet established. Here, we report an apurinic/apyrimidinic site-driven intrinsic nuclease activity of PfAlba3 assisted by divalent metal ions. Surface plasmon resonance and atomic force microscopy confirm sequence non-specific DNA binding by PfAlba3. Upon binding, PfAlba3 cleaves double-stranded DNA (dsDNA) hydrolytically. Mutational studies coupled with mass spectrometric analysis indicate that K23 is the essential residue in modulating the binding to DNA through acetylation-deacetylation. We further demonstrate that PfSir2a interacts and deacetylates K23-acetylated PfAlba3 in favoring DNA binding. Hence, K23 serves as a putative molecular switch regulating the nuclease activity of PfAlba3. Thus, the nuclease activity of PfAlba3, along with its apurinic/apyrimidinic (AP) endonuclease feature identified in this study, indicates a role of PfAlba3 in DNA-damage response that may have a far-reaching consequence in *Plasmodium* pathogenicity.

INTRODUCTION

Nucleases play a fundamental role in a growing number of biological pathways ranging from cellular defense, nutrient regeneration, and apoptosis to nucleic acid metabolism.[1] *Plasmodium falciparum*, the etiological agent of human malignant malaria, has mastered the art of survival by capitalizing on its complex life cycle and intriguingly specialized metabolism to counter host-defense strategies. The oxidative environment under which its intra-erythrocytic stage perpetuates poses a lethal threat to its vulnerable AT-biased genome.[2] Oxidative stress, an inevitable consequence of the parasites' metabolism along with the host immune system as a countermeasure, inflicts DNA damage as a consequence of its interaction with reactive oxygen species (ROS), specifically the hydroxyl radical. Among the several DNA lesions associated, apurinic/apyrimidinic (AP) sites formed due to spontaneous hydrolysis or specific excision of inappropriate or damaged bases by DNA *N*-glycosylases are one of the most frequent to be observed.[3,4] It is estimated that in mammalian cells, around 10,000 bases are lost per day.[5,6] The subsequent loss of an encoding base in the DNA template may end up blocking the DNA and RNA polymerases, thereby stalling DNA replication and transcription. Moreover, translesional DNA synthesis may further culminate into single-nucleotide replacements or deletions/insertions leading to mutations. AP sites are crucial, owing to their high chemical reactivity, and may enhance the production of DNA breaks as well as render DNA-protein and DNA-DNA crosslink. These AP sites, if left untreated, can have deleterious consequences, as they are highly mutagenic and cytotoxic.[7,8] Hence, for maintaining genome integrity, the repair of AP sites is a major mechanism wherein AP endonucleases serve as key enzymes to initiate the repair process. Out of the four nucleobases, adenine and guanine exhibit maximum propensity for impromptu base loss. Considering the fact that the *Plasmodium falciparum* genome exhibits unusually high adenine (A) and thymine (T) content (~80%) and spontaneous de-adenination of DNA occurs naturally, it is quite apparent that an active AP repair process is prevalent. Ten DNA endonucleases encoded by the genome of *Plasmodium falciparum* 3D7 clone have been identified, of which seven are predicted to harbor an endonuclease/exonuclease/phosphatase (IPR005135) domain that plays a crucial role in DNA catalysis.[9] The repair of nuclear DNA in *Plasmodium falciparum* has been proposed to involve homologous recombination, mismatch repair (MMR) pathways, and alternative end joining.[10,11] Putative proteins involved in nucleotide excision repair have also been reported.[12] Base excision repair (BER) in *Plasmodium falciparum* is mediated via long patch repair mechanism by class II AP endonucleases present in the parasite lysate. Recent studies have identified two mitochondrial AP endonucleases in *Plasmodium falciparum*.[13,14] Apart from these two mitochondrial AP endonucleases, three more enzymes (uracil DNA glycosylase, flap endonuclease 1,

The FEBS Journal

FEBS PRESS science publishing by scientists

Structure–function analysis of nucleotide housekeeping protein HAM1 from human malaria parasite *Plasmodium falciparum*

Debanjan Saha[1], Atanu Pramanik[2], Aline Freville[3], Asim Azhar Siddiqui[1], Uttam Pal[2], Chinmoy Banerjee[1], Shiladitya Nag[1], Subhashis Debsharma[1], Saikat Pramanik[1], Somnath Mazumder[4], Nakul C. Maiti[2], Saumen Datta[2], Christiaan van Ooij[3] and Uday Bandyopadhyay[1,5]

1 Division of Infectious Diseases and Immunology, CSIR-Indian Institute of Chemical Biology, Kolkata, India
2 Division of Structural Biology & Bioinformatics, CSIR-Indian Institute of Chemical Biology, Kolkata, India
3 Department of Infection Biology, London School of Hygiene & Tropical Medicine, UK
4 Department of Zoology, Raja Peary Mohan College, Uttarpara, India
5 Department of Biological Sciences, Bose Institute, Kolkata, India

Keywords
CRISPR-Cas9/DiCre; molecular dynamics; non-canonical bases; *Plasmodium falciparum*; X-ray crystallography

Correspondence
U. Bandyopadhyay, Division of Infectious Diseases and Immunology, CSIR-Indian Institute of Chemical Biology, 4, Raja S. C. Mullick Road, Jadavpur, Kolkata – 700032, West Bengal, India; Department of Biological Sciences, Bose Institute, Unified Academic Campus, EN 80, Sector V, Bidhannagar, Kolkata – 700091, West Bengal, India
Tel: +918910865252
E-mail: udayb@jcbose.ac.in

(Received 20 January 2024, revised 29 March 2024, accepted 20 June 2024)

doi:10.1111/febs.17216

Non-canonical nucleotides, generated as oxidative metabolic by-products, significantly threaten the genome integrity of *Plasmodium falciparum* and thereby, their survival, owing to their mutagenic effects. *Pf*HAM1, an evolutionarily conserved inosine/xanthosine triphosphate pyrophosphohydrolase, maintains nucleotide homeostasis in the malaria parasite by removing non-canonical nucleotides, although structure–function intricacies are hitherto poorly reported. Here, we report the X-ray crystal structure of *Pf*HAM1, which revealed a homodimeric structure, additionally validated by size-exclusion chromatography–multi-angle light scattering analysis. The two monomeric units in the dimer were aligned in a parallel fashion, and critical residues associated with substrate and metal binding were identified, wherein a notable structural difference was observed in the β-sheet main frame compared to human inosine triphosphate pyrophosphatase. *Pf*HAM1 exhibited Mg^{++}-dependent pyrophosphohydrolase activity and the highest binding affinity to dITP compared to other non-canonical nucleotides as measured by isothermal titration calorimetry. Modifying the *pfham1* genomic locus followed by live-cell imaging of expressed mNeonGreen-tagged *Pf*HAM1 demonstrated its ubiquitous presence in the cytoplasm across erythrocytic stages with greater expression in trophozoites

Abbreviations
8-oxodG, 8-oxo-2′-deoxyguanosine; ATP, adenosine-5′-triphosphate; BLAST, basic local alignment search tool; Cas9, CRISPR-associated protein 9; CD, circular dichroism; cKO, conditional knockout; CRISPR, clustered regularly interspaced short palindromic repeats; DDT, dichlorodiphenyltrichloroethane; DLS, dynamic light scattering; DMSO, dimethyl sulfoxide; EDTA, ethylenediaminetetraacetic acid; EGS, ethylene glycol bis(succinimidyl succinate); ELISA, enzyme-linked immunosorbent assay; FACS, fluorescence-activated cell sorting; FPLC, fast protein liquid chromatography; gDNA, genomic DNA; GTP, guanosine-5′-triphosphate; HAP, 6-N-hydroxylaminopurine; IDP, inosine-5′-diphosphate; IgG, immunoglobulin G; IMP, inosine-5′-monophosphate; IPTG, isopropyl ?-D-1-thiogalactopyranoside; ITC, isothermal calorimetry; ITP, inosine-5′-triphosphate; ITPases, inosine triphosphate pyrophosphatase; MALDI-TOF-MS, matrix-assisted laser desorption ionization/Time-of-flight/Mass spectrometry; MD, molecular dynamics; mNG, mNeon Green; MSA, multiple sequence alignment; NTP, nucleotide triphosphate; OD, optical density; OPLS, optimized potentials for liquid simulations; PAM, protospacer adjacent motif; PBS, phosphate-buffered saline; PCR, polymerase chain reaction; PDB, protein data bank; Pf, *Plasmodium falciparum*; qRT, quantitative real time; RBC, red blood cell; RMSD, root mean square deviation; ROS, reactive oxygen species; SDS-PAGE, sodium dodecyl-sulphate polyacrylamide gel electrophoresis; SEC-MALS, size exclusion chromatography/multi-angle light scattering; SEM, standard error of the mean; sgRNA, single guide RNA; SLI, selection-linked integration; SPC, simple point charge; UTP, uridine-5′-triphosphate; WT, wild type; XDP, xanthosine-5′-diphosphate; XMP, xanthosine-5′-monophosphate; XRC, x-ray crystallography; XTP, xanthosine-5′-triphosphate.

iScience

CellPress
OPEN ACCESS

Article

Plasmodium falciparum Alba6 exhibits DNase activity and participates in stress response

Shiladitya Nag,[1] Chinmoy Banerjee,[1] Manish Goyal,[2] Asim Azhar Siddiqui,[1] Debanjan Saha,[1] Somnath Mazumder,[1,3] Subhashis Debsharma,[1] Saikat Pramanik,[1] Shubhra Jyoti Saha,[1] Rudranil De,[4] and Uday Bandyopadhyay[1,5,6,*]

SUMMARY

Alba domain proteins, owing to their functional plasticity, play a significant role in organisms. Here, we report an intrinsic DNase activity of PfAlba6 from *Plasmodium falciparum*, an etiological agent responsible for human malignant malaria. We identified that tyrosine28 plays a critical role in the Mg^{2+} driven 5′-3′ DNase activity of PfAlba6. PfAlba6 cleaves both dsDNA as well as ssDNA. We also characterized PfAlba6-DNA interaction and observed concentration-dependent oligomerization in the presence of DNA, which is evident from size exclusion chromatography and single molecule AFM-imaging. PfAlba6 mRNA expression level is up-regulated several folds following heat stress and treatment with artemisinin, indicating a possible role in stress response. PfAlba6 has no human orthologs and is expressed in all intra-erythrocytic stages; thus, this protein can potentially be a new anti-malarial drug target.

INTRODUCTION

Malaria is one of the deadliest tropical diseases and claims millions of lives all over the world.[1] Advancement of genomic research and combinatorial therapeutics initially curbed the deadliness of the disease.[2] Still, the rapid emergence of drug-resistant *Plasmodium* sp. urgently needs more effective and advanced anti-malarial pharmacotherapeutics.[3–7] The emergence of resistant *Plasmodium* sp. is much faster than the invention of new therapeutics; therefore, improved strategies for identifying new drug targets require urgent attention.[8] First-line anti-malarial drugs like chloroquine, mefloquine, Malarone, and artemisinin instigate parasite genome instability and culminate in apoptosis-like death.[9–11] Various studies have proposed that artemisinin has multiple cellular targets involving reactive oxygen species (ROS), which leads to oxidative stress in the parasites.[12] *Plasmodium falciparum* has a plethora of DNA damage repair proteins to protect its unique structural organization.[13–15] Available genome information of *P. falciparum* facilitated us uncovering those putative parasite proteins, which are highly conserved in parasites with no human orthologs and are essential for drug-induced DNA stress response. Thus, they may serve as promising drug targets. Interestingly, the *Plasmodium* genome is 82% A + T rich, higher than any other organism.[16] We investigated the DNA-interacting protein families of *P. falciparum* to understand how the parasite nucleic acid functions with such a unique genomic makeup.[16–20]

Apart from histones, the *Plasmodium* genome encodes a unique DNA-RNA binding protein family, crucial for maintaining genetic and epigenetic functions under such unique genome organization.[21–27] Previously, genomic and transcriptomics data identified nuclear proteins from the *P. falciparum* genome that are small, basic and dimeric, belonging to the Alba (Acetylation Lowers Binding Affinity) superfamily. The Alba proteins came into the limelight after their identification as sequence-independent DNA binding proteins from archaeal hyper-thermophiles.[28–30] It has been proposed that Alba's acetylation occurs reversibly, with the non-acetyl form having greater affinity toward the DNA.[28–31] In *Sulfolobus solfataricus*, the acetylation and deacetylation are catalyzed by a homolog of Pat (protein acetyltransferase) and Sir2 protein (a sirtuin family NAD-dependent deacetylase), respectively.[28,32,33] Both in Euryarchaea (histone present) and Crenarchaea (histone absent), Alba proteins are a significant architectural DNA binding protein, playing an essential role in the organization and regulation of the genome.[29,34–36] However, studies have revealed that these Alba proteins are also associated with the RNA through the arginine–glycine–glycine repeat (RGG) present at the C terminal region where binding is modulated by methylation at the arginine in the RGG box.[34,37–44] Alba protein is not restricted to the Archaeal family and plants possess this protein where it plays important roles in oxidative stress tolerance.[45,46]

[1]Division of Infectious Diseases and Immunology, CSIR-Indian Institute of Chemical Biology, 4, Raja S. C. Mullick Road, Jadavpur, Kolkata 700032, West Bengal, India
[2]Department of Molecular & Cell Biology, School of Dental Medicine, Boston University Medical Campus, Boston, MA, USA
[3]Department of Zoology, Raja Peary Mohan College, 1 Acharya Dhruba Pal Road, Uttarpara, West Bengal 712258, India
[4]Amity Institute of Biotechnology, Amity University, Kolkata, Plot No: 36, 37 & 38, Major Arterial Road, Action Area II, Kadampukur Village, Newtown, Kolkata, West Bengal 700135, India
[5]Division of Molecular Medicine, Bose Institute, Unified Academic Campus, EN 80, Sector V, Bidhan Nagar, Kolkata, West Bengal 700091, India
[6]Lead contact
*Correspondence: ubandyo_1964@yahoo.com
https://doi.org/10.1016/j.isci.2024.109467

Zoospectra 2022

Two Day International Conference

organized by

Department of Zoology, University of Calcutta

Certificate of Participation

Prof./Dr./Smt./Sri. SAIKAT PRAMANIK

of DIV. OF INFECTIOUS DISEASES AND IMMUNOLOGY, CSIR-IICB has participated and/or successfully presented a Poster/Oral Presentation entitled

IMPACT OF ACUTE MENTAL STRESS ON GASTROPATHY AND GUT-MITOCHONDRIAL BIOGENESIS : ROLE OF GR SIGNALLING

in Zoospectra 2022, a two day international conference organized by the Department of Zoology, University of Calcutta held on 5th & 6th December, 2022

8.12.22

Prof. (Dr.) Ena Ray Banerjee
Head of the Department
Department of Zoology
University of Calcutta

Prof. (Dr.) Gautam Aditya
Joint Convenor
Zoospectra 2022

Dr. Sujay Ghosh
Joint Convenor
Zoospectra 2022

International Conference
on
MECHANISTIC AND THERAPEUTIC APPROACHES IN HUMAN AND ANIMAL HEALTH

Organised by

Department of Zoology
Cooch Behar Panchanan Barma University
West Bengal, India

Certificate of Appreciation

This is to certify that Prof. / Dr. / Mr. / Mrs. / Ms. Mr. Saikat Pramanik
of Indian Institute of Chemical Biology *participated and presented a paper in the International Conference on Mechanistic and Therapeutic Approaches in Human and Animal Health, organised by the Department of Zoology, Cooch Behar Panchanan Barma University from 6th-8th December, 2021.*

Title of the Paper presented:

Impaired mitochondrial biogenesis and functionality contributes to gastropathy in Stress-related Mucosal Disease (SRMD): A mechanistic study.

Hadida Yasmin Saikat Pramanik — *Organising Secretary*

Pradip Kumar Das — *Chairperson*

JADAVPUR UNIVERSITY

KOLKATA-700 032

NO.: CW/19052/ 0773

MARK SHEET

(For Ph.D/M. Phil. Course Work)

Results of the PH.D. COURSE WORK EXAMINATION, 2021

In SCIENCE

Name SAIKAT PRAMANIK Class Roll No. 202020502011

Examination Roll No. PHDLSBT21211 Registration No.– of

held in AUGUST, 2021

Subject Code / Name	Credit Hr.(c_i)	Marks
COMPULSORY UNITS::		
EX/LSBT/PHD/1.1 REVIEW OF LITERATURE & RESEARCH METHODOLOGY	4	82
ELECTIVE UNITS ::	4	66
EX/LSBT/PHD/1.2A :: TISSUE CULTURE TECHNIQUES		
EX/LSBT/PHD/1.2B :: MICROBIOLOGY		
EX/LSBT/PHD/1.2C :: PRINCIPLE OF MOLECULAR BIOLOGY TECHNIQUES		
EX/LSBT/PHD/1.2D :: INTRODUCTION TO MOLECULAR BIOLOGY TECHNIQUES		

Total Marks : 148 (out of 200) **Remarks:** P

Prepared by : Checked by :

Date of issue : 27 / 10 / 2021

Controller of Examinations

No. Sc. 0430

Jadavpur University

Registration Certificate

Shri/~~Sm~~ Saikat Pramanik

has been registered as a student of Ph.D. programme of this university

His/~~her~~ Registration Number is SLSBT1104119

Kolkata 27th August 2019

24.02.21

Registrar

যাদবপুর বিশ্ববিদ্যালয়
কলকাতা-৭০০০৩২, ভারত

*JADAVPUR UNIVERSITY
KOLKATA-700 032, INDIA

Ref.No.: D-7/Sc/869/19 Dated: 21.8.19

To
Sri Saikat Pramanik
C/O. – Dr. Uday Bandyopadhyay, Sr. Principal Scientist
Division of Infectious Diseases and Immunology
Indian Institute of Chemical Biology
4, Raja S.C. Mullick Road, Jadavpur
Kolkata–700032.

INDEX No: 41/19/Life Sc./26

Dear Sir,

With reference to your application for the registration for Ph.D.(Science) degree of Jadavpur University, I am to inform you that you are permitted to register your name on payment of requisite fees for Ph.D. programme of Rs.22,000/- (Rupees Twenty-Two Thousands Only), payable in three installments (Rs.8000/- + Rs.8000/- + Rs.6000/-). It may be noted that this offer is provisional until all the documents mentioned below are submitted.

The registration will be valid from the date on which the fees are paid and shall remain valid for six years from that date. Subsequently the period of registration may be extended as per Regulation 2017 if the grounds for extension satisfy the Research Advisory Committee, Ph.D. Research Committee and the Doctorate Committee accordingly. An application requesting extension and citing the grounds for the same must be submitted in due time, duly forwarded and recommended by the supervisor(s), before the date on which the validity of the registration expires.

The scheme of the work and title of the thesis, if not submitted along with the application, shall have to be submitted within two years from the date of registration or within one year from the date of successful completion of the course work result of the candidate. Otherwise, the registration is liable to cancellation as per Regulations 2017 of the University.

If the registration fee is not paid within one month from the date of issue of this letter, your application stated above will be treated as cancelled. A report on the progress of the research work shall have to submit once in every six months from the date of registration as per Regulation 2017. The registration is liable to cancellation if the progress of work is not satisfactory. It may be noted that you will have to fulfill the condition as per Regulation 2017 and have to complete the course work within two years from the date of registration.

Yours faithfully,

(Dr. Atiskumar Chattopadhyay)
Principal Secretary
Faculty Council of Science.

Mode of payment as follows:

1st instalment – within 30 days.
2nd instalment – within 180 days
3rd instalment – within 355 days.

List of required documents:

i) Migration Certificate in Original. → 27/8/19
ii) Nil.